frontiers | Research Topics

Theories, methods, and practices of wetland degradation and restoration

Edited by
Zhenguo Niu, Yijian Zeng, Haitao Wu, Guangxuan Han and Sheel Bansal

Published in
Frontiers in Ecology and Evolution
Frontiers in Environmental Science

ISSN 1664-8714
ISBN 978-2-8325-2916-4
DOI 10.3389/978-2-8325-2916-4

About Frontiers

Frontiers is more than just an open access publisher of scholarly articles: it is a pioneering approach to the world of academia, radically improving the way scholarly research is managed. The grand vision of Frontiers is a world where all people have an equal opportunity to seek, share and generate knowledge. Frontiers provides immediate and permanent online open access to all its publications, but this alone is not enough to realize our grand goals.

Frontiers journal series

The Frontiers journal series is a multi-tier and interdisciplinary set of open-access, online journals, promising a paradigm shift from the current review, selection and dissemination processes in academic publishing. All Frontiers journals are driven by researchers for researchers; therefore, they constitute a service to the scholarly community. At the same time, the *Frontiers journal series* operates on a revolutionary invention, the tiered publishing system, initially addressing specific communities of scholars, and gradually climbing up to broader public understanding, thus serving the interests of the lay society, too.

Dedication to quality

Each Frontiers article is a landmark of the highest quality, thanks to genuinely collaborative interactions between authors and review editors, who include some of the world's best academicians. Research must be certified by peers before entering a stream of knowledge that may eventually reach the public - and shape society; therefore, Frontiers only applies the most rigorous and unbiased reviews. Frontiers revolutionizes research publishing by freely delivering the most outstanding research, evaluated with no bias from both the academic and social point of view. By applying the most advanced information technologies, Frontiers is catapulting scholarly publishing into a new generation.

What are Frontiers Research Topics?

Frontiers Research Topics are very popular trademarks of the *Frontiers journals series*: they are collections of at least ten articles, all centered on a particular subject. With their unique mix of varied contributions from Original Research to Review Articles, Frontiers Research Topics unify the most influential researchers, the latest key findings and historical advances in a hot research area.

Find out more on how to host your own Frontiers Research Topic or contribute to one as an author by contacting the Frontiers editorial office: frontiersin.org/about/contact

Theories, methods, and practices of wetland degradation and restoration

Topic editors

Zhenguo Niu — Aerospace Information Research Institute, Chinese Academy of Sciences (CAS), China

Yijian Zeng — University of Twente, Netherlands

Haitao Wu — Northeast Institute of Geography and Agroecology, Chinese Academy of Sciences (CAS), China

Guangxuan Han — Yantai Institute of Coastal Zone Research, Chinese Academy of Sciences (CAS), China

Sheel Bansal — United States Geological Survey (USGS), United States Department of the Interior, United States

Citation

Niu, Z., Zeng, Y., Wu, H., Han, G., Bansal, S., eds. (2023). *Theories, methods, and practices of wetland degradation and restoration*. Lausanne: Frontiers Media SA. doi: 10.3389/978-2-8325-2916-4

Table of contents

frontiers in Ecology and Evolution

ORIGINAL RESEARCH
published: 14 September 2021
doi: 10.3389/fevo.2021.721628

Freshwater Releases Into Estuarine Wetlands Change the Determinants of Benthic Invertebrate Metacommunity Structure

*Dandan Liu[1,2], Hongxian Yu[2], Kangle Lu[1], Qiang Guan[1] and Haitao Wu[1]**

[1] Key Laboratory of Wetland Ecology and Environment, Northeast Institute of Geography and Agroecology, Chinese Academy of Sciences, Changchun, China, [2] Department of Wetland Science, College of Wildlife Resources, Northeast Forestry University, Harbin, China

In recent years, the relative importance of the processes driving metacommunity composition has aroused extensive attention and become a powerful approach to identify community patterns and their regulatory mechanisms. We investigated variations in the composition of benthic community in restored wetlands and natural wetlands in the Yellow River Delta (Shandong Province, China). First, spatial structures within each wetland were modeled with Moran eigenvector maps. Next, the variation in community structure among local environmental and spatial variables was partitioned using constrained ordination, and the "elements of metacommunity structure" analysis was used to determine the patterns of best fit for species distributions within metacommunities. Finally, the null model was used to analyze non-random patterns of species co-occurrence. The community structure of benthic invertebrates in restored wetlands and natural wetlands differed significantly. The benthic invertebrate metacommunity structure showed a nested distribution in restored wetlands and a quasi-Clementsian structure in natural wetlands. Pure environmental fractions and pure spatial fractions were critical in regulating benthic invertebrate metacommunities of restored wetlands. In natural wetlands, pure spatial fractions and the interaction between environmental and spatial factors (shared fractions) played a major role in the metacommunity. A species co-occurrence analysis showed that species co-occurred more frequently than expected by chance, demonstrating that biotic interactions were not the main driver of metacommunity structures in both wetland types. Accordingly, the benthic invertebrate metacommunity in estuarine wetlands following freshwater releases was mostly determined by environmental and spatial effects, which resulted in a metacommunity with nested distribution. These results are important for biodiversity protection and ecosystem management of estuarine wetlands in the Yellow River Delta.

Keywords: benthic invertebrates, community assembly, estuarine wetlands, metacommunity, variance partitioning

OPEN ACCESS

Edited by:
Weihua Guo,
Shandong University, China

Reviewed by:
Keila Stark,
University of British Columbia, Canada
Junhong Bai,
Beijing Normal University, China

***Correspondence:**
Haitao Wu
wuhaitao@neigae.ac.cn

Specialty section:
This article was submitted to Conservation and Restoration Ecology, a section of the journal Frontiers in Ecology and Evolution

Received: *07 June 2021*
Accepted: *20 August 2021*
Published: *14 September 2021*

Citation:
Liu D, Yu H, Lu K, Guan Q and Wu H (2021) Freshwater Releases Into Estuarine Wetlands Change the Determinants of Benthic Invertebrate Metacommunity Structure. Front. Ecol. Evol. 9:721628. doi: 10.3389/fevo.2021.721628

INTRODUCTION

The mechanisms underlying both the patterns and maintenance of biodiversity within communities have been a core research topic in community ecology (Rosenzweig, 1995). Understanding the relative importance of processes driving the composition of community is the main way to reveal the drivers of community assembly (Bell, 2010; Caruso et al., 2011). According

to niche and neutral theory, community assembly depends on abiotic factors, biotic interactions, priority effects (i.e., competitive dominance due to early colonization), and dispersal processes (Leibold et al., 2004). Discerning the relative importance of these factors has been a major challenge for understanding the assembly of ecological communities (Holyoak et al., 2005; Hildrew, 2009; Heino et al., 2015a). However, the relative importance of these factors varies with biota and spatiotemporal scales (Qian and Ricklefs, 2007; Qian, 2009; Logue et al., 2011; Heino et al., 2012). The degree to which the influence of these factors when the focus is on local-scale communities remains crucial (Heino et al., 2017). Therefore, knowledge on the determinants of local taxonomic diversity is the key to understanding ecological community composition (Daniel et al., 2019) and protecting biodiversity (Heino, 2013c).

In terrestrial, freshwater, and marine systems, the effects of spatial and environmental gradients on community composition have been widely studied (Soininen et al., 2007; Heino and Tolonen, 2017). Environmental gradients are closely related to species distribution in freshwater ecosystems (Heino and Soininen, 2010; Heino, 2011; Saito et al., 2015). For example, previous studies have shown that environmental factors, including lake size, depth, pH, nutrients, and biotic interactions, such as predation, are the main determinants of species distribution patterns in lakes (Heino and Tolonen, 2017). Due to dispersal barriers and isolation effects, the spatial positioning of lakes affects species colonization patterns. Species distributions are also affected by dispersal and other stochastic forces (Tonkin et al., 2015). Considerable variability amongst regions and benthic invertebrate groups has been reported, and environmental variables and species classification appear to be more important than spatial variables in driving the structure of ecological communities (Cottenie, 2005; Thornhill et al., 2017). Additionally, increasing evidence supports the importance of species sorting signals along geographical and environmental gradients in aquatic ecosystems (Heino, 2013a; Alahuhta et al., 2018) and emphasizes the influence of biotic interactions on biological community (García-Girón et al., 2020). Biotic interactions were the primary driving force of beta diversities of multiple organismal groups in ponds and, to a lesser extent, the abiotic environment (García-Girón et al., 2020). Hence, more biological groups and different aquatic ecosystems should be examined to gain a more general picture of the patterns of community organization at local scales (Cai et al., 2017).

The metacommunity concept has the potential to integrate local and regional dynamics within a general community ecology framework, providing a valuable analytical opportunity to identify community patterns and their regulatory mechanisms (Thompson et al., 2020). It refers to communities of interacting species connected by dispersal and responding to local environmental conditions (Leibold and Chase, 2017). Metacommunity theory integrates the abiotic environment, biotic interactions, and dispersal events as drivers of biological diversity across spatial scales. Assessing the relative importance of these drivers is a core objective of metacommunity ecology (Meynard et al., 2013; Brown et al., 2017). During the development of the metacommunity framework, six species distribution patterns (i.e., the nested subset, chessboard, Clementine gradient, Gleason gradient, uniform interval gradient, and random pattern) were identified, and each pattern was regulated by a specific mechanism (Leibold and Mikkelson, 2002; Leibold et al., 2004). Therefore, the metacommunity approach provides a research framework for identifying the mechanisms underlying species co-existence and community assembly at local scales (Leibold et al., 2004; Heino et al., 2017; Hill et al., 2017; Guo et al., 2019; Liu et al., 2019).

Different aquatic ecosystems exhibit fundamental differences in environmental heterogeneity, connectivity, and spatial extension, which provides challenges and opportunities for examining the organization of metacommunities at local scales (Brown et al., 2011; Heino, 2011; Lindstrom and Langenheder, 2012; Heino et al., 2015a). Estuarine wetlands which are transitional areas between land and sea are affected by the interactions among multiple systems including rivers, oceans, wetlands, and upland catchments (Yang et al., 2017a, 2019). Because of extensive interactions between freshwater and saltwater, estuarine wetlands form unique ecological patterns and exhibit biogeochemical cycles and biological communities different from lakes, rivers, and oceans. In estuarine wetlands, benthic invertebrates are directly involved in the material circulation and energy flow of ecosystems, and are sensitive to environmental changes and disturbances. Therefore, they are often used as biological indicator for bioassessments (Guan et al., 2017; Wu et al., 2017, 2019; Lu et al., 2019; Guan and Wu, 2021). In recent years, due to the multiple influences of natural factors and human activities, many estuarine wetlands have been degraded, their biodiversity has been diminished, and their ecosystem structure and function have been compromised. To prevent further degradation of the ecosystems, the management of the reserve has carried out ecological restoration projects for the degraded wetlands in the Yellow River Delta. However, restoration measures included the construction of levees for impoundments which blocked the connectivity between the restored wetlands and the sea. The diversity of benthic invertebrates might respond to the resulting changes in the physical and chemical properties of the water body, and the driving factors of community structure in restored wetland may differ from those in wetlands directly connected to the sea. Therefore, it is important to evaluate the benthic invertebrate metacommunity patterns and drivers after long-term freshwater releases, which can provide basic data and theoretical support for biodiversity conservation and restoration, as well as ecosystem management of the estuarine wetlands of the Yellow River Delta.

Most previous studies have focused primarily on community assembly mechanisms in freshwater ecosystems such as lakes, streams, and ponds, and few empirical studies have been performed in estuarine wetlands using similar approaches as in freshwater systems (Tonkin et al., 2018). In the present study, we assessed the responses of benthic invertebrate metacommunities to ecological restoration utilizing freshwater releases and compared them with nearby natural wetlands, which have not received freshwater releases (i.e., reference areas).

Our main goals were to: (1) assess the differences in benthic invertebrate community structure between restored and natural wetlands; and (2) identify the major factors driving benthic invertebrate metacommunity structure in the two types of wetlands. Our findings may help wetland managers to assess the ecological effects of freshwater releases, provide valuable insights for enhancing the restoration of estuarine wetland biodiversity, and improve the management of wetland ecosystems.

MATERIALS AND METHODS

Study Site

The Yellow River Delta estuarine wetland is located within Shandong Province, China (37°34.768′ ∼ 38°12.310′ N, 118°32.981′ ∼ 119°20.450′ E), between Bohai and Laizhoubays (**Figure 1**). This area is a typical fan-shaped delta encompassing a binary phase structure of river sediments covering a marine layer. As this wetland is located at mid-latitudes, it has a warm-temperate semi-humid continental monsoonal climate. The study area is characterized by annual average temperatures between 11.7 and 12.6°C, including an extreme maximum temperature of 41.9°C, an extreme minimum temperature of −23.3°C, a frost-free period of 211 days, and annual precipitation between 530 and 630 mm.

Since 2010, the Yellow River Delta Nature Reserve Administration has carried out a large-scale restoration project in degraded estuarine wetlands, reshaping the wetlands' hydrological situation. The restoration measures include the construction of tidal barriers and water diversion canals and the implementation of freshwater releases through the Qingshuigou flow path of the Yellow River from June to July every year, normally for 20–30 days (Li et al., 2016; Yang et al., 2017b). After 5 years of freshwater releases, the landscape of the restored area has changed dramatically (Dong et al., 2014; Yang et al., 2017a). This project has successfully expanded the area of reed wetlands, improved the water and salt conditions, and increased the biodiversity of the Yellow River Delta Wetland (Yang et al., 2019).

The barriers between the restored and natural wetland are earth embankments, which limits the extent of freshwater releases and creates different habitat features on either side, while preventing the entry of seawater during high tides and storms. Sampling sites in restored wetlands were located at least 100 m from the barriers to ensure no connectivity with natural wetlands (**Figure 1**).

Sample Processing and Analysis

In October 2017 and May 2018, benthic invertebrates were collected from 32 sampling sites (19 restored wetlands and 13 natural wetlands) in the Yellow River Delta Wetland. Benthic invertebrates were collected at each sampling site using a 1 mm mesh D-shaped sweep net with a diameter of 35 cm. This net was dragged horizontally from the inside of the water body to the shore and scraped the benthic surface (Wu et al., 2017). Our sampling plan captured different subhabitats. Four sweeps were performed in each site and mixed into a composite sample, stored in a numbered plastic bag, preserved in 95% alcohol, and returned to the laboratory for identification and classification. Benthic invertebrates were separated from associated materials and identified to the genus or species level (Morse et al., 1994).

A YSI multi probe water quality system (556MPS; Yellow Springs Instruments, United States) was used to measure the physicochemical properties of the water of the two types of wetlands. Measurements included pH, electrical conductivity (Cond), dissolved oxygen (DO), salinity, total dissolved solids (TDS), oxidation-reduction potential (ORP), chloride ions (Cl^-), and chlorophyll-a (Chl-a). In addition, total nitrogen (TN), total phosphorus (TP), total suspended solids (TSS), total organic carbon (TOC), total carbon (TC), inorganic carbon (IC), and dissolved organic carbon (DOC), as well as nitrate (NO_3^-), ammonium (NH_4^+), sulfate (SO_4^-), carbonate (CO_3^-), and bicarbonate ion (HCO_3^-) concentrations were analyzed in water samples following the Surface Water Environmental Quality Standards of China (GB3838–2002). Some of the measured water quality variables showed significant differences between the two types of wetlands (**Figure 2**, $p < 0.05$).

Statistical Analyses

Benthic Invertebrate Community Structures and Water Quality

The Shannon-Wiener diversity index (H'), the Simpson index (λ), and the Number of species (S) were calculated to compare benthic invertebrate community structures in both restored and natural wetlands. First, all environmental variables and biodiversity indices were tested for normal distribution using the Kolmogorov-Smirnov test prior to analyses. Then, independent sample t-tests were used to analyze differences in water quality variables and biodiversity indices between restored and natural wetlands. The biodiversity indices were calculated with the "Picante" package in R (R Core Team, 2020). The Kolmogorov-Smirnov test and the independent samples t-test were calculated by SPSS statistics version 21.

Non-metric multidimensional scaling (NMDS) was used to identify differences in the spatial distribution of benthic invertebrate metacommunities structure between different wetlands based on species abundance data of each sampling site. Differences were tested by analysis of similarities (ANOSIM). NMDS and ANOSIM were calculated using the "metaMDS" and "anosim" functions of the "vegan" package in R.

Statistical Analysis of Environmental and Spatial Data

To determine the key environmental variables affecting the benthic invertebrate community, detrended correspondence analysis (DCA) based on benthic invertebrate abundances was used to test for linearity, and axis lengths were all greater than 4. Therefore, canonical correspondence analysis (CCA) was selected for subsequent analysis. The data of the benthic invertebrate metacommunities was optimized by eliminating rare species with a frequency of occurrence less than or equal to 2. The optimized species data and environmental data (except pH) were $\log_{10}(x+1)$ transformed prior to CCA. Then, a forward selection process was performed based on the adjusted R^2 to choose significant environmental variables (Dray et al., 2006;

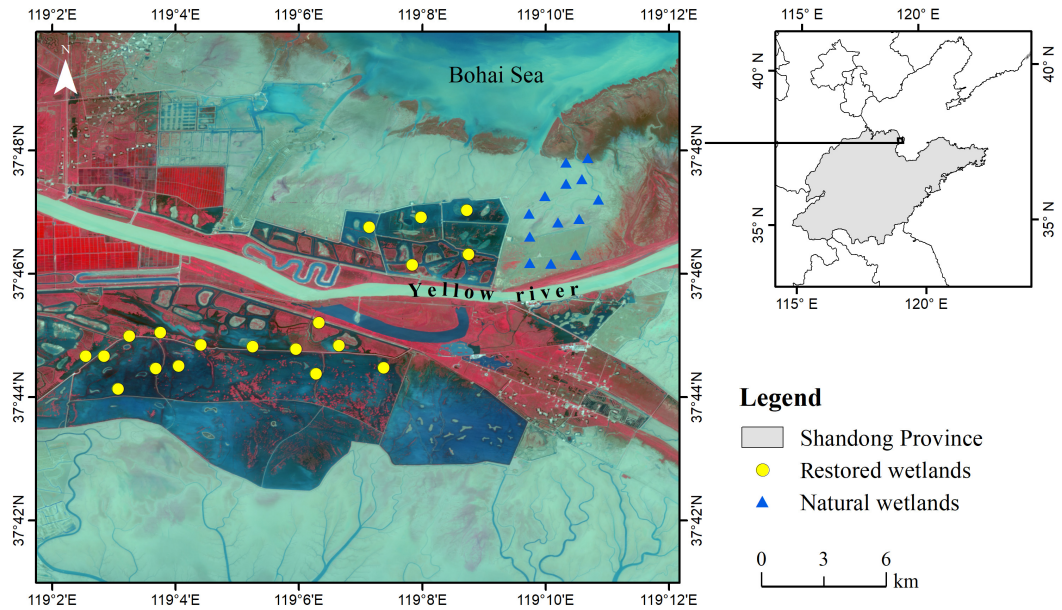

FIGURE 1 | Sampling sites in restored and natural wetlands in the Yellow River Delta.

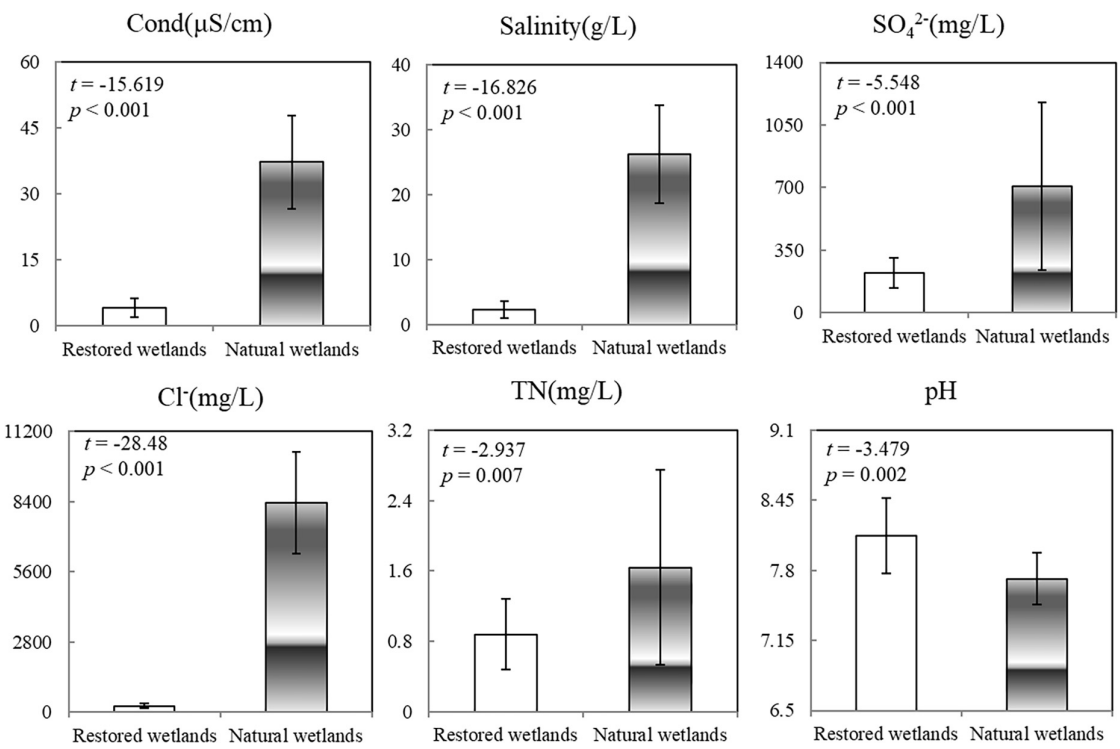

FIGURE 2 | Significant differences in water quality variables between restored and natural wetlands.

Blanchet et al., 2008). DCA and CCA were performed using the "vegan" package in R.

Moran's eigenvector maps (MEM) were used to model spatial structures among sites within the estuarine wetlands derived from the geographic coordinates of the study sites (Dray et al., 2006). The MEM analysis produces a set of orthogonal spatial variables, representing the spatial variation across a range of spatial scales (Dray et al., 2006; Declerck et al., 2011). These variables can be used as explanatory variables in direct gradient analysis to describe spatial patterns

in communities (Borcard and Legendre, 2002; Dray et al., 2012; Heino et al., 2017). In our study, MEM spatial eigen functions were computed using the "PCNM" function of the "PCNM" package in R (Legendre et al., 2012).

Variation Partitioning

To explain the relative contribution of environmental filtering and the effects of the spatial factors, variation partitioning was applied on redundancy analysis models (RDA) for the significant environmental variables and spatial variables. The final results of this analysis included four parts: pure environmental factors [(E), representing environmental controls], the interaction of environmental and spatial factors [(E+S)], pure spatial factors [(S), representing dispersal limitation], and the unexplained variation (1-[E+S], Peres-Neto et al., 2006). We reported adjusted R^2 values for all analyses because they are unbiased estimates of the explained variation (Peres-Neto et al., 2006). Variation partitioning analysis was implemented using the "varpart" function of the "vegan" package in R. The significance of explained variables was tested using the function "anova" in the package "vegan" in R.

Elements of Metacommunity Structure Analysis (EMS)

The EMS can be used to determine the patterns of the benthic invertebrate metacommunities in restored and natural wetlands. Here, the analytical approach followed previous studies by Heino et al. (Heino et al., 2015a,b, 2017), and results were interpreted according to Presley et al. (2010). Prior to analysis, the reciprocal average (RA) method was used to rearrange the species presence-absence matrix (sites by species). The RA method generates one or more RA axes by maximizing the maximum correspondence between species scores and site scores (Leibold and Mikkelson, 2002). Our analysis was performed only for the first axis (Gao et al., 2016). Based on the metrics: (1) coherence, (2) species turnover, and (3) boundary clumping, EMS was used to identify the structure of the metacommunity (e.g., random, checkerboard, nestedness, evenly spaced, Clementian, Gleasonian, and quasi structural patterns; Presley et al., 2010; Heino et al., 2015b).

(1) Coherence was evaluated by comparing the observed number of embedded absences (EAbs) in the ordinated matrix to a null distribution of embedded absences from simulated matrices (Leibold and Mikkelson, 2002; Presley et al., 2010). The results of coherence were characterized as: (i) non-significant coherence, i.e., with a random structure, (ii) significantly negative coherence, i.e., EAbs are significantly higher than expected by chance, which is a checkerboard pattern, reflecting competitive exclusion, or (iii) significantly positive coherence, i.e., EAbs are significantly lower than expected by chance, indicating that communities are structured along environmental gradients. Significantly positive coherence refers to nestedness, evenly spaced gradients, and Gleasonian structure or Clementsian structure, which needs to be further analyzed and confirmed by species turnover and boundary clumping (Leibold and Mikkelson, 2002).

(2) Species turnover was measured as the number of times one species replaces (Rep) another from site to site in an ordinated matrix (Presley et al., 2010). The results of species turnover were characterized as: (i) non-significant, i.e., quasi-structure, (ii) significantly negative, i.e., Rep is significantly lower than expected by chance, referring to a nested pattern, or (iii) significantly positive, i.e., Rep is significantly higher than expected by chance, referring to evenly spaced, Gleasonian or Clementsian structures (Presley et al., 2010). The evenly spaced Gleasonian and Clementsian metacommunity structures can be separated based on boundary clumping (Leibold and Mikkelson, 2002). Furthermore, non-significant negative species turnover could indicate quasi-nestedness, and non-significant positive species turnover could indicate quasi-Gleasonian, quasi-Clementsian, or quasi-evenly spaced gradients. Similarly, non-significant positive turnover can be separated by boundary clumping (for details, see Presley et al., 2010).

(3) Boundary clumping was assessed using Morisita's index (I) and a subsequent Chi-squared test comparing observed and expected distributions of range boundary locations. The results of boundary clumping were characterized as: (i) Gleasonian structure, i.e., I-values were close to 1, (ii) Clementsian structure, i.e., I-values were significantly greater than 1, or (iii) evenly spaced distributions, i.e., I-values were significantly greater than 1. A p-level of 0.05 was selected to test the statistical significance in all analyses. All EMS analyses were performed using the "metacom" package in R (Dallas, 2013).

Co-occurrence Analysis

The patterns of species co-occurrence in the benthic invertebrates metacommunity were analyzed using the C-score (Gotelli, 2000; Gotelli and Ulrich, 2012). The C-score (Checkerboard score, Stone and Roberts, 1990) is based on the average co-occurrence rate among all possible pairs of species in a presence-absence matrix. The checkerboard pattern of benthic invertebrates reflects whether competitive interactions among species occur (Gotelli and Mccabe, 2002). Therefore, indices of the C-score have a good power to examine species co-existence patterns at local scales (Gotelli, 2000; Gotelli and Ulrich, 2012). The calculation method of C-score was as:

$$\text{C-score} = \frac{\sum (R_i - S)(R_j - S)}{(R(R-1)/2)}$$

where R is the row totals of sites containing both species, R_i and R_j are the matrix row totals for species i and j, and S is the number of sites in which both species occur (Gotelli and Mccabe, 2002). If the presence-absence data matrices have a significantly higher C-score than randomly generated matrices, then a substantial number of species pairs co-occur (simulated value) less often than by chance (observed value), suggesting that spatial distributions may be structured by interspecific competition. In contrast, low C-scores suggest that several species co-occur more frequently than expected by chance, and species can aggregate in the same metacommunity due to environmental filtering (Gan et al., 2019; Guo et al., 2019).

To compare the significance of results across studies, standardized effect sizes (SES) should be calculated for each matrix. The standardized effect size measures the number of standard deviations that the observed index is above or below

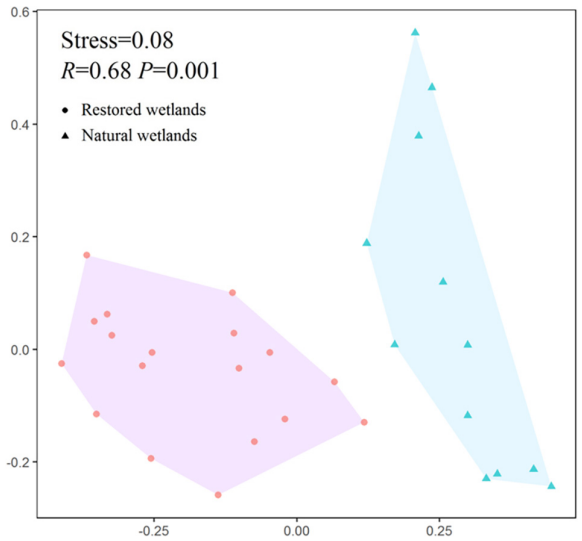

FIGURE 3 | NMDS of benthic invertebrate community composition of the Yellow River Delta based on Bray-Curtis similarities.

the mean index of the simulated communities (Gotelli and Mccabe, 2002). Based on the C-scores from the observed and the simulated communities, the standard effect sizes were calculated as:

$$SES = (C\text{-}observed\ value - C\text{-}simulated\ value)/(C\text{-}simulated\ value)$$

Assuming the SES is normally distributed, the 95% confidence interval of the SES ranges between –2.0 and 2.0 (Gao et al., 2016). C-score analysis was performed using the "EcoSimR" package in R software.

RESULTS

Benthic Invertebrate Community Structure

In total, 96 taxa were recorded at the 32 sites, including 3 phyla, 7 classes, 20 orders, and 59 families. Among these, there were 6 polychaetes, 2 oligochaetes, 58 aquatic insects, 7 bivalves, 13 gastropods, 3 crustaceans, and 7 malacostracans. Aquatic insects were the main components of restored wetlands, accounting for 74.36% of the total number of taxa. However, in natural wetlands, the benthic invertebrate community was mainly composed of annelids, bivalves, malacostracans, and gastropods (**Supplementary Table 1**).

The results of the NMDS (stress = 0.08) analysis showed that the benthic invertebrate community structure of restored and natural wetlands were clearly divided into two groups (**Figure 3**). Furthermore, there were significant differences between these two groups (R = 0.68, p = 0.001, **Figure 2**). The Shannon-Wiener index (H'), the Simpson index (λ), and the Number of species (S) of benthic invertebrates in the restored wetlands of the Yellow River Delta were significantly higher than those of natural wetlands ($p < 0.05$). Diversity indices of benthic invertebrates differed significantly between the two types of wetlands (**Figure 4**).

Metacommunity Structure Analysis in Restored Wetlands

According to the results of the EMS analysis, benthic invertebrate metacommunities showed a significantly positive coherence (i.e., the Abs was significantly lower than expected by chance), indicating that communities were structured along environmental gradients. To distinguish the structures of benthic invertebrate metacommunities, species range turnover and boundary clumping needed to be further evaluated. The results of species turnover showed that the benthic invertebrate metacommunities reflected a nested distribution pattern (i.e., lower turnover than expected by chance, **Table 1** and **Supplementary Figure 1**).

The environmental variables selected in the CCA models, i.e., the main determinants of community structure in restored wetlands, were Cond, Salinity, and ORP. We used the selected main environmental variables and the significant spatial MEM variables (MEM2, MEM4) for further analyses (**Table 2**). According to variance partitioning results, environmental and spatial variables in combination explained 43% of the interpretation rates [(S), (E), and (S+E), **Table 2**]. The amount of variance explained by the pure spatial fraction [27.2%, (E)] and the pure environmental fraction [11%, (S)] were significant ($p < 0.005$, **Table 2**), indicating that environmental and spatial factors played an important role for benthic invertebrates (**Table 2**). The interaction of environmental and spatial factors [4.8%, (E+S)] explained little variation in community composition.

Furthermore, most of the 19 sites in restored wetlands exhibited non-random patterns of species co-existence within sites (**Figure 5**). The SES < –2 indicated an aggregated distribution of benthic invertebrate assemblages. Finally, the species co-occurrence pattern analysis clearly demonstrated that biotic interactions were not the main driver of the metacommunity structure.

Metacommunity Structure Analysis in Natural Wetlands

Based on the results of EMS, benthic invertebrate metacommunities showed positive coherent metacommunity structures, non-significant positive species turnover, and clear boundary clumping. Hence, the benthic invertebrate metacommunities of natural wetlands corresponded best with the Quasi-Clementsian structure (**Table 1** and **Supplementary Figure 1**).

After the forward selection procedure, the CCA and Moran's eigenvector maps identified two statistically significant environmental variables (pH and IC) and one significant spatial variable (MEM1, **Table 2**) for variance partitioning analysis. According to the results of variance partitioning analysis, 50.6% of the total variation in the benthic invertebrate community composition was explained by the spatial and environmental factors in combination [(S), (E), and (S+E); **Table 2**]. The

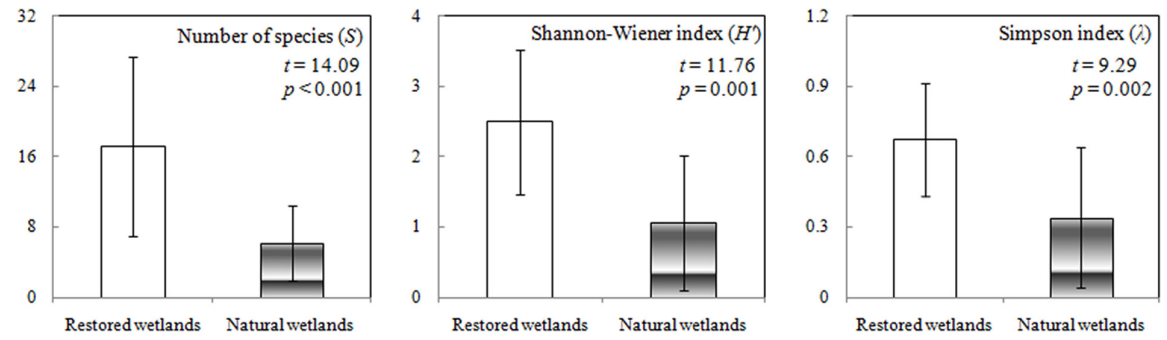

FIGURE 4 | Number of species (*S*), Shannon-Wiener index (*H'*), and Simpson index (λ) of restored and natural wetlands.

TABLE 1 | Results of the elements of metacommunity structure analysis in restored and natural wetlands.

Wetland types	Coherence					Species turnover					Boundary clumping			Interpretation
	Abs	*z*	*p*	simMean	simSD	Rep	*z*	*p*	simMean	simSD	Index	*p*	*df*	
Restored wetlands	531	–9.863	0.001	891	36	10910	–5.111	0.001	19394	1660	1.364	0.001	15	Nested
Natural wetlands	43	–5.876	0.001	112	12	703	0.760	0.447	624	105	1.287	0.044	9	Quasi-Clementsian

TABLE 2 | Results of variation partitioning, showing the contributions of spatial and environmental variables to the variation of restored and natural wetlands.

Wetland types	Fraction	*df*	Adj.R^2	*p*	Variables in the model
Restored wetlands	(E)	3	0.272	0.001	Cond, salinity, ORP
	(S)	2	0.110	0.003	MEM2, MEM4
	(E+S)	0	0.048		Salinity, ORP, Cond, MEM2, MEM4
	1-(E+S)	–	0.570		
Natural wetlands	(E)	2	0.073	0.112	pH, IC
	(S)	1	0.177	0.001	MEM1
	(E+S)	0	0.256		pH, IC, MEM1
	1-(E+S)	–	0.494		

Significance of shared effects [(E+S)] cannot be tested.

amount of variance accounted for by the pure spatial fraction [1.77%, (S)] was significant, but that of the pure environmental fraction [0.73%, (E)] was not. In addition, the amount of variance explained by the shared fraction, which reflected the interaction of environmental and spatial factors [25.6%, (E+S) in **Table 2**], was higher than that of other fractions, indicating that the interaction of environmental and spatial variables was the main driver for benthic invertebrate community composition of natural wetlands.

Furthermore, frequency histograms of standardized effect sizes showed an aggregated distribution among the 13 benthic invertebrate metacommunities in natural wetlands, indicating that biotic interactions were not the main driver of metacommunity structure (**Figure 5**).

DISCUSSION

We examined three sources of variation in community structure, i.e., spatial factors, environmental variables, and biotic interactions. Our results indicated that the benthic invertebrate community structure was significantly altered due to changes in water quality as a result of freshwater releases, and the underlying processes of community composition were also changed. The benthic invertebrate metacommunity structure showed a nested distribution in restored wetlands and a quasi-Clementsian structure in natural wetlands. Further analyses suggested that possible biotic interactions were not the key drivers of metacommunity structure at the local scale in estuarine wetlands. Environmental filtering and dispersal appeared to be key drivers of metacommunity structure in restored wetlands, and dispersal played a major role in regulating benthic invertebrate communities of natural wetlands. At the local scale of estuarine wetlands, however, possible biotic interactions seemed not to play a role in metacommunity structure.

The environmental heterogeneity and water quality changes caused by restoration-related freshwater releases led to changes in benthic invertebrate community composition. Our results showed the benthic invertebrate community structure of restored wetlands and natural wetlands were significantly different. Yang et al. (2019) reported that the composition of macrobenthos functional groups tended to become more diverse after freshwater releases, which is consistent with our findings. Since the implementation of the ecological restoration project of degraded wetlands in the Yellow River Delta, freshwater releases have alleviated the increasing water and salt stress of degraded wetlands. At the same time, freshwater releases had a positive impact on water quality, soil organic matter content, plant communities, and bird communities in degraded wetlands, as well as direct or indirect effects on the species richness and diversity of benthic invertebrate communities (Cui et al., 2009). In another study, we found that salinity is an important indicator to distinguish hydrologic characteristics between the two types of wetlands (Yang et al., 2019). Due to the construction of levees around the degraded wetlands for impoundment, the

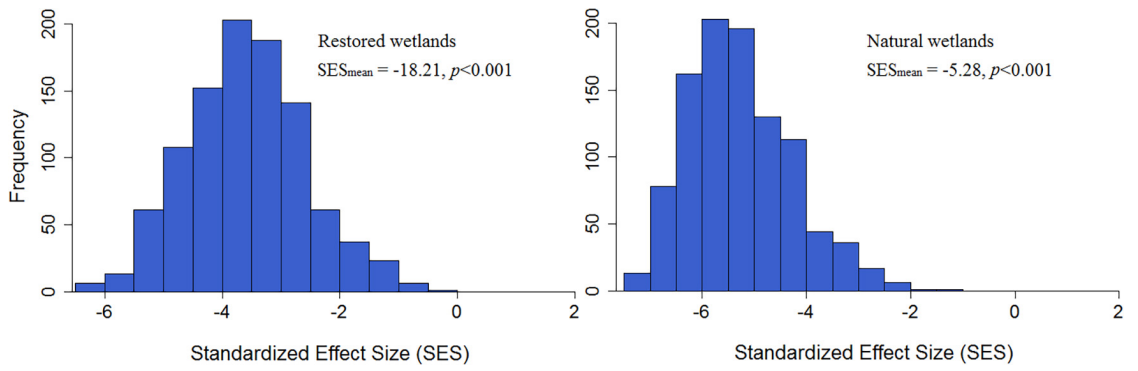

FIGURE 5 | Frequency histograms of standardized effect sizes measured in presence-absence matrices. The blue bars in this figure are standard histograms of simulated metric values.

hydrological connectivity between the freshwater release areas and the ocean has been cut off, and the habitat environment has been greatly changed. Benthic invertebrates are sensitive to environmental changes and disturbances, ultimately leading to significant differences in community composition between the two types of wetlands. Given these potential effects on benthic invertebrate taxa and diversity in both wetland types, there is a need to identify the major drivers of community assembly in these estuarine wetlands.

We found a nested distribution in restored wetlands. It has been shown that nested distribution is not necessarily a result of biotic interactions (Heino, 2009) and may be caused by community size (Verbruggen et al., 2012), spatial isolation (Butaye et al., 2001), and environmental filtering (Heino et al., 2015b). As a result of habitat changes in restored wetlands, sensitive species may disappear along a gradient, and this environmental filtering can cause community nestedness. Indeed, Verbruggen et al. (2012) also confirmed that the varying tolerance levels of taxa for relevant environmental factors might be responsible for the observed nestedness. Therefore, the relative influence of environmental and spatial variables also depends on species traits. Some species exhibit wide environmental tolerances, while others have very specific habitat requirements (Rodil et al., 2017). The presence of suitable habitats and the ability of species to reach these habitats is what affects the extent of species distribution. Explaining differences in species life histories can provide a better understanding of species distribution and coexistence patterns (Corte et al., 2018). In addition, dispersal limitation causes niches to remain vacant, thereby obscuring expected species-environment associations under environmental filtering and potentially resulting in community nestedness (Lekberg and Koide, 2005). We found a quasi-Clementsian structure for the benthic invertebrate metacommunities in natural wetlands. Due to the inherently highly heterogeneous natural wetland systems, species responses to environmental gradients are typically more complex than a simple gain or loss of species along ecological gradients, making Clementsian gradients a frequent occurrence (Ward et al., 2002; Heino et al., 2010; Heino, 2013b). Moreover, natural estuarine wetlands are typically connected to the sea, and the length of the environmental gradient increases with spatial extent, resulting in stronger correlations between species composition and the environment among sites, ultimately leading to a Clementsian structure (Soininen, 2014; Heino et al., 2017).

Variance partitioning allowed us to evaluate the independent contributions of spatial and environmental variables to the observed benthic invertebrate distribution in two wetland types. In restored wetlands, our analyses showed that both environmental and spatial variables explained substantial portions of the variability in benthic invertebrate community composition, although environmental variables had a slightly stronger influence. The Yellow River Delta ecological restoration and protection project blocked the connectivity of the restored wetlands to the sea, and spatial factors, therefore, restricted the dispersal of benthic invertebrate metacommunities. Moreover, habitat changes resulted in higher sensitivity of benthic invertebrates to environmental heterogeneity. Thus environmental filtering played a leading role in determining species composition (Rádková et al., 2015). In natural wetlands, spatial variables played a major role in regulating benthic invertebrate metacommunities, and the interaction between environmental factors and spatial variables was also crucial in the metacommunity. It has been shown that less dispersive species are more strongly affected by spatial processes than highly dispersive species (Rao et al., 2020). Additionally, the mechanisms determining community structure changed according to the spatial scale considered (Rao et al., 2020). The results suggested that the spatial component plays a greater role in metacommunity organization in open estuarine waters (e.g., shallow beaches) than in less open, environmentally controlled aquatic systems (Rodil et al., 2017).

Biotic interactions must be assessed to accurately understand metacommunity organization at local scales (García-Girón et al., 2020). Our results showed that biotic interactions appeared to have little effect on the structure of benthic invertebrate metacommunities of restored and natural wetlands. This may be due to the fact that resource-based niche partitioning and interspecific competition play minor roles in influencing benthic invertebrate communities at small scales (Gao et al., 2016; Guo et al., 2019). Moreover, anthropogenic disturbances and

management measures may also lead to low overall levels of biotic interactions (Ochoa-Hueso, 2016). However, in contrast to our results, Zhao et al. (2019) found that biotic interactions significantly influenced the patterns of biomass, species richness, and community composition of bacteria, diatoms, and shaker mosquitoes along a water depth gradient. This may have been due to the fact that this study only used biotic predictors as surrogates for local biotic constraints and that the role of spatial factors was not considered. However, the exact reasons for these patterns are still not completely understood. Therefore, additional measurements and variables (e.g., food web structure and energy flow, functional properties, and phylogeny) should be considered to analyze the relative contributions of biotic interactions properly.

DATA AVAILABILITY STATEMENT

The original contributions presented in the study are included in the article/**Supplementary Material**, further inquiries can be directed to the corresponding author/s.

AUTHOR CONTRIBUTIONS

DL wrote the manuscript and performed the statistical analysis. HY and HW contributed to conception and design of the study. KL and QG contributed to the experiment data collection. All authors contributed to the article and approved the submitted version.

FUNDING

The study was supported in part by the National Natural Science Foundation of China (Project Nos. 41871099, 41671260, and U20A2083) and the Science and Technology Development Program of Jilin Province (Project No. 20180101080JC).

SUPPLEMENTARY MATERIAL

The Supplementary Material for this article can be found online at: https://www.frontiersin.org/articles/10.3389/fevo.2021.721628/full#supplementary-material

REFERENCES

Alahuhta, J., Lindholm, M., Bove, C. P., Chappuis, E., Clayton, J., Winton, M. D., et al. (2018). Global patterns in the metacommunity structuring of lake macrophytes: regional variations and driving factors. *Oecologia* 188, 1167–1182. doi: 10.1007/s00442-018-4294-0

Bell, T. (2010). Experimental tests of the bacterial distance-decay relationship. *ISME J.* 4, 1357–1365. doi: 10.1038/ismej.2010.77

Blanchet, F. G., Legendre, P., and Borcard, D. (2008). Forward selection of explanatory variables. *Ecology* 89, 2623–2632. doi: 10.1890/07-0986.1

Borcard, D., and Legendre, P. (2002). All-scale spatial analysis of ecological data by means of principal coordinates of neighbour matrices. *Ecol. Modell.* 153, 51–68.

Brown, B. L., Sokol, E. R., Skelton, J., and Tornwall, B. (2017). Making sense of metacommunities: dispelling the mythology of a metacommunity typology. *Oecologia* 183, 643–652. doi: 10.1007/s00442-016-3792-1

Brown, B. L., Swan, C. M., Auerbach, D. A., Grant, E. C., Hitt, N. P., Maloney, K. O., et al. (2011). Metacommunity theory as a multispecies, multiscale framework for studying the influence of river network structure on riverine communities and ecosystems. *J. North Am. Benthol. Soc.* 30, 310–327. doi: 10.1899/10-129.1

Butaye, J., Jacquemyn, H., and Hermy, J. M. (2001). Differential colonization causing non-random forest plant community structure in a fragmented agricultural landscape. *Ecography* 24, 369–380. doi: 10.1111/j.1600-0587.2001.tb00472.x

Cai, Y., Xu, H., Vilmi, A., Tolonen, K. T., Tang, X., and Heino, H. (2017). Relative roles of spatial processes, natural factors and anthropogenic stressors in structuring a lake macroinvertebrate metacommunity. *Sci. Total Environ.* 601–602, 1702–1711. doi: 10.1016/j.scitotenv.2017.05.264

Caruso, T., Chan, Y., Lacap, D. C., Lau, M., Mckay, C. P., and Pointing, S. B. (2011). Stochastic and deterministic processes interact in the assembly of desert microbial communities on a global scale. *ISME J.* 5, 1406–1413. doi: 10.1038/ismej.2011.21

Corte, N. G., Goncalves-Souza, T., Checon, H. H., Siegle, E., Coleman, R. A., and Amaral, A. C. Z. (2018). When time affects space: dispersal ability and extreme weather events determine metacommunity organization in marine sediments. *Mar. Environ. Res.* 136, 139–152. doi: 10.1016/j.marenvres.2018.02.009

Cottenie, K. (2005). Integrating environmental and spatial processes in ecological community dynamics. *Ecol. Lett.* 8, 1175–1182. doi: 10.1111/j.1461-0248.2005.00820.x

Cui, B., Yang, Q., Yang, Z., and Zhang, K. (2009). Evaluating the ecological performance of wetland restoration in the Yellow River Delta. *China Ecol. Eng.* 35, 1090–1103. doi: 10.1016/j.ecoleng.2009.03.022

Dallas, T. (2013). *Metacom: Analysis of the' Elements of Metacommunity Structure', R Package Ver 1.3*.

Daniel, J., Gleason, J. E., Cottenie, K., and Rooney, R. C. (2019). Stochastic and deterministic processes drive wetland community assembly across a gradient of environmental filtering. *Oikos* 128, 1158–1169. doi: 10.1111/oik.05987

Declerck, S. A. J., Coronel, J. S., Legendre, P., and Brendonck, L. (2011). Scale dependency of processes structuring metacommunities of cladocerans in temporary pools of High-Andes wetlands. *Ecography* 34, 296–305. doi: 10.1111/j.1600-0587.2010.06462.x

Dong, G. T., Huang, K., Dang, S. Z., Gu, X. W., and Yang, W. L. (2014). Effect of ecological water supplement on land use and land cover changes in diaokou river. *Adv. Mater. Res.* 864–867, 2403–2407. doi: 10.4028/www.scientific.net/AMR.864-867.2403

Dray, S., Legendre, P., and Peres-Neto, P. R. (2006). Spatial modelling: a comprehensive framework for principal coordinate analysis of neighbour matrices (PCNM). *Ecol. Modell.* 196, 483–493. doi: 10.1016/j.ecolmodel.2006.02.015

Dray, S., Pélissier, R., Couteron, P., Fortin, M. J., Legendre, P., and Wagner, H. H. (2012). Community ecology in the age of multivariate multiscale spatial analysis. *Ecol. Monogr.* 82, 257–275. doi: 10.1890/11-1183.1

Gan, H. J., Zaka, D. R., and Hunter, M. D. (2019). Scale dependency of dispersal limitation, environmental filtering and biotic interactions determine the diversity and composition of oribatid mite communities. *Pedobiologia* 74, 43–53. doi: 10.1016/j.pedobi.2019.03.002

Gao, M. X., Liu, D., Lin, L., and Wu, D. H. (2016). The small-scale structure of a soil mite metacommunity. *Eur. J. Soil Biol.* 74, 69–75. doi: 10.1016/j.ejsobi.2016.03.004

García-Girón, J., Heino, J., García-Criado, F., Fernández-Aláez, C., and Alahuhta, J. (2020). Biotic interactions hold the key to understanding metacommunity organisation. *Ecography* 43, 1180–1190. doi: 10.1111/ecog.05032

Gotelli, N. J. (2000). Null model analysis of species co-occurrence patterns. *Ecology* 81, 2606–2621. doi: 10.2307/177478

Gotelli, N. J., and Mccabe, D. J. (2002). Species co-occurrence: a meta-analysis of J. M. Diamond's assembly rules model. *Ecology* 83, 2091–2096.

Gotelli, N. J., and Ulrich, W. (2012). Statistical challenges in null model analysis. *Oikos* 121, 171–180. doi: 10.1111/j.1600-0706.2011.20301.x

Guan, Q., and Wu, H. T. (2021). Ditches as important aquatic invertebrate habitats: a comparative analysis of their snail (Mollusca: Gastropoda) assemblages with natural wetlands. *Aquat. Sci.* 83:29. doi: 10.1007/s00027-021-00790-y

Guan, Q., Wu, H. T., Lu, K. L., and Darold, P. B. (2017). Longitudinal and lateral variation in snail assemblages along a flood plain continuum. *Hydrobiologia* 79, 345–356. doi: 10.1007/s10750-016-3073-3

Guo, Y. X., Gao, M. X., Liu, J., Zaitsev, A. S., and Wu, D. H. (2019). Disentangling the drivers of ground-dwelling macro-arthropod metacommunity structure at two different spatial scales. *Soil Biol. Biochem.* 130, 55–62. doi: 10.1016/j.soilbio.2018.12.002

Heino, J. (2009). Species co-occurrence, nestedness and guild-environment relationships in stream macroinvertebrates. *Freshw. Biol.* 54, 1947–1959. doi: 10.1111/j.1365-2427.2009.02250.x

Heino, J. (2011). A macroecological perspective of diversity patterns in the freshwater realm. *Freshw. Biol.* 56, 1703–1722. doi: 10.1111/j.1365-2427.2011.02610.x

Heino, J. (2013a). Does dispersal ability affect the relative importance of environmental control and spatial structuring of littoral macroinvertebrate communities? *Oecologia* 131, 971–980. doi: 10.1007/s00442-012-2451-4

Heino, J. (2013b). Environmental heterogeneity, dispersal mode and co-occurrence in stream macroinvertebrates. *Ecol. Evol.* 3, 344–355. doi: 10.1002/ece3.470

Heino, J. (2013c). The importance of metacommunity ecology for environmental assessment research in the freshwater realm. *Biol. Rev.* 88, 166–178. doi: 10.1111/j.1469-185X.2012.00244.x

Heino, J., Grnroos, M., Soininen, J., Virtanen, R., and Muotka, T. (2012). Context dependency and metacommunity structuring in boreal headwater streams. *Oikos* 121, 537–544. doi: 10.1111/j.1600-0706.2011.19715.x

Heino, J., Melo, A. S., Siqueira, T., Soininen, J., Valanko, S., and Bini, L. M. (2015a). Metacommunity organisation, spatial extent and dispersal in aquatic systems: patterns, processes and prospects. *Freshw. Biol.* 60, 845–869. doi: 10.1111/fwb.12533

Heino, J., Mykrä, H., and Rintala, J. (2010). Assessing patterns of nestedness in stream insect assemblages along environmental gradients. *Ecoscience* 17, 345–355. doi: 10.2980/17-4-3263

Heino, J., Nokela, T., Soininen, J., Tolkkinen, M., Virtanen, L., and Virtanen, R. (2015b). Elements of metacommunity structure and communityenvironment relationships in stream organisms. *Freshw. Biol.* 60, 973–988. doi: 10.1111/fwb.12556

Heino, J., and Soininen, J. (2010). Are common species sufficient in describing turnover in aquatic metacommunities along environmental and spatial gradients? *Limnol. Oceanogr.* 55, 2397–2402. doi: 10.4319/lo.2010.55.6.2397

Heino, J., Soininen, J., Alahuhta, J., Lappalainen, J., and Virtanen, R. (2017). Metacommunity ecology meets biogeography: effects of geographical region, spatial dynamics and environmental filtering on community structure in aquatic organisms. *Oecologia* 183, 121–137. doi: 10.1007/s00442-016-3750-y

Heino, J., and Tolonen, K. T. (2017). Ecological drivers of multiple facets of beta diversity in a lentic macroinvertebrate metacommunity. *Limnol. Oceanogr.* 62, 2431–2444. doi: 10.1002/lno.10577

Hildrew, A. G. (2009). Sustained research on stream communities: a model system and the comparative approach. *Adv. Ecol. Res.* 41, 175–312. doi: 10.1016/S0065-2504(09)00404-8

Hill, M. J., Heino, J., Thornhill, I., Ryves, D. B., and Wood, P. J. (2017). Effects of dispersal mode on the environmental and spatial correlates of nestedness and species turnover in pond communities. *Oikos* 126, 1–11. doi: 10.1111/oik.04266

Holyoak, M., Leibold, M. A., Mouquet, N. M., Holt, R. D., and Hoopes, M. F. (2005). *Metacommunities: A Framework for Large-Scale Community Ecology*. Chicago: University of Chicago Press.

Legendre, P., Borcard, D., Blanchet, F. G., and Dray, S. (2012). *MEM Spatial Eigenfunction and Principal Coordinate Analyses. Vers. 2.1-2*.

Leibold, M. A., and Chase, J. M. (2017). *Metacommunity Ecology*. Princeton, NJ: Princeton University Press.

Leibold, M. A., Holyoak, M., Mouquet, N., Amarasekare, P., Chase, J. M., Hoopes, M. F., et al. (2004). The metacommunityconcept: a framework for multi-scale community ecology. *Ecol. Lett.* 7, 601–613. doi: 10.1111/j.1461-0248.2004.00608.x

Leibold, M. A., and Mikkelson, G. M. (2002). Coherence, species turnover, and boundary clumping: elements of meta-community structure. *Oikos* 97, 237–250. doi: 10.1034/j.1600-0706.2002.970210.x

Lekberg, Y., and Koide, R. T. (2005). Is plant performance limited by abundance of arbuscular mycorrhizal fungi? A meta-analysis of studies published between 1988 and 2003. *New Phytol.* 168, 189–204. doi: 10.1111/j.1469-8137.2005.01490.x

Li, M., Yang, W., Sun, T., and Jin, Y. W. (2016). Potential ecological risk of heavy metal contamination in sediments and macrobenthos in coastal wetlands induced by freshwater releases: a case study in the yellow river delta, china. *Mar. Pollut. Bull.* 103, 227–239. doi: 10.1016/j.marpolbul.2015.12.014

Lindstrom, E. S., and Langenheder, S. (2012). Local and regional factors influencing bacterial community assembly. *Environ. Microbiol. Rep.* 4, 1–9. doi: 10.1111/j.1758-2229.2011.00257.x

Liu, J., Gao, M. X., Ma, Y. L., Sun, X. Y., and Wu, D. H. (2019). Spatial and environmental factors are minor structuring forces in a soil collembola metacommunity in a maize agroecosystem. *Pedobiologia* 76:150572. doi: 10.1016/j.pedobi.2019.150572

Logue, J. B., Mouquet, N., Peter, H., and Hillebrand, H. (2011). Empirical approaches to metacommunities: a review and comparison with theory. *Trends Ecol. Evol.* 26, 482–491. doi: 10.1016/j.tree.2011.04.009

Lu, K. L., Wu, H. T., Xue, Z. S., Lu, X. G., and Batzer, D. P. (2019). Development of a multi-metric index based on aquatic invertebrates to assess floodplain wetland condition. *Hydrobiologia* 827, 141–153. doi: 10.1007/s10750-018-3761-2

Meynard, C. N., Lavergne, S., Boulangeat, I., Garraud, L., Es, J. V., and Thuiller, W. (2013). Disentangling the drivers of metacommunity structure across spatial scales. *J. Biogeogr.* 40, 1560–1571. doi: 10.1111/jbi.12116

Morse, J. C., Yang, L. F., and Tian, L. X. (1994). *Aquatic Insects of China Useful for Monitoring Water Quality*. Nanjing: HoHai University Press.

Ochoa-Hueso, R. (2016). Nonlinear disruption of ecological interactions in response to nitrogen deposition. *Ecology* 97, 2802–2814. doi: 10.1002/ecy.1521

Peres-Neto, P. R., Legendre, P., Dray, S., and Borcard, D. (2006). Variation partitioning of species data matrices: estimation and comparison of fractions. *Ecology* 87, 2614–2625.

Presley, S. J., Higgins, C. L., and Willig, M. R. (2010). A comprehensive framework for the evaluation of metacommunity structure. *Oikos* 119, 908–917. doi: 10.1111/j.1600-0706.2010.18544.x

Qian, H. (2009). Global comparisons of beta diversity among mammals, birds, reptiles, and amphibians across spatial scales and taxonomic ranks. *J. Syst. Evol.* 47, 509–514. doi: 10.1111/j.1759-6831.2009.00043.x

Qian, H., and Ricklefs, R. E. (2007). A latitudinal gradient in large-scale beta diversity for vascular plants in North America. *Ecol. Lett.* 10, 737–744. doi: 10.1111/j.1461-0248.2007.01066.x

R Core Team (2020). *R: A Language and Environment for Statistical Computing*. Vienna: R Foundation for Statistical Computing.

Rádková, V., Bojková, J., and Horsák, M. (2015). The role of dispersal mode and habitat specialisation in metacommunity structuring of aquatic macroinvertebrates in isolated spring fens. *Freshw. Biol.* 59, 2256–2267. doi: 10.1111/fwb.12428

Rao, Y., Cai, L., Chen, B., Chen, X., and Lin, S. (2020). How do spatial and environmental factors shape the structure of a coastal macrobenthic community and meroplanktonic larvae cohort? evidence from day a bay. *Mar. Pollut. Bull.* 157:111242. doi: 10.1016/j.marpolbul.2020.111242

Rodil, I. F., Paloma, L. M., Henri, J., Victoria, O., and Anna, V. (2017). The role of dispersal mode and habitat specialization for metacommunity structure of shallow beach invertebrates. *PLoS One* 12:e0172160. doi: 10.1371/journal.pone.0172160

Rosenzweig, M. L. (1995). *Species Diversity in Space and Time*. Cambridge: Cambridge University Press.

Saito, V. S., Soininen, J., Fonseca-Gessner, A. A., and Siqueira, T. (2015). Dispersal traits drive the phylogenetic distance decay of similarity in Neotropical stream metacommunities. *J. Biogeogr.* 42, 2101–2111. doi: 10.1111/jbi.12577

Soininen, J. (2014). A quantitative analysis of species sorting across organisms and ecosystems. *Ecology* 95, 3284–3292. doi: 10.1890/13-2228.1

Soininen, J., Mcdonald, R., and Hillebrand, H. (2007). The distance decay of similarity in ecological communities. *Ecography* 30, 3–12. doi: 10.1111/j.0906-7590.2007.04817.x

Stone, L., and Roberts, A. (1990). The checkerboard score and species distributions. *Oecologia* 85, 74–79. doi: 10.1007/bf00317345

Thompson, P. L., Guzman, M., Meester, L. D., Horváth, Z., Ptacnik, R., Vanschoenwinkel, B., et al. (2020). A process-based metacommunity framework linking local and regional scale community ecology. *Ecol. Lett.* 23, 1314–1329. doi: 10.1111/ele.13568

Thornhill, I., Batty, L., Death, R. G., Friberg, N. R., and Ledger, M. E. (2017). Local and landscape scale determinants of macroinvertebrate assemblages and their conservation value in ponds across an urban land-use gradient. *Biodivers. Conserv.* 26, 1065–1086. doi: 10.1007/s10531-016-1286-4

Tonkin, J. D., Andrea, S., Jähnig, S. C., Peter, H., and Judi, H. (2015). Environmental controls on river assemblages at the regional scale: an application of the elements of metacommunity structure framework. *PLoS One* 10:e0135450. doi: 10.1371/journal.pone.0135450

Tonkin, J. D., Merritt, D. M., Olden, J. D., Reynolds, L. V., and Lytle, D. A. (2018). Flow regime alteration degrades ecological networks in riparian ecosystems. *Nat. Ecol. Evol.* 2, 86–93. doi: 10.1038/s41559-017-0379-0

Verbruggen, E., Heijden, M., Weedon, J. T., and Röling, W. (2012). Community assembly, species richness and nestedness of arbuscular mycorrhizal fungi in agricultural soils. *Mol. Ecol.* 21, 2341–2353. doi: 10.1111/j.1365-294x.2012.05534.x

Ward, J. V., Malard, F., and Tockner, K. (2002). Landscape ecology: a framework for integrating pattern and process in river corridors. *Landsc. Ecol.* 17, 35–45. doi: 10.1023/A:1015277626224

Wu, H. T., Guan, Q., Lu, X. L., and Batzer, D. P. (2017). Snail (Mollusca: Gastropoda) assemblages as indicators of ecological condition in freshwater wetlands of Northeast China. *Ecol. Indic.* 75, 203–209. doi: 10.1016/j.ecolind.2016.12.042

Wu, H. T., Qiang, G., Ma, H. Y., Xue, Z. S., Yang, M. Y., and Batzer, D. P. (2019). Effects of saline conditions and hydrologic permanence on snail assemblages in wetlands of Northeastern China. *Ecol. Indic.* 96, 620–627. doi: 10.1016/j.ecolind.2018.09.043

Yang, M. Y., Lu, K. L., Batzer, D. P., and Wu, H. T. (2019). Freshwater release into estuarine wetlands changes the structure of benthic invertebrate assemblages: a case study from the Yellow River Delta. *Sci. Total Environ.* 687, 752–758. doi: 10.1016/j.scitotenv.2019.06.154

Yang, W., Li, X., Sun, T., Pei, J., and Li, M. (2017a). Macrobenthos functional groups as indicators of ecological restoration in the northern part of china's yellow river delta wetlands. *Ecol. Indic.* 82, 381–391. doi: 10.1016/j.ecolind.2017.06.057

Yang, W., Li, X., Sun, T., Yang, Z., and Li, M. (2017b). Habitat heterogeneity affects the efficacy of ecological restoration by freshwater releases in a recovering freshwater coastal wetland in china's yellow river delta. *Ecol. Eng.* 104, 1–12. doi: 10.1016/j.ecoleng.2017.04.007

Zhao, W. Q., Hu, A., Ni, Z., Wang, Q., and Wang, J. (2019). Biodiversity patterns across taxonomic groups along a lake water-depth gradient: effects of abiotic and biotic drivers. *Sci. Total Environ.* 686, 1262–1271. doi: 10.1016/j.scitotenv.2019.05.381

Conflict of Interest: The authors declare that the research was conducted in the absence of any commercial or financial relationships that could be construed as a potential conflict of interest.

Publisher's Note: All claims expressed in this article are solely those of the authors and do not necessarily represent those of their affiliated organizations, or those of the publisher, the editors and the reviewers. Any product that may be evaluated in this article, or claim that may be made by its manufacturer, is not guaranteed or endorsed by the publisher.

frontiers in Ecology and Evolution

ORIGINAL RESEARCH
published: 16 September 2021
doi: 10.3389/fevo.2021.719844

Numerical Simulation on the Diffusion of Alien Phytoplankton in Bohai Bay

Beibei Zhang[1,2], Amin Pu[1,2,3], Peng Jia[1,2]*, Chenglong Xu[1,2], Qinggai Wang[1,2] and Wenhao Tang[1,2,4]*

[1] The Appraisal Center for Environment and Engineering, Ministry of Environmental Protection, Beijing, China, [2] State Environmental Protection Key Laboratory of Numerical Modeling for Environment Impact Assessment, Beijing, China, [3] Nanjing Water Group Co., Ltd., Nanjing, China, [4] College of Hydrology and Water Resources, Hohai University, Nanjing, China

In order to investigate the motion feature of alien phytoplankton in the Bohai Bay area, this manuscript builds a two-dimensional tide hydrodynamic model coupled with a particle tracking model to simulate the alien phytoplankton movement trajectory and the diffusion processes with different specific growth rates in three major ports of Bohai Bay (Caofeidian port, Tianjin port, and Huanghua port). The results show that the movement of alien phytoplankton is mainly affected by the tidal circulation near the port, and the diffusion trend is basically consistent with the residual flow in Bohai Bay. The distribution density of alien phytoplankton is directly affected by the specific growth rate of the population and is positively related to specific growth rate. The released alien phytoplankton in the three major ports are all concentrated around the ports area. The largest distribution density is in Tianjin port, and the possibility of red tide disasters is also greatest here compared with the other two major ports. It is necessary to strengthen the monitoring of alien organisms in the port area and actively prevent alien phytoplankton from entering Bohai Bay through ship ballast water.

Keywords: alien phytoplankton, tide-induced residual current, particle tracking, numerical simulation, lagrangian method

OPEN ACCESS

Edited by:
Haitao Wu,
Northeast Institute of Geography and Agroecology, Chinese Academy of Science, China

Reviewed by:
Chang Liu,
China Institute of Water Resources and Hydropower Research, China
Gang Zhou,
Chinese Research Academy of Environmental Sciences, China

***Correspondence:**
Amin Pu
pam2111@163.com
Peng Jia
peng.jia@acee.org.cn

Specialty section:
This article was submitted to Conservation and Restoration Ecology, a section of the journal Frontiers in Ecology and Evolution

Received: *03 June 2021*
Accepted: *09 August 2021*
Published: *16 September 2021*

Citation:
Zhang B, Pu A, Jia P, Xu C, Wang Q and Tang W (2021) Numerical Simulation on the Diffusion of Alien Phytoplankton in Bohai Bay. Front. Ecol. Evol. 9:719844. doi: 10.3389/fevo.2021.719844

INTRODUCTION

Bohai Bay is an important economic belt in China, and it is located in the west of Bohai Sea, with unique geographical and important strategic position. There are many ports in Bohai Bay, and some non-inactivated alien phytoplankton (sporangia) may be carried in with ships arriving at the port. Since 2012, Bohai Bay has been the most seriously affected area by foreign phytoplankton (State Oceanic Administration, 2019). Up to 2019, 17 species of alien phytoplankton have been found in Bohai Bay, among which 16 species belong to red tide organisms (Pu et al., 2020). Under the action of suitable hydrometeorology, seawater physical and chemical factors, water nutrients, and other factors, red tide will be triggered, which will cause a serious negative impact on the marine environment and social economy.

Many scholars studied the ecological environment of Bohai Bay, and phytoplankton has become the focus of research. In July 2003, Cao et al. (2004, 2006) detected 31 species of phytoplankton belonging to 19 genera and found red tide organisms in five sites near Luju River in Tianjin port. Wu et al. (2006), by constructing a three-dimensional dynamic ecological coupling model, found that tidal current has an impact on the vertical distribution of phytoplankton and can promote

the formation of red tide when the light and nutrient conditions are appropriate, which provides a dynamic basis for further research on the occurrence of red tide. Liu (2007) summarized the temporal and spatial distribution characteristics of phytoplankton quantity and the distribution of dominant species by analyzing phytoplankton data in Bohai Bay in 2005. The number of phytoplankton cells, the diversity of phytoplankton, and the complexity of community structure in Bohai Bay showed seasonal variation (Liu et al., 2007; Yang et al., 2007). Yin et al. (2007) combined the survey results of Tianjin coastal zone and the ecological survey data of Tianjin coastal area in Bohai Bay from 2008 to 2012 and determined the species composition of phytoplankton in summer in Tianjin coastal area of Bohai Bay. In addition, many studies have shown that the community structure of phytoplankton is affected by multiple environmental factors (Liu X. T., 2011; Yin et al., 2013a,b, 2015; Wang, 2015; Wang et al., 2016; Zhang et al., 2016). Qin et al. (2017) proposed that there are five kinds of alien phytoplankton in Bohai Bay through a large number of research and investigation, and evaluated their ecological risk by constructing an evaluation model. Liu (2019) studied the temporal and spatial distribution characteristics and response relationship of nutrients and phytoplankton communities in Bohai Bay, which provided a scientific basis for further understanding the evolution characteristics of the ecological environment in Bohai Bay under the joint action of human activities and climate change. Pang et al. (2020) constructed the eutrophication evaluation index system of Tianjin coastal waters based on the PSR model, evaluated and verified the eutrophication level of Tianjin coastal waters by using the analytic hierarchy process, and explained that human behavior had a negative impact on the ecosystem of Tianjin coastal waters in Bohai Bay.

At present, most studies on alien phytoplankton in the world stay on their own biological characteristics (Goes et al., 2013; Cristian et al., 2016; Silkin et al., 2016; Belyaeva, 2019), and there are few studies on their transport and diffusion under the influence of hydrodynamic conditions; the relevant studies on phytoplankton in Bohai Bay are also based on the research of Chinese scholars.

The application of numerical simulation technology to predict the movement and diffusion of invasive phytoplankton in Bohai Bay is of great significance in the monitoring and prevention of red tide disaster in Bohai Bay. The particle tracking model is based on the hydrodynamic model and superposed with the particle tracking module to study the transport and diffusion process of particles under the influence of wind and hydrodynamic conditions. The particle tracking model is very suitable for establishing the tracking model and simulating the particle track and tracking trajectory in the water environment. Pablo (2005) used the Lagrange particle tracking method to simulate the movement characteristics of eel population in the upper reaches of the river. Zhang et al. (2012) used the Lagrange method to track the path of jellyfish based on the simulation results of the sea flow field. Han et al. (2013) based on the results of a three-dimensional hydrodynamic model of a puppet lake, using the particle tracking method to simulate the movement characteristics of algae, ignoring the growth and reproduction of algae, and studied the accumulation of algae under different wind directions. Zheng (2014) simulated the drift path and diffusion range of planktonic larvae under the dual influence of wind field and tidal current field based on the three-dimensional hydrodynamic model of the Yellow Sea area and superimposed particle tracking module, and the simulated data were basically consistent with the measured data. The particle tracking method is widely used to study the movement characteristics and migration path of alien phytoplankton, and the results are reasonable and satisfactory. However, previous studies on plankton simulation ignored the growth and reproduction of plankton.

In view of the above shortcomings, based on the numerical simulation of tidal current field in a specific period of Bohai Bay, combined with the residual current theory and particle tracking model, the tide-induced Euler residual current field and tide-induced Lagrangian residual current field are analyzed and compared; combined with the biological characteristics of alien phytoplankton, the Lagrangian particle tracking model is applied to analyze the distribution of alien phytoplankton (sporangia) in three ports of Bohai Bay in order to provide support for the prevention and control of red tide disaster in Bohai Bay.

MATERIALS AND METHODS

Numerical Simulation of the Tidal Current Field in Bohai Bay

In order to conduct a numerical simulation of the tidal current field in Bohai Bay (the area surrounded by CD open boundary and land boundary in **Figure 1**), this study intends to build a tidal hydrodynamic numerical model of Bohai Sea (the area surrounded by AB open boundary and land boundary in **Figure 1**) with a wider coverage and then provide water level for the CD open boundary required by the numerical model of Bohai Bay.

The period of hydrodynamic simulation in Bohai Sea is from April 15 to May 15, 2014, and the simulation time step is 200 s. The model is calibrated by using the data of tidal table water level at four tidal stations in Bohai Sea, and the current field in Bohai Sea can be properly simulated (Pu, 2019) when the eddy viscosity coefficient $C_s = 0.28$, Manning coefficient $M = 48\ \mathrm{m}^{1/3}/\mathrm{s}$, i.e., $n = 0.0208$.

The current model encrypts the calculation grid of the offshore area, with 6,316 nodes and 10,335 grids in the whole Bohai Bay simulation area. The grid division is shown in **Figure 2A**. The open boundary tidal level data of Bohai Bay are obtained from the results of the Bohai Sea current hydrodynamic model mentioned above, and the simulation period and parameter settings are the same as those of the Bohai Sea current model. The simulation results are verified by the measured data of tide level and tidal current stations in Bohai Bay. As shown in **Figure 2B**, T1 and T6 are tide level stations and S1 and S3 are tidal current stations. The simulated results were verified by using the observed values of sea level, velocity, and flow direction of four stations from April 30, 2014, 10:00 to May 1, 2014 10:00 (spring tide period) and from May 12, 2014, 07:00 to May 13, 2014 07:00 (neap tide period).

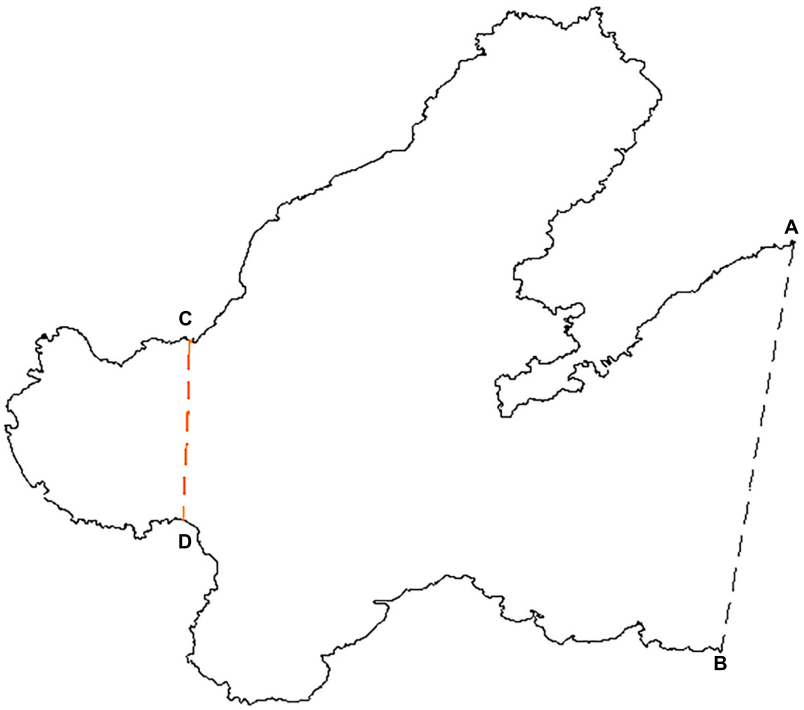

FIGURE 1 | Sketch diagram of the modeling scope of the hydrodynamic model.

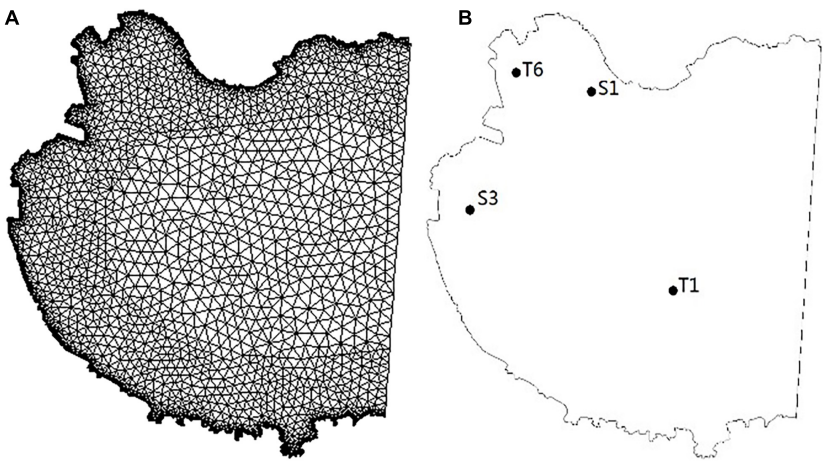

FIGURE 2 | Mesh partition of the hydrodynamic model and tidal current observation points in Bohai Bay. **(A)** Mesh partition. **(B)** Observation points.

The results of **Figures 3**, **4** show that the simulated current field in Bohai Bay is reasonable and feasible, and further simulation work can be carried out based on the flow field results.

Analysis and Comparison of Tide-Induced Residual Current

The non-linear effect of tidal current will produce tide-induced residual current, which will further form tidal circulation and plays an important role in the migration and distribution of material in the sea area. The tide-induced residual current can be described by two methods: Euler residual current and Lagrangian residual current. Euler residual current is the average value of instantaneous velocity at fixed position in the flow field in certain tidal cycles; Lagrangian residual current is the ratio of the displacement of fluid microcluster to the time consumed in a certain tidal cycle (Chen et al., 2020).

Analysis of Euler Residual Current Field

According to the definition of Euler residual current and based on the hydrodynamic field simulation results above, the

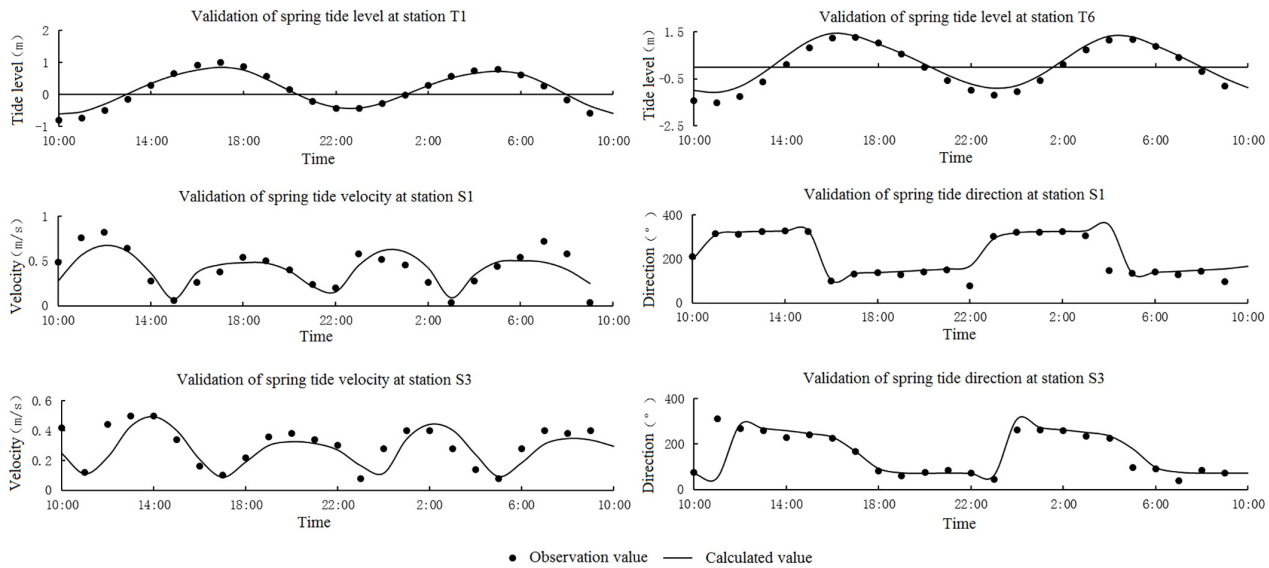

FIGURE 3 | Validation of tide level, current velocity, and direction in Bohai Bay (spring tide).

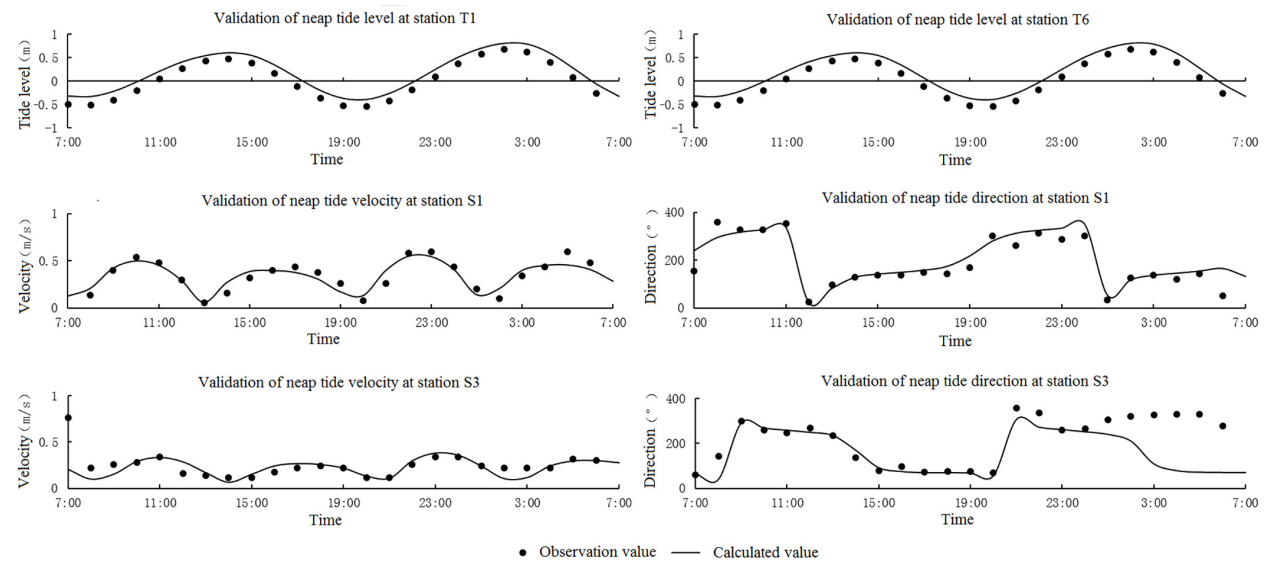

FIGURE 4 | Validation of tide level, current velocity, and direction in Bohai Bay (neap tide).

tide-induced Euler residual current in Bohai Bay is obtained as shown in **Figure 5**. The chart shows that the overall trend of the residual current in Bohai Bay is that seawater flows into Bohai Bay along the coast and flows out from the middle of the open boundary to maintain water balance. The residual current in the middle of Bohai Bay is weak, and it is strong along the coast. The residual current near the coast of Caofeidian port, Dagukou, Dakou River, and Dongfeng port is obviously enhanced. A clockwise circulation is between Dagukou and the west of Caofeidian port, and a counterclockwise circulation is in the southwest of Bohai Bay. A counterclockwise circulation forms in Caofeidian port, and in the south of Caofeidian port another clockwise circulation forms, and the two circulations present a double circulation structure.

Analysis of Lagrangian Residual Current Field

The Lagrangian particle tracking model is constructed to simulate the characteristics of Lagrangian residual current in Bohai Bay. A certain number of tracer particles are released at three locations as shown in **Figure 6**. Under the same hydrodynamic conditions, the particle migration path trajectory is shown in **Figure 7**. The simulation results show that after the particles are released in Caofeidian port, they move mainly in the east–west direction with the longshore current and do not expand to the central

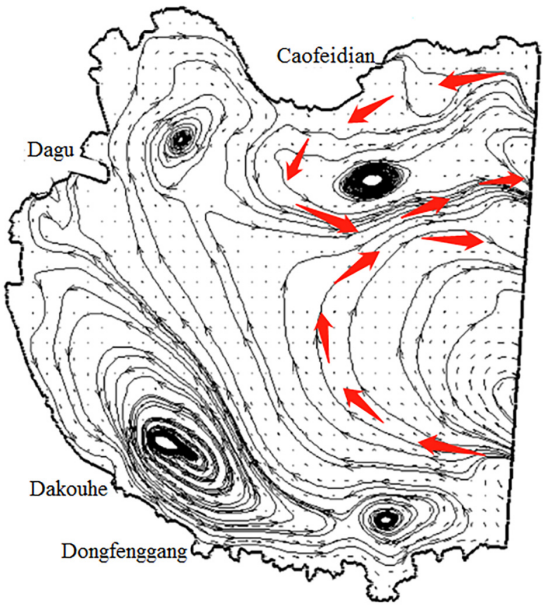

FIGURE 5 | Tide-induced Euler residual current in Bohai Bay.

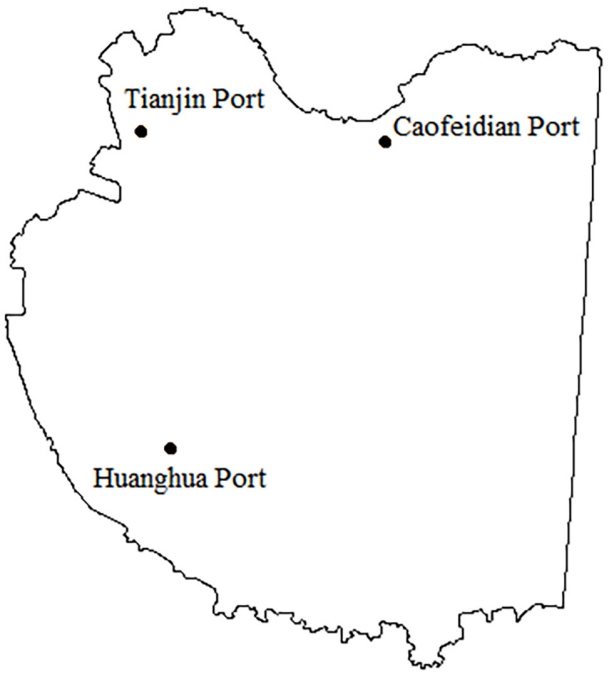

FIGURE 6 | Sketch diagram of Lagrangian particle release position.

area of Bohai Bay. In Tianjin port, the particles released mainly diffuse around the port in the simulation time, and the motion track basically covers the area of Tianjin port. After being released in Huanghua port, the particles move back and forth with the longshore current, and they mainly diffuse along the coast and move to the northwest of Bohai Bay.

Theoretically, with first-order approximation, the Lagrangian residual current is the material transport velocity, and the difference between the Euler residual current and the material transport velocity is a Stokes drift velocity; therefore, the Euler residual current and the Lagrangian residual current are not completely consistent. In practical application, it is generally considered that the difference between the two is small enough to be ignored, but relevant studies show that the difference cannot be ignored under certain conditions (Wei et al., 2003), and it is necessary to use the Lagrangian method to study the material migration in the sea area (Yu and Chen, 1983; Tang, 1987). In view of this, although the shape of the Eulerian residual current field has great reference significance for predicting the motion trend and trajectory range of Lagrangian particles, the final trajectory coverage of Lagrangian particles in the three ports is highly consistent with the shape of Eulerian residual flow field in the three ports. The following work will be conducted based on the Lagrangian method to study the transport characteristics of alien organisms.

Numerical Simulation of Alien Phytoplankton Diffusion

In this study, we continue to use the Lagrangian particle tracking model to characterize the movement of alien phytoplankton by Lagrangian particle trajectory, and simulate the movement of alien phytoplankton (sporangium) in Caofeidian port, Tianjin port, and Huanghua port of Bohai Bay, revealing the movement characteristics of alien phytoplankton in Bohai Bay, so as to provide support for the prevention and control of red tide disaster in Bohai Bay.

Biological Characteristics of Alien Phytoplankton

In order to carry out the relevant simulation work, it is necessary to make clear the mathematical description of the growth, reproduction, and attenuation process of alien phytoplankton in Bohai Bay, so as to reflect its quantitative change process in water. The number of phytoplankton community in water is directly affected by the maximum specific growth rate, zooplankton feeding, competition, population migration, and other factors.

Specific growth rate of phytoplankton

The life process of phytoplankton includes growth and death, and its instantaneous number is the difference between the increment of plant cells and the decrement of plant cells (including sedimentation and death of phytoplankton) in the instantaneous interval. The net growth rate can be expressed by the specific growth rate (μ) of the number of phytoplankton, and μ can be expressed as Equation 1.

In the formula, μ (day^{-1}) is the specific growth rate of phytoplankton, N_1 (cell L^{-1}) is the number of phytoplankton at time t_1, and N_0 (cell L^{-1}) is the number of phytoplankton at t_0.

μ is a non-fixed parameter, which is not only determined by the genetic material of individual cells but also affected by nutritional level, light, temperature, and other external environmental factors. When the phytoplankton population grows in the most suitable environmental conditions, μ is a constant value, called the maximum specific growth rate μ_{max} or

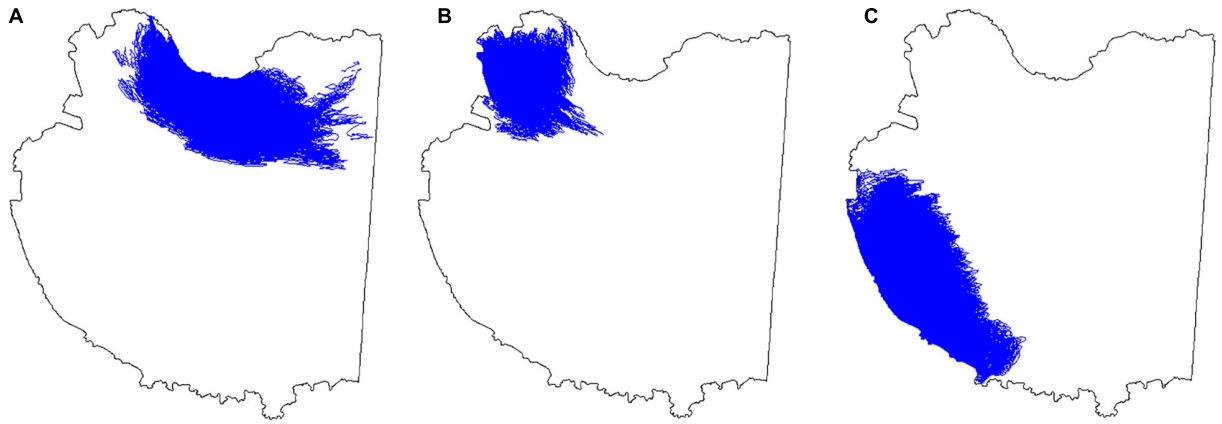

FIGURE 7 | Trajectory of Lagrangian particles in Bohai Bay. **(A)** Caofeidian Port. **(B)** Tianjin Port. **(C)** Huanghua Port.

intrinsic growth rate (Sun and Ning, 2005). Moreover, different phytoplankton have different maximum specific growth rates.

Through the investigation of a large number of literature (Wang et al., 2001; Yu, 2005; Li, 2006; Hu et al., 2010; Liu S. X., 2011; Ma et al., 2012; Ge et al., 2017), the maximum specific growth rates of 17 kinds of alien phytoplankton in Bohai Bay were obtained. The largest intrinsic growth rate of these species was found in *Pseudo-nitzschia pungens* (0.92 day^{-1}), and the smallest was found in *Cochlodinium polykrikoides* (0.42 day^{-1}), with an average of 0.52 day^{-1}.

Feeding rates of zooplankton

In natural waters, zooplankton mainly feed on various phytoplankton and suspended organic matter, and the feeding rate of zooplankton varies in different sea areas. Zhang and Wang (2000) sampled and analyzed the spatial distribution of microzooplankton in the Bohai Sea and calculated the feeding rate of zooplankton as 0.42–0.69 day^{-1} by the dilution method. In order to determine the maximum influence range of alien phytoplankton diffusion as large as possible, the minimum feeding rate of zooplankton 0.42 day^{-1} was taken in this paper.

Specific growth rate of the phytoplankton community

The specific growth rate of the phytoplankton community is not only directly affected by the maximum specific growth rate but also controlled by a variety of factors, including zooplankton feeding, competition, and population migration. According to the research purpose, this manuscript only took the specific growth rate of a single phytoplankton community into consideration, and factors such as population competition and population migration were not considered.

The specific growth rate of phytoplankton community can be expressed as Equation 2.

In Equation 2, μ' is the community specific growth rate, μ_{max} is the maximum specific growth rate, and g is the zooplankton feeding rate.

For 17 species of phytoplankton in Bohai Bay, the maximum specific growth rate of the community was 0.5 day^{-1}, the minimum was 0 day^{-1}, and the average was 0.1 day^{-1}.

Under ideal conditions, without considering the maximum environmental capacity, the growth of a single phytoplankton community conforms to the exponential growth model (Fan et al., 2011) expressed as Equation 3.

In the formula, N_t is the biomass of phytoplankton at time t, N_0 is the biomass of phytoplankton at the initial time, t is the growth time, and μ' is the community specific growth rate.

Influence of temperature factor

Since the viability of phytoplankton sporangium is much better than that of phytoplankton cells, and the survival ability in ballast water is stronger, the alien phytoplankton leaked at the port is mainly the non-inactivated sporangium in ballast water. The sporangium has a certain dormant period, and it will germinate and grow as long as the environment is suitable.

The Bohai Bay region is a temperate continental climate, with low water temperature from December to March. From April to spring, the water temperature gradually increases, and the surface water temperature is high (11–12°C) along the coast, and the offshore water temperature is low (7–8°C). The spores of alien phytoplankton begin to germinate in this season. From April to May, with water temperature gradually increasing, it will be more suitable for the growth of alien phytoplankton, so during the whole simulation period, the alien phytoplankton is in the growth and reproduction period. Therefore, the model particles will be released throughout the simulation time.

Diffusion Simulation of Alien Phytoplankton

Particlization hypothesis of phytoplankton

Considering that the alien phytoplankton in the study area are single-cell organisms and have small volume and mass, under the action of gravity, buoyancy, inertia, and other forces in the sea, they move with the tide. We can learn from the sediment movement research methods to generally analyze the movement of alien phytoplankton.

In order to explore the transport and diffusion law of alien phytoplankton under the tidal current field in Bohai Bay, the research model is appropriately generalized, and the rules are as follows:

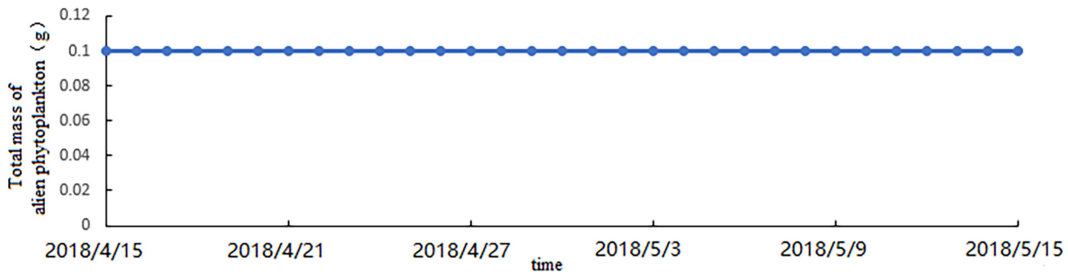

FIGURE 8 | Mass of alien phytoplankton in Bohai Bay ($\mu' = 0$ day^{-1}).

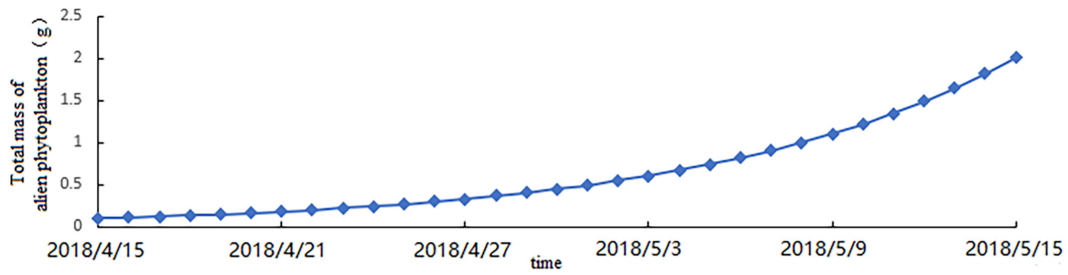

FIGURE 9 | Mass of alien phytoplankton in Bohai Bay ($\mu' = 0.1$ day^{-1}).

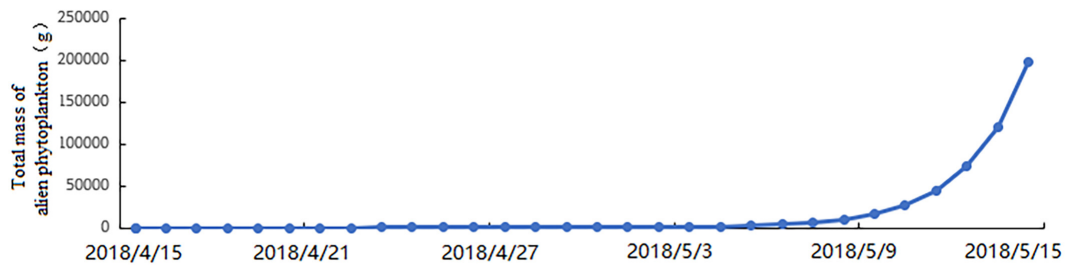

FIGURE 10 | Mass of alien phytoplankton in Bohai Bay ($\mu' = 0.5$ day^{-1}).

(1) Alien phytoplankton is represented by particles, and the movement of phytoplankton is ignored.
(2) Based on the two-dimensional hydrodynamic simulation results, this manuscript only considers the transportation and dispersion of particles in the horizontal direction without considering settlement.

The setting of phytoplankton growth

The maximum distance between the open boundary of Bohai Bay and the port on the land boundary is no more than six nautical miles, with an average water depth of 12.5 m. According to the relevant discharge requirements of the ballast water convention (Fu et al., 2016), under normal circumstances, the possibility of alien phytoplankton spreading from the ballast water replacement site to the Bohai Bay is small. However, in the process of ballast water treatment, due to failure of the treatment technology to inactivate all organisms (Sun, 2014), the ballast water may contain some algae cysts that have not been inactivated, and these cysts will enter the port with ships and be released at the port.

Based on the research results on the invasion pathway of alien phytoplankton in Bohai Bay, the bay is an important economic zone in China, with many coastal ports, among which Caofeidian port, Tianjin port, and Huanghua port are the three largest ports in the bay, and the possibility of alien phytoplankton cyst leakage in the three ports is great. In this study, Caofeidian port, Tianjin port, and the inner bay port of Huanghua port in Bohai Bay are selected as the key research areas. Considering the large area of the port, the point source particles near the central point of the port are selected in this model. The particle release sources are shown in **Figure 6**.

In the model, the instantaneous particle number is the instantaneous total number of alien phytoplankton. The number of phytoplankton sporangium in the cabin is very large, which can reach hundreds of millions (Long et al., 2005). To see the results more clearly, in this study, the number of sporangium leaked at a port is assumed as 10^6.

The 17 species of alien phytoplankton in Bohai Bay are all single-cell organisms with small size, and the mass of a single phytoplankton is about 0.1 μg, so the initial total mass released in the simulation study is 10^5 μg. The growth rates of the 17 alien phytoplankton population are 0–0.5 day^{-1}. In order to more accurately learn the possible diffusion range of alien phytoplankton in Bohai Bay, the transport and diffusion simulations of alien phytoplankton are taken with different growth rates of species community, which are minimum value ($\mu' = 0$ day^{-1}), average value ($\mu' = 0.1$ day^{-1}), and maximum value ($\mu' = 0.5$ day^{-1}), respectively.

As mentioned above, the number of phytoplankton increased exponentially with time during the simulation period. Accordingly, the time series file of particle release rate changing with time should be established in the model. **Figures 8–10** show changes of total mass of alien phytoplankton corresponding to different specific growth rates of phytoplankton communities in the simulation period. The mass of particles released by the particle tracking model over time should meet this rule.

The setting of simulation conditions

Based on the flow field simulation of the study area, the particle tracking model was coupled to simulate the transport and diffusion of particles released at specific locations during April 15 to May 15, 2014. At the initial time, the tracer particles are released at Caofeidian port, Tianjin port, and Huanghua port, respectively. The instantaneous trajectory was output once per hour, and 720 movement moments are recorded. The description of simulated working conditions is shown in **Table 1**.

RESULTS

Figures 11–13 show the density profile of released alien phytoplankton under different working conditions in three ports after 30 days of simulation.

Through the simulation and analysis of particle diffusion trajectory, particle number, diffusion range, and diffusion trend in Caofeidian port, Tianjin port, and Huanghua port, the following information can be obtained: the movement of alien phytoplankton is mainly affected by the tidal circulation in the port area; for different release quantities, the diffusion trend and diffusion range of alien phytoplankton in the same area are basically the same, that is, the number of alien phytoplankton will not have a significant impact on the diffusion range in the study area, but the release quantity will have a direct impact on the density distribution of alien phytoplankton in the study area, and the larger the amount of phytoplankton released, the greater the phytoplankton density in the water body.

TABLE 1 | Working conditions setting of phytoplankton community specific growth rate in each port.

Working conditions	Instruction
Condition 1	Minimum specific growth rate of alien phytoplankton community $\mu' = 0$ day^{-1}
Condition 2	Average specific growth rate of alien phytoplankton community $\mu' = 0.1$ day^{-1}
Condition 3	Maximum specific growth rate of alien phytoplankton community $\mu' = 0.5$ day^{-1}

DISCUSSION

The existing application of the particle tracking model is basically based on the application background, which simplifies the research object to particles with no life characteristics (even the simulation research on the migration of aquatic community is the same), that is, the research object can only drift with the current and has no active ability. In this study, based on the investigation of the species and growth characteristics of alien phytoplankton in Bohai Bay, the concept of specific growth rate is used to endow the particle (alien phytoplankton) with "reproductive capacity," that is, measures are taken to make the particle (alien phytoplankton) propagate with time, and its number in the water area continues to increase. The improved application of the model makes it more suitable for the actual scene under specific conditions than the conventional particle tracking model. It should be pointed out that the specific growth rate data used in the study are not measured in Bohai Bay, and there are some differences in the specific growth rate values of different researchers for the same phytoplankton. In order to ensure that the research results have a sufficient margin of safety, the specific growth rate data with larger values are selected in this study. It is necessary to measure the specific growth rate of alien phytoplankton one by one in Bohai Bay to provide basic support for more accurate research.

Considering that the scale of movement of phytoplankton is negligible compared with the tidal current field, the movement characteristics of phytoplankton such as its own movement and sedimentation are ignored in this study, and only the drift and diffusion in the horizontal direction are considered. In fact, this is also the limitation of the conventional particle tracking model, which is difficult to fully reflect the autonomous activity of aquatic organisms, and then more accurately reflect the relationship between them and the water ecology and hydrodynamic environment. To solve this problem, the model based on the theory of ecological agent (such as the agent-based model, ABM, which is developed by DHI) can be used to define intelligent individuals (such as planktonic larvae, fish, and mammals) and their states (weight, morphology, and habits) and describe the interaction and response relationship with hydrodynamic and aquatic ecological conditions. However, the application of this model needs to be based on the comprehensive and in-depth study of aquatic biological characteristics.

Some red tides contain biotoxins. If a red tide disaster occurs, on the one hand, it will endanger the life of shellfish, fish, shrimp, crab, and other marine life in Bohai Bay; disrupt the ecological balance; and cause serious economic losses to marine fisheries. On the other hand, it will also threaten human health and life safety. If aquatic organisms containing red tide biotoxins are eaten, they may cause poisoning or even death. Thus, it is necessary to simulate and predict the movement trajectory of invasive phytoplankton and the areas where red tides may occur

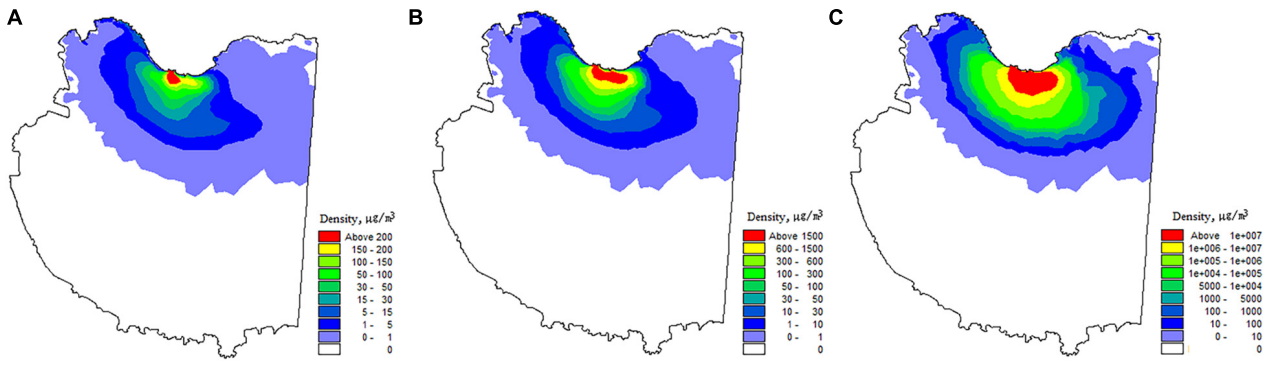

FIGURE 11 | The density profile of alien phytoplankton under different conditions in Caofeidian port. **(A)** Condition 1. **(B)** Condition 2. **(C)** Condition 3.

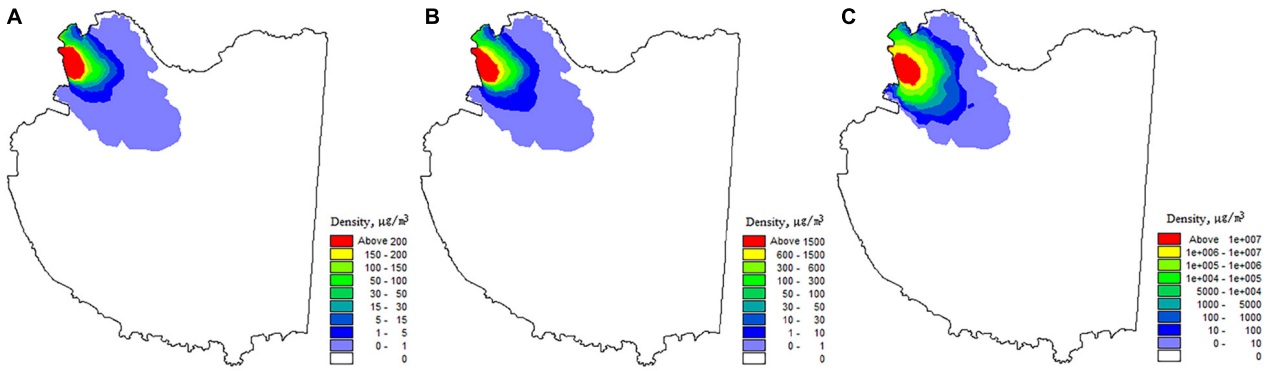

FIGURE 12 | The density profile of alien phytoplankton under different conditions in Tianjin port. **(A)** Condition 1. **(B)** Condition 2. **(C)** Condition 3.

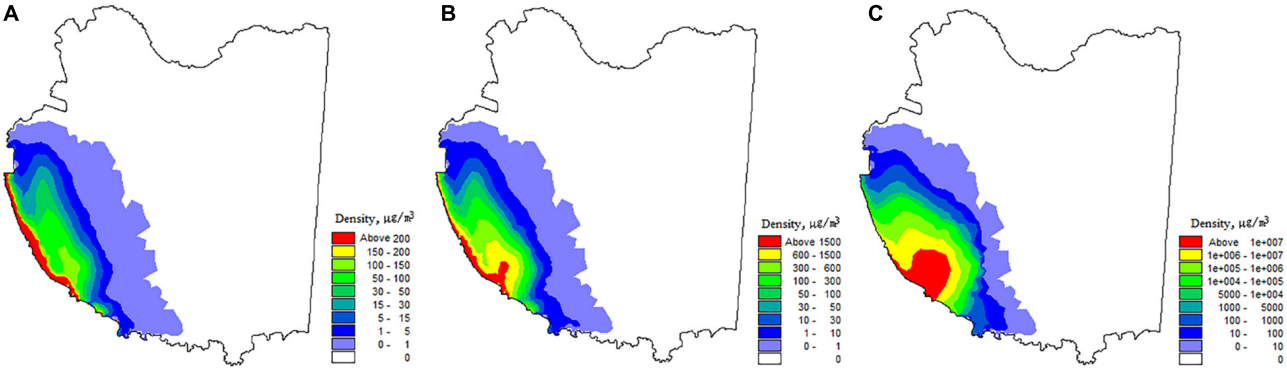

FIGURE 13 | The density profile of alien phytoplankton under different conditions in Huanghua port. **(A)** Condition 1. **(B)** Condition 2. **(C)** Condition 3.

and then prevent and curb the development of red tide organisms as soon as possible. These measures are of great significance to public health management.

CONCLUSION

Under the condition of neglecting the movement of phytoplankton and sedimentation, tracer particles were used to represent alien phytoplankton in this study. Based on the hydrodynamic numerical simulation technology of Bohai Bay, the movement law of alien phytoplankton in the three ports of Bohai Bay was explored through particle transport and diffusion simulation under various conditions. The conclusions and suggestions are as follows:

(1) The movement of phytoplankton in Bohai Bay is mainly affected by the hydrodynamic condition of the region,

namely, tidal circulation. Influenced by the hydrodynamic force in Bohai Bay, the alien phytoplankton will be transported and spread around the port after entering Caofeidian port, Tianjin port, and Huanghua port. The floating plants in Caofeidian port have the largest influence range, and the influence range of Tianjin port is the smallest, but more is still gathered around the core area of each port.

(2) The specific growth rate of phytoplankton will directly affect the distribution density of alien phytoplankton entering Caofeidian port, Tianjin port, and Huanghua port. The higher the specific growth rate, the higher the density of alien phytoplankton in the water.

(3) In view of the fact that it is difficult for the alien phytoplankton to leave the Bohai Bay area driven by hydrodynamic conditions after entering the three port areas, and with the increase of the number of reproduction, and under the effect of the external environment (nutrient content in the water, hydrometeorological conditions, seawater physical and chemical factors, etc.), the possibility of subsequent red tide disasters increases correspondingly. It is necessary to strengthen the monitoring of alien organisms in the port area and actively prevent alien phytoplankton from entering Bohai Bay through ship ballast water.

(4) The specific growth rates of 17 alien phytoplankton species (including 16 species of red tide organisms) in Bohai Bay may be measured through experiments, and the red tide occurrence areas of each species in this area can be simulated and predicted by combining with the numerical model in Bohai Bay, so as to provide more targeted support for the monitoring, prevention, and ballast water treatment of red tide disasters in this area and better provide reference for public health management services for the society.

EQUATIONS

Equation 1:

$$\mu = \frac{\ln N_1 - \ln N_0}{t_1 - t_0}$$

Equation 2:

$$\mu = \mu_{\max} - g$$

Equation 3:

$$N_t = N_0 e^{\mu' t}$$

DATA AVAILABILITY STATEMENT

The original contributions presented in the study are included in the article/supplementary material, further inquiries can be directed to the corresponding authors.

AUTHOR CONTRIBUTIONS

BZ wrote the manuscript. AP provided review and comments. BZ and CX analyzed the data. QW was responsible for the methods used in the study. AP and PJ conceived the research idea of this study and provided review and comments. WT revised the content of the article and was responsible for the overall submission. All the authors were engaged in the final manuscript preparation and agreed to the publication of this manuscript.

FUNDING

This work was financially supported by the National Key Research and Development Program of China (2017YFC1 404602 and 2016YFC0500402-3).

REFERENCES

Belyaeva, P. G. (2019). Invasions of diatom algae in the kama and votkinsk reservoirs. *Rus. J. Biol. Invas*. 10, 118–125. doi: 10.1134/S2075111719020036

Cao, C. H., Sun, Z. N., Wang, X. K., and Li, D. J. (2006). Preliminary study on net-phytoplankton community and red tide causative species in Tianjin sea area, Bohai Sea. *J. Tian. Univ. Sci. Technol*. 3, 34–37. doi: 10.13364/j.issn.1672-6510.2006.03.010

Cao, C. H., Zhang, G. X., Wang, X. K., and Wang, M. T. (2004). Studies on phytoplankton and red tide causitive species in Tianjin Harbour, the Bohai Sea. *Transact. Oceanol. Limnol*. 4, 46–51. doi: 10.13984/j.cnki.cn37-1141.2004.04.009

Chen, X. Y., Mao, X. Y., and Jiang, W. S. (2020). Numerical Study of the lagrangian residual velocity induced by internal tide. *Period. Ocean Univ. China* 50, 1–10. doi: 10.16441/j.cnki.hdxb.20190426

Cristian, A., Sarma, S., and Nandini, S. (2016). Allelopathic activity and chemical analysis of crude extracts from the macrophyte *Egeria densa* on selected phytoplankton species. *Allelop. J*. 37, 147–160.

Fan, S. P., Wang, Y. F., Feng, M. Q., and Zheng, B. M. (2011). Particle tracing random simulation on advection diffusion of pollutants. *Eng. J. Wuhan Univ*. 44, 32–36.

Fu, L. D., Xu, J. W., Wu, G. T., and Gao, Z. M. (2016). Analysis of the current situation of ship ballast water convention and the implementation countermeasures. *Ship Ocean Eng*. 45, 93–96.

Ge, H. X., Chen, Z., Li, J., Feng, Y. Y., Liu, S. T., and Zhao, F. Z. (2017). Effect of pH level and N/P ratio on growth and competition of the microalgae *Tetraselmis helgolandica* and *Prorocentrum minimum*. *J. Fish. Sci. China* 24, 587–595. doi: 10.3724/SP.J.1118.2017.16206

Goes, J. I., Gomes, H., and Chekalyuk, A. M. (2013). Influence of the Amazon River discharge on the biogeography of phytoplankton communities in the western tropical north Atlantic. *Progr. Oceanogr*. 120, 29–40. doi: 10.1016/j.pocean.2013.07.010

Han, T., Fan, Y. L., Zhang, L., Du, Y. Y., Gu, H. B., and Jiang, K. R. (2013). Effect and numerical simulation of algae-isolation with fence in water soune of Lake Ruileihu. *Environ. Sci. Technol*. 26, 32–35.

Hu, Z. X., Xu, N., Duan, S. S., Li, A. F., and Zhang, C. W. (2010). Effects of urea on the growth of *Phaeocystis globosa*, Scrippsiella tro-choidea, *Skeletonema costatum*. *Acta Sci. Circumst*. 30, 1265–1270. doi: 10.13671/j.hjkxxb.2010.06.011

Li, Y. (2006). *The Eco-Physiological Studies of Phosphorus on the Growth of Prorocentrum Donghaiense*. Master's thesis. Guangzhou, GD: Jinan University.

Liu, H. (2019). *The Variations of Nutrients and Phytoplankton on Assemblages in the Bohai Bay and Their Correlation Analysis*. Doctor's thesis. Yantai, SD: Chinese Academy of Sciences (Yantai Institute of Coastal Zone Research). doi: 10.27841/d.cnki.gytha.2019.000005

Liu, S. J. (2007). *Ecological Research of Phytoplankton in Bohai Bay*. Master's thesis. Tianjin: Tianjin University. doi: 10.7666/d.y1357761

Liu, S. J., Tao, J. H., and Zhao, H. P. (2007). Diversity analyse of phytoplankton in the Bohai Ba. *J. Hebei Univ. Eng. (Nat. Sci. Ed.)* 1, 74–77. doi: 10.3969/j.issn.1673-9469.2007.01.020

Liu, S. X. (2011). *Research and Application of Pigment Biomarkers of Common Phytoplankton Species in the Coast of China*. Master's thesis. Qingdao, SD: Ocean University of China. doi: 10.7666/d.y1928373

Liu, X. T. (2011). *Studies on Community Structure and Size-Fractioned Structure of Phytoplankton in Yellow River Estuary and Its Adjacent in Summer and Autumn*. Master's thesis. Qingdao, SD: Ocean University of China.

Long, H., Lin, S. P., Liang, J. R., Gao, Y., Yu, Q. B., and Gao, Y. H. (2005). Harm and monitoring of alien algae introduced into ballast water. *Plant Quar*. 19, 289–291.

Ma, F. F., Li, X., and Lv, S. H. (2012). Influence of inorganic nitrogen and phosphorus on the growth of Cochlodinium geminatum. *J. Saf. Environ*. 12, 1–4. doi: 10.3969/j.issn.1009-6094.2012.04.001

Pablo, G. M. (2005). A model for the upstream motion of elvers in the Adour River. *Compt. Rend. Biol*. 328, 367–378. doi: 10.1016/j.crvi.2004.09.012

Pang, W. B., Zhang, Q. F., Chen, Y. Z., Tu, J. B., and Ma, Y. Y. (2020). Eutrophication evaluation of Tianjin coastal waters in Bohai Bay based on PSR model and analytic hierarchy process. *Transact. Oceanol. Limnol*. 6, 111–118. doi: 10.13984/j.cnki.cn37-1141.2020.06.014

Pu, A. M. (2019). *Simulation Study on the Transport and Diffusion of Alien Phytoplankton in Bohai Bay*. Master's thesis. Nanjing, JS: HoHai University.

Pu, A. M., Zhang, B. B., Jia, P., and Wang, Q. G. (2020). Analysis of alien phytoplankton species and their invasion routes in Bohai Bay. *J. Agricult. Resour. Environ*. 37, 477–483. doi: 10.13254/j.jare.2019.0118

Qin, X. B., Zhou, R., Peng, S. T., Zhang, Z. Y., Liu, Y. R., and Zhao, Y. (2017). The alien phytoplankton species and their ecological risk assessment in Bohai Bay. *J. Water. Harbor* 38, 192–197. doi: 10.3969/j.issn.1005-8443.2017.02.015

Silkin, V. A., Abakumov, A. I., and Pautova, L. A. (2016). Mechanisms of regulation of invasive processes in phytoplankton on the example of the north-eastern part of the Black Sea. *Aquatic Ecol*. 50, 221–234. doi: 10.1007/s10452-016-9570-7

State Oceanic Administration (2019). *Bulletin on the State of China's Marine Environment[EB/OL]*. Available online at: http://www.coi.gov.cn/gongbao/huanjing/ (accessed March 6, 2019).

Sun, H. D. (2014). Progress of ship ballast water treatment technology. *China Water Transport (Lat. Half Month)* 14, 12–13.

Sun, J., and Ning, X. R. (2005). Marine phytoplankton specific growth rate. *Adv. Earth Sci*. 20, 73–80. doi: 10.3321/j.issn:1001-8166.2005.09.003

Tang, Y. X. (1987). An outline of researches on tide-induced residual current. *J. Oceanogr. Huang. Bohai Seas* 5, 73–80.

Wang, H. (2015). *Research on Seasonal Variations of Zooplankton Community and Environment in Coastal Waters of the Caofeidian*. Master's thesis. Qingdao, SD: Hebei Normal University. doi: 10.7666/d.Y2789499

Wang, Y., Liu, L. S., Zhu, Y. Z., Lin, K. X., Zhou, J., and Yang, X. (2016). The community structure of phytoplankton sampled by nets in the coastal seawaters of Bohai bay in spring and autumn. *Mar. Environ. Sci*. 35, 564–570. doi: 10.13634/j.cnki.mes.2016.04.014

Wang, Z. F., Zhang, Q., and Lv, H. Y. (2001). Effects of temperature, salinity, light and pH on the growth of red tide organisms prorocentrum micans. *Oceanol. Limnol. Sin*. 32, 15–18. doi: 10.3321/j.issn:0029-814X.2001.01.003

Wei, H., Hainbucher, D., Pohlmann, T., Feng, S., and Suendermann, J. (2003). Tidal-induced lagrangian and eulerian mean circulation in the Bohai Sea. *J. Mar. Syst*. 44, 141–151. doi: 10.1016/j.jmarsys.2003.09.007

Wu, Y. S., Liu, C., and Wang, Z. Y. (2006). Effect of tidal turbulence on the vertical distribution of phytoplankton in the Bohai Sea. *J. Hydrodyn*. 2, 276–284. doi: 10.3969/j.issn.1000-4874.2006.02.018

Yang, S. M., Dong, S. G., Li, F., Xu, Z. J., and Wu, Y. P. (2007). Study on ecological environment in Bohai Bay I. Species composition and abundance of phytoplankton. *Mar. Environ. Sci*. 2007, 442–445. doi: 10.3969/j.issn.1007-6336.2007.05.010

Yin, C. L., Zhang, Q. F., Cao, C. H., Liu, Y., and Cui, J. (2013a). Net-phytoplankton community in the Tianjin nearshore waters of Bohai Bay in spring of 2012. *J. Mar. Sci*. 31, 80–89. doi: 10.3969/j.issn.1001-909X.2013.04.013

Yin, C. L., Zhang, Q. F., Cui, J., Liu, Y., Xu, Y. S., and Ma, Y. Y. (2007). Phytoplankton composition in Bohai Bay Tianjin coastal area in summer from 2008 to 2012. *Adv. Mar. Sci*. 5, 442–445. doi: 10.3969/j.issn.1671-6647.2013.04.011

Yin, C. L., Zhang, Q. F., Niu, X. F., Shi, H. M., Xu, Y. S., and Tu, J. B. (2015). Primary productivity and net-phytoplankton composition in the Tianjin nearshore waters of Bohai Bay from 2012 to 2013. *J. Mar. Sci*. 33, 82–92. doi: 10.3969/j.issn.1001-909X.2015.02.012

Yin, C. L., Zhang, Q. F., Shi, H. P., Xu, Y. S., Ma, Y. Y., Cui, J., et al. (2013b). Net-phytoplankton community in the nearshore waters of Bohai in 2011. *Transact. Oceanol. Limnol*. 3, 152–160. doi: 10.13984/j.cnki.cn37-1141.2013.03.017

Yu, G. Y., and Chen, S. J. (1983). Numerical modeling of the circulation and the pollutant dispersion in Jiaozhou Bay III. The Lagrangian residual current and the pollutant dispersion. *J. Shand. Coll. Oceanol*. 13, 1–14. doi: 10.16441/j.cnki.hdxb.1983.01.001

Yu, P. (2005). *Effect of Temperature, Irradiance and Population Interaction on the Growth of Phytoplankton of East China Sea*. Master's thesis. Qingdao, SD: Ocean University of China. doi: 10.7666/d.y828410

Zhang, H. Y., Zhao, L., and Wei, H. (2012). Origin of the giant jellyfish in Qingdao offshore in summer. *Oceanol. Limnol. Sin*. 43, 62–668. doi: 10.1007/s11783-011-0280-z

Zhang, P. R. Y., Li, D. L., Peng, Y. Y., Gao, Y., Zhang, J. W., Yang, W. Y., et al. (2016). The characteristic of phytoplankton community structureinthe coastal area of Tianjin. *Transact. Oceanol. Limnol*. 6, 53–59. doi: 10.13984/j.cnki.cn37-1141.2016.06.007

Zhang, W. C., and Wang, R. (2000). Microzooplankton and their grazing pressure on phytoplankton in Bohai Sea. *Oceanol. Limnol. Sin*. 31, 252–258. doi: 10.3321/j.issn:0029-814X.2000.03.004

Zheng, Q. (2014). *Temporal and Spatial Distribution Prediction of Patinopecten Yessoensis Planktonic Larvae in Northern Yellow Sea*. Master's thesis. Dalian, LN: Dalian Ocean University.

Conflict of Interest: AP is employed by Nanjing Water Group Co., Ltd.

The remaining authors declare that the research was conducted in the absence of any commercial or financial relationships that could be construed as a potential conflict of interest.

frontiers in Ecology and Evolution

ORIGINAL RESEARCH
published: 21 October 2021
doi: 10.3389/fevo.2021.731735

Air Warming and Drainage Influences Soil Microarthropod Communities

Hui Zhang[1,2,3], Xin Sun[4,5], Dong Liu[1], Haitao Wu[1] and Huai Chen[2]*

[1] Key Laboratory of Wetland Ecology and Environment, Northeast Institute of Geography and Agroecology, Chinese Academy of Sciences, Changchun, China, [2] Key Laboratory of Mountain Ecological Restoration and Bioresource Utilization & Ecological Restoration and Biodiversity Conservation Key Laboratory of Sichuan Province, Chengdu Institute of Biology, Chinese Academy of Sciences, Chengdu, China, [3] University of Chinese Academy of Sciences, Beijing, China, [4] Key Laboratory of Urban Environment and Health, Institute of Urban Environment, Chinese Academy of Sciences, Xiamen, China, [5] J.F. Blumenbach Institute of Zoology and Anthropology, University of Göttingen, Göttingen, Germany

The degradation of wetlands due to climate change is of critical concern to human beings worldwide. Little is known about the potential synergistic effects of simultaneous water level reduction and warming on the underground wetland ecosystems. We conducted a 5-month field experiment in the Sanjiang Plain, utilizing open-top chambers and water level automatic control systems to investigate such synergistic effects. Soil springtails (Collembola) and mites (Acari) in the top (0–20 cm) soil layers were sampled to calculate their density, diversity, and to screen for indicator species. Warming significantly influenced soil springtail communities, slightly increasing the total density and total abundance under the natural water level while reducing them under a constant water level. In addition, *Anurida maritima* and *Vertagopus laricis*, two indicators for the natural water level, had the highest densities in the natural water level treatment and under the combined treatment of warming and natural water level, respectively. *Cheiroseius sinicus* and *Malaconothrus tardus* had the highest densities in warming under the 0 cm water level, significantly higher than the other three treatments. This study also revealed the importance of maintaining fluctuating water levels for microarthropod communities influenced by global warming, providing a theoretical basis for water level control in wetland restoration.

Keywords: climate change, collembola, mites, indicator species, wetland restoration

OPEN ACCESS

Edited by:
Hideyuki Doi,
University of Hyogo, Japan

Reviewed by:
Rentao Liu,
Ningxia University, China
Ender Makineci,
Istanbul University-Cerrahpasa, Turkey

****Correspondence:***
Haitao Wu
wuhaitao@iga.ac.cn

Specialty section:
This article was submitted to Conservation and Restoration Ecology, a section of the journal Frontiers in Ecology and Evolution

Received: *28 June 2021*
Accepted: *23 September 2021*
Published: *21 October 2021*

Citation:
Zhang H, Sun X, Liu D, Wu H and Chen H (2021) Air Warming and Drainage Influences Soil Microarthropod Communities. Front. Ecol. Evol. 9:731735. doi: 10.3389/fevo.2021.731735

HIGHLIGHTS

- Air warming increased the density and richness of springtails (Collembola), while no significant effects on the density and richness of soil mites (Acari).
- Springtails were more sensitive to warming and drainage than mites.
- *Anurida maritima* (springtails) and *Vertagopus laricis* (springtails) had the highest densities in the natural water level and warming under the natural water level, respectively. Besides, *Cheiroseius sinicus* (mites) and *Malaconothrus tardus* (mites) had the highest densities in warming under the 0 cm water level. These four indicator species characterized warming and water level changes in wetlands.
- Natural water level fluctuations are important for soil microarthropods protection.

INTRODUCTION

Soil fauna are a crucial part of the terrestrial biosphere, and plays an important role in ecosystem function and plant community dynamics (Brussaard, 1998; Geisen and Bonkowski, 2018; Phillips et al., 2019; van den Hoogen et al., 2019; Hallam and Hodson, 2020; Oliverio et al., 2020). Driven by resource heterogeneity, nutrient availability, and abiotic conditions, they could impose direct or indirect and positive or negative feedbacks on aboveground biology by altering rates of nutrient mineralization and the spatial distribution of nutrient availability, rhizospheric hormones and the soil environment (Wang and Ran, 2008). The composition and diversity of soil fauna are closely related to soil properties (physical, chemical, and microbial characteristics), vegetation, and climate (Wardle et al., 2005; Liu et al., 2012; Phillips et al., 2020; Vazquez et al., 2020), among which some sensitive species can also act as indicators to indicate environmental changes (Liang et al., 2001; Sun et al., 2021). It is noteworthy that changes in composition and distribution patterns of soil fauna are likely to impact ecosystem processes and functions (Koltz et al., 2018).

Among soil fauna, soil microarthropods (most fungi-/detritivores) such as Collembola, oribatid mites (Acari: Oribatida), and enchytraeids (Oligochaeta: Enchytraeidae) take part in important ecosystem functions such as decomposition, nutrient mobilization, soil mixing, and aggregate formation (Lindberg, 2003; Semenina and Tiunov, 2020). Climate change impacts soil fauna's growth, development, and reproduction, impacting soil microarthropod communities' abundance, and composition, by altering the soil microenvironment. Climate change can also indirectly influence the soil microarthropod communities' structure by changing the resource availability and composition of the soil food web (Kardol et al., 2011; Zhang and Wu, 2020).

The effect of warming on soil microarthropods is controversial, as some studies have found that warming significantly reduced the biomass and diversity of springtails (Makkonen et al., 2011; Chang et al., 2019), as well as significantly changing the composition and diversity of soil fauna (Briones et al., 2009; Kardol et al., 2011). In contrast, others have found that warming either increased the total abundance of springtails (Orchesellides) in grasslands of the Songnen Plain, northeast China (Yan et al., 2015) or had no significant effect on the abundance of soil collembola and mites. The different results were possibly related to water content of ecosystems. In humid area, the warming effect was positive or insignificant. However, in relatively arid areas, warming had a negative effect on soil microarthropods, and the variation of precipitation often had a more significant effect on soil microarthropods than warming. For example, one study conducted on a semiarid grassland in Duolun County showed that an increase in rainfall significantly increased the abundance of soil mites and springtails, but warming had no significant effect on soil microarthropods (Wu et al., 2014). Drought increased the abundance of soil microarthropods while reducing their biomass, it also increased the abundance of small mites (body length 0.20 mm), and decreased the abundance of large mites (body length >0.40 mm) in the sandy forest soils (the water level is between 5 and 30%) (Xu et al., 2012). In comparison, warming only slightly affected the animal population (Xu et al., 2012). This was similar to a meta-analysis that identified that the soil microbiota responded more strongly to changes in precipitation than warming (Blankinship et al., 2011). Nevertheless, other studies have found that changes in precipitation can have no significant impact on soil microarthropods (Kardol et al., 2011; Darby and Neher, 2012).

Wetlands provide critical ecosystem functions, including water storage and flood regulation, water quality purification, and local climate regulation. However, the annual average temperature of the Sanjiang Plain and the average temperature of the growing season has increased over the past 60 years, with projections to rise continuously over the next 30 years (Liu, 2016; Meng, 2016). Concurrently, the water levels of the marsh have declined significantly, and the ecosystem has degraded under human drainage disturbance and global change. Yet, research into the relationships between climate change and vegetation coverage, phenology, NDVI (the Normalized Difference Vegetation Index), and the carbon budget of the Sanjiang Plain is limited (Liu et al., 2019; Shen et al., 2019a,b; Zhang et al., 2019). There is also insufficient research into the potential impact of climate warming and drainage on soil microarthropods in the marsh of the Sanjiang Plain.

In this study, we conducted a 5-month simulation experiment of warming and drainage on the marsh of the Sanjiang Plain. We examined the influence of warming and wetland drainage on soil microarthropod community composition, diversity, and vertical distribution. The influence of mild drainage on the wetland soil ecosystem provides a theoretical basis for further understanding how these important and fluctuating abiotic effects can influence wetland soil ecosystems. We also screened soil microarthropod communities for species sensitive to climate change and wetland drainage to enrich the existing wetland evaluation index system. Wetlands are flooded or seasonally flooded areas with higher water content. As a result, we hypothesize that continued drainage will significantly reduce the density and abundance of soil microarthropods, while warming had a positive effect on it. This article mainly focuses on mites and springtails in this article because they are two critical classes of soil fauna and were the most dominant microarthropod groups collected across all treatments.

MATERIALS AND METHODS

Sample Collection and Processing

Field samples were collected in August, September, and November of 2018, and data were averaged for these analyses. One soil column was taken from each subplot at each sampling time, immediately wrapped with plastic, and then transported to the laboratory. The soil samples were then placed in a Tullgren-type extractor (Yin, 1992) for 72 h to extract the soil arthropods. The extracted arthropods were preserved in 70% ethanol and identified to taxonomic species or morphospecies

using applicable keys (Balogh and Balogh, 1992; Bellinger et al., 1996-2019; Yin, 1998; Krantz and Walter, 2009).

Site and Plot Description

The field study was conducted from June 2018 to November 2018, in the marshes at the Sanjiang Mire Wetland Experimental Station (47°13′50′N, 133°13′10′E, 55 m above the sea level), Chinese Academy of Sciences. The marshes are located in the Sanjiang Plain, a low-lying floodplain, in the Heilongjiang Province, Northeast China. This region has a temperate moist monsoon climate, with a mean annual temperature of 1.9°C (−21°C in January and 22°C in July) and mean annual precipitation of 600 mm (≥60% between July and September). *Carex lasiocarpa*, *Carex pseudocuraica*, and *Carex meyeriana* are the dominant grass species, often grown with co-occurring *Deyeuxia angustifolia* and *Glyceria spiculosa*.

In this study, the dominant vegetation in our experiment is *C. lasiocarpa*, and the water depth in this study area usually fluctuated up and down by 10 cm. Our main purpose was to simulate the fluctuation and the same of water level and found their different impacts on soil fauna communities. So we chose the fluctuation water level of natural wetlands and the constant water level of 0 and −10 cm. The water levels could be controlled independently, and the specific design and operation of the experiment have been previously described in detail (Tan et al., 2018). In brief, this set of automatic water level control equipment was able to realize the multi-loop automatic control and the function of replenishing and draining simultaneously, consisting of control center, horizontal self-priming centrifugal pump, water ring vacuum pump, electrode hydraulic gauge, water refill solenoid valve, drainage solenoid valve, remote pressure gauge, air compressor, vacuum tank, pneumatic valve, water refill diverters, drainage diverters, water refill pipes, and drainpipes (**Figure 1**). When the actual water level is lower than the set water level, the water supply system starts to work. Otherwise, the control center will start the drainage system.

Besides, a method of open-top chambers (OTC) was used for the calefaction treatments. The basic function of the OTCs is to increase the air temperature and soil temperature by passively trapping the long wavelength solar radiation. It is also common method for soil fauna researches (Kardol et al., 2011; Makkonen et al., 2011; Yan et al., 2015). In a hexagon-based pyramid shape, the OTC was made of polymethyl-methacrylate sheet [length: width: height = 100: 65 (top) or 280 (bottom): 230 cm]. Each chamber had a door (100 cm width and 180 cm height) to ensure access. The control treatment contained only frame without polymethyl-methacrylate sheet. The air temperature was measured minutely using air temperature sensors (HMP155, Vaisala, Helsinki, Finland), and the results showed an average increase of 2.5°C in atmospheric temperature during the sampling period (see **Supplementary Figure 1**). All measured temperatures were stored in data loggers (CR1000, Campbell, NY, Untied States) throughout the plant growing season from June to December 2018. Thus, the 12 subplots were split into four treatments; namely, the natural water level (CK), warming under the natural water level (OTC), warming under the reference water level (the constant water level, about 20–40 cm, based on the suitable water level of the dominant vegetation) (0 cm × OTC), and warming under 10 cm below the reference water level (the constant water level) (−10 cm × OTC), including interaction designs of water-level and warming (**Table 1** and **Figure 2**).

Before the experiment, 36 soil columns were collected using a PVC pipe (diameter = 110 mm, length = 200 mm) in a relatively flat wetlands outside the plots to avoid the original differences between plots and to reduce the direct collection of soil samples that could influence our treatments. To prevent species loss during collection, we carefully and immediately wrapped the soil samples with plastic wrap after obtaining them, marked the soil surface, placed the soil columns according to the direction of collecting soil columns, and transported them to the study site. Three soil column samples were placed into one subplot with their plastic wrap removed. The sampling design excluded the dispersal ability of these animals and the possibility of species turnover.

Statistical Analysis

Abundance data were expressed as numbers per square meter. Diversity indices (Margalef Richness, Pielou Evenness, and Shannon–Wiener index) were calculated in Primer 7.0 to characterize arthropod communities and the influence of warming and water level. The specific formula is as follows: Margalef Richness ($M = \frac{(s-1)}{lnN}$), Shannon–Wiener index ($H = -\sum_{i=1}^{s} P_i \ln P_i$), and Pielou Evenness ($E = H/\ln S$), where S, total number of species; N, total number of individuals in the sample; Pi, the proportion of the entire community made up of species. Dominance (%) of a species was expressed as its proportion in the community (dominant, common, and rare species), and the number of individuals of a species was accounted for >10, 1–10, and <1% of the total numbers, respectively. One-way ANOVA analyses were performed to determine the statistical significance of the warming treatment on density measures, the number of species and to test for differences in the diversity indexes between treatments using Tukey's Studentized Range (HSD) test ($p < 0.05$). Figures were created by using Origin 2018 (Origin Lab, Northampton, MA, United States).

Indicator species analysis was based on the abundance of soil springtails and mites under four treatments ($n = 3$) in PCORD Version 5.0, using Dufrene and Legendre's (1997) indicator value method (IVM) (Dai et al., 2006; Iqbal et al., 2018; Kamran et al., 2020). The equations for determining the indicator species were presented in **Supplementary Material**. Indicator value (IV), ranging from 0 (no indication) to 100 (perfect indication), were tested for statistical significance using a Monte Carlo technique. Only significant species were list ($p < 0.05$) in the results.

RESULTS

Springtails

Community Composition and Structure

The community structure of soil collembola varied significantly across our treatments, with increasing temperature under two constant water level significantly reducing the number of species

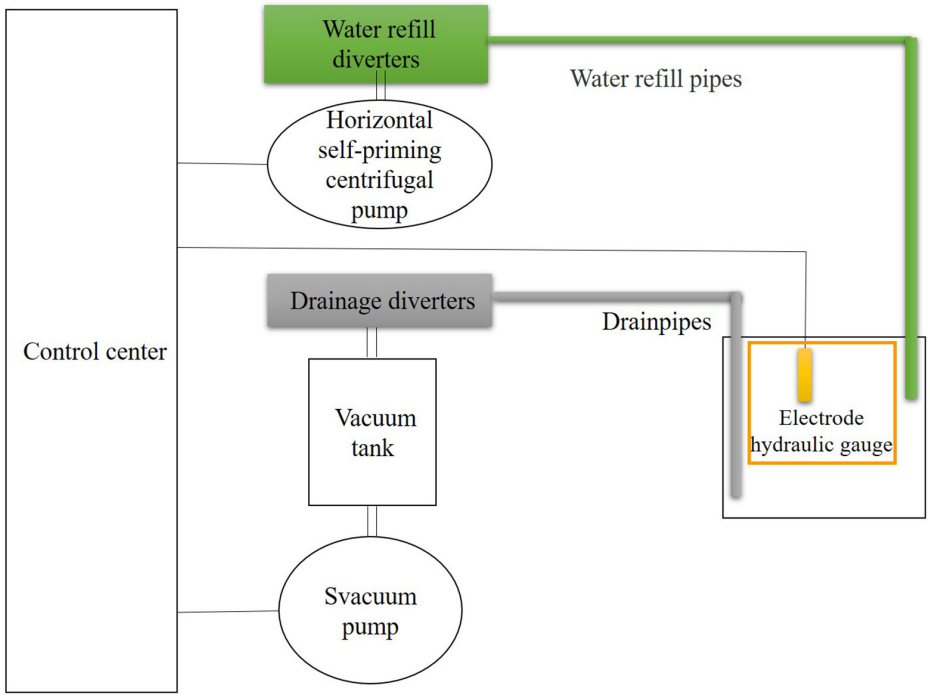

FIGURE 1 | Sketch of automatic water-level control equipment in one subplot (modified from Tan et al., 2018).

TABLE 1 | The design of this experiment.

Treatments	Water level	Warming or not	Replicates	Soil columns	Sampling times
CK	The natural water level	No	3	9	3
OTC	The natural water level	Yes	3	9	3
0 cm × OTC	The constant water level	Yes	3	9	3
−10 cm × OTC	The constant water level	Yes	3	9	3

Treatment codes: CK, control (the natural water level); OTC, warming under the natural water level; 0 cm × OTC, warming under the reference water level (the constant water level, about 20–40 cm, based on the suitable water level of the dominant vegetation); and −10 cm × OTC, warming under 10 cm below the reference water level (the constant water level). Soil columns were collected in August, September, and November of 2018, and data were averaged for these analyses.

of collembola (**Table 2**). There were 20 species identified in the natural water level treatment (CK); the dominant species was *Folsomia octoculata,* which accounted for 41.86% of all individuals, while the most common species included *Lepidocyrtus szeptyckii*, *Desoria infuscata*, and *Anurida maritima*. Overall a total of 12 species accounted for 53.02%, with only 7 species accounting for 4.27%. There were also 20 species in the warming treatment (OTC); the dominant species were *Desoria olivacea* and *F. octoculata*, accounting for 10.25 and 54.81%, respectively. The common species included *Desoria tigrina* and *Parisotoma ekmani*, and an additional seven species accounted for 20.63%. There were 11 rare species, accounting for only 3.85%. There were eight species in total in the warming under 0 cm water level treatment (0 cm × OTC). *D. olivacea*, *F. octoculata,* and *Tomocerus nigrus* were the dominant species, accounting for 51.65%; there were four common species, accounting for 23.99%; and *D. infuscata* was the rarest species, accounting for 0.37%. Finally, there were 13 species in the warming treatment at −10 cm water level (−10 cm × OTC). *D. olivacea* and *F. octoculata* were the dominant species, accounting for 18.36 and 63.99%, respectively; common species (14.68%) included *D. tigrina*, *Vertagopus laricis*, and *A. maritima*, while five rare species accounted for 2.96%.

The Density and Diversity Dynamics of Springtails

The results of the one-way analysis of variance revealed that the soil collembola density ($F = 14.064$, $p = 0.034$) and the number of species under different treatments ($F = 3.832$, $p = 0$) were significantly different (**Figure 3**). During warming at the natural water level, the density and number of species were consistently higher than other treatments, with the lowest abundances always present in the warming treatment at the 0 cm water level. At the same time, the Margalef richness index ($F = 10.801$, $p = 0.001$) of collembola was significantly different under the four treatments, with higher abundances in the natural water level and its warming treatment (**Figure 4**). Warming at 0 cm water level treatment had a high uniformity, and the natural water level had high diversity.

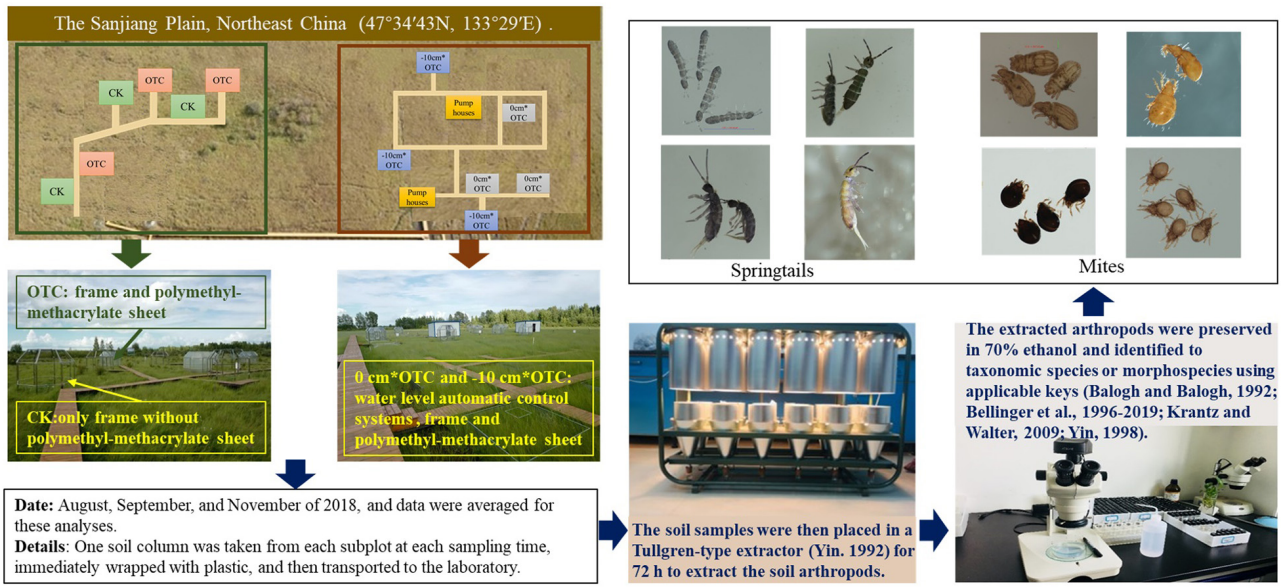

FIGURE 2 | The study site, experimental design, and some kinds of soil microarthropods.

Analysis of Indicator Species

The indicator species analysis of the four treatments (**Table 3**) exhibited two indicator species: *A. maritima* ($p = 0.0196$) in the natural water level and *V. laricis* ($p = 0.0172$) in the warming treatment. Collembola *A. maritima* existed under the natural water level, warming and warming treatment at −10 cm water level (densities were 912 ± 228, 614 ± 162, and 246 ± 35 ind./m^2, respectively), but was not present at 0 cm water level in the warming treatments. The density of *V. laricis* increased significantly after warming (4069 ± 1187/m^2), significantly higher than in the other three treatments were 1789 ± 914, 561 ± 246, and 316 ± 0 ind./m^2, respectively.

Mites

Community Composition and Structure

A total of 1290 mites were captured in three samplings in 2018, belonging to nine families and ten genera (**Table 1**). The dominant species were *Geolaelaps praesternaliodes*, *Malaconothrus tardus*, and *Zetomimus furcatus*, which accounted for 32.48, 37.52, and 13.72% of all individuals, respectively. Common species include *Cheiroseius sinicus* and *Geolaelaps dailingensis*, accounting for 15.12% of the total catch, while four rare species accounted for only 1.16%.

There were also significant differences in the community composition of soil mites under various treatments (**Table 2**). There were nine species identified under the natural water level. The dominant species were *G. praesternaliodes*, *M. tardus*, and *Z. furcatus*, accounting for 37.25, 33.04, and 10.20%, respectively; five common species accounted for 19.24%; *Belba compta* was a rare species that only accounted for 0.44%. After warming treatment, there were eight species. The dominant species were consistent with the natural water level plots, but the proportions varied, respectively, 33.33, 29.17, and 24.56%; there were three common species, accounting for 11.84%. The other two species were rare, accounting for 1.10%. There were eight kinds of warming treatments under 0 cm water level. Compared with the first two treatments, the dominant species (*Z. furcatus*) was significantly reduced; there were three common taxa, accounting for 19.74%, and the remaining two species were rare, accounting for 0.86%. There were eight species after warming at −10 cm water level. Compared with the dominant species at 0 cm water level, the dominant species accounted for 52 and 31.33%, respectively; common species included *C. sinicus* and *Banksinoma akhtyamovi*. Four species accounted for 15.33% of the total catch, and two rare species accounted for 1.16% of the total catch.

The Density and Diversity Dynamics of Mites

According to the Shannon–Wiener diversity index ($F = 3.904$, $p = 0.032$), there were also significant differences across treatments, with a significantly higher diversity of mites under natural water level and warming treatment, than under warming at 0 cm water level (**Figure 5**). Although, the soil mites density ($F = 0.387$, $p = 0.764$), number of species ($F = 1.379$, $p = 0.290$), Pielou evenness index ($F = 2.532$, $p = 0.099$), and Margalef richness index ($F = 1.062$, $p = 0.397$) did not significantly differ (**Figures 5**, **6**). The natural water level had higher uniformity and diversity than increasing temperatures under the 0 cm water level.

Indicator Species Analysis

There were two indicator species of mites, *C. sinicus* ($p = 0.0426$) and *M. tardus* ($p = 0.0022$) (**Table 3**). The density of *C. sinicus* under the four treatments were 631 ± 192, 263 ± 71, 1052 ± 219, and 281 ± 126 ind./m^2. The density of *M. tardus* under the four treatments was 2613 ± 562, 2333 ± 596, 5437 ± 345, and 1649 ± 345 ind./m^2.

TABLE 2 | Soil microarthropod community composition and dominance in four treatments (n = 3) in the Sanjiang Plain.

		CK		OTC		0 cm × OTC		−10 cm × OTC		Total	
Order/family	**Specie**	**Dominance**		**Dominance**		**Dominance**		**Dominance**		**Dominance**	
Collembola Arthropleona											
Entomobryinae	*Homidia phjongiangica* (Szeptycki, 1973)	–		0.09	+	–		–		0.05	+
	Lepidocyrtus szeptyckii (Rusek, 1985)	2.23	++	0.45	+	–		0.7	+	0.9	+
Isotominae	*Desoria choi* (Lee, 1977)	0.1	+	0.36	+	–		–		0.22	+
	Desoria infuscata (Murphy, 1959)	2.33	++	0.4	+	0.37	+	–		0.83	+
	Desoria olivacea (Tullberg, 1871)	8.43	++	10.25	+++	25.09	+++	18.36	+++	11.91	+++
	Desoria tigrina (Nicolet, 1842)	7.27	++	4.27	++	9.23	++	7.17	++	5.76	++
	Desoria violacea (Tullberg, 1877)	0.97	+	0.76	+	–		0.35		0.71	+
	Folsomia octoculata (Handschin, 1925)	41.86	+++	54.81	+++	37.27	+++	63.99	+++	51.67	+++
	Parisotoma ekmani (Fjellberg, 1977)	5.91	++	5.44	++	–		0.35	+	4.49	++
	Pseudisotoma sensibilis (Tullberg, 1877)	0.19	+	0.18	+	–		–		0.15	+
	Vertagopus laricis (Martynova, 1975)	9.88	++	10.43	++	5.9	++	1.57	++	8.76	++
Neanurinae	*Anurida maritima* (Guérin-Méneville, 1836)	5.04	++	1.57	++	–		1.22	++	2.29	++
	Lobellina decipiens (Yosii, 1965)	0.78	+	0.45	+	7.01	++	2.1	++	1.2	++
Onychiurinae	*Allonychiurus songi* (Sun & Wu, 2012)	1.07	++	2.2	++	–		–		1.46	++
Poduridae	*Podura aquatica* (Linnæus, 1758)	1.65	++	0.63	+	–		–		0.76	+
Tomoceridae	*Tomocerina varia* (Folsom, 1899)	0.58	+	0.04	+	–		–		0.17	+
	Tomocerus nigrus (Sun, Liang & Huang, 2006)	8.14	++	5.8	++	13.28	+++	2.62	++	6.44	++
	Tomocerus sp. 1	0.68	+	–		–		–		0.17	+
Collembola Symphypleona											
Sminthuridídae	*Arrhopalites minor* (Park & Kang, 2007)	1.07	++	0.36	+	–		0.52	+	0.54	+
	Sminthurides aquaticus (Bourlet, 1842)	0.97	++	0.13	+	–		0.52	+	0.39	+
	Sminthurides malmgreni (Tullberg, 1877)	0.87	+	1.35	++	1.85	++	0.52	+	1.15	++
The number of species (dominant, common and rare species)		20 (1:12:7)		20 (3:6:11)		8 (3:4:1)		13 (2:5:6)		21 (2:8:11)	
Parasitiformes Mesostigmata											
Blattisociidae	*Cheiroseius sinicus* (Yin & Bei, 1991)	7.98	++	3.29	++	12.88	+++	5.33	++	6.9	++
Laelapidae	*Geolaelaps dailingensis* (Ma and Yin, 1998)	2.22	++	–		1.29	++	–		1.01	++
	Geolaelaps praesternaliodes (Ma & Yin, 1998)	37.25	+++	33.33	+++	9.01	++	52	+++	32.48	+++
Acariformes Oribatida											
Banksinoma	*Banksinoma akhtyamovi* (Rjabinin, 1993)	1.77	++	4.61	++	0.43	+	1.33	++	2.48	++
Bellidae	*Belba compta* (Kulczynski, 1902)	0.44	+	–		–		0.67	+	0.23	+
Malaconothridae	*Malaconothrus tardus* (Michael, 1888)	33.04	+++	29.17	+++	66.52	+++	31.33	+++	37.52	+++
Scheloribatidae	*Scheloribates latipes* (C.L. Koch, 1844)	5.99	++	3.95	++	5.58	++	2	++	4.73	++
Suctobelbidae	*Suctobelbella longidentata* (Chinone, 2003)	1.11	++	0.88	+	–		–		0.7	+
Tectocepheidae	*Tectocepheus velatus* (Michael, 1880)	–		0.22	+	0.43	+	0.67	+	0.23	+
Zetomimidae	*Zetomimus furcatus* (Warburton & Pearce, 1905)	10.2	+++	24.56	+++	3.86	++	6.67	++	13.72	+++
The number of species (dominant, common and rare species)		9 (3:5:1)		8 (3:3:2)		8 (2:4:2)		8 (2:4:2)		10 (3:4:3)	

The dominance of the Collembola and Oribatida was calculated separately.

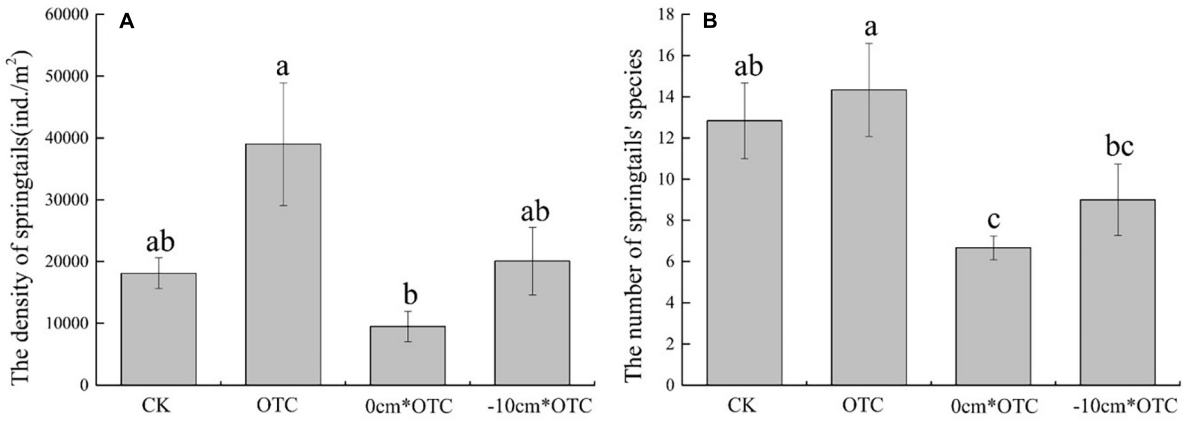

FIGURE 3 | Soil springtail density **(A)** and number of species **(B)** in different treatments. Data are means ± SE (n = 3) and different letters indicate significant differences between treatments (a, b, and c) at $p < 0.05$.

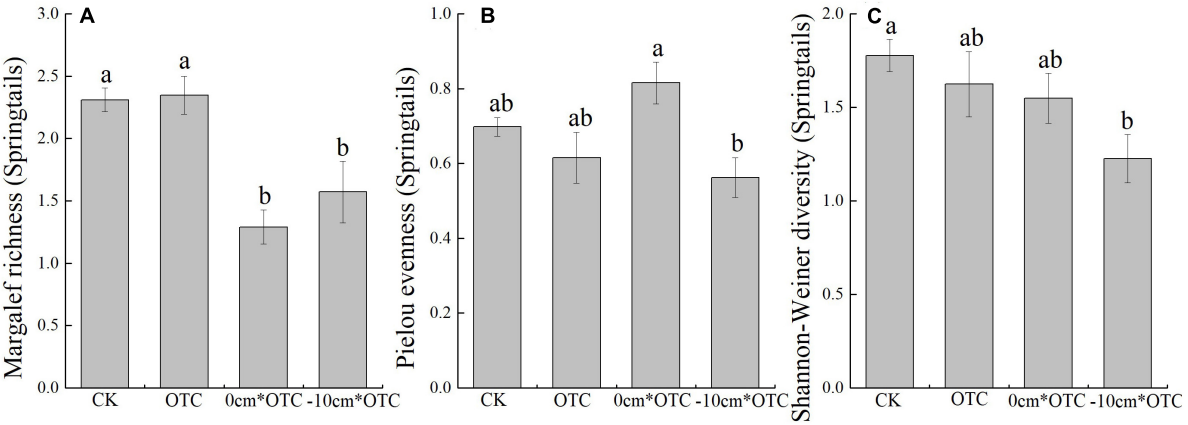

FIGURE 4 | Soil springtail diversity indexes in different treatments: **(A)** Margalef richness, **(B)** Pielou evenness, and (C) Shannon–Wiener index. Data are means ± SE (n = 3) and different letters indicate significant differences between treatments (a and b) at $p < 0.05$.

TABLE 3 | Indicator species analysis of four treatments in the Sanjiang Plain marshlands.

Treatments	Indicator species	Indicator value	*p*
OTC	*Vertagopus laricis* (Martynova, 1975) (Springtails)	60.4	0.0172
CK	*Anurida maritima* (Guérin-Méneville, 1836) (Springtails)	51.5	0.0196
0 cm × OTC	*Cheiroseius sinicus* (Yin & Bei, 1991) (Mites)	47.2	0.0426
0 cm × OTC	*Malaconothrus tardus* (Michael, 1888) (Mites)	45.2	0.0022

Only significant species were list, $p < 0.05$.

DISCUSSION

Our results demonstrate that single and combined effects of warming and drainage can influence soil microarthropod's abundance and community structure, which are important regulators of ecosystem processes. Further, we found that the major taxonomic groups of soil microarthropods, i.e., collembola and mites, differed in their response to our climate change treatments, which appears to be more complex than we assumed. Besides, the results confirmed our hypothesis that warming alone slightly increased the density and abundance of springtails (CK vs. OTC). It supports the view that warming in humid areas has a positive effect or no effect on soil fauna. And the synergistic effect of warming and drainage also increased the density and abundance of springtails (0 cm × OTC vs. −10 cm × OTC).

Previous studies have identified that 3 years of temperature increases have significantly increased the abundance of total collembola and its dominant species *Orchesellides* sp1 in the Songnen Grasslands (Yan et al., 2015). In this study, warming under different water levels impacted the community

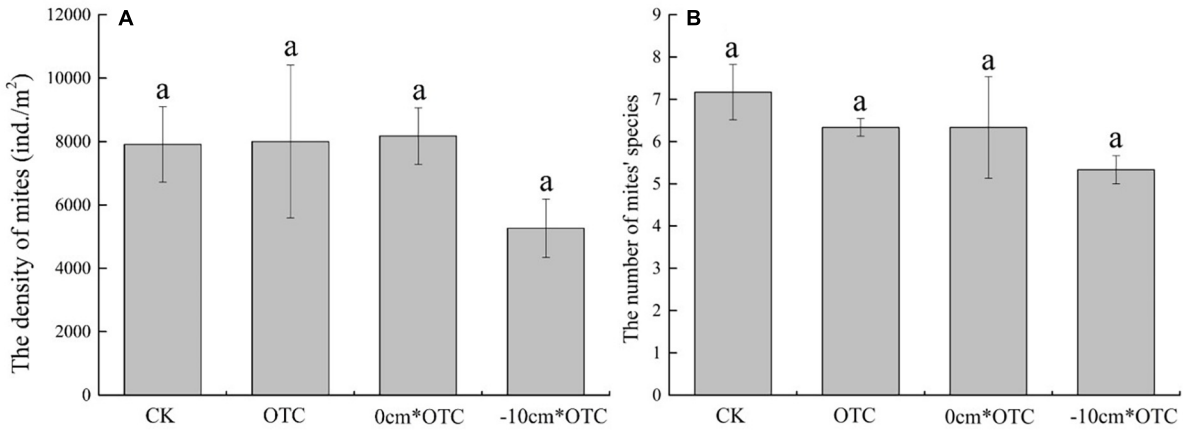

FIGURE 5 | Soil mites density **(A)** and number of species **(B)** in different treatments. Data are means ± SE (n = 3), and the same letter indicate insignificant differences between treatments (a) at $p < 0.05$.

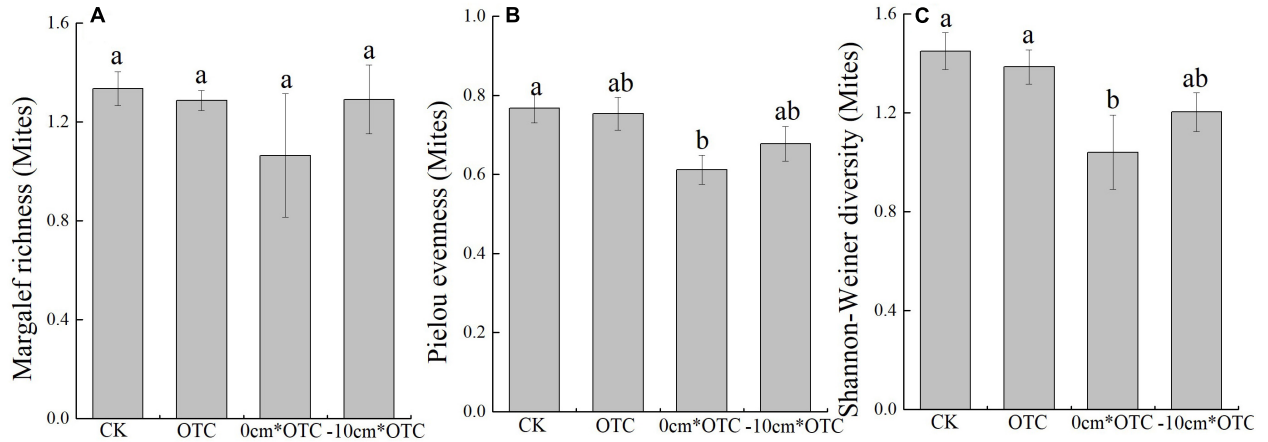

FIGURE 6 | Soil mites diversity indexes in different treatments: **(A)** Margalef richness, **(B)** Pielou evenness, and **(C)** Shannon–Wiener index. Data are means ± SE (n = 3) and different letters indicate significant differences between treatments (a and b) at $p < 0.05$.

composition of soil microarthropods in the marsh of the Sanjiang Plain, which may influence ecosystem functioning. Warming has also increased the density of collembola under the natural water levels. Conversely, other studies found that increasing temperatures can result in decreasing population densities of Prostigmata (Briones et al., 2009), nematodes (Simmons et al., 2009; Mueller et al., 2016), and springtails (Holmstrup et al., 2017). However, variation in these ecosystems could explain these differences. Compared with the natural water level, the number of collembola species decreased from 20 to 8 species under the temperature increase at 0 cm water level. Makkonen et al. (2011) also found that increased temperature reduced the number of collembola species in subarctic regions, decreasing from 14 species to 12. This may result from some species of springtails being unable to adapt to the changing environment when faced with temperature change, inducing the migration or death of species. Many previous studies have also shown that the adverse effects of warming on soil fauna may be caused by decreased soil moisture concentrations (Xu et al., 2012; Chang et al., 2019). Due to the increase in vegetation and soil surface evaporation, the increase in temperature usually leads to a dry environment, resulting in shifts in the composition of the collembola community to a low-water preference species. Compared with springtails, the number of species of oribatid varied less after treatment exposure, displaying a greater ability to adapt. In the context of warming, it often appears that springtails are more influenced by warming than mites in some ecosystems, but the opposite is also apparent in other ecosystems (Blankinship et al., 2011; Bokhorst et al., 2017).

Soil fauna can represent suitable indicator organisms for evaluating soil quality, soil biological effects, ecosystem succession, or the degree of disturbance (David and Gillon, 2009; Shao et al., 2015; Venuste et al., 2018; Srut et al., 2019). Indicator species analysis based on the abundance of soil springtails and mites under four treatments helped us to screen out four indicator species. The density of *A. maritima* (springtail) was

significantly reduced at the constant water level. *A. maritima* (springtail) had the highest density after the warming at the natural fluctuating water levels, demonstrating adaptability to warming. Two species of mites, *C. sinicus* and *M. tardus*, were indicators in the 0 cm water level warming treatment. Their densities were significantly higher than in the other treatment groups, exhibiting tolerance to warming and constant water level.

Drainage and water level fluctuation impact the community composition and diversity of plants and soil fauna. The relationship between water level change and plant population characteristics, species diversity and life history have been studied. Researches showed that fluctuation and its frequency are important factors affecting the growth, reproduction, and population distribution of wetland plants (Gattringer et al., 2018; Yao et al., 2021). Water fluctuation increased number of shoot nodes and shoot length of the communities, and may increase the vegetative spread of submerged macrophyte communities (Wang et al., 2016), and biomass accumulation in roots rather than in shoots and the ability to asexually propagate were important for the survival of these species during water fluctuation (Wei et al., 2019). Short-term decline of the water table may increase the primary productivity by shifting dominant species of hygrophytes to mesophytes in the Zogie wetlands (Cao et al., 2017). Meanwhile, plant diversity or functional characteristics often lead to changes in soil fauna resources and habitat environment. Collembola density and diversity significantly increased with plant species and plant functional group richness (Eisenhauer et al., 2011; Sabais et al., 2011). In forest area, the mean species richness of the collembolan communities increased by 47%, when the number of plant species increased from one (spruce) to three (spruce beech and fir) (Chauvat et al., 2011). In this study, the density, species number and abundance of springtails under the natural water level and its warming treatment were significantly higher than the warming treatment under the constant water level. This increase was also observed in the diversity of mites. This phenomenon were likely due to increased root and microbial biomass in the natural water level, and elevated quantity and quality of plant residues serving as food resources for springtails and mites. It is also recommended that the natural water level fluctuations of the wetland should be maintained, when wetland restoration is conducted under the influence of future warming. Otherwise, we were aware of this study also had deficiencies. A long-term, comprehensive research is needed for indicating the effect of warming and water level on wetland plants, soil fauna, and soil properties.

CONCLUSION

After the wetlands, under different water levels, in the Sanjiang Plain were warmed, the composition of the soil microarthropod community was significantly changed. Warming increased the density and richness of collembola under the natural water level, but decreased the density and richness of springtails under the constant water level. The diversity of mites under the natural water level and its warming treatment was significantly higher than that of the warming treatment at the 0 cm water level. Besides, *A. maritima* and *V. laricis*, two indicators for the natural water level, had the highest densities in the natural water level and warming under the natural water level, respectively. *C. sinicus* and *M. tardus* had the highest densities in warming under the 0 cm water level, significantly higher than the other three treatments. We have also shown that in the context of global warming, maintaining natural water level fluctuations is of great significance to the composition and diversity of soil microarthropod communities.

DATA AVAILABILITY STATEMENT

The original contributions presented in the study are included in the article/**Supplementary Material**, further inquiries can be directed to the corresponding author.

AUTHOR CONTRIBUTIONS

HZ performed the field investigation, collected the data, conducted the statistical analysis, and wrote the manuscript. XS and DL carried on the classification and identification to the collembola and mites, respectively. HW designed the study and, reviewed and edited the manuscript. HC provided pertinent comments, improved the discussion, and polished the article. All authors read and approved the final manuscript.

FUNDING

This study was supported by the National Natural Science Foundation of China Joint Fund (Regional Innovation and Development Joint Fund) (U20A2083), the National Key R&D Program of China (2017YFC0505901), the National Natural Science Foundation of China (41671260 and 41871099), and Jilin Scientific and Technological Development Program (20180101080JC).

ACKNOWLEDGMENTS

We are grateful to Qiang Guan, Kangle Lu, and Ke Zhang from Northeast Institute of Geography and Agroecology, Chinese Academy of Sciences for sampling.

SUPPLEMENTARY MATERIAL

The Supplementary Material for this article can be found online at: https://www.frontiersin.org/articles/10.3389/fevo.2021.731735/full#supplementary-material

Supplementary Figure 1 | Air temperature time-series within or outside the open-top chambers in natural water level during the experiment.

REFERENCES

Balogh, J., and Balogh, P. (1992). *The Oribatid Mite Genera of the World. vol. 1*. Budapest: Hungarian Natural History Museum, 1–263.

Bellinger, P. F., Christiansen, K. A., and Janssens, F. (1996-2019). *Checklist of the Collembola of the World*. Available online at: http://www.collembola.org (accessed 1996).

Blankinship, J. C., Niklaus, P. A., and Hungate, B. A. (2011). A meta-analysis of responses of soil biota to global change. *Oecologia* 165, 553–565. doi: 10.1007/s00442-011-1909-0

Bokhorst, S., Convey, P., Huiskes, A., Van Bodegom, P. M., and Aerts, R. (2017). Dwarf shrub and grass vegetation resistant to long-term experimental warming while microarthropod abundance declines on the Falkland Islands. *Austral Ecol.* 42, 984–994. doi: 10.1111/aec.12527

Briones, M. J. I., Ostle, N. J., Mcnamara, N. P., and Poskitt, J. (2009). Functional shifts of grassland soil communities in response to soil warming. *Soil Biol. Biochem.* 41, 315–322. doi: 10.1016/j.soilbio.2008.11.003

Brussaard, L. (1998). Soil fauna, guilds, functional groups and ecosystem processes. *Appl. Soil Ecol.* 9, 123–135. doi: 10.1016/s0929-1393(98)00066-3

Cao, R., Wei, X., Yang, Y., Xi, X., and Wu, X. (2017). The effect of water table decline on plant biomass and species composition in the Zoige peatland: a four-year in situ field experiment. *Agric. Ecosyst. Environ.* 247, 389–395. doi: 10.1016/j.agee.2017.07.008

Chang, L., Wang, B., Yan, X., Ma, L., Reddy, G. V. P., and Wu, D. (2019). Warming limits daytime but not nighttime activity of epigeic microarthropods in Songnen grasslands. *Appl. Soil Ecol.* 141, 79–83. doi: 10.1016/j.apsoil.2019.05.012

Chauvat, M., Titsch, D., Zaytsev, A. S., Zaytsev, A. S., and Wolters, V. (2011). Changes in soil faunal assemblages during conversion from pure to mixed forest stands. *For. Ecol. Manag.* 262, 317–324. doi: 10.1016/j.foreco.2011.03.037

Dai, X., Page, B., and Duffy, K. J. (2006). Indicator value analysis as a group prediction technique in community classification. *South Afr. J. Bot.* 72, 589–596. doi: 10.1016/j.sajb.2006.04.008

Darby, B. J., and Neher, D. A. (2012). Stable isotope composition of microfauna supports the occurrence of biologically fixed nitrogen from cyanobacteria in desert soil food webs. *J. Arid Environ.* 85, 76–78.

David, J.-F., and Gillon, D. (2009). Combined effects of elevated temperatures and reduced leaf litter quality on the life-history parameters of a saprophagous macroarthropod. *Global Change Biol.* 15, 156–165. doi: 10.1111/j.1365-2486.2008.01711.x

Dufrene, M., and Legendre, P. (1997). Species assemblages and indicator species: the need for a flexible asymmetrical approach. *Ecol. Monogr.* 67, 345–366. doi: 10.2307/2963459

Eisenhauer, N., Milcu, A., Sabais, A. C. W., Bessler, H., Brenner, J., Engels, C., et al. (2011). Plant diversity surpasses plant functional groups and plant productivity as driver of soil biota in the long term. *PLoS One* 6:e16055. doi: 10.1371/journal.pone.0016055

Gattringer, J. P., Ludewig, K., Harvolk-Schoning, S., Donath, T. W., and Otte, A. (2018). Interaction between depth and duration matters: flooding tolerance of 12 floodplain meadow species. *Plant Ecol.* 219, 973–984. doi: 10.1007/s11258-018-0850-2

Geisen, S., and Bonkowski, M. (2018). Methodological advances to study the diversity of soil protists and their functioning in soil food webs. *Appl. Soil Ecol.* 123, 328–333. doi: 10.1016/j.apsoil.2017.05.021

Hallam, J., and Hodson, M. E. (2020). Impact of different earthworm ecotypes on water stable aggregates and soil water holding capacity. *Biol. Fertil. Soils* 56, 607–617. doi: 10.1007/s00374-020-01432-5

Holmstrup, M., Damgaard, C., Schmidt, I. K., Arndal, M. F., Beier, C., and Mikkelsen, T. N. (2017). Long-term and realistic global change manipulations had low impact on diversity of soil biota in temperate heathland. *Sci. Rep.* 7:11.

Iqbal, M., Khan, S. M., Khan, M. A., Ahmad, Z., and Ahmad, H. (2018). A novel approach to phytosociological classification of weeds flora of an agro-ecological system through Cluster, Two Way Cluster and Indicator Species Analyses. *Ecol. Indic.* 84, 590–606. doi: 10.1016/j.ecolind.2017.09.023

Kamran, S., Khan, S. M., Ahmad, Z., Rahman, A. U., Iqbal, M., Manan, F., et al. (2020). The role of graveyards in species conservation and beta diversity: a vegetation appraisal of sacred habitats from Bannu, Pakistan. *J. For. Res.* 31, 1147–1158. doi: 10.1007/s11676-019-00893-1

Kardol, P., Reynolds, W. N., Norby, R. J., and Classen, A. T. (2011). Climate change effects on soil microarthropod abundance and community structure. *Appl. Soil Ecol.* 47, 37–44. doi: 10.1016/j.apsoil.2010.11.001

Koltz, A. M., Classen, A. T., and Wright, J. P. (2018). Warming reverses top-down effects of predators on belowground ecosystem function in Arctic tundra. *Proc. Natl. Acad. Sci. U.S.A.* 115, E7541–E7549.

Krantz, G. W., and Walter, D. E. (2009). *A Manual of Acarology*. Lubbock, TX: Texas Tech University Press.

Liang, W. J., Ge, T. K., and Duan, Y. X. (2001). Bioindication of soil fauna to soil health. *J. Shenyang Agric. Univ.* 32, 70–72.

Lindberg, N. (2003). *Soil Fauna and Global Change (Responses to Experimental Drought, Irrigation, Fertilisation and Soil Warming). Swedish University of Agricultural Sciences.* Doctoral Thesis. Uppsala: Swedish University of Agricultural Sciences.

Liu, W. P. A., Janion, C., and Chown, S. L. (2012). Collembola diversity in the critically endangered Cape Flats Sand Fynbos and adjacent pine plantations. *Pedobiologia* 55, 203–209. doi: 10.1016/j.pedobi.2012.03.002

Liu, X. (2016). *Effects of Climate Change on the Net Primary Productivity of Wetlands in Sanjiang Plain*. Doctoral Thesis. Changchun.

Liu, X. H., Zhang, Y., Dong, G. H., and Jiang, M. (2019). Difference in carbon budget from marshlands to transformed paddy fields in the Sanjiang Plain, Northeast China. *Ecol. Eng.* 137, 60–64. doi: 10.1016/j.ecoleng.2018.03.013

Makkonen, M., Berg, M. P., Van Hal, J. R., Callaghan, T. V., Press, M. C., and Aerts, R. (2011). Traits explain the responses of a sub-arctic Collembola community to climate manipulation. *Soil Biol. Biochem.* 43, 377–384. doi: 10.1016/j.soilbio.2010.11.004

Meng, H. (2016). *Research on the Impact of Climate Change on the Marsh Distribution and its Risk Assessment in the Sanjiang Plain.* Doctoral Thesis. Changchun.

Mueller, K. E., Blumenthal, D. M., Carrillo, Y., Cesarz, S., Ciobanu, M., and Hines, J. (2016). Elevated CO2 and warming shift the functional composition of soil nematode communities in a semiarid grassland. *Soil Biol. Biochem.* 103, 46–51. doi: 10.1016/j.soilbio.2016.08.005

Oliverio, A. M., Geisen, S., Delgado-Baquerizo, M., Maestre, F. T., Turner, B. L., and Fierer, N. (2020). The global-scale distributions of soil protists and their contributions to belowground systems. *Sci. Adv.* 6:Eaax8787. doi: 10.1126/sciadv.aax8787

Phillips, H. R. P., Guerra, C. A., Bartz, M. L. C., Briones, M. J. I., Brown, G., Crowther, T. W., et al. (2019). Global distribution of earthworm diversity. *Science* 366, 480–485.

Phillips, H. R. P., Heintz-Buschart, A., and Eisenhauer, N. (2020). Putting soil invertebrate diversity on the map. *Mol. Ecol.* 29, 655–657. doi: 10.1111/mec.15371

Sabais, A. C. W., Scheu, S., and Eisenhauer, N. (2011). Plant species richness drives the density and diversity of Collembola in temperate grassland. *Acta Oecol. Int. J. Ecol.* 37, 195–202. doi: 10.1016/j.actao.2011.02.002

Semenina, E. E., and Tiunov, A. V. (2020). Assimilation of aboveground litter carbon versus soil carbon by Collembola and Lumbricidae in spruce forest: a litter replacement experiment. *Polish J. Ecol.* 68, 172–180.

Shao, Y. H., Zhang, W. X., Liu, S. J., Wang, X. L., and Fu, S. L. (2015). Diversity and function of soil fauna. *Acta Ecol. Sin.* 35, 6614–6625.

Shen, X. J., Liu, B. H., Xue, Z. S., Jiang, M., Lu, X. G., and Zhang, Q. (2019a). Spatiotemporal variation in vegetation spring phenology and its response to climate change in freshwater marshes of Northeast China. *Sci. Total Environ.* 666, 1169–1177. doi: 10.1016/j.scitotenv.2019.02.265

Shen, X. J., Xue, Z. S., Jiang, M., and Lu, X. G. (2019b). Spatiotemporal change of vegetation coverage and its relationship with climate change in freshwater marshes of Northeast China. *Wetlands* 39, 429–439. doi: 10.1007/s13157-018-1072-z

Simmons, B. L., Wall, D. H., Adams, B. J., Ayres, E., Barrett, J. E., and Virginia, R. A. (2009). Long-term experimental warming reduces soil nematode populations in the McMurdo Dry Valleys, Antarctica. *Soil Biol. Biochem.* 41, 2052–2060. doi: 10.1016/j.soilbio.2009.07.009

Srut, M., Menke, S., Hockner, M., and Sommer, S. (2019). Earthworms and cadmium - Heavy metal resistant gut bacteria as indicators for heavy metal

pollution in soils? *Ecotoxicol. Environ. Saf.* 171, 843–853. doi: 10.1016/j.ecoenv.2018.12.102

Sun, X., Li, Q., Yao, H. F., Liu, M. Q., Wu, D. H., Zu, D., et al. (2021). Soil fauna and soil health. *Acta Pedol. Sin.* 58, 1073–1083.

Tan, W. W., Sun, Y., Song, C. C., Zhang, X. H., Han, Z., and Qiao, T. H. (2018). Design and construction of water-level and air temperature co-regulated plot in sanjiang plain experimental station of wetland ecology. *Chin. Acad. Sci. Wetland Sci.* 16, 114–119.

van den Hoogen, J., Geisen, S., Routh, D., Ferris, H., Traunspurger, W., Wardle, D. A., et al. (2019). Soil nematode abundance and functional group composition at a global scale. *Nature* 572, 194–198.

Vazquez, E., Teutscherova, N., Lojka, B., Arango, J., and Pulleman, M. (2020). Pasture diversification affects soil macrofauna and soil biophysical properties in tropical (silvo)pastoral systems. *Agric. Ecosyst. Environ.* 302:107083. doi: 10.1016/j.agee.2020.107083

Venuste, N., Beth, K. A., Frederic, F., Lombart, K. M. M., Wouter, D., and Donat, N. (2018). Use of soil and litter ants (Hymenoptera: Formicidae) as biological indicators of soil quality under different land uses in Southern Rwanda. *Environ. Entomol.* 47, 1394–1401.

Wang, P., Zhang, Q., Xu, Y. S., and Yu, F. H. (2016). Effects of water level fluctuation on the growth of submerged macrophyte communities. *Flora* 223, 83–89. doi: 10.1016/j.flora.2016.05.005

Wang, S. J., and Ran, H. H. (2008). Feedback mechanisms of soil biota to aboveground biology in terrestrial ecosystems. *Biodriversity Sci.* 16, 407–416. doi: 10.3724/sp.j.1003.2008.07356

Wardle, D. A., Williamson, W. M., Yeates, G. W., and Bonner, K. I. (2005). Trickle-down effects of aboveground trophic cascades on the soil food web. *Oikos* 111, 348–358. doi: 10.1111/j.0030-1299.2005.14092.x

Wei, G. W., Chen, Y., Sun, X. S., Chen, Y. H., Luo, F. L., and Yu, F. H. (2019). Growth responses of eight wetland species to water level fluctuation with different ranges and frequencies. *PLoS One* 14:e0220231. doi: 10.1371/journal.pone.0220231

Wu, T., Su, F., Han, H., Du, Y., Yu, C., and Wan, S. (2014). Responses of soil microarthropods to warming and increased precipitation in a semiarid temperate steppe. *Appl. Soil Ecol.* 84, 200–207.

Xu, G. L., Kuster, T. M., Gunthardt-Goerg, M. S., Dobbertin, M., and Li, M. H. (2012). Seasonal exposure to drought and air warming affects soil Collembola and mites. *PLoS One* 7:e43102. doi: 10.1371/journal.pone.0043102

Yan, X., Ni, Z., Chang, L., Wang, K., and Wu, D. (2015). Soil warming elevates the abundance of Collembola in the songnen plain of China. *Sustainability* 7, 1161–1171. doi: 10.3390/su7021161

Yao, X. C., Cao, Y., Zheng, G. D., Devlin, A. T., Li, X., Li, M. H., et al. (2021). Ecological adaptability and population growth tolerance characteristics of Carex cinerascens in response to water level changes in Poyang Lake, China. *Sci. Rep.* 11:4887.

Yin, W. Y. (1992). *Subtropical Soil Animals of China*. Beijing: Science Press.

Yin, W. Y. (1998). *Pictorial Keys to Soil Animals of China*. Beijing: Science Press.

Zhang, H., and Wu, H. T. (2020). Research progresses in effects of climate warming on soil fauna community structure. *Chin. J. Ecol.* 39, 655–664.

Zhang, J. Q., Zhang, B., Ma, B., Cao, B., Liang, J. J., and Ma, S. Q. (2019). Spatial-temporal variation of NDVI in Sanjiang Plain and its response to climate change. *J. Desert Res.* 39, 206–213.

Conflict of Interest: The authors declare that the research was conducted in the absence of any commercial or financial relationships that could be construed as a potential conflict of interest.

Publisher's Note: All claims expressed in this article are solely those of the authors and do not necessarily represent those of their affiliated organizations, or those of the publisher, the editors and the reviewers. Any product that may be evaluated in this article, or claim that may be made by its manufacturer, is not guaranteed or endorsed by the publisher.

frontiers in Ecology and Evolution

ORIGINAL RESEARCH
published: 12 January 2022
doi: 10.3389/fevo.2021.816918

Variation in Bacterial Community Structure in Rhizosphere and Bulk Soils of Different Halophytes in the Yellow River Delta

Yinghan Zhao[1,2], Tian Li[1], Pengshuai Shao[1], Jingkuan Sun[1], Wenjing Xu[1,2] and Zehao Zhang[1,2]*

[1] Shandong Provincial Key Laboratory of Eco-Environmental Science for Yellow River Delta, Binzhou University, Binzhou, China, [2] National Positioning Observation and Research Station of Taishan Forest Ecosystem/Key Laboratory of Silviculture in the Lower Yellow River of State Forestry and Grassland Administration, College of Forestry, Shandong Agricultural University, Taian, China

OPEN ACCESS

Edited by:
Guangxuan Han,
Yantai Institute of Coastal Zone Research, Chinese Academy of Sciences (CAS), China

Reviewed by:
Hui Wang,
University of Jinan, China
Fei-Hai Yu,
Taizhou University, China

***Correspondence:**
Tian Li
912litian@163.com

Specialty section:
This article was submitted to Conservation and Restoration Ecology, a section of the journal Frontiers in Ecology and Evolution

Received: 17 November 2021
Accepted: 15 December 2021
Published: 12 January 2022

Citation:
Zhao Y, Li T, Shao P, Sun J, Xu W and Zhang Z (2022) Variation in Bacterial Community Structure in Rhizosphere and Bulk Soils of Different Halophytes in the Yellow River Delta. Front. Ecol. Evol. 9:816918. doi: 10.3389/fevo.2021.816918

Soil microorganisms play the important role in driving biogeochemical cycles. However, it is still unclear on soil microbial community characteristics and microbial driving mechanism in rhizosphere and bulk soils of different halophyte species. In this study, we analyzed bacterial communities in the rhizosphere and bulk soils of three typical halophytes in the Yellow River Delta, i.e., *Phragmites communis*, *Suaeda salsa*, and *Aeluropus sinensis*, by high-throughput sequencing. The contents of total carbon, total nitrogen, and available phosphorus in rhizosphere soils of the three halophytes were significantly higher than those in bulk soils, which suggested a nutrient enrichment effect of the rhizosphere. Rhizosphere soil bacterial α-diversity of *P. communis* was higher than that in bulk soil, whereas bacterial α-diversity in rhizosphere soil of *S. salsa* and *A. sinensis* was lower than those in bulk soil. The dominant bacterial phyla were *Proteobacteria*, *Actinobacteria*, *Chloroflexi*, and *Bacteroidetes*, which accounted for 31, 20.5, 16.3, and 10.3%, respectively. LDA effect size (LEfSe) analysis showed that the bacterial species with significant differences in expression abundance was obviously different in the rhizosphere and bulk soil of three halophytes. The principal component analysis (PCoA) showed that bacterial community composition was greatly different between rhizosphere and bulk soils of *P. communis* and *S. salsa*, while no difference in *A. sinensis*. Changed bacterial community composition was mainly ascribed to salinity in rhizosphere and bulk soils. Additionally, salinity was positively correlated with *Bacteroidetes* and negatively correlated with *Actinobacteria* and *Acidobacteria*. Our study clarified the variation in bacterial community structure between rhizosphere and bulk soils with soil physicochemical properties, which proved a biological reference to indicate the characteristics of saline and alkaline land.

Keywords: rhizosphere microorganisms, high-throughput sequencing, bacterial community diversity, halophytes, Yellow River Delta

INTRODUCTION

Soil salinization is a global ecological and environmental problem, which seriously affects vegetation restoration and the sustainable development of regional ecosystems. Salinized soil can influence the composition and function of plant communities by inhibiting soil microbial activities and soil nutrients (Albdaiwi et al., 2019). In China, the area of saline-alkali land is about 99.13 million hectares (Zhu et al., 2018). The Yellow River Delta is the main distribution area of saline-alkali soil with high salinity and low land utilization (Xia et al., 2019).

Soil microorganisms respond quickly to the changing external soil environment, and bacterial community structure is generally considered to be an important indicator for evaluating soil nutrients (Chourasiya et al., 2017). In recent years, the use of microorganisms to improve the soil environment and promote the restoration of vegetation in saline soil has increasingly become a hot spot (Berendsen et al., 2012). There is a close relationship among plants, soil, and microorganisms, and they interact with each other (Yuan et al., 2016). Studies have found that soils with different types of salt, pH, soil texture, and nutrient have different microbial communities (Yamamoto et al., 2018). Plants can change soil physicochemical properties by releasing root exudates, shaping rhizosphere microbial communities (Raaijmakers et al., 2009); meanwhile, rhizosphere microorganisms would affect rhizosphere soil (Bakker et al., 2015). In addition, the types and quantities of root exudates released by different plants are different; therefore, different halophytes result in the differences in microbial community structure between rhizosphere and bulk soils (Ladygina and Hedlund, 2010).

Recent studies have reported the characteristics of microbial communities in forest and farmland ecosystems (Teurlincx et al., 2018; Liang et al., 2019; Shao et al., 2019; Liu et al., 2021) and research on microbial communities in saline-alkali lands should be paid more attention. Salinity is one of the main factors affecting soil microbial diversity and composition in saline-alkali areas (Zhang et al., 2018; Yang and Sun, 2020; Zhao et al., 2020). The vegetation in saline-alkali areas is dominated by halophytes, which have an important impact on soil microbial communities (Cao et al., 2014). Rathore et al. (2017) have reported that halophytes enhanced soil microbial activities and promoted ecosystem health. Yamamoto et al. (2018) studied bacterial communities in the rhizosphere, root inner layer, and blank soil of two halophytes (*Glaux maritima* and *Salicornia europaea*) in saline-alkali land and found that soil bacterial community functions of different plant types were significantly different. Jing et al. (2018) showed that planting *Atriplex triangularis* and *Suaeda glauca* for 3 months changed rhizosphere soil properties and bacterial community. Additionally, the research of Tian et al. (2020) on the microbial communities in rhizospheres of plants in salinized soil in North Yinchuan showed that *Medicago sativa* and *Achnatherum splendens* significantly improved the functional diversity of soil microbial community and enzyme activity. These studies reflect the influence of plant species on the rhizosphere microbial community. Soil microbial communities shape some unique salt-tolerant mechanisms adapting to long-term salinity stress for halophytes in saline-alkali land (Bell et al., 2015). Therefore, the study on rhizosphere soil microorganisms of different halophyte species can help us to further understand the salt tolerance of halophytes and their interaction with rhizosphere soil microorganisms and find some specific flora related to plant growth and soil improvement.

Halophytes have formed different salt tolerance strategies undergoing long-term salinity stress (Mansour and Salama, 2004). There were varying degrees in the connection between plants and soil due to different salt tolerance strategies (Li et al., 2021). Thus, we hypothesized whether the differences in the relationship between halophytes and soil could cause the heterogeneity of soil microorganisms around plant roots? In this study, we selected three different types of typical halophytes (salt-repellent plant—*Phragmites communis*, salt-accumulating plant—*Suaeda salsa,* and salt-secreting plant—*Aeluropus sinensis*) in the Yellow River Delta (1) to explore the heterogeneity of bacterial community structure and ecological function of different types of halophytes in the rhizosphere and bulk soils; (2) to detect the relationship of the bacterial community with soil physicochemical properties; (3) to clarify different salt tolerance strategies of halophytes impacts on rhizosphere soil microorganisms.

MATERIALS AND METHODS

Study Area

The study area is located in the Hekou District of Dongying City in the Yellow River Delta (37°35′–38°12′ N, 118°33′–119°20′ E) (**Figure 1**), with a semi humid continental monsoon climate. The annual average temperature is 12.1°C. The terrain is relatively flat, mostly sandy, and muddy soil, which is easy to compact and has poor ventilation. The dominant plants are *P. communis*, *S. salsa*, *A. sinensis*, and *Tamarix chinensis*, etc.

Soil Sample Collection

In June 2020, three plant communities (*P. communis*, *S. salsa*, and *A. sinensis*) were scattered in 3 sampling areas, and each sample area was divided into 1 *1 m regional quadrats, randomly selected healthy plants in the quadrat, and shovel in the depth of 0–20 cm. Large pieces of soil without roots were shaken off and removed the soil around the roots as bulk soil. The soil attached to the root system (0–0.5 cm from the root) as the rhizosphere soil was carefully brushed, and the mixed roots in the rhizosphere soil were completely removed. A total of 18 soil samples were collected, and then, the samples of each sample point were divided into two parts: one was placed in a 50-ml sterilization centrifuge tube, placed in an ice box, brought back to the laboratory within 24 h, and frozen and dried at −80°C for soil microbial analysis (Wang W. C. et al., 2019); another portion were put into the ziplock bags with a written label, brought back to the laboratory, and dried naturally for the determination of soil physicochemical properties.

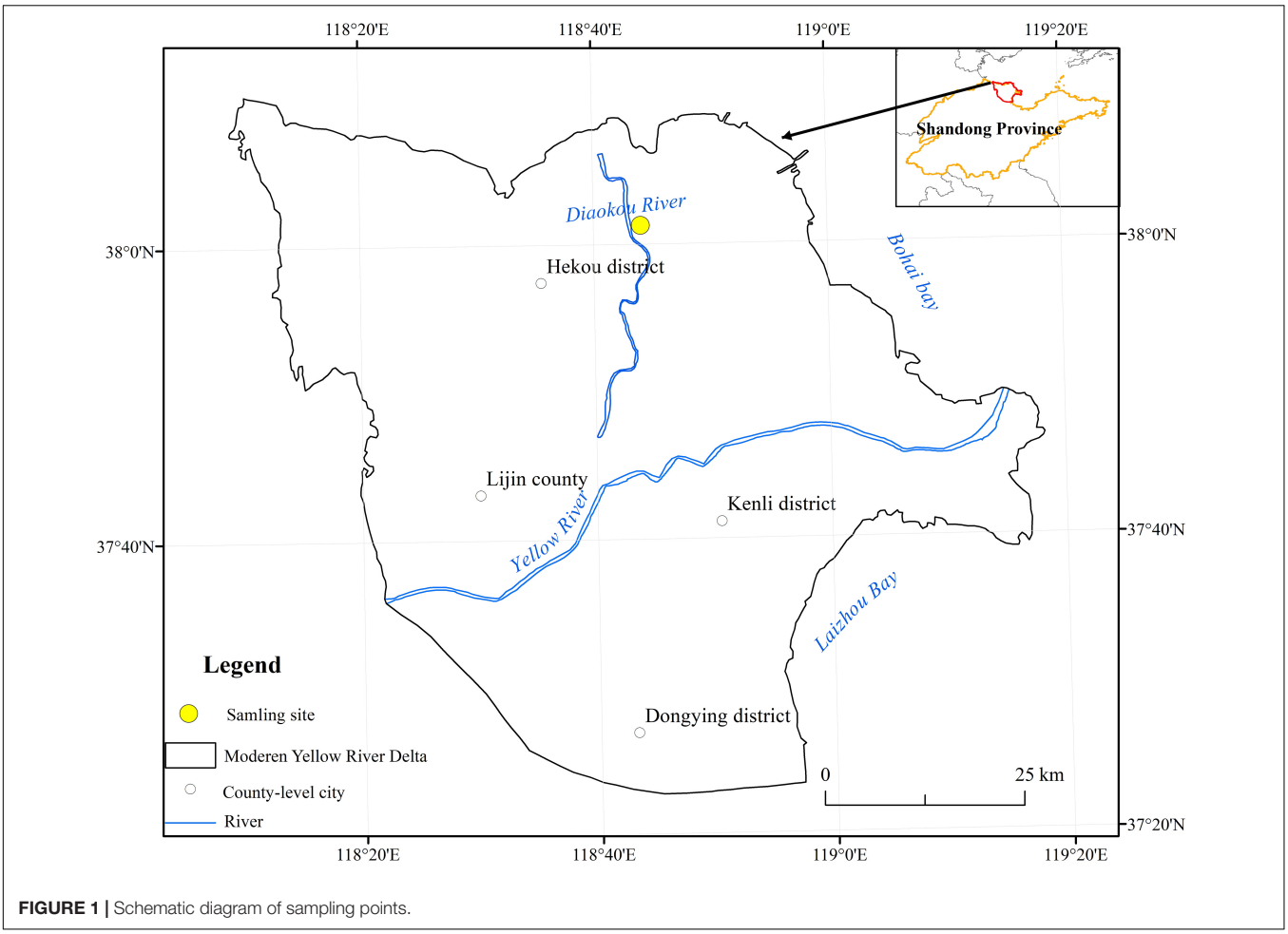

FIGURE 1 | Schematic diagram of sampling points.

Extraction of Total DNA From Soil and PCR Amplification of 16SrRNA Gene

Three repeated soils in the rhizosphere and bulk of different plants were all extracted with Omega's "Soil DNA Kit," primers 338F ACTCCTACGGGAGGCAGCAG and 806R: GGACTACHVGGGTWTCTAAT were used to amplify in the 16SV3-V4 region (Haas et al., 2011), the products were detected by 2% agarose gel electrophoresis, and purified by using AxyPrep DNA Gel Extraction Kit. The MiSeqPE300 platform of Illumina company (Shanghai Majorbio Bio-Pharm Technology Co., Ltd., China) was used for high-throughput sequencing. Qiime2 processed the original DNA data, and the obtained effective sequences were clustered by OTU for further analysis (PRJNA782205).

Analysis of Soil Physicochemical Properties

Three repeated soils of rhizosphere and bulk of different halophytes were air-dried. The physicochemical properties of soil pH, salt ion concentration, organic carbon (OC), total carbon (TC), total nitrogen (TN), and available phosphorus (aP) were measured. Soil pH was measured by pH meter; soil salt was measured by conductivity meter; OC was measured by potassium dichromate volumetric method (Ye et al., 2019), the TC and TN were measured by element analyzer, and the aP was measured by $NaHCO_3$ extraction-molybdenum antimony anti-colorimetry (Wang et al., 2011).

Data Analysis

SPSS 23.0 was used for statistical analysis. CANOCO software was used to analyze the relationship between soil bacterial community diversity and soil physicochemical properties by RDA analysis. Bacterial community analyses (network analysis, LEfSe analysis, and PCoA) were carried out with the help of the platform.[1]

RESULTS

Soil Physicochemical Properties

The analysis of the physicochemical properties of the rhizosphere and bulk soils in different halophytes was shown in **Figure 2**. There were significant differences in soil nutrient contents.

[1]https://bioincloud.tech/#/

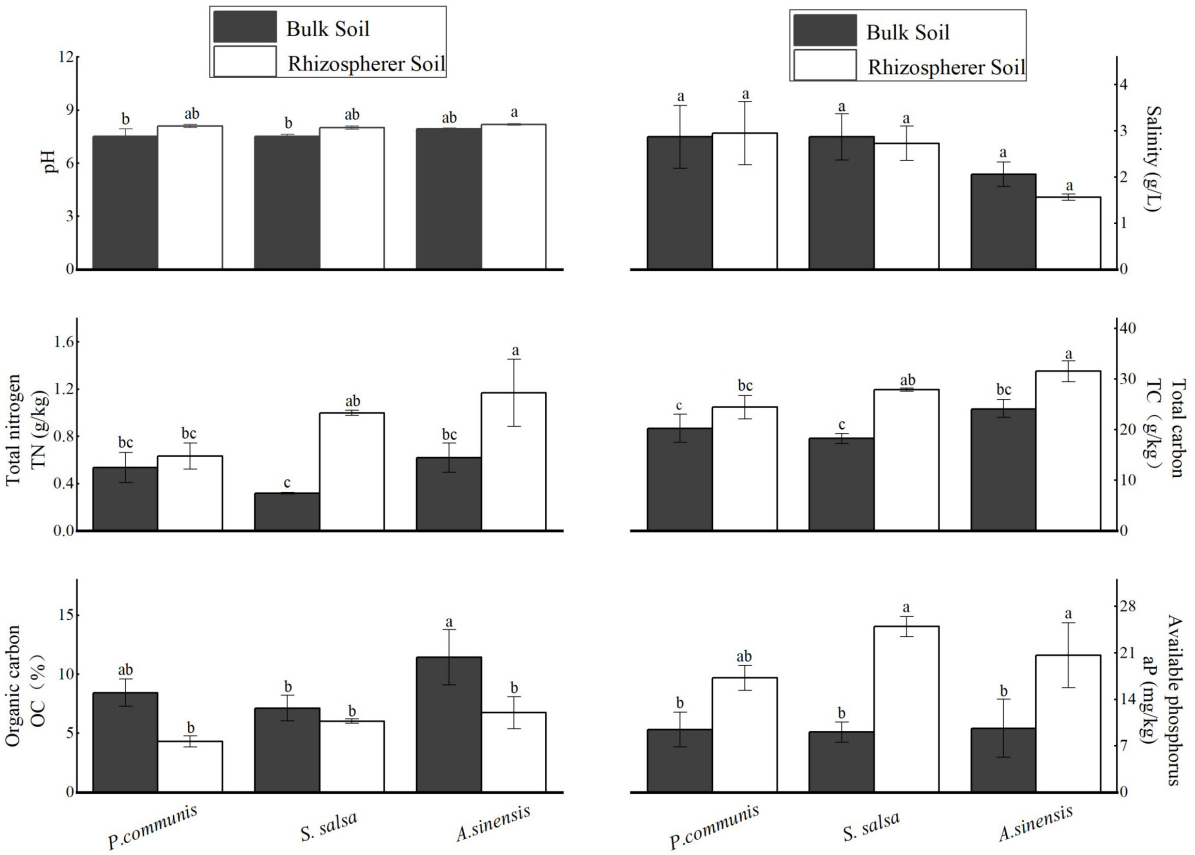

FIGURE 2 | Physicochemical factors in the rhizosphere and bulk soils of different halophytes. Different letters denote significant differences at $P < 0.05$.

The contents of TN, TC, and aP in *S. salsa* and *A. sinensis* rhizosphere soils were significantly higher than those in bulk soils ($p < 0.05$). The content of OC in rhizosphere soil of *A. sinensis* was significantly higher than that in rhizosphere soil.

For the bulk soils of different halophytes, the OC content of *A. sinensis* was significantly higher than that of *S. salsa*. For rhizosphere soils of different halophytes, the TN and TC contents of *A. sinensis* were significantly higher than that of *S. salsa* and *P. communis*.

α-Diversity Analysis

As shown in **Table 1**, the number of OTUs, Chao1 index, Shannon index, and faith in rhizosphere and bulk soils of the three halophytes had a similar change trend. The number of OTUs, Chao1 index, and Faith_pd index in *A. sinensis* were significantly different ($p < 0.05$). The number of OTUs, Chao1 index, and Faith_pd index in *A. sinensis* rhizosphere soil were significantly lower than those in *P. communis* and *S. salsa* rhizosphere soil.

Bacterial Community Structure

Relative Abundance Comparison

At the phylum level, the abundance of the top 10 bacterial phyla in the rhizosphere and bulk soils of *P. communis* and *S. salsa* has changed (**Figure 3**). The relative abundance of *Proteobacteria* was the highest. The weighted heatmap (**Figure 4**) showed that *Bacteroidetes*, *Proteobacteria*, *Firmicutes*, and *Acidobacteria*, etc., in rhizosphere soil and *Chloroflexi*, *Actinobacteria*, and *Nitrospirae*, etc., in bulk soil were different among three different types of halophytes. In addition, the relative abundance of *Bacteroidetes* in *P. communis* rhizosphere soil was significantly higher than that in bulk soil; the relative abundance of *Planctomycetes* in *S. salsa* rhizosphere soil was significantly higher than that in bulk soil. The relative abundance of *Nitrospirae* in rhizosphere soil of *A. sinensis* was slightly lower than that in bulk soil.

At the genus level, the bacterial abundance of rhizosphere and bulk soils of three halophytes have changed, and the sum of the relative abundance of the top ten bacterial genera in bulk soils was all higher than their rhizosphere soils. According to the weighted heatmap, *Pelobacteriae*, *A4b*, *Hypomycobiaceae*, and *Acidimicrobiales*, etc., in rhizosphere soil and *Bacillus, Alphaproteobacteria*, etc., in bulk soil were different among three different types of halophytes.

Comparison of Dominant Bacteria

In this study, the phyla of relative abundance (RA) > 10% were regarded as the dominant phyla (**Table 2** and **Figure 5**), including

TABLE 1 | α-diversity in the rhizosphere and bulk soils of different halophytes.

Sample	OTUs	Chao1	Shannon	Faith_pd	Simpson
Bulk_ Ph	1,122.3 ± 157.68ab	1,122.36 ± 157.69ab	9.01 ± 0.31a	106.85 ± 12.25a	0.994 ± 0a
Rhizosphere_ Ph	1,253.7 ± 197.74a	1,253.92 ± 197.73a	9.04 ± 0.31a	110.06 ± 11.16a	0.994 ± 0a
Bulk_ Su	1,156 ± 82.14ab	1,156.44 ± 82.3ab	9.3 ± 0.15a	101.76 ± 6.81ab	0.996 ± 0a
Rhizosphere_ Su	1,059.67 ± 98.4ab	1,059.92 ± 98.2ab	9.29 ± 0.1a	101.33 ± 6.56ab	0.997 ± 0a
Bulk_ Ae	1,201.33 ± 13.53ab	1,201.6 ± 13.47ab	9.21 ± 0.1a	102.79 ± 1.85ab	0.995 ± 0a
Rhizosphere_ Ae	824 ± 88.71c	824.33 ± 88.52c	8.98 ± 0.2a	77.1 ± 5.69c	0.996 ± 0a

Ph, Phragmites communis; Su, Suaeda salsa; Ae, Aeluropus sinensis. Different letters denote significant differences at P < 0.05.

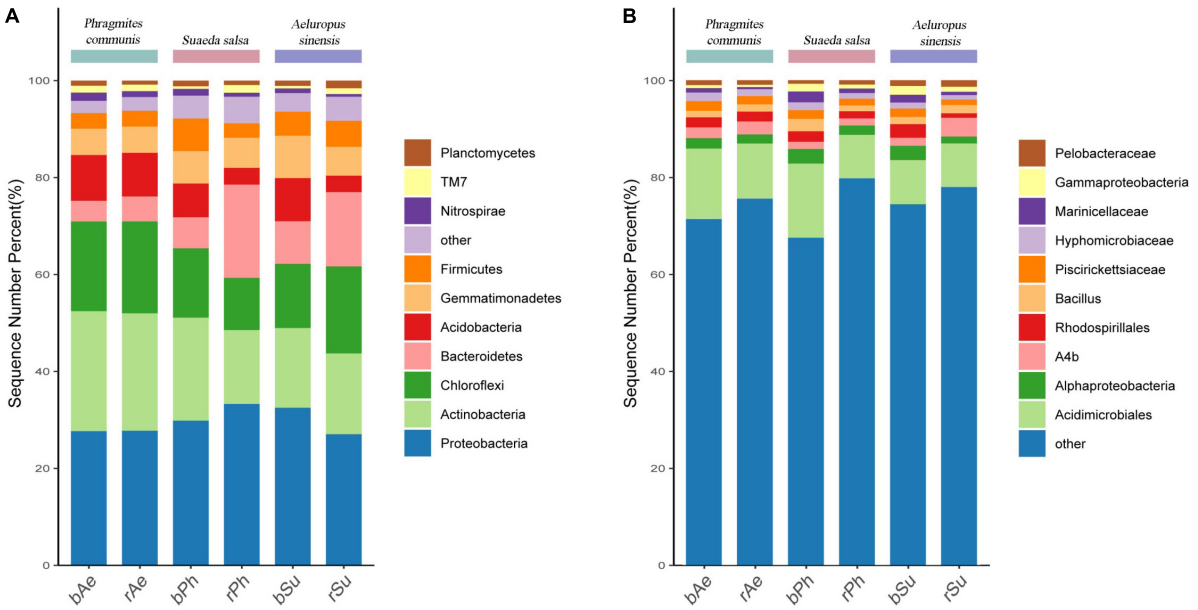

FIGURE 3 | Table of relative abundance of the top 10 bacterial phyla **(A)** and genera **(B)** in the rhizosphere and bulk soils of different halophytes.

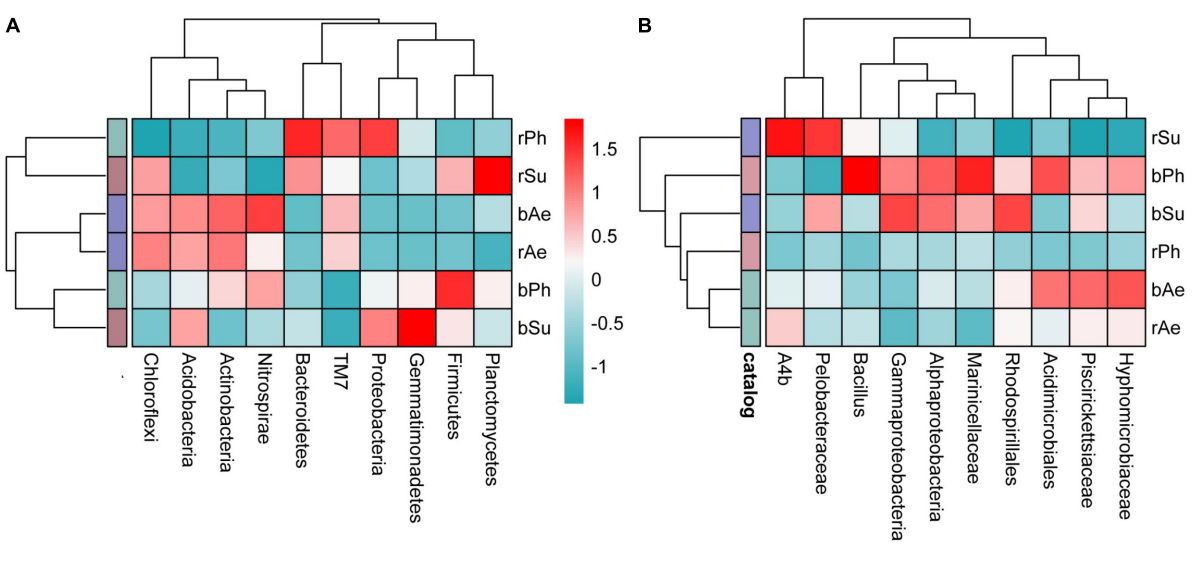

FIGURE 4 | Heatmap of the top 10 bacterial phyla **(A)** and genera **(B)** in the rhizosphere and bulk soil of different halophytes. The range from red to blue represents the relative abundance from high to low.

TABLE 2 | The dominant phyla in the rhizosphere and bulk soil of different halophytes.

Halophytes	Conditions	Dominant bacterial phylum
P. communis	Bulk soil	*Proteobacteria, chloroflexi, actinobacteria*
	Rhizosphere soil	*Proteobacteria, chloroflexi, actinobacteria, bacteroidetes*
S. salsa	Bulk soil	*Proteobacteria, actinobacteria, chloroflexi*
	Rhizosphere soil	*Proteobacteria, chloroflexi, actinobacteria, bacteroidetes*
A. sinensis.	Bulk soil	*Proteobacteria, actinobacteria, chloroflexi*
	Rhizosphere soil	*Proteobacteria, actinobacteria, chloroflexi*

Proteobacteria (RA: 27–35%), *Actinobacteria* (RA: 11–25%), *Chloroflexi* (RA: 11–19%), and *Bacteroidetes* (RA: 4–20%). For *Bacteroidetes*, the relative abundance of the rhizosphere soil in *P. communis* showed significant changes, which was higher than that in bulk soil ($p < 0.05$). The significant differences of the four dominant bacteria in the rhizosphere soil of the three halophytes were mainly between *A. sinensis* and *P. communis*. Results showed that the abundance of *Actinobacteria* and *Chloroflexi* in *A. sinensis* rhizosphere soil was significantly higher than those in *P. communis* rhizosphere soil, but the abundance of *Bacteroidetes* was significantly lower than that in *P. communis* rhizosphere soil.

Analysis of Bacterial Symbiosis System

Symbiotic network analysis was carried out for bacterial species in the rhizosphere and bulk soil of three different halophytes (**Figure 6**), and the number of edges connected between all bacterial species and other nodes was calculated. There were 59 in rhizosphere soil (**Figure 6A**) and 42 in bulk soil (**Figure 6B**). The positive correlation connecting lines (95%) observed in rhizosphere soil was significantly more than the negative correlation (5%). *BRC1*, *Planctomycetes*, *OP11,* and *Verrucomicrobia* played a central role in the network analysis diagram (connectivity > 7), which were the key phylum in rhizosphere soil, but their abundance was relatively low. *Verrucomicrobia* and *BCR1* had 9 connecting lines, and the relative abundance was less than 1%. *Actinobacteria* with high relative abundance (RA > 15%) had only one connecting line in the network structure analysis. In bulk soil (**Figure 6B**), the positive correlation connecting line (57%) was more than the negative correlation (43%). *BRC1*, *Actinobacteria,* and *Thermi* (connecting line ≥ 6) had relatively high connectivity. In addition, there was 8 positive correlation connecting lines in *Planctomycetes* in rhizosphere soil, whereas the number of connecting lines was 0 in bulk soil.

Significant Difference Analysis

The results of LEfSe analysis (**Figure 7**) showed that there were 76 distinct microbial between the rhizosphere and bulk soils of the three halophytes (LDA > 2). Significantly different bacteria between bulk and rhizosphere soil of *P. communis* were 6 and 12, which included *Gammaproteobacteria* (*Proteobacteria*), *Burkholderiaceae* (*Proteobacteria*), *Flavobacteriaceae* (*Bacteroidetes*), and *Erythrobacteraceae* (*Bacteroidetes*), etc. The *S. salsa* were 7 and 17, including *Alteromonadales* (*Proteobacteria*), *Chromatiales* (*Proteobacteria*), *Cytophagaceae* (*Bacteroidetes*), *Rhodobacteraceae* (*Proteobacteria*), and *Geodermatophilaceae* (*Proteobacteria*), etc., and the *A. sinensis* were 10 and 26, including *Betaproteobacteria* (*Proteobacteria*), *Myxococcaceae* (*Proteobacteria)*, *Alphaproteobacteria* (*Proteobacteria*), *Rubrobacteraceae* (*Proteobacteria*), and *Flavisolibacteria* (*Bacteroidetes*), etc. The bacteria with significant differences in the rhizosphere soil of *A. sinensis* were the most, and *Phragmites communis* were the least.

Correlation Between Soil Bacterial Groups and Physicochemical Properties

Based on Bray–Curtis similarity coefficient, the bacterial community composition of three halophytes was significantly different (**Figure 8**). The confidence ellipse of *P. communis* and *S. salsa* indicated that there was a great difference in the bacterial community structure between the rhizosphere and bulk soil in the two halophytes. The confidence ellipse of *A. sinensis* rhizosphere and bulk soil samples was clustered together, indicating that their composition was relatively similar.

At the OTU level, the first and second axes of RDA explained 21.63 and 20.19% of the variation in bacterial community composition, respectively (**Figure 9**). According to the length of rays, the bacterial community structure of the three halophytes was strongly affected by soil, salinity, and pH. The salinity was located in the first quadrant, with an obtuse angle with other environmental factors, which was negatively correlated with TN, TC, aP, OC, and pH. The pH located in the third quadrant, which had a positive correlation with OC, TN, TC, and aP. According to the position of the samples on the RDA diagram, the rhizosphere and bulk samples of *A. sinensis* were gathered together, and the nutrient content was relatively rich. Among the top eight phyla of relative abundance (RA > 2%), *Acidobacteria*, *Bacteroidetes,* and *Actinobacteria* had a great impact on the composition of the bacterial community. *Bacteroidetes* were located in the first quadrant, and *Acidobacteria* and *Actinobacteria* were located in the third quadrant. Salt was positively correlated with *Bacteroidetes* and negatively correlated with *Actinobacteria* and *Acidobacteria*. pH was positively correlated with *Actinomycetes* and negatively correlated with *Acidobacteria* and *Bacteroidetes*.

DISCUSSION

Characteristics of Physicochemical Properties in Rhizosphere and Bulk Soils of Different Halophytes

In saline soil, the root system of halophytes can affect the physicochemical properties of soil and the structure of the rhizosphere microbial community by regulating the salt content, forming a microenvironment that is conducive to plant growth and development (Lau and Lennon, 2012; Lareen et al., 2016). There are salt gland cells in the salt-secreting plant *A. sinensis*,

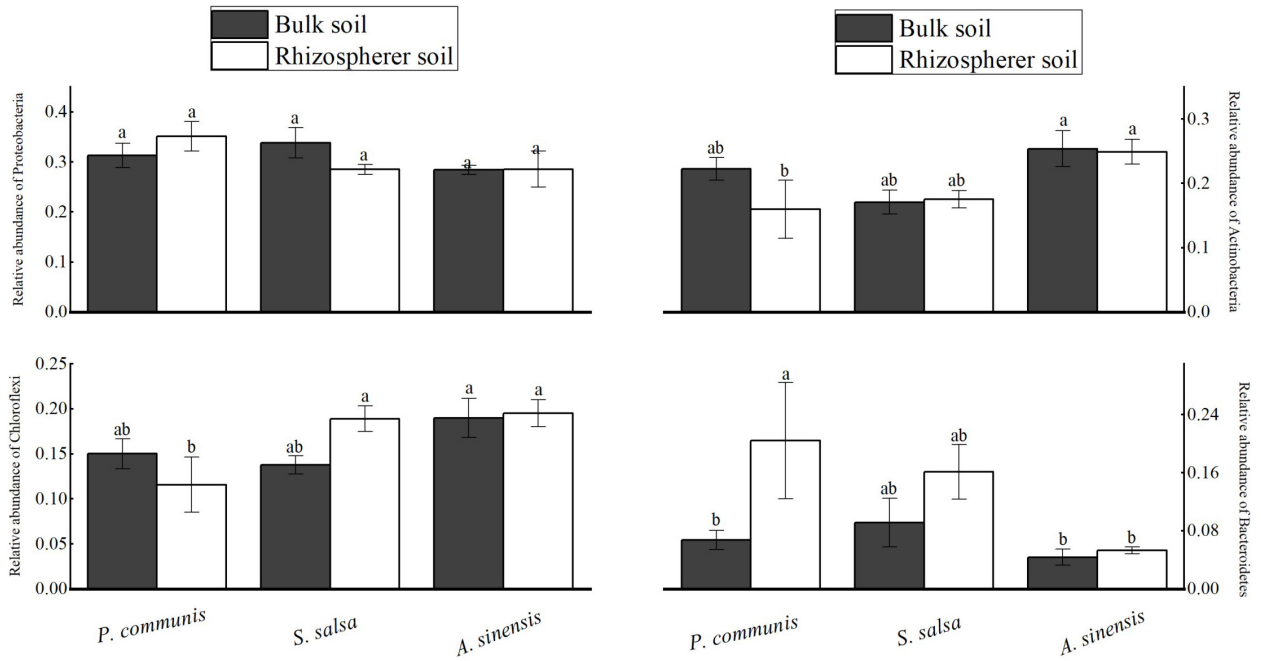

FIGURE 5 | Comparative analysis of relative abundance (RA) > 10% in the rhizosphere and bulk soils of different halophytes. Different letters denote significant differences at $P < 0.05$.

which can absorb soil salt and secrete the salt *in vitro* (Wu et al., 2020). The salt-accumulating plant *S. salsa* can absorb the salt from the soil and accumulate in the fleshy stems and leaves (Jia et al., 2021). Therefore, the salt content of *A. sinensis* and *S. salsa* was less in the rhizosphere than in bulk soil. The salt content in the rhizosphere of the salt-repellent plant *P. communis* was higher than that in bulk soil because its roots restrict the transport of Na^+ to the ground and transport Na^+ from the plant to the root soil (Peng et al., 2016).

Plant mucus secreted by plant roots, sloughed cells and tissues, and soluble products of broken cells contribute to the TC of plant rhizosphere soil (Ai et al., 2015), resulting in higher TC content of three plant rhizosphere soils than that in bulk soil. In addition, the sugar and amino acids secreted by plant roots will increase the availability of soil nitrogen and phosphorus (Smith, 2007), explaining higher content of TN and aP in rhizosphere soil than bulk soil. The results suggest that the root systems of the three halophytes can significantly increase soil carbon, nitrogen, and phosphorus content.

Among the three halophytes, OC content in *A. sinensis* rhizosphere was significantly lower than bulk soil, and it was not significant in the soil of *P. communis* and *S. salsa*. This result is similar to the determination results of rhizosphere and bulk soil organic carbon of *Amorpha fruticose* by An et al. (2011) and *Agropyron cristatum* by Song et al. (2014). It may be caused by the high utilization rate of rhizosphere microorganisms.

High-quality soil is the basic condition to ensure plant growth and development. Soil salt content and pH have a great impact on microbial community structure and plant growth and development (Nacke et al., 2011). In this study, the salt content of the rhizosphere soil of the three plants was not significantly different, but the salt content of rhizosphere soil in *A. sinensis* was relatively low, which was related to the fact that *A. sinensis* belongs to salt-secreting plants. In the three halophytes, the TN content of rhizosphere soil was different, which showed that *A. sinensis* is significantly higher than *P. communis*, which was the result of different rhizosphere precipitation caused by different halophytes. RDA also showed that *P. communis* could survive in soils with low carbon, nitrogen, and high salt content. For different plants, the types of organic acids secreted by roots are different, resulting in differences in the ability to compete with phosphate for adsorption sites (Chen et al., 2002). Therefore, the content of aP in rhizosphere soil of three halophytes was different. We found that the root system of *S. salsa* can improve the content of soil aP, and *A. sinensis* was more dependent on the content of nutrients in the soil than *P. communis* and *S. salsa*, which was consistent with the results of soil physicochemical properties. Therefore, *P. communis* and *S. salsa* have greater survival advantages in nutrient poor saline-alkali soil than *A. sinensis*.

Effects of Different Halophytes in the Rhizosphere and Bulk Soils on Bacterial Community Diversity

The RDA showed that soil salinity was the main factor affecting the characteristics of the bacterial community. Soil salinity was positively correlated with bacterial community α-diversity, which was consistent with the results of Nie et al. (2009) in the Yellow River Delta. The results showed that mild salt stress promoted the survival and reproduction of salt tolerant and halophilic bacteria in the soil. In addition, the diversity and richness of bacterial community in *A. sinensis* rhizosphere soil were significantly lower

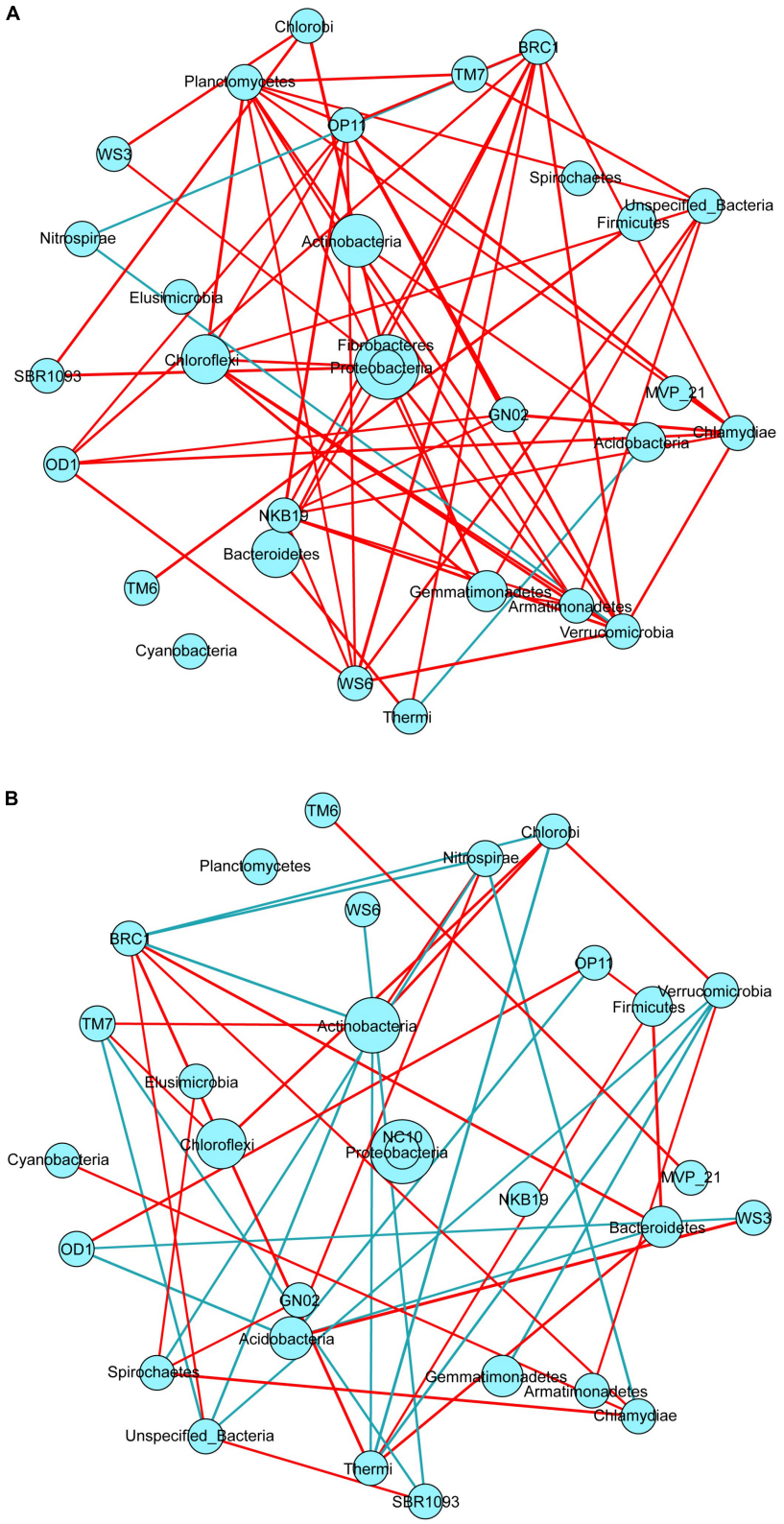

FIGURE 6 | Symbiotic network analysis of soil bacterial communities in the rhizosphere **(A)** and bulk **(B)** of three halophytes (correlation threshold > 0.5). Nodes in the network diagram represent bacterial gates, and the size of each node is in direct proportion to the relative abundance. The red connection line represents a positive correlation between bacteria, whereas the blue connection line represents a negative correlation between bacteria.

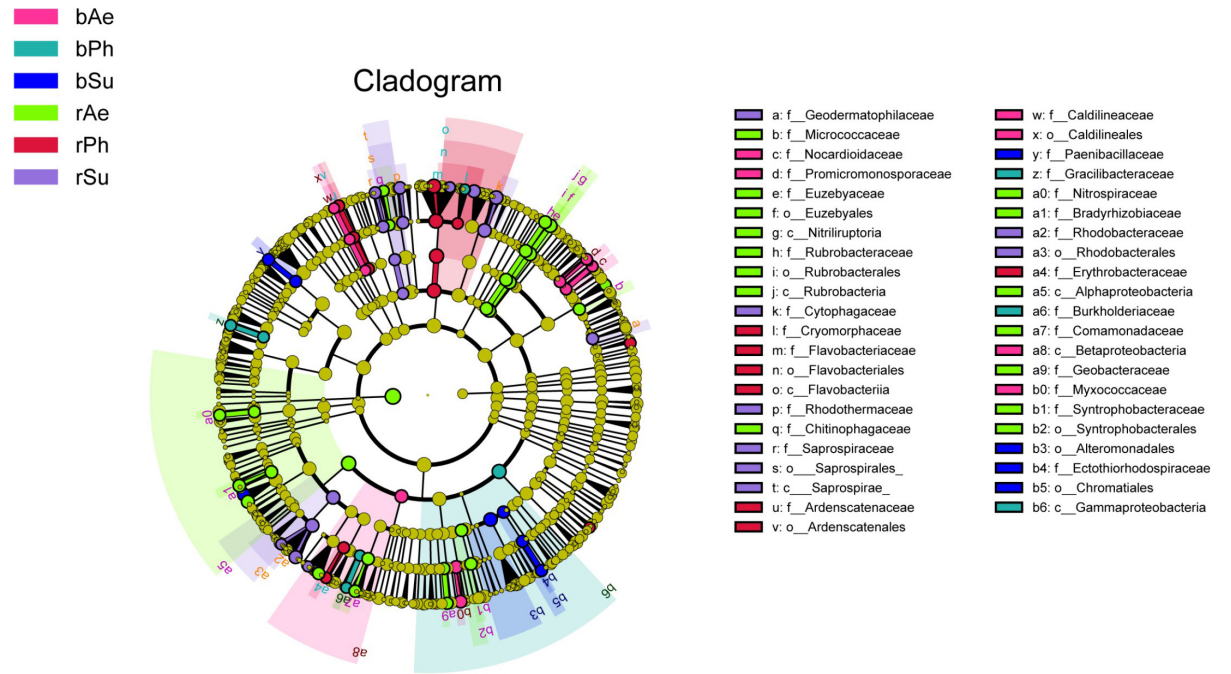

FIGURE 7 | LEfSe analysis of bacteria with a significant difference in classification level between rhizosphere and bulk soil of three halophytes (LDA > 2). c_, Class; o_, Order; f_, Family.

than that in bulk soil ($p < 0.05$), and there was an obvious negative rhizosphere effect, which was related to the fact that *A. sinensis* belongs to salt-secreting plants. The salt content of rhizosphere soil was less than bulk soil due to the salt resistance mechanism of *A. sinensis*, decreasing rhizosphere soil bacterial community diversity. There was no significant difference in bacterial community diversity between rhizosphere and bulk soils of *P. communis*, *S. salsa*, but it was still consistent with the regular pattern of rhizosphere and bulk soil in *A. sinensis*, which further showed that the soil bacterial community in this area needed appropriate salt induction and stimulation to have higher diversity and richness.

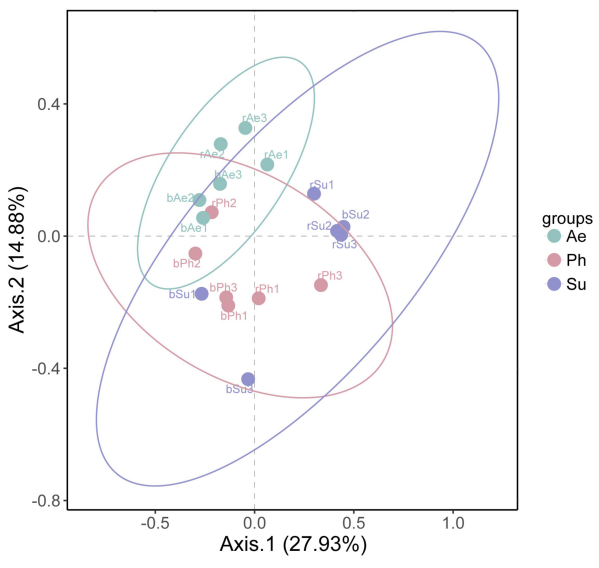

FIGURE 8 | PCoA sequence of microbial communities in rhizosphere and bulk soil of different halophytes.

In this study, the differences in bacterial diversity and richness of three halophytes rhizosphere soil showed that *P. communis* was significantly higher than *A. sinensis*, which was caused by the unique physiological process of different plants. Studies had shown that abscission and secretion were positively correlated with the growth of plant roots, the more vigorous the growth of plant roots, the more abscission and secretion in soil (Cao et al., 2017). Compared with the other two halophytes, the rhizome of *P. communis* is larger, sturdy, and well-developed, which makes the bacterial community in the rhizosphere soil of *P. communis* have higher diversity and richness.

Effects of Rhizosphere and Bulk Soils of Different Halophytes on Bacterial Community Structure

In this study, the relative abundance of the *Proteobacteria* was significantly higher than that of other phyla, which included many nitrogen-fixing bacteria (Delmont et al., 2018). The relative abundance of *Proteobacteria* in the rhizosphere soil of the three halophytes did not change significantly compared with that in the bulk soil. This result was not in line with the research on the rhizosphere and bulk soil of *Lycium ruthenicum* by Li et al. (2018) and also was different from Wang X. T. et al. (2019)

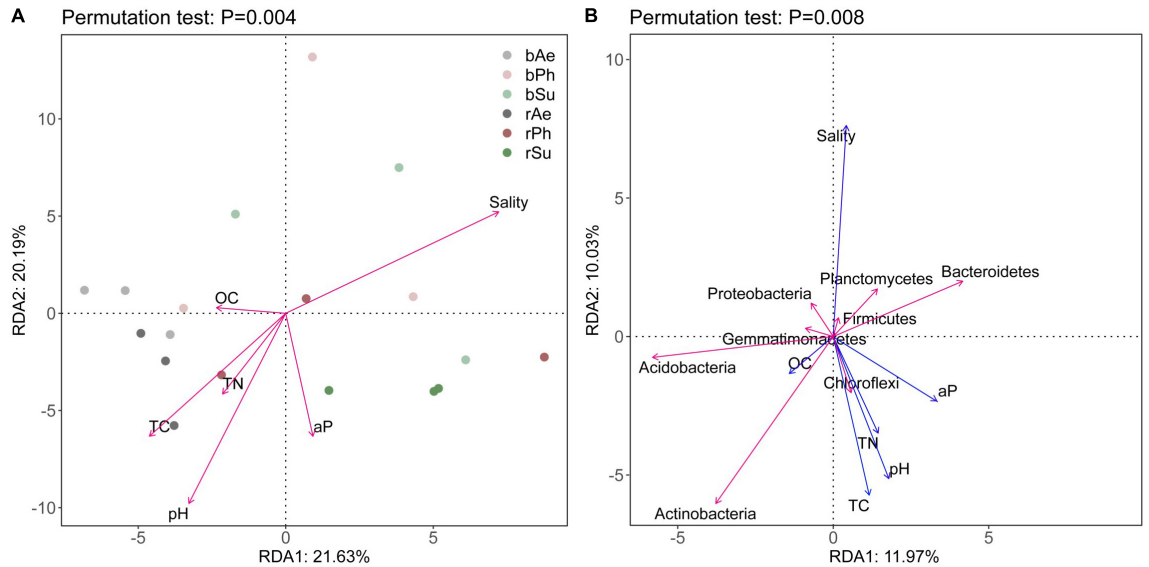

FIGURE 9 | RDA of environmental factors and bacterial communities in rhizosphere and bulk soils of different halophytes: **(A)** correlation between soil physicochemical properties and bacterial community and **(B)** correlation between soil physicochemical properties and dominant bacteria.

on the rhizosphere effect of rice (*Orvaa sativa*) and wheat (*Triticum aestivwm*). Studies have shown that the changes in soil nitrogen content can cause differences in the signal molecules secreted by the different plant roots and then selected bacterial species. In particular, the higher nitrogen content in the soil will cause the nitrogen-fixing bacteria in *proteobacteria* to be replaced by non-nitrogen-fixing bacteria (Zheng et al., 2020). In this study, although the content of TN in *P. communis* rhizosphere soil was significantly lower than that of *A. sinensis*, there was no significant difference in *Proteobacteria*. This reflects that among the three halophytes, *P. communis* can survive under the condition of low nitrogen, and the low nitrogen microenvironment of the rhizosphere does not significantly inhibit the survival of *Proteobacteria*, which suggests that *P. communis* rhizosphere may contribute to the increase of the relative abundance of nitrogen-fixing bacteria in some soils. In addition, it also showed that although the nitrogen content in rhizosphere soil of *A. sinensis* is significantly higher than that in bulk soil, it was still at a low level, which should be related to the lack of nitrogen in this area.

Plant roots have a great influence on the construction of key bacterial species in the soil bacterial community. Compared with bulk soil, the rhizosphere soil bacterial community co-occurrence network had stronger connectivity and higher modularity, suggesting that plant rhizosphere soil had the ability to resist external environmental disturbance and recovery (Zhou et al., 2019). In the plant rhizosphere soil, there were many bacteria with low abundance with high network connectivity, such as *Planctomycetes*, *Verrucomicrobia*, and *OP11*. These bacteria have important ecological functions for the diversity of plant rhizosphere soil bacterial community, the stability of community structure, and the health of host plants (Nuccio et al., 2016). This result can provide theoretical guidance for the future selection of plant rhizosphere growth-promoting bacteria. By comparing the rhizosphere and bulk soils of three halophytes, most of the bacteria with significant differences between the rhizosphere and bulk soils of three halophytes belong to *Proteobacteria*.

CONCLUSION

Different types of halophytes had stronger effects on rhizosphere soil nutrients than on pH and salinity, and the rhizosphere soil nutrient content of different plant species was higher than that of bulk soil. However, their enrichment ability was different, and *A. sinensis* (salt-secreting) and *S. salsa* (salt-accumulating) had stronger rhizosphere nutrient accumulation ability than *P. communis* (salt-repellent). Plant species affected the diversity and richness of rhizosphere soil bacteria. Among the three halophytes, the diversity and richness of rhizosphere soil bacteria in *P. communis* and *S. salsa* were higher than that of *A. sinensis*. Different plant species made for the composition of dominant bacteria and significantly different microbial flora in rhizosphere soil and bulk soil. The number of significant differences bacteria in the expression abundance of *A. sinensis* rhizosphere soil was higher than that of *S. salsa* and *P. communis*, and the discovery of these significantly different microbial flora caused by plant species provided a basis for the excavation and utilization of specific microbial resources. Some low abundance phyla in plant rhizosphere soil were key phyla rather than high abundance dominant phyla, suggesting that attention should be paid attention to this kind of key phyla. Plant species can lead to differences in bacterial community structure. The bacterial community structure of *P. communis* and *S. salsa* in rhizosphere soil and bulk soil was quite different, while *A. sinensis* was not obvious, suggesting that *P. communis* and *S. salsa* had more obvious effects on the bacterial community structure of rhizosphere soil than *A. sinensis*. Soil salinity and pH were

the main factors affecting the bacterial community structure in the three types of halophytes. Salinity was positively correlated with bacterial community diversity, suggesting that moderate salt induction and excitation can promote the increase of bacterial diversity and richness in the rhizosphere soil of halophytes.

DATA AVAILABILITY STATEMENT

The datasets presented in this study can be found in online repositories. The names of the repository/repositories and accession number(s) can be found below: NCBI (accession: PRJNA782205).

AUTHOR CONTRIBUTIONS

YZ was the executor of this experimental research, completed data analysis, and wrote the first draft of the manuscript. TL was the designer and person in charge of the experimental project, guiding the experimental design, data analysis, thesis writing and modification, and fund support. PS guided data processing methods, experimental methods, and data sorting. JS supervised the experimental research process and fund support. WX and ZZ participated in sample determination experiments and data sorting. All authors contributed to the article and approved the submitted version.

FUNDING

The funding was supported by the National Natural Science Foundation of China (41971119, 42171059, and 32101387), the Natural Science Foundation of Shandong Province (ZR2019MD024 and ZR2020QD004), and the Science, and Technology Support Plan for Youth Innovation of Colleges and Universities (2019KJD010).

REFERENCES

Ai, C., Sun, J. W., Wang, X. B., Liang, G. Q., He, P., and Zhou, W. (2015). Research progress on relationship between plant rhizosphere deposition and soil microorganism. *J. Plant Nutr. Fertil.* 21, 1343–1351. doi: 10.11674/zwyf.2015.0530

Albdaiwi, R. N., Khyami, H. H., Ayad, J. Y., Alananbeh, K. M., and Al-Sayaydeh, R. (2019). Isolation and characterization of halotolerant plant growth promoting rhizobacteria from durum wheat (*Triticum turgidum* subsp. durum) cultivated in saline areas of the dead sea region. *Front. Microbiol.* 10:1639. doi: 10.3389/fmicb.2019.01639

An, S. S., Li, G. H., and Chen, L. D. (2011). Soil microbial functional diversity between rhizosphere and non- rhizosphere of typical plants in the hilly area of southern Nixia. *Acta Ecol. Sin.* 31, 5225–5234.

Bakker, M. G., Chaparro, J. M., Manter, D. K., and Vivanco, J. M. (2015). Impacts of bulk soil microbial community structure on rhizosphere microbiomes of Zea mays. *Plant Soil.* 392, 115–126. doi: 10.1007/s11104-015-2446-0

Bell, C. W., Asao, S., Calderon, F., Wolk, B., and Wallenstein, M. D. (2015). Plant nitrogen uptake drives rhizosphere bacterial community assembly during plant growth. *Soil Biol. Biochem.* 85, 170–182. doi: 10.1016/j.soilbio.2015.03.006

Berendsen, R. L., Pieterse, C. M. J., and Bakker, P. A. H. M. (2012). The rhizosphere microbiome and plant health. *Trends Plant Sci.* 17, 478–486. doi: 10.1016/j.tplants.2012.04.001

Cao, D., Shi, F. C., Koike, T., Lu, Z. H., and Sun, J. K. (2014). Halophyte plant communities affecting enzyme activity and microbes in saline soils of the Yellow River Delta in China. *Clean Soil Air Water* 42, 1433–1440. doi: 10.1002/clen.201300007

Cao, Y. C., Yang, R., Li, S., Wang, Z. X., He, W. X., and Geng, Z. C. (2017). Characteristics of microbial community in forest soil between rhizosphere and non-rhizosphere in summer and autumn in Qinling Mountains, China. *Acta Ecol. Sin.* 37, 1667–1676. doi: 10.5846/stxb201509151898

Chen, Y. L., Guo, Y. Q., Han, S. J., Zou, C. J., Zhou, Y. M., and Cheng, G. L. (2002). Effect of root derived organic acids on the activation of nutrients in the rhizosphere soil. *J. For. Res.* 13, 115–118. doi: 10.1007/BF02857233

Chourasiya, D., Sharma, M. P., Maheshwari, H. S., Ramesh, A., Sharma, S. K., and Adhya, T. K. (2017). "Microbial diversity and soil health in tropical agroecosystems," in *Advances in Soil Microbiology. Recent Trends and Future Prospects*, eds T. Adhya, B. Mishra, K. Annapurna, D. Verma, and U. Kumar (Singapore: Springer), 19–35. doi: 10.1007/978-981-10-7380-9_2

Delmont, T. O., Quince, C., Shaiber, A., Esen, O. C., Lee, S. T., Rappéet, M. S., et al. (2018). Author correction: nitrogen-fixing populations of Planctomycetes and *Proteobacteria* are abundant in surface ocean metagenomes. *Nat. Microbiol.* 3, 963–963. doi: 10.1038/s41564-018-0209-4

Haas, B. J., Gevers, D., Earl, A. M., Feldgarden, M., Ward, D. V., Giannoukos, G., et al. (2011). Chimeric 16S rRNA sequence formation and detection in Sanger and 454-pyrosequenced PCR amplicons. *Cold Spring Harb. Lab. Press* 21, 494–504. doi: 10.1101/gr.112730.110

Jia, L., Liu, L. Y., Wang, P. S., Li, Z. M., Zhang, J. L., Tian, X. M., et al. (2021). Salt-tolerance and soil improvement mechanism of Suaeda salsa: research progress. *Chin. Agric. Sci. Bull.* 37, 73–80.

Jing, C. L., Xu, Z. C., Zou, P., Tang, Q., Li, Y. Q., You, X. W., et al. (2018). Coastal halophytes alter properties and microbial community structure of the saline soils in the Yellow River Delta, China. *Appl. Soil Ecol.* 134, 1–7.

Ladygina, N., and Hedlund, K. (2010). Plant species influence microbial diversity and carbon allocation in the rhizosphere. *Soil Biol. Biochem.* 42, 162–168. doi: 10.1016/j.soilbio.2009.10.009

Lareen, A., Burton, F., and Schafer, P. (2016). Plant root-microbe communication in shaping root microbiomes. *Plant Mol. Biol.* 90, 575–587. doi: 10.1007/s11103-015-0417-8

Lau, J. A., and Lennon, J. T. (2012). Rapid responses of soil microorganisms improve plant fitness in novel environments. *Proc. Natl. Acad. Sci. U.S.A.* 109, 14058–14062. doi: 10.1073/pnas.1202319109

Li, T., Sun, J. K., and Fu, Z. Y. (2021). Halophytes differ in their adaptation to soil environment in the Yellow River Delta: effects of water source, soil depth, and nutrient stoichiometry. *Front. Plant Sci.* 12:675921. doi: 10.3389/fpls.2021.675921

Li, Y., He, X. M., Yang, X. D., Zhang, X. N., and Lv, G. H. (2018). The microbial community diversity of the rhizosphere and bulk soils of *Lycium ruthenicum* in different habitats. *Acta Ecol. Sin.* 38, 5983–5995. doi: 10.5846/stxb201711082002

Liang, M. X., Liu, X. B., Parker, I. M., Johnson, D., Zheng, Y., Luo, S., et al. (2019). Soil microbes drive phylogenetic diversity-productivity relationships in a subtropical forest. *Sci. Adv.* 5, eaax5088–eaax5096. doi: 10.1126/sciadv.aax5088

Liu, M. X., Li, B., Xu, L., and Yu, R. (2021). Characteristics of culturable microbial community in rhizosphere/non-rhizosphere soil of *Potentilla Fruticosa* population in alpine meadow elevation gradient. *Front. Soil Sci.* 1:741012. doi: 10.3389/fsoil.2021.741012

Mansour, M. M. F., and Salama, K. H. A. (2004). Cellular basis of salinity tolerance in plants. *Environ. Exp. Bot.* 52, 113–122.

Nacke, H., Thürmer, A., Wollherr, A., Will, C., Hodac, L., Herold, N., et al. (2011). Pyrosequencing-based assessment of bacterial community structure along different management types in German forest and grassland soils. *PLoS One* 6:e17000. doi: 10.1371/journal.pone.0017000

Nie, M., Zhang, X. D., Wang, J. Q., Jiang, L. F., Yang, J., Quan, Z. X., et al. (2009). Rhizosphere effects on soil bacterial abundance and diversity in the Yellow River Deltaic ecosystem as influenced by petroleum contamination and soil

salinization. *Soil Biol. Biochem.* 41, 2535–2542. doi: 10.1016/j.soilbio.2009.09.012

Nuccio, E. E., Anderson, F. J., Estera, K. Y., Pett-Ridge, J., Valpine, P., Brodie, E. L., et al. (2016). Climate and edaphic controllers influence rhizosphere community assembly for a wild annual grass. *Ecology* 97, 1307–1318. doi: 10.1890/15-0882.1

Peng, Z., He, S. P., Gong, W. F., Pan, Y. E., Jia, Y. H., Lu, Y. L., et al. (2016). Transcriptome analysis of transcription factors in upland cotton seedlings under NaCl stress. *Acta Agron. Sin.* 43, 354–370. doi: 10.3724/SP.J.1006.2017.00354

Raaijmakers, J. M., Paulitz, T. C., Steinberg, C., Alabouvette, C., and Moënne-Loccoz, Y. (2009). The rhizosphere: a playground and battlefield for soilborne pathogens and beneficial microorganisms. *Plant Soil* 321, 341–361. doi: 10.1007/s11104-008-9568-6

Rathore, A. P., Chaudhary, D. R., and Jha, B. (2017). Seasonal patterns of microbial community structure and enzyme activities in coastal saline soils of perennial halophytes. *Land Degrad. Dev.* 28, 1779–1790. doi: 10.1002/ldr.2710

Shao, P. S., Liang, C., Rubert, N. K., Li, X. Z., Xie, H. T., and Bao, X. L. (2019). Secondary successional forests undergo tightly-coupled changes in soil microbial community structure and soil organic matter. *Soil Biol. Biochem.* 128, 56–65. doi: 10.1016/j.soilbio.2018.10.004

Smith, F. A. (2007). Plant roots. growth, activity and interaction with soils. *Ann. Bot.* 100, 151–152. doi: 10.1093/aob/mcm099

Song, X., Zhang, L. J., Dai, W. A., Zhou, Z. Y., Li, X. Z., Zhou, Y. Y., et al. (2014). Effect of *Amorpha fruticose* planting on soil nutrient characteristics at rhizosphere and non-rhizosphere in Tibetan Plateau. *Pratac. Sci.* 31, 1226–1232.

Teurlincx, S., Heijboer, A., Veraart, A. J., Kowalchuk, G. A., and Declerck, S. A. (2018). Local functioning, landscape structuring: drivers of soil microbial community structure and function in peatlands. *Front. Microbiol.* 9:2060. doi: 10.3389/fmicb.2018.02060

Tian, P. Y., Chen, C., Zhao, H., Zhang, Y., and Dai, J. X. (2020). Enzyme activities and microbial communities in rhizospheres of plants in salinized soil in North Yinchuan, China. *Acta Pedol. Sin.* 57, 217–226. doi: 10.11766/trxb201807050359

Wang, W. C., Zhai, S. S., Xia, Y. Y., Wang, H., Ruan, D., Zhou, T., et al. (2019). Ochratoxin A induces liver inflammation: involvement of intestinal microbiota. *Microbiome* 7, 151–165. doi: 10.1186/s40168-019-0761-z

Wang, X. T., Chen, R. R., Jing, Z. W., Feng, Y. Z., Yao, T. Y., and Lin, X. G. (2019). Comparative study on rhizosphere effects and bacterial communities in the rhizospheres of rice and wheat. *Acta Pedol. Sin.* 56, 443–453. doi: 10.11766/trxb201806020042

Wang, X. X., Han, Z., Bai, Z. H., Tang, J. C., Ma, A. Z., He, J. Z., et al. (2011). Archaeal community structure along a gradient of petroleum contamination in saline-alkali soil. *J. Environ. Sci.* 23, 1858–1864. doi: 10.1016/S1001-0742(10)60640-7

Wu, X.-X., Bai, T. H., Zhang, L., and Bao, A. K. (2020). Research progress on mechanisms underlying salt secretion in recretohalophytes. *Plant Physiol. J.* 56, 2526–2532. doi: 10.13592/j.cnki.ppj.2020.0370

Xia, J. B., Ren, J. Y., Zhang, S. Y., Wang, Y. H., and Fang, Y. (2019). Forest and grass composite patterns improve the soil quality in the coastal saline-alkali land of the Yellow River Delta, China. *Geoderma* 349, 25–35.

Yang, C., and Sun, J. (2020). Soil salinity drives the distribution patterns and ecological functions of fungi in saline-alkali land in the Yellow River Delta, China. *Front. Microbiol.* 11:594284. doi: 10.3389/fmicb.2020.594284

Yamamoto, K., Shiwa, Y., Ishige, T., Sakamoto, H., Keisuke, T., Masataka, U., et al. (2018). Bacterial diversity associated with the rhizosphere and endosphere of two halophytes: glaux maritima and Salicornia Europaea. *Front. Microbiol.* 9:2878. doi: 10.3389/fmicb.2018.02878

Ye, W. Y., Liao, H. P., Xu, Y. Y., Xie, X. Z., Ni, M. Y., Hu, H. L., et al. (2019). Rhizosphere soil bacterial community of juncao by high-throughput sequencing techniques. *Chin. J. Trop. Crops* 40, 1783–1788. doi: 10.3969/j.issn.1000-2561.2019.09.016

Yuan, Z., Druzhinina, I. S., Labbé, J., Redman, R., Qin, Y., Rodriguez, R., et al. (2016). Specialized microbiome of a halophyte and its role in helping non-host plants to withstand salinity. *Sci. Rep.* 6, 32467–32480. doi: 10.1038/srep32467

Zhang, Q. Q., Steven, A. W., Liang, Y. C., and Chu, G. X. (2018). Soil microbial activity and community structure as affected by exposure to chloride and chloride-sulfate salts. *J. Arid Land* 10, 737–749. doi: 10.1007/s40333-018-0014-1

Zhao, Q. Q., Bai, J. H., Gao, Y. C., Zhao, H. X., Zhang, G. L., and Cui, B. S. (2020). Shifts in the soil bacterial community along a salinity gradient in the Yellow River Delta. *Land Degrad. Dev.* 31, 2255–2267. doi: 10.1002/ldr.3594

Zheng, M. H., Chen, H., Li, D. J., Luo, Y. Q., and Mo, J.-M. (2020). Substrate stoichiometry determines nitrogen fixation throughout succession in southern Chinese forests. *Ecol. Lett.* 23, 336–347. doi: 10.1111/ele.13437

Zhou, Z. D., Gao, T., Zhu, Q., Yan, T. T., Li, D. C., Xue, J. H., et al. (2019). Increases in bacterial community network complexity induced by biochar-based fertilizer amendments to karst calcareous soil. *Geoderma* 337, 691–700. doi: 10.1016/j.geoderma.2018.10.013

Zhu, J. F., Cui, Z. R., Wu, C. H., Deng, C., Chen, J. H., and Zhang, H. X. (2018). Research advances and prospect of saline and alkali land greening in China. *World For. Res.* 31, 70–75. doi: 10.13348/j.cnki.sjlyyj.2018.0034.y

Conflict of Interest: The authors declare that the research was conducted in the absence of any commercial or financial relationships that could be construed as a potential conflict of interest.

Publisher's Note: All claims expressed in this article are solely those of the authors and do not necessarily represent those of their affiliated organizations, or those of the publisher, the editors and the reviewers. Any product that may be evaluated in this article, or claim that may be made by its manufacturer, is not guaranteed or endorsed by the publisher.

frontiers in Ecology and Evolution

ORIGINAL RESEARCH
published: 20 January 2022
doi: 10.3389/fevo.2021.801608

Effect of Wetland Restoration and Degradation on Nutrient Trade-Off of *Carex schmidtii*

Dongjie Zhang[1], Jiangbao Xia[1], Jingkuan Sun[1], Kaikai Dong[1], Pengshuai Shao[1], Xuehong Wang[2] and Shouzheng Tong[3]**

[1] Shandong Key Laboratory of Eco-Environmental Science for Yellow River Delta, Binzhou University, Binzhou, China, [2] The Institute for Advanced Study of Coastal Ecology, Key Laboratory of Ecological Restoration and Conservation of Coastal Wetlands in Universities of Shandong, Ludong University, Yantai, China, [3] Northeast Institute of Geography and Agroecology, Chinese Academy of Sciences, Changchun, China

Plant nutrient trade-off, a growth strategy, regulates nutrient stoichiometry, allocation and stoichiometric relationships, which is essential in revealing the stoichiometric mechanism of wetland plants under environmental fluctuations. Nonetheless, how wetland restoration and degradation affect nutrient trade-off of wetland plants was still unclear. In this study, field experiments were conducted to explore the dynamic of nutrient stoichiometry and nutrient limitation of *Carex schmidtii* under wetland restoration and degradation. Plant nutrient stoichiometry and stoichiometric relationships among natural (NW), restored (RW), and degraded (DW) tussock wetlands were examined. Results showed that nutrient stoichiometry of *C. schmidtii* was partly affected by wetland restoration and degradation, and growth stages. The N:P and N:K ratios indicated N-limitation for the growth of *C. schmidtii*. Robust stoichiometric scaling relationships were quantified between some plant nutrient concentrations and their ratios of *C. schmidtii*. Some N- and P-related scaling exponents are varied among NW, RW, and DW. PCA indicated that wetland restoration and degradation had significantly affected on the nutrient trade-offs of *C. schmidtii* (May∼August). Compared to NW, nutrient trade-off in RW was more similar to DW. *Carex schmidtii* had significant correlation between most nutrients and their ratios, and the SEM indicated that plant P and K concentrations had a high proportional contribution to plant C and N concentrations. Insights into these aspects are expected to contribute to a better understanding of nutrient trade-off of *C. schmidtii* under wetland restoration and degradation, providing invaluable information for the protection of *C. schmidtii* tussock wetlands.

Keywords: ***Carex schmidtii*** **tussocks, nutrient trade-off, wetland restoration and degradation, nutrient dynamics, stoichiometric relationship**

OPEN ACCESS

Edited by:
Zhenguo Niu,
Aerospace Information Research Institute, Chinese Academy of Sciences (CAS), China

Reviewed by:
Dario Liberati,
University of Tuscia, Italy
Xinhou Zhang,
Nanjing Normal University, China

****Correspondence:***
Dongjie Zhang
zhangdongjie14@mails.ucas.ac.cn
Shouzheng Tong
tongshouzheng@iga.ac.cn

Specialty section:
This article was submitted to Conservation and Restoration Ecology, a section of the journal Frontiers in Ecology and Evolution

Received: *25 October 2021*
Accepted: *13 December 2021*
Published: *20 January 2022*

Citation:
Zhang D, Xia J, Sun J, Dong K, Shao P, Wang X and Tong S (2022) Effect of Wetland Restoration and Degradation on Nutrient Trade-Off of Carex schmidtii. Front. Ecol. Evol. 9:801608. doi: 10.3389/fevo.2021.801608

INTRODUCTION

Plant nutrient trade-off focus on the mass balance of multiple elements and nutrient distribution and stoichiometric relationships, controlling plant growth and eco-physiological responses to environmental fluctuations in wetland ecosystems (Elser et al., 2000; Güsewell and Koerselman, 2002; He et al., 2019; Chen et al., 2020). Biomass nutrient stoichiometry indicates the limits

of elements on plant growth and explains plant functional diversity, community structure, and vegetation patterns based on the availability of nutrients (Busch et al., 2018; Peng et al., 2019; Yu et al., 2020; Sardans et al., 2021). Dynamic nutrient stoichiometry, availability, and limitation imply plant nutrition status at different growth stages (Zhang et al., 2019a; Bratt et al., 2020). Plant nutrient trade-off and stoichiometric relationship regarding biomass nutrients can regulate the dynamic equilibrium of nutrients and maintain the stoichiometric homeostasis or flexibility in plants and the ecosystem (Wright et al., 2004; Yu et al., 2015; Tian et al., 2018). Therefore, the research on plant nutrient trade-off helps clarify the mechanism of stoichiometric homeostasis or flexibility and nutrient balance of wetland plants under environmental fluctuations.

Carbon (C), nitrogen (N), phosphorus (P), and potassium (K) are the main biogenic elements and composition element of plant organisms (Lawniczak et al., 2010; Wright et al., 2011; Rong et al., 2015; Chiwa et al., 2019; Wan et al., 2020). Plant C concentration is closely related to carbon fixation during photosynthesis (Hartmann et al., 2020). N and P, as essential components of higher plants, provide source elements for the synthesis and transformation of protein and nucleic acids (Elser et al., 1996; Huang et al., 2021). Previous studies reported that approximately 75% of a leaf's organic N concentrated in chlorophyll, thylakoid proteins, and associated cofactors and enzymes (Loomis, 1997). Phosphorus, in form of phosphate, ATP, and phospholipid, is the main components of the nucleus and has profound effects on plant eco-physiological processes (Elser et al., 1996; Ghimire et al., 2017). K is involved in the production, transportation and storage of carbohydrates in plants, playing a role in leaf turgor maintenance and promoting protein synthesis and activating certain enzymes or coenzymes (Gierth and Mäser, 2007; Chiwa et al., 2019). Previous studies have reported that C, N, P, and their ratios are closely associated with plant growth and adaptation to environmental changes (Rong et al., 2015; Pan et al., 2020; Zhang et al., 2021a). However, limited studies focused on the roles that the stoichiometric relationship between K and other nutrient elements in the adaption mechanism of plants to environmental stresses in restored and degraded wetlands.

Nutrient availability and limitation drive ecosystem development, affecting species competition of the vegetation and plant growth (Güsewell and Koerselman, 2002; Zhang et al., 2019a). The N:P ratio and N:K ratio regulate plant eco-physiological processes and resource acquisition (Koerselman and Meuleman, 1996; Hoosbeek et al., 2002; Peng et al., 2019), the dynamic change of which can also precisely reflect the gradual nutrient limitation and shifts in nutrient availability. Koerselman and Meuleman (1996) reported that the N:P ratio < 14 indicates N limitation and N:P ratio > 16 indicates P limitation, while $14 <$ N:P ratio < 16 indicates co-limitation of N and P. Similarly, N:K ratio < 1.2 indicates that the N limitation and N:K ratio > 1.4 indicates K limitation for plant growth (Hoosbeek et al., 2002). There have been a number of studies that investigated the nutrient availability and limitation of wetland plants across species at a global or zonal scale (Güsewell et al., 2003; Tian et al., 2018), but the nutrient limitation for the growth of single species at different growth stages in wetland system, especially in restored and degraded wetlands has received limited attention.

Nutrient trade-off regulates C, N, P, K, affecting nutrient availability and limitation of plants (Rong et al., 2015; Branco et al., 2018; Zhang et al., 2021a). Nutrient trade-off in the soil-plant system determines nutrient capture and usage of wetland plants, as well as control plant growth and community functioning (Van de Waal et al., 2010; Song et al., 2014). Additionally, nutrient trade-off is closely related to the ability of the plant to maintain stoichiometric homoeostasis despite changes in environmental gradients (Yu et al., 2011). It was reported that the strong stoichiometric relationships between plant nutrients and their ratios could be quantified by a power function as $i = \beta j^{\alpha}$, where i and j indicate plant nutrient concentrations and their ratios, respectively; α and β indicate the scaling exponent and normalization constant, which are the slope and the "elevation" or Y-intercept of the log-log linear i vs. j regression line, respectively (Wright et al., 2004; Reich et al., 2010; Tian et al., 2018). The scaling exponent α was widely applied to quantified the stoichiometric relationship between N and P across species under multiple nutrient environments (Tian et al., 2019; Guo et al., 2020; Zhao et al., 2021). However, limited studies focus on the scaling exponent related to C and K.

Momoge Wetland Nature Reserve (MWNR), an international wetland, appeals to a variety of rare birds like white stork, northern goshawk, lesser kestrel, and white-naped crane (Jiang et al., 2016; Ding et al., 2021). *Carex schmidtii*, a native tussock-forming species, is widely distributed in the riparian wetland along the Nenjiang River in MWNR (Zhang et al., 2019b; Qi et al., 2021a), which has abundant root systems and storage of biological elements (i.e., C, N, P, Si), and was capable of supporting a rich plant diversity (Lawrence and Zedler, 2011; Opdekamp et al., 2012; Zhang et al., 2019a; Qi et al., 2021a). Therefore, *C. schmidtii* tussock wetlands play important roles in nutrient cycling and biodiversity supporting. However, *C. schmidtii* tussocks are degrading on this area due to climate change and human activities (Pan et al., 2006; Zhang et al., 2019a; Qi et al., 2021b) and the management and conservation of tussock wetlands has become an urgent necessity. In recent years, with the strengthening of wetland conservation in China, many wetland restoration projects have been implemented, and comprehensive and deepening wetland restoration and protection are further developed for tussock wetlands (Guo et al., 2016; Zhang et al., 2019b; Qi et al., 2021c). Wetland restoration engineering has been conducted to restore tussocks, especially in semi-arid zones, utilizing seedbanks, transplanting rhizomes, creating microtopography, and regulating hydrological conditions (Zhang et al., 2019b; Wang M. et al., 2020; Qi et al., 2021c). It is recorded that a restoration project was conducted in 2008 by planting *C. schmidtii* tussocks, and significant recovery effect was achieved in the initial stage of restoration project. After 10 years, biodiversity and plant growth performance have been well investigated (Zhang et al., 2021b). However, despite the importance of nutrient trade-off for the

ecological adaptation of wetland species, how plant C, N, P, and K of *C. schmidtii* respond to wetland restoration and degradation is still unclear. Meanwhile, the variation of plant nutrient trade-off of *C. schmidtii* during growth stages also need to be identified.

Previous studies have advanced the understanding of eco-physiological responses and growth of *C. schmidtii* to environmental fluctuations (Yan et al., 2015; Zhang et al., 2019b). The structure and biodiversity of *C. schmidtii* community under multiple environments was also evaluated to imply the restoration of tussock wetlands (Guo et al., 2016; Qi et al., 2021c). However, nutrient limitation and trade-off of wetland plants, especially *C. schmidtii* in restored (RW) and degraded (DW) tussock wetlands have received limited attention. In this study, plant samples were collected, and C, N, P, and K of *C. schmidtii* were determined. The purposes of this study are: (1) to examine nutrient stoichiometry of *C. schmidtii* at the entire growth stages; (2) to identify how wetland restoration and degradation alter nutrient stoichiometry and scaling exponents of *C. schmidtii*; (3) to reveal nutrient limitation and trade-off of *C. schmidtii* in RW and DW. Three hypotheses were made: (1) Wetland restoration and degradation significantly affected the nutrient trade-off of *C. schmidtii*; (2) Wetland restoration relieved the nutrient limitation for the growth of *C. schmidtii* compared to DW; (3) The development of nutrient balance achieved in RW with reference to natural tussock wetland (NW) is opposite of that in DW. The findings of nutrient stoichiometry and stoichiometric relationship of *C. schmidtii* are expected to help protect and manage *C. schmidtii* tussock wetlands.

MATERIALS AND METHODS

Study Area

The study area is in the eastern of MWNR (45°42′– 46°18′N, 122°27′–124°04′E) in Jilin province, Northeast China. The MWNR characterized by a continental monsoon climate, covers a total area of 1.44×10^3 km^2 with the mean annual temperature of 4.2°C and a frost-free period of 160 days. The mean annual precipitation is approximately 412 mm and 70–80% of the precipitation falls in July and August. Dominant soil types are marsh and meadow soil. The typical marsh plants are *Phragmites australis*, *Typha orientalis*, *Bolboschoenus planiculmis*, *C. schmidtii*, *Deyeuxia angustifolia*, *Suaeda glauca*, and *Trapa japonica* (Ding et al., 2021; Qi et al., 2021a).

Carex schmidtii tussocks were widely distributed in the riparian wetland along the downstream of the Nenjiang River in MNNR. However, a large area of *C. schmidtii* tussock wetland degraded due to climate change and human activity. Therefore, wetland restoration was conducted in this area, and *C. schmidtii* tussock was recognized as the prior choice for the wetland restoration (Zhang et al., 2019b). *C. schmidtii* tussocks were collected from local wetlands and cut into uniform pieces. The ridge and furrow micro-topography were artificially constructed

FIGURE 1 | *Carex schmidtii* in natural **(A)**, restored **(B)**, and degraded **(C)** tussock wetlands (Zhang et al., 2021b).

in degraded wetland, and *C. schmidtii* tussocks were uniformly planted on the ridge at a density of 9 tussocks/m^2 in the spring of 2008 (Qi et al., 2021c; Zhang et al., 2021b), and then the area of RW was 0.08 km^2 after 10 years' natural restoration (**Figure 1B**). Moreover, NW (**Figure 1A**) without anthropogenic disturbance and DW (**Figure 1C**) were also selected to study the nutrient trade-off of *C. schmidtii*. Properties of soil nutrients and plant growth of *C. schmidtii* in this zone referred to Zhang et al. (2019a, 2021b).

Experiment Design and Field Sampling

A total of 2500 m^2 sampling site was fixed in NW, RW, and DW, respectively. The landform of RW is gentle without water storage structure. The NW and DW closed to RW were selected. The landform of NW is typical saucer-shaped depressions without anthropogenic disturbance. The landform of DW, a damaged saucer depression whose hydrological connection with other wetlands was destroyed due to building roads, but the water storage structures (low-lying terrain gathering water) of DW remained. It is noted that serious drought occurred in RW from June to July referring to the average soil water content (**Supplementary Figure 1**). The soil water content was determined using five-point sampling method in sampling plot in the middle of each month. Considering the same climatic conditions in this zone, the absence of water storage structure and hydrological connection with other wetlands led to serious drought in RW. Field sampling was carried out every month from May to September. Three fixed experimental plots with 5 m × 5 m were set in the three wetlands (sampling site), respectively, and the distance of each experimental plot was 20 m. Aboveground biomass of *C. schmidtii* was gained in a 1 m × 1 m sample in each experimental plot (Zhang et al., 2021b). A total of fifteen

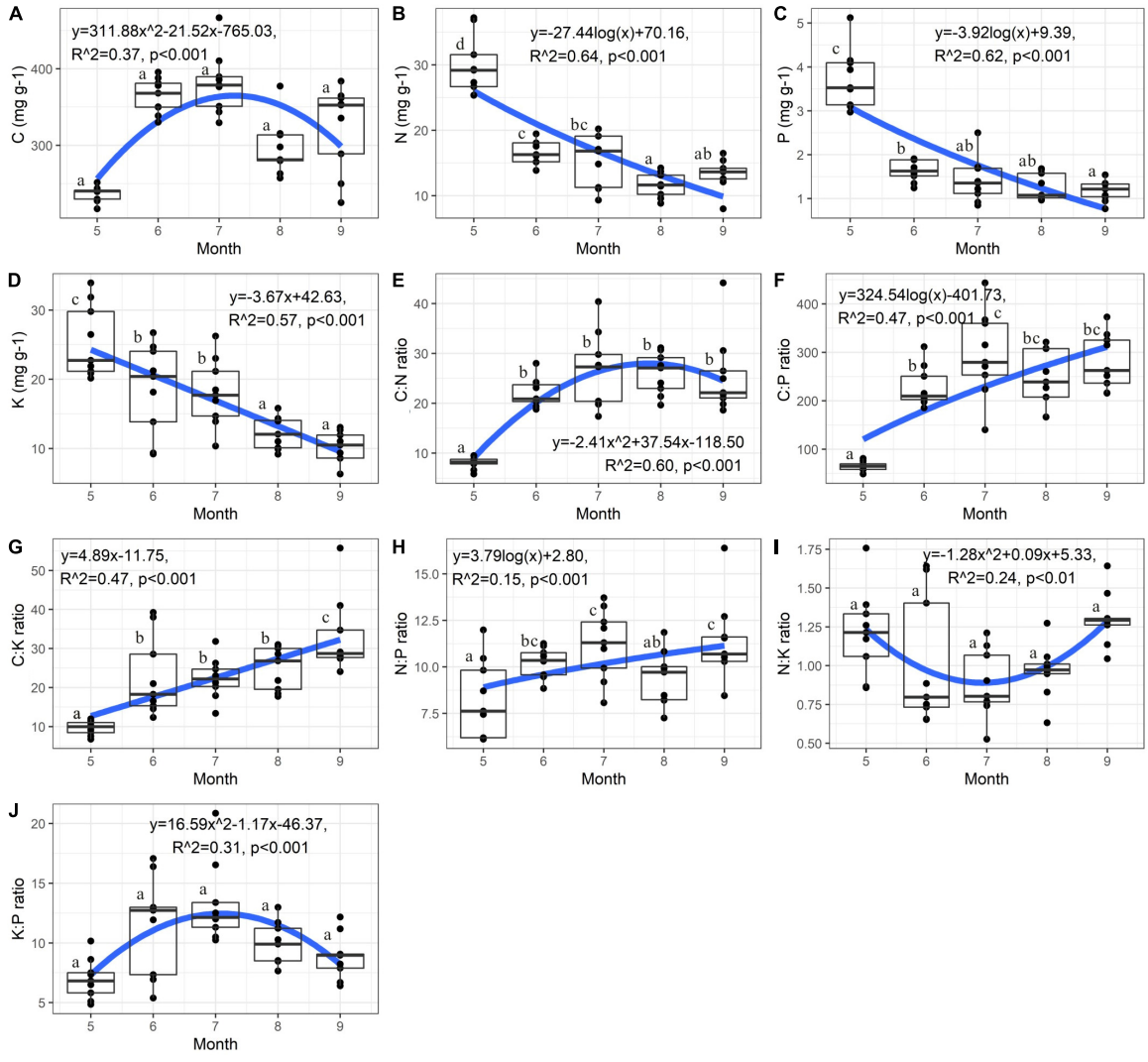

FIGURE 2 | Variation of nutrient stoichiometry of *Carex schmidtii* at the entire growth stages. **(A)** C concentration, **(B)** N concentration, **(C)** P concentration, **(D)** K concentration, **(E)** C:N ratio, **(F)** C:P ratio, **(G)** C:K ratio, **(H)** N:P ratio, **(I)** N:K ratio, and **(J)** K:P ratio. Fitting was applied to describe the dynamic of nutrient. NW, Natural tussock wetland; RW, Restored tussock wetland; DW, Degraded tussock wetland.

samples were gained in each wetland during the entire growth stages (May∼ September).

Determination of C, N, P, and K Concentrations of *Carex schmidtii*

Plant samples collected from in NW, RW, and DW were killed at 120°C for 2 h, and dried at 65°C to a constant weight, and then ground into powder and sieved through a 0.25 mm sieve. Plant C concentration was measured with a TOC analyzer (Multi N/C 2100, Jena, Germany). Plant samples were digested by sulfuric acid (with a mass fraction (ω) of = 98% and a density (ρ) of 1.84 g/cm^3) and hydrogen peroxide (ω = 30%; ρ = 1.13 g/cm^3) at 375°C using a muffle furnace until the liquid was clear, and then the clear liquid was cooled to room temperature to make up the volume. Plant N and P concentrations were determined using Kjeldahl determination

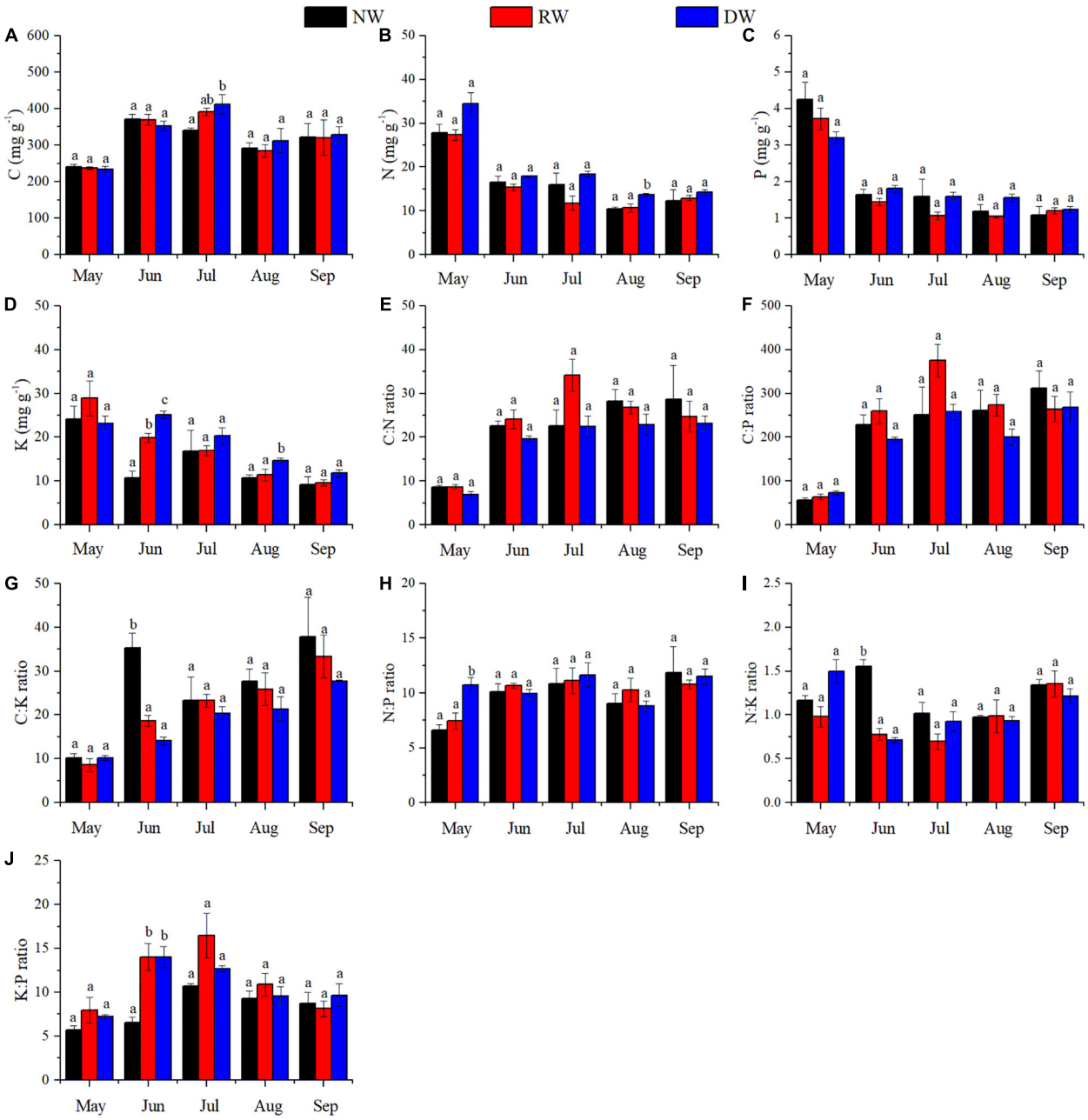

FIGURE 3 | Effect of wetland restoration and degradation on C, N, P, and K stoichiometry of *Carex schmidtii* at the entire growth stages (means ± se, *n* = 3). **(A)** C concentration, **(B)** N concentration, **(C)** P concentration, **(D)** K concentration, **(E)** C:N ratio, **(F)** C:P ratio, **(G)** C:K ratio, **(H)** N:P ratio, **(I)** N:K ratio, and **(J)** K:P ratio. NW, Natural tussock wetland; RW, Restored tussock wetland; DW, Degraded tussock wetland. Different letters stand for significant differences at the 0.05 significance level in NW, RW, and DW in the same growth stage.

and the Molybdenum-Antimony-Spectropho-Tometric Method with an automatic chemistry analyzer (Smartchem 300, Advanced Monolithic Systems, Graz, Italy), respectively. Plant K concentration was determined with an atomic emission spectrophotometer (I-7500, Shimadzu, Japan; Zhang et al., 2021a). All nutrient ratios were calculated as mass ratios.

Data Analysis

Plant C, N, P, and K concentrations and their ratios were gain from the 1 m × 1 m sample in each experimental plot, and checked for normality and homogeneity before the further analyses. Plant P concentration was log-transformed to meet the normality. When the assumptions of homoscedasticity were not met, permutational ANOVA was implemented in R 4.0.1 (package "lmPerm"). Effect of growth stage on nutrient concentration and their ratios of *C. schmidtii* were evaluated using one-way analysis of variance (ANOVA), and fitting was applied to describe the relationship between nutrient stoichiometry. Duncan's multiple range test was employed to determine the differences at the 0.05 significance level. In order to clarify how wetland restoration and degradation alter nutrient stoichiometry of *C. schmidtii*, the differences in the nutrient stoichiometry of *C. schmidtii* among NW, RW, and DW at each growth stage (Month) were examined with ANOVA. The nutrient stoichiometric relationships of *C. schmidtii* were determined using the general scaling function $\mathrm{Lg}\ i = \alpha\ \mathrm{Lg}\ j + \beta$, where i and j indicate C, N, P, K concentrations and their ratios of *C. schmidtii*, respectively; α and β indicate the scaling exponent and normalization constant, which are the slope and the "elevation" or Y-intercept of the log-log linear i vs. j regression line, respectively (Tian et al., 2018; Zhang et al., 2021a). $\alpha < 1$ indicates a faster change in an element concentration in proportion to other element concentration, vice versa when $\alpha > 1$. Ordinary least square (OLS) regression was performed to determine the scaling relationship under different treatments (package "lmodel2" in R) among three tussock wetlands. The correlation between plant C, N, P, and K concentrations and their ratios of *C. schmidtii* were performed with R ("PerformanceAnalytics" package, "corrr" package). Principal component analysis (PCA) was performed to identify the difference of nutrient trade-offs among NW, RW, and DW using the "FactomineR" and "factoextra" packages in R. Structural equation model (SEM) analysis was performed to evaluate the pathways and flux between biomass nutrients and their ratios of *C. schmidtii* in R ("sem" package).

RESULTS

Ecological Stoichiometry of *Carex schmidtii* and Its Dynamic

The mean values of C, N, P, and K concentrations of *C. schmidtii* in tussock wetland were 320.59 ± 9.34, 17.34 ± 1.08, 1.84 ± 0.16, 16.92 ± 1.03 mg g^{-1}, respectively (**Supplementary Table 1**). The mean values of C:N, C:P, C:K, N:P, N:K, and K:P ratios were 21.62 ± 1.30, 222.66 ± 14.88, 22.51 ± 1.53, 10.10 ± 0.31, 1.07 ± 0.05, 10.11 ± 0.51, respectively. It is noted that the N:P ratio was < 14 and N:K ratio was < 1.2, indicating N-limitation for the growth of *C. schmidtii*.

Plant nutrients and their ratios were significantly affected by the growth stage except plant C concentration, N:K and K:P ratios (**Supplementary Table 2** and **Figure 2**). The C:N ratio of *C. schmidtii* increased initially and then decreased with growth time (**Figure 2E**). Plant C:N ratio in May was 8.09, significantly lower than that in other 4 months (**Figure 2E**). The average value of C concentration and K:P ratio was 381.25 mg g^{-1} and 13.28 in July, 60.89% and 90.52% greater than that in May, respectively (**Figures 2A,J**). The highest plant N, P, and K concentrations were 29.88 mg g^{-1}, 3.73 mg g^{-1}, and 25.43 mg g^{-1} in May, and then significantly decreased over time (**Figures 2B–D**). The C:P, C:K, and N:P ratios were 65.13, 9.64, and 8.28 in May, respectively, and then increased during the following growth stages (**Figures 2F–H**). It is noted that the mean N:P ratio is < 14 in each month (**Figure 2H**). The N:K ratio of *C. schmidtii* decreased initially and then increased during the entire growth stages (**Figure 2I**). The N:K ratio in May and September was 1.21 and 1.30, respectively, but it was < 1.2 from June to August.

Effects of Wetland Restoration and Degradation on Ecological Stoichiometry of *Carex schmidtii* at Each Growth Stage

Wetland restoration and degradation affected the N:P ratio of *C. schmidtii* in May significantly (**Figure 3H** and **Table 1**). The highest N:P ratio was 10.75 recorded in DW, 44.32% greater than the value in RW and 61.99% greater than the value in NW. In June, significant differences in K concentration, C:K, N:K, and K:P ratios were identified among NW, RW, and DW. Plant K concentration of *C. schmidtii* in DW was 25.15 mg g^{-1}, higher than that in NW (10.81 mg g^{-1}) and RW (19.93 mg g^{-1}, **Figure 3**). The highest C:K ratio was 35.28 in NW, 1.90 times higher than that in RW and 2.51 times higher than that in DW. The N:K ratio, ranging from 0.71 to 1.56, displayed a pattern similar to the C:K ratio. Plant C concentration of *C. schmidtii*

TABLE 1 | Results (*p*-values) of permutational ANOVAs on the effects of wetland restoration and degradation on ecological stoichiometry of *Carex schmidtii* during the growth stages.

	Growth stages				
	May	**June**	**July**	**August**	**September**
C	0.725	0.342	**<0.05**	0.638	1.000
N	0.075	0.351	0.686	**<0.05**	0.396
P	0.064	0.554	0.961	0.102	0.458
K	0.961	**<0.001**	0.438	**<0.05**	0.140
C:N ratio	0.066	0.187	1.000	0.108	0.667
C:P ratio	0.082	0.540	0.902	0.263	0.448
C:K ratio	1.000	**<0.001**	0.655	0.151	0.250
N:P ratio	**<0.05**	0.863	0.581	0.882	0.745
N:K ratio	0.155	**<0.01**	0.667	0.804	0.405
K:P ratio	0.27	**<0.05**	0.516	0.725	0.556

Bold indicates p < 0.05.

was significantly affected by wetland restoration and degradation in July (**Figure 3**). The mean C concentration of *C. schmidtii* was 411.60 mg g^{-1} in DW, 20.58% higher than the lowest C concentration of *C. schmidtii* in NW. There are significant differences in N and K concentrations of *C. schmidtii* among NW, RW, and DW in August (**Figure 3**). Plant N and K results

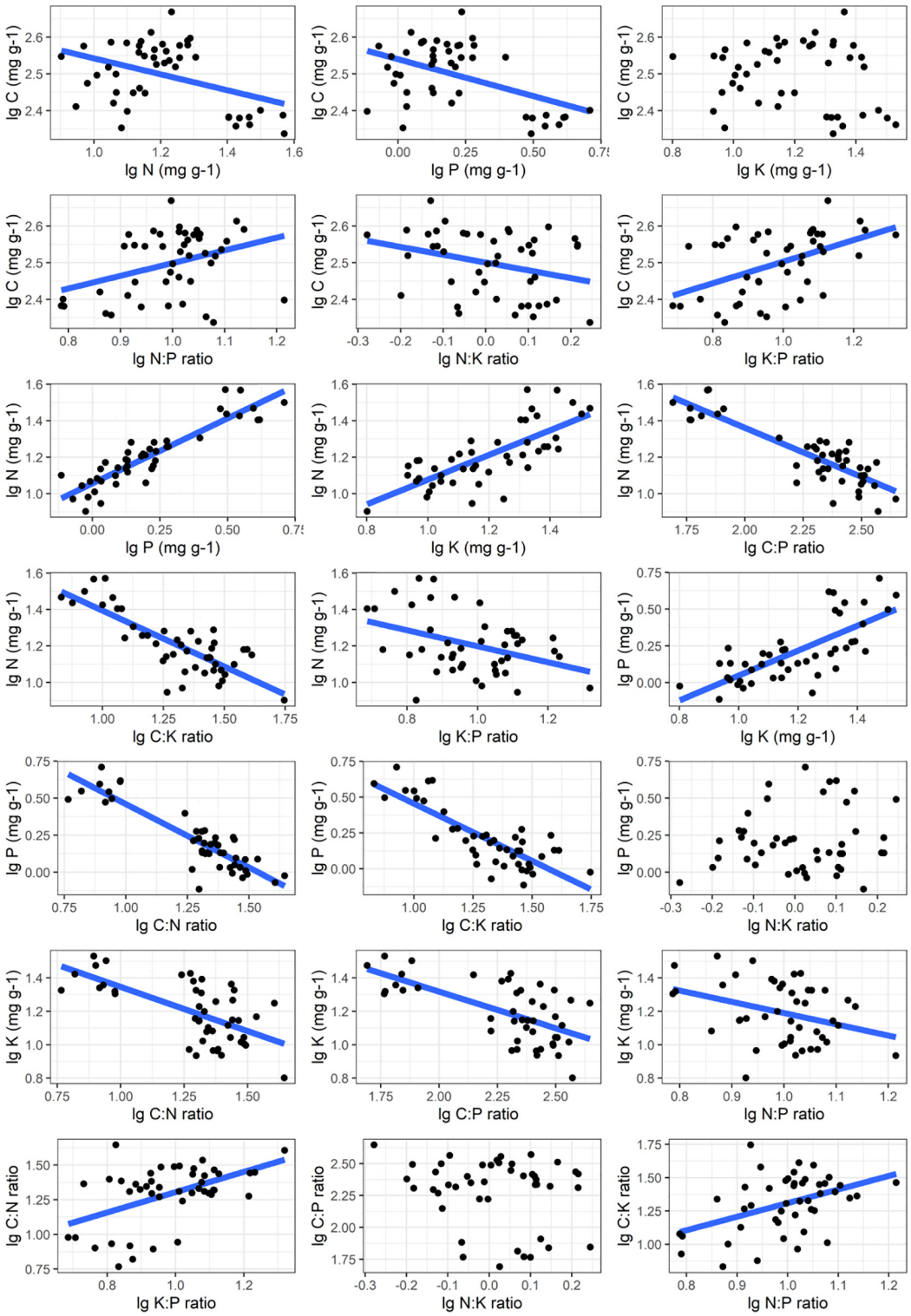

FIGURE 4 | Nutrient stoichiometric relationships of *Carex schmidtii*. The relationships between C, N, P, K and the corresponding ratios of *C. schmidtii* are fitted.

TABLE 2 | Summary of fitting results (Lg $i = \alpha$ Lg $j + \beta$) between C, N, P, K concentrations and their ratios of *Carex schmidtii* under natural (NW), restored (RW), and degraded wetlands (DW).

i∼*j*	Wetland Type	α (95%CI)	R^2	*p*
C∼ N	NW	−0.148 (−0.401∼0.104)	0.110	0.226
	RW	−0.263 (−0.590∼0.064)	0.189	0.106
	DW	−0.357 (−0.659∼−0.055)	0.334	**<0.05**
C∼P	NW	−0.126 (−0.295∼0.043)	0.167	0.131
	RW	−0.242 (−0.463∼−0.021)	0.300	**<0.05**
	DW	−0.378 (−0.678∼−0.079)	0.365	**<0.05**
C∼K	NW	−0.159 (−0.380∼0.062)	0.157	0.144
	RW	−0.093 (−0.396∼0.216)	0.030	0.545
	DW	−0.017 (−0.432∼0.399)	0.001	0.932
C∼N:P ratio	NW	0.254 (−0.115∼0.622)	0.146	0.16
	RW	0.663 (0.118∼1.208)	0.347	**<0.05**
	DW	0.063 (−0.845∼0.971)	0.002	0.882
C∼ N:K ratio	NW	0.175 (0.325∼0.676)	0.042	0.462
	RW	−0.196 (−0.608∼0.217)	0.075	0.324
	DW	−0.501 (−0.833∼−0.171)	0.452	**<0.01**
C∼K:P ratio	NW	0.139 (−0.239∼0.517)	0.046	0.441
	RW	0.325 (0.023∼0.627)	0.294	**<0.05**
	DW	0.572 (0.250∼0.894)	0.531	**<0.01**
N∼P	NW	0.632 (0.461∼0.801)	0.831	**<0.001**
	RW	0.689 (0.546∼0.832)	0.893	**<0.001**
	DW	0.930 (0.686∼1.174)	0.839	**<0.01**
N∼K	NW	0.794 (0.540∼1.048)	0.778	**<0.001**
	RW	0.604 (0.241∼0.968)	0.498	**<0.01**
	DW	0.699 (0.172∼1.226)	0.387	**<0.05**
N∼C:P ratio	NW	−0.521 (−0.695∼−0.347)	0.764	**<0.001**
	RW	−0.494 (−0.656∼−0.332)	0.770	**<0.001**
	DW	−0.604 (−0.807∼−0.400)	0.760	**<0.001**
N∼C:K ratio	NW	−0.618 (−0.862∼−0.374)	0.697	**<0.001**
	RW	−0.550 (−0.820∼−0.280)	0.598	**<0.001**
	DW	−0.759 (−1.063∼−0.455)	0.691	**<0.001**
N∼K:P ratio	NW	−0.705 (−1.462∼−0.052)	0.237	0.066
	RW	−0.463 (−0.987∼0.061)	0.219	0.079
	DW	−0.563 (−1.246∼0.120)	0.196	0.098
P∼K	NW	1.151 (0.789∼1.513)	0.784	**<0.001**
	RW	0.816 (0.309∼1.322)	0.482	**<0.01**
	DW	0.722 (0.219∼1.225)	0.425	**<0.01**
P∼C:N ratio	NW	−1.056 (−1.372∼−0.739)	0.800	**<0.001**
	RW	−0.925 (−1.148∼−0.703)	0.861	**<0.001**
	DW	−0.606 (−0.792∼−0.421)	0.793	**<0.001**
P∼C:K ratio	NW	−0.922 (−1.245∼−0.598)	0.744	**<0.001**
	RW	−0.793 (−1.134∼−0.452)	0.660	**<0.001**
	DW	−0.783 (−1.048∼−0.517)	0.757	**<0.001**
P∼N:K ratio	NW	−0.378 (−2.015∼1.259)	0.019	0.626
	RW	0.257 (−0.702∼1.217)	0.025	0.572
	DW	0.483 (−0.169∼1.135)	0.165	0.133
K∼C:N ratio	NW	−0.786 (−1.059∼−0.514)	0.750	**<0.01**
	RW	−0.500 (−0.911∼−0.090)	0.348	**<0.05**
	DW	−0.271 (−0.601∼0.060)	0.194	0.1
K∼C:P ratio	NW	−0.575 (−0.772∼−0.378)	0.754	**<0.001**
	RW	−0.391 (−0.708∼−0.075)	0.354	**<0.05**
	DW	−0.280 (−0.609∼0.048)	0.207	0.088
K∼N:P ratio	NW	−0.976 (−1.776∼−0.176)	0.348	**<0.05**
	RW	−0.997 (−2.153∼0.159)	0.211	0.085
	DW	−0.107 (−1.415∼1.201)	0.002	0.862
C:N ratio ∼ K:P ratio	NW	0.844 (−0.088∼1.776)	0.227	0.072
	RW	0.788 (0.122∼1.453)	0.335	**<0.05**
	DW	1.135 (0.268∼2.003)	0.381	**<0.05**
C:P ratio ∼ N:K ratio	NW	0.554 (−1.336∼2.443)	0.030	0.538
	RW	−0.453 (−1.682∼0.776)	0.046	0.44
	DW	−0.985 (−1.849∼−0.122)	0.318	**<0.05**
C:K ratio ∼ N:P ratio	NW	1.230 (0.276∼2.184)	0.374	**<0.05**
	RW	1.660 (0.450∼2.870)	0.403	**<0.05**
	DW	0.171 (−1.438∼1.779)	0.004	0.822

α, Scaling exponents; β, elevation; CI, Confidence interval.
Bold indicates $p < 0.05$.

recorded the highest value in DW with a value of 13.68 mg g^{-1} and 14.73 mg g^{-1}, respectively. No significant differences in the nutrient stoichiometry of *C. schmidtii* were identified among the three wetlands in September. N:P ratio was < 14 in NW, RW, and DW every month. Moreover, N:K ratio of the three wetlands was between 1.2 and 1.4 in September, but less than 1.2 from May to August except for that in DW in May and that in NW in June.

Effects of Wetland Restoration and Degradation and Growth Stage on the Scaling Exponent of *Carex schmidtii*

The robust relationships between C, N, P, K concentrations and the corresponding ratios of *C. schmidtii* (except C∼K, P∼N:K ratio, C:P ratio∼ N:K ratio) are quantified with the power function (Lg $i = \alpha$ Lg $j + \beta$; **Figure 4** and **Supplementary Table 3**). Plant C concentration decreases with the N, P concentrations and N:K ratio in DW, but increases with K:P ratio in RW and DW (**Table 2** and **Supplementary Figures 2–4**). The scaling exponent of C∼P decreases from -0.242 in RW to -0.378 in DW, while that of C∼K:P ratio increases from 0.325 to 0.572. Plant N concentration increases with P and K concentrations, while decreases with C:P ratio and C:K ratio in the three wetlands (**Table 2**). Plant P concentration increases with K concentration, but decreases with the C:P and C:N ratios in the three wetlands (**Table 2**). Plant K concentration decreases with C:N and C:P ratios in NW and RW. Plant K concentration increases with the N:P ratio in NW. The C:N ratio of *C. schmidtii* increases with the K:P ratio in RW and DW. The C:P ratio of *C. schmidtii* decreases with N:K ratio in DW. Plant C:K ratio increases with increasing the N:P ratio.

Principal Component Analysis of Nutrients and Their Ratios of *Carex schmidtii*

The PCA has summarized 90.52% of the total variability. The first two components reveal 79.9% of the total variability (**Supplementary Figure 5**). Plant C, N, P, K concentrations, and

C:N, C:P, C:K, N:P ratios are important contributors to the PC1. The PC2 is formed based on plant K concentration, N:K, K:P, and C:K ratios. The nutrient trade-off in NW is different from that in DW and RW due to the positions along PC2 (**Supplementary Figure 5**). In May, the nutrient trade-off in DW had significant differences with NW and RW along PC1 (**Figures 5A,B**). In June, wetland restoration and degradation affect the plant nutrient trade-off significantly (**Figures 5C,D**). The nutrient trade-offs in NW, RW, and DW are occupied with different positions along PC1 and PC2. In July, the first two components reveal 81.3% of the total variability. The nutrient trade-offs in DW and NW are different from that in RW because they occupied unique positions in the PCA (**Figures 5E,F**). Significant differences in nutrient trade-offs are observed in August between DW and RW along PC1 due to the unique positions in the PCA (**Figures 5G,H**). No significant effects of wetland restoration and degradation were found on the nutrient balances along PC1 and PC2 in September (**Figures 5I,J**).

The Coupling Relationships of Biomass Nutrients and Their Ratios of *Carex schmidtii*

Significant correlations between some nutrients and the corresponding ratios are observed ($0.30 \leq |r| \leq 0.92$, **Figure 6**). Positive relationships are observed between C, N:P ratio, and K:P ratio. In contrast, opposite trends are observed between C, N, P, and K concentrations. Plant N concentration has positive effects on plant P and K concentrations, but it is restricted by the C:P, C:K, and K:P ratios. Plant P concentration is related to plant K concentration and C:N ratio. Plant K concentration is negatively associated with the C:N, C:P, and N:P ratios. Besides, the plant C:N ratio is moderately associated with K:P ratio. The C:K ratio exhibits weak positive relationship with N:P ratio.

The biomass nutrients and their ratios of *C. schmidtii* are explored using the SEM. **Figure 7A** shows 53.34% of the variation in plant P concentration, 35.81% of the variation in plant C concentration, and 79.88% of the variation in plant N concentration. Plant K concentration has positive influences on C, N, and P concentrations. Plant P concentration has a negative effect on plant C concentration but a positive affection on plant N concentration. As shown in **Figure 7B**, the K:P ratio promotes plant C concentration and N:P ratio but inhibits the N:K ratio. However, the N:K ratio can improve the plant C concentration and N:P ratio. In the SEM of plant N concentration and other nutrient ratios, the variables explain 95.59% of the variation in C:P ratio and 75.23% of the variation for plant N concentration (**Figure 7C**). The C:P, C:K, and K:P ratios negatively affect plant N concentration of *C. schmidtii*. The SEM results in **Figure 7D** show that plant C:N and C:K ratios negatively affect plant P concentration. The N:K ratio positively influenced C:K ratio, and the C:K ratio contributed to C:N ratio. The variables in the model explain 62.58% of the variation in plant P concentration. In the SEM of plant K concentration, C:N, C:P, and N:P ratios

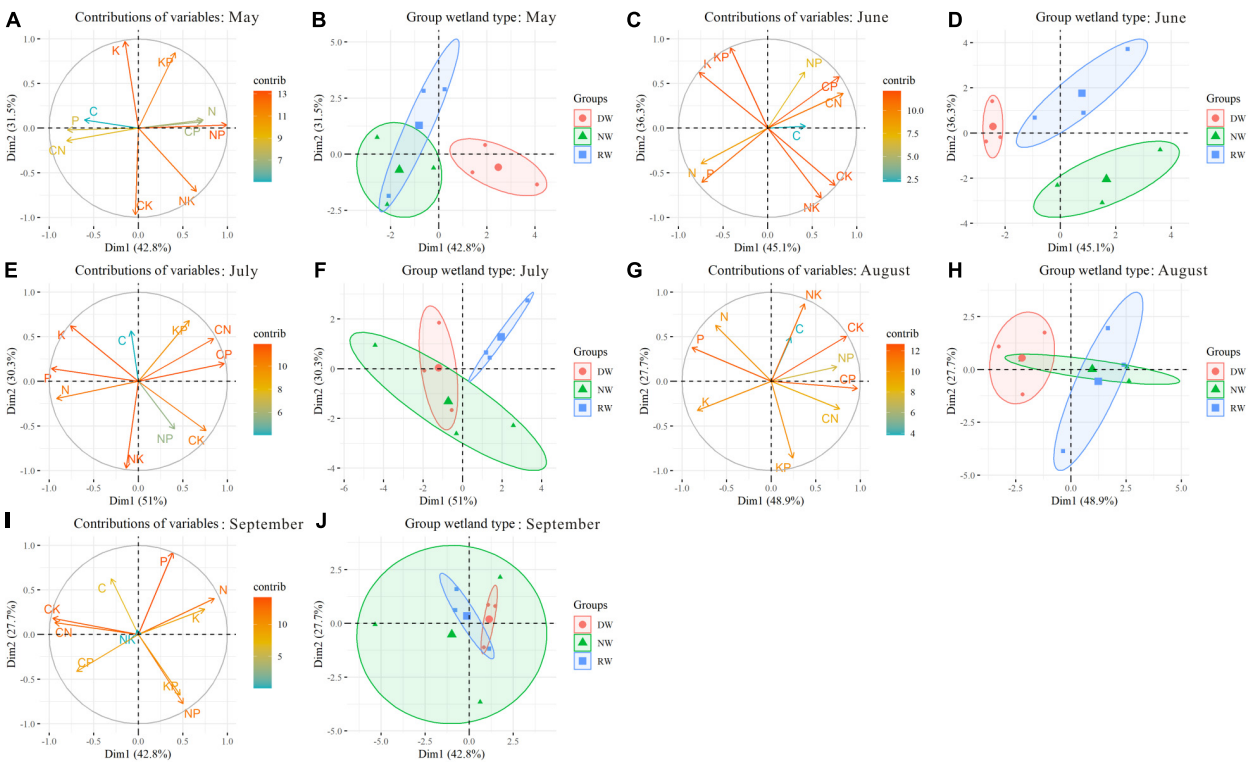

FIGURE 5 | The locations of nutrient stoichiometry in *Carex schmidtii* reared on wetland type during growth stages. May: **(A,B)**; June: **(C,D)**; July: **(E,F)**; August: **(G,H)**; September: **(I,J)**. Markers represent individual sample locations, while the ellipses represent 95% confidence interval for each group.

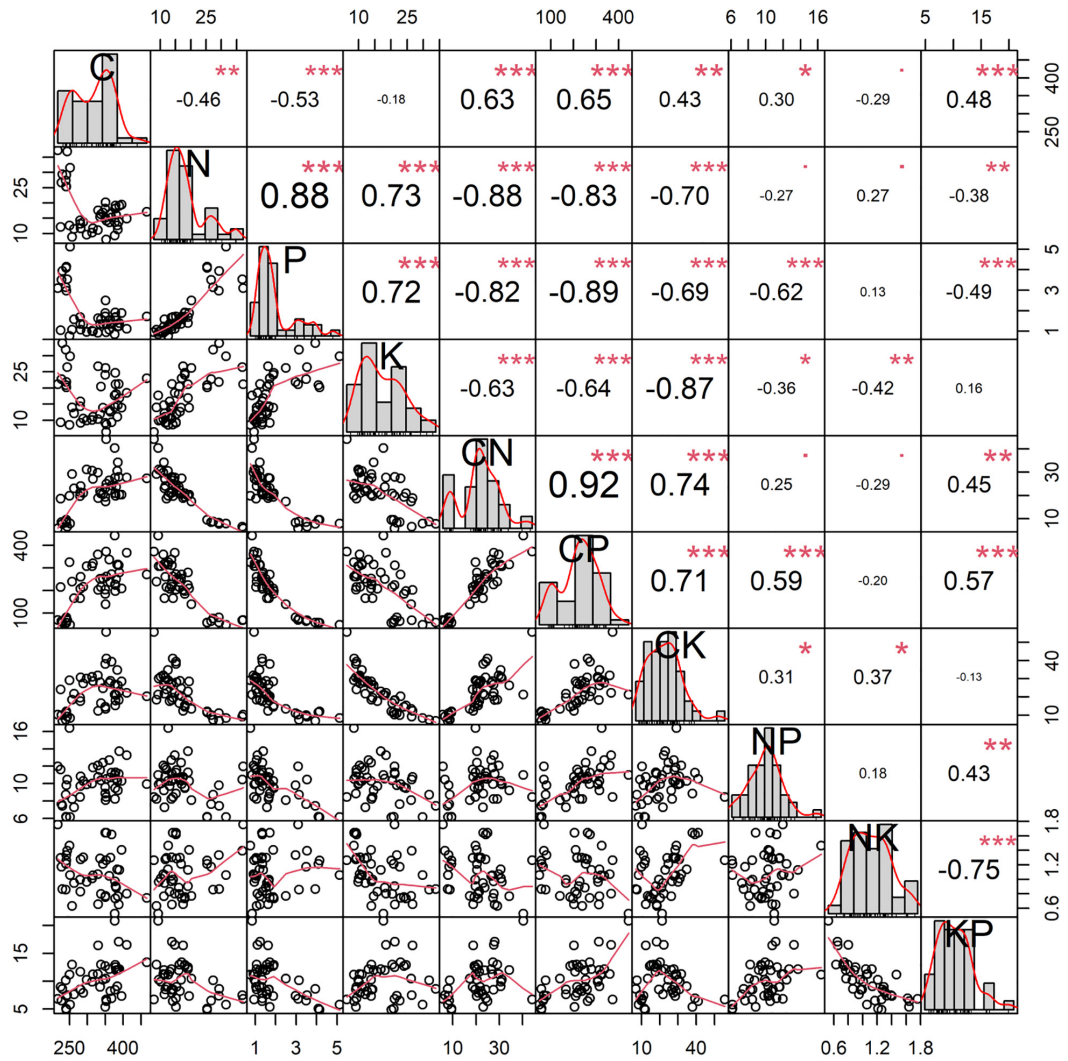

FIGURE 6 | The correlations between C, N, P, and K concentrations and the corresponding ratios of *Carex schmidtii*. *$p < 0.05$; **$p < 0.01$; ***$p < 0.001$.

(**Figure 7E**), the C:N ratio and N:P ratio explain 44.29% of the variation of plant P concentration by negatively affecting plant P concentration.

DISCUSSION

Environmental changes can affect plant growth and nutrient stoichiometry across species at global and regional scales (Elser et al., 2000; Güsewell et al., 2003; Lawniczak et al., 2010; Hu et al., 2018). Wetland restoration can alter degraded habitats, promote plant growth and improve community biomass. However, wetland degradation due to changes in hydrological conditions and soil environment results in plant dwarfism, and even incomplete life history of plants. All these are closely associated with plant eco-physiological processes and nutrient requirements (Zhang et al., 2019a; Wang M. et al., 2020; Qi et al., 2021c). The effects of wetland restoration and degradation on soil properties are interactive, providing both positive and negative effects (Wang G. et al., 2019; Cui et al., 2021). Wetland restoration can alleviate soil nutrient degradation, affecting N-related stoichiometry in the soil-plant system (Wang G. et al., 2020). However, few studies have explored the effect of wetland restoration and degradation on wetland plants with plant nutrient stoichiometry. This study found that wetland restoration and degradation partly altered nutrient stoichiometry of *C. schmidtii*, inconsistent with the original hypothesis. Wetland restoration and degradation effects on the nutrient stoichiometry of *C. schmidtii* are closely related to plant growth stages, nutrient acquisition and utilization (Guo et al., 2016; Zhang et al., 2019a). In the early growth stage (May∼June), nutrients sourced from the root system contributed to rapid growth and biomass accumulation of *C. schmidtii* seedlings in NW and RW (Lawrence et al., 2013; Rong et al., 2015; Zhang et al., 2021b), diluting plant N, P and K concentrations. Additionally, a large number of seeds of *C. schmidtii* form and fall off in NW and RW, also

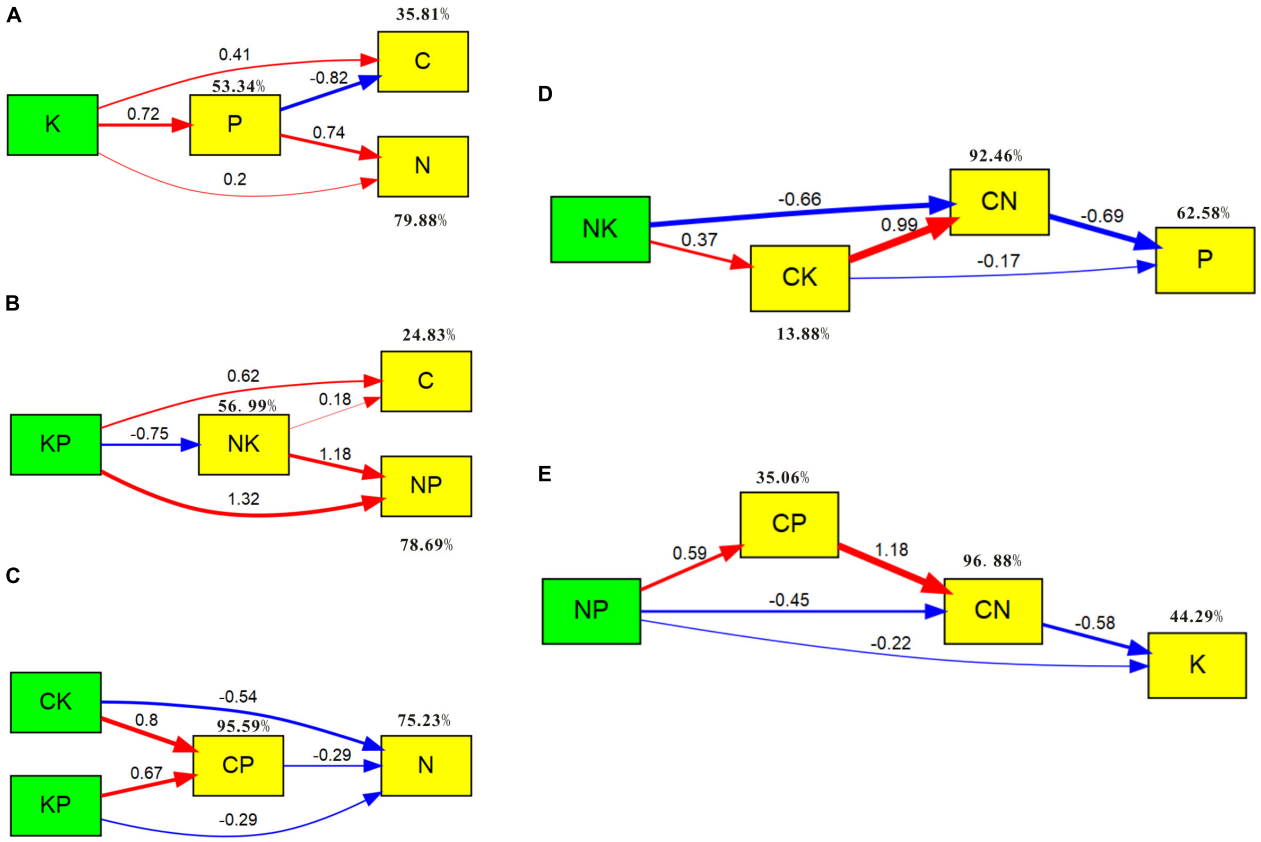

FIGURE 7 | SEM of plant C, N, P, K concentrations and the corresponding ratios. Red and blue solid arrows indicate the significant positive and negative pathways, respectively. Numbers in the arrows indicate the path coefficients. Percentage values close to the variables refer to the proportion of explained variance (R^2) by the model. **(A)** The SEM of plant C, N, P, and K concentrations (χ^2 = 0.428, p = 0.513, GFI = 0.995). **(B)** The SEM of plant C concentration, N:P ratio (NP), K:P ratio (KP), and N:K ratio (NK; χ^2 = 0.000, p = 0.987, GFI = 1.000). **(C)** The SEM of plant N concentration, C:K ratio (CK), C:P ratio (CP), and K:P ratio (χ^2 = 0.774, p = 0.379, GFI = 0.991). **(D)** The SEM of plant P concentration, C:N ratio (CN), C:K ratio, and N:K ratio (χ^2 = 0.009, p = 0.925, GFI = 1.000). **(E)** The SEM of plant K concentration, C:N ratio, C:P ratio, and N:P ratio (χ^2 = 1.511, p = 0.219, GFI = 0.983).

reducing plant nutrients. Compared to NW and RW, long-term degradation of *C. schmidtii* tussocks results in low germination rate and slow growth of *C. schmidtii* in DW (Wang X. et al., 2019), this being related to a low consumption of K and a high N:P ratio in plants. In July, a higher C concentration were found in DW (**Figure 3A**), promoting root extension and resists adversity. A similar pattern of plant N and K concentrations is found among the three wetlands in August, and a rapid biomass accumulation and postponement of growth peak of *C. schmidtii* contributes to a high plant N and K concentrations in DW (Zhang et al., 2021b). At the end of the growth, plant C, N, P, and K concentrations and the corresponding ratios are consistent among the three wetlands. Besides, the nutrient stoichiometry of *C. schmidtii* varies among growth stages, being consistent with previous studies about *C. schmidtii* in field and laboratory experiments (Zhang et al., 2021a).

Stoichiometric indices of N:P, N:K, and K:P ratios are important proxies to reflect the gradual and dynamic nutrient availability and limitation of plants (Koerselman and Meuleman, 1996; Olde Venterink et al., 2003). However, the stoichiometric indices provide a different focus on plant nutrient limitation (Güsewell et al., 2003). Both N:P and N:K ratio indicate N-limitation; N:P and K:P ratios imply for P- and N + P-limitation; N:K and K:P ratios indicate K- and K + N-limitation (Olde Venterink et al., 2003). The criteria for nutrient limitation are still controversial. The N:P ratio with a threshold of 14 and 16, and the N:K ratio with a threshold of 1.2 and 1.4 are applied to identify nutrient limitation (Koerselman and Meuleman, 1996; Güsewell et al., 2003). The N:P ratios are < 14 in NW, RW, and DW at entire growth stages, indicating N-limitation for the growth of *C. schmidtii* (**Figure 3H** and **Supplementary Figure 6**). Similarly, the N:K ratio indicates an N-limitation during May–August for most cases (<1.2) and a co-limitation of N and K in September (between 1.2 and 1.4). Besides, K-limitation for plant growth is identified in DW in May and in NW in June (>1.4). In particular, N-limitation for plant growth is gradually reduced in NW and RW (**Supplementary Figure 6**). However, the N:K ratio in RW indicates that N-limitation increases before decreases over time and finally shifts into the co-limitation of N and K (**Supplementary Figure 6**). In DW, K-limitation shifts into N-limitation in the early growth stage and the N-limitation gradually decreases over

time (**Supplementary Figure 6**). Plants in NW are (1) limited by N in the early growth stage; (2) shifted to K-limitation in July; (3) and then returned to N-limitation with an increasing trend; (4) at the end of growth stage, N-limitation decreases and turns into co-limitation of N and K (**Supplementary Figure 6**). The results are consistent with previous studies, revealing that N can limit the growth of *C. schmidtii* according to soil N:P ratio in the field (Zhang et al., 2019a). Results are partly in line with the second hypothesis that both N:P and N:K ratios indicate that RW strengthen N-limitation in the early growth stages and reduce N-limitation in the end of growth stages of *C. schmidtii* compared with DW. Besides, RW relieves K-limitation of *C. schmidtii* in the early growth stages. Therefore, improving the degree of N-limitation of *C. schmidtii* in the early growth stage provides valuable information for restoring tussock wetlands.

Trade-off between biomass nutrients and the corresponding ratios reveal the integration, relevance, and dynamic nature of nutrient homeostasis or flexibility in plants (Yan et al., 2019; Zhang et al., 2021a). Plant internal states drive nutrient homeostasis or flexibility by modulating nutrient trade-off (Reich et al., 2010; Rong et al., 2015; Julian et al., 2020). Scaling exponent and PCA describe the stoichiometric relationships and give invaluable information for nutrient trade-off (Zhang et al., 2021a). Besides, scaling exponents based on the empirical model ($\mathrm{Lg}\, i = \alpha\, \mathrm{Lg}\, j + \beta$) are vital to predict plant growth and functioning (Tian et al., 2019). Wetland restoration and degradation alter plant nutrient trade-off, especially N∼ and P∼ scaling exponents. Compared with DW, the scaling exponents of N∼P, N∼C:P ratio, N∼C:K ratio, P∼K, P∼C:N ratio and P∼C:K ratio in RW is more closed to NW. However, partly C-related (C∼) and K-related (K∼) scaling exponents are absent due to the non-robust fit, indicating nutrient flexibility of *C. schmidtii*. PCA shows that the nutrient trade-offs in RW are much more similar to DW, other than NW (**Supplementary Figure 5**), indicating that *C. schmidtii* in RW has not yet returned to its best natural level according to NW. Plant nutrient trade-offs in RW and NW developed in the opposite directions (**Supplementary Figure 5**). While the plant nutrient trade-off in DW gradually approaches NW from May to August (**Figure 5**). Therefore, how to effectively restore tussock wetlands warrants further studies and more validations. Besides, plant nutrient ratios explain 44.29∼75.23% of N, P, and K concentrations and moderately explain plant C concentration. Plant K and P concentrations explain 79.88% of plant N concentration and explain 35.81% of plant C concentration.

Planting tussocks and regulating hydrological conditions were successfully applied to restore tussock wetland (Lawrence and Zedler, 2011; Guo et al., 2016; Zhang et al., 2019b; Qi et al., 2021c). Plant nutrient trade-off in RW approached DW other than NW in view of the entire growth stage, opposite to the original goal of wetland restoration. The results are closely related to the gentle landform of RW. The absence of water storage structure results in frequent drought (**Supplementary Figure 1**) and the limitation of the growth of *C. schmidtii* tussocks. Thus, hydrological management for tussock planting is recommended to recovery the growth of *C. schmidtii* tussocks.

CONCLUSION

The nutrient stoichiometry of *C. schmidtii* was partly affected by wetland restoration and degradation but varied among growth stages. The growth of *C. schmidtii* was N-limited in the field during the entire growth stages. Significant stoichiometric scaling relationships were quantified between plant C, N, P, K concentrations and the corresponding ratios of *C. schmidtii* (except for C∼K, K∼N:P ratio, C:P ratio∼ N:K ratio). N-related (N∼) and P-related (P∼) scaling exponents effectively quantified the stoichiometric relationship in natural (NW), restored (RW) and degraded tussock wetlands, indicating changes in an element concentration in proportion to another element concentration (DW; except for N∼K:P ratio and P∼N:K ratio). Wetland restoration and degradation altered nutrient scaling exponent compared with NW. PCA indicated that wetland restoration and degradation had significant effects on the nutrient balances from May to August. The nutrient trade-off in RW was much more similar to DW, other than NW. *Carex schmidtii* had strong stoichiometric relationships between their nutrients and ratios. The structural equation model indicated that plant P and K concentrations had a high proportional contribution to plant C and N concentrations. These findings help in understanding nutrient trade-off of *C. schmidtii* under wetland restoration and degradation. Efficient evaluation of nutrient limitation and trade-off of plants are important to reveal the stoichiometric mechanism of *C. schmidtii* in NW, RW, and DW, providing invaluable information for the restoration and protection of *C. schmidtii* tussock wetlands. The coupling relationships among community diversity performance, plant growth and eco-physiological responses, and nutrient trade-off of *C. schmidtii*in tussock wetlands warrant needs to be studied further.

DATA AVAILABILITY STATEMENT

The original contributions presented in the study are included in the article/**Supplementary Material**, further inquiries can be directed to the corresponding authors.

AUTHOR CONTRIBUTIONS

DZ, ST, and XW designed the study. DZ collected the data. DZ, KD, and PS analyzed the data. ST, JX, and JS lead the writing with all co-authors. All authors gave final approval for publication.

FUNDING

This research was supported by the National Natural Science Foundation of China (Nos. 42101111 and 41871101), the Ph.D. research startup foundation of Binzhou University (No. 2021Y14), the Science and Technology Development Project of Jilin Province, China (No. 20190201115JC), and the Shandong Provincial Natural Science Foundation (No. ZR2021QD101).

ACKNOWLEDGMENTS

We thank for the help of Qing Qi and Mingye Zhang. We would like to express their gratitude to EditSprings (https://www.editsprings.com/) for the expert linguistic services provided.

SUPPLEMENTARY MATERIAL

The Supplementary Material for this article can be found online at: https://www.frontiersin.org/articles/10.3389/fevo.2021.801608/full#supplementary-material

REFERENCES

Branco, P., Egas, M., Elser, J. J., and Huisman, J. (2018). Eco-evolutionary dynamics of ecological stoichiometry in plankton communities. *Am. Nat.* 192, E1–E20. doi: 10.1086/697472

Bratt, A. R., Finlay, J. C., Welter, J. R., Vculek, B. A., and Van Allen, R. E. (2020). Co-limitation by N and P characterizes phytoplankton communities across nutrient availability and land Use. *Ecosystems* 23, 1121–1137. doi: 10.1007/s10021-019-00459-6

Busch, V., Klaus, V. H., Penone, C., Schäfer, D., Boch, S., Prati, D., et al. (2018). Nutrient stoichiometry and land use rather than species richness determine plant functional diversity. *Ecol. Evol.* 8, 601–616. doi: 10.1002/ece3.3609

Chen, Y., Stagg, C. L., Cai, Y., Lü, X., Wang, X., Shen, R., et al. (2020). Scaling responses of leaf nutrient stoichiometry to the lakeshore flooding duration gradient across different organizational levels. *Sci. Total Environ.* 740:139740. doi: 10.1016/j.scitotenv.2020.139740

Chiwa, M., Sheppard, L. J., Leith, I. D., Leeson, S. R., Tang, Y. S., and Cape, J. N. (2019). P and K additions enhance canopy N retention and accelerate the associated leaching. *Biogeochemistry* 142, 413–423. doi: 10.1007/s10533-019-00543-y

Cui, H., Ou, Y., Wang, L., Liang, A., Yan, B., and Li, Y. (2021). Dynamic changes in microbial communities and nutrient stoichiometry associated with soil aggregate structure in restored wetlands. *Catena* 197:104984. doi: 10.1016/j.catena.2020.104984

Ding, Z., Liu, Y., Lou, Y., Jiang, M., Li, H., and Lü, X. (2021). How soil ion stress and type influence the flooding adaptive strategies of *Phragmites australis* and *Bolboschoenus planiculmis* in temperate saline–alkaline wetlands? *Sci. Total Environ.* 771:144654. doi: 10.1016/j.scitotenv.2020.144654

Elser, J. J., Dobberfuhl, D. R., MacKay, N. A., and Schampel, J. H. (1996). Organism size, life history, and N:P stoichiometry. *Bioscience* 46, 674–684. doi: 10.2307/1312897

Elser, J. J., Fagan, W. F., Denno, R. F., Dobberfuhl, D. R., Folarin, A., Huberty, A., et al. (2000). Nutritional constraints in terrestrial and freshwater food webs. *Nature* 408, 578–580. doi: 10.1038/35046058

Ghimire, B., Riley, W. J., Koven, C. D., Kattge, J., Rogers, A., Reich, P. B., et al. (2017). A global trait-based approach to estimate leaf nitrogen functional allocation from observations. *Ecol. Appl.* 27, 1421–1434. doi: 10.1002/eap.1542

Gierth, M., and Mäser, P. (2007). Potassium transporters in plants–involvement in K+ acquisition, redistribution and homeostasis. *FEBS Lett.* 581, 2348–2356. doi: 10.1016/j.febslet.2007.03.035

Guo, J., Jiang, H., Bian, H., He, C., and Gao, Y. (2016). Effects of hydrologic mediation and plantation of Carex schmidtii Meinsh on peatland restoration in China's Changbai Mountain region. *Ecol. Eng.* 96, 187–193. doi: 10.1016/j.ecoleng.2016.01.015

Guo, Y., Yan, Z., Gheyret, G., Zhou, G., Xie, Z., and Tang, Z. (2020). The community-level scaling relationship between leaf nitrogen and phosphorus changes with plant growth, climate and nutrient limitation. *J. Ecol.* 108, 1276–1286. doi: 10.1111/1365-2745.13369

Güsewell, S., and Koerselman, M. (2002). Variation in nitrogen and phosphorus concentrations of wetland plants. *Perspect. Plant Ecol. Evol. Syst.* 5, 37–61. doi: 10.1078/1433-8319-0000022

Güsewell, S., Koerselman, W., and Verhoeven, J. T. (2003). Biomass N: P ratios as indicators of nutrient limitation for plant populations in wetlands. *Ecol. Appl.* 13, 372–384.

Hartmann, H., Bahn, M., Carbone, M., and Richardson, A. D. (2020). Plant carbon allocation in a changing world-challenges and progress: introduction to a virtual issue on carbon allocation. *New Phytol.* 227, 981–988. doi: 10.1111/nph.16757

He, N., Liu, C., Piao, S., Lawren, S., Xu, L., Luo, Y., et al. (2019). Ecosystem traits linking functional traits to macroecology. *Trends Ecol. Evol.* 34, 200–210. doi: 10.1016/j.tree.2018.11.004

Hoosbeek, M. R., Van Breemen, N., Vasander, H., Buttler, A., and Berendse, F. (2002). Potassium limits potentialgrowth of bog vegetation underelevated atmospheric CO2 and N deposition. *Glob. Change Biol.* 8, 1130–1138. doi: 10.1046/j.1365-2486.2002.00535.x

Hu, M., Peñuelas, J., Sardans, J., Sun, Z., Wilson, B. J., Huang, J., et al. (2018). Stoichiometry patterns of plant organ N and P in coastal herbaceous wetlands along the East China Sea: implications for biogeochemical niche. *Plant Soil* 431, 273–288. doi: 10.1007/s11104-018-3759-6

Huang, Y., Lou, C., Luo, L., and Wang, X. C. (2021). Insight into nitrogen and phosphorus coupling effects on mixotrophic *Chlorella vulgaris* growth under stably controlled nutrient conditions. *Sci. Total Environ.* 752:141747. doi: 10.1016/j.scitotenv.2020.141747

Jiang, H., Wen, Y., Zou, L., Wang, Z., He, C., and Zou, C. (2016). The effects of a wetland restoration project on the Siberian crane (*Grus leucogeranus*) population and stopover habitat in Momoge National Nature Reserve, China. *Ecol. Eng.* 96, 170–177. doi: 10.1016/j.ecoleng.2016.01.016

Julian, P., Gerber, S., Bhomia, R. K., King, J., Osborne, T. Z., and Wright, A. L. (2020). Understanding stoichiometric mechanisms of nutrient retention in wetland macrophytes: stoichiometric homeostasis along a nutrient gradient in a subtropical wetland. *Oecologia* 193, 969–980. doi: 10.1007/s00442-020-04722-9

Koerselman, W., and Meuleman, A. F. M. (1996). The vegetation N: P ratio: a new tool to detect the nature of nutrient limitation. *J. Appl. Ecol.* 33, 1441–1450. doi: 10.2307/2404783

Lawniczak, A. E., Zbierska, J., Choiński, A., and Szczepaniak, W. (2010). Response of emergent macrophytes to hydrological changes in a shallow lake, with special reference to nutrient cycling. *Hydrobiologia* 656, 243–254. doi: 10.1007/s10750-010-0436-z

Lawrence, B. A., and Zedler, J. B. (2011). Formation of tussocks by sedges: effects of hydroperiod and nutrients. *Ecol. Appl.* 21, 1745–1759.

Lawrence, B. A., Fahey, T. J., and Zedler, J. B. (2013). Root dynamics of *Carex stricta*-dominated tussock meadows. *Plant Soil.* 364, 325–339. doi: 10.1007/s11104-012-1360-y

Loomis, R. S. (1997). On the utility of nitrogen in leaves. *Proc. Natl. Acad. Sci. U.S.A.* 94, 13378–13379. doi: 10.1073/pnas.94.25.13378

Olde Venterink, H., Wassen, M. J., Verkroost, A. W. M., and De Ruiter, P. C. (2003). Species richness–productivity patterns differ between N-, P-, and K-limited wetlands. *Ecology* 84, 2191–2199. doi: 10.1890/01-0639

Opdekamp, W., Teuchies, J., Vrebos, D., Chormański, J., Schoelynck, J., Van Diggelen, R., et al. (2012). Tussocks: biogenic silica hot-spots in a riparian wetland. *Wetlands* 32, 1115–1124. doi: 10.1007/s13157-012-0341-5

Pan, X., Zhang, D., and Quan, L. (2006). Interactive factors leading to dying-off *Carex tato* in Momoge wetland polluted by crude oil, Western Jilin, China. *Chemosphere* 65, 1772–1777. doi: 10.1016/j.chemosphere.2006.04.063

Pan, Y., Cieraad, E., Armstrong, J., Armstrong, W., Clarkson, B. R., Colmer, T. D., et al. (2020). Global patterns of the leaf economics spectrum in wetlands. *Nat. Commun.* 11:4519. doi: 10.1038/s41467-020-18354-3

Peng, Y., Peng, Z., Zeng, X., and Hou, J. H. (2019). Effects of nitrogen-phosphorus imbalance on plant biomass production: a global perspective. *Plant Soil* 436, 245–252. doi: 10.1007/s11104-018-03927-5

Qi, Q., Zhang, D., Zhang, M., Tong, S., An, Y., Wang, X., et al. (2021a). Hydrological and microtopographic effects on community ecological characteristics of *Carex schmidtii* tussock wetland. *Sci. Total Environ.* 780:146630. doi: 10.1016/j.scitotenv.2021.146630

Qi, Q., Zhang, D., Zhang, M., Tong, S., Wang, W., and An, Y. (2021b). Spatial distribution of soil organic carbon and total nitrogen in disturbed *Carex tussock* wetland. *Ecol. Indic.* 120:106930. doi: 10.1016/j.ecolind.2020.106930

Qi, Q., Zhang, D., Tong, S., Zhang, M., Wang, X., An, Y., et al. (2021c). The driving mechanisms for community expansion in a restored *Carex tussock* wetland. *Ecol. Indic.* 121:107040. doi: 10.1016/j.ecolind.2020.107040

Reich, P. B., Oleksyn, J., Wright, I. J., Niklas, K. J., Hedin, L., and Elser, J. J. (2010). Evidence of a general 2/3-power law of scaling leaf nitrogen to phosphorus among major plant groups and biomes. *Proc. R. Soc. Lond. B Biol. Sci.* 277, 877–883. doi: 10.1098/rspb.2009.1818

Rong, Q., Liu, J., Cai, Y., Lu, Z., Zhao, Z., Yue, W., et al. (2015). Leaf carbon, nitrogen and phosphorus stoichiometry of *Tamarix chinensis* Lour. in the Laizhou Bay coastal wetland, China. *Ecol. Eng.* 76, 57–65. doi: 10.1016/j.ecoleng.2014.03.002

Sardans, J., Janssens, I. A., Ciais, P., Obersteiner, M., and Peñuelas, J. (2021). Recent advances and future research in ecological stoichiometry. *Perspect. Plant Ecol. Evol. Syst.* 50:125611. doi: 10.1016/j.ppees.2021.125611

Song, Z., Liu, H., Zhao, F., and Xu, C. (2014). Ecological stoichiometry of N: P: Si in China's grasslands. *Plant Soil* 380, 165–179. doi: 10.1007/s11104-014-2084-y

Tian, D., Yan, Z., Ma, S., Ding, Y., Luo, Y., Chen, Y., et al. (2019). Family-level leaf nitrogen and phosphorus stoichiometry of global terrestrial plants. *Sci. China Life Sci.* 62, 1047–1057. doi: 10.1007/s11427-019-9584-1

Tian, D., Yan, Z., Niklas, K., Han, W., Kattge, J., Reich, P., et al. (2018). Global leaf nitrogen and phosphorus stoichiometry and their scaling exponent. *Natl. Sci. Rev.* 5, 728–739. doi: 10.1093/nsr/nwx142

Van de Waal, D. B., Verschoor, A. M., Verspagen, J. M., van Donk, E., and Huisman, J. (2010). Climate-driven changes in the ecological stoichiometry of aquatic ecosystems. *Front. Ecol. Environ.* 8, 45–152. doi: 10.1890/080178

Wan, S. Z., Yang, G. S., and Mao, R. (2020). Responses of leaf nitrogen and phosphorus allocation patterns to nutrient additions in a temperate freshwater wetland. *Ecol. Indic.* 110:105949. doi: 10.1016/j.ecolind.2019.105949

Wang, G., Jiang, M., Wang, M., and Xue, Z. (2020). Element composition of soils to assess the success of wetland restoration. *Land Degrad. Dev.* 31, 1641–1649. doi: 10.1002/ldr.3561

Wang, G., Otte, M. L., Jiang, M., Wang, M., Yuan, Y., and Xue, Z. (2019). Does the element composition of soils of restored wetlands resemble natural wetlands? *Geoderma* 351, 174–179. doi: 10.1016/j.geoderma.2019.05.032

Wang, M., Wang, S., Wang, G., and Jiang, M. (2020). Soil seed banks and restoration potential of tussock sedge meadows after farming in Changbai Mountain, China. *Mar. Freshw. Res.* 71, 1099–1106. doi: 10.1071/MF19025

Wang, X., Zhang, D., Qi, Q., Tong, S., An, Y., Lu, X., et al. (2019). The restoration feasibility of degraded *Carex Tussock* in soda-salinization area in arid region. *Ecol. Indic.* 98, 131–136. doi: 10.1016/j.ecolind.2018.08.066

Wright, I. J., Reich, P. B., Westoby, M., Ackerly, D. D., Baruch, Z., Bongers, F., et al. (2004). The worldwide leaf economics spectrum. *Nature* 428, 821–827. doi: 10.1038/nature02403

Wright, S. J., Yavitt, J. B., Wurzburger, N., Turner, B. L., Tanner, E. V. J., Sayer, E. J., et al. (2011). Potassium, phosphorus or nitrogen limit root allocation, tree growth, or litter production in a lowland tropical forest. *Ecology* 92, 1616–1625. doi: 10.1890/10-1558.1

Yan, H., Liu, R., Liu, Z., Wang, X., Luo, W., and Sheng, L. (2015). Growth and physiological responses to water depths in *Carex schmidtii* Meinsh. *PLoS One* 10:e0128176. doi: 10.1371/journal.pone.0128176

Yan, Z., Hou, X., Han, W., Ma, S., Shen, H., Guo, Y., et al. (2019). Effects of nitrogen and phosphorus supply on stoichiometry of six elements in leaves of *Arabidopsis thaliana*. *Ann. Bot.* 123, 441–450. doi: 10.1093/aob/mcy169

Yu, M. F., Tao, Y., Liu, W., Xing, W., Liu, G., Wang, L., et al. (2020). C, N, and P stoichiometry and their interaction with different plant communities and soils in subtropical riparian wetlands. *Environ. Sci. Pollut. Res.* 27, 1024–1034. doi: 10.1007/s11356-019-07004-x

Yu, Q., Elser, J. J., He, N., Wu, H., Chen, Q., Zhang, G., et al. (2011). Stoichiometric homeostasis of vascular plants in the Inner Mongolia grassland. *Oecologia* 166, 1–10. doi: 10.1007/s00442-010-1902-z

Yu, Q., Wilcox, K., Pierre, K. L., Knapp, A. K., Han, X., and Smith, M. D. (2015). Stoichiometric homeostasis predicts plant species dominance, temporal stability, and responses to global change. *Ecology* 96, 2328–2335. doi: 10.1890/14-1897.1

Zhang, D., Qi, Q., Tong, S., Wang, J., Zhang, M., Zhu, G., et al. (2021a). Effect of hydrological fluctuation on nutrient stoichiometry and trade-off of *Carex schmidtii*. *Ecol. Indic.* 120:106924. doi: 10.1016/j.ecolind.2020.106924

Zhang, D., Sun, J., Cui, Q., Jia, X., Qi, Q., Wang, X., et al. (2021b). Plant growth and diversity performance after restoration in *Carex schmidtii* tussock wetlands, Northeast China. *Comm. Ecol.* 22, 391–401. doi: 10.1007/s42974-021-00062-7

Zhang, D., Qi, Q., Tong, S., Wang, X., An, Y., Zhang, M., et al. (2019a). Soil degradation effects on plant diversity and nutrient in tussock meadow wetlands. *J. Soil Sci. Plant Nutr.* 19, 535–544. doi: 10.1007/s42729-019-00052-9

Zhang, D., Qi, Q., Wang, X., Tong, S., Lv, X., An, Y., et al. (2019b). Physiological responses of *Carex schmidtii* Meinsh to alternating flooding-drought conditions in the Momoge wetland, northeast China. *Aquat. Bot.* 153, 33–39. doi: 10.1016/j.aquabot.2018.11.010

Zhao, M., Luo, Y., Chen, Y., Shen, H., Zhao, X., Fang, J., et al. (2021). Varied nitrogen versus phosphorus scaling exponents among shrub organs across eastern China. *Ecol. Indic.* 121:107024. doi: 10.1016/j.ecolind.2020.107024

Conflict of Interest: The authors declare that the research was conducted in the absence of any commercial or financial relationships that could be construed as a potential conflict of interest.

Publisher's Note: All claims expressed in this article are solely those of the authors and do not necessarily represent those of their affiliated organizations, or those of the publisher, the editors and the reviewers. Any product that may be evaluated in this article, or claim that may be made by its manufacturer, is not guaranteed or endorsed by the publisher.

frontiers in Ecology and Evolution

ORIGINAL RESEARCH
published: 27 January 2022
doi: 10.3389/fevo.2021.798520

Positive Effects on Alfalfa Productivity and Soil Nutrient Status in Coastal Wetlands Driven by Biochar and Microorganisms Mixtures

Qian Cui, Jiangbao Xia, Ling Peng, Ximei Zhao and Fanzhu Qu*

Shandong Key Laboratory of Eco-Environmental Science for the Yellow River Delta, Binzhou University, Binzhou, China

OPEN ACCESS

Edited by:
Zhenguo Niu, Aerospace Information Research Institute, Chinese Academy of Sciences (CAS), China

Reviewed by:
Mingxiang Zhang, Beijing Forestry University, China
Qingxue Guo, Hangzhou Normal University, China
Pifu Cong, National Marine Environmental Monitoring Center, China
Shouzheng Tong, Northeast Institute of Geography and Agroecology, Chinese Academy of Sciences (CAS), China

***Correspondence:**
Jiangbao Xia
xiajb@163.com

Specialty section:
This article was submitted to Conservation and Restoration Ecology, a section of the journal Frontiers in Ecology and Evolution

Received: *20 October 2021*
Accepted: *22 December 2021*
Published: *27 January 2022*

Citation:
Cui Q, Xia J, Peng L, Zhao X and Qu F (2022) Positive Effects on Alfalfa Productivity and Soil Nutrient Status in Coastal Wetlands Driven by Biochar and Microorganisms Mixtures. Front. Ecol. Evol. 9:798520. doi: 10.3389/fevo.2021.798520

Biochar application in reclaiming degraded soils and improving plant productivity has been recognized as a promising technology. Yet, the impacts of biochar and mixtures with compound effective microorganisms (CEM) on alfalfa growth and soil quality in coastal wetlands are poorly understood. A greenhouse experiment was set to systematically reveal the impacts of biochar and biochar combined with CEM on alfalfa growth traits, nutrient uptake, biomass, soil quality, and enzyme activities. Eight treatments were included: (1) control (CK−CEM), (2) 10-g/kg biochar (B_{10}−CEM); (3) 20-g/kg biochar (B_{20}−CEM); (4) 30-g/kg biochar (B_{30}−CEM), (5) CEM without biochar (CK + CEM); (6) 10-g/kg biochar with CEM (B_{10} + CEM), (7) 20-g/kg biochar with CEM (B_{20} + CEM), (8) 30-g/kg biochar with CEM (B_{30} + CEM). The utilization of biochar promoted seed germination, height, and tissue nutrient contents of alfalfa, and the combined biochar with CEM showed greater effects. Alfalfa biomass showed the maximum value in the B_{20} + CEM treatment, and the biomass of root, shoot, leaf in the B_{20} + CEM treatment increased by 200, 117.3, 144.6%, respectively, relative to the CK−CEM treatment. Alfalfa yield in the CK + CEM, B_{10} + CEM, B_{20} + CEM, B_{30} + CEM treatments was 71.91, 84.11, 138.5, and 120.5% higher than those in the CK−CEM treatment. The use of biochar and CEM decreased soil salinity and elevated soil nutrient content effectively. Biochar elevated soil organic carbon (SOC) and microbial biomass carbon (MBC), NH_4^+, NO_3^-, and enzymatic activities, and the positive impacts of biochar combined with CEM were additive. The combined addition of 20-g/kg biochar with CEM showed the pronounced improvement effects on improving soil fertility and nutrient availability as well as soil enzyme activities. Path analysis indicated that the application of biochar mixture with CEM promoted alfalfa biomass by regulating plant nutrient uptake, soil quality (soil nitrogen, SOC, MBC, NH_4^+, NO_3^-), and soil enzymatic activities (sucrase, urease, and alkaline phosphatases). Thus, incorporation of suitable biochar and CEM can serve as an effective measure to promote alfalfa productivity and restore coastal wetlands soils.

Keywords: biochar, alfalfa growth, alfalfa nutrient uptake, soil quality, soil enzyme activities

HIGHLIGHTS

- Biochar addition decreased soil salinity and elevated soil organic carbon, NH_4^+ and sucrase activity effectively.
- Combined use of 20 g/kg biochar with microorganisms mixtures performed well in improving alfalfa growth.
- Alfalfa total biomass increased depend on the rise of plant potassium uptake, soil organic carbon, NH_4^+, and NO_3^-.
- An appropriate dosage of biochar combined with microorganisms mixtures is effective to ameliorate coastal wetlands.

INTRODUCTION

Soil salinization with potentially nutrient deficiency has become a global issue concerning the sustainable development of food security and human livelihoods (Saifullah et al., 2018; Hassani et al., 2020). As a typical part of saline-alkali soil, coastal wetlands are considered as one of the most productive ecosystems on Earth and contributors to valuable service (Kirwan and Megonigal, 2013; Zhao et al., 2018). Recently, anthropogenic activities and seawater encroachment have resulted in high salinization, shallow groundwater, and soil function deterioration, which would cause soil degradation and threaten crop productivity in coastal wetlands (Stagg et al., 2017; Liu et al., 2018). Severe soil depletion, low nutrient deficiency, and poor vegetation coverage occur on coastal wetlands, aggravating plant productivity and unsustainable land use (Huang et al., 2012; Li et al., 2021). Consequently, the restoration of coastal wetlands is particularly critical, and soil amendments with the advantages of being effective, sustainable, and environmentally friendly are urgently needed for improving soil health and rehabilitating vegetation (Luo et al., 2017).

Biochar is a carbonous coproduct generated by pyrolysis organic biomass that has received growing attentions in pieces of research of ecological issues, soil restoration, and soil carbon sequestration (Lehmann, 2007; Chávez-García and Siebe, 2019; Cooper et al., 2020). Biochar has been advocated as a suitable conditioner that can remediate salt-affected soils by reducing salinity stress and promoting soil nutrient status (Kim et al., 2016; Ali et al., 2017; Gunarathne et al., 2020). Biochar has been proved to increase soil aggregate stability and water retention (Palansooriya et al., 2019; Caban et al., 2020), stimulate nutrient utilization efficiency (Biederman and Harpole, 2013; Chen et al., 2018), boost soil microbial proliferation and activities (Pokharel et al., 2020), and improve plant nutrient uptake and productivity (Lashari et al., 2015). Biochar can diminish sodium (Na^+) absorption by plants and mitigate salt stress to plant growth and physiology in salt-affected soils (Akhtar et al., 2015; Saifullah et al., 2018). Furthermore, biochar application can stimulate the plant nutrients absorption ability *via* promoting biochar-root interactions and increasing the efficiency of nutrient absorption by the roots (Olmo et al., 2016; Jeffery et al., 2017). However, inappropriate use of biochar to salt-affected soils may increase salinity and alkalinity and inhibit soil nutrient supply, which have an adverse impact on plant performance (Sigua et al., 2016; Luo et al., 2017). Thus, the effect of biochar on soil and plant quality under salinity conditions depends on soil type, plant feature, biochar feedstock type, biochar pyrolysis terms, and biochar addition rate.

Recently, compound effective microorganisms (CEM), a wide range of beneficial and non-pathogenic microorganisms, has been adopted as microbial fertilizers to improve soil quality (Talaat et al., 2015). The benefits of CEM have been highlighted in salt-affects soils for diminishing the detrimental impact of saline stress, enhancing beneficial microbial activities and soil nutrient cycling, accelerating decay of soil organic matter, which are favorable for plant productivity (Hu and Qi, 2013; Olle and Williams, 2013; Talaat, 2019). The amendment of biochar within microorganism mixtures showed encouraging results in promoting plant yield under saline conditions than single addition of biochar or other soil amendments (Akhtar et al., 2015; Talaat et al., 2015; Wang et al., 2021). For example, El-Mageed et al. (2020) found that the combined use of biochar and CEM maximized pepper growth and production more by improving favorable soil characteristics, photosynthetic availability, and nutritional status than biochar addition alone. Wang et al. (2021) reported that biochar mixture with plant growth-promoting rhizobacteria improved microbial diversity, enzyme activity, and nitrogen availability from tomato soil. In general, biochar mixture with microorganisms provides a favorable environment for microorganisms and produces remarkable effects on soil quality and plant growth. Thus, the combination of biochar with microorganisms is considered as a promising and effective measure for improving plant yield and remediating nutrient-poor soil.

Adding soil conditioner is an effective and eco-friendly approach to remediate soil degradation and improve salinity soil function of coastal wetlands (Sun et al., 2016). The additive positive effects on soil nutrient status and plant growth have been proved in salt-affected soils amended with the mixture of biochar and other fertilizer or microorganisms (Luo et al., 2017; Saifullah et al., 2018). Furthermore, planting halophytes in coastal wetlands is a bioremediation strategy to restore the degraded soil and improve the efficiency of land usage (Cai et al., 2021). Alfalfa is a preferred halophyte to adapt to saline environment and develop grass and livestock breeding in salt-affected regions. Alfalfa is a considerable important forage crop and has many prominent advantages, including high yield, nutritional quality, drought tolerance, and adaptation to infertile habitat (Cao et al., 2012; Zhang et al., 2019). In addition, combinations of biochar with microorganism mixtures or other amendments applied to soil showed effective effects on alfalfa yield (Liu et al., 2020; Raklami et al., 2021). However, previous reviews on restoring coastal wetlands soils have focused on sole biochar addition or combined with other organic materials (Kim et al., 2016; Luo et al., 2017). It is still unclear if the use of biochar with microorganism mixtures affects soil nutrient status and plant yield in coastal wetlands. Here, we hypothesize that biochar combined with CEM would improve soil nutrient availability, enhance soil enzyme activities, and promote plant nutrient uptake and alfalfa growth. The main objectives of this study were: (1) to clarify the changes in plant

growth traits, plant nutrient content, and soil nutrient content, following biochar and CEM inputs, and (2) to evaluate the potential mechanisms affecting alfalfa growth in coastal wetlands.

MATERIALS AND METHODS

Soil Sample and Experiment Preparation

The soil was randomly sampled from topsoil samples (0–20 cm) of the coastal wetlands in the Nature Reserve of the Yellow River Delta (37°45′N, 118°59′E) in the Shandong Province, China. Soil samples were transferred to a laboratory, and stones and roots were removed. The soil samples were air-dried and passed through a 2-mm sieve; then, all the samples were homogenized thoroughly. The soil had a salt content of 0.6%, pH of 7.49, soil organic matter of 9.23 g/kg, total nitrogen (TN) of 0.42 g/kg, available phosphate (AP) of 3.9 mg/kg.

Phragmites australis was chosen as a raw material for biochar mainly due to well-developed aerenchym and high carbon fixation capacity, which is suitable for the requirement of biochar (Liang et al., 2019). Biochar was produced from *Phragmites australis* shoot by combustion anaerobically for 2 h at 400°C in a muffle furnace (Leibo Terry Equipment Co., Ltd., Tianjin, China). The pyrolysis temperature of 400°C was selected due to its highest yield and relatively stable properties. The biochar sample was passed through a 2-mm sieve and homogenized completely before addition. Biochar contains 40.5% yield, 58.34% total carbon (TC), 1.18% TN, 4.11% hydrogen (H), 36.75% oxygen (O), 14.19 C/H, 0.70 (O + H)/C, an 8.65 m^2/g specific surface area, 1.83-nm average pore width, with a pH of 7.65. CEM contains a series of composite strains, and the main strains are photosynthetic bacteria, lactic acid bacteria, fermenting fungi, yeast, and actinomycetes. The quantity of colony forming units (CFU) units in each strain exceeded 10^4/ml.

Experiment Design and Measurements

This pot experiment comprised eight treatments in five replicates. These treatments were: (1) soil alone (CK−CEM); (2) 10-g/kg biochar (B_{10}−CEM, w/w); (3) 20-g/kg biochar (B_{20}−CEM); (4) 30-g/kg biochar (B_{30}−CEM); (5) CEM without biochar (CK + CEM); (6) 10-g/kg biochar with CEM (B_{10} + CEM); (7) 20-g/kg biochar with CEM (B_{20} + CEM); (8) 30-g/kg biochar with CEM (B_{30} + CEM). Soils samples with or without biochar addition were weighed (450-g dry mass) into a series of plastic pots (15 cm × 13 cm × 10 cm) with a hole and a tray in the bottom. Each pot was filled with deionized water to adjust the soil moisture to 60–70% of its water-holding capacity during the experiment. The CEM solution was diluted with deionized water to a concentration of 0.5 and then added to each pot. This diluted concentration was chosen because the alfalfa seed germination rate showed the highest in the pre-experiment. The dosage of the CEM was 4 ml/pot from the CEM solution in the treatments with CEM at the age of irrigation, while the treatments without CEM were added with double distilled water.

This experiment was conducted in a greenhouse. Alfalfa seeds were surface sterilized with 10% H_2O_2 for 0.5 h and rinsed. Fifteen alfalfa seeds were sown and then thinned to five plants per pot after short-term growth (3- to 5-cm height aboveground). The alfalfa grew in May 2019 and harvested in September 2019. The alfalfa was watered daily, and weeds in each pot were eradicated to ensure the growth of alfalfa. The number of seed germination was counted after the seeds were germinated. The height of alfalfa was measured in each plastic pot before harvesting. After harvesting, alfalfas aboveground parts and roots were rinsed, wiped with absorbent paper, and oven-dried at 70°C for 48 h. The soil sample in each pot was collected, mixed, and stored at 4°C for the measurement of soil property.

Soil pH was measured by deionized water at a 1:5 ratio (soil/water) with a pH meter, and soil salt content was measured using the gravimetric method. An elemental analyzer was used to analyze soil TC and TN. The Olsen method was conducted to measure AP, and the NH_4Ac extraction plus flame photometry method was used to analyze available potassium (AK). Soil organic carbon (SOC) was analyzed by the elemental analyzer after being treated with hydrochloric acid (HCl, 1 mol/L) for removal of inorganic carbon. The chloroform fumigation-extraction method was adopted to determine microbial biomass carbon (MBC; Vance et al., 1987). After the soil samples were extracted with potassium chloride (KCl) solution, an AA3 automated flow injection analysis (Auto Analyzer III, Seal, Germany) was used to determine soil NH_4^+ and NO_3^-. Soil sucrase, urease, and alkaline phosphatase activities were measured based on these methods and procedures (Tan et al., 2014). An elemental analyzer was used to analyze plant TN, the molybdenum-antimony colorimetry method was used to test plant total phosphorus (TP), and the flame photometer was used to determine plant total potassium (TK).

Statistical Analysis

All statistical analyses were conducted *via* SPSS 19.0. The influences of biochar, CEM, and their interactions on alfalfa seed germination, height, biomass, nutrient contents, and soil fertility change were tested by two-way ANOVA. The significance of differences in alfalfa growth parameters, soil properties, and soil enzymatic activities was analyzed *via* one-way ANOVA. Pearson correlation analysis was used to explore the relationship of plant parameters with soil quality. Path analysis was performed to ascertain hypothetical pathways by which soil quality and plant nutrient might explain plant biomass. Path analysis was conducted using the AMOS 21.0 version (IBM SPSS Amos 21.0 software). The data were fit to the model using maximum likelihood estimation. We selected the χ^2 test and the root mean square error of approximation to assess the fitness of the model.

RESULTS

Plant Growth, Biomass, and Nutrient Status

Compared with the CK−CEM treatment, seed germination significantly increased by 50–81.25% and 56.25–118.7% under −CEM treatments and +CEM treatments, respectively ($p < 0.05$, **Figure 1A**). The application of biochar and CEM increased alfalfa height among different treatments, and the highest plant height in

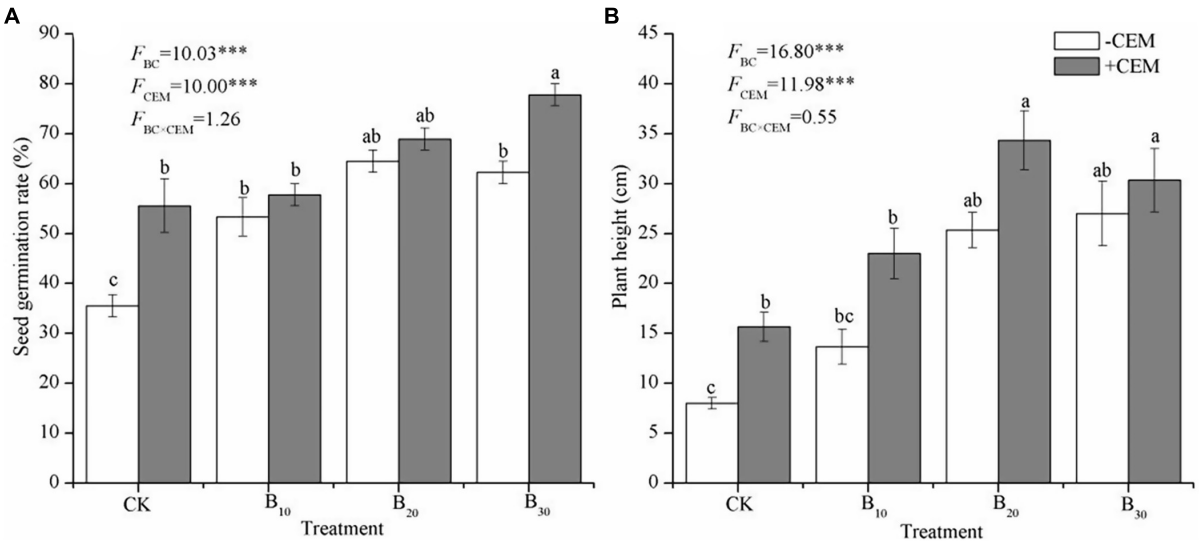

FIGURE 1 | Alfalfa seed germination rate **(A)** and alfalfa plant height **(B)** under different treatments. Bars and error bars show means ± SE (n = 5). Different lowercase letters referred to significant difference between treatments ($p < 0.05$). The F_{BC}, F_{CEM}, and $F_{BC \times CEM}$ are F and the degree of freedom of two-way ANOVAs. ***$p < 0.001$.

the B_{20} + CEM treatment reached to 34.33 ± 2.96 cm ($p < 0.05$, **Figure 1B**). The influences of biochar and CEM on plant biomass (root, shoot, leaf, aboveground, and total) varied with a biochar level (**Figure 2**). Alfalfa biomass enhanced with the increase of the biochar level in −CEM treatments, and the alfalfa biomass elevated and then declined with the increase of the biochar level in +CEM treatments. The B_{20} + CEM treatment showed the highest biomass among all the treatments, and the biomass of root, shoot, leaf, aboveground, and total was significantly higher than the CK−CEM treatment by 200, 117.3, 144.6, 123.2, and 138.5%, respectively ($p < 0.05$).

The contents of root TN, shoot TN, and leaf TN in other treatments were 60.24–226.6%, 46.46–143.5%, and 33.98–93.73% higher, respectively, than those in the CK−CEM treatment ($p < 0.05$, **Figures 3A–C**). Single biochar amendment or mixture with CEM significantly increased root TP concentrations by 57.58–155.3%, shoot TP concentrations by 36.89–117.6%, leaf TP concentrations by 31.81–108.8%, root TK concentrations by 41.28–138.9%, shoot TK concentrations by 64.55–209.8%, and leaf TK concentrations by 20.85–98.32%, respectively ($p < 0.05$, **Figures 3D–I**), compared with the CK−CEM treatment. Biochar elevated the contents of plant TN, TP, and TK in the −CEM treatments, while biochar increased the concentrations of plant TN, TP, and TK first and then decreased in +CEM treatments. The maximum TN, TP, and TK contents in plant tissues were detected in the B_{20} + CEM treatment. The interactive application of biochar and CEM led to more improved performance on alfalfa growth and nutrient absorption than the individual addition of either biochar or CEM.

Soil Properties and Fertility

Biochar addition with or without CEM had no significant influence on soil pH (**Table 1**). The soil salinity in the B_{10} + CEM, B_{20} + CEM, and B_{30} + CEM treatments was significantly reduced by 38.76, 44.14, and 45.48% than the CK−CEM treatment ($p < 0.05$, **Table 1**). The use of biochar and CEM improved soil TC, and the highest value in the B_{20} + CEM treatment was 50.13% higher than the CK−CEM treatment. Compared with that of CK−CEM treatment, soil TN treated with biochar application alone increased by 17.89–70.36%, while soil TN treated with biochar combined with CEM enhanced by 60.12–114.7% ($p < 0.05$, **Table 1**). Soil AP and AK in the B_{20} + CEM treatment significantly elevated by 44.06 and 18.35% ($p < 0.05$), respectively, compared with the CK−CEM treatment. Biochar amendment alone enhanced soil fertility, whereas the use of 30-g/kg biochar combined with CEM exerted a negative influence on soil fertility.

Soil Nutrient Availability and Enzyme Activities

Compared with the CK−CEM treatment, the B_{10}−CEM, B_{20}−CEM, B_{30}−CEM, B_{10} + CEM, B_{20} + CEM, B_{30} + CEM treatments enhanced SOC by 15.58, 65.07, 135.9, 12.65, 34.95, 157.94, and 140.3%, respectively (**Figure 4A**). Likewise, biochar addition alone significantly enhanced soil MBC by 41.44–86.50%, while biochar mixture with CEM enhanced soil MBC by 43.31–97.33% ($p < 0.05$, **Figure 4B**). Under the −CEM and +CEM treatments, soil NH_4^+ and NO_3^- were significantly increased by 44.95–198.1% and 36.42–104.7% relative to the CK−CEM treatment, and the enhanced effects on soil NH_4^+ were greater than soil NO_3^- ($p < 0.05$, **Figures 4C,D**). Biochar, CEM, and their interaction enhanced soil sucrase activity by 23.64–125.7%, urease activity by 19.35–74.45%, and alkaline phosphatase activity by 13.86–113.8%, as compared to the CK−CEM treatment, respectively (**Figure 5**). Notably, the increase amplitude of soil sucrase activity was more pronounced

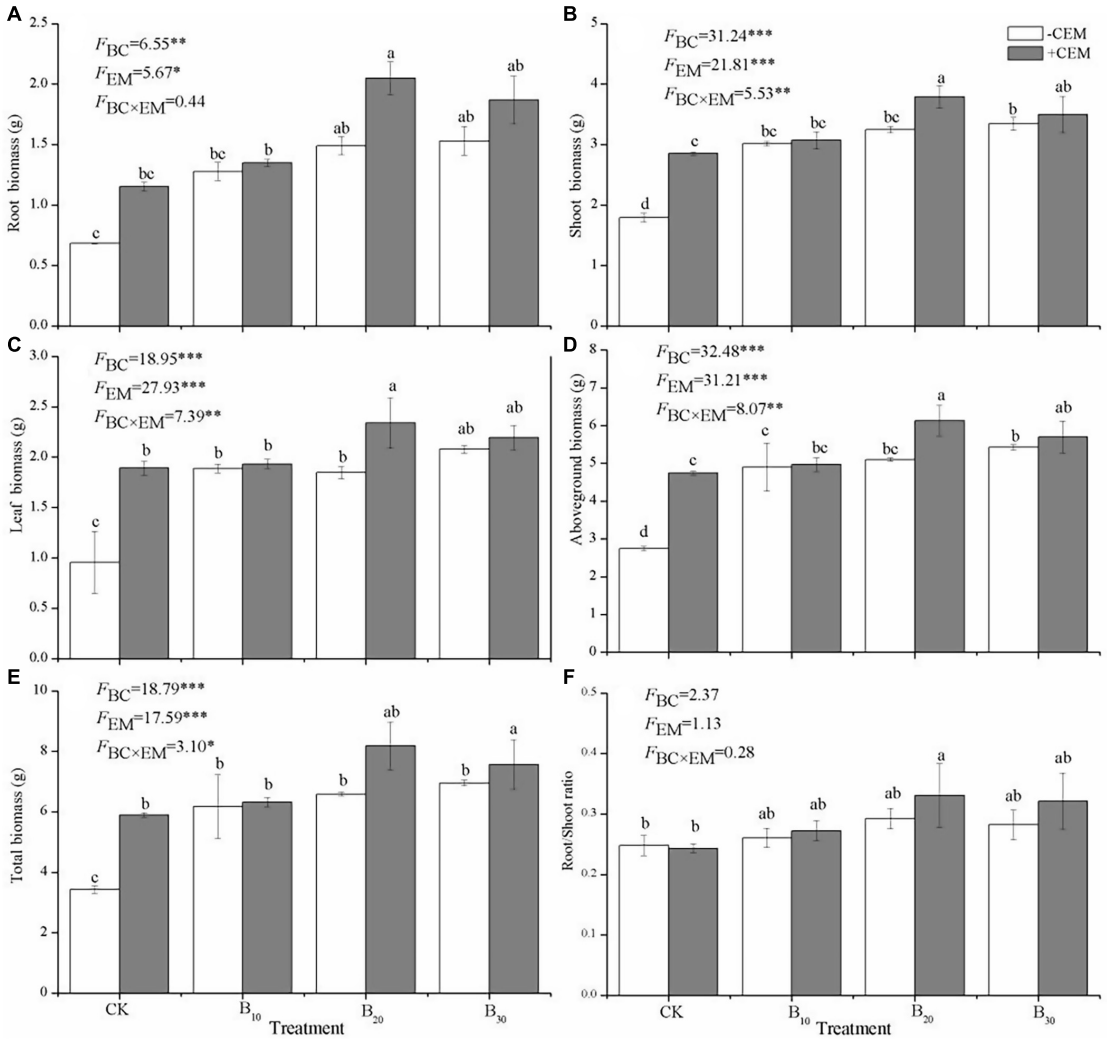

FIGURE 2 | Root biomass **(A)**, shoot biomass **(B)**, leaf biomass **(C)**, aboveground biomass **(D)**, total biomass **(E)**, and root/shoot ratio **(F)** under different treatments. Different lowercase letters referred to significant difference between treatments ($p < 0.05$). The F_{BC}, F_{CEM}, and $F_{BC \times CEM}$ are F and the degree of freedom of two-way ANOVAs. ***$p < 0.001$, **$p < 0.01$, *$p < 0.05$.

than alkaline phosphatase and urease activity, and the B_{20} + CEM treatment emerged the highest value among all the treatments.

Linkages Between Soil Nutrient Status and Plant Biomass

Significant positive correlations between plant biomass with nutrient contents of plant tissue, soil TN, SOC, MBC, NH_4^+, and NO_3^- were detected in this experiment (**Table 2**). The various pathways of biochar and CEM addition on soil nutrient and further on alfalfa biomass were quantified by SEM. The root mass, shoot mass, leaf mass, and total mass were explained by 54, 62, 70, and 72% using the path analysis (**Figure 6**). The amendment of biochar and CEM enhanced the contents of soil enzyme activities, TN, SOC, MBC, NH_4^+, and NO_3^-, and then positively promoted plant tissue nutrient absorption, and hence improved plant biomass. Soil TN, SOC, MBC, NH_4^+, and NO_3^- positively affected root TN and TK, and subsequently, root TN and TK strongly impacted root mass (**Figure 6A**). Likewise, soil NH_4^+, NO_3^-, and SOC were positively correlated with shoot TK, and hence, shoot TK mainly affected shoot mass (**Figure 6B**). Soil TN, MBC, NH_4^+, and NO_3^- positively influenced leaf TN, and SOC, NH_4^+, and NO_3^- positively affected leaf TK, and thus, leaf mass was positively driven by leaf TN and TK (**Figure 6C**). With regard to total biomass, soil NH_4^+, NO_3^-, and SOC positively affected total TK, and hence, total mass was explained by total TK (**Figure 6D**).

DISCUSSION

Promotion of Alfalfa Growth and Nutrient Absorption

In accordance with our hypothesis, appropriate application of biochar and CEM in coastal wetland soils resulted in an increase

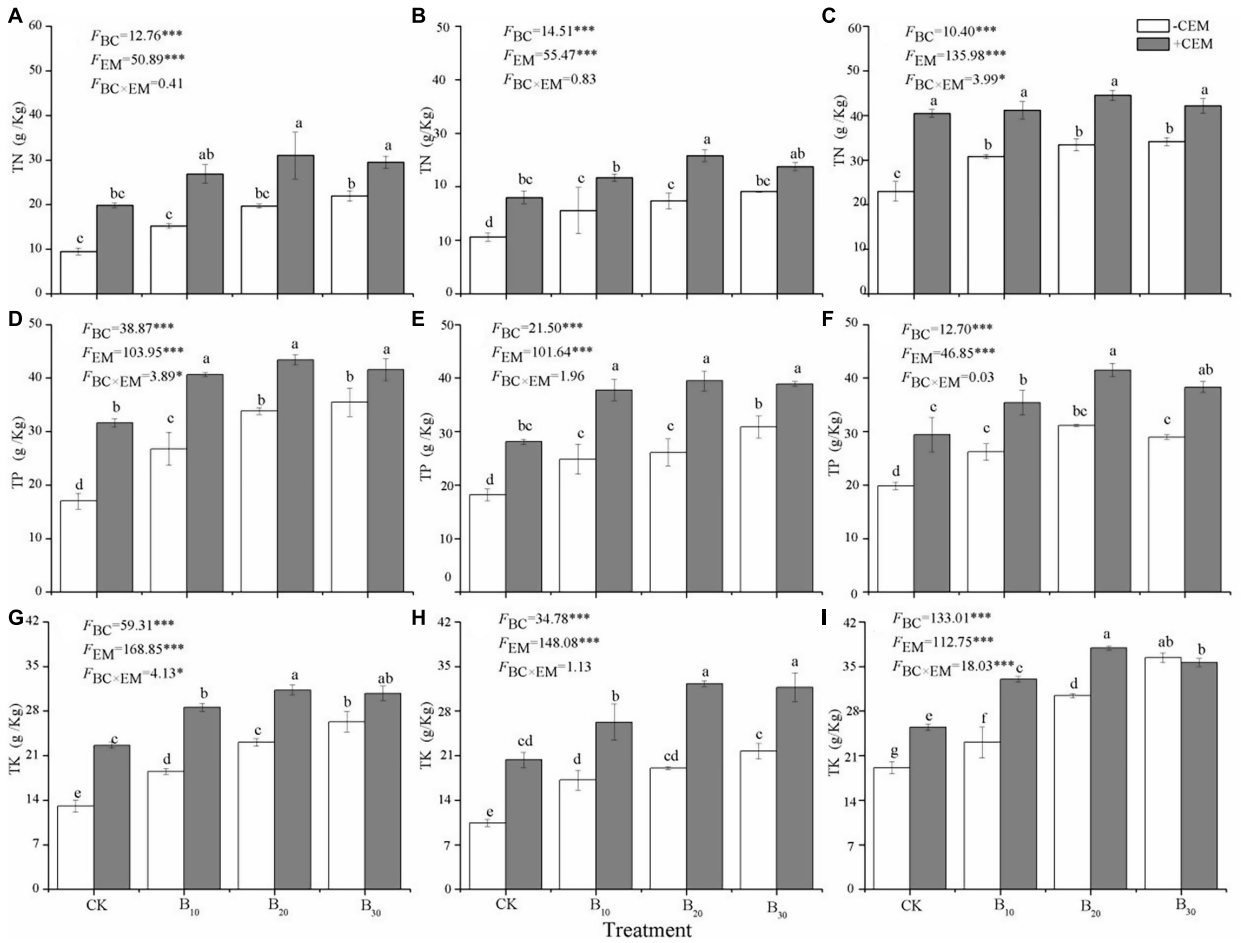

FIGURE 3 | Root TN **(A)**, shoot TN **(B)**, leaf TN **(C)**, root TP **(D)**, shoot TP **(E)**, leaf TP **(F)**, root TK **(G)**, shoot TK **(H)**, and leaf TK **(I)** under different treatments. TN, total nitrogen; TP, total phosphorus; TK, total potassium. Different lowercase letters referred to significant difference between treatments ($p < 0.05$). The F_{BC}, F_{CEM}, and $F_{BC \times CEM}$ are F and the degree of freedom of two-way ANOVAs. ***$p < 0.001$ and *$p < 0.05$.

in alfalfa seed germination, height and biomass, indicating that improved alfalfa growth was regulated by many benefits from the presence of biochar (Zhang et al., 2019; Liu et al., 2020). These results were similar to previous studies, which documented that biochar promoted plant growth, yield, and soil quality in salinity soils (Kim et al., 2016; Saifullah et al., 2018). The improved soil physicochemical and biological properties and elevated soil nutrient induced by biochar may be responsible for these results, which can provide nutrient supply with ongoing alfalfa growth (Agegnehu et al., 2017; Ali et al., 2017; Mehmood et al., 2020). As revealed by the path analysis, the improvement of plant biomass may be due to the stimulated nutrient cycling of alfalfa caused by the enhanced soil quality and enzyme activities. These following factors dominated the promotion of biochar on alfalfa growth: (i) improved soil TN, NH_4^+, NO_3^-, SOC, MBC, soil sucrase, urease, and alkaline phosphatase activities (El-Naggar et al., 2019); (ii) stimulated plant TN, TP, and TK concentration (Agegnehu et al., 2017); (iii) decreased soil salinity stress to alfalfa (Lashari et al., 2015).

The promotion impacts of biochar mixture with CEM on alfalfa growth were stronger than sole biochar addition, implying that biochar combined with CEM can have a stronger cooperative effect. These profound lifting effects could be ascribed to the increased beneficial microorganism activity induced by CEM, thus facilitating alfalfa growth through accelerating decomposition of soil organic matter (Talaat, 2019). Moreover, the interior of biochar could offer suitable habitats for the survival of microorganisms, leading to boosted microbial activities and nutrient release. The combined use of biochar and CEM can further promote alfalfa growth through alleviating salt stress and increasing photosynthetic capacity in salted-affected soils (Akhtar et al., 2015; El-Mageed et al., 2020). However, the CEM + B_{20} treatment accelerated alfalfa growth, while the CEM + B_{30} treatment inhibited alfalfa growth. Therefore, the combined use of biochar with CEM should be kept at an appropriate level, which may generate greater noticeable effects.

The amendment of biochar and CEM caused a significant increase in concentrations of alfalfa tissue nutrient (TN, TP, and TK), identifying the positive response of biochar in contributing to plant nutrient uptake as proved by several findings (Biederman and Harpole, 2013; Sigua et al., 2016). Improved soil properties, soil nutrient availability, and plant

TABLE 1 | Soil properties and fertility under different treatments.

Treatment	pH	Soil salt content (%)	TC (g/kg)	TN (g/kg)	AP (mg/kg)	AK (mg/kg)
CK−CEM	7.25 ± 0.04^{a}	0.58 ± 0.01^{a}	18.70 ± 0.62^{d}	0.54 ± 0.08^{b}	17.70 ± 0.75^{d}	199.23 ± 3.46^{c}
B_{10}−CEM	7.16 ± 0.01^{a}	0.50 ± 0.03^{b}	19.39 ± 0.10^{d}	0.64 ± 0.06^{b}	21.1 ± 0.65^{bc}	210.16 ± 5.31^{bc}
B_{20}−CEM	7.16 ± 0.03^{a}	0.42 ± 0.03^{c}	21.70 ± 0.70^{c}	0.65 ± 0.08^{b}	22.07 ± 0.52^{b}	215.53 ± 6.79^{b}
B_{30}−CEM	7.21 ± 0.04^{a}	0.39 ± 0.02^{cd}	26.05 ± 0.77^{ab}	0.92 ± 0.09^{ab}	23.63 ± 0.84^{ab}	225.50 ± 3.55^{b}
CK + CEM	7.17 ± 0.02^{a}	0.36 ± 0.01^{cd}	21.95 ± 0.90^{bc}	0.76 ± 0.21^{b}	18.27 ± 0.52^{cd}	216.46 ± 3.98^{b}
B_{10} + CEM	7.15 ± 0.03^{a}	0.35 ± 0.01^{d}	24.09 ± 0.69^{b}	0.86 ± 0.03^{ab}	20.00 ± 0.75^{c}	221.80 ± 2.90^{b}
B_{20} + CEM	7.12 ± 0.03^{a}	0.32 ± 0.01^{d}	28.08 ± 0.90^{a}	1.16 ± 0.13^{a}	25.50 ± 0.31^{a}	235.80 ± 1.90^{a}
B_{30} + CEM	7.13 ± 0.03^{a}	0.31 ± 0.01^{d}	27.91 ± 0.86^{ab}	1.00 ± 0.15^{ab}	24.03 ± 0.67^{a}	228.96 ± 4.56^{ab}
BC	1.38	12.86***	32.40***	2.98	37.99***	8.78**
CEM	4.22	84.89***	58.61***	9.84**	3.24	18.56**
BC × CEM	0.55	4.43*	3.35*	1.11	4.27*	1.46

*Different lowercase letters behind values referred to significant differences between the same columns ($p < 0.05$). The given are F values of two-way ANOVAs. ***$p < 0.001$, **$p < 0.01$, *$p < 0.05$. Data were mean values with standard deviation in parentheses (n = 5).*

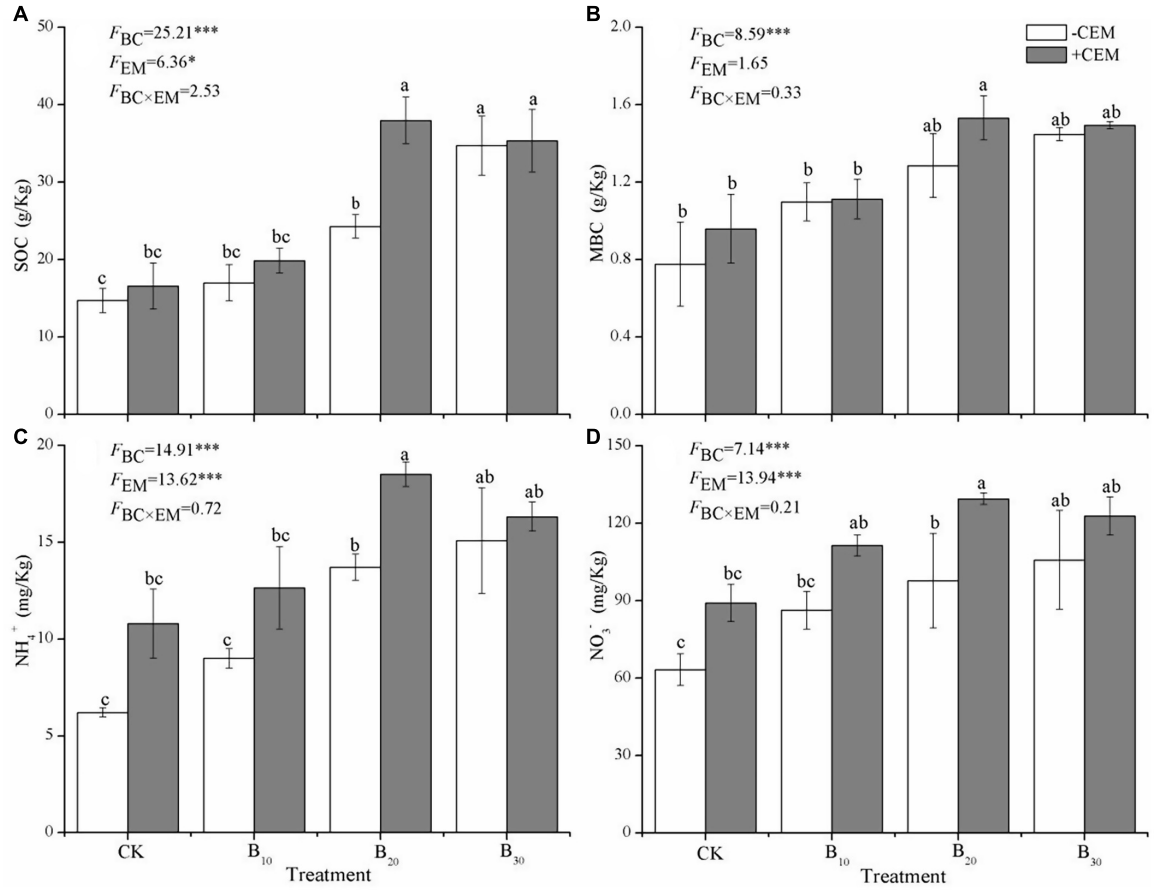

FIGURE 4 | SOC **(A)**, MBC **(B)**, NH_4^+ **(C)**, and NO_3^- **(D)** under different treatments. SOC, soil organic carbon; MBC, microbial biomass carbon; NH_4^+, ammonium nitrogen; NO_3^-, nitrate nitrogen. Different lowercase letters referred to significant difference between treatments ($p < 0.05$). The F_{BC}, F_{CEM}, and $F_{BC \times CEM}$ are *F* and the degree of freedom of two-way ANOVAs. ***$p < 0.001$ and *$p < 0.05$.

photosynthetic parameter after biochar is applied may contribute to the boosted plant nutrient uptake (Palansooriya et al., 2019). Notably, biochar combined with CEM was more effective in stimulating alfalfa nutrient uptake compared to single biochar application. The CEM could provide photosynthetic bacteria for soil to promote photosynthesis and endogenous phytohormones synthesis (Talaat, 2019). Thus, the EM combined with biochar could alleviate salinity stress and elevate the contents of plant TN, TP, and TK. Hence, biochar combined with CEM could provide a survival advantage for alfalfa growth by acquiring

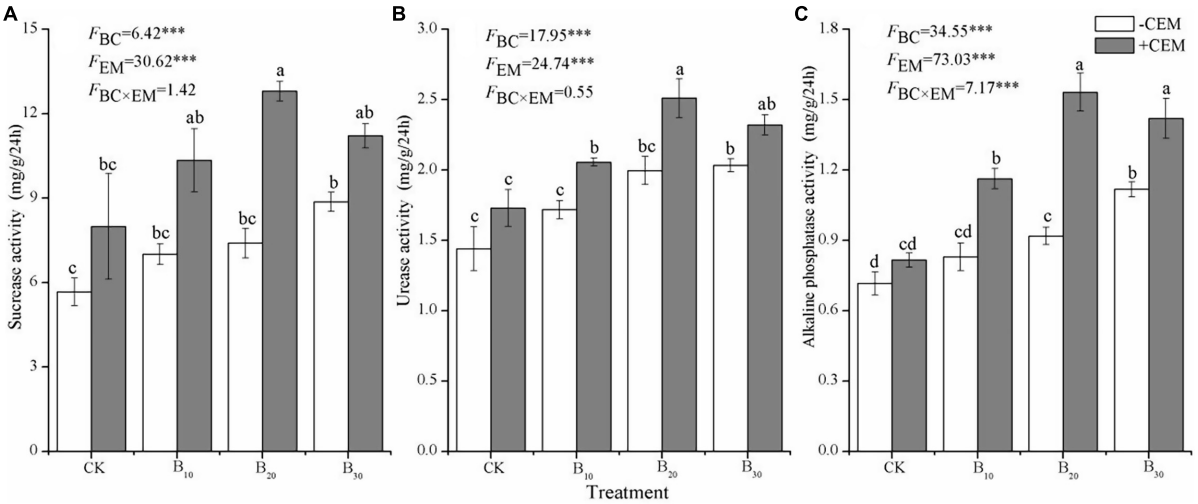

FIGURE 5 | Soil sucrase activity **(A)**, soil urease activity **(B)**, and soil alkaline phosphatase activity **(C)** under different treatments. Different lowercase letters referred to significant difference between treatments ($p < 0.05$). The F_{BC}, F_{CEM}, and $F_{BC \times CEM}$ are F and the degree of freedom of two-way ANOVAs. ***$p < 0.001$.

more nutrients in soil and improving plant absorption (Agegnehu et al., 2017). In general, nutrient contents of alfalfa tissues could generate dramatically active effect on improving alfalfa growth by modulating nutrient supply (Zhang et al., 2019).

Amelioration of Soil Salinity and Fertility

As an excellent soil conditioner, biochar plays a crucial role in reducing soil salinity *via* improving leaching of soluble salts and declining salt accumulation of surface soils (Saifullah et al., 2018). Biochar addition or combined with CEM reduced soil salinity by 12.97–45.48%, suggesting that biochar addition can alleviate salt stress and offer a suitable environment for alfalfa growth. Moreover, the adsorption of salts on the biochar surfaces or fine pores might be a reason for reducing soil salinity. Another possible explanation for decreased soil salinity could be the cover of biochar that helped downward saline water movement, contributing to the falling soil salinity in topsoil (Hammer et al., 2015; Gunarathne et al., 2020). Biochar addition could facilitate salts leaching by meliorating soil hydraulic conductivity and porosity (Chaganti et al., 2015). Moreover, extensive results carried out confirmed that planting alfalfa was an effective plant-assisted strategy to prevent salinization and promote soil quality in inland regions (Qadir et al., 2001; Cao et al., 2012). Thus, alfalfa planting combined with the amendment of biochar and CEM could also help inhibit salt accumulation in coastal wetlands.

TABLE 2 | Pearson correlations analyses between plant parameters and soil quality.

Parameters	Height	RB	SB	LB	TB
Root TN	0.67**	0.56**	0.79**	0.79**	0.72**
Shoot TN	0.72**	0.64**	0.72**	0.75**	0.75**
Leaf TN	0.66**	0.61**	0.91**	0.76**	0.73**
Root TP	0.75**	0.64**	0.68**	0.64**	0.76**
Shoot TP	0.67**	0.65**	0.90**	0.78**	0.76**
Leaf TP	0.69**	0.61**	0.69**	0.69**	0.70**
Root TK	0.81**	0.68**	0.94**	0.81**	0.81**
Shoot TK	0.78**	0.73**	0.91**	0.78**	0.80**
Leaf TK	0.85**	0.70**	0.68**	0.78**	0.80**
Soil TN	0.55**	0.63**	0.88**	0.73**	0.68**
SOC	0.77**	0.56**	0.82**	0.61**	0.64**
MBC	0.63**	0.58**	0.90**	0.59**	0.65**
NH_4^+	0.85**	0.62**	0.87**	0.71**	0.75**
NO_3^-	0.67**	0.65**	0.81**	0.71**	0.72**

*RB, Root biomass; SB, Shoot biomass; LB, Leaf biomass; TB, Total biomass. **$p < 0.01$.*

Biochar makes a critical difference in improving soil fertility and rehabilitating salt-affected soils *via* the improvement in soil functions, such as aggregation formation, a nutrient cycle, and microorganism development (El-Naggar et al., 2019; Gunarathne et al., 2020). Our analysis confirmed that biochar application elevated soil content of TC, TN, AP, and AK, and the enhanced effects become even more significant when biochar is combined with CEM. The high content of nutrients in biochar may elevate soil nutrient status and promote nutrient transformation considerably (Kim et al., 2016; Gunarathne et al., 2020). Besides, the porous structure and super absorption of biochar may enhance soil fertility through reserving nutrients and releasing nutrient slowly (Ding et al., 2016). The increased soil aggregation and water holding ability induced by biochar addition were responsible for stabilizing soil structure, which was conducive to decreasing nutrient leaching and increasing nutrient contents (Agegnehu et al., 2017; El-Naggar et al., 2019; Zhao et al., 2020). In addition, the more pronounced improvement of soil fertility caused by the addition of biochar with CEM may also ascribe the beneficial microorganisms that boost soil nutrient cycling and organic matter decomposition, thereby improving soil nutrient supply (Talaat, 2019; El-Mageed et al., 2020).

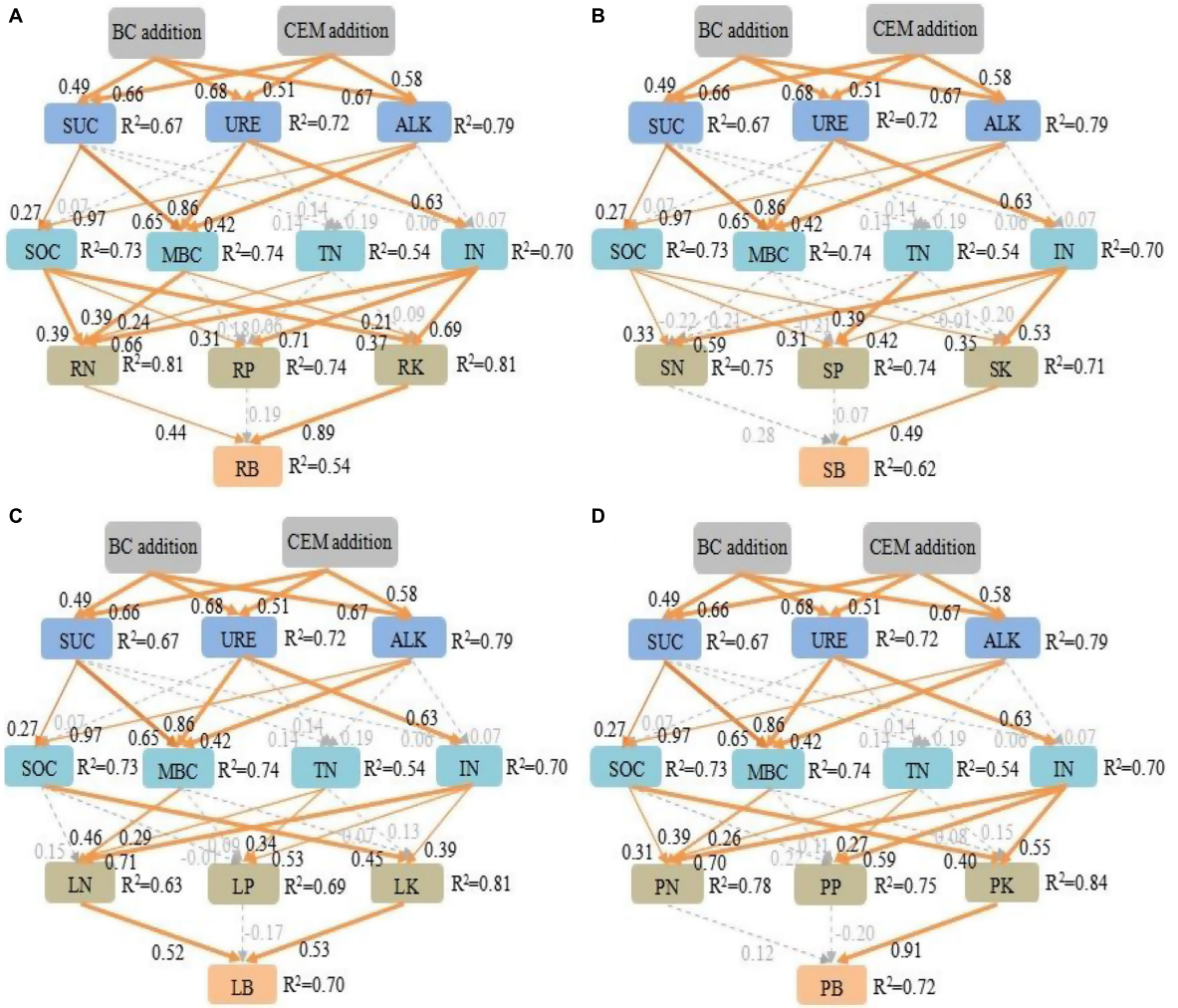

FIGURE 6 | The structure equation model investigates the plausible pathways by which biochar addition and CEM addition affected root biomass **(A)**, shoot biomass **(B)**, leaf biomass **(C)**, and plant total biomass **(D)**. Goodness-of-fit statistics for the model: root biomass: $\chi^2 = 118$, df = 45, $p < 0.05$, root mean square error of approximation (RMSEA) = 0.26. Shoot biomass: $\chi^2 = 127$, df = 45, $p < 0.05$, shoot mean square error of approximation (RMSEA) = 0.28. Leaf biomass: $\chi^2 = 113.6$, df = 45, $p < 0.05$, leaf mean square error of approximation (RMSEA) = 0.25. Plant total biomass: $\chi^2 = 153.9$, df = 45, $p < 0.05$, total mean square error of approximation (RMSEA) = 0.32. Orange solid arrows from thick to thin indicate positive pathways ($p < 0.001$, $p < 0.01$, and $p < 0.05$) and light dashed gray arrows indicate non-significant relationships ($p > 0.05$). The numbers next to arrows are standardized path coefficients, and the arrow width represents the strength of the relationship. The proportion of the variation (R^2) values occurs aside each response variable in the model. SUC, sucrase activity; URE, urease activity; ALK, alkaline phosphatase activity; SOC, soil organic carbon; MBC, microbial biomass carbon; TN, total nitrogen; IN, NH_4^+ and NO_3^-; RN, root total nitrogen; RP, root total phosphorus; RK, root total potassium; SN, shoot total nitrogen; SP, shoot total phosphorus; SK, shoot total potassium; LN, leaf total nitrogen; LP, leaf total phosphorus; LK, leaf total potassium; PN, plant total nitrogen; PP, plant total phosphorus; PK, plant total potassium; RB, root biomass; SB, shoot biomass; LB, leaf biomass; PB, plant total biomass.

Enhancement of Soil Organic Carbon, Microbial Biomass Carbon, NH_4^+, and NO_3^- Availability

Considerable reviews from field or laboratory experiments confirmed that biochar could be used to reduce carbon mineralization and sequestrate soil carbon (Lehmann, 2007; Agegnehu et al., 2016; Liu et al., 2021). We showed that SOC and MBC were facilitated under the application of biochar and CEM, as supported by a meta-analysis study by Liu et al. (2016), who revealed biochar addition elevated SOC and MBC by 40 and 18%, respectively. The increased soil SOC and MBC following biochar and CEM addition may be explained by several reasons: (i) the inertness and rich polychromatic acids of biochar may store carbon in soil and increase the mineralization of SOC *via* activating soil microbial activity and preserving labile soil organic matter (Cooper et al., 2020); (ii) the amendment of biochar and CEM would be more beneficial for accelerating soil carbon decomposition through improving soil aeration and modulating microbial diversity (Talaat, 2019; Liu et al., 2021); (iii) the promoted plant biomass and endogenous carbon formation or exogenous carbon input induced by biochar and

CEM would increase soil aggregation formation and strengthen fertility conservation (Liu et al., 2016; Caban et al., 2020).

Amendment of biochar and CEM led to improvements in soil NH_4^+ and NO_3^- availabilities, which may be closely connected with stimulated soil N recycling in coastal wetland soil. Increases in soil NH_4^+ and NO_3^- may have been linked to the alteration of soil N mineralization to immobilization and the negatively charged biochar surface, in turn influencing plants N absorption (Jones et al., 2012; Lentz et al., 2014; Agegnehu et al., 2017). The improvement of N immobilization and the reduction of N leaching following biochar addition may also be responsible for altering the nitrification rate and enhancing NH_4^+ content (Sun et al., 2017). The CEM supplement modified the diversity and abundance of beneficial microorganisms in salt-affected soils, which, in turn, stimulated soil organic matter turnover and N availability (Olle and Williams, 2013; Talaat, 2019). The path analysis suggested that soil NH_4^+ and NO_3^- were closely correlated with enzyme activities, indicating that biochar and CEM addition may accelerate N transformations by enhancing soil enzyme and microbial activities (Lehmann et al., 2011; Ameloot et al., 2015). Furthermore, the stimulated soil inorganic N availability after biochar and CEM addition was beneficial for alfalfa growth and productivity.

Stimulation of Soil Enzyme Activities

In this study, the mixture of biochar and CEM exerted a beneficial impact on soil sucrase, urease, and alkaline phosphatase activities. Biochar application directly drives changes in soil enzyme activities by targeting diverse soil substrates for the decomposition of SOC (Sinsabaugh, 2010). The priming effect on soil microbial and enzyme activities induced by biochar may stimulate microbial growth by increasing the SOC bioavailability (Pokharel et al., 2020). Significantly, the most likely mechanisms promoting enzyme activities included the following parts: (i) improved soil aggregate formation and water retention (Palansooriya et al., 2019); (ii) enhanced nutrients supply for microbes through improving flows of air, water, and nutrients within soil substrates (Liu et al., 2016); (iii) decreased salinity and provided sufficient carbon sources for microorganisms (Mehmood et al., 2020; Liu et al., 2021). In addition, CEM as a microbial inoculant contained many species of microorganisms and produced biologically active agents that can stimulate the decomposition of organic materials and soil enzyme activities (Talaat, 2019). Soil enzymes are good indicators of soil quality due to the crucial role in influencing microbial activity and nutrient cycling (Pokharel et al., 2020). In our case, soil sucrase, urease, and alkaline phosphatase activities were directly associated with SOC, MBC, and inorganic N, implying that the elevated soil enzyme activities and nutrient availability would be helpful to ameliorate soil quality and promote alfalfa growth (Chávez-García and Siebe, 2019; El-Naggar et al., 2019). Thus, the use of biochar combined with CEM in coastal wetlands soils showed encouraging results, resulting in increased soil enzyme activities, ameliorated soil quality, and improved alfalfa nutrient absorption and growth.

CONCLUSION

Biochar addition alone and combined with CEM decreased soil salt and improved alfalfa growth, nutrient uptake, soil fertility, SOC, MBC, NH_4^+, NO_3^-, and enzyme activities in coastal wetlands. As compared with the CK−CEM treatment, alfalfa mass in the B_{10}−CEM, B_{20}−CEM, B_{30}−CEM, CK + CEM, B_{10} + CEM, B_{20} + CEM, B_{30} + CEM treatment enhanced by 20.01, 91.93, 102.8, 71.91, 84.11, 138.5, and 120.5%, respectively. The B_{20} + CEM treatment could achieve the best performance in terms of elevating soil quality and enzyme activities, contributing to the highest nutrient concentration and growth of alfalfa. Alfalfa biomass was regulated by elevated plant nutrient uptake through promoting soil quality, such as SOC, MBC, TN, NH_4^+, NO_3^-, soil sucrase, urease, and alkaline phosphatase activities. Together, applying biochar compositing with CEM into coastal saline-alkali soils could take as an efficient management practice to accelerate soil nutrient cycling and improve alfalfa productivity. This study could provide effective coastal wetlands restoration approach, and further research should be confirmed in the field.

DATA AVAILABILITY STATEMENT

The original contributions presented in the study are included in the article/supplementary material, further inquiries can be directed to the corresponding author.

AUTHOR CONTRIBUTIONS

QC contributed to data curation, formal analysis, methodology, and writing of the original draft. JX contributed to data curation and supervision. LP contributed to visualization, methodology, and investigation. XZ contributed to conceptualization and formal analysis. FQ contributed to review and editing. All authors reviewed, edited, and approved the manuscript.

FUNDING

This study was funded by the Joint Funds of the National Natural Science Foundation of China (U2006215), the National Natural Science Foundation of China (41901118), Natural Science Foundation of Shandong Province (ZR2019PD012), Shandong Key Laboratory of Coastal Environmental Processes, YICCAS (2019SDHADKFJJ10), and Taishan Scholars Program of Shandong Province, China (No. TSQN201909152).

REFERENCES

Agegnehu, G., Bass, A. M., Nelson, P. N., and Bird, M. I. (2016). Benefits of biochar, compost and biochar-compost for soil quality, maize yield and greenhouse gas emissions in a tropical agricultural soil. *Sci. Total Environ.* 543, 295–306. doi: 10.1016/j.scitotenv.2015.11.054

Agegnehu, G., Srivastava, A. K., and Bird, M. I. (2017). The role of biochar and biochar-compost in improving soil quality and crop performance: a review. *Appl. Soil Ecol.* 119, 156–170. doi: 10.1016/j.apsoil.2017.06.008

Akhtar, S. S., Andersen, M. N., Naveed, M., Zahir, Z. A., and Liu, F. (2015). Interactive effect of biochar and plant growth-promoting bacterial endophytes on ameliorating salinity stress in maize. *Funct. Plant Biol.* 42, 770–781. doi: 10.1071/FP15054

Ali, S., Rizwan, M., Qayyum, M. F., Ok, Y. S., Ibrahim, M., Riaz, M., et al. (2017). Biochar soil amendment on alleviation of droughtand salt stress in plants: a critical review. *Environ. Sci. Pollut. Res.* 24, 12700–12712. doi: 10.1007/s11356-017-8904-x

Ameloot, N., Sleutel, S., Das, K. C., Kanagaratnam, J., and De Neve, S. (2015). Biochar amendment to soils with contrasting organic matter level: effects on N mineralization and biological soil properties. *Glob. Change Biol. Bioenergy* 7, 135–144. doi: 10.1111/gcbb.12119

Biederman, L. A., and Harpole, W. S. (2013). Biochar and its effects on plant productivity and nutrient cycling: a meta-analysis. *Glob. Change Biol. Bioenergy* 5, 202–214. doi: 10.1111/gcbb.12037

Caban, M., Folentarska, A., Lis, H., Kobylis, P., Bielicka-Giełdon, A., Kumirska, J., et al. (2020). Critical study of crop-derived biochars for soil amendment and pharmaceutical ecotoxicity reduction. *Chemosphere* 248:125976. doi: 10.1016/j.chemosphere.2020.125976

Cai, J. F., Jiang, F., Liu, X. S., Sun, K., Wang, W., Zhang, M. X., et al. (2021). Biochar-amended coastal wetland soil enhances growth of Suaeda salsa and alters rhizosphere soil nutrients and microbial communities. *Sci. Total Environ.* 788:147707. doi: 10.1016/j.scitotenv.2021.147707

Cao, J., Li, X., Kong, X., Zed, R., and Dong, L. (2012). Using alfalfa (*Medicago sativa*) to ameliorate salt-affected soils in Yingda irrigation district in Northwest China. *Acta Ecol. Sin.* 32, 68–73. doi: 10.1016/j.chnaes.2011.12.001

Chaganti, V. N., Crohn, D. M., and Šimůnek, J. (2015). Leaching and reclamation of a biochar and compost amended saline-sodic soil with moderate SAR reclaimed water. *Agric. Water Manag.* 158, 255–265. doi: 10.1016/j.agwat.2015.05.016

Chávez-García, E., and Siebe, C. (2019). Rehabilitation of a highly saline-sodic soil using a rubblebarrier and organic amendments. *Soil Tillage Res.* 189, 176–188. doi: 10.1016/j.still.2019.01.003

Chen, M., Alim, N., Zhang, Y. T., Xu, N., and Cao, X. D. (2018). Contrasting effects of biochar nanoparticles on the retention and transport of phosphorus in acidic and alkaline soils. *Environ. Pollut.* 239, 562–570. doi: 10.1016/j.envpol.2018.04.050

Cooper, J., Greenberg, I., Ludwig, B., Hippich, L., Ficher, D., Glaser, B., et al. (2020). Effect of biochar and compost on soil properties and organic matter in aggregate size fractions under field conditions. *Agric. Ecosyst. Environ.* 295:106882. doi: 10.1016/j.agee.2020.106882

Ding, Y., Liu, Y. G., Liu, S. B., Li, Z. W., Tan, X. F., and Huang, X. X. (2016). Biochar to improve soil fertility: a review. *Agron. Sustain. Dev.* 36, 35–52. doi: 10.1007/s13593-016-0372-z

El-Mageed, T. A. A., Rady, M. M., Taha, R. S., El Azeam, S. A., Simpson, C. R., and Semida, W. M. (2020). Effects of integrated use of residual sulfur-enhanced biochar with effective microorganisms on soil properties, plant growth and short-term productivity of *Capsicum annuum* under salt stress. *Sci. Hortic.* 261:108930. doi: 10.1016/j.scienta.2019.108930

El-Naggar, A., Lee, S. S., Rinklebe, J., Farooq, M., Song, H., Sarmah, A. K., et al. (2019). Biochar application to low fertility soils: a review of current status, and future prospects. *Geoderma* 337, 536–554. doi: 10.1016/j.geoderma.2018.09.034

Gunarathne, V., Senadeera, A., Gunarathne, U., Biswas, J. K., Almaroai, Y. A., and Vithanage, M. (2020). Potential of biochar and organic amendments for reclamation of coastal acidic-salt affected soil. *Biochar* 2, 107–120. doi: 10.1007/s42773-020-00036-4

Hammer, E. C., Forstreuter, M., Rillig, M. C., and Kohler, J. (2015). Biochar increases arbuscular mycorrhizal plant growth enhancement and ameliorates salinity stress. *Appl. Soil Ecol.* 96, 114–121. doi: 10.1016/j.apsoil.2015.07.014

Hassani, A., Azapagic, A., and Shokri, N. (2020). Predicting long-term dynamics of soil salinity and sodicity on a global scale. *Proc. Natl. Acad. Sci. U.S.A.* 117, 33017–33027. doi: 10.1073/pnas.2013771117

Hu, C., and Qi, Y. C. (2013). Long-term effective microorganisms application promote growth and increase yields and nutrition of wheat in China. *Eur. J. Agron.* 46, 63–67. doi: 10.1016/j.eja.2012.12.003

Huang, L. B., Bai, J. H., Chen, B., Zhang, K. J., Huang, C., and Liu, P. P. (2012). Two-decade wetland cultivation and its effects on soil properties in salt marshes in the Yellow River Delta, China. *Ecol. Inform.* 10, 49–55. doi: 10.1016/j.ecoinf.2011.11.001

Jeffery, S., Memelink, I., Hodgson, E., Jones, S., van de Voorde, T. F., Bezemer, T. M., et al. (2017). Initial biochar effects on plant productivityderive from N fertilization. *Plant Soil* 13, 1–4. doi: 10.1007/s11104-016-3171-z

Jones, D. L., Rousk, J., Edwards-Jones, G., DeLuca, T. H., and Murphy, D. V. (2012). Biochar-mediated changes in soil quality and plant growth in a three year field trial. *Soil Biol. Biochem.* 45, 113–124. doi: 10.1016/j.soilbio.2011.10.012

Kim, H. S., Kim, K. R., Yang, J. E., Ok, Y. S., Owens, G., Nehls, T., et al. (2016). Effect of biochar on reclaimed tidal land soil properties and maize (*Zea mays* L.) response. *Chemosphere* 142, 153–159. doi: 10.1016/j.chemosphere.2015.06.041

Kirwan, M. L., and Megonigal, J. P. (2013). Tidal wetland stability in the face of human impactsand sea-level rise. *Nature* 504, 53–60. doi: 10.1038/nature12856

Lashari, M. S., Ye, Y., Ji, H., Li, L., Kibue, G. W., Lu, H., et al. (2015). Biochar-manure compost in conjunction with pyroligneous solution alleviated salt stress and improved leaf bioactivity of maize in a saline soil from central China: a 2-year field experiment. *J. Sci. Food Agric.* 95, 1321–1327. doi: 10.1002/jsfa.6825

Lehmann, J. (2007). A handful of carbon. *Nature* 447, 143–144. doi: 10.1038/447143a

Lehmann, J., Rillig, M. C., Thies, J., Masiello, C. A., Hockaday, W. C., and Crowley, D. (2011). Biochar effects on soil biota-a review. *Soil. Biol. Biochem.* 43, 1812–1836. doi: 10.1016/j.soilbio.2011.04.022

Lentz, R. D., Ippolito, J. A., and Spokas, K. A. (2014). Biochar and manure effects on net nitrogen mineralization and greenhouse gas emissions from calcareous soil under corn. *Soil Sci. Soc. Am. J.* 78, 1641–1655. doi: 10.2136/sssaj2014.05.0198

Li, K. S., Li, Q. X., Geng, Y. H., and Liu, C. X. (2021). An evaluation of the effects of microstructural characteristics and frost heave on the remediation of saline-alkali soils in the Yellow River Delta, China. *Land Degrad. Dev.* 32, 1325–1337. doi: 10.1002/ldr.3801

Liang, J. F., An, J., Gao, J. Q., Zhang, X. Y., Song, M. H., and Yu, F. H. (2019). Interactive effects of biochar and AMF on plant growth and greenhouse gas emissions from wetland microcosms. *Geoderma* 346, 11–17. doi: 10.1016/j.geoderma.2019.03.033

Liu, J., Jiang, B. S., Shen, J. L., Zhu, X., Yi, W. Y., Li, Y., et al. (2021). Contrasting effects of straw and straw-derived biochar applications on soil carbon accumulation and nitrogen use efficiency in double-rice cropping systems. *Agric. Ecosyst. Environ.* 311:107286. doi: 10.1016/j.agee.2020.107286

Liu, M. H., Zhuo, Z. J., Chen, L., Wang, L. Q., Ji, L. Z., and Xiao, Y. (2020). Influences of arbuscular mycorrhizae, phosphorus fertiliser and biochar on alfalfa growth, nutrient status and cadmium uptake. *Ecotoxicol. Environ. Saf.* 196:110537. doi: 10.1016/j.ecoenv.2020.110537

Liu, S. L., Hou, X. Y., Yang, M., Cheng, F. Y., and Coxixo, A. (2018). Factors driving the relationships between vegetation and soil properties in the Yellow River Delta, China. *Catena* 165, 279–285. doi: 10.1016/j.catena.2018.02.004

Liu, S. W., Zhang, Y. J., Zong, Y. J., Hu, Z. Q., Wu, S., Zhou, J., et al. (2016). Response of soil carbon dioxide fluxes, soil organic carbon and microbial biomass carbon to biochar amendment: a meta-analysis. *Glob. Change Biol. Bioenergy* 8, 392–406. doi: 10.1111/gcbb.12265

Luo, X. X., Liu, G. C., Xia, Y., Chen, L., and Jiang, Z. X. (2017). Use of biochar-compost to improve properties and productivity of the degraded coastal soil in the Yellow River Delta, China. *J. Soils Sediments* 17, 780–789. doi: 10.1007/s11368-016-1361-1

Mehmood, I., Qiao, L., Chen, H. Q., Tang, Q. Y., Woolf, D., and Fam, M. S. (2020). Biochar addition leads to more soil organic carbon sequestration under a maize-rice cropping system than continuous flooded rice. *Agric. Ecosyst. Environ.* 298:106965. doi: 10.1016/j.agee.2020.106965

Olle, M., and Williams, I. H. (2013). Effective microorganisms and their influence on vegetable production-a review. *J. Hortic. Sci. Biotechnol.* 88, 380–386. doi: 10.1080/14620316.2013.11512979

Olmo, M., Villar, R., Salazar, P., and Alburquerque, J. A. (2016). Changes in soil nutrient availability explain biochar's impact on wheat root development. *Plant Soil* 399, 333–343. doi: 10.1007/s11104-015-2700-5

Palansooriya, K. N., Ok, Y. S., Awad, Y. M., Lee, S. S., Sung, J. K., Koutsospyros, A., et al. (2019). Impacts of biochar application on upland agriculture: a review. *J. Environ. Manage.* 234, 52–64. doi: 10.1016/j.jenvman.2018.12.085

Pokharel, P., Ma, Z., and Chang, S. X. (2020). Biochar increases soil microbial biomass with changes in extra-and intracellular enzyme activities: a global meta-analysis. *Biochar* 2, 65–79. doi: 10.1007/s42773-020-00039-1

Qadir, M., Schubert, S., Ghafoor, A., and Murtaza, G. (2001). Amelioration strategies for sodic soils: a review. *Land Degrad. Dev.* 12, 357–386. doi: 10.1002/ldr.458

Raklami, A., Tahiri, A. I., Bechtaoui, N., Abdelhay, E. G., Pajuelo, E., Baslam, M., et al. (2021). Restoring the plant productivity of heavy metal-contaminated soil using phosphate sludge, marble waste, and beneficial microorganisms. *J. Environ. Sci.* 99, 210–221. doi: 10.1016/j.jes.2020.06.032

Saifullah, Dahlawi, S., Naeem, A., Rengel, Z., and Naidu, R. (2018). Biochar application for the remediation of salt-affected soils: challenges and opportunities. *Sci. Total Environ.* 625, 320–335.

Sigua, G. C., Novak, J. M., Watts, D. W., Johnson, M. G., and Spokas, K. (2016). Efficacies of designer biochars in improving biomass and nutrient uptake of winter wheat grown in a hard setting subsoil layer. *Chemosphere* 142, 176–183. doi: 10.1016/j.chemosphere.2015.06.015

Sinsabaugh, R. L. (2010). Phenol oxidase, peroxidase and organic matter dynamics of soil. *Soil. Biol. Biochem.* 42, 391–404. doi: 10.1016/j.soilbio.2009.10.014

Stagg, C. L., Schoolmaster, D. R., Krauss, K. W., Cormier, N., and Conner, W. H. (2017). Causal mechanisms of soil organic matter decomposition:deconstructing salinity and flooding impacts in coastal wetlands. *Ecology* 98, 2003–2018. doi: 10.1002/ecy.1890

Sun, H. J., Lu, H. Y., Chu, L., Shao, H. B., and Shi, W. M. (2017). Biochar applied with appropriate rates can reduce N leaching, keep N retention and not increase NH3 volatilization in a coastal saline soil. *Sci. Total Environ.* 575, 820–825. doi: 10.1016/j.scitotenv.2016.09.137

Sun, J., He, F., Shao, H. B., Zhang, Z. H., and Xu, G. (2016). Effects of biochar application on *Suaeda salsa* growth and saline soil properties. *Environ. Earth Sci.* 75:630. doi: 10.1007/s12665-016-5440-9

Talaat, N. B. (2019). Effective microorganisms: an innovative tool for inducing common bean (*Phaseolus vulgaris* L.) salt-tolerance by regulating photosynthetic rate and endogenous phytohormones production. *Sci. Hortic.* 250, 254–265. doi: 10.1016/j.scienta.2019.02.052

Talaat, N. B., Ghoniem, A. E., Abdelhamid, M. T., and Shawky, B. T. (2015). Effective microorganisms improve growth performance, alter nutrients acquisition and induce compatible solutes accumulation in common bean (*Phaseolus vulgaris* L.) plants subjected to salinity stress. *Plant Growth Regul.* 75, 281–295. doi: 10.1007/s10725-014-9952-6

Tan, X., Kong, L., Yan, H., Wang, Z., He, W., and Wei, G. (2014). Influence of soil factors on the soil enzyme inhibition by Cd. *Acta Agric. Scand. Sect. B Soil Plant Sci.* 64, 666–674. doi: 10.1080/09064710.2014.953985

Vance, E. D., Brookes, P. C., and Jenkinson, D. S. (1987). An extraction method for measuring soil microbial biomass C. *Soil. Biol. Biochem.* 19, 703–707. doi: 10.1016/0038-0717(87)90052-6

Wang, Y., Li, W. Q., Du, B. H., and Li, H. H. (2021). Effect of biochar applied with plant growth-promoting rhizobacteria (PGPR) on soil microbial community composition and nitrogen utilization in tomato. *Pedosphere* 31, 872–881. doi: 10.1016/S1002-0160(21)60030-9

Zhang, F. G., Liu, M. H., Li, Y., Che, Y. Y., and Xiao, Y. (2019). Effects of arbuscular mycorrhizal fungi, biochar and cadmium on the yield and element uptake of *Medicago sativa*. *Sci. Total Environ.* 655, 1150–1158. doi: 10.1016/j.scitotenv.2018.11.317

Zhao, Q. Q., Bai, J. H., Zhang, G. L., Jia, J., Wang, W., and Wang, X. (2018). Effects of water and salinity regulation measures on soil carbon sequestration in coastal wetlands of the Yellow River Delta. *Geoderma* 319, 219–229. doi: 10.1016/j.geoderma.2017.10.058

Zhao, W., Zhou, Q., Tian, Z. Z., Cui, U. T., Liang, Y., and Wang, H. Y. (2020). Apply biochar to ameliorate soda saline-alkali land, improve soil function and increase corn nutrient availability in the Songnen Plain. *Sci. Total Environ.* 722:137428. doi: 10.1016/j.scitotenv.2020.137428

Conflict of Interest: The authors declare that the research was conducted in the absence of any commercial or financial relationships that could be construed as a potential conflict of interest.

Publisher's Note: All claims expressed in this article are solely those of the authors and do not necessarily represent those of their affiliated organizations, or those of the publisher, the editors and the reviewers. Any product that may be evaluated in this article, or claim that may be made by its manufacturer, is not guaranteed or endorsed by the publisher.

frontiers in Ecology and Evolution

ORIGINAL RESEARCH
published: 24 February 2022
doi: 10.3389/fevo.2022.856479

Responses of Above- and Belowground Carbon Stocks to Degraded and Recovering Wetlands in the Yellow River Delta

*Pengshuai Shao, Hongyan Han, Hongjun Yang, Tian Li, Dongjie Zhang, Jinzhao Ma, Daixiang Duan and Jingkuan Sun**

Shandong Key Laboratory of Eco-Environmental Science for the Yellow River Delta, Binzhou University, Binzhou, China

Wetlands reserve a large amount of organic carbon (C), playing a key role in contributing global C stocks. It is still uncertain to evaluate wetland C stocks due to wetland disturbance or degradation. In this study, we performed the degraded and recovering wetlands to estimate aboveground C stocks and soil organic C (SOC) stocks at the depth of 1 m in the Yellow River Delta. Our results showed that the recovering wetland sequestered 1.67 Mg C ha^{-1} aboveground, approximately three times higher than those (0.56 Mg C ha^{-1}) of degraded wetland, and recovering wetland stored more SOC of 51.86 Mg C ha^{-1} in the top 1 m soils, approximately two times higher than those (26.94 Mg C ha^{-1}) of degraded wetland. These findings indicate that the transformation between degraded and recovering wetlands is associated with the conversion of wetland C sources and sinks. The shifts in aboveground C stocks and SOC stocks were mainly attributed to changed biotic (i.e., aboveground biomass and photosynthetic C) and abiotic (i.e., soil water, salinity, SOC and N contents, and SOC compounds) factors. The improved soil water, salinity, and nutrient enhance C reservoir, sequestering more C in aboveground vegetation and storing more SOC *via* photosynthetic C input of plant litter and root exudates in recovering wetland than in degraded wetland with poor soil conditions. The relationships among wetland C stocks, plant, and soil properties indicate plant-soil interaction driving wetland ecosystem C stocks in degraded and recovering wetlands. Our research suggests that wetland restoration highlights a positive response to "carbon neutrality" by efficiently sequestering C above- and belowground.

Keywords: wetland C stocks, aboveground biomass, soil organic carbon, wetland degradation, wetland restoration

OPEN ACCESS

Edited by:
Guangxuan Han,
Yantai Institute of Coastal Zone Research (CAS), China

Reviewed by:
Weiqi Wang,
Fujian Normal University, China
Guan Bo,
Ludong University, China

***Correspondence:**
Jingkuan Sun
sunjingkuan@bzu.edu.cn

Specialty section:
This article was submitted to Conservation and Restoration Ecology, a section of the journal Frontiers in Ecology and Evolution

Received: *17 January 2022*
Accepted: *28 January 2022*
Published: *24 February 2022*

Citation:
Shao P, Han H, Yang H, Li T, Zhang D, Ma J, Duan D and Sun J (2022) Responses of Above- and Belowground Carbon Stocks to Degraded and Recovering Wetlands in the Yellow River Delta. Front. Ecol. Evol. 10:856479. doi: 10.3389/fevo.2022.856479

INTRODUCTION

Wetlands serve as the carbon (C) sink and reservoir, playing an important role in global ecosystem C stocks (Duarte et al., 2013), although they occupy only 5–8% of the earth's area, accounting for 20–30% of global C storage (Xiao et al., 2019). However, a large number of wetlands have been degraded in the past decades due to reclamation, construction projects, or climate warming (Xu W. et al., 2019). Wetland degradation associated with the loss of plant biomass and soil C implies that wetlands are transformed from C sink to C source, exacerbating global climate warming

(Baustian et al., 2021). To alleviate climate warming and enhance wetland ecosystem functions, the governments and scientists pay more attention to the protection and restoration of wetlands (Crooks et al., 2018). Studies have reported that wetland restoration can greatly recover above- and belowground ecosystem structures and function, such as increasing plant diversity and biomass, storing more C in soils, and structuring stable linkage among plant, microorganism, and soil (Ma et al., 2017; Orth et al., 2020). Based on the goal of C neutrality, it is necessary to evaluate wetland C stocks and clarify the regulation mechanism of soil organic C (SOC) storage during the degradation and restoration of wetlands.

Wetland C budgets are attributed to the balance between plant C input and soil C loss (Spivak et al., 2019). The disturbed wetlands would influence plant C assimilation and soil organic matter (SOM) decomposition. Wetland degradation, such as wetland converting to saline-alkali land, exacerbates soil salinity and nutrient stress, which result in the decline in plant productivity and soil microbial C degradation (Herbert et al., 2015; Servais et al., 2019). The unbalance between the input and output of organic matter affects wetland C turnover and storage. Despite plant-derived C contribution to wetland C stocks through litter and root exudates, C quality (defined as labile and recalcitrant C compounds) also plays a crucial role in mediating wetland C retention (Xia et al., 2021). Labile C compounds (e.g., carbohydrates) are easily degraded by microorganisms with a fast turnover rate (Shao et al., 2021). Recalcitrant C compounds contain macromolecular substances such as aromatic C compounds and lignin, which are resistant to be degraded and persist in soils for decades or even centuries, contributing to ecosystem C storage (Suseela et al., 2013). However, the empirical evidence is still lacking to assess above- and belowground C reservoirs in disturbed wetlands through integrating C quantity and quality.

Phragmites australis (*P. australis*) is the dominant species with strong photosynthetic capacity, widely spreading over wetland ecosystems (Guan et al., 2017). The change in wetland dominated by *P. australis* can exhibit substantial effects on wetland ecosystem C stocks. Using complementary approaches of C estimation, natural ^{13}C isotope, and mid-infrared spectroscopy (mid-IR), we evaluated above- and belowground C stocks and illustrated the plant-soil interaction of degraded and recovering wetlands in the Yellow River Delta. The goal of this study was to (1) assess the responses of wetland C stocks (i.e., plant C and SOC stocks) to degraded and recovering wetlands, (2) detect the dynamics of SOC compounds in degraded and recovering wetlands, and (3) explore how plant and soil parameters regulated above- and belowground C immobilization in our studied wetlands.

MATERIALS AND METHODS

Site Description and Sampling

Soil and plant samples were taken in July 2020 from the degraded and recovering estuarine wetlands, located in the Yellow River Delta National Nature Reserve (118°33′–119°20′E, 37°35′–38°12′N, established in 1992), Eastern China. The mean annual precipitation is 530–630 mm, mainly occurring in summer (∼70%); mean annual temperature is 11.7–12.6°C. The studied soils are classified as an alluvial soil formed by alluvial sediment of the Yellow River, with average pH of 8.57 (**Table 1**). Roads built for oil exploitation and transportation interrupted Yellow River water into wetland, exacerbating soil salinization and decreased aboveground biomass, and ultimately resulting in wetland degradation (**Figure 1**). In recent years, the governments have performed the rehabilitation engineering to recover wetland by diverting Yellow River water into degraded wetland, leading to wetland restoration with the increase in aboveground biomass (**Figure 1**). Both degraded and recovering wetlands are dominated by *P. australis* (**Figure 1**).

Sampling plots were conducted with a randomized within-wetland nested design. Six 30 m × 30 m plots were randomly selected in each degraded and recovering wetland. To weaken the spatial heterogeneity, we collected aboveground vegetation and soil cores (i.e., 0–10 cm, 10–20 cm, 20–40 cm, 40–60 cm, and 60–100 cm) from five random subplots. Plant and soil samples from subplots were then integrated to the plot level by mixing samples into one representative plant and soil sample, respectively. Sixty soil samples were collected with two wetland types × six plots × five depths. Plant samples were used to measure plant C content, natural ^{13}C isotope, and aboveground biomass, subsequently to calculate aboveground C stock. Soil samples were sieved (<2 mm) to remove residues and roots. Each soil sample was divided into two subsamples to analyze (1) water content (fresh soil subsamples), and (2) electrical conductivity (EC), pH, SOC and TN contents, natural ^{13}C isotope, and SOC compounds (air-dried soil subsamples).

Measurement and Calculation of Aboveground Plant Parameters

Leaf photosynthetic rate of *P. australis* was measured with a Li-6400XT photosynthesis system (Li-COR Inc., Lincoln, NE, United States). The harvested *P. australis* (1 m × 1 m subplot) were oven-dried to measure aboveground biomass. Plant subsamples grounding by ball milling (MM400, Retsch, Germany) and sieving (0.15 mm) were used to analyze plant C content and natural ^{13}C isotope (i.e., $\delta^{13}C$) on an elemental analysis with isotope-ratio mass spectrometry (EA-IRMA) (Elementar, Langenselbold, Germany). We estimated aboveground C stocks using the following formula: Aboveground C stocks (Mg C ha^{-1}) = plant C content (g kg^{-1}) × aboveground biomass (kg m^{-2})/100.

Soil Physicochemical Analysis and SOC Stock Estimation

Fresh soil samples were oven-dried (105°C for 48 h) to measure soil water content (SWC). We prepared soil slurries (1:5 w/v) to analyze EC and pH using an electrode meter (Jenco 6173, Jenco, United States). After sieving to 0.15 mm, soil samples were provided to calculate SOC by the potassium dichromate oxidation method, to determine soil nitrogen (N) with the

TABLE 1 | Effects of wetland degradation and restoration on soil physicochemical properties, including soil water content, electrical conductivity, pH, bulk density, and total nitrogen content.

	Soil water content (%)			Electrical conductivity (dS m^{-1})			pH			Bulk density (g cm^{-3})			Soil nitrogen content (g kg^{-1})		
Depth (cm)	Degradation	Restoration	*Statistical value*	Degradation	Restoration	*Statistical value*	Degradation	Restoration	*Statistical value*	Degradation	Restoration	*Statistical value*	Degradation	Restoration	*Statistical value*
0-10	9.09 ± 0.64	15.20 ± 1.04	*−5.02****	3.20 ± 0.51	1.38 ± 0.24	*3.22***	8.40 ± 0.10	8.82 ± 0.14	*−2.53**	1.34 ± 0.06	1.04 ± 0.06	*3.58***	0.10 ± 0.01	0.70 ± 0.04	*−14.66****
10-20	13.17 ± 2.06	20.64 ± 1.16	*−3.06**	2.64 ± 0.45	1.94 ± 0.20	*2.54**	8.54 ± 0.06	8.65 ± 0.12	*−0.80*	1.72 ± 0.02	1.48 ± 0.03	*6.04****	0.07 ± 0.02	0.80 ± 0.02	*−29.53****
20-40	11.63 ± 1.58	25.42 ± 2.11	*−5.24****	2.56 ± 0.38	2.33 ± 0.29	*0.48*	8.57 ± 0.05	8.53 ± 0.08	*0.42*	1.93 ± 0.04	1.75 ± 0.02	*3.95***	0.04 ± 0.01	0.13 ± 0.01	*−5.70****
40-60	8.13 ± 0.30	10.93 ± 0.75	*−3.46***	2.63 ± 0.27	2.57 ± 0.17	*0.19*	8.62 ± 0.05	8.55 ± 0.05	*0.92*	1.95 ± 0.02	1.80 ± 0.06	*2.64**	0.03 ± 0.01	0.04 ± 0.01	*−1.05*
60-100	17.32 ± 1.37	27.06 ± 1.28	*−5.19****	2.91 ± 0.27	2.75 ± 0.12	*0.56*	8.55 ± 0.03	8.50 ± 0.02	*1.71*	1.97 ± 0.06	1.83 ± 0.01	*2.46*$^{\wedge}$	0.03 ± 0.01	0.08 ± 0.02	*−2.64**

The symbols of ***, **, *, *and* $^{\wedge}$ *represent statistical significance with* $p < 0.001$, $p < 0.01$, $p < 0.05$, *and* $p < 0.1$, *respectively.*

elemental analyzer (Elementar vario EL III, Germany), and to analyze soil $\delta^{13}C$ after removing carbonate on an EA-IRMA (Elementar, Langenselbold, Germany). Soil bulk density (BD) was measured using an oven-dried soil sample collected with a bulk sampler. Finally, we calculated SOC stocks using the following formula: SOC stocks (Mg C ha^{-1}) = SOC content (%) × BD (g cm^{-3}) × soil depth (cm).

Soil samples (sieved to 0.15 mm) were thoroughly mixed with potassium bromide (soil:KBr = 1:40 w/w), which were used to analyze SOC compounds on a Thermo Nicolet 6,700 infrared spectrometer (Thermo Electron Scientific Instruments Corp., Madison, WI, United States). Reflectance spectra (4,000–400 cm^{-1}) were measured with 64 scans at a resolution of 4 cm^{-1}. Relative spectral peak areas at 1,630 and 1,050 cm^{-1} represent aromatic C compounds and carbohydrates, respectively (Shao et al., 2019).

Statistical Analysis

To test whether plant and soil parameters differed between degraded and recovering wetlands, we performed paired sample *t*-tests with the evaluation of normality assumption and homogenous variance using the SAS V.8.1 software (SAS Institute Inc., Cary, NC, United States). Generalized linear models (GLM) were used to determine relationships among plant parameters, soil properties, and wetland C stocks including above- and belowground C stocks.

RESULTS

Responses of Soil Physicochemical Properties to Degraded and Recovering Wetlands

Soil physicochemical properties, including SWC, EC pH, BD, and soil N content, significantly responded to degraded and recovering wetlands in different soil depths (**Table 1**). Wetland restoration greatly increased SWC and soil N content of 0–100 cm compared with degraded wetland (all $p < 0.05$). Surface soil EC (0–10 cm and 10–20 cm) in recovering wetland was lower than degraded wetland (both $p < 0.05$), whereas no change in soils of 20–100 cm ($p > 0.05$). For soil pH, wetland restoration only led to the increase in soil pH of 0–10 cm ($p < 0.05$). In addition, recovering wetland showed lower soil BD than degraded wetland at the five soil depths (all $p < 0.05$, except marginal significance at 60–100 cm).

Responses of Plant Properties and Aboveground C Stocks to Degraded and Recovering Wetlands

Our study demonstrated that wetland degradation and restoration significantly influenced aboveground biomass, leaf photosynthesis rate, and plant $\delta^{13}C$ (**Figure 1**). Compared with degraded wetland, recovering wetland substantially increased aboveground biomass and leaf photosynthesis rate by 199.0% ($p < 0.001$) and 195.7% ($p < 0.001$), respectively. The plant $\delta^{13}C$ was higher in degraded wetland (−26.67‰)

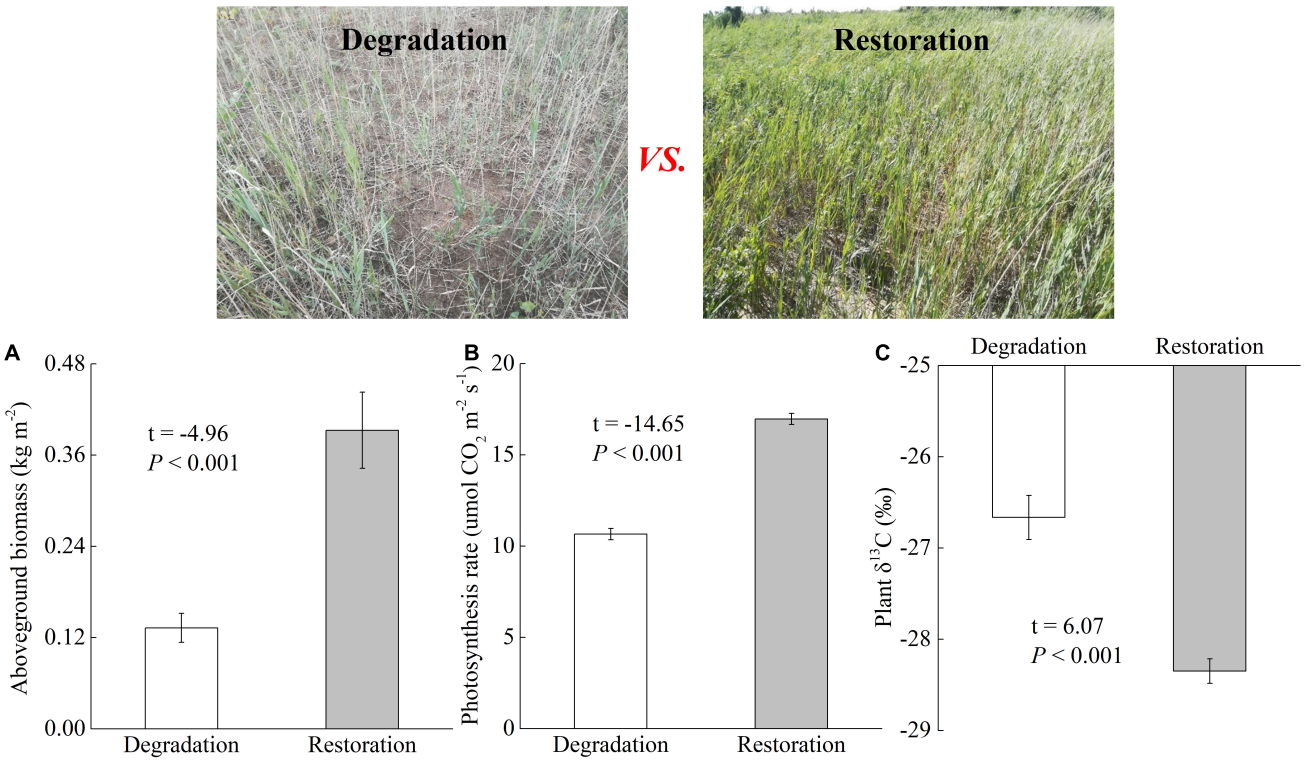

FIGURE 1 | Effects of wetland degradation and restoration on aboveground biomass **(A)**, leaf photosynthesis rate **(B)**, and natural plant $\delta^{13}C$ **(C)**.

than in recovering wetland (−28.35‰). In addition, our study estimated aboveground C stocks that were significantly changed from 0.56 Mg C ha^{-1} to 1.67 Mg C ha^{-1} as a conversion of degraded wetland to recovering wetland ($p < 0.001$; **Figure 2**).

Responses of Soil C Parameters to Degraded and Recovering Wetlands

The SOC content and soil $\delta^{13}C$ were greatly changed in degraded and recovering wetlands at the depth of 0-40 cm; no change was found at the depth of 40-100 cm (**Figure 3**). In comparison with wetland degradation, wetland restoration significantly increased the SOC content by 304.6, 517.6, and 98.62% at depth of 0-10 cm, 10–20 cm, and 20–40 cm, respectively (all $p < 0.05$). Soil $\delta^{13}C$ in recovering wetland was significantly lower than that in degraded wetland at depths of 0–10 cm (−38.39‰ vs. −35.65‰), 10–20 cm (−38.92‰ vs. −35.64‰), and 20–40 cm (−39.04‰ vs. −38.21‰) (all $p < 0.05$).

Wetland restoration led to a significant increment in SOC stocks, which increased by 6.09 Mg C ha^{-1} (0–10 cm, $p < 0.001$), 11.64 Mg C ha^{-1} (10–20 cm, $p < 0.001$), and 4.39 Mg C ha^{-1} (20–40 cm, $p < 0.001$) as degraded wetland converting to recovering wetland, whereas slight increment in SOC stocks at the depth of 40–60 cm (**Figure 4**). We evaluated SOC stocks of 0–100 cm and found that SOC stocks were greatly lower in degraded wetland (26.94 Mg C ha^{-1}) than recovering wetland (51.86 Mg C ha^{-1}) (**Figure 4A**).

The SOC compounds were estimated using the mid-IR technology (**Figure 5**). We found that wetland restoration resulted in significant reduction of soil aromatic C compounds (relative abundance, 1,630 cm^{-1}) at the depth of 0-40 cm (all

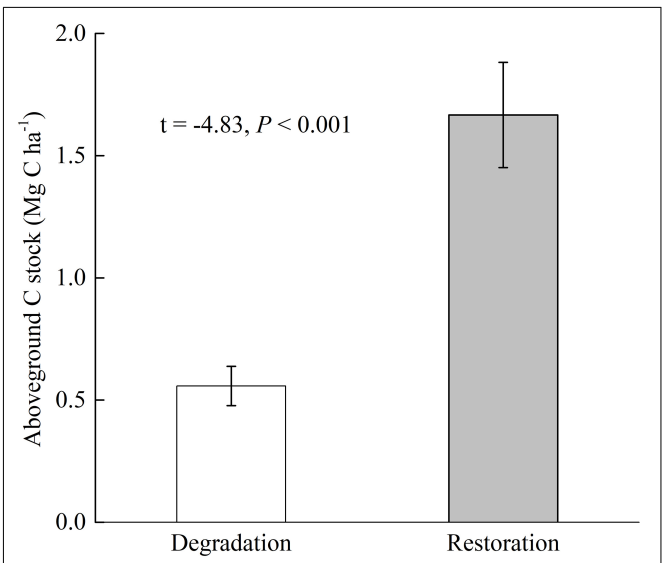

FIGURE 2 | The evaluation of aboveground carbon (C) stocks in degraded and recovering wetlands.

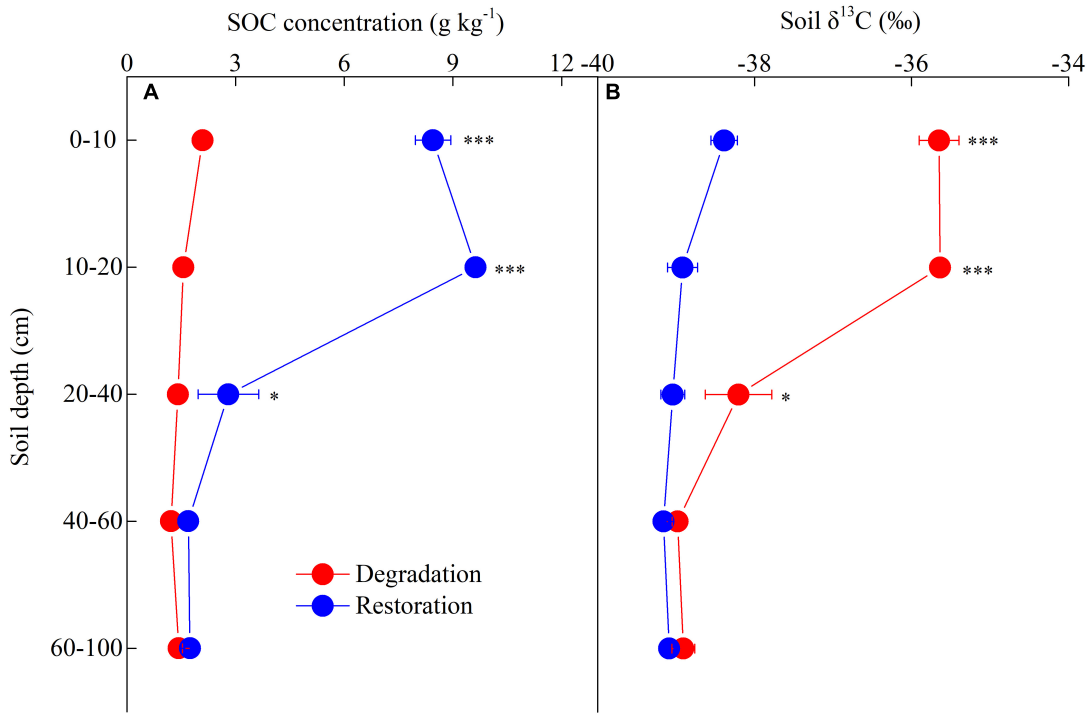

FIGURE 3 | Effects of wetland degradation and restoration on soil organic C (SOC) concentration **(A)** and natural soil $\delta^{13}C$ **(B)** at a soil depth of 0–100 cm. The symbols of *** and * represent statistical significance with $p < 0.001$ and $p < 0.05$, respectively.

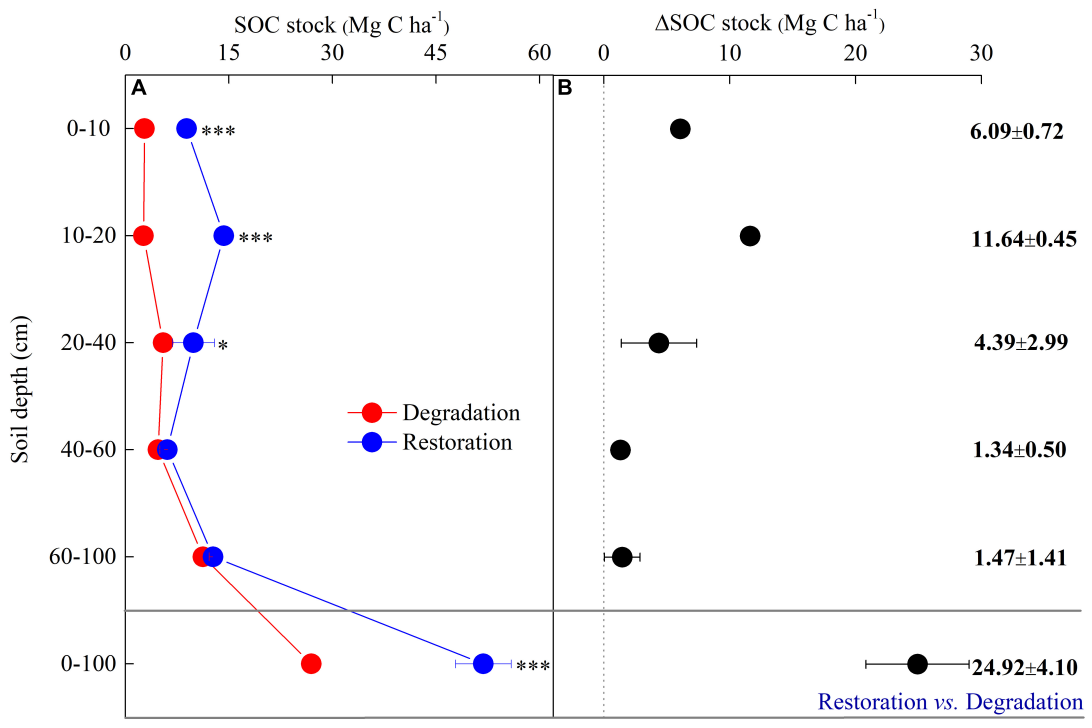

FIGURE 4 | Variations of soil organic C (SOC) stocks **(A)** and Δ SOC stocks **(B)** of 0–100 cm in degraded and recovering wetlands. The symbols of *** and * represent statistical significance with $p < 0.001$ and $p < 0.05$, respectively.

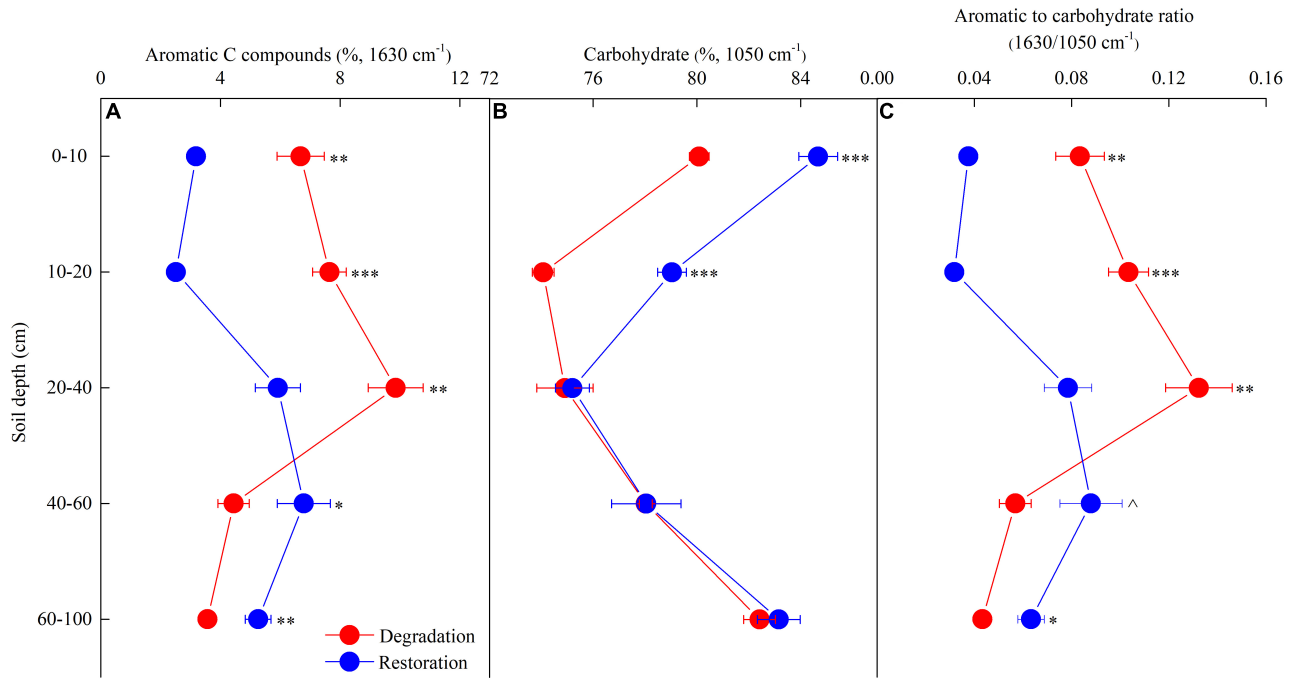

FIGURE 5 | Effects of wetland degradation and restoration on soil organic C (SOC) compounds (i.e., aromatic C compounds, **A**; and carbohydrates, **B**) and the ratio of aromatic C compounds to carbohydrates **(C)** at a soil depth of 0–100 cm. The symbols of ***, **, *, and ^ represent statistical significance with $p < 0.001$, $p < 0.01$, $p < 0.05$, and $p < 0.1$, respectively.

$p < 0.01$), while significant increase in aromatic C compounds at the depth of 40-100 cm (both $p < 0.05$, **Figure 5A**). The relative abundance of carbohydrates (1,050 cm^{-1}) was higher in recovering wetland than degraded wetland at the soil depth of 0–20 cm and did not change at a soil depth of 40-100 cm (**Figure 5B**). In addition, the ratio of aromatic C compounds to carbohydrates showed similar changes with aromatic C compounds in degraded and recovering wetlands at soil depth of 0–100 cm (**Figure 5C**).

Correlations of Above- and Belowground C Stocks With Plant and Soil Parameters in Degraded and Recovering Wetlands

Generalized linear models showed that aboveground C stocks were tightly and positively related with SWC ($R^2 = 0.54$, $p < 0.01$), soil N content ($R^2 = 0.69$, $p < 0.001$), leaf photosynthesis rate ($R^2 = 0.69$, $p < 0.001$), and aboveground biomass ($R^2 = 0.99$, $p < 0.01$), whereas negatively associated with soil EC ($R^2 = 0.60$, $p < 0.01$) and not related with plant C content ($R^2 = 0.19$, $p = 0.09$) in degraded and recovering wetlands (**Figure 6**).

In addition, SOC stocks of 0-100 cm showed positive relationships with SWC ($R^2 = 0.66$, $p < 0.001$), leaf photosynthesis rate ($R^2 = 0.72$, $p < 0.001$), aboveground biomass ($R^2 = 0.79$, $p < 0.001$), SOC content ($R^2 = 0.93$, $p < 0.001$), and carbohydrate ($R^2 = 0.57$, $p = 0.003$), while negative relationships with soil EC ($R^2 = 0.48$, $p < 0.01$), soil BD ($R^2 = 0.61$, $p = 0.002$), soil $\delta^{13}C$ ($R^2 = 0.72$, $p < 0.001$), aromatic C compounds ($R^2 = 0.54$, $p = 0.004$), and ratio of aromatic C compounds to carbohydrates ($R^2 = 0.54$, $p = 0.004$) (**Figure 7**).

DISCUSSION

Impacts of Wetland Degradation and Restoration on Aboveground C Stocks

Our study found that aboveground C stocks in recovering wetland (1.67 Mg C ha^{-1}) was approximately three times of aboveground C stocks in degraded wetland (0.56 Mg C ha^{-1}). This finding indicates that wetland restoration can recover and enhance plant C sequestration (Renzi et al., 2019; Sapkota and White, 2020).

The aboveground C stocks are originated from plant C content and aboveground biomass (Dayathilake et al., 2020). In this study, aboveground C stocks were tightly related with aboveground biomass and slightly associated with the plant C content, suggesting aboveground biomass was the predominant factor driving aboveground C stocks in degraded and recovering wetlands (Sharma et al., 2020). The prior studies have reported that the shift in aboveground biomass is ascribed to varied biotic and abiotic factors, such as soil water level, salinity, nutrient, and plant photosynthesis (Hayes et al., 2017; Zhai et al., 2022).

In degraded wetland, the increased soil environmental stress, such as low water availability and high salinity, restrains plant growth, development, and physiological characteristics (Cui et al., 2018). Water deficit and salinity stress influence

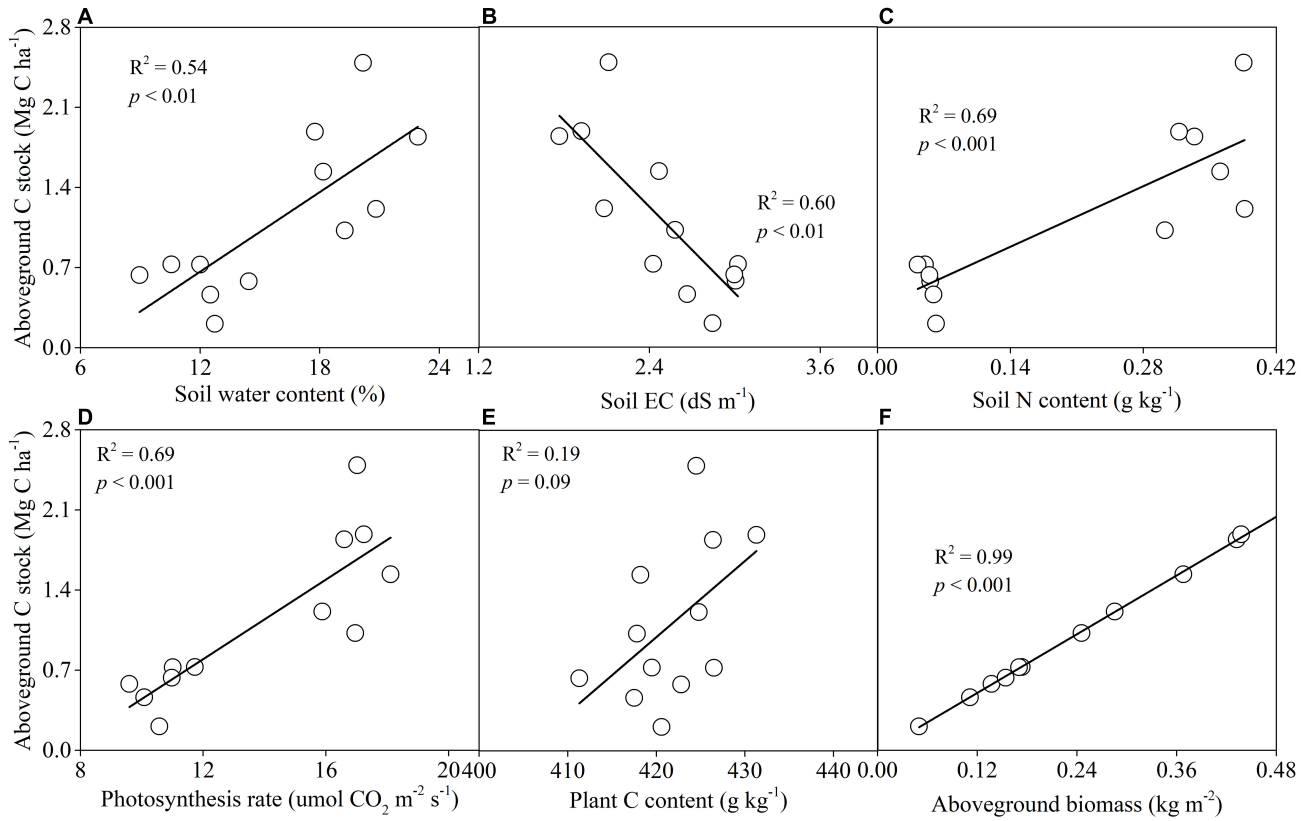

FIGURE 6 | The relationships of aboveground C stocks with soil properties (weighted average of 0–100 cm) and plant properties in degraded and recovering wetlands. Soil properties include soil water content **(A)**, soil EC **(B)**, soil N content **(C)**, photosynthesis rate **(D)**, plant C content **(E)**, and aboveground biomass **(F)**.

plant productivity *via* the following two reasons: one is to control seedling germination and the other is to regulate CO_2 assimilation of vegetation leaf (Ma et al., 2020). Under drought and salinity stress, the first response of vegetation is a decline in seedling germination and, subsequently, the reduction in plant growth, which negatively affects aboveground biomass. In addition, drought and salinity stress can impact leaf physiological characteristics to keep vegetation adaption in the severe environmental conditions (Munns et al., 2020). For example, the low stomatal conductance in degraded wetland (**Supplementary Figure 1b**) suppresses CO_2 into leaf intercellular spaces, thus reducing plant CO_2 assimilation and the photosynthesis rate (also represented by natural plant $\delta^{13}C$), subsequently resulting in low plant productivity and C sequestration.

Soil nutrients are also the key and limited factors driving plant productivity (Hayes et al., 2017). Wetland degradation leads to a large amount of soil nutrient loss due to increased surface SOM decomposition, wind erosion, or water erosion, exacerbating wetland nutrient limitation (Song et al., 2014; Wu et al., 2021). In our degraded wetland, soil N content was so scarce, which cannot satisfy plant N requirement. Low N availability held low plant productivity and showed negative feedback to wetland C sequestration.

In contrast to degraded wetland, recovering wetland sequestered more C in aboveground vegetation, which was ascribed to the improving soil conditions and plant physiological characteristics. The increasing soil water and nutrient level stimulate the vegetation growth, metabolism, and development associated with strong photosynthetic C assimilation, causing higher aboveground biomass in recovering wetland, exhibiting a positive feedback to wetland C stocks (Zhao et al., 2016; Dronova et al., 2021).

Impacts of Wetland Degradation and Restoration on SOC Stocks

Wetland soils contain a large amount of organic C, which generally serves as C sinks due to the slow decomposition rate of SOM (Stagg et al., 2018). However, wetland disturbances, such as human activities, result in wetland degradation, inducing soil C loss by increased surface SOM decomposition or erosion (Kirwan and Megonigal, 2013; Baustian et al., 2021). In our study, roads built for oil exploitation led to wetland degradation of *P. australis*. The degraded wetland stored SOC stocks of 26.94 Mg C ha^{-1} in top soil 100 cm, approximately less than two times of recovering wetland SOC stocks (51.86 Mg C ha^{-1}). Compared with recovering wetland, degraded wetland substantially diminished SOC stocks, especially at a soil depth of 0-40 cm. The dynamics of SOC stocks in degraded and recovering wetlands suggest that wetland degradation induces substantial

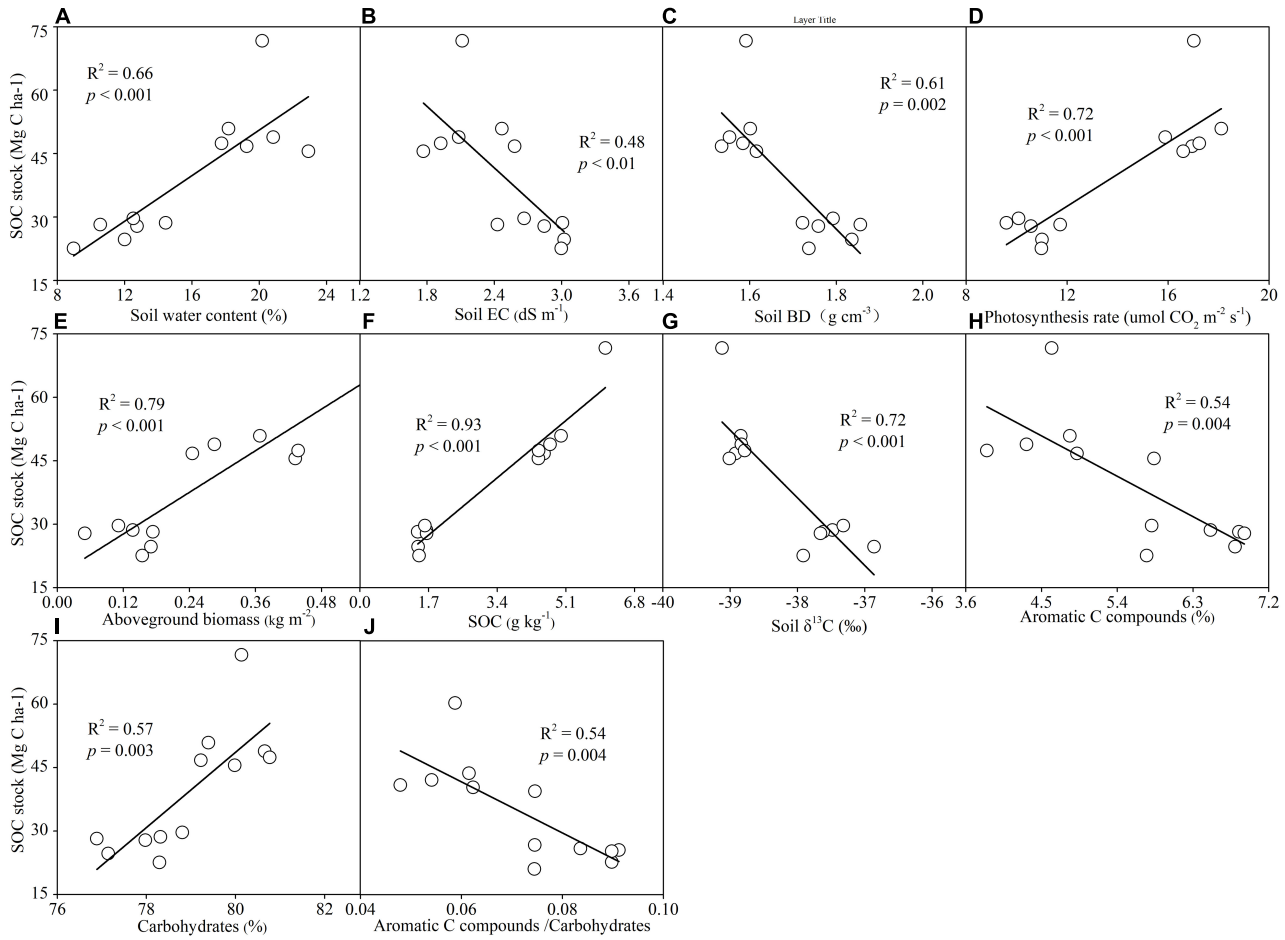

FIGURE 7 | The relationships of soil organic C (SOC) stocks with soil properties (weighted average of 0–100 cm) and plant properties in degraded and recovering wetlands. Soil properties include soil water content **(A)**, soil EC **(B)**, soil BD **(C)**, photosynthesis rate **(D)**, aboveground biomass **(E)**, SOC **(F)**, soil $\delta^{13}C$ **(G)**, aromatic C compounds **(H)**, carbohydrates **(I)**, and aromatic C compounds/carbohydrates **(J)**.

loss of SOC, and recovering the degraded wetland and protecting the existing wetlands are the effective approaches to restore and enhance C reservoir in wetland soils.

The variations of SOC stocks in degraded and recovering wetlands are likely due to the restoration of water and vegetation (Zhao et al., 2018). After wetland restoration, freshwater input increases the flooding period of wetland that led to more SOC retention in anaerobic soils because of the constrained SOM decomposition by microorganisms (Keller et al., 2015). Previous studies have reported that vegetation restoration can promote SOC accumulation (Chu et al., 2019). Wetland SOC storage originated from enhanced plant production is mainly through two pathways, namely, (1) more inputs of aboveground plant litter or (2) increased input of photosynthetic C *via* root excretion (Billah et al., 2022). These are supported by our finding that SOC stocks were tightly associated with the aboveground biomass and leaf photosynthesis rate. Recovering wetland had high available water and nitrogen supply to plant, stimulating plant growth, and subsequently contributing SOC pool through dead aboveground plant residues (Li et al., 2022). In addition, decreased soil salinity stress can relieve the salinity effect on leaf physiology, such as the increase in stomatal conductance, which induces more plant CO_2 fixation (Cui et al., 2018). Combined with high available water and nitrogen supply, vegetation in recovering wetland showed a higher photosynthesis rate, releasing more C into soils *via* root exudates, and thus enhancing SOC stocks. Compared with degraded wetland, recovering wetland substantially increased SOC stocks, especially at a soil depth of 0–40 cm (mainly root active layers), indicating that aboveground vegetation plays an important role in regulating SOC accumulation and restoration.

We observed that the changes in SOC quality (represented by specifically spectral peak of mid-IR) can influence SOC stocks in degraded and recovering wetlands (Yang et al., 2022). SOC stocks were positively associated with carbohydrates and negatively with aromatic C compounds and ratio of aromatic C compounds to carbohydrates. These correlations suggest that a greater proportion of carbohydrates in soils increases SOC storage. The aromatic C compounds are relatively stable and recalcitrant SOM compounds, which mainly are originated from plant residues (Suseela et al., 2013). Carbohydrates, as

labile SOM compounds, are derived from root exudates (Shao et al., 2021). Although the aboveground plant residues input increases the aromatic C compound, the ratio of aromatic C compounds to carbohydrates is lower in recovering wetland than in degraded wetland. The increased photosynthesis rate of recovering wetlands continuously input C of low molecular weight (e.g., glucose, fructose, and sucrose), performing great contribution to SOC storage. In addition, low natural ^{13}C isotope can represent high photosynthetic C retention in soils (Xia et al., 2021), which further corroborates the impact of carbohydrates on SOC stocks in recovering wetland, especially in topsoil of 40 cm. The shifts in the SOC quality (e.g., carbohydrates, aromatic C compounds) and their tight relationships suggest that the SOC quality is also the major driver of belowground C retention and storage.

Soil BD is a comprehensive proxy to indicate soil structure, reflect soil compaction, porosity, and fertility, and play a crucial role in affecting SOC stocks (Zhao et al., 2018). The negative relationship between SOC stocks and BD was observed under wetland degradation and restoration. Although wetland degradation increased soil BD, SOC concentration of 40 cm is substantially lower compared with that in recovering wetland. Wetland degradation results in a large amount of SOC loss due to low plant productivity and surface soil erosion (Baustian et al., 2021). The lower SOC concentration amplifies its negative effect on SOC stocks, leading to the negative feedback of BD to SOC stocks in degraded wetland.

Effects of Plant-Soil Interactions on Wetland C Stocks

Our study illustrated that biotic (i.e., aboveground biomass and photosynthetic C) and abiotic (i.e., soil water, salinity, SOC, and N contents) factors predominately determine wetland C stocks, including aboveground C stocks and SOC stocks. Soil and plant parameters do not separately influence SOC stocks, whereas plant-soil interaction mediates wetland C stocks in degraded and recovering wetlands. The conversion between disturbed wetland and protected wetland results in the shifts of plant community that is a key linkage of above- and belowground ecosystems (Xu S. et al., 2019). On the one hand, dead plant residues and root exudates supply C and nutrients to soils, persisting in soils in the form of SOM through mineral associations or aggregate occlusion (Maietta et al., 2019), and then contributing SOC stocks. On the other hand, the new C input, especially photosynthetic C, primes the SOM decomposition to release nutrients to the plant (Chen et al., 2019). The nutrient recycling promotes the plant growth and photosynthetic C fixation, enhancing aboveground C stocks. Therefore, we revealed that plant-soil interactions and their feedbacks to fluctuant wetland ecosystems play an important role in regulating SOC cycling and storage.

CONCLUSION

Our study demonstrates that wetland restoration is expected to be an efficient approach to offset C loss resulting from wetland degradation. Wetland restoration contained higher aboveground C stocks and SOC stocks, which of the summary was approximately two times of degraded wetland C stocks. We observed that the restoration of water, nutrient, and vegetation were the key factors to enhance the sequestration and storage of organic C above- and belowground in recovering wetland, tightly associated with high photosynthetic C fixation in plant (represented by aboveground biomass) and photosynthetic C input to soils (represented by soil natural $\delta^{13}C$ and carbohydrates). We suggested that plant–soil interactions and their feedbacks to environmental change need to be considered to evaluate SOC stocks in wetlands.

DATA AVAILABILITY STATEMENT

The raw data supporting the conclusions of this article will be made available by the authors, without undue reservation.

AUTHOR CONTRIBUTIONS

PS analyzed the data and wrote the manuscript. HH helped perform statistical analyses. HY, TL, DZ, JM, and DD helped collect soil samples. JS supervised the writing of this manuscript. All authors contributed to the article and approved the submitted version.

FUNDING

This work was supported by the Natural Science Foundation of Shandong Province (ZR2020QD004 and ZR2020QC040) and the National Natural Science Foundation of China (32101387, 41971119, and 42171059).

SUPPLEMENTARY MATERIAL

The Supplementary Material for this article can be found online at: https://www.frontiersin.org/articles/10.3389/fevo.2022.856479/full#supplementary-material

REFERENCES

Baustian, M. M., Stagg, C. L., Perry, C. L., Moss, L. C., and Carruthers, T. J. (2021). Long-term carbon sinks in marsh soils of coastal Louisiana are at risk to wetland loss. *J. Geophys. Res. Biogeosci.* 126:e2020JG005832. doi: 10.1029/2020JG005832

Billah, M. M., Bhuiyan, M. K. A., Islam, M. A., Das, J., and Hoque, A. (2022). Salt marsh restoration: an overview of techniques and success indicators. *Environ. Sci. Pollut. Res.* 29, 15347–15363. doi: 10.1007/s11356-021-18305-5

Chen, L., Liu, L., Qin, S., Yang, G., Fang, K., Zhu, B., et al. (2019). Regulation of priming effect by soil organic matter stability over a broad geographic scale. *Nat. Commun.* 10:5112. doi: 10.1038/s41467-019-13119-z

Chu, X., Han, G., Xing, Q., Xia, J., Sun, B., Li, X., et al. (2019). Changes in plant biomass induced by soil moisture variability drive interannual variation in the net ecosystem CO_2 exchange over a reclaimed coastal wetland. *Agric. For. Meteorol.* 264, 138–148. doi: 10.1016/j.agrformet.2018.09.013

Crooks, S., Sutton-Grier, A. E., Troxler, T. G., Herold, N., Bernal, B., Schile-Beers, L., et al. (2018). Coastal wetland management as a contribution to the US National Greenhouse Gas Inventory. *Nat. Clim. Change* 8, 1109–1112. doi: 10.1038/s41558-018-0345-0

Cui, L., Li, G., Ouyang, N., Mu, F., Yan, F., Zhang, Y., et al. (2018). Analyzing coastal wetland degradation and its key restoration technologies in the coastal area of Jiangsu, China. *Wetlands* 38, 525–537. doi: 10.1007/s13157-018-0997-6

Dayathilake, D. D. T. L., Lokupitiya, E., and Wijeratne, V. P. I. S. (2020). Estimation of aboveground and belowground carbon stocks in urban freshwater wetlands of Sri Lanka. *Carbon Balance Manage.* 15:17. doi: 10.1186/s13021-020-00152-5

Dronova, I., Taddeo, S., Hemes, K. S., Knox, S. H., Valach, A., Oikawa, P. Y., et al. (2021). Remotely sensed phenological heterogeneity of restored wetlands: linking vegetation structure and function. *Agric. For. Meteorol.* 296:108215. doi: 10.1016/j.agrformet.2020.108215

Duarte, C. M., Losada, I. J., Hendriks, I. E., Mazarrasa, I., and Marbà, N. (2013). The role of coastal plant communities for climate change mitigation and adaptation. *Nat. Clim. Change* 3, 961–968. doi: 10.1038/nclimate1970

Guan, B., Yu, J., Hou, A., Han, G., Wang, G., Qu, F., et al. (2017). The ecological adaptability of *Phragmites australis* to interactive effects of water level and salt stress in the Yellow River Delta. *Aquat. Ecol.* 51, 107–116. doi: 10.1007/s10452-016-9602-3

Hayes, M. A., Jesse, A., Tabet, B., Reef, R., Keuskamp, J. A., and Lovelock, C. E. (2017). The contrasting effects of nutrient enrichment on growth, biomass allocation and decomposition of plant tissue in coastal wetlands. *Plant Soil* 416, 193–204. doi: 10.1007/s11104-017-3206-0

Herbert, E. R., Boon, P., Burgin, A. J., Neubauer, S. C., Franklin, R. B., Ardón, M., et al. (2015). A global perspective on wetland salinization: ecological consequences of a growing threat to freshwater wetlands. *Ecosphere* 6, 1–43. doi: 10.1890/ES14-00534.1

Keller, J. K., Anthony, T., Clark, D., Gabriel, K., Gamalath, D., Kabala, R., et al. (2015). Soil organic carbon and nitrogen storage in two southern California salt marshes: the role of pre-restoration vegetation. *Bull. South. Calif. Acad. Sci.* 114, 22–32.

Kirwan, M. L., and Megonigal, J. P. (2013). Tidal wetland stability in the face of human impacts and sea-level rise. *Nature* 504, 53–60. doi: 10.1038/nature12856

Li, J., Han, G., Wang, G., Liu, X., Zhang, Q., Chen, Y., et al. (2022). Imbalanced nitrogen–phosphorus input alters soil organic carbon storage and mineralisation in a salt marsh. *Catena* 208:105720. doi: 10.1016/j.catena.2021.105720

Ma, Y., Dias, M. C., and Freitas, H. (2020). Drought and salinity stress responses and microbe-induced tolerance in plants. *Front. Plant Sci.* 11:591911. doi: 10.3389/fpls.2020.591911

Ma, Z., Zhang, M., Xiao, R., Cui, Y., and Yu, F. (2017). Changes in soil microbial biomass and community composition in coastal wetlands affected by restoration projects in a Chinese delta. *Geoderma* 289, 124–134. doi: 10.1016/j.geoderma.2016.11.037

Maietta, C. E., Bernstein, Z. A., Gaimaro, J. R., Buyer, J. S., Rabenhorst, M. C., Monsaint-Queeney, V. L., et al. (2019). Aggregation but not organo-metal complexes contributed to C storage in tidal freshwater wetland soils. *Soil Sci. Soc. Am. J.* 183, 252–265. doi: 10.2136/sssaj2018.05.0199

Munns, R., Day, D. A., Fricke, W., Watt, M., Arsova, B., Barkla, B. J., et al. (2020). Energy costs of salt tolerance in crop plants. *New Phytol.* 225, 1072–1090. doi: 10.1111/nph.15864

Orth, R. J., Lefcheck, J. S., McGlathery, K. S., Aoki, L., Luckenbach, M. W., Moore, K. A., et al. (2020). Restoration of seagrass habitat leads to rapid recovery of coastal ecosystem services. *Sci. Adv.* 6:eabc6434. doi: 10.1126/sciadv.abc6434

Renzi, J. J., He, Q., and Silliman, B. R. (2019). Harnessing positive species interactions to enhance coastal wetland restoration. *Front. Ecol. Evol.* 7:131. doi: 10.3389/fevo.2019.00131

Sapkota, Y., and White, J. R. (2020). Carbon offset market methodologies applicable for coastal wetland restoration and conservation in the United States: a review. *Sci. Total Environ.* 701:134497. doi: 10.1016/j.scitotenv.2019.134497

Servais, S., Kominoski, J. S., Charles, S. P., Gaiser, E. E., Mazzei, V., Troxler, T. G., et al. (2019). Saltwater intrusion and soil carbon loss: testing effects of salinity and phosphorus loading on microbial functions in experimental freshwater wetlands. *Geoderma* 337, 1291–1300. doi: 10.1016/j.geoderma.2018.11.013

Shao, P., Liang, C., Rubert-Nason, K., Li, X., Xie, H., and Bao, X. (2019). Secondary successional forests undergo tightly-coupled changes in soil microbial community structure and soil organic matter. *Soil Biol. Biochem.* 128, 56–65. doi: 10.1016/j.soilbio.2018.10.004

Shao, P., Lynch, L., Xie, H., Bao, X., and Liang, C. (2021). Tradeoffs among microbial life history strategies influence the fate of microbial residues in subtropical forest soils. *Soil Biol. Biochem.* 153:108112.

Sharma, S., MacKenzie, R. A., Tieng, T., Soben, K., Tulyasuwan, N., Resanond, A., et al. (2020). The impacts of degradation, deforestation and restoration on mangrove ecosystem carbon stocks across Cambodia. *Sci. Total Environ.* 706:135416. doi: 10.1016/j.scitotenv.2019.135416

Song, K., Wang, Z., Du, J., Liu, L., Zeng, L., and Ren, C. (2014). Wetland degradation: its driving forces and environmental impacts in the Sanjiang Plain, China. *Environ. Manage.* 54, 255–271. doi: 10.1007/s00267-014-0278-y

Spivak, A. C., Sanderman, J., Bowen, J. L., Canuel, E. A., and Hopkinson, C. S. (2019). Global-change controls on soil-carbon accumulation and loss in coastal vegetated ecosystems. *Nat. Geosci.* 12, 685–692. doi: 10.1038/s41561-019-0435-2

Stagg, C. L., Baustian, M. M., Perry, C. L., Carruthers, T. J., and Hall, C. T. (2018). Direct and indirect controls on organic matter decomposition in four coastal wetland communities along a landscape salinity gradient. *J. Ecol.* 106, 655–670. doi: 10.1111/1365-2745.12901

Suseela, V., Tharayil, N., Xing, B., and Dukes, J. S. (2013). Labile compounds in plant litter reduce the sensitivity of decomposition to warming and altered precipitation. *New Phytol.* 200, 122–133. doi: 10.1111/nph.12376

Wu, Y., Xu, N., Wang, H., Li, J., Zhong, H., Dong, H., et al. (2021). Variations in the diversity of the soil microbial community and structure under various categories of degraded wetland in Sanjiang Plain, northeastern China. *Land Degrad. Dev.* 32, 2143–2156. doi: 10.1002/ldr.3872

Xia, S., Song, Z., Li, Q., Guo, L., Yu, C., Singh, B. P., et al. (2021). Distribution, sources, and decomposition of soil organic matter along a salinity gradient in estuarine wetlands characterized by C: N ratio, $\delta^{13}C$–$\delta^{15}N$, and lignin biomarker. *Glob. Change Biol.* 27, 417–434. doi: 10.1111/gcb.15403

Xiao, D., Deng, L., Kim, D. G., Huang, C., and Tian, K. (2019). Carbon budgets of wetland ecosystems in China. *Glob. Change Biol.* 25, 2061–2076. doi: 10.1111/gcb.14621

Xu, S., Liu, X., Li, X., and Tian, C. (2019). Soil organic carbon changes following wetland restoration: a global meta-analysis. *Geoderma* 353, 89–96.

Xu, W., Fan, X., Ma, J., Pimm, S. L., Kong, L., Zeng, Y., et al. (2019). Hidden loss of wetlands in China. *Curr. Biol.* 29, 3065–3071. doi: 10.1016/j.cub.2019.07.053

Yang, R., Wang, L., Chen, L., and Zhang, Z. (2022). Assessment of soil quality using VIS–NIR spectra in invaded coastal wetlands. *Environ. Earth Sci.* 81:19.

Zhai, Z., Luo, M., Yang, Y., Liu, Y., Chen, X., Zhang, C., et al. (2022). Trade-off between microbial carbon use efficiency and microbial phosphorus limitation under salinization in a tidal wetland. *Catena* 209:105809. doi: 10.1016/j.catena.2021.105809

Zhao, Q., Bai, J., Huang, L., Gu, B., Lu, Q., and Gao, Z. (2016). A review of methodologies and success indicators for coastal wetland restoration. *Ecol. Indic.* 60, 442–452.

Zhao, Q., Bai, J., Zhang, G., Jia, J., Wang, W., and Wang, X. (2018). Effects of water and salinity regulation measures on soil carbon sequestration in coastal wetlands of the Yellow River Delta. *Geoderma* 319, 219–229.

Conflict of Interest: The authors declare that the research was conducted in the absence of any commercial or financial relationships that could be construed as a potential conflict of interest.

Publisher's Note: All claims expressed in this article are solely those of the authors and do not necessarily represent those of their affiliated organizations, or those of the publisher, the editors and the reviewers. Any product that may be evaluated in this article, or claim that may be made by its manufacturer, is not guaranteed or endorsed by the publisher.

frontiers in Ecology and Evolution

ORIGINAL RESEARCH
published: 21 March 2022
doi: 10.3389/fevo.2022.840784

Deposition Flux, Stocks of C, N, P, S, and Their Ecological Stoichiometry in Coastal Wetlands With Three Plant Covers

Shudong Du[1], Junhong Bai[1], Qingqing Zhao[2], Chen Wang[1,3]*, Yanan Guan[1], Jia Jia[4], Guangliang Zhang[1] and Chongyu Yan[1]*

[1] State Key Laboratory of Water Environment Simulation, School of Environment, Beijing Normal University, Beijing, China, [2] Shandong Provincial Key Laboratory of Applied Microbiology, Ecology Institute, Qilu University of Technology (Shandong Academy of Sciences), Jinan, China, [3] Research and Development Center for Watershed Environmental Eco-Engineering, Beijing Normal University, Zhuhai, China, [4] Henan Key Laboratory of Ecological Environment Protection and Restoration of Yellow River Basin, Yellow River Institute of Hydraulic Research, Zhengzhou, China

OPEN ACCESS

Edited by:
Haitao Wu,
Northeast Institute of Geography and Agroecology (CAS), China

Reviewed by:
Xu Chen,
China University of Geosciences Wuhan, China
Weiqi Wang,
Fujian Normal University, China
Jiang Bao Xia,
Binzhou University, China

***Correspondence:**
Junhong Bai
junhongbai@163.com
Chen Wang
wangchen90@bnu.edu.cn

Specialty section:
This article was submitted to Conservation and Restoration Ecology, a section of the journal Frontiers in Ecology and Evolution

Received: *21 December 2021*
Accepted: *18 February 2022*
Published: *21 March 2022*

Citation:
Du S, Bai J, Zhao Q, Wang C, Guan Y, Jia J, Zhang G and Yan C (2022) Deposition Flux, Stocks of C, N, P, S, and Their Ecological Stoichiometry in Coastal Wetlands With Three Plant Covers. Front. Ecol. Evol. 10:840784. doi: 10.3389/fevo.2022.840784

The depositional flux of coastal wetlands and the deposition rate of biogenic elements greatly affect the carbon sink storage. Ecological stoichiometry is an important ecological indicator, which can simply and intuitively indicate the biogeochemical cycle process of the region. This study investigated the soil deposition flux, stocks, and ecological stoichiometric ratios of C, N, P, and S under different water and salt conditions based on ^{137}Cs dating technology in the Yellow River Delta (YRD) of China. The results showed that the deposition fluxes were 0.38 cm/year for PV wetlands, 1.08 cm/yr for PA wetlands, and 1.06 cm/yr for SS wetlands. Similarly, PA wetlands showed higher deposition fluxes of C, N, and S compared with SS and PV wetlands. PA wetlands had higher stocks of C (5.86 kg/m^2), N (0.36 kg/m^2) and S (0.36 kg/m^2) in the top 1-m soil layer compared with PV and SS wetlands. However, the highest deposition rate of P (9.82 g/yr/m^2) was observed in SS wetlands among the three wetlands. Three accumulative hotspots of C, N, and S in soil profiles of PA and SS wetlands were observed at soil depths of 0–10, 40–60, and 90–100 cm, whereas one accumulative hotspot of P was at the soil depth of 10–12 cm in SS wetlands and 80–82 cm in PA wetlands. PV wetlands showed higher accumulations of C, P, and S in the top 10 cm soil layer and N at the soil depth of 90–100 cm. The higher top concentration factors in these three wetlands indicated that the dominant input of plant residues was the main reason. The ratios of C/N and C/N/P of each sampling site were higher in the surface soils and decreased with depth. The ratios of C/P and N/P were larger in the surface layer (0–20 cm), the middle layer (40–60 cm), and the deep layer (90–100 cm). The ratios of N/P and C/N/P were relatively lower, indicating that these studied wetlands were N-limited ecosystems. The results implied that the coastal wetlands in the YRD have huge storage potential of biogenic elements as blue carbon ecosystems.

Keywords: water and salt conditions, deposition flux, ecological stoichiometry, topsoil concentration factor, soil profiles

INTRODUCTION

Coastal wetlands, sea-land interlaced belts and buffer zones are important areas for the strong exchange of materials and energy between the ocean and land. They play a vital role in regulating global environmental changes and serving as sources and sinks of carbon (C), nitrogen (N), phosphorus (P), and sulfur (S). C, N, P, and S are important constituent elements in the soil. Their contents and stocks can directly affect the soil quality, nutrient cycling, and ecological functions of the coastal wetland ecosystems (Bai et al., 2012; Feng et al., 2017; Lu et al., 2018).

The regulation of biological elements with different soil profiles in the coastal wetland is not obvious because coastal wetlands are subject to the combined effects of erosion and sedimentation under the two-way regulation of tidal current and runoff. Taking soil organic carbon (SOC) as an example, the SOC pool is composed of the active pool and the inert pool, which leads to different stability in the soil profile due to high spatial heterogeneity. In addition, soil animals and microorganisms could decompose SOC and nitrogen into CO_2, CH_4 or N_2O, which would exacerbate the heterogeneity of soil carbon or nitrogen pools (Wu et al., 2013, 2015).

Many studies have shown that SOC is mainly distributed in the upper soil layer of the soil profile and it tends to gradually decrease from the surface to the bottom (Wang et al., 2010). However, the current research on the SOC storage of coastal wetlands is mainly concentrated on the surface soil (0–30 cm) of the Yellow River Delta (YRD) region, and there are few studies on the contribution rate of the deep SOC storage to the carbon pool (Luo et al., 2020). Therefore, it is not enough to accurately reflect the soil carbon pool of coastal wetlands by studying the biogenic elements in surface soils. For the study of the distribution form of soil biogenic elements and ecological stoichiometry in the soil, a deeper soil profile should be selected.

The ecological stoichiometric ratio provides important insights for studying the energy and material cycles in estuarine ecosystems (Coynel et al., 2016). In addition, each ecological stoichiometric ratio is of great significance to the biogeochemical cycle of C, N, P, and S in the soil. For example, the soil C/N ratio is a sensitive indicator used to measure soil quality (Elser et al., 2003); the C/P ratio and C/S ratio are considered to be symbols of the mineralization ability of phosphorus and sulfur in the soil. Previous studies have focused on the stoichiometric ratios of soil and the effects of various environmental factors, such as vegetation types and rainfall, on the ecological stoichiometric ratios of soil at different soil depths in forests, karst, and grasslands (Yang et al., 2014; Fan et al., 2015; Wang et al., 2018). Some researchers have presented the impacts of the ecological stoichiometric ratios on various ecological functions in the ecosystems and the interactions between microbes and the ecological stoichiometric ratios in the abovementioned ecosystems. Although the stoichiometric ratios in coastal wetlands are more important due to the impacts of historical sedimentation and strong exchange between marine and terrestrial materials of coastal wetlands, only few studies have been conducted on the relations between sedimentation and ecological stoichiometry in coastal wetlands.

The Yellow River is one of the rivers with the highest sediment content in the world, and the relationship between its sedimentation flux and the stocks of soil biogenic elements is also a problem that needs to be revealed. As the most fragile and sensitive new delta in the world, the YRD has extremely precious ecological value. In recent years, governance along the Yellow River has also received great attention from the Chinese government. Therefore, it is necessary to study the soil deposition rate of the YRD and enhance the sequestration capacity of these elements and soil quality management of the coastal wetlands. The primary objectives of this study were to: (1) analyze the depth of the distributions of the contents and stocks of C, N, P, and S along soil profiles with different water and salt conditions in the YRD; (2) investigate the deposition rates of C, N, P, and S in the soil using the ^{137}Cs dating technique in coastal wetlands; and (3) identify the changes in ecological stoichiometric ratios of C, N, P, and S with depth along the soil profiles.

MATERIALS AND METHODS

Study Area

The study area is located in the YRD (N 37°35′-38°12′, E 118°33′-119°20′), Dongying city, Shandong Province, China. It has a warm temperate semihumid monsoon climate with four distinct seasons, rain and heat at the same time, small regional climate differences, and a frost-free period of 196 days (Cui et al., 2008). The annual average sunshine hours are 2,590–2,830 h, and the

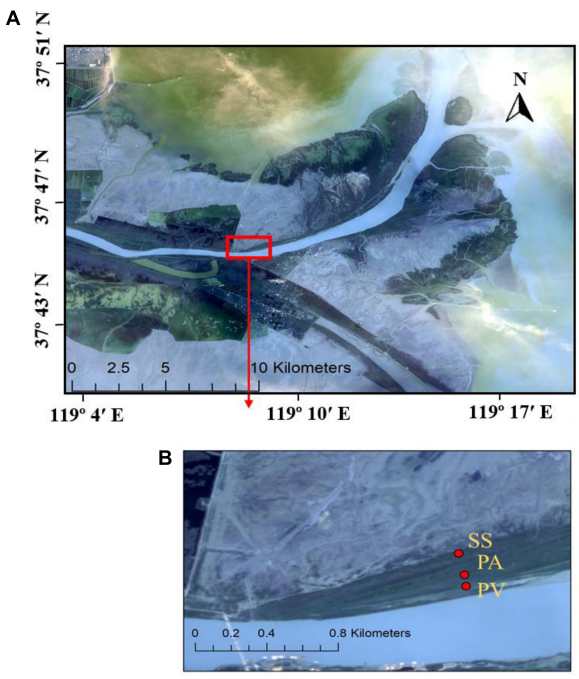

FIGURE 1 | Location map of sampling sites in the YRD. **(A)** The location of sampling belt in the YRD, **(B)** the location of sampling sites in the sampling belt.

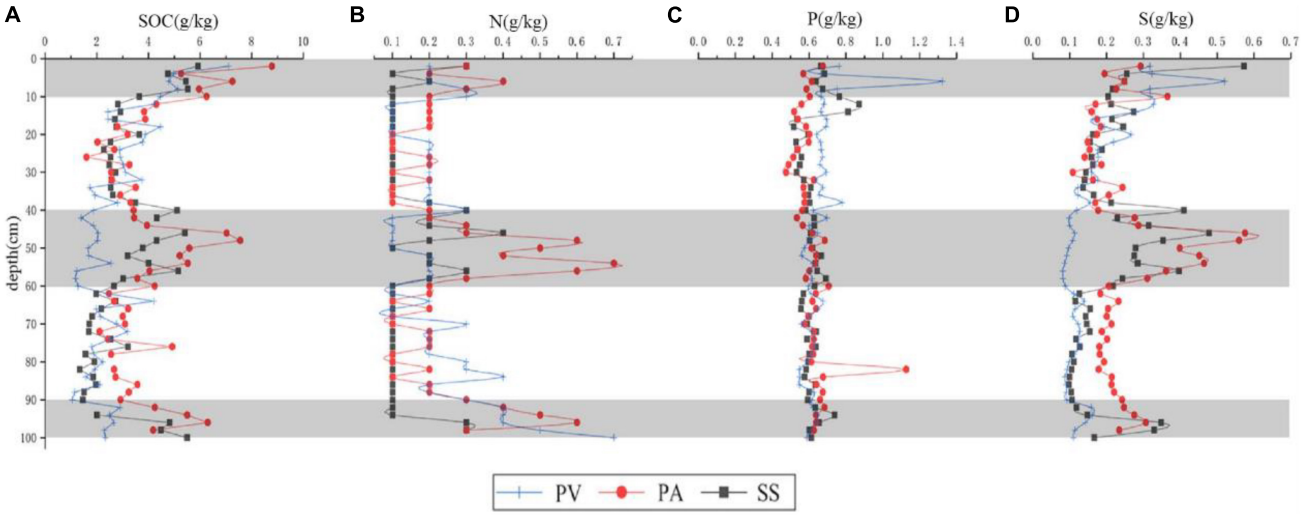

FIGURE 2 | Changes in the contents of C **(A)**, N **(B)**, P **(C)**, and S **(D)** along different soil profiles in PV, PA, and SS wetlands.

annual average temperature is 12.1°C. The annual precipitation is 551.6 mm, 70% of which is concentrated in the period from June to August. The annual evaporation is 1,962 mm. The spring evaporation is strong, and the evaporation accounts for approximately 51.7% of the year. The drought index is as high as 3.56 (Gao et al., 2012). The main vegetation types are herbs, such as *Pteris violata*, *Phragmites australis*, *Triarrhena sacchariflora*, *Suaeda salsa*, *Myriophyllum spicatum*, and *Limoninum sinense*; shrubs, such as *Tamarix chinensis*; and trees, such as *Salix matsudana* (Cheng et al., 2021). There are more than 40 families, 110 genera, and 160 species. *Phragmites australis*, *Pteris violate,* and *Suaeda salsa* are the main dominant species in this area.

Three sampling sites were selected along one sampling belt perpendicular to the riverbed in the coastal wetlands on the north bank of the Yellow River (**Figure 1**), including *Pteris violata* wetlands (PV), *Phragmites australis* wetlands (PA), and *Suaeda salsa* wetlands (SS). Among them, PA wetlands can be affected by underground seawater and freshwater when the water and sediment regulation project of the YRD is implemented in July. Comparatively, SS wetlands are dominantly affected by tidal water.

Sample Collection and Analysis

The soil samples were collected by excavating the soil profiles at a depth of 0–100 cm at intervals of 2 cm. After removing visible plant residues and stones, the soil samples were air-dried for 2 or 3 weeks. One replicate was sampled at each point for analyzing relevant indicators. One part of the air-dried samples were ground through sieving using a 20-mesh for the determination of ^{137}Cs labeling. Another part of the sample was further ground to pass through a 100-mesh sieve for determining soil properties. SOC was measured by the potassium dichromate dilution thermal-colorimetric method. Total nitrogen (N) was measured on an elemental analyzer (CHNOS elemental analyzer, Vario EL, Germany). Total phosphorus (P) and total sulfur (S) were determined by inductively coupled plasma atomic emission spectroscopy (ICP/AES) after digestion in an $HClO_4$-HNO_3-HF mixture in Teflon tubes. Quality assurance and quality control were assessed using duplicates, method blanks, and standard reference materials (GBW07401) from the Chinese Academy of Measurement Sciences with each batch of samples (1 blank and 1 standard for every 10 samples). The recoveries of samples spiked with standards ranging from 95 to 106%. ^{137}Cs value in the soil was determined using a high-purity germanium gamma spectrometer in the laboratory of the Geography Department, Beijing Normal University.

Stocks and Topsoil Concentration Factors

The stocks of C, N, P, and S were calculated as follows:

$$CS = \sum BD_i \times C_i \times T$$

$$NS = \sum BD_i \times N_i \times T$$

$$PS = \sum BD_i \times P_i \times T$$

$$SS = \sum BD_i \times S_i \times T$$

where CS, NS, PS, and SS are the stocks of C, N, P, and S per unit area (kg/m^2), respectively; C_i, N_i, P_i, and S_i are the average contents of C, N, P and S in the soil layer i (i = 1, 2, 3, 4, and 5); and T is the thickness of soil layer i (cm). The topsoil concentration factor is calculated by the stocks in the top 10 cm and the stocks in the top 100 cm.

Statistical Analysis and Graphing

One-way ANOVA was used to identify the significant difference in C, N, P, and S contents and stocks between different wetlands. The difference was considered to be significant if $P < 0.05$. Data processing was performed using Excel 2019 software

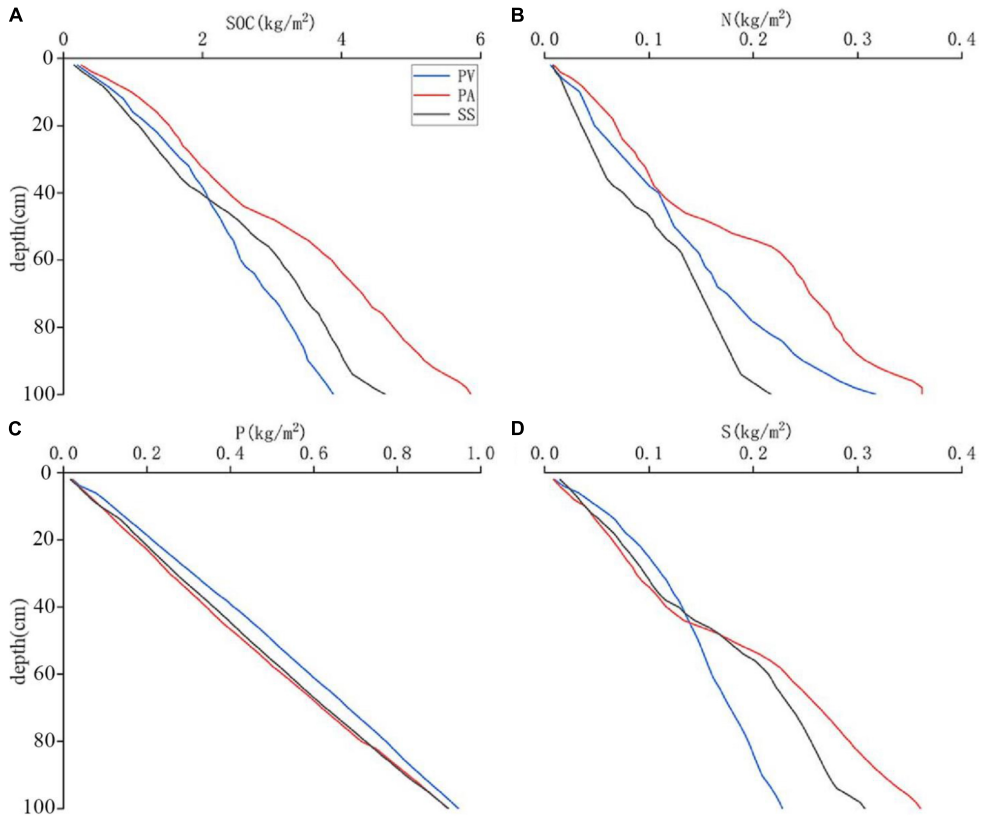

FIGURE 3 | Accumulative distributions of the stocks of C **(A)**, N **(B)**, P **(C)**, and S **(D)** along with different soil profiles in PV, PA, and SS wetlands.

package software, and graphs were created by Origin 2017 software package.

RESULTS

Contents and Stocks of C, N, P and S

The highest average contents of C, N, and S in the PA wetland were 3.91, 0.24, and 0.24 g/kg, respectively, and the PV wetland had the highest average contents of P (0.65 g/kg) (**Figure 2**). SOC content in PA wetlands was significantly higher than that in PV wetlands ($P < 0.05$). Three layers with high concentrations of C, N, and S in soil profiles were observed in PA and SS wetlands at soil depths of 0–10 cm, 40–60 cm, and 90–100 cm. In PV wetlands, higher concentrations of C (5.29 g/kg) and S (0.36 g/kg) appeared in surface soils (0–10 cm) and N (0.48 g/kg) at soil depths of 90–100 cm, respectively. However, P contents showed different depth distributions in three wetlands, with an accumulative peak at the soil depth of 4–6 cm (3.70 g/kg) in PV wetlands, 10–12 cm (2.58 g/kg) in SS wetlands, and 80–82 cm (3.36 g/kg) in PA wetlands.

SOC stocks in 1-m depth reached approximately 6 kg/m^2 in PA wetlands, slightly higher than that in the PV (3.55 kg/m^2) and SS (5 kg/m^2) wetlands (**Figure 3**). In contrast, low soil N stocks (0.36 kg/m^2, PA; 0.22 kg/m^2, SS; and 0.32 kg/m^2, PV) were observed in the YRD. Unlike C and N, three wetlands showed similar soil P stocks (0.92 kg/m^2) in 1-m depth. Similar to N, PA wetlands exhibited the largest soil S stocks (0.36 kg/m^2), followed by SS wetlands (0.31 kg/m^2), while the lowest soil S stocks (0.23 kg/m^2) in PV wetlands were observed. SOC stocks in three accumulative hotspots in PA wetlands were 97.79 g/m^2 in top 10 cm soils, 148.25 g/m^2 for the 40–60 cm soil depth, and 66.32 g/m^2 for the 90–100 cm soil depth, also 64.67, 113.86, and 59.25 g/m^2 in SS wetlands, respectively. Soil TN stocks in three accumulative hotspots were 4.09 g/m^2 (0–10 cm), 12.14 g/m^2 (40–60 cm), and 5.36 g/m^2 (90–100 cm) in PA wetlands, with TS stocks of 3.87, 11.50, and 3.65 g/m^2, respectively. In SS wetlands, TN and TS stocks were 2.05 and 5.03 g/m^2 in the top 10 cm, 5.88 and 2.81 g/m^2 for the 40–60 cm soil depth, and 3.52 and 1.99 g/m^2 for the 90–100 cm soil depth. Soil P stocks in the accumulative hotspot were 9.85 g/m^2 for the 10–20 cm soil depth in SS wetland and 11.25 g/m^2 for the 80–90 cm soil depth in the PA wetland. In contrast, the accumulative hotspot of C, P, and S stocks appeared in top 10 cm soils of PV wetlands (with the levels of 74.06, 11.67, and 3.83 g/m^2, respectively), whereas the accumulative hotspot of N appeared in the 90–100 cm soil depth (6.96 g/m^2).

Soil Concentration Factors and Deposition Rates

The top concentration factors of C, N, P, and S in each wetland were all more than 0.10, which indicated that the accumulation of

TABLE 1 | Topsoil concentration factors of C, N, P, and S in PV, PA, and SS wetlands.

	SOC	N	P	S
PV	0.22	0.11	0.14	0.26
PA	0.19	0.13	0.11	0.12
SS	0.16	0.11	0.12	0.15

these elements was mainly affected by plant secretions (**Table 1**). Among them, the topsoil concentration factor of C fell within the scope of 0.16–0.22, following the order PV > PA > SS. As for soil N, their topsoil concentration factors in the three wetlands were relatively low. The followed order of topsoil concentration factors of both P and S was PV > SS > PA. The topsoil concentration factors of C, N, P, and S in the PA wetlands were higher than that of PV and SS wetlands. After ^{137}Cs isotope dating, the depth of the soil layer represented in the year 1963 was identified at the 20-cm soil depth in PV wetland, 56-cm soil depths in PA, and 58-cm soil depths in SS wetlands. As shown in **Figure 4**, the deposition rate of sediments in PV wetland was 0.38 cm/yr, 1.08 cm/yr in PA wetland, and 1.06 cm/yr in SS wetland.

Deposition Fluxes of C, N, P and S

Different deposition rates of C, N, P, and S in three wetlands were also observed. PA wetlands exhibited the highest deposition rate of C (71.17 g/yr/m^2), N (4.35 g/yr/m^2), and S (4.34 g/yr/m^2), while the lowest deposition rate appeared in PV wetlands (**Figure 5**). In contrast, the highest deposition rate of P followed the order SS wetlands (9.82 g/yr/m^2) > PA wetlands (9.70 g/yr/m^2) > PV wetlands (4.08 g/yr/m^2). The contents of four elements in three wetlands showed a similar pattern with depth along soil profiles (**Figure 2**). Except for N, the contents of C, P, and S in the top 15-cm soils were relatively high, then declined significantly at approximately 20-cm soil depth and kept stable. However, at soil depth of approximately 40 cm, the contents of C, N, and S in the soil increased significantly again, but the change of P content was not obvious at this depth. At approximately 60-cm soil depth, the contents of these four elements again fell to a relatively stable level, to the soil layer of approximately 90–100 cm.

Ecological Stoichiometric Ratios

The soil C/N ratios in the three wetlands remained relatively stable (**Figure 4**). PV wetlands showed a higher range of the C/N ratios than PA and SS wetlands. This indicated that the C/N ratios at higher ranges in low-salinity wetlands were lower than that in middle-salinity and high-salinity wetlands. The highest C/P ratios were observed in PA wetlands, followed by those in SS wetlands, while the lowest value appeared in PV wetlands. Similarly, both C/N and C/P ratios were higher in surface soils of the three wetlands, and higher ratios also appeared at soil depths of 40–60 and 90–100 cm in PA and SS wetlands. However, this was not the case in PV wetlands. PA wetlands showed higher C/S ratios in upper soils than deeper soils, while a fluctuating change was observed along soil profiles in PV and SS wetlands. The C/N/P of SS wetlands was significantly higher than that of PA wetlands; the C/N/P of PA wetlands was significantly higher than that of PV wetlands ($P < 0.05$). N/P ratios decreased along soil profiles in PV wetlands, and a fluctuation was observed in PA and SS wetlands with higher ratios at the soil depths of 40–60 and 90–100 cm.

DISCUSSION

Depth Distributions of the Contents of C, N, P and S Along Soil Profiles

Higher contents of C, N, P, and S in surface soils (0–10 cm) of the three wetlands were generally observed, which was associated with exogenous inputs of plant litters, sedimentation by freshwater, and seawater input (Saintilan et al., 2013). The contents of C and N in the surface soils were higher than that in the deep soils in coastal wetlands (Wang et al., 2016). The

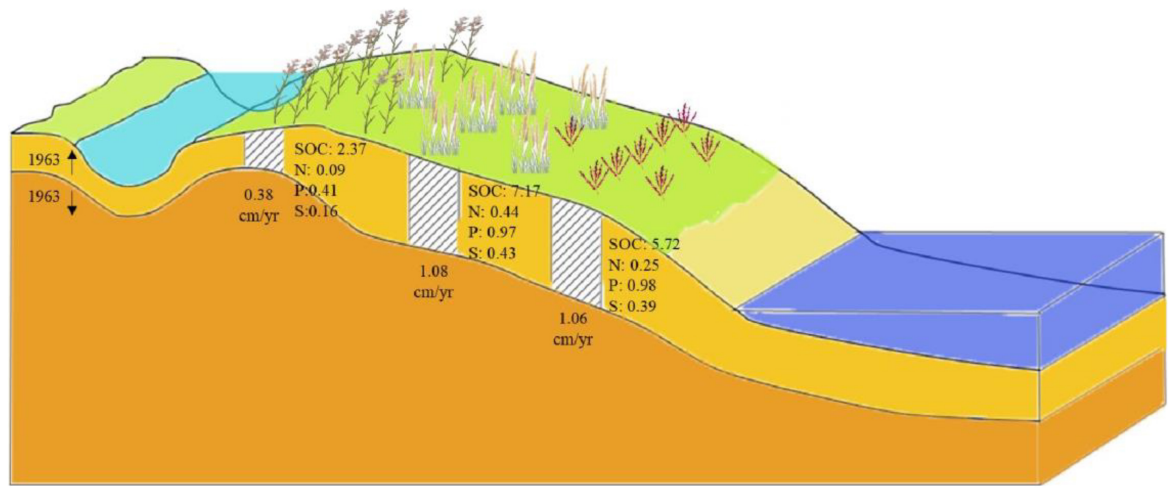

FIGURE 4 | Soil sedimentation rate and sedimentation flux of C, N, P, and S in the YRD.

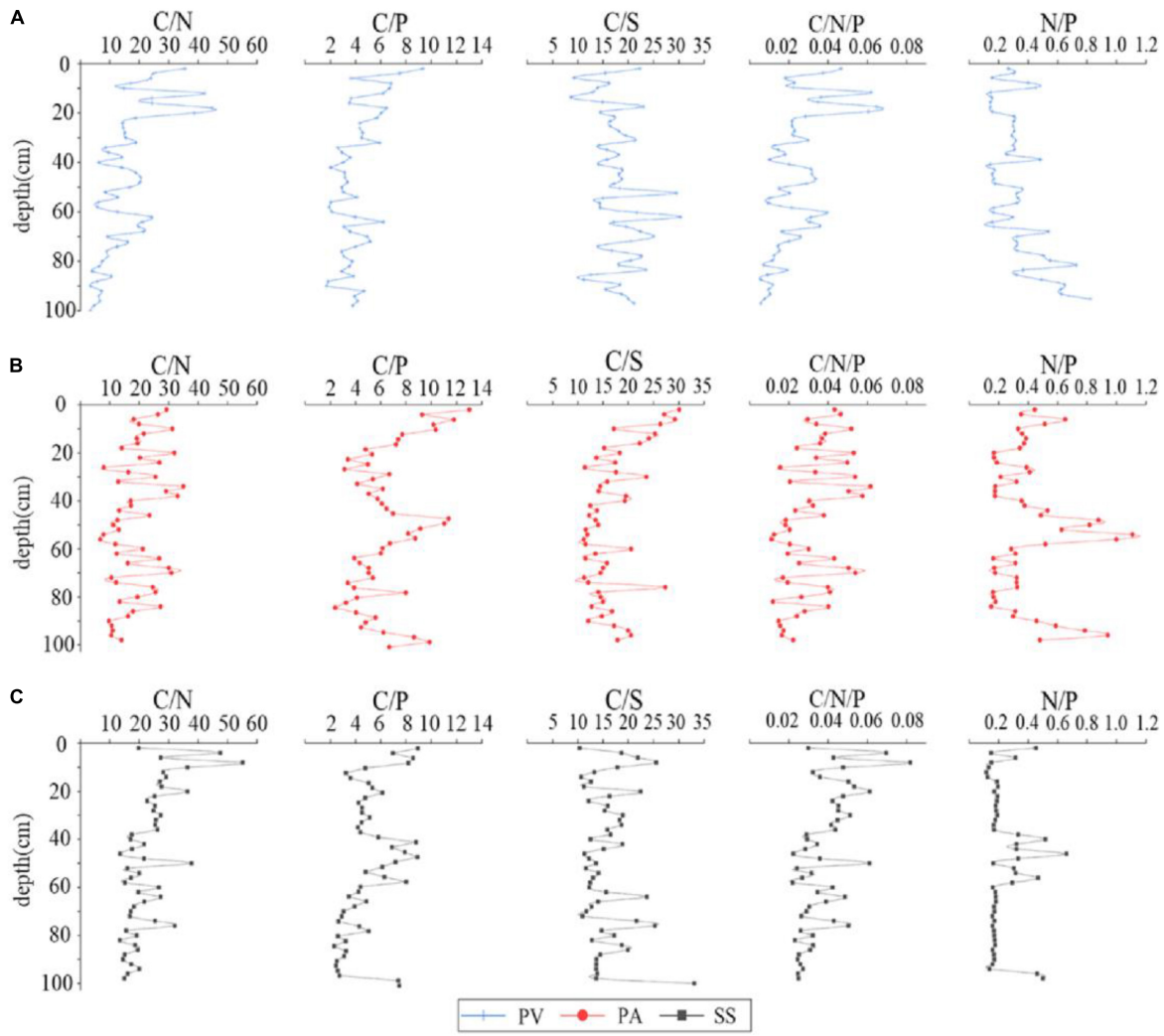

FIGURE 5 | Depth distributions of the ecological stoichiometric ratios along soil profiles under different water and salt conditions. PV **(A)**, PA **(B)**, SS **(C)**.

reason might be that the surface soils are more easily affected by environmental changes (Salome et al., 2010). In addition, higher contents of C, N, and S in the three wetlands were also observed at soil depths of 40–60 and 90–100 cm, which was associated with historical input and sedimentation. Over the past years, historical plant death and sedimentation due to flooding or Yellow River runoff might contribute to the elemental accumulation in deep soils. According to the annual Yellow River Yearbook, the Yellow River was diverted in 1964, which may have caused a large number of plants to be buried underground at this stage and converted into biogenic elements, such as C, N, P, and S. Another reason might be related to the high content of silt and clay in these layers since soil C content has a linear relationship with the composition content of clay + silt in the YRD (Zhao et al., 2020). Additionally, microbial activity and leaching could also cause C, N, and S in the surface soil to migrate downward (Wang et al., 2010).

TABLE 2 | Organic carbon density and sampling time of different coastal wetlands.

Region	SOCD (kg/m^2)	Sampling season	source
This study Yellow River Estuary in China	1.47–1.89	Autumn	This study
Other studies on the coastal wetlands of the Yellow River Estuary in China	1.17–2.41	Summer	Yu et al., 2013
Chongming East Coastal Area, China	2.32	Spring	Jiang et al., 2015
Tidal Flat Area, Shanghai, China	1.38	Autumn	Shi et al., 2010
New wetlands on the east coast of the U.S.	1.58 ± 0.11	Autumn	Krull and Craft, 2009
Mature wetlands on the east coast of the U.S.	5.83 ± 0.25	Autumn	Krull and Craft, 2009

Soil Deposition and Stocks of C, N, P and S in Soil Profiles

Compared with PA and SS wetlands, PV wetlands showed lower soil deposition at the rate of 0.38 cm/yr, which could be ascribed to the strong erosion by river water in PV wetland and higher

sediment deposition in PA (1.08 cm/yr) and SS (1.06 cm/yr) wetlands affected by the flow-sediment regulation in July and sediment input by tidal flow (Bai et al., 2020). Our results fell within the range by DeLaune et al. (2003) that the deposition rate of Louisiana estuarine wetlands affected by freshwater input was 0.10–1.11 cm/yr. Ding et al. (2016) also reported that the deposition rate of tidal flats in the YRD was 0.58 cm/yr, which was lower than that of PA and SS wetlands and higher than that of PV wetland observed in this study. This indicated that tidal flats underwent much stronger hydraulic erosion by tidal flow than coastal salt marshes (Ding et al., 2016). Moreover, river flow might have a much stronger erosion than tidal flow in the study area.

In general, the stocks of C, N, P, and S in PA wetlands were higher than those of PV and SS wetlands. This might be associated with less erosion by runoff or tidal flow in PA wetlands. Moreover, higher plant biomass of *Phragmites australis* and high litter inputs in PA wetlands than PV and SS wetlands could explain higher levels of these elements (Lu et al., 2018). Additionally, higher salinity in SS wetland may inhibit the accumulation of SOC (Zhao et al., 2017). The SOC stocks in this study were 1.47–1.89 kg/m^2 at the top 30 cm soils, which was within the range of the previous results (1.17–2.14 kg/m^2) (Yu et al., 2013). Compared with other Chinese coastal wetlands, the SOC storage in the YRD was lower than that of the Chongming Dongtan coastal wetland (2.32 kg/m^2) (Jiang et al., 2015), but higher than that in the Shanghai tidal flats (1.38 kg/m^2) (Shi et al., 2010; **Table 2**). The possible explanation was that the YRD is a newly formed wetland, vegetation types and different runoff or tidal flow conditions would also lead to different SOC storage in different regions. The organic carbon storage in the YRD is close to that of the new wetlands, but much lower than the mature wetlands on the eastern coast of the United States (Krull and Craft, 2009). This was because the vegetation of mature wetlands had gradually evolved into more advanced large plants, and more SOC was imported into the soil. This also indicated that wetland protection and restoration will help to improve the YRD's carbon storage.

The SOC content of the three accumulative hotspots of PA wetlands accounted for 16.69% (0–10 cm), 25.30% (40–60 cm), 11.32% (90–100 cm) of the total soil profile; and 13.97% (0–10 cm), 24.60% (40–60 cm), 12.97% (90–100 cm) in the SS wetlands. The proportion of SOC in the three accumulative hotspots of PA and SS wetlands exceeded 40% (PA: 53.31%, SS: 51.36%). SOC stocks of PV wetlands in the top 10 cm soils accounted for 19.1% of the soil profiles. The SOC storage in the 0–10 cm hot zone showed PV > PA > SS, which may be related to the difference of soil salinity. In the deep hot zone (90–100 cm), it was just the opposite (PV < PA < SS). The results showed that the increase in salinity might accelerate the downward migration of SOC.

The proportion of N in the three accumulative hotspots of PA and SS wetlands exceeded 40% (PA: 59.6%, SS: 52.8%). The proportion of S in the three accumulative hotspots of PA and SS wetlands exceeded 40% (PA: 52.8%, SS: 52.0%). The distribution of P is relatively uniform in the entire section, and only a significant jump occurs in some soil layers. Similar to the Chongming Dongtan wetlands (Jiang et al., 2015), the nitrogen content of the YRD also showed a high peak at a depth of about 10 cm. In addition, according to the C/N comparison with other wetlands, the YRD is a nitrogen-restricted area (Cheng et al., 2021). Compared with PV wetlands, the stocks of C and S in both PA and SS wetlands increased significantly at soil depths below 40 cm. The possible reason was higher historical inputs and underground seawater inputs. Additionally, the root input of these wetland plants is mainly concentrated at a depth above 40 cm. The assimilation and utilization of nutrients by the root system make the soil at 0–40 cm less neutralized by C and S (Wang Z. et al., 2019).

Top concentration factors for three wetlands showed higher stocks of C, N, P, and S in surface soils (0–10 cm), indicating that plant-soil cycling is the dominant factor influencing the biogeochemical processes of nutrients in the YRD. This was in agreement with the results of Bai et al. (2016). The topsoil concentration factor of C, P, and S in PV wetlands was higher than that of PA and SS wetlands. This may be associated with the effects of freshwater and seawater in PV and SS wetlands, respectively. Compared with SS wetland impacted by tidal water, the salinity of SS wetland was higher than that of PV due to the impacts of tidal flooding in SS wetlands with worse plant growth. Appropriate water conditions and lower salinity would have a positive effect on the topsoil concentration factor since water and salinity conditions can greatly influence vegetation covers and plant growth. Therefore, SS wetlands had a lower surface enrichment factor than PV wetlands. Additionally, higher salinity in SS wetlands might enhance the leaching effect of soil nutrients (Wang X. et al., 2019).

Changes in Ecological Stoichiometric Ratios Along Soil Profiles

The C/N ratio of the soil has been proven to be an important indicator for the ability of microorganisms to decompose soil organic matter (Canfora et al., 2017). If C/N < 9 it represents the stage of accelerating the decomposition of soil organic matter; C/N ratio between 9 and 11 indicates a dynamic equilibrium stage; and C/N > 11 can indicate the process of complete humification (Thomsen et al., 2008). Parolari and Porporato (2016) also proposed that when C/N > 10, the mineralization of SOC began to be restricted. Generally, the C/N ratios in this study were within the range of 10–50, except for a few low-value points. This indicated that soil organic matter is in the process of complete humification in the YRD, and the mineralization of organic carbon in this area had been inhibited to a certain extent. Cleveland and Liptzin (2007) observed that the soil C/N ratio was relatively consistent across various ecosystem types, although the soil was characterized by high biological diversity, structural complexity, and spatial heterogeneity (Yang et al., 2010). Our results in the current study showed that the C/N ratio in the surface soils was higher than that in deeper soils in PV and SS wetlands ($P < 0.05$). Although there was no statistically significant value, the soil C/N ratios tended to decrease with soil depth in PV and SS wetlands. However, the soil C:N ratios were relatively unstable in the PA wetland.

The C/P ratio is usually an indicator for the mineralization ability of soil organic phosphorus, and C/S represents the effect of the microbial biomass of the site on the availability of soil S (Heinze et al., 2010). When the ratios of C/P and C/S in a certain area are high, the limits of P and S during the decomposition of soil organic matter are not conducive for the growth of plants in the area. In contrast, low C/P and C/S ratios will contribute to the release of nutrients during the decomposition of organic matter and increase the available P and S levels in the soil. In addition, Reddy and DeLaune (2008) presented that the initial S mineralization would occur when the C/S ratio is less than 200, and the initial S immobilization will occur when the C/S ratio is in access of 400. In this study, the low ratios of C/P (2–7) and C/S (10–35) indicated that the mineralization of P and S, instead of immobilization, is the main process in the YRD (**Figure 4**), resulting in lower accumulation in this region. Compared with other coastal wetlands in China, the soil nutrients in the YRD are relatively low (Zhang et al., 2012, 2013), indicating that the exchange of carbon and nutrients between the YRD and the external environment might be very active (Cao et al., 2015). Soil N/P and C/N/P also could be used as indicators of nutrient restriction types. In the current study, The N/P ratios in three wetlands were less than 1.2, which was similar to the results of Gao et al. (2012). Similarly, the C/N/P ratios were between 0 and 0.1. Therefore, the YRD is a nitrogen-limited area, and the accumulated SOC content in this area was relatively less than N and P.

CONCLUSION

The deposition and ecological stoichiometric of C, N, P, and S were investigated in coastal wetlands along a sampling belt of the YRD in this study. The results showed three accumulative hotspots of C, N, and S in soil profiles in PA and SS wetlands (0–10, 40–60, and 90–100 cm), and one accumulative hotspot of P in SS (10–20 cm) and PA (80–90 cm) wetlands. In PV wetlands, one accumulative hotspot of C, P, and S appeared in the top 10 cm, whereas N at the soil depth of 90–100 cm. Generally, due to the erosion of rivers, higher soil deposition rates and deposition fluxes of C, N, P, and S were observed in PA and SS wetlands compared with PV wetlands. Topsoil concentration factors showed that the area was mainly affected by the input of plant residues, while the leaching effect gradually strengthens with increasing salinities. The ecological stoichiometry further verified that coastal wetlands in the YRD were nitrogen-limited ecosystems and in the stage of accelerating the decomposition of soil organic matter. Improving the degree of salinization in this area, increasing the vegetation coverage of YRD, and reducing the erosion effect of rivers on soil will not only help to improve the ecological stability of this area but also increase the blue carbon storage of YRD and make better use of YRD's carbon sink function.

DATA AVAILABILITY STATEMENT

The original contributions presented in the study are included in the article/supplementary material, further inquiries can be directed to the corresponding authors.

AUTHOR CONTRIBUTIONS

SD and CW contributed to the writing of the manuscript. SD, QZ, and JJ involved in the field work and data collection. JB and QZ contributed to concept of study. JB, CW, YG, JJ, GZ, and CY provided important guidance on methods and writing. All authors contributed critically to drafts and gave approval for publication.

FUNDING

This study was financially supported by the Joint Funds of the National Natural Science Foundation of China (No. U2006215) and the National Natural Science Foundation of China (No. 42107490).

ACKNOWLEDGMENTS

We acknowledge all colleagues for their contributions to the fieldwork.

REFERENCES

Bai, J., Wang, J., Yan, D., Gao, H., Xiao, R., Shao, H., et al. (2012). Spatial and temporal distributions of soil organic carbon and total nitrogen in two marsh wetlands with different flooding frequencies of the Yellow River Delta, China. *CLEAN–Soil Air Water* 40, 1137–1144. doi: 10.1002/clen.201200059

Bai, J., Yu, L., Du, S., Wei, Z., Liu, Y., Zhang, L., et al. (2020). Effects of flooding frequencies on soil carbon and nitrogen stocks in river marginal wetlands in a ten-year period. *J. Environ. Manage.* 267:110618. doi: 10.1016/j.jenvman.2020.110618

Bai, J., Zhang, G., Zhao, Q., Lu, Q., Jia, J., Cui, B., et al. (2016). Depth-distribution patterns and control of soil organic carbon in coastal salt marshes with different plant covers. *Sci. Rep.* 6:34835. doi: 10.1038/srep34835

Canfora, L., Salvati, L., Benedetti, A., and Francaviglia, R. (2017). Is soil microbial diversity affected by soil and groundwater salinity? Evidences from a coastal system in central Italy. *Environ. Monit. Assess.* 189:319. doi: 10.1007/s10661-017-6040-1

Cao, L., Song, J., Li, X., Yuan, H., Li, N., Duan, L., et al. (2015). Geochemical characteristics of soil C, N, P, and their stoichiometrical significance in the coastal wetlands of Laizhou Bay, Bohai Sea. *CLEAN–Soil Air Water* 43, 260–270. doi: 10.1002/clen.201300752

Cheng, Q., Chang, H., Yang, X., Wang, D., and Wang, W. (2021). Salinity and nutrient modulate soil bacterial communities in the coastal wetland of the Yellow River Delta, China. *Environ. Sci. Pollut. Res.* 28, 14621–14631. doi: 10.1007/s11356-020-11626-x

Cleveland, C. C., and Liptzin, D. (2007). C: N: P stoichiometry in soil: is there a "Redfield ratio" for the microbial biomass? *Biogeochemistry* 85, 235–252. doi: 10.1007/s10533-007-9132-0

Coynel, A., Gorse, L., Curti, C., Schafer, J., Grosbois, C., Morelli, G., et al. (2016). Spatial distribution of trace elements in the surface sediments of a major

European estuary (Loire Estuary, France): Source identification and evaluation of anthropogenic contribution. *J. Sea Res.* 118, 77–91. doi: 10.1016/j.seares.2016.08.005

Cui, B., He, Q., and Zhao, X. (2008). Ecological thresholds of Suaeda salsa to the environmental gradients of water table depth and soil salinity. *Acta Ecol. Sin.* 28, 1408–1418. doi: 10.1016/s1872-2032(08)60050-5

DeLaune, R. D., Jugsujinda, A., Peterson, G. W., and Patrick, W. H. Jr. (2003). Impact of Mississippi River freshwater reintroduction on enhancing marsh accretionary processes in a Louisiana estuary. *Estuar. Coast. Shelf Sci.* 58, 653–662. doi: 10.1016/s0272-7714(03)00177-x

Ding, X. G., Wang, J. S., Zhao, G. M., Yuan, H. M., Wang, J., and Ye, S. Y. (2016). Accretion rate and controlling factors of carbon and nutrients during coastal wetland evolution in Yellow River Delta. *Geol. Chin.* 43, 319–328. doi: 10.12029/gc20160124

Elser, J. J., Acharya, K., Kyle, M., Cotner, J., Makino, W., Markow, T., et al. (2003). Growth rate–stoichiometry couplings in diverse biota. *Ecol. Lett.* 6, 936–943. doi: 10.1046/j.1461-0248.2003.00518.x

Fan, H., Wu, J., Liu, W., Yuan, Y., Hu, L., and Cai, Q. (2015). Linkages of plant and soil C: N: P stoichiometry and their relationships to forest growth in subtropical plantations. *Plant Soil* 392, 127–138. doi: 10.1007/s11104-015-2444-2

Feng, J., Zhou, J., Wang, L., Cui, X., Ning, C., Wu, H., et al. (2017). Effects of short-term invasion of Spartina alterniflora and the subsequent restoration of native mangroves on the soil organic carbon, nitrogen and phosphorus stock. *Chemosphere* 184, 774–783. doi: 10.1016/j.chemosphere.2017.06.060

Gao, H., Bai, J., Xiao, R., Yan, D., Huang, L., and Huang, C. (2012). Soil net nitrogen mineralization in salt marshes with different flooding periods in the Yellow River Delta, China. *CLEAN–Soil Air Water* 40, 1111–1117. doi: 10.1002/clen.201200031

Heinze, S., Raupp, J., and Joergensen, R. G. (2010). Effects of fertilizer and spatial heterogeneity in soil pH on microbial biomass indices in a long-term field trial of organic agriculture. *Plant Soil* 328, 203–215. doi: 10.1007/s11104-009-0102-2

Jiang, J., Huang, X., Li, X., Yan, Z., Li, X., and Ding, W. (2015). The Organic Carbon Reserve of Wet Beach Wetlands and Its Relationship with Soil Physical and Chemical Factors– Taking Chongming Dongtan as an Example. *J. Ecol. Rural Environ.* 31, 540–547.

Krull, K., and Craft, C. (2009). Ecosystem development of a sandbar emergent tidal marsh, Altamaha River Estuary, Georgia, USA. *Wetlands* 29, 314–322. doi: 10.1672/06-178.1

Lu, Q., Bai, J., Zhang, G., Zhao, Q., and Wu, J. (2018). Spatial and seasonal distribution of carbon, nitrogen, phosphorus, and sulfur and their ecological stoichiometry in wetland soils along a water and salt gradient in the Yellow River Delta, China. *Phys. Chem. Earth Parts A/B/C* 104, 9–17. doi: 10.1016/j.pce.2018.04.001

Luo, Z., Luo, Y., Wang, G., Xia, J., and Peng, C. (2020). Warming-induced global soil carbon loss attenuated by downward carbon movement. *Glob. Change Biol.* 26, 7242–7254. doi: 10.1111/gcb.15370

Parolari, A. J., and Porporato, A. (2016). Forest soil carbon and nitrogen cycles under biomass harvest: stability, transient response, and feedback. *Ecol. Model.* 329, 64–76. doi: 10.1016/j.ecolmodel.2016.03.003

Reddy, K. R., and DeLaune, R. D. (2008). *Biogeochemistry of wetlands: science and applications*. Boca Raton: CRC press.

Saintilan, N., Rogers, K., Mazumder, D., and Woodroffe, C. (2013). Allochthonous and autochthonous contributions to carbon accumulation and carbon store in southeastern Australian coastal wetlands. *Estuar. Coast. Shelf Sci.* 128, 84–92. doi: 10.1016/j.ecss.2013.05.010

Salome, C., Nunan, N., Pouteau, V., Lerch, T. Z., and Chenu, C. (2010). Carbon dynamics in topsoil and in subsoil may be controlled by different regulatory mechanisms. *Glob. Change Biol.* 16, 416–426. doi: 10.1111/j.1365-2486.2009.01884.x

Shi, L., Zheng, L., Mei, X., Yu, L., and Jia, Z. (2010). Characteristics of Soil organic carbon and total nitrogen under different land use types in Shanghai. *J. Appl. Ecol.* 21, 2279–2287. doi: 10.13287/j.1001-9332.2010.0325

Thomsen, I. K., Petersen, B. M., Bruun, S., Jensen, L. S., and Christensen, B. T. (2008). Estimating soil C loss potentials from the C to N ratio. *Soil Biol. Biochem.* 40, 849–852. doi: 10.1016/j.soilbio.2007.10.002

Wang, L., Wang, P., Sheng, M., and Tian, J. (2018). Ecological stoichiometry and environmental influencing factors of soil nutrients in the karst rocky desertification ecosystem, southwest China. *Glob. Ecol. Conserv.* 16, e00449. doi: 10.1016/j.gecco.2018.e00449

Wang, T., Kang, F., Cheng, X., Han, H., and Ji, W. (2016). Soil organic carbon and total nitrogen stocks under different land uses in a hilly ecological restoration area of North China. *Soil Till. Res.* 163, 176–184. doi: 10.1016/j.still.2016.05.015

Wang, X., Jiang, Z., Li, Y., Kong, F., and Xi, M. (2019). Inorganic carbon sequestration and its mechanism of coastal saline-alkali wetlands in Jiaozhou Bay, China. *Geoderma* 351, 221–234. doi: 10.1016/j.geoderma.2019.05.027

Wang, Y., Li, Y., Ye, X., Chu, Y., and Wang, X. (2010). Profile storage of organic/inorganic carbon in soil: From forest to desert. *Sci. Total Environ.* 408, 1925–1931. doi: 10.1016/j.scitotenv.2010.01.015

Wang, Z., Zhang, H., He, C., Liu, C., Liang, X., and Chen, X. (2019). Spatiotemporal variability in soil sulfur storage is changed by exotic Spartina alterniflora in the Jiuduansha wetland, China. *Ecol. Eng.* 133, 160–166. doi: 10.1016/j.ecoleng.2019.04.014

Wu, H., Lu, M., Lu, X., Guan, Q., and He, X. (2015). Interactions between earthworms and mesofauna has no significant effect on emissions of CO2 and N2O from soil. *Soil Biol. Biochem.* 88, 294–297. doi: 10.1016/j.soilbio.2015.06.005

Wu, H., Lu, X., Wu, D., Song, L., Yan, X., and Liu, J. (2013). Ant mounds alter spatial and temporal patterns of CO2, CH4 and N2O emissions from a marsh soil. *Soil Biol. Biochem.* 57, 884–891. doi: 10.1016/j.soilbio.2012.10.034

Yang, Y., Chen, Y., Li, W., and Chen, Y. (2010). Distribution of soil organic carbon under different vegetation zones in the Ili River Valley, Xinjiang. *J. Geogr. Sci.* 20, 729–740. doi: 10.1007/s11442-010-0807-4

Yang, Y., Fang, J., Ji, C., Datta, A., Li, P., Ma, W., et al. (2014). Stoichiometric shifts in surface soils over broad geographical scales: evidence from China's grasslands. *Glob. Ecol. Biogeogr.* 23, 947–955. doi: 10.1111/geb.12175

Yu, J., Wang, Y., Dong, H., Wang, X., Li, Y., Zhou, D., et al. (2013). Estimation of soil organic carbon storage in coastal wetlands of modern Yellow River Delta based on landscape pattern. *Wetl. Sci.* 11, 1–6. doi: 10.13248/j.cnki.wetlandsci.2013.01.006

Zhang, Z. S., Song, X. L., Lu, X. G., and Xue, Z. S. (2013). Ecological stoichiometry of carbon, nitrogen, and phosphorus in estuarine wetland soils: influences of vegetation coverage, plant communities, geomorphology, and seawalls. *J. Soil. Sediment.* 13, 1043–1051. doi: 10.1007/s11368-013-0693-3

Zhang, Z., Lu, X., Song, X., Guo, Y., and Xue, Z. (2012). Soil C, N and P stoichiometry of Deyeuxia angustifolia and Carex lasiocarpa wetlands in Sanjiang Plain, Northeast China. *J. Soil. Sediment.* 12, 1309–1315. doi: 10.1007/s11368-012-0551-8

Zhao, Q., Bai, J., Lu, Q., and Zhang, G. (2017). Effects of salinity on dynamics of soil carbon in degraded coastal wetlands: implications on wetland restoration. *Phys. Chem. Earth, Parts A/B/C* 97, 12–18. doi: 10.1016/j.pce.2016.08.008

Zhao, Q., Bai, J., Wang, X., Zhang, W., Huang, Y., Wang, L., et al. (2020). Soil organic carbon content and stock in wetlands with different hydrologic conditions in the Yellow River Delta, China. *Ecohydrol. Hydrobiol.* 20, 537–547. doi: 10.1016/j.ecohyd.2019.10.008

Conflict of Interest: The authors declare that the research was conducted in the absence of any commercial or financial relationships that could be construed as a potential conflict of interest.

Publisher's Note: All claims expressed in this article are solely those of the authors and do not necessarily represent those of their affiliated organizations, or those of the publisher, the editors and the reviewers. Any product that may be evaluated in this article, or claim that may be made by its manufacturer, is not guaranteed or endorsed by the publisher.

frontiers | Frontiers in Ecology and Evolution

ORIGINAL RESEARCH
published: 04 April 2022
doi: 10.3389/fevo.2022.855453

Comparing the Effectiveness of Biodiversity Conservation Across Different Regions by Considering Human Efforts

Kaikai Dong[1,2], Zhaoli Liu[2], Ying Li[2], Ziqi Chen[2,3], Guanglei Hou[2] and Jingkuan Sun[1]*

[1] Shandong Key Laboratory of Eco-Environmental Science for the Yellow River Delta, Binzhou University, Binzhou, China, [2] Northeast Institute of Geography and Agroecology, Chinese Academy of Sciences, Changchun, China, [3] College of Geo-Exploration Science and Technology, Jilin University, Changchun, China

The effective allocation of funds is of significant importance for biodiversity conservation, but there is currently no scientific method for comparing the effectiveness of biodiversity conservation across different regions. Existing studies omit differences in the ecological background, such as the terrain, climate, hydrology, soil, and ecosystem, or do not differentiate between the impacts caused by humans and nature. To address these limitations, we take habitat quality as a proxy for biodiversity and quantify the human-induced habitat quality changes as a means of measuring the efforts of management departments, with the background differences eliminated using a reference condition index. The method is applied to the San Jiang Plain Wetlands and Northwest Tibet Qiang Tang Plateau Biodiversity National Key Ecological Function Region in China. The results show that the effects of human activities on habitat improvement or degradation are overestimated or underestimated if there is no differentiation between human and natural causes. Human-induced habitat quality changes broadly reflect the human efforts toward biodiversity conservation. By considering the human efforts and background differentiation, the proposed method allows the effectiveness of biodiversity conservation to be compared across different regions. This study provides a scientific reference for China's transfer payment policy and for the biodiversity funds allocated in other countries. Furthermore, our results will guide the practice of improving habitat quality and biodiversity.

Keywords: effectiveness assessment, biodiversity conservation, regional comparison, reference condition, human efforts, background differentiation, habitat quality

OPEN ACCESS

Edited by:
Zhenguo Niu,
Aerospace Information Research Institute (CAS), China

Reviewed by:
Luan Zhaoqing,
Nanjing Forestry University, China
Jianjun Zhao,
Northeast Normal University, China
Xlaodong Wang,
Changchun Normal University, China

***Correspondence:**
Zhaoli Liu
liuzhaoli@iga.ac.cn

Specialty section:
This article was submitted to Conservation and Restoration Ecology, a section of the journal Frontiers in Ecology and Evolution

Received: *15 January 2022*
Accepted: *11 March 2022*
Published: *04 April 2022*

Citation:
Dong K, Liu Z, Li Y, Chen Z, Hou G and Sun J (2022) Comparing the Effectiveness of Biodiversity Conservation Across Different Regions by Considering Human Efforts. Front. Ecol. Evol. 10:855453. doi: 10.3389/fevo.2022.855453

INTRODUCTION

As a highly effective tool for biodiversity conservation, protected areas (PAs) have expanded rapidly around the globe, and currently cover 15% of the terrestrial surface (UNEP-WCMC et al., 2020). However, habitat loss and degradation in PAs remain serious areas of concern (Almond et al., 2020). One important reason is the scarcity of funds and resources (Coad et al., 2019; Reed et al., 2020). Generally, when more funds and resources are allocated for PAs, the effects of biodiversity conservation are more effective better. However, such funds are limited, which greatly restricts

the protection effects. Therefore, the effective allocation of funds is a key issue in biodiversity conservation (Coad et al., 2019).

The most effective means of allocating funds is particularly important in China. To improve the national biodiversity level, China has designated several key ecological function regions, which are types of PAs (Fan et al., 2012). The Ministry of Ecology and Environment measures the protection work of local government management departments by quantitatively assessing the effectiveness of biodiversity conservation, and then takes actions such as administrative management, policy changes, and capital investment. Specifically, the central government provides transfer payment after measuring the biodiversity conservation efforts made by the management of these ecological function regions (Zheng et al., 2019). Those regions that have made greater efforts are rewarded with more funds, whereas those that have made lesser efforts may have funds deducted. Therefore, it is imperative to develop a method that can be used to compare the biodiversity conservation efforts between different ecological function regions.

To date, most assessment studies for biodiversity conservation effectiveness have focused on a single PA, such as in before–after comparisons (Liu et al., 2001; Gaveau et al., 2007), inside–outside comparisons, and matching comparisons (Andam et al., 2008; Joppa and Pfaff, 2011; Geldmann et al., 2019; Terraube et al., 2020). For example, Gaveau et al. (2007) compared the deforestation rates inside and outside PAs in Sumatra, while Geldmann et al. (2019) assessed the effectiveness of PAs at resisting anthropogenic pressures using matching analysis. Different from the above, Zheng et al. (2012) used key species numbers, endangered species numbers, and rare species numbers to compare the effectiveness of biodiversity conservation between different national wetland nature reserves in China. However, this evaluation could not reflect the true differences among protection effectiveness because there was no background differentiation between the ecological environment in different regions. For example, they gave the Sanjiangyuan nature reserve a poor conservation effectiveness grade just because its low ecological background, this result was not convincing and cannot stimulate the enthusiasm for the related management department. Furthermore, differences in ecological background can also lead to obvious differences in the difficulty of conducting ecological construction and protection, and the need for funds (Liu et al., 2020). For example, the afforestation cost in the western area of the Hexi Corridor in Gansu Province is as high as $4722 per hectare because of the fragile natural ecological environment, whereas the afforestation cost in Ergun, Inner Mongolia, is only $1416 per hectare because of its superior natural condition (Liu et al., 2017). The assessment results cannot be applied in practice without considering these differences.

To eliminate ecological background differentiation, Dong et al. (2018) developed a method of comparing the effectiveness of biodiversity conservation between different regions. They selected national natural reserves inside biodiversity ecological function regions as reference areas, and used the habitat quality of these reference areas as reference conditions reflecting the biological background. The degree of difference between the habitat quality of the ecological function region and its corresponding reference condition was then used to measure the effectiveness of biodiversity conservation between different regions. Although this approach successfully eliminates the ecological background differentiation, it does not differentiate between human-induced and nature-induced habitat change. When the central government transfers funding, human efforts should only be used to compare the effectiveness of biodiversity conservation. Here, human efforts include both positive impacts (ecological restoration) and negative human impacts (crop expansion and urbanization) on biodiversity. If natural processes are incorporated, the assessment results will be biased. Therefore, it is imperative to develop a method that considers both human efforts and ecological background differentiation.

In this study, we take the San Jiang Plain Wetlands (SJPW) and Northwest Tibet Qiang Tang Plateau Biodiversity National Key Ecological Function Region as study areas, and compare the effectiveness of biodiversity conservation from 1990–2018 by considering both human efforts and ecological background differences. The main objectives were as follows: (1) construct a human-induced habitat quality change index to measure human efforts on biodiversity conservation; (2) develop a method for comparing the effectiveness of biodiversity conservation across different regions. Our study provides a scientific reference for national transfer payment.

MATERIALS AND METHODS

Study Area

The SJPW and Northwest Tibet Qiang Tang Plateau (NTQTP) Biodiversity National Key Ecological Function Region were chosen as study areas (**Figure 1**). SJPW (45°0′57″–48°27′47″N, 129°29′52″–135°5′12″E) is located in the downstream area of the Songhua River near the confluence with Wusuli River in Heilongjiang Province. It extends over seven counties and has a total area of 48,000 km^2. There are many national nature reserves in the district, such as Dongfanghong Wetlands National Nature Reserve. More than 150 species of rare birds inhabit the area, including eight first-class protected animals such as red-crowned cranes and white storks. The area has a temperate humid and semi-humid continental monsoon climate, with an average annual rainfall of 500–650 mm and an average temperature of 1.4–4.3°C. From 2015–2018, the land-use changes induced by crop expansion, urbanization, and land degradation covered 4824, 102, and 1 km^2, respectively. Land-use changes induced by ecological restoration covered 590 km^2. Therefore, SJPW is still suffering from intensive positive and negative human impacts.

Northwest Tibet Qiang Tang Plateau is located in the northwestern part of the Tibet Autonomous Region, covering five counties and extending over a total area of 490,000 km^2. Selincuo and Qiangtang National Nature Reserves lie inside this district. Several rare and endemic species inhabit the region, such as the Tibetan antelope, Tibetan wild donkey, and wild yak. The area belongs to the climate region of the Qinghai–Tibet Plateau, with an average annual rainfall of 100–300 mm, an average annual temperature of less than 0°C, and an average temperature of less than −10°C in the coldest month. From 2015 to 2018,

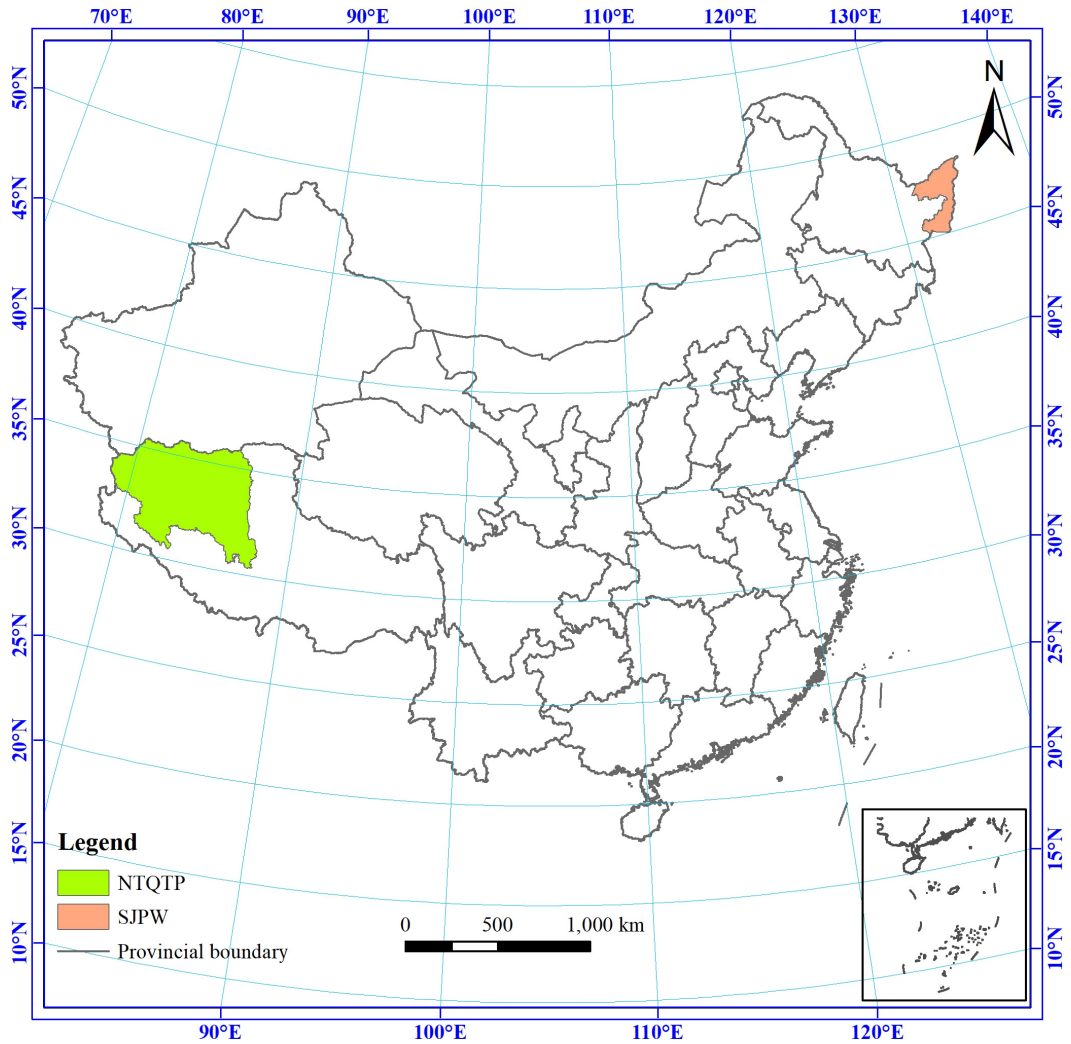

FIGURE 1 | Locations of study areas.

land-use changes induced by land degradation and ecological restoration covered 1,261 and 1,684 km^2, respectively; there was no crop expansion and only 3 km^2 of urbanization-induced land-use changes.

In summary, there are obvious differences between the two regions in terms of the protection target species and environmental factors such as terrain, climate, hydrology, and soil. The positive/negative human impacts in the two regions are also different. We therefore chose these two regions as our study areas.

Data Sources

For this study, land use data from 1980, 1990, 1995, 2000, 2005, 2010, 2015, and 2018 with a spatial resolution of 1,000 m was downloaded from the Resource and Environmental Science and Data Center of China. The data were transformed and resampled from a vector format, which was produced by manual digitalization with a scale of 1:10,0000. The total classification accuracy is more than 90%. There are six first-class land types (cropland, forestland, grassland, water body, built-up areas, and unused land) and 25 second-class land types. Land use was reclassified according to the habitat classification framework developed by Song and Deng (2017) and Tang et al. (2021); see **Table 1**.

The boundaries of SJPW and NTQTP were taken from the "National Planning for Key Function Areas" document (State Council of the People's Republic of China, 2010). The boundaries of national nature reserves were obtained from the Resource and Environmental Science and Data Center.[1]

Methods

In this study, habitat quality was used as a proxy for biodiversity. To measure the degree of effort made by biodiversity management departments, human-induced habitat

[1]https://www.resdc.cn/

TABLE 1 | Land-use reclassification.

Original land-use classification		Land-use reclassification
1 Cropland	11 Paddy land	1 Cropland 11, 12
	12 Dry land	
2 Forestland	21 Forest	2 Forestland 21, 24
	22 Shrub	3 Shrub 22
	23 Open forest savanna	4 Open forest savanna 23
	24 Others	
3 Grassland	31 Dense grass	5 Grassland 31, 32, 33
	32 Moderate grass	
	33 Sparse grass	
4 Water body	41 Streams and rivers	6 Wetlands 41, 42, 43, 44, 45, 46, 64
	42 Lakes	
	43 Reservoir and ponds	
	44 Permanent ice and snow	
	45 Beach and shore	
	46 Bottomland	
5 Built-up areas	51 Urban built-up	7 Urban built-up 51
	52 Rural settlements	8 Rural settlements 52
	53 Other Construction land	9 Construction land 53
6 Unused land	61 Sandy land	10 Unused land 61, 62, 63, 65, 66, 67
	62 Gobi	
	63 Salina	
	64 Swampland	
	65 Bare soil	
	66 Bare rock	
	67 Others	

quality changes were computed by differentiating between human-induced land-use changes. A reference condition index, which reflects the ecological background, was then constructed. Finally, a comparable regional index of biodiversity conservation effectiveness was developed based on the reference condition index.

Human-Induced Habitat Quality Changes Index

Habitat Quality

There is mounting evidence that habitat quality can be used as a proxy for biodiversity (Leh et al., 2013; Sallustio et al., 2017; Yi et al., 2018). The InVEST (Integrated Valuation of Ecosystem Services and Tradeoffs) model, jointly developed by Stanford University, The Nature Conservancy (TNC), and the World Wildlife Foundation (WWF), has been widely used for estimating habitat quality (Baral et al., 2014; Liu et al., 2021b; Mengist et al., 2021; Wu et al., 2021). Terrado et al. (2016) found that there was a significant correlation between the results estimated by the model and biodiversity observations, demonstrating the reliability of the model. Therefore, the InVEST model was used to estimate habitat quality as a representation of the biodiversity level.

In the InVEST model, habitat quality is determined by four factors: (1) the weights of different threat sources; (2) the relative sensitivity of each habitat to each threat source; (3) the distance between the habitat and the threat source; and (4) the degree of habitat protection. The formula for calculating the habitat quality Q_{xj} is as follows:

$$Q_{xj} = H_j\left(1 - D_{xj}^z/(D_{xj}^z + k^z)\right) \quad (1)$$

where Q_{xj} is the habitat quality of cell x of land-use type j; H_j is the habitat suitability of land-use type j, which can be assigned a value ranging from 0 to 1 (where 1 indicates the highest habitat suitability and 0 indicates no habitat suitability); D_{xj} is the threat level of cell x of land-use type j; k is the half-saturation constant [when $(1 - D_{xj}^z/(D_{xj}^z + k^z)) = 0.5$, $k = D_{xj}$]; and $z = 2.5$ is a scaling factor. D_{xj} is calculated as follows:

$$D_{xj} = \sum_{r=1}^{R}\sum_{y=1}^{Y_r}\left(w_r/\sum_{r=1}^{R} w_r\right) r_y i_{rxy} \beta_x S_{jr} \quad (2)$$

where r denotes an ecological threat; R is the total number of ecological threats; y is a cell within ecological threat layer r; Y_r is the total number of raster cells within ecological threat layer r; w_r is the weight of ecological threat r, indicating the relative impact of a certain threat factor; β_x is the accessibility level in grid cell x, where 1 indicates complete accessibility; S_{jr} is the sensitivity of land-use type j to threat r, and i_{rxy} is the impact of threat r that originates in grid cell y. We calculate i_{rxy} as follows:

$$i_{rxy} = 1 - \frac{d_{xy}}{d_{rmax}} \quad \text{Linear} \quad (3)$$

$$i_{rxy} = exp\left(-\left(\frac{2.99}{d_{rmax}}\right) d_{xy}\right) \quad \text{Exponent} \quad (4)$$

In this study, cropland, urban areas, rural settlements, and construction land were selected as the major threat factors to natural habitat. The habitat suitability of each habitat, the habitat sensitivity to the threat factors, the scope of impacts, the weights, and the maximum weighting distances were determined according to previous studies (He et al., 2017; Sun et al., 2019; Tang et al., 2021). The specific parameters can be found in **Supplementary Tables 1, 2**.

Definition of Human-Induced Land-Use Changes

Land-use changes can be divided into human-induced land-use changes and nature-induced land-use changes. Following Liu et al. (2021a), we defined the conversions between forestland, grassland, wetlands, shrubland, and open forest savanna as natural-induced land-use changes. Other conversions were defined as human-induced land-use changes (see **Figure 2**), covering four situations: (1) that induced by cropland expansion, i.e., the transfer from other land-use types to cropland; (2) that induced by urbanization, including the transfer to urban areas, rural settlements, and others; (3) that induced by land degradation, including the transfer to unused land; and (4) that induced by ecological restoration, including the transfer to forestland, grassland, and wetlands.

Human-Induced Habitat Quality Changes Index

Human-induced habitat quality changes reflect the human impacts of biodiversity maintenance capacity. These include

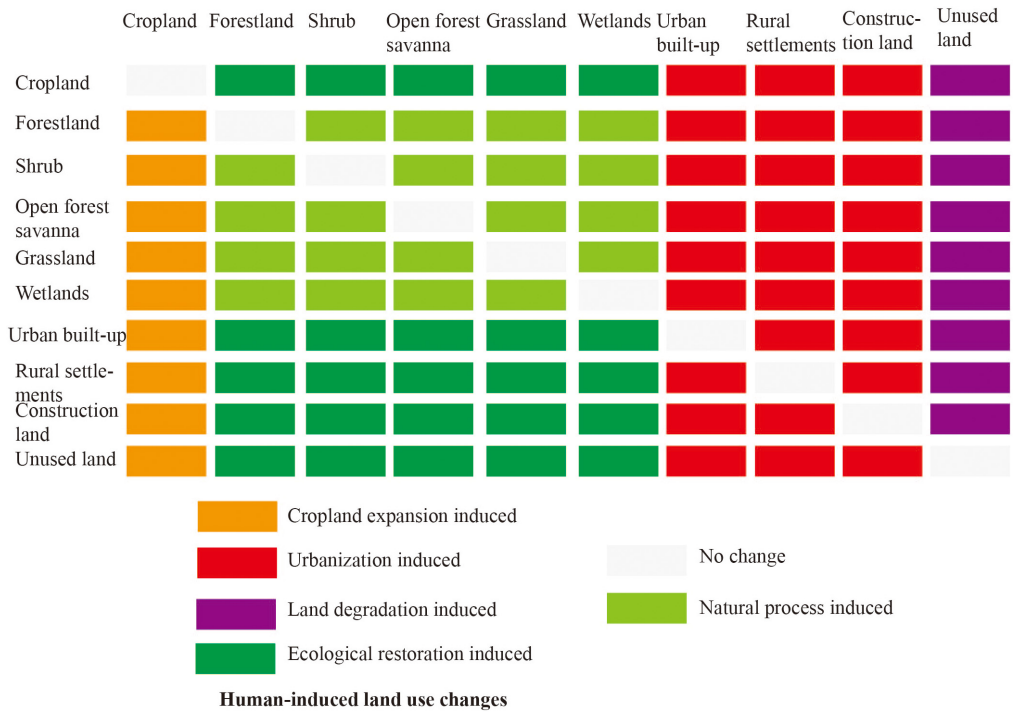

FIGURE 2 | Definition of human-induced land-use changes.

positive impacts, which improve the ability for biodiversity maintenance, and negative impacts, which damage the potential for biodiversity maintenance.

The human-induced habitat quality changes index (*HHQCI*) was calculated as follows: (**Figure 3**) (1) based on the land-use change map from year T1 to year T2, calculated using ArcGIS, the human-induced land-use changes are obtained using the "Con" function in ArcGIS; (2) using the land-use map of year T1, the habitat quality map can be calculated using the InVEST model, and the human-induced habitat quality map from year T1 to year T2 can be obtained by imputing the human-induced changes from year T1 to year T2; (3) the spatial distribution of *HHQCI* from year T1 to year T2 can be calculated by subtracting the human-induced habitat quality map from year T1 to year T2 from the habitat quality map of year T1 using the raster calculator in the ArcGIS platform.

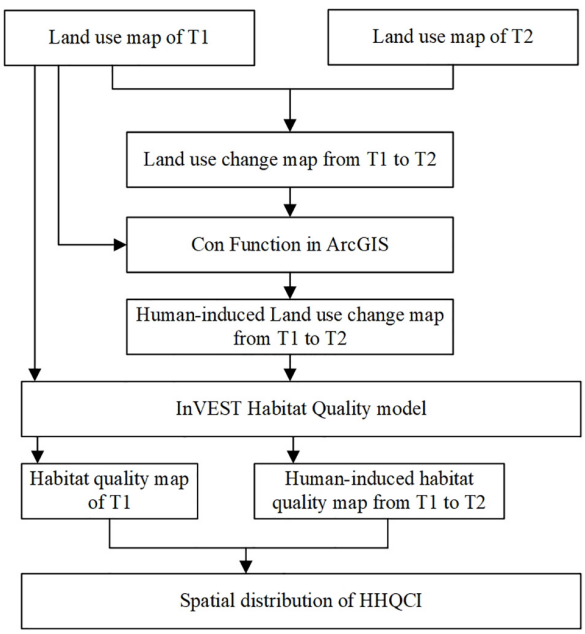

FIGURE 3 | Flowchart of HHQCI calculation.

Reference Condition Index

Reference conditions are widely used in restoration ecology. The reference condition refers to attribute values or characteristics of a reference ecosystem. Generally, several principles should be followed in selecting the reference conditions: (1) the reference should be the best of the existing conditions; (2) there should be little human disturbance; and (3) the reference condition should be achievable by the current sites if they are managed better.

The core areas of national nature reserves always suffer less human disturbance. Therefore, the optimum habitat quality value of the core area of national nature reserve located in the ecological function Regions from 1980–2018 were used to determine the reference condition index (*RCI*) through the following formula:

$$RCI = MAX(HQ_{1980}, HQ_{1990}, HQ_{1995}, HQ_{2000}, HQ_{2005}, HQ_{2010}, HQ_{2015}, HQ_{2018}) \quad (5)$$

TABLE 2 | HHQCI and total habitat quality changes and their biases from 1980–2018.

Year	SJPW			NTQTP		
	HHQCI	THQC	Bias	HHQCI	THQC	Bias
1980–1990	−0.103832	−0.113682	0.009849	0.000000	0.000000	0.000000
1990−−1995	−0.048314	−0.046866	−0.001448	−0.073423	−0.074927	0.001504
1995–2000	−0.025431	−0.023915	−0.001516	0.073425	0.074929	0.001504
2000–2005	−0.007303	−0.007125	−0.000178	−0.000256	−0.000253	−0.000002
2005–2010	−0.020722	−0.007563	−0.013159	−0.168142	−0.151838	−0.016303
2010–2015	−0.017267	−0.016773	−0.000494	−0.000081	0.000025	−0.000056
2015–2018	−0.078042	−0.075649	−0.002392	0.001230	0.001356	0.000126
1980–2018	−0.305471	−0.167501	−0.137970	−0.167501	−0.150707	−0.016794

TABLE 3 | Human-induced land-use changes from 1980–2018 (units: km^2).

Year	SJPW				NTQTP			
	Crop expansion	Urbanization	Land degradation	Ecological restoration	Crop expansion	Urbanization	Land degradation	Ecological restoration
1980–1990	5863	203	2	301	0	0	0	0
1990–1995	4119	77	5	1113	0	2	72123	23694
1995–2000	2122	25	1	776	0	0	23696	72124
2000–2005	449	4	0	99	0	0	105	14
2005–2010	5264	510	4	3671	4	2	137026	22713
2010–2015	940	19	0	2	0	2	208	172
2015–2018	4824	102	1	590	0	3	1261	1684
1980–2018	17759	641	3	941	3	6	136899	22891

where HQ_{1980}, HQ_{1990}, HQ_{1995}, HQ_{2000}, HQ_{2005}, HQ_{2010}, HQ_{2015}, and HQ_{2018} represent the habitat quality of the core area of the national nature reserves in 1980, 1990, 1995, 2000, 2005, 2010, 2015, and 2018, respectively.

Biodiversity Conservation Effectiveness Regional Comparable Index

Based on *HHQCI* and *RCI*, the biodiversity conservation effectiveness regional comparable index (*CEI*) was constructed as follows:

$$CEI_{i,j} = \frac{HHQCI_{i,j}}{RCI} \quad (6)$$

where $CEI_{i,j}$ is the *CEI* from year *i* to year *j*; $HHQCI_{i,j}$ is the *HHQCI* from year *i* to year *j*; and *RCI* is the reference condition index.

RESULTS

Human-Induced Habitat Quality and Total Habitat Quality Changes From 1990–2018

Human-induced habitat quality changes index and the total habitat quality changes (THQC) are presented in **Table 2**, along with their biases in SJPW and NTQTP. For the period 1980–2018, the HHQCI values in SJPW and NTQTP are −0.3055 and −0.1675, respectively. This is because the two regions have undergone severe human-induced land-use disturbances over this time (see **Table 3**). For SJPW, the land-use changes induced by crop expansion, urbanization, and land degradation cover 641, 641, and 3 km^2, respectively, while ecological restoration-induced land-use changes extended across 941 km^2. For NTQTP, although there were very low levels of crop expansion and urbanization, land degradation affected 136,899 km^2, almost six times the area of ecological restoration. The HHQCI values of each time period in SJPW are negative, meaning that the habitat condition was consistently destroyed by human activities. The worst stage is 1980–1990, with an HHQCI value of −0.1038. In this period, crop expansion (5,863 km^2) and urbanization (203 km^2) induced severe land-use changes, while ecological restoration was applied to only 301 km^2. The period of least human disturbance was 2000–2005, when the HHQCI value is −0.0073 and cropland expansion and urbanization covered only 449 and 4 km^2, respectively. The HHQCI values of NTQTP are positive, negative, and zero, meaning that human impacts had positive and negative efforts on NTQTP. The maximum HHQCI value in NTQTP is 0.0734, from the period 1995–2000, when ecological restoration-induced land-use changes reached 72,124 km^2. The minimum value is −0.1681 in 2005–2010, when land degradation had a severe impact.

The biases were obtained by subtracting the absolute values of THQC and HHQCI. Positive biases indicate that human impacts are underestimated, while negative values indicate an overestimation of human impacts. For the period 1980–2018, the human impacts on SJPW and NTQTP would all be underestimated if we did not differentiate the human-induced habitat quality changes, having bias values of −0.137970 and −0.016794, respectively. The degree of underestimation is not the same, and will generally be different when using HHQCI to quantify the efforts of management departments. For different

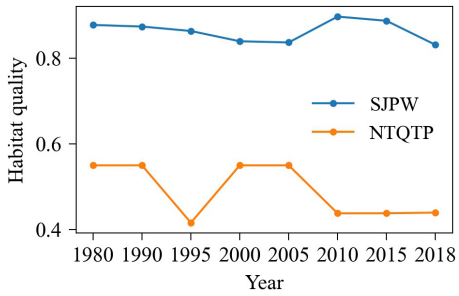

FIGURE 4 | Habitat quality changes of the core areas of national nature reserves in SJPW and NTQTP from 1980–2018.

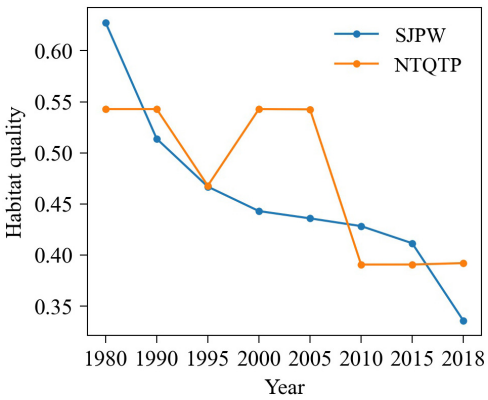

FIGURE 5 | Habitat quality changes in SJPW and NTQTP from 1980–2018.

time periods, the biases of SJPW are all negative, except for 1980–1990. The maximum bias value is −0.013159 from the period 2005–2010. There is no bias in NTQTP from 1980–1990, as there is no change of habitat quality over this period. The maximum bias value is from 2005–2010, where the underestimation of habitat quality reaches 0.016303. Therefore, it is important to use HHQCI instead of THQC to measure human efforts, as this provides a more rational basis for the allocation of biodiversity funds.

Reference Condition Index of San Jiang Plain Wetlands and Northwest Tibet Qiang Tang Plateau

Figure 4 shows the habitat quality changes of the core areas of the national nature reserves in SJPW and NTQTP from 1980–2018. It is clear that the habitat quality of the core areas in SJPW is much better than in NTQTP. Specifically, the habitat quality of nature reserves in SJPW decreases from 1980–2005, climbs to a peak in 2010, and declines again thereafter. Thus, the reference year for SJPW is 2010 and its RCI value is 0.897. The habitat quality of nature reserves in NTQTP first decreases from 1980–1995, then increases from 1995–2005, before decreasing again from 2005–2018. Therefore, the reference year for NTQTP is 1980 and its RCI value is 0.5500.

Habitat Quality and Conservation Effectiveness From 1980–2018

Figure 5 shows the habitat quality of SJPW and NTQTP from 1980–2018. The habitat quality of SJPW shows a consistent downward trend, decreasing from 0.6275 in 1990 to 0.3360 in 2018. The habitat quality of NTQTP exhibits a decreasing–increasing–decreasing. The maximum value of the habitat quality in NTQTP is 0.54288 in 1980 and 1990, and the minimum value is 0.39079 in 2010. Comparing the two areas, it can be seen that, with the exception of 2010 and 2015, the habitat quality of NTQTP is much better than that in SJPW. **Figure 6** shows the spatial distribution of habitat quality changes in SJPW and NTQTP from 1980–2018. In general, the habitat quality degradation in SJPW (mean value of −0.2932) is much more serious than that in NTQTP (mean value of −0.1509). The habitat quality change in both SJPW and NTQTP from 1980–2018 exhibits obvious spatial differences. This is especially true in SJPW, where the habitat quality degradation is severe in the northern and southern regions, while habitat quality improvements are scattered across the whole region. In NTQTP, the habitat quality improvement is better in the northwest of the region.

Figure 7 shows the CEI of SJPW and NTQTP from 1990–2018. The conservation efforts in SJPW are most effective from 2000–2005, with a CEI value of −0.008. The worst period for SJPW is from 1980–1990, when the CEI is −0.1157. The effectiveness of conservation efforts in NTQTP is best from 1995–2000, with a CEI value of 0.1335. The least-effective conservation efforts occur from 2005–2010, with a CEI of −0.3057. In general, the conservation effectiveness of NTQTP is better than that in SJPW, except from 1990–1995 and 2005–2010. **Figure 8** shows the spatial distribution of CEI in SJPW and NTQTP from 1980–2018. In general, the CEI in SJPW (mean value of −0.3405) is much worse than that in NTQTP (mean value of −0.3046). For SJPW, high CEI values are distributed in the middle and northwest parts of the region, while lower values are mainly distributed in the northeast part. For NTQTP, high values of CEI can be found in the northwest part, with lower values sporadically distributed in the southwest part of the region.

DISCUSSION

To stimulate biodiversity conservation initiatives in management departments, China implemented the transfer payment policy. Transfer funds are allocated according to the assessment results of the effectiveness of biodiversity conservation. To ensure the equality of the policy, the protection effectiveness caused by human efforts should be comparable. Additionally, the different ecological backgrounds of different regions should be considered. These two aspects make it challenging to compare the effectiveness of biodiversity efforts across different regions.

Several studies have used the inside–outside comparison method to differentiate between the impacts of humans and nature (Mao et al., 2021; Mu et al., 2021). For example, Mu et al. (2021) combined a land-use dynamic index and landscape

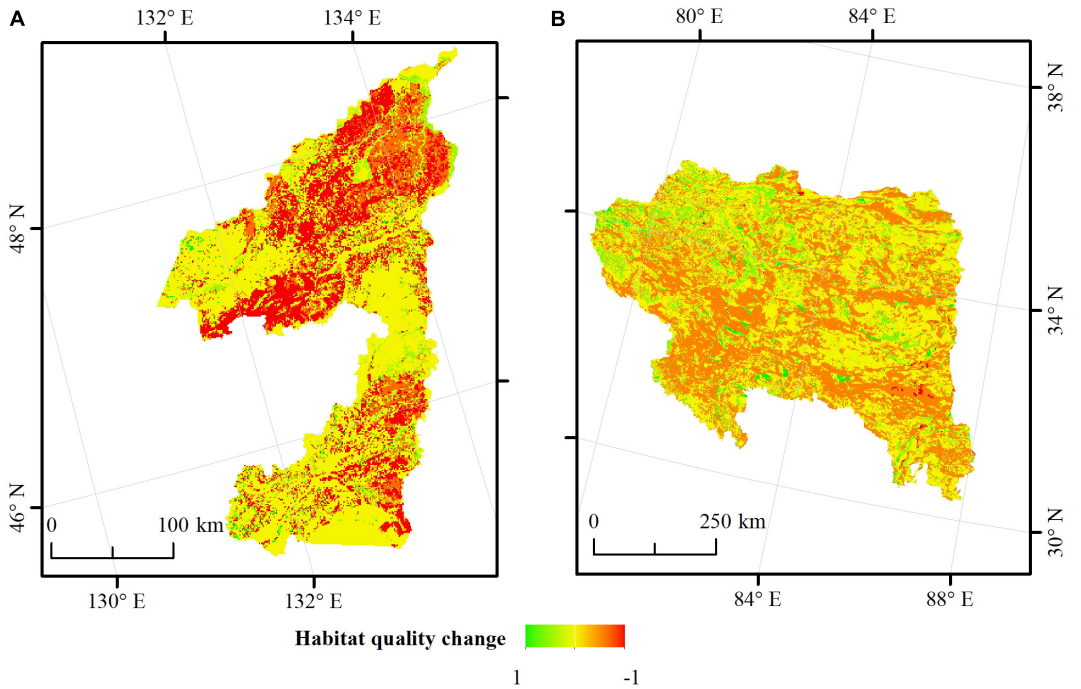

FIGURE 6 | Spatial distribution of habitat quality changes in SJPW **(A)** and NTQTP **(B)** from 1980–2018.

fragmentation dynamic index to assess the effectiveness of 92 wetland national nature reserves in China. They used sub-catchments containing PAs as references and distinguished the human- and nature-induced changes using statistical analysis. Their method takes the potential hypothesis that the natural conditions inside and outside the PAs are the same. Any differences between the changes inside and outside the PAs are then assumed to be caused by humans. However, the habitat outside the PAs can suffer positive or negative human disturbance, leading to overestimated or underestimated human impacts on the PAs. Gong et al. (2017) used changes in the distance between pandas and threat sources to measure the degree of human efforts. However, the distance to the threat source is only one aspect reflecting human efforts toward biodiversity protection. In this study, we used the human-induced habitat quality to reflect the efforts made by management departments. Human-induced habitat quality was estimated by the InVEST model, which considers habitat suitability, threat sources, and the distance to threat sources. Therefore, our method is much more comprehensive and reasonable.

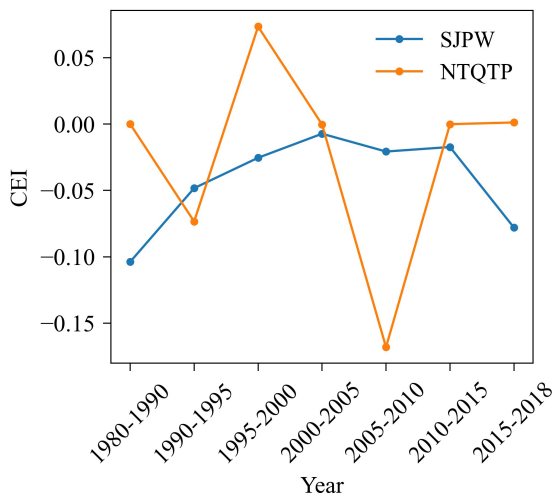

FIGURE 7 | CEI of SJPW and NTQTP from 1980–2018.

Our study found that the total habitat quality changes may overestimate or underestimate the human impacts on habitat improvement or degradation, and the biases between total habitat quality changes and human-induced habitat quality changes are different in SJPW and NTQTP. This implies that if the human impacts are not differentiated, the effects of the efforts made by management departments will not be equitably reflected. Clarifying the causes of human-induced changes also guides the practice for improving habitat quality.

National nature reserves in China are the most strictly PAs for biodiversity conservation and suffer relatively little human disturbance (Xu et al., 2017). We used the optimum habitat quality of national nature reserves inside the ecological function regions as the reference condition, and applied the ratio of human-induced habitat quality changes to the reference condition value to eliminate the background differentiation. In our previous study (Dong et al., 2018), the distance to the reference was used as a metric of conservation effectiveness. If the changes in the distance to the reference remained the

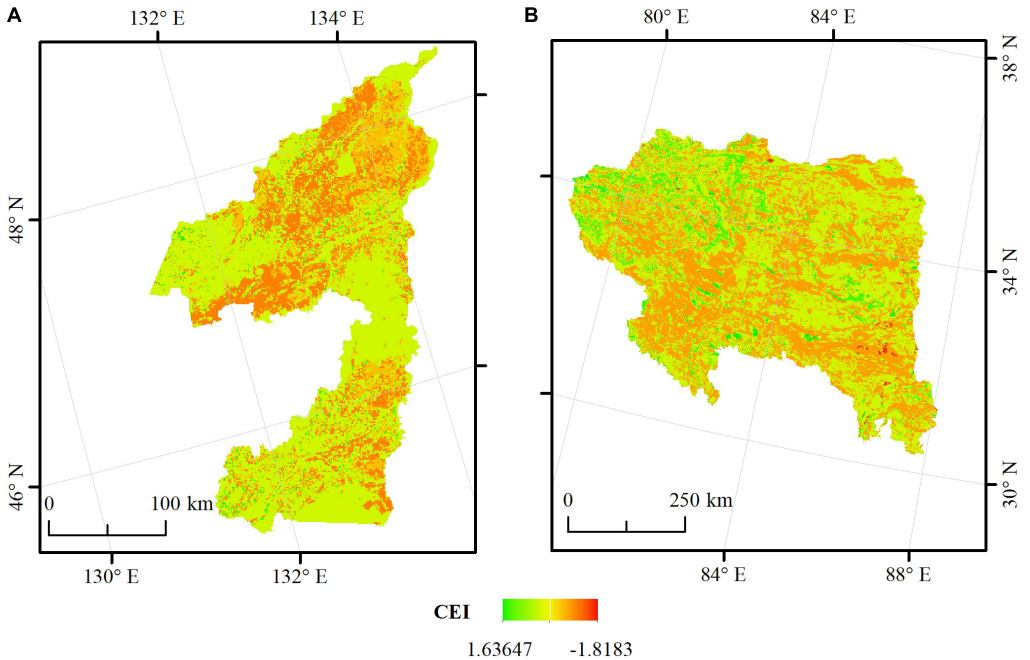

FIGURE 8 | Spatial distribution of CEI in SJPW **(A)** and NTQTP **(B)** from 1980–2018.

same between different regions, the conservation effectiveness was assumed to be equivalent. However, because there are large differences in the ecological background and recovery difficulties among different regions, the same conservation effectiveness value does not reflect the same human effort. Therefore, in this study, the ratio of human-induced habitat quality changes to the reference condition was used to eliminate the background difference.

Our results show that direct assessment using habitat quality produces different outcomes from assessment using CEI. Habitat quality is the same as the species richness index selected by Zheng et al. (2012) when they conducted a spatial comparison of national nature reserves. Both metrics reflect the biodiversity maintenance ability of the ecosystem itself, and do not consider the ecological background and restoration difficulties. The assessment results are therefore not convincing.

Equality is one of the most important principles in determining whether the central government will pay transfer funding across different regions. If biodiversity funds are not allocated equally, the policy will not perform well in terms of stimulating biodiversity conservation. To ensure equality, our method first distinguishes the human impacts and natural process impacts on habitat quality improvement or degradation. Positive and negative human impacts are then used to represent the human efforts made by management departments. However, this is not sufficient, because there are large differences in the ecological background of different regions, leading to large differences in the difficulty of restoration. Hence, a reference condition index was constructed and the ratio of human-induced habitat quality changes to the reference condition index was calculated to eliminate the background differences between different regions. Based on these two aspects, we believe our method provides a scientific reference for China's transfer payment policy, as well as for the allocation of biodiversity funds in other countries.

There are some limitations to this study. First, except for habitat quality, hunting and invasive species pressures can also cause changes in the effectiveness of biodiversity conservation. However, this limitation does not affect the practicality of the proposed method. Second, habitat quality was estimated by the InVEST model, which cannot reflect habitat quality differences across regions that have the same land-use type. This leads to the omission of positive or negative human impacts in regions of the same land-use type, such as wetland degradation. Third, the InVEST model cannot measure the ecological background differences related to terrain, climate, hydrology, soil, and the ecosystem. Fortunately, this does not influence the rationality of our method, which eliminates the ecological background differences by constructing a reference condition index. These aspects will be considered further in future research.

CONCLUSION

In this study, we developed a method for comparing the effectiveness of biodiversity conservation between different regions. Using habitat quality as a proxy for biodiversity, human-induced habitat quality changes were used to represent the human efforts of management departments. A reference condition index was then constructed to represent the reference state, and the ratio of human-induced habitat quality changes to the reference condition index was calculated to eliminate the background differences between different regions. The

main conclusions are as follows: (1) Human-induced habitat quality changes broadly reflect human efforts toward biodiversity conservation. (2) The application of the proposed method to SJPW and NTQTP has demonstrated its utility in comparing the effectiveness of biodiversity conservation across different regions. This study provides a significant reference for China's transfer payment policy. It also gives an insight into ecological compensation in other countries. Furthermore, our results will guide the management of habitat enhancement and biodiversity conservation.

DATA AVAILABILITY STATEMENT

The original contributions presented in the study are included in the article/**Supplementary Material**, further inquiries can be directed to the corresponding author.

AUTHOR CONTRIBUTIONS

KD wrote the manuscript and performed the data analysis. ZL conceived the manuscript. YL, ZC, GH, and JS reviewed and edited the manuscript. All authors contributed to the article and approved the submitted version.

FUNDING

This study was supported by the National Natural Science Foundation of China (42001266).

ACKNOWLEDGMENTS

We thank Jing Tang at Northeast Institute of Geography and Agroecology, Chinese Academy of Sciences for her helpful suggestions.

SUPPLEMENTARY MATERIAL

The Supplementary Material for this article can be found online at: https://www.frontiersin.org/articles/10.3389/fevo.2022.855453/full#supplementary-material

REFERENCES

Almond, R. E., Grooten, M., and Peterson, T. (2020). *Living Planet Report 2020-Bending the Curve of Biodiversity Loss*. WWF, Gland: World Wildlife Fund: Switzerland

Andam, K. S., Ferraro, P. J., Pfaff, A., Sanchez-Azofeifa, G. A., and Robalino, J. A. (2008). Measuring the effectiveness of protected area networks in reducing deforestation. *Proc. Natl. Acad. Sci. U.S.A.* 105, 16089–16094. doi: 10.1073/pnas.0800437105

Baral, H., Keenan, R. J., Sharma, S. K., Stork, N. E., and Kasel, S. (2014). Spatial assessment and mapping of biodiversity and conservation priorities in a heavily modified and fragmented production landscape in north-central victoria. *Austral. Ecol. Indic.* 36, 552–562. doi: 10.1016/j.ecolind.2013.09.022

Coad, L., Watson, J. E., Geldmann, J., Burgess, N. D., Leverington, F., Hockings, M., et al. (2019). Widespread shortfalls in protected area resourcing undermine efforts to conserve biodiversity. *Front. Ecol. Environ.* 17:259–264. doi: 10.1002/fee.2042

Dong, K. K., Hou, G. L., Xu, D. D., He, H. L., and Liu, Z. L. (2018). A method to compare the biodiversity conservation effectiveness between regions based on a reference condition. *Sustainability.* 10:3694. doi: 10.3390/su10103694

Fan, J., Sun, W., Zhou, K., and Chen, D. (2012). Major function oriented zone: new method of spatial regulation for reshaping regional development pattern in China. *Chin. Geogr. Sci.* 22, 196–209. doi: 10.1007/s11769-012-0528-y

Gaveau, D. L., Wandono, H., and Setiabudi, F. (2007). Three decades of deforestation in southwest sumatra: have protected areas halted forest loss and logging, and promoted re-growth? *Biol. Conserv.* 134, 495–504. doi: 10.1016/j.biocon.2006.08.035

Geldmann, J., Manica, A., Burgess, N. D., Coad, L., and Balmford, A. (2019). A global-level assessment of the effectiveness of protected areas at resisting anthropogenic pressures. *Proc. Natl. Acad. Sci. U.S.A.* 116, 23209–23215. doi: 10.1073/pnas.1908221116

Gong, M., Fan, Z., Zhang, X., Liu, G., Wen, W., and Zhang, L. (2017). Measuring the effectiveness of protected area management by comparing habitat utilization and threat dynamics. *Biol. Conserv.* 210, 253–260. doi: 10.1016/j.biocon.2017.04.027

He, J. H., Huang, J. L., and Li, C. (2017). The evaluation for the impact of land use change on habitat quality: a joint contribution of cellular automata scenario simulation and habitat quality assessment model. *Ecol. Model.* 366, 58–67. doi: 10.1016/j.ecolmodel.2017.10.001

Joppa, L. N., and Pfaff, A. (2011). Global protected area impacts. *Proc. R. Soc. Lond. Ser. B.* 278, 1633–1638. doi: 10.1098/rspb.2010.1713

Leh, M. D. K., Matlock, M. D., Cummings, E. C., and Nalley, L. L. (2013). Quantifying and mapping multiple ecosystem services change in West Africa. *Agric. Ecosyst. Environ.* 165, 6–18. doi: 10.1016/j.agee.2012.12.001

Liu, B., Pan, L. B., Qi, Y., Guan, X., and Li, J. S. (2021a). Land use and land cover change in the yellow river basin from 1980 to 2015 and its impact on the ecosystem services. *Land.* 10:1080. doi: 10.3390/land10101080

Liu, C., Cheng, K., Liu, H., Cheng, T. F., and He, D. (2017). Research on transfer payment of national key ecological function regions——taking five counties in gansu and two counties in inner mongolia as examples. *For. Econ.* 3, 3–15. doi: 10.13843/j.cnki.lyjj.2017.03.001

Liu, G. H., Wen, Y. H., Xie, J., and Liu, H. J. (2020). Evolution of transfer payment policy for national key ecological function areas and suggestions for improvement. *Environ. Prot.* 48, 9–14. doi: 10.14026/j.cnki.0253-9705.2020.17.002

Liu, J. G., Linderman, M., Ouyang, Z. Y., An, L., Yang, J., and Zhang, H. M. (2001). Ecological degradation in protected areas: the case of wolong nature reserve for giant pandas. *Science.* 292, 98–101. doi: 10.1126/science.1058104

Liu, Y. X., Liu, S. L., Wang, F. F., Sun, Y. X., Li, M. Q., Wang, Q. B., et al. (2021b). Responses of habitat quality and animal biodiversity to grazing activities on the Qinghai-Tibet Plateau. *Front. Ecol. Evol.* 9:349. doi: 10.3389/fevo.2021.681775

Mao, D. H., Wang, Z. M., Wang, Y. Q., Choi, C. Y., Jia, M. M., Jackson, M. V., et al. (2021). Remote observations in China's ramsar sites: wetland Dynamics, anthropogenic threats, and implications for sustainable development goals. *J. Remote Sens.* 2021:9849343. doi: 10.34133/2021/9849343

Mengist, W., Soromessa, T., and Feyisa, G. L. (2021). Landscape change effects on habitat quality in a forest biosphere reserve: implications for the conservation of native habitats. *J. Clean. Prod.* 329:129778. doi: 10.1016/j.jclepro.2021.129778

Mu, Y. L., Li, X. W., Liang, C., Li, P., Guo, Y., Liang, F. Y., et al. (2021). Rapid landscape assessment for conservation effectiveness of wetland national nature reserves across the Chinese mainland. *Glob. Ecol. Conserv.* 31:e01842. doi: 10.1016/j.gecco.2021.e01842

Reed, J., Oldekop, J., Barlow, J., Carmenta, R., Geldmann, J., Ickowitz, A., et al. (2020). The extent and distribution of joint conservation-development funding in the tropics. *One Earth.* 3, 753–762. doi: 10.1016/j.oneear.2020.11.008

Sallustio, L., De Toni, A., Strollo, A., Di Febbraro, M., Gissi, E., Casella, L., et al. (2017). Assessing habitat quality in relation to the spatial distribution

of protected areas in Italy. *J. Environ. Manage.* 201, 129–137. doi: 10.1016/j.jenvman.2017.06.031

Song, W., and Deng, X. Z. (2017). Land-use/land-cover change and ecosystem service provision in China. *Sci. Total Environ.* 576, 705–719. doi: 10.1016/j.scitotenv.2016.07.078

State Council of the People's Republic of China. (2010). *National Key Functional Zoning Plan*. Zhongnanhai: State Council of the People's Republic of China.

Sun, X. Y., Jiang, Z., Liu, F., and Zhang, D. Z. (2019). Monitoring spatio-temporal dynamics of habitat quality in Nansihu Lake basin, eastern China, from 1980 to 2015. *Ecol. Indicators.* 102, 716–723. doi: 10.1016/j.ecolind.2019.03.041

Tang, L. P., Ke, X. L., Chen, Y. Y., Wang, L. Y., Zhou, Q. S., Zheng, W. W., et al. (2021). Which impacts more seriously on natural habitat loss and degradation? Cropland expansion or urban expansion? Land. Degrad. *Dev.* 32, 946–964. doi: 10.1002/ldr.3768

Terrado, M., Sabater, S., Chaplin-Kramer, B., Mandle, L., Ziv, G., and Acuña, V. (2016). Model development for the assessment of terrestrial and aquatic habitat quality in conservation planning. *Sci. Total Environ.* 540, 63–70. doi: 10.1016/j.scitotenv.2015.03.064

Terraube, J., Helle, P., and Cabeza, M. (2020). Assessing the effectiveness of a national protected area network for carnivore conservation. *Nat. Commun.* 11:2957. doi: 10.1038/s41467-020-16792-7

UNEP-WCMC, IUCN and NGS (2020). *Protected Planet Live Report 2020*. Nairobi: UNEP-WCMC UNEP IUCN.

Wu, L. L., Sun, C. G., and Fan, F. L. (2021). Estimating the characteristic spatiotemporal variation in habitat quality Using the InVEST model—a case study from Guangdong–Hong Kong–Macao greater bay area. *Remote. Sens.* 13:1008. doi: 10.3390/rs13051008

Xu, W. H., Xiao, Y., Zhang, J. J., Yang, W., Zhang, L., Hull, V., et al. (2017). Strengthening protected areas for biodiversity and ecosystem services in China. *Proc. Natl. Acad. Sci. U.S.A.* 114, 1601–1606. doi: 10.1073/pnas.1620503114

Yi, H., Güneralp, B., Kreuter, U. P., Güneralp, I., and Filippi, A. M. (2018). Spatial and temporal changes in biodiversity and ecosystem services in the San Antonio River Basin, Texas, from 1984 to 2010. *Sci. Total Environ* 619, 1259–1271. doi: 10.1016/j.scitotenv.2017.10.302

Zheng, H., Wang, L., Peng, W., Zhang, C., Li, C., Robinson, B. E., et al. (2019). Realizing the values of natural capital for inclusive, sustainable development: Informing China's new ecological development strategy. *Proc. Natl. Acad. Sci. U.S.A.* 116:8623. doi: 10.1073/pnas.1819501116

Zheng, Y. M., Zhang, H. Y., Niu, Z. G., and Gong, P. (2012). Protection efficacy of national wetland reserves in China. *Chin. Sci. Bull* 57, 1116–1134. doi: 10.1007/s11434-011-4942-9

Conflict of Interest: The authors declare that the research was conducted in the absence of any commercial or financial relationships that could be construed as a potential conflict of interest.

The handling editor ZN declared a shared affiliation with the author(s) ZL, YL, ZC, and GH at the time of review.

Publisher's Note: All claims expressed in this article are solely those of the authors and do not necessarily represent those of their affiliated organizations, or those of the publisher, the editors and the reviewers. Any product that may be evaluated in this article, or claim that may be made by its manufacturer, is not guaranteed or endorsed by the publisher.

frontiers | Frontiers in Ecology and Evolution

SYSTEMATIC REVIEW
published: 08 April 2022
doi: 10.3389/fevo.2022.865516

Economic Evaluation and Systematic Review of Salt Marsh Restoration Projects at a Global Scale

Jiang-Jing Wang[1], Xiu-Zhen Li[1,2], Shi-Wei Lin[1] and Yu-Xi Ma[1]*

[1] State Key Laboratory of Estuarine and Coastal Research, Institute of Eco-Chongming, East China Normal University, Shanghai, China, [2] Yangtze Delta Estuarine Wetland Ecosystem Observation and Research Station, Ministry of Education and Shanghai Science and Technology Committee, Shanghai, China

Restoring degraded and damaged salt marshes has become an important initiative in the coastal wetlands management around the world. Evaluating the economic output of salt marsh restoration is of great significance for identifying the current state of knowledge gaps related to conservation activities and economic benefits. To address this question, we conducted an overview of global salt marsh restoration projects, and their financial expenses and restoration benefits in the past 40 years. The results showed that most of the saltmarsh restoration projects are near megacities and larger rivers, and restoration techniques of different regions depend on the types of disturbance factors such as climate change, extreme weather events, and land use change. With limited resources, fund allocation between protected areas and unprotected areas in middle-income countries is often unbalanced, indicating a mismatch between conservation efforts and regional needs. Although restoration projects are expensive, the evidence in this article implies that most salt marsh restoration projects could recover their financial expense in the finite time, especially for large-scale restoration activities. Besides, the great carbon sequestration potential would make salt marsh restoration projects more profitable under current efforts to promote carbon sequestration for combating global warming.

Keywords: salt marshes, ecological restoration, restoration cost, restoration outcome, mismatch, carbon

OPEN ACCESS

Edited by:
Guangxuan Han,
Yantai Institute of Coastal Zone Research (CAS), China

Reviewed by:
Chuan Tong,
Fujian Normal University, China
Dongdong Shao,
Beijing Normal University, China

***Correspondence:**
Xiu-Zhen Li
xzli@sklec.ecnu.edu.cn

Specialty section:
This article was submitted to Conservation and Restoration Ecology, a section of the journal Frontiers in Ecology and Evolution

Received: *30 January 2022*
Accepted: *07 March 2022*
Published: *08 April 2022*

Citation:
Wang J-J, Li X-Z, Lin S-W and Ma Y-X (2022) Economic Evaluation and Systematic Review of Salt Marsh Restoration Projects at a Global Scale. Front. Ecol. Evol. 10:865516. doi: 10.3389/fevo.2022.865516

INTRODUCTION

Coastal salt marshes usually occur in the intertidal zone of moderate to low-energy shorelines along estuaries, bays, and tidal rivers and have characteristics of both marine and terrestrial environments (Broome et al., 1988; Doody, 2008). They sustain a rich, dynamic, and productive ecological zone that plays an important role in biological diversity and human welfare (Mitsch and Gosselink, 2015). They not only provide abundant resources for production and daily life but also serve as nursery and shelter places for numerous species, including benthic fauna, fish, and migratory birds. Moreover, they provide a significant number of vital ecosystem services, including water purification, flooding mitigation, carbon sinks, climate stabilization, nutrient cycling, and coastal protection, and socioeconomic benefits (e.g., sightseeing and tourism, recreation, education, and research spaces; Barbier et al., 2011; Tang et al., 2018; Stewart-Sinclair et al., 2020). Although salt marshes occupied relatively small geographical space, less than 1% of the earth's surface area, the

economic value generated from related ecosystem services, culture, and employment was estimated around US$ 8,722 billion/year, approximately 29% of the global coastal wetland value of each year (Costanza et al., 2014; The United Nations Ocean Conference, 2017; Li et al., 2018).

Despite their importance, salt marshes were still under enormous pressure and disappeared at an unpredictable speed in the global scale (Scott et al., 2014). Triggered by climate change, sea level rise, and extreme weather events and disturbed by urbanization expansion and intensive human activities, 20–50% of salt marshes were predicted to be either lost or degraded during the current century (Barbier et al., 2011; Kirwan and Megonigal, 2013). Salt marsh degradation and loss have induced declinations in ecosystem resilience and biodiversity, which lead to the reduction of supporting ability and collapse of maintaining ability (Koch et al., 2009; DeLaune and White, 2012). Eventually, those processes would have an adverse effect on environmental and economic benefits. Even without considering other ecosystem services' loss, the annual economic loss of carbon emissions caused by the loss and degradation of salt marshes can reach US$ 6.4–97 million (Coverdale et al., 2014). In this context, salt marsh rehabilitation and restoration is an effective initiative to stop further degradation process and to restore the integrity, health, and sustainability of the degraded salt marsh ecosystem (Saintilan, 2013; Adam, 2019), especially in areas where natural recovery is relatively slow or facing biological or physical obstacles (Society for Ecological Restoration, 2004). Some successful salt marsh ecological restoration projects have been conducted around the world, such as the San Francisco Bay, the Gulf of Mexico, the Bay of Fundy, and the Yangtze River Estuary (Cornelisen, 1998; Roman and Burdick, 2012; Liu et al., 2016). These projects generated numerous environmental, economic, and social benefits, such as increase of ecosystem services, conservation of biodiversity, supplying of products, and jobs creation. For example, the report from the Restore America's Estuaries website[1] gave a message that coastal habitat restoration work in the Chesapeake Bay, the Great Lakes, and Everglades boosted US$ 4.3 billion economic output and supported more than 3,200 jobs (Restore America's Estuaries, 2011).

Although salt marsh restoration projects reinforce ecosystem function and generate relatively high benefits, people still pay less attention to salt marsh restoration and wrongly consider them as "net-cost" projects based on inadequate analysis (De Groot et al., 2013; Secretariat of the Convention on Biological Diversity, 2020). The cost of ecological restoration is relatively expensive, ranging from tens of thousands of dollars (for seagrass, salt marsh, and mangrove) to millions (for coral reefs; Spurgeon, 1999; Bullock et al., 2011). The high up-front cost and long-term nature of investment cannot match investors' desire for liquidity and might reduce their investment interests (Wainaina et al., 2020). However, some studies posed new evidence and suggested that salt marsh restoration projects were profitable (Mok, 2019; Taillardat et al., 2020). Besides, salt marshes and mangroves play an important role in keeping coastlines stable and could considerably reduce coastal infrastructure costs, which might make restoration engineering and sustainable management of marine ecosystems more economical (Hochard et al., 2019; van Zelst et al., 2021).

There is very substantial literature about salt marsh restoration and rehabilitation technologies and methods, restoration result evaluation indicators and their framework, and their application and accounting for specific sites, including reviews of them (Adam, 2019). However, interdisciplinary research among restoration ecology, society, and economy is lacking. While Spurgeon (1999) and Bayraktarov et al. (2016) had carried out some surveys about the cost and benefit of restoration, they focused on different marine and coastal ecosystems. Similarly, Su et al. (2021) analyzed the cost and benefit of mangrove restoration. But there have been few studies on salt marsh ecosystem restoration projects' cost and benefit at a global scale. Furthermore, the location preference (i.e., bias) phenomenon or mismatches between conservation efforts and regional demands might occur during restoration because of limited resources, invalid communication, lack of adaptive management, and weak links between conservation science and practice, among other reasons (Zhang et al., 2018). In fact, mismatches between restoration efforts and needs had been well documented in coral reefs, avian conservation, amphibians, and other conservation actions (Lawler et al., 2006; Fisher et al., 2011). Besides, although the number of marine-protected areas has increased over the past decade, the levels of protection investment of "areas of importance for ecosystem services" have not been effectively studied (United Nations Environment Programme -World Conservation Monitoring Centre et al., 2018).

Actually, the theoretical framework among ecological restoration goals, restoration technologies and methods, restoration projects' cost, and ecological policies should be better tailored to overcome people's prejudice about salt marsh restoration (Blignaut et al., 2013). Economic evaluation of restoration projects should be interpreted cautiously to determine if similar mismatches exist in salt marsh restoration activities. Further analysis of salt marsh restoration is necessary for us to understand the relationship between restoration projects' attributes and budget. Therefore, we conducted a systematic literature review to better identify knowledge gaps related to conservation activities and economic benefits, which was critical to improve practice and justify further investment in salt marsh restoration. We assessed the distribution, protection status, geographical area, duration, disturbance factors, techniques, cost, and outcome in relation to different restoration projects, to address the following three questions:

1. What are the spatial and temporal characteristics of global salt marsh restoration projects, as well as disturbance factors and restoration techniques and their changing patterns?
2. According to the financial cost of different restoration projects, is there a mismatch existing between conservation fund allocation and regional ecological service supplication?

[1] http://www.estuaries.org/

3. How long might it take for salt marsh restoration projects to pay for themselves? What is the impact of carbon ecosystem services and types of ecosystem services on this outcome?

METHODS

Literature Collection

We searched the peer-reviewed literature to identify quantitative studies about the economic costs and benefits of salt marsh restoration. In the first step, we first searched using the title search term "salt marsh," "ecosystem restoration," "ecological rehabilitation," and "coastal restoration" or their combination in the Google Scholar, Web of Science (WOS), and China National Knowledge Infrastructure (CNKI) online version database, respectively. Our search period is mainly focused from 1980 to 2001. After removing invalid, irrelevant, and repetitive articles, we did further screening according to the abstract and preliminarily obtained 232 relevant articles. We updated other restoration projects' data and supplemented additional useful information of all restoration projects by browsing governments' ecological and environmental department websites, non-profit organizations' websites, and influential ecological protection websites' databases. We also looked through relevant physical books, conference reports, and other "gray materials." Some effective messages, such as citations and personal communications, enabled us to figure out the connection of diverse information sources. According to the international principles and standards of ecological restoration practice proposed by Gann et al. (2019), the ecological restoration projects and experiments included in our analysis should meet some specific standards. We modified them for following practical reasons: (1) Stakeholders participation, (2) many types of knowledge used for ecological restoration, (3) a reference system, and (4) clear indicators for ecological assessment and restoration. For this study, 133 primary studies that had feasible economic data finally met the above criteria.

Restoration Cost and Benefit Data

As for the restoration cost, to eliminate the impact of inflation and regional disparity, we used consumer price index (CPI), purchasing power parity (PPP), and discount rate (DIS) to convert all value data into 2020 (base year). The calculation methods of three indices were derived from Hanley and Black (2006); Bayraktarov et al. (2016), and Wei et al. (2018). More details are shown in the **supplementary material**. A discount rate reflects a society's relative valuation on today's wellbeing versus wellbeing in the future. Since small changes in the discount rate would have a great influence on future benefits, huge errors might occur by roughly applying one or several discount rates to all restoration projects (Hanley et al., 2009). Therefore, we summarized the corresponding countries' discount rates (**Table 1**) and applied the exact value according to every restoration projects' reference year. We assumed a constant discount rate of 4.7% (value of 1978–2017) for the years after 2017 for the United States as relevant data are unavailable during this period. Similarly, the discount rate of China is 4.5% after 2011. All restoration projects were divided into two categories, namely, completed projects and ongoing projects. The completed projects' reference year used for monetary converting was chosen according to the following priority order: (1) funding year, (2) project year, (3) data collection year, and (4) publication year minus one. In contrast, those unfinished projects' reference year selection method was much easier. We defined all of them as 2021. All economic data were derived from the National Bureau of Statistics of China[2] and the World Bank website[3].

We recorded every sites' monetary value generated from restoration action. In addition, we replenished extra benefit data from the latest ESVD database (Ecosystem Service Value database, 2020) developed by De Groot et al. (2012). Every benefit value of the ESVD database was assigned to geographically overlapping or adjacent restoration sites through spatial analysis. Using the same way, further supplementary benefit data were obtained from official reports, monitoring data documents, and other relevant information. Detailed gray information sources are also available in the **Supplementary Material**. As mentioned above, benefit value data were also converted into 2020 to ensure data consistency. Finally, we calculated how many years were needed for the restoration projects to recover their cost (t_y) with the following equation:

$$\boldsymbol{Cost2020\$} = \sum_{t=1}^{t_y} \boldsymbol{Benefit2020\$}\ (1+i)^{t_y}$$

In this equation, the symbol "i" represented the discount rate of each country in different periods. *Cost2020$* and *Benefit2020$* represented the total cost and benefit of the restoration project in 2020.

Since most selected studies do not have valid monitoring and running cost data, we assumed that all restoration projects in this research did not need human actively interfering and managing after restoration activities. This meant the monitoring and running cost was excluded from the calculation of t_y for simplification. Besides, due to the lack of the carbon sequestration benefit in most restoration projects, we also applied the simple and empirical model proposed by Burden et al. (2019, Figure 1f) to replenish these restoration projects' new carbon stock situation after 2020. An open-access software called GetData Graph Digitizer was used to obtain data from the graph. The carbon price range was \$ 5–30/t CO_2 e, taking into account current carbon prices in compliance and voluntary markets across the world (Mok, 2019). So, \$ 5/t CO_2 e was supposed to be a low-carbon value, while \$ 30/t CO_2 e was regarded as a high-carbon value in this study. We calculated t_y of restoration sites based on three different benefit data evaluations (i.e., original, high-carbon value, and low carbon) to assess salt marsh carbon sequestration potential value contribution under a warmer climate.

[2]http://www.stats.gov.cn/english/

[3]https://www.worldbank.org/en/home

TABLE 1 | Social discount rates in some countries.

Countries and area	Time	Discount rates (%)	Calculation methods	References
The United States	1954~1976	5.3	SRTP	Kula, 1987
	1978~2017	4.7	SRTP	Nesticò and Maselli, 2020
Canada	1954~1976	5.4	SRTP	Kula, 1987
		10.0	SOC	Zhuang et al., 2007
Australia	Before 1991	8.0	SOC	Zhuang et al., 2007
		6.5	Other	Abelson and Dalton, 2018
The United Kingdom	1970~2001	4.2	SRTP	Evans and Sezer, 2004
European Union (Spain, Netherlands, Denmark, Portugal)		3.0	SRTP	Evans and Sezer, 2005
The Republic of Korea		3~4.5	Weighted average approach	Song, 2016
The People's Republic of China		8.0	Weighted average approach	Zhuang et al., 2007
	2001~2011	4.5	SRTP	Wang et al., 2013
South Africa		10.1	Weighted average approach	Du Preez, 2004
India		12	SOC	Zhuang et al., 2007

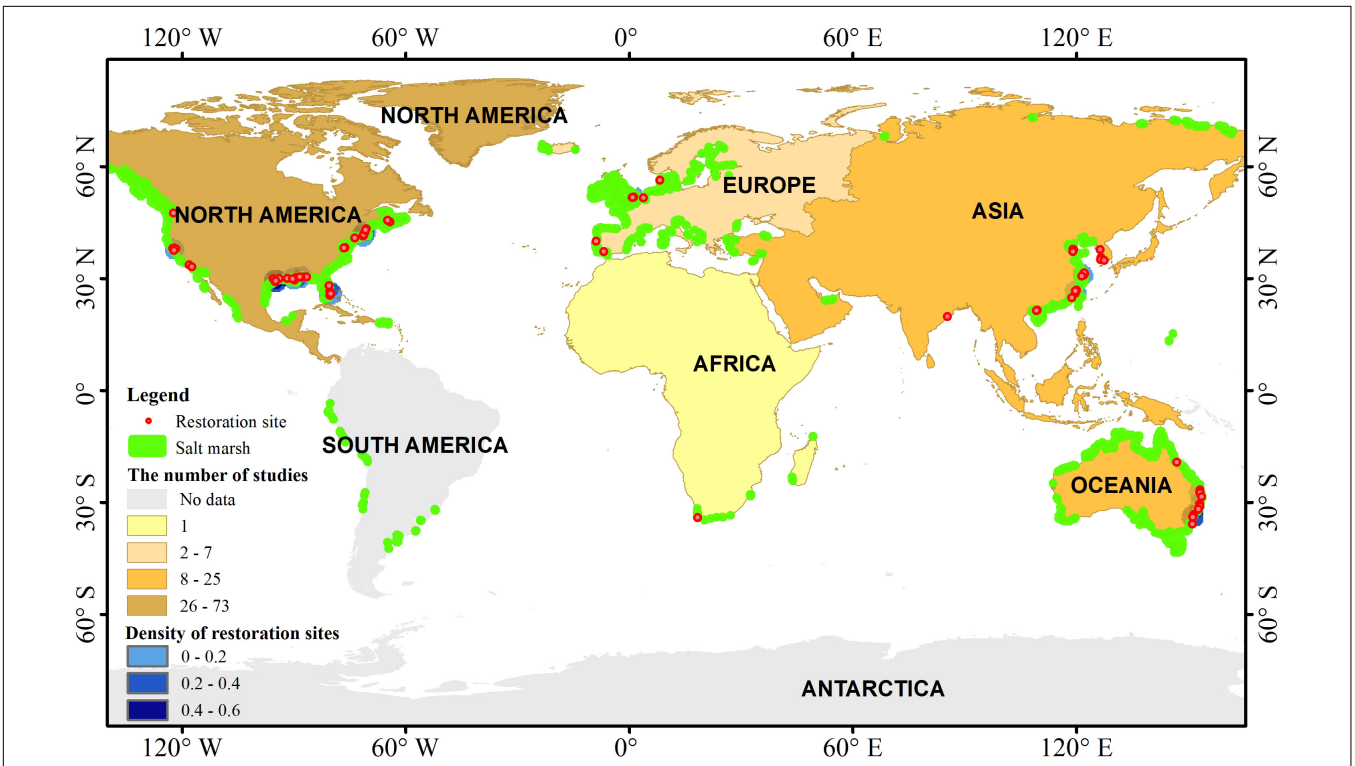

FIGURE 1 | Spatial distribution of the global salt marsh ecological restoration projects used for this study.

Analysis

Apart from the cost and benefit data of salt marsh restoration projects, geographical location, disturbance reasons, actions, and outcomes were also included in the analysis. For experimental restoration projects with multiple restoration sites and different cost data, every site was regarded as a single study when doing a cost-benefit analysis. But when we counted other information frequency, including degradation factor, restoration technologies, and generated ecosystem services, we regarded all restoration sites of an experimental restoration project as a study, since there was usually a strong similarity among different sites. We also combined the Ramsar wetland website[4] and Protected planet website[5] data to evaluate every single site protection situation for spatial analysis. Salt marshes areas with human management and conservation, such as ecological reserves, marine parks, and national wetlands, were all defined as "protected" status in this article, while other salt marshes were defined as "unprotected" status. In this article, we assumed that protected areas represent

[4]https://rsis.ramsar.org/ris-search?selectlayer=centroids-ramsar_sdi%3Aunboundaries

[5]https://www.protectedplanet.net/en

areas where restoration efforts and resources are concentrated, which generally have a higher restoration priority than non-protected areas.

RESULTS

Distribution of Restoration Projects

A total of 117 studies with reasonable data were incorporated into our spatial analysis. Compared with Africa and Europe, North America and Asia had more restoration projects data publicly available, similar to Zhang et al. (2018). As shown in **Figure 1**, global salt marsh restoration projects had an obvious spatial distribution pattern. Most of the restoration projects were concentrated in the San Francisco Bay, the Gulf of Mexico, and Maine Bay in the United States, Yangtze Estuary in China, and the New South Wales region of Australia. The distribution of high-density value of restoration sites was adjacent to larger rivers (i.e., Mississippi and Yangtze River) and megacities (i.e., New York, Sydney, and Shanghai). This pattern reflected that intensive human activities and rapid economic development may accelerate the transformation of salt marsh and the degradation process of this ecosystem, which in turn induces intensive restoration activities in the later period. A further issue that emerged from the data was that salt marsh restoration activities dominated by people might have an evident location preference, with emphasis on those degradation areas used to sustain high ecosystem services and have a strong influence on surrounding residents.

There was a surge of restoration projects during the period of 1990–2000 and 2013–2021 around the world (**Figure 2**). Not only the number of restoration studies showed an obvious upward trend between 1990 and 2000 but also the cumulative restoration area and cost increased rapidly. This reflected that intensive and large-scale restoration projects were carried out during this period, and people's investment enthusiasm was gradually ramping up, but it dropped down in the next decade. Although the cumulative cost was gradually climbing during the period from 2001 to 2012, the cumulative restoration area remained virtually unchanged. The number of restoration studies in North America dropped, while the number of restoration studies grew in Asia and Oceania, despite of fluctuation. Fluctuations of the number of restoration studies in North America might have a relationship with the global financial crisis that happened in 2008 because a recent study verified the relationship between gross domestic product (GDP) and the number of salt marsh restoration projects in the United States (Li et al., 2019). From 2013, the cumulative total cost started to dramatically increase till 2021. This meant that the government and people began to understand the importance of salt marsh ecosystem protection. For example, the Chinese State Council issued a public announcement to strictly control coastal wetlands reclamation in 2018 (Gu et al., 2018). Besides, heavy disasters also accelerated wetland legislation processes and salt marsh restoration and creation projects in disaster-stricken areas. After Hurricane Sandy devastated the New England area in 2012, the United States government allocated funds to salt marsh restoration projects in Rhode Island to improve the resistance in coastal and estuarine areas. The growth of salt marsh restoration projects in recent years would deliver a positive signal to ecological scientists and conservationists and encourage their work, especially when we started the "UN Decade on Ecosystem Restoration" (2021–2030; Waltham et al., 2020).

Degradation Factors and Restoration Methods

We also collected other useful information about restoration projects for analysis. **Table 2** showed more details about restoration methods that were used in this study. With regard to disturbance and stress factors, different continents shared some common characteristics. Obviously, extreme weather events and climate change were the main physical stress factors to induce salt marshes' ecosystem degradation and loss in the five continents. Marshland conversion affected by human activities, such as enclosure, aquaculture, and urbanization, were the dominant anthropogenic factors for the loss of salt marshes (**Figure 3A**). The number of studies reported about dams and hydrology change in North America was significantly different from other continents. The United States used to consider salt marsh as mosquito nurseries and thus carried out long-term and massive physical landfilling and water impoundment activities in the past century (Taylor, 2011). This may have explained why North America showed the largest number in hydrological connectivity and managed realignment approaches (**Figure 3B**). There had been 3,869 dams removed between 1950 and 2016, about a third of which occurred in America (Secretariat of the Convention on Biological Diversity, 2020). Besides, the beneficial use of dredged materials and hard structure construction were also popular in North America. Although the planting vegetation method was widely applied across the world, using fences for avoiding animals disturbance was also popular in Oceania.

The number of studies that recorded different stress factors and restoration methods changed with time and showed different patterns. The number of studies that recorded land use change, dam, and hydrology change declined during the period 1991–2021 (**Figure 4A**). In contrast, the number of studies of climate change and contamination increased with time. Overall, almost every restoration method experienced an earlier increase and later decrease, whereas a dissimilar increase trend could be seen in the number of studies that documented vegetation restoration and removing disturbance methods (**Figure 4B**). The emerging shoreline protection concept, living shorelines and nature-based solutions, might prompt vegetation restoration technology flourishing in recent years (Bilkovic et al., 2016).

Unbalanced Restoration Cost Allocation

As shown from **Table 3**, the number of restoration sites located in the protected area was significantly less than those in unprotected areas, probably due to the limited space of protected salt marshes. According to the Global Biodiversity Outlook 5, at least 10% of coastal and marine zone are effectively conserved by 2020 (Chape et al., 2005; Secretariat of the Convention on Biological Diversity, 2020). The

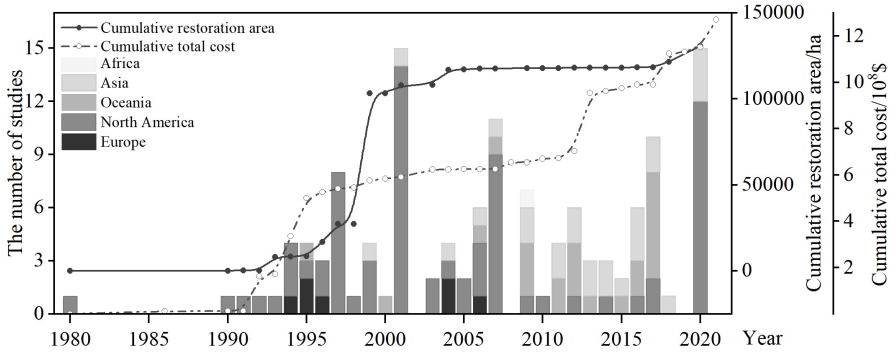

FIGURE 2 | Temporal distribution of the global salt marsh ecological restoration projects used for this study.

TABLE 2 | Salt marsh restoration methods and techniques.

Methods	Techniques	Note	References
Vegetation restoration	Planting vegetation	Native vegetation communities were promoted by sowing seeds, transplanting propagules and small plants in areas where vegetation propagules or seed dispersal are restricted	Lindig-Cisneros and Zedler, 2002
	Seed bank	The seed bank is an important seed source for the secondary succession of the vegetation community after disturbance	Bossuyt and Honnay, 2008
	Bio-geomorphologic	Using positive and negative feedback mechanisms between plant growth and dynamic geomorphological processes to assist ecological restoration	
Removing disturbance	Fence	Fencing is used to reduce livestock and tourist impact on restoration sites	Laegdsgaard, 2006
	Decontamination	To remove contamination from soil and water, including chemicals, radioactive materials, rubbish and other harmful materials	
Invasion control	Physical, chemical, biological control and integrated control methods	Use a variety of methods to eliminate invasive species	
Sediment and substrate	Dredged material	The dredged materials are used to raise the elevation of the restoration sites, which offsets the direct or indirect impacts of sediment reduction and sea level rise, thereby promoting the establishment and growth of vegetation	Hardy and Wu, 2020
	Micro-topography	Micro-topography manipulation is the typical way to imitate or recover the natural topographic heterogeneity for the degraded salt marsh restoration. Artificially alter the landform and elevation of tidal flats to form diverse habitats under the influence of rainwater and tide.	Wang et al., 2020
Hydrological restoration	Managed realignment	Shore-hardening structures are removed selectively to allow natural coastal environments to be maintained or reestablished locally	Neal et al., 2005
	Hydrological connectivity	Hydrological connectivity was originally defined as being the water-mediated transfer of matter, energy and/or organisms within or between the elements of the hydrological cycle. Degradation areas can be restored by changing the variation of key factors that affect plant history process.	Li et al., 2021; Wang et al., 2021
Hard structure	Culverts, spillways, breakers, dykes and other constructions	Hard structures, such as groins and breakwaters, are built on the foreshore to prevent or mitigate erosion.	Schoonees et al., 2019

cumulative restoration area and mean total cost per hectare values were variable in different income countries. Although middle-income countries restored and created more area in comparison with high-income countries, their expense allocation of restoration sites under different protection statuses was more unbalanced than high-income countries. Except for hard structure cost, we found that almost all the cost for the restoration of unprotected sites in high-income countries were higher than those in middle-income countries, regardless of the three different monetary conversion methods. In contrast to earlier findings, however, the cost of the six restoration methods listed in **Table 3** for protected sites in the high-income country was either lower or roughly equal with those in the middle-income country.

No matter which monetary conversion method was applied, vegetation restoration, removing disturbance, and hard structure restoration methods need more financial investment in comparison with invasion control, hydrological restoration, and sediment and substrate recovery (**Figure 5**). Although removing disturbance and hard structure restoration methods were more expensive, middle-income countries still invested more

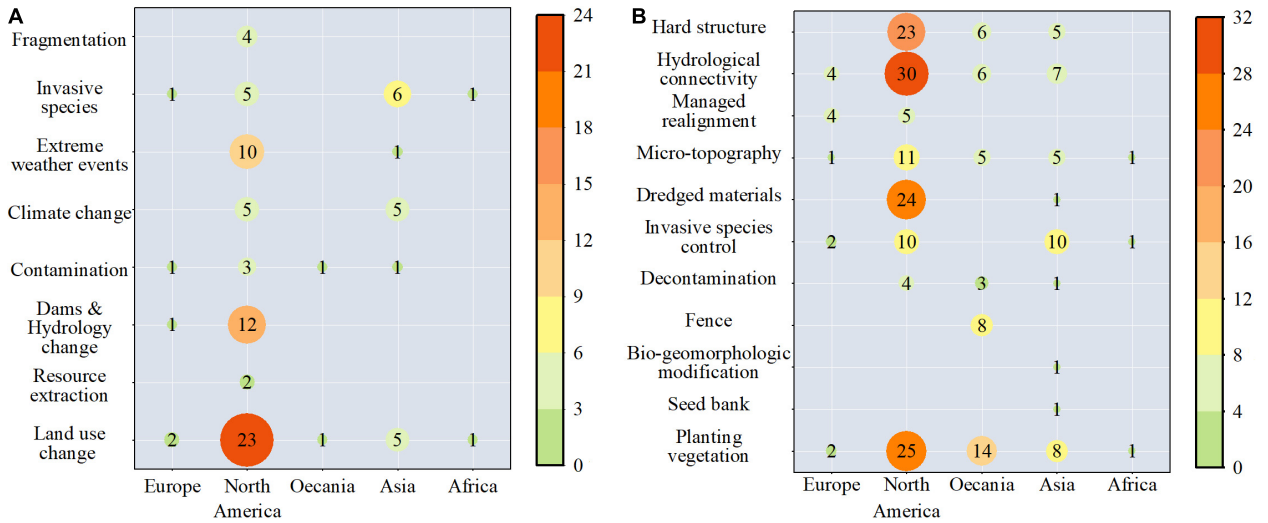

FIGURE 3 | Salt marsh ecological restoration projects' degradation factors **(A)** and restoration techniques **(B)** in the five continents. Numbers are the count of projects.

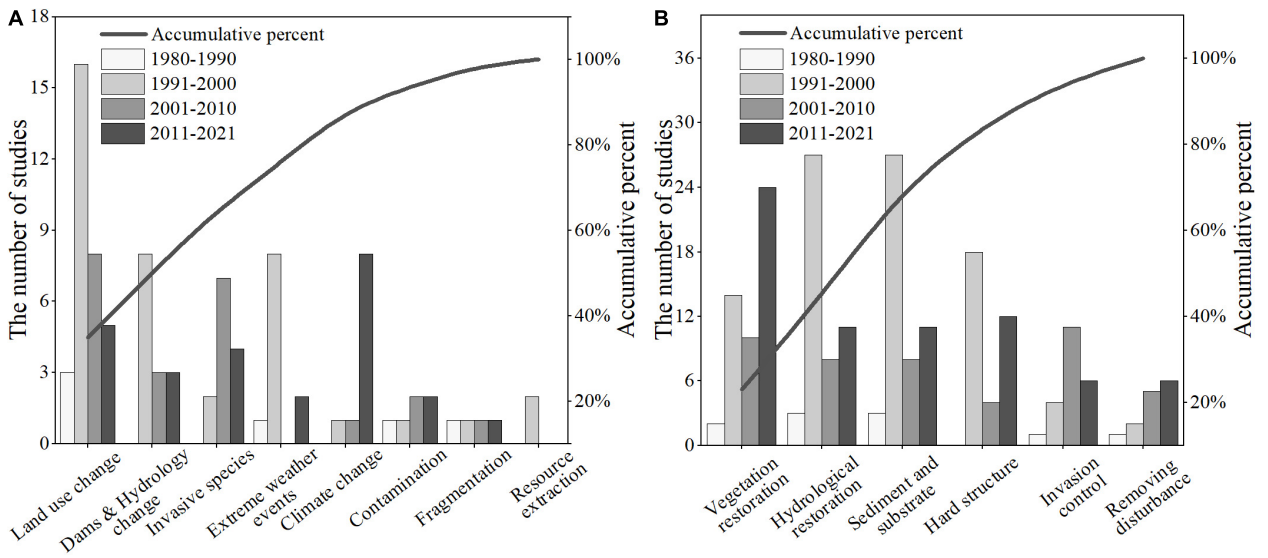

FIGURE 4 | Salt marsh ecological restoration projects' degradation factors **(A)** and restoration methods **(B)** in the past four decades.

money for those methods in protected sites than high-income countries. The invasion control cost in protected areas in the middle-income countries was biased by an expensive ecological project in Shanghai, China, which spent over one billion RMB for wiping out the invasive species and promoting birds' habitats. After removing anomaly data, the mean total cost of invasion control restoration approach for one hectare would drop to US$ 4,369–6,596. Overall, middle-income countries paid more attention to the salt marsh restoration projects in the protected area, such as Ramsar sites, wildlife management areas, refuges, ecological reserves, marine parks, and marine protected areas. Since they are generally faced with more economic and resource limitations than high-income countries, restoration projects for ecological hot spots tend to get funds and public support relatively easy because they have particular importance for biodiversity and ecosystem services.

Restoration Benefits and the Year to Recover the Cost

We analyzed all ecosystem services generated from effective managed action and documented ecosystem services only used for monetization of every restoration project. Then, we calculated the year to recover the cost of every restoration project in three different benefit data evaluations based on CPI, PPP, and DIS value conversion methods by combining with the restoration

TABLE 3 | Restoration cost in protected and unprotected restoration sites in the middle-income and high-income countries and other useful information (only minimum and maximum value of the three monetary conversion methods presented).

Country		Middle-income country		High-income country	
Restoration Sites' Status		**Protected**	**Unprotected**	**Protected**	**Unprotected**
Percentage of studies (%)		6.8%	11.3%	19.5%	62.4%
The cumulative restoration area (ha)		83,505	1,777	11,568	33,919
Mean total cost per hectare ($/ha)		956,609∼1,418,770	495,067∼876,564	472,101∼633,032	454,285∼694,724
Mean total cost of different restoration methods per hectare ($/ha)	Invasion control	7,953,495∼11,781,099	4,369∼6,596	31,930∼72,014	15,781∼23,157
	Hydrological restoration	24,235∼37,008	6,090∼9,945	26,489∼50,373	37,532∼64,623
	Sediment and substrate	24,235∼37,008	6,090∼9,945	26,489∼50,373	37,532∼64,623
	Vegetation restoration	89,319∼133,875	26,945∼42,756	123,338∼179,867	90,765∼139,724
	Removing disturbance	634,567∼960,478	No data	79,324∼130,417	48,531∼74,207
	Hard structure	103,152∼153,837	66,262∼108,197	59,909∼84,555	56,136∼97,023

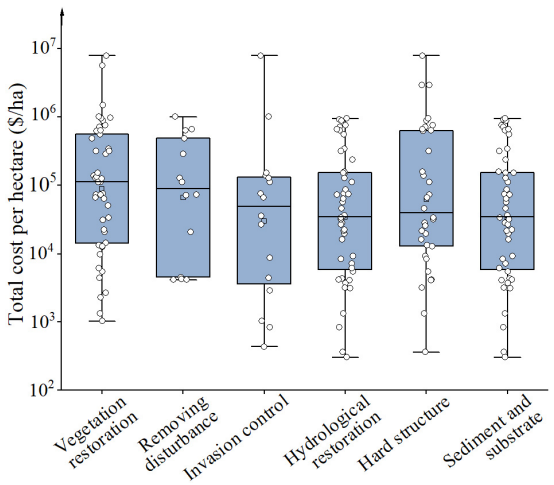

FIGURE 5 | Salt marsh ecological restoration methods and their total cost per hectare.

projects' cost data. We found that most benefit data only included one or two types of ecosystem service value, namely, production or ecotourism. According to the rough benefit data estimation, nearly one-fifth of the restoration projects that are based on the ordinary benefit data evaluation could return their investment cost in a short period of time (less than 5 years). If time is extended to 30 years, the proportion of restoration projects with recovered cost will increase to about 40%, of which nearly half (47%) are located in protected areas. As **Figure 6** showed, salt marsh restoration projects located in the protected area needed less time to recover costs than those in unprotected areas, either in high-income countries or in middle-income countries. Therefore, ecological hotspots produced enormous ecological benefits and human welfare in return to the high financial support. However, there were still 19% of restoration projects located in unprotected areas whose cost recovery period was significantly lower than the mean cost recovery period. The mismatch between ecological investment and returns in some unprotected areas presented in this study could raise our recognition of the remaining restoration gaps in global salt marsh restoration. In addition, restoring and recreating salt marsh can contribute to carbon sequestration and climate mitigation (Johnson et al., 2018). But, we found that carbon sequestration value was often overlooked in most restoration projects' benefit evaluations. After adding carbon sequestration value to restoration projects without carbon benefit data, our findings showed that the cost recovery period for those restoration projects had been reduced, regardless of whether they were under low-carbon value or high-carbon value. The information presented in this study suggested that the tremendous carbon sequestration benefit of salt marsh habitat restoration and creation could make corresponding restoration activities more profitable.

DISCUSSION

Restoration Scale and Cost

Until recently, most coastal restoration projects were still costly and at small scales in comparison with terrestrial ecosystem restoration projects, with a limited success rate. To achieve the expected success of the large-scale coastal zone management, we need to think broadly about the relationship between restoration scale and cost because it is vital for restoration site selection and financial resource division. Some scholars believe that large-scale restoration size would diminish and share construction and management expenses as a result of the economy of scale theory, which is more thrifty (Berger, 1997). However, other scientists find no obvious linear relationship between restoration area and restoration cost per unit area (Bayraktarov et al., 2016). In this study, salt marsh restoration projects are dominated by small-scale experimental restoration, ranging from 1 ha to 76,000 ha. The total cost and cost per hectare irregularly and dramatically fluctuate when restoration size is scaled up. However, after using the natural breaks method to divide all restoration projects into several categories to maximize single category similarities, we found restoration cost and benefit value

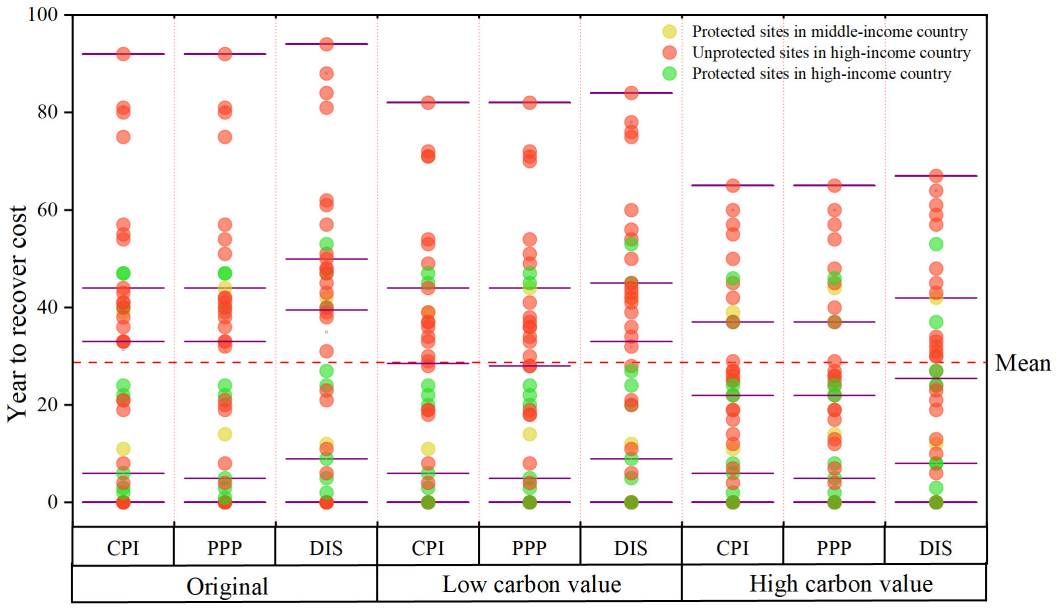

FIGURE 6 | Year to recover the cost of salt marsh ecological restoration projects based on three different benefit data evaluations. The purple lines represent the max, min, median, and two quartile values.

TABLE 4 | Restoration cost and benefit of different scales (only minimum and maximum value of the three monetary conversion methods presented).

Area	(0–471)	(471–1400)	(1400–4238)	>4238
Mean duration time (year)	2.50	7.25	8.67	5.40
Mean total cost ($)	6,509,325~8,769,151	13,623,094~15,168,969	34,423,676~43,898,802	62,010,124~64,805,808
Mean total cost per hectare ($/ha)	565,139~825,752	23,855~26,583	12,112~14,979	6,354~6,925
Mean benefit per hectare ($/ha•a)	6103	1011	No data	16070
Mean cost recovery time (year)	33~46	8~20	No data	0~1

presented different changing patterns as the restoration scale increased (**Table 4**). With the increase of the restoration scale, the mean total cost of restoration projects has risen significantly. But the mean benefit per hectare showed a trend of decrease first and then increase. It reached the lowest point when restoration size ranged from 471 ha to 1,400 ha and then increased to a high level as restoration scaled up. This can be caused by the relationship between ecological services, landscape scale, ecosystem service assessment methods, and people's willingness to pay. Further research is needed to provide evidence for explaining the relationship between restoration scale and cost. Besides, since small-scale and short-time restoration activities had the highest unit mean cost and relatively lower benefit, it was foreseeable that small-scale restoration activities would take longer time to recover the original expenses than large-scale restoration.

Although substantial literature have focused on restoration scale, cost, and their correlations, all the studies reviewed so far, however, suffer from the difficulty of data collection. When collecting data from the same country and adjacent geographical area, scientists tended to draw a conclusion that restoration cost has a regression relationship with scale when complicated factors were simplified, such as GDP, technologies, funding sources, and policies. Some of these factors have been proven to affect the restoration budget (Stewart-Sinclair et al., 2020).

Mismatch Phenomenon

Although we have recognized that unbalanced funding allocation and regional biases of salt marsh restoration projects would probably provoke a mismatch between restoration efforts and social expectations, corresponding practical reasons are diverse and complex. One potential explanation is that endangered species richness and the degree of ecosystem degradation vary widely across the world. Regarding degradation areas that have lost tremendous ecological services and are faced with severe human encroachment, scientists are predisposed to understand their threats and consider them as conservation priority areas (Lawler et al., 2006). Due to the greater ecosystem services value in ecological hotspots and reserves, restoration projects happening in these areas would receive more attention and funds than unprotected zones (**Table 3**). Various restoration and creation activities, such as lowering water levels on impounded former wetlands, filling in with dredged material, or creating new habitats by removing tidal barriers, are all associated with the transformation of different land use forms. There is a trade-off between former land use and salt marsh restoration activities.

The buffer effect of salt marshes against storm surge is critical to coastal cities with high population density and economic values. However, an important predictor of salt marsh services value is the income level of the particular affected community, which means the salt marsh value in high-income areas is higher in "avoided damage cost" method than that in middle-income areas. Therefore, we inadvertently created a justification to over-invest in marshes in high-income areas and underinvest in middle-low-income areas (zu Ermgassen et al., 2021). The salt marsh assessment and land trade-off offered an intrinsic explanation about why most of the restoration sites are adjacent to megacities. Another factor that affects ecological funds allocation is regional administrative capacity and policies, rather than environmental needs or population size (Borgström et al., 2016). Government funding is still the main source for coastal habitat restoration (Zhang et al., 2018). Except for North America and Europe, private protection was rarely considered in other regions, and subnational protection was least considered in Asia (McKinley et al., 2020). On the other hand, some mismatches are mainly derived from English literature. Africa and South America have many countries and regions where English is not the primary official language or a secondary foreign language, which means non-English literature cannot be accessed even if they do exist in native language (Lawler et al., 2006).

Limitations and Uncertainties

Although we endeavored to search salt marsh restoration projects and their cost and benefit data, cost data are still quite limited for deep research. The Economics of Ecosystems and Biodiversity project conducted a study of more than 2,000 recovery cases and found that less than 5% of the cases provided meaningful cost data (Neßhöver et al., 2011). The quality of the cost data varied in different projects (Bullock et al., 2011). Similarly, a report by Wortley et al. (2013) indicated that only 3.9% of restoration projects interpreted the economic results of restoration projects. Bayraktarov et al. (2016) and Li et al. (2019) also pointed out the problem of restoration cost data accessibility. In addition, multiple projects with a certain degree of relevance are often implemented within a long duration in some specific geographic areas, with repetitive and somewhat different records from different sources such as academic journals, news, bloggers, reports, and webpages. Establishing advanced and available coastal wetland restoration databases might be helpful to improve the analysis results. However, only some developed countries owned public available ecosystem restoration databases, while most developing countries still need time to establish their restoration database and share the data.

To simplify the research questions, we used simplified cost-benefit analysis as a "decision rule" for identifying a preferred option in our study. But, it is subject to the uncertainties of different monetary conversion methods. CPI, PPP, and DIS are the most common and widely used monetary conversion methods in environmental management projects, such as coastal protection, wild animal protection, and their cultural services (Narayan et al., 2016; Wei et al., 2018). But they reflect different economic concepts and consumption differences, which would cause uncertainties in our final calculation results (Bayraktarov et al., 2016; Ma et al., 2020). When we compared the three monetary conversion methods, DIS usually had the highest value, while the difference between CPI and PPP was not obvious (**Figure 7**). Different discount rates also affect our results. In the DIS method, different discount rates can produce contradictory results, and there is no consensus on which discount rate should be applied for restoration projects (Bullock et al., 2011). Turner et al. (2007) considered that fixed negative, positive, and zero discount rates were not suitable for longtime restoration projects because climate change and other various factors may affect consequences. Gowdy et al. (2010) suggested that variable discount rates should be used for assessing the long-term impacts of environmental change. Considering the differences among countries and years, we used various discount rates for every

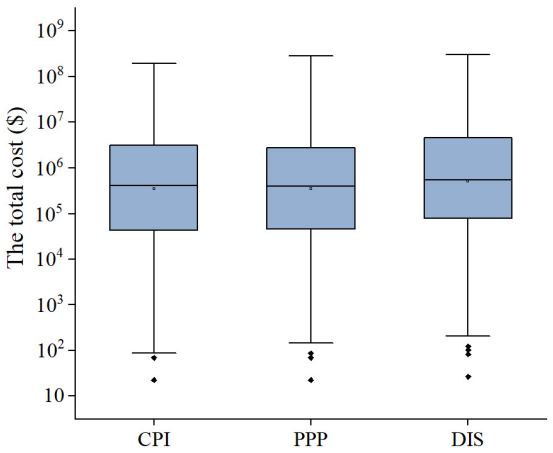

FIGURE 7 | The total cost of salt marsh ecological restoration projects in different monetary conversion methods.

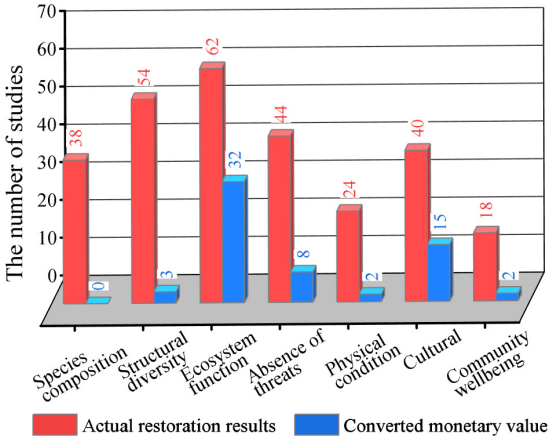

FIGURE 8 | Comparison between actual restoration results and converted monetary values. The red bar represents the number of studies of specific restoration results that either improved or were generated due to salt marsh restoration projects in a total of 133 studies. Similarly, the blue bar represents the number of studies with restoration economic results reported. Not all natural restoration benefits were converted into monetary value.

single restoration project to minimize inherent uncertainties in the DIS method. Moreover, in the actual situation, a certain restoration project usually lasted for several years, and their investment is in batches, including long-term maintenance cost and original construction cost. For practical reasons, we used a specific year during the implementation period and removed maintenance and running costs from the calculation, which would reduce costs and thereby affect the results' accuracy.

Another uncertainty is from the economic evaluation of restoration outcomes. We must distinguish between the "restoration outcomes" and the "restoration benefits." Restoration outcomes cover all the results produced by the restoration action, while the restoration benefits are more inclined toward the beneficial ones for human. Sometimes, ecosystem benefits generated from restoration activities return over long periods of time, which might be overlooked because they are hard to monetize. For example, local residents' health improvement associated with environmental changes could be absent from ecological assessment documents of restoration activities. After summarizing the natural and economic results of 133 selected restoration studies, we found that ecosystem services generated from restoration actions are not consistent with reported monetary benefit calculation (**Figure 8**). In fact, most benefit data only recorded benefit values of fish and shrimp production, raw materials, and ecotourism. Ecosystem services, such as residents' sense of experience from restoration activities and the value of specific native species, were absent from the benefit data. Without species composition, biodiversity, and physical condition improvement benefit data generated from restoration activities, we could draw an inexact conclusion that the costs of salt marsh restoration outweigh the benefits. In addition, the potential negative impacts and opportunity cost of land use change caused by restoration activities should be further taken into account because the overall result of cost-effectiveness of ecological restoration was sensitive to manipulation of market and economic data. In the materials collected, we barely found any observed bad effects or failure lessons of restoration. In the future, the uncertainties can be alleviated by conducting surveys and interviews with relevant participators and management organizations of restoration projects. Further work is required to understand the multiple values of salt marshes across the globe.

CONCLUSION

Our results showed that most ecological restoration projects were geographically close to large rivers and megacities and formed two restoration booms during the periods of 1990–2000 and 2013–2021. Restoration methods were based on the types of natural disturbances and anthropogenic threats, while planting vegetation was becoming more popular. Although the number of restoration projects is increasing in recent years, middle-income countries tend to spend more salt marsh restoration efforts in protected areas than that in unprotected areas. As for restoration benefits, most restoration projects could recover their original investment in a relatively short period under the imprecise monetary valuation of limited ecosystem services. The great carbon sequestration potential would make salt marsh restoration projects more profitable in the future, as carbon neutral policies are being adopted by many countries to combat global warming. Compared with large-scale restoration activities, small-scale experimental restoration projects are more expensive and make it difficult to recover their costs. Our study provides obvious evidence that middle-income countries have not adequately recognized the contributions of salt marsh restoration in unprotected areas yet. Restoration can significantly increase natural capital and the flow of services and benefits to human society. More efforts are needed to make these links explicit and provide evidence to convince society that the benefits outweigh the investment costs. Our results could help to bridge policymakers and ecologists in their joint efforts to improve restoration planning and implementation.

DATA AVAILABILITY STATEMENT

The original contributions presented in the study are included in the article/**Supplementary Material**, further inquiries can be directed to the corresponding author.

AUTHOR CONTRIBUTIONS

J-JW: conceptualization, data acquisition, methodology, analysis, writing—original draft, review, and editing. X-ZL: supervision, editing, and funding acquisition. S-WL: conceptualization and polishing. Y-XM: polishing. All authors contributed to the article and approved the submitted version.

FUNDING

This work was sponsored by the National Natural Science Foundation of China (42141016), and the National Key R&D Program of China (2017YFC0506000).

SUPPLEMENTARY MATERIAL

The Supplementary Material for this article can be found online at: https://www.frontiersin.org/articles/10.3389/fevo.2022.865516/full#supplementary-material

REFERENCES

Abelson, P., and Dalton, T. (2018). Choosing the social discount rate for Australia. *Aust. Econ. Rev.* 51, 52–67. doi: 10.1111/1467-8462.12254

Adam, P. (2019). "Salt marsh restoration," in *Coastal Wetlands: an Integrated Ecosystem Approach*, eds G. M. E. Perillo, E. Wolanski, D. R. Cahoon, and C. S. Hopkinson (Amsterdam: Elsevier), 817–861. doi: 10.1016/b978-0-444-63893-9.00023-x

Barbier, E. B., Hacker, S. D., Kennedy, C., Koch, E. W., Stier, A. C., and Silliman, B. R. (2011). The value of estuarine and coastal ecosystem services. *Ecol. Monog.* 81, 169–193. doi: 10.1890/10-1510.1

Bayraktarov, E., Saunders, M. I., Abdullah, S., Mills, M., Beher, J., Possingham, H. P., et al. (2016). The cost and feasibility of marine coastal restoration. *Ecol. Appl.* 26, 1055–1074. doi: 10.1890/15-1077.1

Berger, L. (1997). *Costs for Wetland Creation and Restoration Projects in the Glaciated Northeast*. Washington DC: United States Environmental Protection Agency.

Bilkovic, D. M., Mitchell, M., Mason, P., and Duhring, K. (2016). The Role of Living Shorelines as Estuarine Habitat Conservation Strategies. *Coast. Manag.* 44, 161–174. doi: 10.1080/08920753.2016.1160201

Blignaut, J., Esler, K. J., de Wit, M. P., Le Maitre, D., Milton, S. J., and Aronson, J. (2013). Establishing the links between economic development and the restoration of natural capital. *Curr. Opin. Environ. Sustain.* 5, 94–101. doi: 10.1016/j.cosust.2012.12.003

Borgström, S., Zachrisson, A., and Eckerberg, K. (2016). Funding ecological restoration policy in practice—patterns of short-termism and regional biases. *Land Use Policy* 52, 439–453. doi: 10.1016/j.landusepol.2016.01.004

Bossuyt, B., and Honnay, O. (2008). Can the seed bank be used for ecological restoration? An overview of seed bank characteristics in European communities. *J. Veg. Sci.* 19, 875–884. doi: 10.3170/2008-8-18462

Broome, S. W., Seneca, E. D., and Woodhouse, W. W. Jr. (1988). Tidal salt marsh restoration. *Aquat. Bot.* 32, 1–22. doi: 10.1016/0304-3770(88)90085-X

Bullock, J. M., Aronson, J., Newton, A. C., Pywell, R. F., and Rey-Benayas, J. M. (2011). Restoration of ecosystem services and biodiversity: conflicts and opportunities. *Trends Ecol. Evol.* 26, 541–549. doi: 10.1016/j.tree.2011.06.011

Burden, A., Garbutt, A., and Evans, C. D. (2019). Effect of restoration on saltmarsh carbon accumulation in Eastern England. *Biol. Lett.* 15:20180773. doi: 10.1098/rsbl.2018.0773

Chape, S., Harrison, J., Spalding, M., and Lysenko, I. (2005). Measuring the extent and effectiveness of protected areas as an indicator for meeting global biodiversity targets. *Phil. Trans. R. Soc. B.* 360, 443–455. doi: 10.1098/rstb.2004.1592

Cornelisen, C. D. (1998). *Restoration of Coastal Habitats and Species in the Gulf of Maine*. Portland: Gulf of Marine Council on the Marine Environment.

Costanza, R., De Groot, R., Sutton, P., Van der Ploeg, S., Anderson, S. J., Kubiszewski, I., et al. (2014). Changes in the global value of ecosystem services. *Glob. Environ. Change* 26, 152–158. doi: 10.1016/j.gloenvcha.2014.04.002

Coverdale, T. C., Brisson, C. P., Young, E. W., Yin, S. F., Donnelly, J. P., and Bertness, M. D. (2014). Indirect human impacts reverse centuries of carbon sequestration and salt marsh accretion. *PLoS One* 9:e93296. doi: 10.1371/journal.pone.0093296

De Groot, R., Blignaut, J., Van Der Ploeg, S., Aronson, J., Elmqvist, T., and Farley, J. (2013). Benefits of investing in ecosystem restoration. *Conserv. Biol.* 27, 1286–1293. doi: 10.1111/cobi.12158

De Groot, R., Brander, L., Van der Ploeg, S., Costanza, R., Bernard, F., Braat, L., et al. (2012). Global estimates of the value of ecosystems and their services in monetary units. *Ecosyst. Serv.* 1, 50–61. doi: 10.1016/j.ecoser.2012.07.005

DeLaune, R. D., and White, J. R. (2012). Will coastal wetlands continue to sequester carbon in response to an increase in global sea level: a case study of the rapidly subsiding Mississippi river deltaic plain. *Clim. Change* 110, 297–314. doi: 10.1007/s10584-011-0089-6

Doody, J. P. (2008). *Saltmarsh Conservation, Management and Restoration*. Dordrecht: Springer.

Du Preez, M. (2004). The discount rate for public sector conservation projects in South Africa. *Afr. Dev. Rev.* 16, 456–471. doi: 10.1111/j.1017-6772.2004.00100.x

Evans, D. J., and Sezer, H. (2004). Social discount rates for six major countries. *Appl. Econ. Lett.* 11, 557–560. doi: 10.1080/135048504200028007

Evans, D. J., and Sezer, H. (2005). Social discount rates for member countries of the European Union. *J. Econ. Stud.* 32, 47–59. doi: 10.1108/01443580510574832

Fisher, R., Radford, B. T., Knowlton, N., Brainard, R. E., Michaelis, F. B., and Caley, M. J. (2011). Global mismatch between research effort and conservation needs of tropical coral reefs. *Conserv. Lett.* 4, 64–72. doi: 10.1111/j.1755-263X.2010.00146.x

Gann, G. D., McDonald, T., Walder, B., Aronson, J., Nelson, C. R., Jonson, J., et al. (2019). International principles and standards for the practice of ecological restoration. *Restor. Ecol.* 27, S1–S46. doi: 10.1111/rec.13035

Gowdy, J., Howarth, R. B., and Tisdell, C. (2010). "Discounting, ethics and options for maintaining biodiversity and ecosystem integrity," in *The Economics of Ecosystems and Biodiversity: Ecological and Economic Foundations*, ed. P. Kumar (London: Routledge), 257–278.

Gu, J., Luo, M., Zhang, X., Christakos, G., Agusti, S., Duarte, C. M., et al. (2018). Losses of salt marsh in China: trends, threats and management. *Estuar. Coast. Shelf Sci.* 214, 98–109. doi: 10.1016/j.ecss.2018.09.015

Hanley, N., Barbier, E. B., and Barbier, E. (2009). *Pricing Nature: Cost-Benefit Analysis and Environmental Policy*. Cheltenham: Edward Elgar Publishing.

Hanley, N., and Black, A. R. (2006). Cost-benefit analysis and the water framework directive in Scotland. *Integr. Environ. Assess. Manag.* 2, 156–165. doi: 10.1002/ieam.5630020208

Hardy, T., and Wu, W. (2020). Impact of different restoration methods on coastal wetland loss in Louisiana: Bayesian analysis. *Environ. Monit. Assess.* 193:1. doi: 10.1007/s10661-020-08746-9

Hochard, J. P., Hamilton, S., and Barbier, E. B. (2019). Mangroves shelter coastal economic activity from cyclones. *PNAS* 116, 12232–12237. doi: 10.1073/pnas.1820067116

Johnson, B. J., Lovelock, C. E., and Herr, D. (2018). "Climate Regulation: Salt Marshes and Blue Carbon," in *The Wetland Book: Structure and Function, Management, and Methods*, eds C. M. Finlayson, M. Everard, K. Irvine, R. J. McInnes, B. A. Middleton, A. A. V. Dam, et al. (Dordrecht: Springer), 1185–1196. doi: 10.1007/978-90-481-9659-3_213

Kirwan, M. L., and Megonigal, J. P. (2013). Tidal wetland stability in the face of human impacts and sea-level rise. *Nature* 504, 53–60. doi: 10.1038/nature12856

Koch, E. W., Barbier, E. B., Silliman, B. R., Reed, D. J., Perillo, G. M. E., Hacker, S. D., et al. (2009). Non−linearity in ecosystem services: temporal and spatial variability in coastal protection. *Front. Ecol. Environ.* 7:29–37. doi: 10.1890/080126

Kula, E. (1987). Social interest rate for public sector appraisal in the United Kingdom, the United States and Canada. *Project Appraisal* 2, 169–174. doi: 10.1080/02688867.1987.9726623

Laegdsgaard, P. (2006). Ecology, disturbance and restoration of coastal saltmarsh in Australia: a review. *Wetl. Ecol. Manag.* 14, 379–399. doi: 10.1007/s11273-005-8827-z

Lawler, J. J., Aukema, J. E., Grant, J. B., Halpern, B. S., Kareiva, P., Nelson, C. R., et al. (2006). Conservation science: a 20−year report card. *Front. Ecol. Environ.* 4:473–480. doi: 10.1890/1540-929520064[473:CSAYRC]2.0.CO;2

Li, S., Xie, T., Pennings, S. C., Wang, Y., Craft, C., and Hu, M. (2019). A comparison of coastal habitat restoration projects in China and the United States. *Sci. Rep.* 9:14388. doi: 10.1038/s41598-019-50930-6

Li, X., Bellerby, R., Craft, C., and Widney, S. E. (2018). Coastal wetland loss, consequences, and challenges for restoration. *Anthropocene Coast.* 1, 1–15. doi: 10.1139/anc-2017-0001

Li, Y., Xu, J., Wright, A., Qiu, C., Wang, C., and Liu, H. (2021). Integrating two aspects analysis of hydrological connectivity based on structure and process to support muddy coastal restoration. *Ecol. Indic.* 133:108416. doi: 10.1016/j.ecolind.2021.108416

Lindig-Cisneros, R., and Zedler, J. B. (2002). Halophyte recruitment in a salt marsh restoration site. *Estuaries* 25, 1174–1183. doi: 10.1007/bf02692214

Liu, Z., Cui, B., and He, Q. (2016). Shifting paradigms in coastal restoration: six decades' lessons from China. *Sci. Total Environ.* 56, 205–214. doi: 10.1016/j.scitotenv.2016.05.049

Ma, Y. X., Li, X. Z., Lin, S. W., Xie, Z. L., and Xue, L. M. (2020). Ecosystem services valuation and its uncertainty in wetlands surrounding Chongming. *Chin. J. Ecol.* 39, 1875–1883. doi: 10.13292/j.1000-4890.202006.011

McKinley, E., Pagès, J. F., Alexander, M., Burdon, D., and Martino, S. (2020). Uses and management of saltmarshes: a global survey. *Estuar. Coast. Shelf Sci.* 243:106840. doi: 10.1016/j.ecss.2020.106840

Mitsch, W. J., and Gosselink, J. G. (2015). *Wetlands*. New York: John Wiley & Sons.

Mok, J. (2019). *Creating Added Value for Korea's tidal flats: Using Blue Carbon as an Incentive for Coastal Conservation*. [PhD thesis]. California: the University of California.

Narayan, S., Beck, M. W., Reguero, B. G., Losada, I. J., Van Wesenbeeck, B., Pontee, N., et al. (2016). The effectiveness, costs and coastal protection benefits of natural and nature-based defences. *PLoS One* 11:e0154735. doi: 10.1371/journal.pone.0154735

Neal, W. J., Bush, D. M., and Pilkey, O. H. (2005). "Managed Retreat," in *Encyclopedia of Coastal Science. Encyclopedia of Earth Science Series*, ed. M. L. Schwartz (Dordrecht: Springer), 602–606. doi: 10.1007/978-3-319-48657-4_201-2

Nesticò, A., and Maselli, G. (2020). A protocol for the estimate of the social rate of time preference: the case studies of Italy and the USA. *J. Econ. Stud.* 47, 527–545. doi: 10.1108/JES-02-2019-0081

Neßhöver, C., Aronson, J., Blignaut, J., Eppink, F., Vakrou, A., Wittmer, H., et al. (2011). "Investing in ecological infrastructure," in *The Economics of Ecosystems and Biodiversity in National and International Policy Making*, ed. P. T. Brink (London: Routledge), 401–442.

Restore America's Estuaries. (2011). *Jobs and Dollars: Big Returns from Coastal Habitat Restoration*. Available online at: https://estuaries.org/wp-content/uploads/2019/01/Jobs-and-Dollars_2011.pdf (accessed November 2, 2021).

Roman, C. T., and Burdick, D. M. (2012). *Tidal Marsh Restoration-A Synthesis of science and management*. Washington DC: Island press.

Saintilan, N. (2013). "Rehabilitation and management of saltmarsh habitats," in *Workbook for Managing Urban Wetlands in Australia*, ed. S. Paul (Sydney: Sydney Olympic Park Authority), 309–320.

Schoonees, T., Mancheño, A. G., Scheres, B., Bouma, T. J., Silva, R., Schlurmann, T., et al. (2019). Hard structures for coastal protection, towards greener designs. *Estuar. Coast.* 42, 1709–1729. doi: 10.1007/s12237-019-00551-z

Scott, D. B., Frail-Gauthier, J., and Mudie, P. J. (2014). *Coastal Wetlands of the World: Geology, Ecology, Distribution and Applications*. Cambridge: Cambridge University Press.

Secretariat of the Convention on Biological Diversity (2020). *Global Biodiversity Outlook 5*. Available online at: https://www.cbd.int/gbo5 (accessed January 21, 2022)

Society for Ecological Restoration (2004). *The SER International Primer on Ecological Restoration*. Available online at: https://www.ser-rrc.org/resource/the-ser-international-primer-on/ (accessed January 21, 2022)

Song, J. (2016). *An Empirical Investigation of Social Discount Rate: Case of Korea.* Available online at: https://www.dbpia.co.kr/Journal/articleDetail?nodeId=NODE07097608 (accessed March 25, 2022).

Spurgeon, J. (1999). The Socio-Economic Costs and Benefits of Coastal Habitat Rehabilitation and Creation. *Mar. Pollut. Bull.* 37, 373–382. doi: 10.1016/s0025-326x(99)00074-0

Stewart-Sinclair, P. J., Purandare, J., Bayraktarov, E., Waltham, N., Reeves, S., Statton, J., et al. (2020). Blue restoration–building confidence and overcoming barriers. *Front. Mar. Sci.* 7:541700. doi: 10.3389/fmars.2020.541700

Su, J., Friess, D. A., and Gasparatos, A. (2021). A meta-analysis of the ecological and economic outcomes of mangrove restoration. *Nat. Commun.* 12:5050. doi: 10.1038/s41467-021-25349-1

Taillardat, P., Thompson, B. S., Garneau, M., Trottier, K., and Friess, D. A. (2020). Climate change mitigation potential of wetlands and the cost-effectiveness of their restoration. *Interface Focus* 10:20190129. doi: 10.1098/rsfs.2019.0129

Tang, J., Ye, S., Chen, X., Yang, H., Sun, X., Wang, F., et al. (2018). Coastal blue carbon: concept, study method, and the application to ecological restoration. *Sci. CHIN. Earth Sci.* 61, 637–646. doi: 10.1007/s11430-017-9181-x

Taylor, D. S. (2011). Removing the sands (sins?) of our past: dredge spoil removal and saltmarsh restoration along the Indian River Lagoon, Florida (USA). *Wetl. Ecol. Manag.* 20, 213–218. doi: 10.1007/s11273-011-9236-0

The United Nations Ocean Conference (2017). *Factsheet: People and Oceans*. Available online at: https://www.un.org/sustainabledevelopment/wp-content/uploads/2017/05/Ocean-fact-sheet-package.pdf (accessed January 21, 2022)

Turner, R. K., Burgess, D., Hadley, D., Coombes, E., and Jackson, N. (2007). A cost–benefit appraisal of coastal managed realignment policy. *Glob. Environ. Change* 17, 397–407. doi: 10.1016/j.gloenvcha.2007.05.006

United Nations Environment Programme -World Conservation Monitoring Centre, International Union for Conservation of Nature, and National Geographic Society (2018). *Protected Planet Report 2018*. Available online at: https://portals.iucn.org/library/node/48344 (accessed January 21, 2022).

van Zelst, V., Dijkstra, J. T., van Wesenbeeck, B. K., Eilander, D., Morris, E. P., Winsemius, H. C., et al. (2021). Cutting the costs of coastal protection by integrating vegetation in flood defences. *Nat. Commun.* 12:6533. doi: 10.1038/s41467-021-26887-4

Wainaina, P., Minang, P. A., Gituku, E., and Duguma, L. (2020). Cost-benefit analysis of landscape restoration: a stocktake. *Land* 9:465. doi: 10.3390/land9110465

Waltham, N. J., Elliott, M., Lee, S. Y., Lovelock, C., Duarte, C. M., Buelow, C., et al. (2020). UN Decade on Ecosystem Restoration 2021–2030—what chance for success in restoring coastal ecosystems? *Front. Mar. Sci.* 7:71. doi: 10.3389/fmars.2020.00071

Wang, D., Bai, J., Wang, W., Ma, X., Guan, Y., Gu, C., et al. (2020). Micro-topography manipulations facilitate Suaeda Salsa marsh restoration along the lateral gradient of a tidal creek. *Wetlands* 40, 1657–1666. doi: 10.1007/s13157-020-01308-2

Wang, H. Z., Du, S. Y., and Zeng, X. F. (2013). Evaluating China's Social Discount Rate Based on SRTP. *Stat. Decis.* 21, 18–21. doi: 10.13546/j.cnki.tjyjc.2013.21.012

Wang, Q., Xie, T., Luo, M., Bai, J., Chen, C., Ning, Z., et al. (2021). How hydrological connectivity regulates the plant recovery process in salt marshes. *J. Appl. Ecol.* 58, 1314–1324. doi: 10.1111/1365-2664.13879

Wei, F. W., Costanza, R., Dai, Q., Stoeckl, N., Gu, X. D., Farber, S., et al. (2018). The Value of Ecosystem Services from Giant Panda Reserves. *Curr. Biol.* 28, 2174–2180. doi: 10.1016/j.cub.2018.05.046

Wortley, L., Hero, J.-M., and Howes, M. (2013). Evaluating ecological restoration success: a review of the literature. *Restor. Ecol.* 21, 537–543. doi: 10.1111/rec.12028

Zhang, Y. S., Cioffi, W. R., Cope, R., Daleo, P., Heywood, E., Hoyt, C., et al. (2018). A global synthesis reveals gaps in coastal habitat restoration research. *Sustainability* 10:1040. doi: 10.3390/su10041040

Zhuang, J., Liang, Z., Lin, T., and De Guzman, F. (2007). *Theory and Practice in the Choice of Social Discount Rate for Cost-Benefit Analysis: a Survey*. Los Baños: ERD working paper series.

zu Ermgassen, P. S., Baker, R., Beck, M. W., Dodds, K., zu Ermgassen, S. O., Mallick, D., et al. (2021). Ecosystem services: delivering decision-making for salt marshes. *Estuar. Coast.* 44, 1691–1698. doi: 10.1007/s12237-021-00952-z

Conflict of Interest: The authors declare that the research was conducted in the absence of any commercial or financial relationships that could be construed as a potential conflict of interest.

Publisher's Note: All claims expressed in this article are solely those of the authors and do not necessarily represent those of their affiliated organizations, or those of the publisher, the editors and the reviewers. Any product that may be evaluated in this article, or claim that may be made by its manufacturer, is not guaranteed or endorsed by the publisher.

frontiers | Frontiers in Ecology and Evolution

ORIGINAL RESEARCH
published: 14 April 2022
doi: 10.3389/fevo.2022.721244

Physiological Responses of Typical Wetland Plants Following Flooding Process—From an Eco-Hydrological Model Perspective

Chengliang Liu[1], Yijian Zeng[1], Zhongbo Su[1] and Demin Zhou[2,3]**

[1] Department of Water Resources, Faculty of Geo-Information Science and Earth Observation, University of Twente, Enschede, Netherlands, [2] College of Resource Environment and Tourism, Capital Normal University, Beijing, China, [3] Key Laboratory of 3D Information Acquisition and Application of Ministry, Capital Normal University, Beijing, China

OPEN ACCESS

Edited by:
Carlos Freitas, Federal University of Amazonas, Brazil

Reviewed by:
Yu An, Northeast Institute of Geography and Agroecology (CAS), China
Ji-Zhong Wan, Qinghai University, China

***Correspondence:**
Zhongbo Su
z.su@utwente.nl
Demin Zhou
zhoudemin@cnu.edu.cn

Specialty section:
This article was submitted to Conservation and Restoration Ecology, a section of the journal Frontiers in Ecology and Evolution

Received: *06 June 2021*
Accepted: *07 March 2022*
Published: *14 April 2022*

Citation:
Liu C, Zeng Y, Su Z and Zhou D (2022) Physiological Responses of Typical Wetland Plants Following Flooding Process—From an Eco-Hydrological Model Perspective. Front. Ecol. Evol. 10:721244. doi: 10.3389/fevo.2022.721244

Anaerobics increase resistance to gas transport and microbial activity in flooded soils. This may result in the presence of aerenchyma in the roots of some wetland plants. Increased aerenchyma airspaces enable oxygen to be transported from the above-ground plant parts to the submerged roots and rhizosphere. Nevertheless, there is still a lack of studies linking field experiments and eco-hydrological modeling to the parameterization of the physiological responses of typical wetland plant species to natural flooding events. Furthermore, from the modeling perspective, the contribution of aerenchyma was not sufficiently considered. The goal of this study was to develop and apply an eco-hydrological model capable of simulating various patterns of plant physiological responses to natural flooding events based on key processes of root oxygen diffusion and aerenchyma functioning in a variably-saturated wetland soil environment. Eco-hydrological experiments were conducted accordingly, with surface water level, root-zone soil water content, soil temperature, leaf net photosynthesis rate and root morphology monitored simultaneously *in situ* at a site dominated by meadow species *Deyeuxia angustifolia* (Kom.) Y. L. Chang and invaded shrub species *Salix rosmarinifolia* Linn. var. *brachypoda* (Trautv.et Mey.) Y.L. Chou in a typical natural floodplain wetland. The results are as follows: (1) Root oxygen respiration rates are strongly correlated with leaf net photosynthesis rates of the two plant types, particularly under flooding conditions during the growing season; (2) Meadow species with a preference for wet microhabitats has a competitive advantage over first-year invading shrub species during flooding events; and (3) an aerenchyma sub-model could improve the eco-hydrological model's accuracy in capturing plant physiological responses. These findings have the potential to contribute to the management of wetland and its restorations.

Keywords: soil water dynamics, riparian habitat, inland wetlands, flooding, photosynthesis, root oxygen respiration

INTRODUCTION

Along flooding gradients, plant zonation is widely observed and extensively described (Ewing, 1996; Zhou et al., 2009, 2013; Kirwan and Guntenspergen, 2015; Pedersen et al., 2017; Haak et al., 2017; Wright et al., 2017). Typically, plant zonation is attributed to differences in flood tolerance, more specifically, the ability of plants to tolerate hypoxic rooting conditions (Armstrong et al., 1994; Reddy and DeLaune, 2008). The hydrological regime, particularly the dynamics of the water table due to seasonal flooding, has an effect on soil features by regulating the area and duration of saturation (Rubol et al., 2012), which indicates the occurrence and intensity of anaerobic soil conditions. The primary constraint imposed by flooding on wetland plants is the exchange of gas. In flooded soils, anaerobics improve resistance to gas transportation and microbial activities. This could occur in a matter of hours in freshly flooded soils. The impact could also be accelerated at high temperatures (Armstrong et al., 2000).

Seasonal flooding tolerance is characterized by distinct physiological features include, among others, leaf net photosynthesis rate (LNPR) (Pezeshki, 2001; Dalmagro et al., 2016), aerenchyma abundance (Laan et al., 1989; Wright et al., 2017), and root oxygen respiration (Armstrong et al., 2019). The amount of internal oxygen in plants depends both on the root respiration rate and the soil microbe respiration (Kumari and Gupta, 2017). Root oxygen respiration is crucial for maintaining vital physiological and metabolic pathways (Glenz et al., 2006), particularly in wetland plants. Leaf photosynthesis is a critical physiological activity because it directly reflects the ability of growth and nutrient absorption (Lai et al., 2012; Pezeshki et al., 2018). It was found that a significant portion of the oxygen diffusing to the roots during the day may originate from photosynthetic activity (Evans, 2004). Typically, photosynthesis is a major source of oxygen for plants and rhizosphere in submerged species (Jackson and Armstrong, 1999). Submergence of photosynthetically active organs hinders the immediate supply of photosynthetically generated oxygen to the roots (Armstrong et al., 2019), as well as significant fluctuations in radial oxygen loss (ROL), which has a direct impact on the sediment oxidation (Waters et al., 1989; Pedersen et al., 1995, 2017). Aerenchyma acts as a conduit for oxygen in the root system, which is critical for wetland plants to survive in anoxic conditions (Armstrong et al., 1991). Through aerenchyma, oxygen needed by wetland plants can be transported from the above-ground plant parts to the rhizosphere of the submerged roots. Numerous wetland plants' roots contain a barrier that prevents oxygen from diffusing into the basal zones, thereby increasing longitudinal oxygen diffusion along the aerenchyma toward the root tips (Armstrong et al., 2000; Colmer, 2003), and ensuring oxygenation in the aerobic zone surrounding the growing tips (Striker et al., 2007). It is now widely accepted that the aerenchyma can act as ecological engineers by conferring the capacity to tolerate soil saturation (Jones et al., 1994; Booth and Loheide, 2010). Above all, fine root traits, specifically the aerenchyma, can be used to evaluate the wetland plants' functional characteristics to adapt to flooding stress (Purcell et al., 2019). However, from the eco-hydrological modeling perspective, the contribution of aerenchyma was not sufficiently considered.

To date, the effect of hydrology and soil physics on plant physiological responses to flooding has been investigated most extensively under controlled experimental conditions (DeLaune et al., 1990; Casanova and Brock, 2000; Hough-Snee et al., 2015; Kirwan and Guntenspergen, 2015; Byun et al., 2017; Zhang et al., 2019). While the effects of seasonal flooding on a few species under specific conditions have been determined in controlled experiments, the ability of wetlands plants to survive in natural settings was not extensively reported. It has been reported that plant communities with greater diversity in natural conditions are commonly more resistant to environmental disturbances and can respond positively to some mild flooding events than plants grown in monoculture or under controlled conditions (Reich et al., 2001; Isbell et al., 2015; Wright et al., 2015; Fischer et al., 2016; Cesarz et al., 2017). The majority of field studies on the interactions between abiotic factors and plant physiological responses have been conducted in salt marshes with low species diversity (Pezeshki et al., 1987; Pezeshki, 1998; Abou Jaoudé et al., 2012; Watson et al., 2015; Yan et al., 2018). Few model studies on the relationships between abiotic features and plant physiological responses have been conducted in natural inland seasonal flooding wetlands, but little is known about the root oxygen respiration rate (RORR) and aerenchyma functioning of typical wetland plants (Zhou et al., 2016; Pezeshki et al., 2018). Furthermore, there is still a need for a systematic method to link field experiments and eco-hydrological modeling to improve the parameterization of the physiological responses of typical wetland plant species to natural flooding events. Understanding the plant physiological responses enables us to gain insight into the functional characteristics of seasonal wetland environments. This may be especially important for natural floodplain wetlands, where the social and ecological importance is extremely high, while being seriously affected by drainage and reclamation with an estimated 95 km^2/year loss globally (Coleman et al., 2008).

This study aims to bridge the above-mentioned research gap by deploying a process-based eco-hydrological model and *in-situ* field experiments, applied to a natural floodplain wetland located in northeastern Heilongjiang Province, China. A site-scale eco-hydrological experiment was conducted in No.139 Monitoring Transect (EMT-139) of Honghe National Nature Reserve (HNNR) to compare the response patterns of two typical wetland plants to a natural flooding process. The LNPRs of flood-tolerant meadow species *Deyeuxia angustifolia* (Kom.) Y. L. Chang (MeS) and invading shrub species *Salix rosmarinifolia* Linn. var. *brachypoda* (Trautv.et Mey.) Y.L. Chou (ShS) were monitored in relations to the flooding regimes, root-zone soil moisture content (RZ-SWC), soil temperature (ST), and soil physio-chemical variables. Furthermore, a process-based eco-hydrological model specifically for calculating RORR was proposed for simulating plant physiological responses to natural flooding events. The following three hypotheses were tested: 1. The MeS with a preference for wet habitats has a competitive advantage over first-year invading ShS during flooding events; 2. The RORR is strongly correlated with the LNPR of the two plant types, particularly under flooding conditions during the growing

season; and 3. The aerenchyma sub-model may improve the eco-hydrological model's performance in accurately capturing the physiological dynamics of the plants in responses to natural flooding events.

MATERIALS AND METHODS

Study Area

The Sanjiang Plain is a cool temperate continental climate region with the most extensive and concentrated aquatic habitats in China, including freshwater marshes, marshy meadows, shrubs, forests, etc. (Zhou et al., 2009; Niu et al., 2012). The HNNR is located northeast of the Sanjiang Plain in Heilongjiang Province (47°42′18″–47°52′00″ N, 133°34′38″ –133°46′29″ E). The HNNR is designated as a Ramsar Wetland of International Importance (Gardner and Davidson, 2011). It is well-known for the Sanjiang Plain's "unique gene pool of wildlife" (Zhou et al., 2013). This wetland is 251 square kilometers in size. The annual precipitation averages 579.3 millimeters, while annual evaporation averages 1,166 mm. Between July and September, approximately 50–70% of the precipitation occurs. Each year, for more than 5 months, the soils freeze to depths of 160–180 cm (Li et al., 2011). Seasonal flooding is prevalent in the EMT-139 (**Figure 1**), resulting in a varying hydrological gradient that is either fully saturated, seasonally saturated, or unsaturated. In the EMT-139, two typical wetland plant types, the MeS and ShS, were compared and analyzed. The MeS is widespread wetland plant species in the Sanjiang Plain. It can survive and thrive under a variety of soil and water conditions. The MeS usually sparsely covered with shrubs, maintaining an open character. The ShS is also native plant community to certain marshy areas in the Sanjiang Plain and is well-adapted to dry soil conditions. However, when moisture levels in the upper soil layers are low due to insufficient rainfall and flooding, the local habitat becomes ideal for the ShS, allowing it to expand extensively. In the EMT-139, growing season in the year 2017 was marked by the invasion of the ShS over MeS.

Eco-Hydrological Modeling Framework

The eco-hydrological model building process is depicted in **Figure 2**. To begin, we simulated the root zone soil water content (RZ-SWC) of the MeS and ShS in the variably-saturated soil column. By comparing the soil water retention curve, the RZ-SWC, and the moisture at which capillary bonds rupture, the effective soil layers for the main growing root tips were identified. The optimal soil layer for the MeS root growth was found to be between 10 and 20 cm (Zhang et al., 2015), whereas the optimal soil layer for the ShS was between 30 and 40 cm (Blume-Werry et al., 2019). The second stage involved calculating the oxygen concentration in bulk soil at the macroscale using the simulated RZ-SWC from step 1 (Cook, 1995; Bartholomeus et al., 2008). The third step was to calculate oxygen concentration at the outer

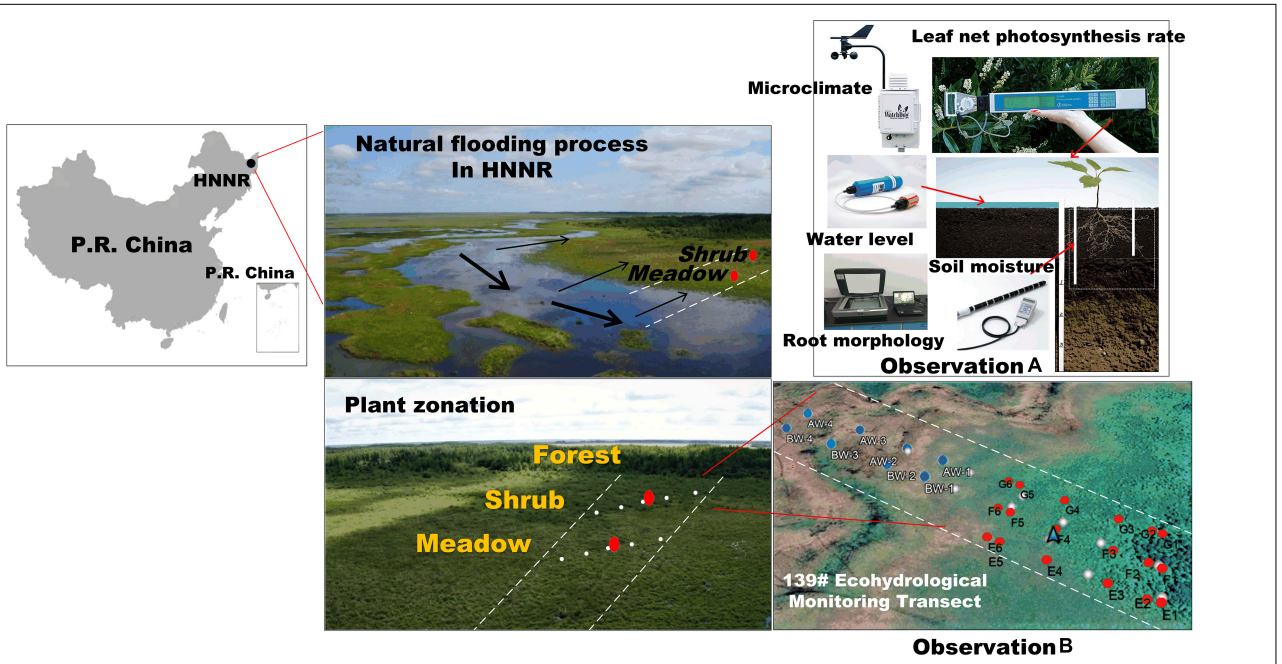

FIGURE 1 | Eco-hydrological experiments in an eco-hydrological monitoring transect (EMT-139) along a seasonal river in the HNNR in Heilongjiang Province, China. Observation B depicts the experimental transects established in the year 2011 (Li et al., 2011). *In-situ* eco-hydrological monitoring experiments were conducted continuously along this transect between the year 2011 and 2020. The observation matrix (red dots) covered the multi-layers' root-zone soil water contents (RZ-SWCs) at the transitional zone, whereas the observation matrix (blue dots) represented the *in-situ* monitoring of the surface water level (SWL) of the seasonal Nongjiang River; The observation matrix (white dot) represented the check observations of the RZ-SWCs. Observation A illustrates the detailed eco-hydrological monitoring of each PFT on a site by site basis, which included *in-situ* monitoring of the leaf net photosynthesis rate (LNPR), RZ-SWC, SWL, and soil temperature (ST), as well as root and soil sampling of the meadow species (MeS) and shrub species (ShS).

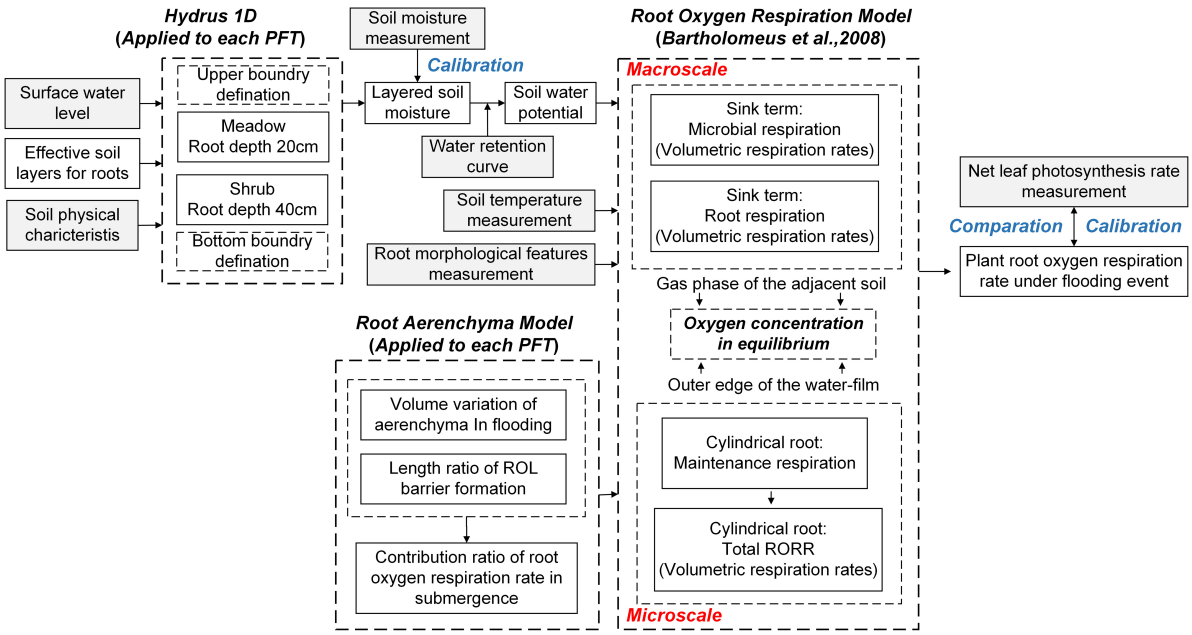

FIGURE 2 | The model framework of the present study (building process of the eco-hydrological model). Gray-colored boxes underlines the data from field experiments.

edge of the water-film adjacent to the root from macroscale to microscale. Following step 3, a new root aerenchyma model was developed in step 4 to account for the microscale physiological function of aerenchyma during flooding events. Finally, based on Bartholomeus et al. (2008), we simulated the RORR-MeS and RORR-ShS at the microscale, evaluated the biotic and abiotic parameter sensitivities of the new model, and investigated the link between the RORR and LNPR.

Root Zone Soil Water Content

The RZ-SWCs of the MeS and ShS were quantitatively simulated by solving the Richards Equation in the variably-saturated wetland soil environment using the USDA Salinity Laboratory's HYDRUS1D software (Simunek et al., 2005). The top 10 cm soil layer was defined as the organic surface layer (Bai et al., 2005), which contains finely divided organic matter and dead roots. This layer is in direct contact with the hydro-meteorological conditions at the surface and mineral soil layers beneath. Thus, in the parameterization scenario, the upper boundary condition was set to the variable pressure head, while the bottom layer was set to the variable flux. The model domain was extended to a depth of one meter, and a simulation period from 24 June to 1 October 2017 with a time step of 1 day.

Root Oxygen Respiration Rate

At the macroscale, microbial and root respiration were defined as two separate sink terms in the soil columns. Each term was defined using a reference value at $z = 0$ ($R_{microbial\_z0}$ and R_{root_z0} (kg O^2 m^{-3} d^{-1} soil) and an exponential shape factor [$Z_{microbial}$ and Z_{root} (m)] (Cook, 1995; Bartholomeus et al., 2008). The equilibrium was assumed to be achieved at soil depth z (m) in wetland soils. The oxygen concentration $C_{bulksoil}$ in the gas phase at soil depth z was calculated as follows under both flooding and non-flooding conditions:

$$C_{bulksoil} = C_{(atm,fw)} - \left(Z^2_{microbial} \cdot \frac{R_{microbial\_z0}}{D_{soil}}\right)\left(1 - exp\left(-\frac{z}{Z_{microbial}}\right)\right) - \left(Z^2_{root} \cdot \frac{R_{root\_z0}}{D_{soil}}\right)\left(1 - exp\left(-\frac{z}{Z_{root}}\right)\right) \quad (1)$$

where $C_{(atm,fw)}$ is used to express the oxygen concentration (kg O^2 m^{-3} d^{-1} soil) in the atmosphere or flooding water, respectively. D_{soil} is the mean diffusivity of the soil (m^2 d^{-1}).

Microbial respiration varies due to soil water dynamics and soil temperature, therefore the volumetric microbial respiration rates $R_{microbial}$ (kg O_2 m^{-3} soil d^{-1}) in the bulk soil were expressed as:

$$R_{microbial} = R_{microbial\_z0} exp\left(-z/Z_{microbial}\right) \quad (2)$$

$$R_{microbial\_z0} = \mu \beta f_{\varphi} Q_{10\_microbial}^{(T_{soil} - T_{ref})/10} \quad (3)$$

where μ is organic carbon content of the soil (kg C m^{-3} soil), β is vegetation dependent respiration rate (kg O^2 kg^{-1} C d^{-1}), f_{φ} is the factor which represents the reduction of microbial activity due to soil moisture availability (Probert et al., 1998; Arora, 2003), T_{soil} is soil temperature (K) at certain depth (m), T_{ref} is reference temperature (K), $Q_{10\_microbial}$ is relative increase in microbial respiration.

The oxygen concentration at the outer edge of the water-film C_{wfedge} and the gas phase of the adjacent soil $C_{bulksoil}$ were considered to be in equilibrium, thus the macro-to-microscale transformation was as follows:

$$C_{bulksoil} = C_{wfedge}/\alpha_B \quad (4)$$

where α_B is the Bunsen solubility coefficient for oxygen (m^3 gas m^{-3} liquid) (Weiss, 1970).

At the microscale, the total water-film respiration rate $r_{waterfilm}$ of a cylindrical root was calculated as follows:

$$r_{waterfilm} = r_{waterfilm\_z0} exp(-z/Z_{microbial}) \quad (5)$$

$$r_{waterfilm\_z0} = 0.5(\mu A)\beta Q_{10\_microbial}^{(T_{soil}-T_{ref})/10} \quad (6)$$

where T_{soil} (°C) is the soil temperature at certain soil depth, A is the area of the water-film cross-section (m^2). The cylindrical root oxygen respiration rate (μmol m^{-2} s^{-1}) at the micro-scale were calculated (Lemon and Wiegand, 1962; De Willigen and Van Noordwijk, 1984; Bartholomeus et al., 2008) as follows:

$$r_{cylin\_root} = \frac{4\pi C_{wfedge} D_{waterfilm} - r_{waterfilm} + 2r_{waterfilm} log_{10}^{(1+R_2)} M^{\frac{R_1}{R_2}}}{1 + R_1 log_{10}^{(1+R^2)}} \quad (7)$$

where $M = (1R_2)^2 (2R_2)$, $R_1 = D_{root}/D_{waterfilm}$, $R_2 = WFT_{waterfilm}/RS_{root}$. $WFT_{waterfilm}$ is the water-film thickness (m), RS_{root} is the root radius (m) of the cylindrical root, $D_{waterfilm}$ is the diffusivity of the water-film (m^2 d^{-1}). For a detailed definition and description of the equations and parameters used in the RORR simulation, please refer to Bartholomeus et al. (2008).

Root Aerenchyma

Upon soil waterlogging, oxygen transports through the gas conducting tissue (inducible and secondary aerenchyma) can occur *via* simple diffusion or pressure flow (Armstrong et al., 2000; Evans, 2004). In aerenchyma, oxygen is transported *via* diffusion through the pipe to the root tips. In this model, the cylindrical root's aerenchyma pipe structure was treated as a circular truncated cone (CTC) by summing up the volumes of all the individual aerenchyma pipes. The oxygen concentration in the aerenchyma is maintained at a constant level. Increased aerenchyma volume ratio during soil emergence in flooding-tolerant meadow and first-year invading shrub could, above all, correspond to increased oxygen respiration rates per unit time.

According to Montagnoli et al. (2019), volume variation of aerenchyma $P_{aerenchyma\_(MeS,\ ShS)}$ of both plant types under non-flooding and flooding conditions can be expressed as follows:

$$P_{aerenchyma\_(MeS,ShS)} = \frac{V_F}{V_{NF}} = \frac{R_F^2 + R_F \cdot r_F + r_F^2}{R_{NF}^2 + R_{NF} \cdot r_{NF} + r_{NF}^2} \quad (8)$$

where, V_F and V_{NF} are the aerenchyma volumes (m^3) under flooding and non-flooding conditions, respectively. R_F and r_F indicate lower and upper bases of the CTC under flooding conditions (m), while R_{NF} and r_{NF} are the lower and upper bases of the CTC under non-flooding conditions (m). $P_{aerenchyma}$ was determined using data from greenhouse experiments (Maricle and Lee, 2002), in which the amount of aerenchyma along the lengths of roots was determined under flooding and non-flooding conditions.

Following submergence, an out cortex ROL barrier with a length ratio $\frac{Barrier_{(MeS,\ ShS)}}{Length_{(MeS,\ ShS)}}$ formed accordingly. Therefore, available oxygen to cultivate root tips was formulated at an update ratio $R_{(MeS,\ ShS)}$:

$$R_{(MeS,ShS)} = \frac{Length_{(MeS,ShS)}}{Length_{(MeS,ShS)} - Barrier_{(MeS,ShS)}} \quad (9)$$

However, in comparison with the MeS, the ROL barrier in roots of ShS was inadequate. This resulted in the insufficient oxygen transport to root tips during flooding, thereby poor oxygenation of the rhizosphere zone (Blom, 1999). According to ROL experiment results in Watanabe et al. (2017) and Yamauchi et al. (2018), the $\frac{Barrier_{(MeS,ShS)}}{Length_{(MeS,ShS)}}$ after flooding were set to 0.625, 0.325 in the present study, respectively.

All in all, the contribution rate $CAR_{Flooding}$ of both aerenchyma and the ROL on the RORRs during flooding can be formulated as follows:

$$CAR_{Flooding\_MeS} = P_{aerenchyma\_MeS} Q_{10\_aerenchyma\_MeS}^{(T_{soil\_MeS}-T_{ref})/10} exp(R_{MeS}) \quad (10)$$

$$CAR_{Flooding\_ShS} = P_{aerenchyma\_ShS} Q_{10\_aerenchyma\_ShS}^{(T_{soil\_ShS}-T_{ref})/10} \quad (11)$$

where, $Q_{10\_aerenchyma\_(MeS,ShS)}$ is the rate of relative increase in aerenchyma activity intensity with a temperature increase of 10°C, with values of 1.1 and 1.2 for the MeS and ShS, respectively. In the current study, this indicates the increased respiration intensity induced due to increases in soil and rhizosphere temperature.

Eco-Hydrological Experiments in the No.139 Monitoring Transect

The shrub encroachment in the year 2017 was driven by the colonization of *Salix rosmarinifolia* Linn. var. *brachypoda* (Trautv.et Mey.) Y.L. Chou into former meadow areas. Current study categorized *Deyeuxia angustifolia* (Kom.) Y. L. Chang and *Salix rosmarinifolia* Linn. var. *brachypoda* (Trautv.et Mey.) Y.L.Chou into two plant functional types (PFTs): flood-tolerant meadow and first-year invading shrub. This classification system can be used to evaluate the physiological response of two representative plant types in the EMT-139 to seasonal flooding events. For each PFT, 10 samples were randomly selected that appeared to be healthy in appearance and stood approximately 60 cm high for the MeS and 130 cm high for the ShS. For each sample, the LNPR was measured daily with the CI-340 Handheld

Photosynthesis System (CID Bio-Science, Inc., United States) during the early to mid-morning hours. Young leaves of each sample were placed into the leaf chamber and the measurement results were recorded when the screen displayed a stable value, which typically took 2–5 min. On 16 September 2017, four individual plants of each PFT were harvested (above- and below-ground). We used the data collected during this period because the plant's maximum biomass occurs during this vegetative stage. The entire root systems were carefully harvested and rinsed with tap water, and the fresh mass was recorded. The root systems were oven-dried for 48 h at 65°C and then weighed. Sections of the fresh root system were carefully separated from each species and scanned immediately at a resolution of 600 dpi with a flat-bed transparent lighting system using an Expression 10000 XL 3.49 scanner (Epson Telford Ltd., United Kingdom). WinRHIZO Pro2012b software (Regent Instruments, Inc., Canada) was used to analyze the root images for the average diameter (mm), specific root length (SRL, m g^{-1}), and specific root area (SRA, cm^3 g^{-1}), etc. The root total organic carbon (TOC, g kg^{-1}) and total nitrogen (TN) (ROC, g kg^{-1}) were then measured with a Nitrogen analyzer multi N/C 2100 (Analytik Jena AG, Germany) using a dry combustion method.

Hydrological experiments in the EMT-139 measured the basic hydrological conditions for plants across the growing season. Simultaneous measurements of precipitation, surface water, and soil water content were made. It contains surface water level (SWL) (m), multi-layer RZ-SWCs (volume moisture content, cm^3/cm^3), micrometeorological variables, and determination of soil water retention curve from 24 June 2017 to 1 November 2017. Odyssey capacitance water level loggers (Dataflow Systems Ltd., New Zealand) were installed in eight PVC pipes (AW1-AW4, BW1- BW4) to monitor the actual SWL along the Nongjiang River's cross section in the EMT-139 (**Figure 1**). The RZ-SWCs were measured using a Delta-T Devices PR2 profile probe (Delta-T Devices Ltd., United Kingdom). The instrument was one meter in length and was placed into thin wall-mounted tubes with sensor pairs at 10, 20, 30, 40, 60, and 100 cm depth. There were 24 PR2 sites in the EMT-139 and the RZ-SWCs were measured manually. The WatchDog 2000 Series Weather Station (Spectrum Technologies, Inc., United States) was installed in the central part of the EMT-139. Since June 2017, microclimate data series had been recorded every 6 h, which contained precipitation, wind speed, air temperature, air humidity, solar radiation, etc. Water retention curve is a critical soil hydraulic characteristic that must be considered when solving soil water flow equations (Zeng et al., 2011). The water potential of soil samples was determined using the WP4C Soil Water Potential Lab Instrumentation (METER Group, Inc., United States). By using RETC software (Salinity Laboratory, USDA), the Van Genuchten equation (Van Genuchten, 1980) was fitted to the measured RZ-SWCs and soil matric potential data (**Table 1**).

Data Analyses

The simulated RZ-SWC values by HYDRUS1D were compared to those measured *in-situ* in EMT-139. The Relative Root Mean Square Error (RRMSE) (Zeng, 2013) and coefficient of determination (R^2) were used to evaluate the simulation

TABLE 1 | Measured soil physical and chemical properties and root morphology within the observation sites in the EMT-139.

Plant type	Soil depth	Soil hydraulic parameters[a]					Soil chemical properties[b]			Biomass (dry weight)		Root morphology[c]	
EMT-139	(cm)	θ_s (cm^3 cm^{-3})	θ_r (cm^3 cm^{-3})	α (cm^{-1})	N (−)	K_s (mm day^{-1})	TN (g kg^{-1})	TC (g kg^{-1})	SOC (g kg^{-1})	Aboveground (g)	Root (g)	SRL (m g^{-1})	SRA (cm^3g^1)
MeS	0–10	0.76	0.13	0.04	1.27	3181.60	13.43	128.43	221.42	1.07	0.09	28.03	362.34
	10–20	0.54	0.10	0.02	1.34	257.60	5.15	15.78	63.57				
	20–30	0.49	0.10	0.02	1.30	103.80	3.31	8.86	21.24				
	30–50	0.46	0.10	0.02	1.28	62.50	2.25	3.65	10.78				
	50–70	0.47	0.10	0.02	1.24	77.70	2.08	2.53	4.35				
	70—-100	0.46	0.10	0.02	1.21	63.40	1.67	1.58	2.72				
ShS	0–10	0.68	0.12	0.02	1.31	1708.90	6.31	71.05	122.48	7.57	3.20	3.63	49.24
	10–20	0.58	0.11	0.02	1.33	565.90	1.97	14.25	38.42				
	20–30	0.50	0.10	0.01	1.39	151.20	2.20	3.62	24.57				
	30–50	0.44	0.09	0.01	1.32	44.10	1.97	4.04	6.96				
	50–70	0.44	0.10	0.02	1.21	49.80	2.01	4.02	6.93				
	70–100	0.45	0.10	0.02	1.23	60.40	2.33	4.60	7.93				

[a]*Soil hydraulic parameters of Van Genuchten equation were fitted using RETC software.*
[b]*Values shown averaged over soil samples in EMT-139.*
[c]*Values shown averaged over root samples in EMT-139.*

performance. The data analyses were done by using the OriginPro (OriginLab Corporation, United States).

$$RRMSE = \frac{\sqrt{\sum_{i=1}^{N_M}(M_i - S_i)^2 / N_M}}{Max\left(M_1, M_2, \ldots\ldots, M_{N_M}\right) - Min\left(M_1, M_2, \ldots\ldots, M_{N_M}\right)} \quad (12)$$

$$R^2 = 1 - \frac{\sum_{i=0}^{N_M}(M_i - S_i)^2}{\sum_{i=0}^{N_M}\left(M_i - \overline{M}\right)^2} \quad (13)$$

where N_M is the number of the soil moisture measurements; M_i and C_i are the value of soil moisture measurements and HYDRUS1D simulations; $Max\left(M_1,\ M_2, \ldots\ldots, M_{N_M}\right)$ and $Min\left(M_1,\ M_2, \ldots\ldots, M_{N_M}\right)$ are the maximum and minimum values of the soil misture measurements, respectively; $\overline{M}$ is the mean of the soil moisture measurements. The *RRMSE* and R^2 are dimensionless. The lower the *RRMSE*, the closer the simulated values approach the observed values, while higher R^2 values indicates better agreement.

The RORRs of the MeS and ShS were simulated and compared to the measured LNPRs in the EMT-139. The performance of correlations was evaluated by the Pearson Correlation Coefficient (PCC) and coefficient of determination (R^2).

$$PCC = 1 - \frac{\sum_{i=0}^{N_M}\left(SR_i - \overline{SR}\right)\left(ML_i - \overline{ML}\right)}{\sqrt{\sum_{i=0}^{N_M}\left(SR_i - \overline{SR}\right)^2}\sqrt{\sum_{i=0}^{N_M}\left(ML_i - \overline{ML}\right)^2}} \quad (14)$$

where SR_i and ML_i are the value of the RORR simulations and LNPR measurements; $\overline{SR}$ and $\overline{ML}$ are the mean of the RORR simulations and LNPR measurements. The PCC value range from −1 to +1. A value of +1 indicates total positive linear correlation, 0 indicates that there is no linear correlation, and −1 is total negative linear correlation.

RESULTS

Soil Properties and Morphological Characteristics of the Roots

The physio-chemical properties of the soil profile, the biomass and root morphological characteristics of the two plant types observed in the EMT-139 are shown in **Table 1**. The vertical permeability of multi-layer soil profiles was found to vary due to layered deposition or biological activity-induced soil gradient characteristics. Additionally, as a key soil-water characteristic, the saturated hydraulic conductivity (Ks) of the 0–10 cm layer of the MeS is much greater than the ShS', indicating a higher water flow rate, and a more efficient partitioning of rainfall and surface water into soil water storage. Moreover, the saturated hydraulic conductivity, the concentrations of total nitrogen, total carbon, and organic carbon of both soils were quite low below 40 cm depth, showing that these dense, impervious, and low-nutrient layers isolated the groundwater interaction and were unfavorable for root system penetration and growth. Furthermore, despite the lower above- and below-ground biomass, the MeS' specific root length (SRL) and specific root area (SRA) were approximately eight times larger than the ShS', reflecting a stronger capacity for adapting to environmental changes throughout the growing season.

Simulation Results of the Root-Zone Soil Moisture Content

Figure 3 depicted the observed and simulated RZ-SWCs of the MeS and ShS. The simulation results were generally in good agreement with the observations. The RRMSE values of RZ-SWC at 20 cm depth in MeS and 40 cm in ShS were 0.229 and 0.117, while the R^2 values were 0.650 and 0.906, respectively. The simulated RZ-SWCs in the MeS and ShS could follow the general trend of the observations over the study period. Better agreements with the observations were achieved in the ShS. Exceptions were noted during the flooding periods and thereafter, when the simulated results of MeS were a bit higher than the observed recession curves, while the ShS' were slightly lower. The upper boundary condition specifications may partially explain the overestimated simulated results. It was assumed that surface water directly infiltrated into the underlying mineral profiles, disregarding any horizontal runoff processes of this layer, therefore promoting soil columns with higher water input and consequently increasing the simulated RZ-SWC of MeS; Underestimated ShS' may had been influenced by the flow and redistribution of water in "horizontal soil columns" of varying textures. In the field condition, a fairly obvious leaching layer was observed at approximately 40 cm depth in the EMT-139 along the riverside, which may also contributed to the underestimation.

Simulation Results of the Root Oxygen Respiration Rate

Notably, simulated RORRs of the MeS and ShS were generally in good agreement with the measured LNPRs (**Figure 4**). Better correlations were achieved in the MeS. The MeS and ShS had PCC values of 0.847 and 0.850, respectively, while R^2 value were 0.717 and 0.722. It is noteworthy that the RORR simulation results for the MeS and ShS could almost follow the general trend of the LNPR observation values over the study period. As illustrated in **Figures 4A,B**, surface flooding from 31th July 2017 immediately suppressed the RORRs and LNPRs in both plant types. A noticeable trend was the sharp decline following the occurrence of surface water flooding. Interestingly, the RORR-MeS increased from a trough value 0.22 μmol m^{-2} s^{-1} within 1–2 days and recovered to nearly normal level within approximately 10 days. However, for the ShS, the RORR value dropped dramatically shortly after the surface flooding, and remained nearly constant at an average value of 0.30 μmol m^{-2} s^{-1} onwards, which indicated a deadly flooding impact on the root functioning of the ShS. This demonstrated an advantageous effect of flooding on shrub expansion restriction (Myers-Smith et al., 2015).

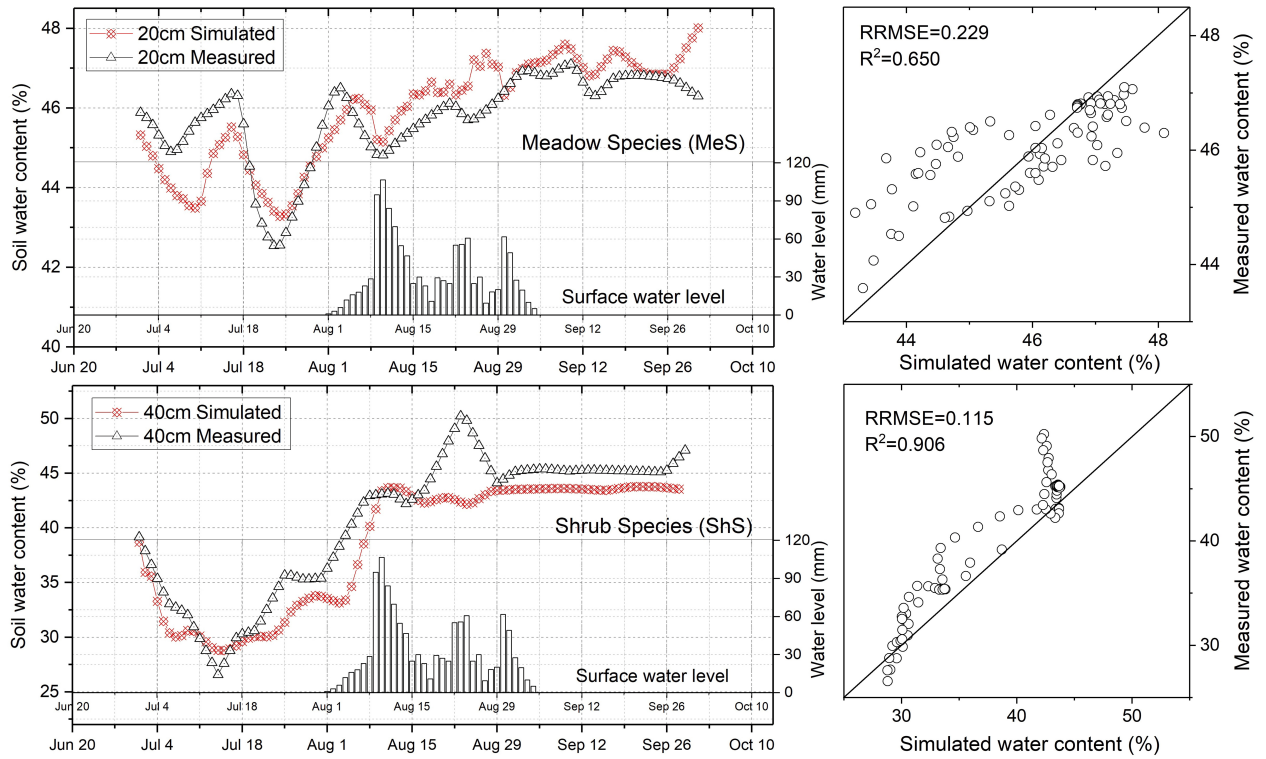

FIGURE 3 | Observed and simulated RZ-SWCs of the MeS and ShS at certain soil depths. Scatter tracks illustrate the difference between the observed and simulated RZ-SWCs by displaying the mean radically root square error (RRMSE) and the determination coefficient (R^2).

Influence of the Aerenchyma Sub-Model to the Root Oxygen Respiration Rate Simulation Results

The effect of the aerenchyma sub-model on simulation results of the RORR for the MeS and ShS was investigated. As indicated in **Figure 5**, the simulated values of the RORR-MeS and RORR-ShS during periods of surface flooding were considerably underestimated (18.96 and 16.37%, respectively) without the aerenchyma sub-model. This emphasized the critical role of the aerenchyma's physiological function under flooding stress. Developing appropriate aerenchyma models would assist in quantifying the dynamics of plant physiological responses to flooding events.

DISCUSSION

The Performance of Current Eco-Hydrological Model

In this study, we simulated the physiological responses of typical wetland plants to natural flooding events by using a process-based eco-hydrological model. Additionally, a new root aerenchyma sub-model was developed and incorporated into the above-mentioned model. This sub-model contained key processes of root oxygen diffusion and ROL during soil submergence. The aerenchyma model improved the precision of root oxygen respiration rate simulation, thereby would enhance the understanding of the structure and function of aerenchyma in wetland plants during seasonal flooding events. Furthermore, soil moisture was successfully simulated in variably saturated wetland conditions under the assumption that the wetland surface litter layer was specified as a 10 cm top soil layer. When surface flooding water was present, the simulation results closely matched the observations. Overall, we improved the model reliability in representing the eco-hydrological processes and parameterization of abiotic and biotic factors, which were both considered concurrently when simulating the RORR-MeS and RORR-ShS. Notably, we observed an exception that the RORR-ShS value did not vary significantly in comparison to the LNPR-ShS value before the rainy season. We hypothesize that this could be due to the ShS' unique physiological characteristics, which enabled it to maintain a steady RORR during dry seasons, thereby establish stable whole-plant source-sink relationships in this stage (Pregitzer et al., 2000).

Relationship of the Root Oxygen Respiration Rate and Leaf Net Photosynthesis Rate

The present study confirmed previous findings that oxygen diffusing to the roots and rhizosphere during the day may be a result of photosynthetic activities (Caffrey and Kemp, 1991; Evans, 2004). Moreover, in submerged species, photosynthesis

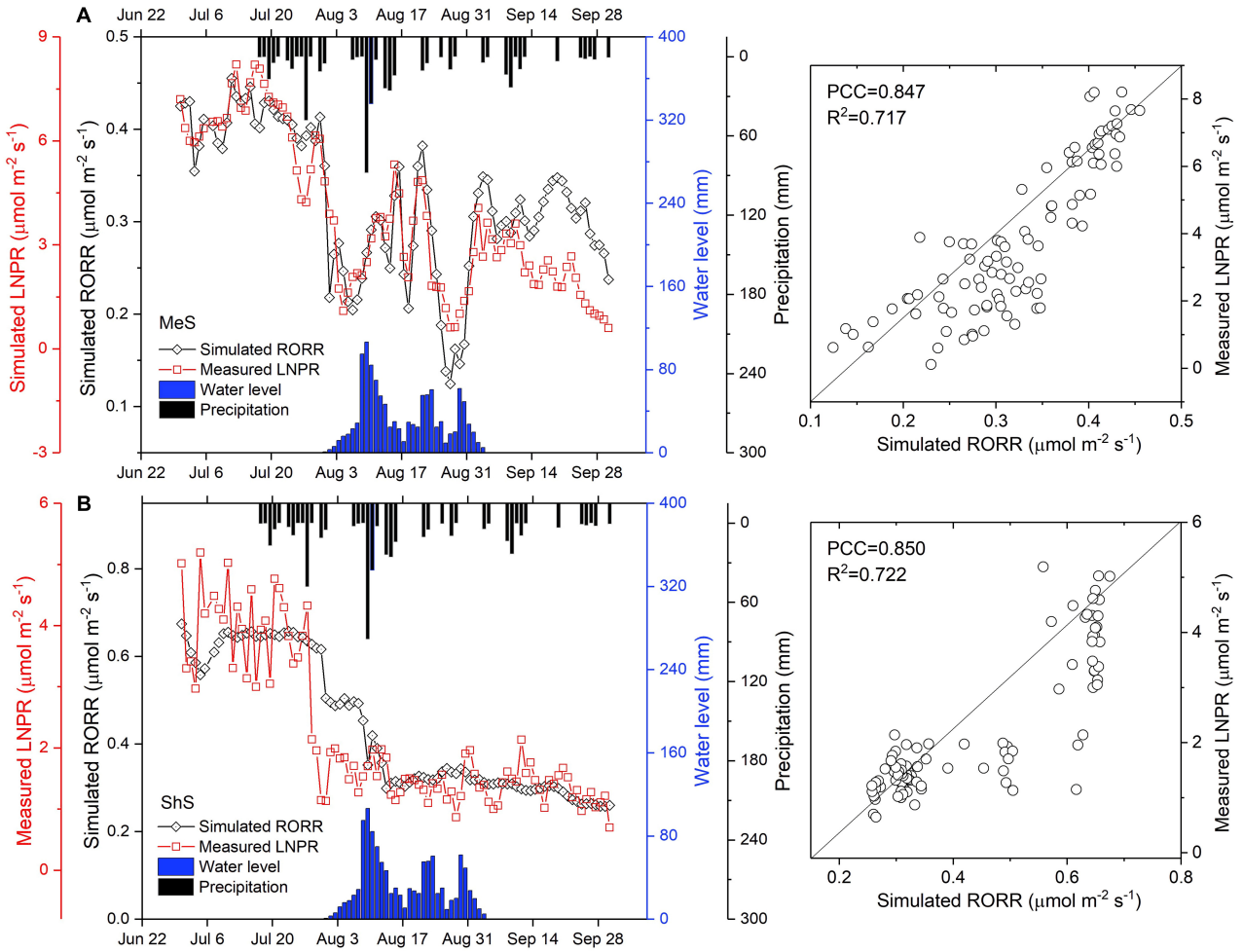

FIGURE 4 | Simulated root oxygen respiration rate (RORR) and measured leaf net photosynthesis rate (LNPR) of the MeS **(A)** and ShS **(B)** under the influence of rainfall and surface water level. Scatter tracks demonstrate the relationship between the observed and simulated values of the MeS and ShS by displaying Pearson Correlations Coefficients (PCC) and the determination coefficient (R^2).

was a significant source of oxygen for the fine root and rhizosphere (Jackson and Armstrong, 1999). Diurnal changes in root respiration strongly correlated with rates of net photosynthesis (Lai et al., 2016). As illustrated in **Figures 4A,B**, during the initial stage of seasonal flooding, when the rhizosphere was hypoxic, both leaf photosynthetic capacity and root oxygen respiration rate of the Mes and ShS were significantly affected. However, the MeS with a preference for wet microhabitats had a competitive advantage over first-year invading ShS under flooding stress, which was consistent with previous researches (Jung et al., 2008; Gattringer et al., 2017, 2018). Flooding had a detrimental effect on the ShS due to the physiological dysfunctions caused by soil anaerobiosis (Kozlowski, 2002). To summarize, the RORRs correlated positively with the LNPRs in both plant types during flooding events. However, it should be noted that, from 31st August onwards, there was a noticeable recovery (averaged 0.32 μmol m^{-2} s^{-1}) of the RORR-MeS, which outnumbered the LNPR-MeS as a whole during this period. This may help explain, at least in part, why fine root production exceeded above-ground production. That is, as evidenced by measurement data from a variety of biomes, seasonal variation in root production cannot always be attributed to above-ground production (Abramoff and Finzi, 2015). Therefore, typical wetland plants may increase the level of RORR to prepare for the next life-cycle stage.

Influences of the Root-Zone Soil Moisture Content and Soil Temperature on the Root Oxygen Respiration Rate

Monte Carlo methods were used to evaluate the sensitivity of the RORR to root-zone soil water stress associated with the soil temperature (Hammersley, 2013). To begin, the RZ-SWC was randomly selected from normal distributions using the mean and standard deviation values from the HYDRUS1D simulation results. Then, the RORR-MeS and RORR-ShS were simultaneously simulated, with the inputs from the normalized RZ-SWC and ST. The RORR's sensitivity to RZ-SWC and ST was

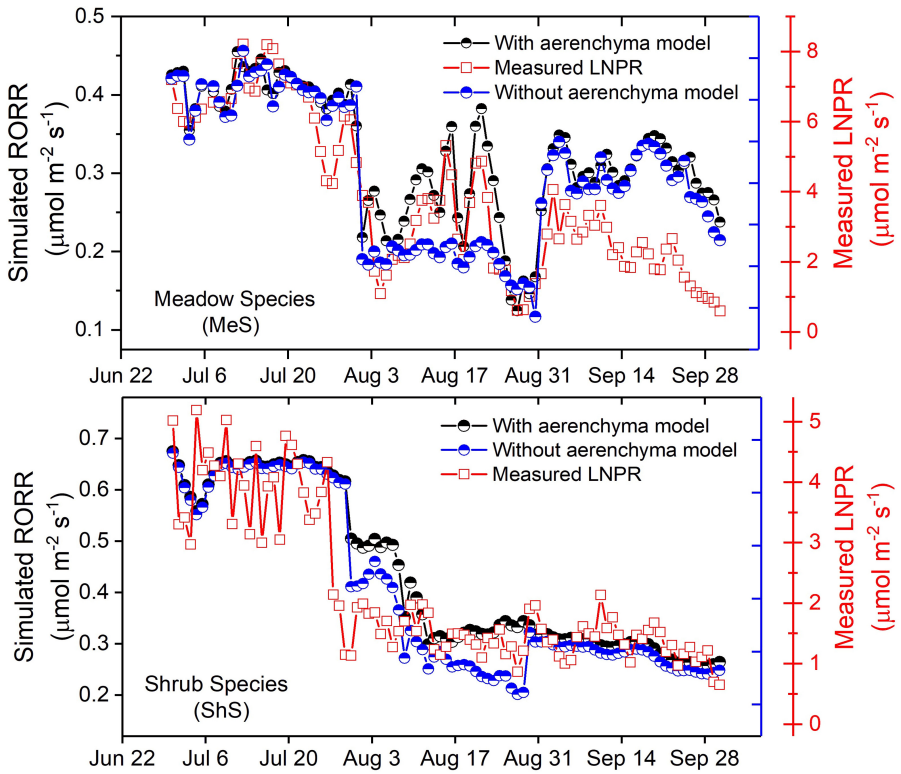

FIGURE 5 | Comparison of the RORR and LNPR simulation results of the MeS and ShS with and without the aerenchyma sub-model.

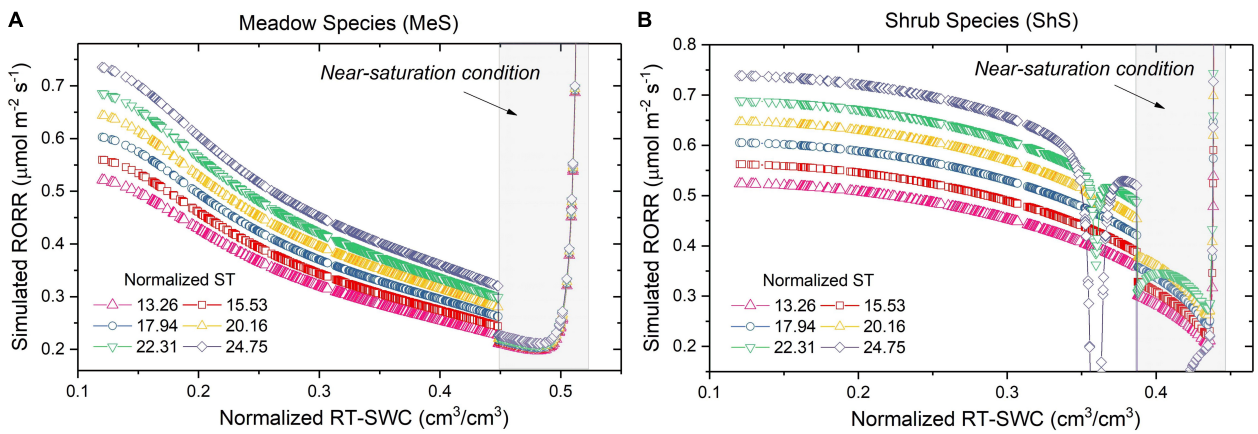

FIGURE 6 | Sensitivity of the RORRs to RZ-SWCs at various ST (ranging from 13.26 to 24.75°C) for the MeS **(A)** and ShS **(B)**. Gray areas indicates the near-saturation conditions.

then visualized by using linear regression methods. Sensitivity analysis reveals that the RZ-SWC had a ST-dependent effect as illustrated in **Figures 6A,B**. Interestingly, the RORR-MeS was more susceptible to ST fluctuations than the RORR-ShS under low RZ-SWC conditions. By contrast, the RORR-ShS (**Figure 6B**) was more sensitive to ST fluctuations than the RORR-MeS at the state of near saturation, with the RORR-MeS exhibited no apparent ST dependence (**Figure 6A**) at this stage. It is noted that RORR-ShS was more sensitive to the ST above approximately 20 °C, which resulted in a significant decrease in RORR-ShS values. In other words, the ST over 20 °C caused more RORR damage to the roots of the ShS than to the MeS'. Moreover, the RORR-MeS was more stable over a wider range of RZ-SWC values (upper limit: 0.53 cm^3/cm^3) than the RORR-ShS (upper limit: 0.44 cm^3/cm^3). Notably, the RORR-MeS could recover, at least to some extent, before the state of full saturation. This reflects a stronger capacity of the MeS adjusting the root oxygen respiration function under flooding conditions.

Above all, sensitivity analysis demonstrated that the RORR responses may differ according to plant types and stages in relations to the combined effects of temperature and soil saturation, as evidenced by Calleja-Cabrera et al. (2020). The MeS appeared to respond to the combined stresses more effectively by increasing oxygen partitioning to the roots, thereby promoting rhizosphere oxidation and fine root growth. When both stresses were present, in contrast to the MeS, the harmful effects were amplified for the ShS, because they were more intolerant to relatively high RZ-SWC and ST (Atkin et al., 2000).

Limitations of the Current Study

This study has two main limitations. The first limitation is the observational error in natural wetlands. The hydrological complexity of the seasonal flooding intensified the difficulty of *in-situ* multi-layered soil moisture measurement. This may partially resulted in not good agreement (with the RRMSE values 0.229, and the R^2 values 0.650) of the simulated RZ-SWC-MeS with the observations. Second, the current eco-hydrological model did not include all the key physiological processes to adapt to flooding stress. For example, flooding-induced adventitious roots (They contain aerenchyma cells as well) have been described for a number of Central European shrub species (Glenz et al., 2006), which can also maintain the root respiration *via* rapid oxygen absorption. Therefore, in order to more effectively simulate the physiological response to seasonal flooding events, the adventitious roots should be incorporated into the eco-hydrological model in the future.

CONCLUSION

A process-based eco-hydrological model for the physiological responses of typical wetland plant species to natural flooding events, has been developed and validated with the data from *in-situ* field measurements from a natural wetland in northeastern China. The new root aerenchyma sub-model was able to improve the precision of root oxygen respiration rate simulation. The results presented here show that we improved the model reliability in representing the eco-hydrological processes and parameterization of abiotic and biotic factors. The study also shows a strong correlation between the root oxygen respiration rate and the leaf net photosynthesis rate during natural flooding events. This would contribute to eco-hydrological modeling science with a new way of understanding the key processes in floodplain wetlands. This would also assist in more accurate assessments and predictions of vegetation dynamics for wetland management and restoration initiatives. Restoration of degraded or destroyed freshwater wetlands can be achieved by designing regulatory flooding processes that efficiently restore native flood-tolerant wetland vegetation and restrict woody plant invasion. This study will be expanded in the future to deal with the physiological responses at a larger spatio-temporal scale by developing a more comprehensive eco-hydrological model, thereby providing mathematical tools for exploring the spatio-temporal patterns of plant physiological responses in natural floodplain wetlands.

DATA AVAILABILITY STATEMENT

The original contributions presented in the study are included in the article/**Supplementary Material**, further inquiries can be directed to the corresponding author/s.

AUTHOR CONTRIBUTIONS

CL, YZ, ZS, and DZ conceived and designed the study. YZ, ZS, and DZ establish the context for field experiments and simulations. CL conducted experiments and simulations and wrote the manuscript. All authors contributed to developing the model and provided feedback on earlier drafts and approved the final version for submission.

FUNDING

This work was supported by grants from the National Natural Science Foundation of China (NSFC41671509).

ACKNOWLEDGMENTS

We would like to express our gratitude to the Sanjiang Experimental Station of Wetland Ecology, Northeast Institute of Geography and Agroecology, Chinese Academy of Sciences, for supporting the Eco-Hydrological Experiments in this study.

SUPPLEMENTARY MATERIAL

The Supplementary Material for this article can be found online at: https://www.frontiersin.org/articles/10.3389/fevo.2022.721244/full#supplementary-material

REFERENCES

Abou Jaoudé, R., de Dato, G., and De Angelis, P. (2012). Photosynthetic and wood anatomical responses of *Tamarixafricana* poiret to water level reduction after short-term fresh-and saline-water flooding. *Ecol. Res.* 27, 857–866. doi: 10.1007/s11284-012-0963-3

Abramoff, R. Z., and Finzi, A. C. (2015). Are above-and below-ground phenology in sync? *New Phytol.* 205, 1054–1061. doi: 10.1111/nph.13111

Armstrong, W., Beckett, P. M., Colmer, T. D., Setter, T. L., and Greenway, H. (2019). Tolerance of roots to low oxygen: 'Anoxic' cores, the phytoglobin-nitric oxide cycle, and energy or oxygen sensing. *J. Plant Physiol.* 239, 92–108. doi: 10.1016/j.jplph.2019.04.010

Armstrong, W., Brändle, R., and Jackson, M. B. (1994). Mechanisms of flood tolerance in plants. *Acta Bot. Neerl.* 43, 307–358. doi: 10.1111/j.1438-8677.1994.tb00756.x

Armstrong, W., Cousins, D., Armstrong, J., Turner, D., and Beckett, P. (2000). Oxygen distribution in wetland plant roots and permeability barriers to gas-exchange with the rhizosphere: a microelectrode and modelling study with phragmites australis. *Ann. Bot.* 86, 687–703. doi: 10.1006/anbo.2000.1236

Armstrong, W., Justin, S., Beckett, P., and Lythe, S. (1991). Root adaptation to soil waterlogging. *Aquat. Bot.* 39, 57–73. doi: 10.1016/0304-3770(91)90022-w

Arora, V. K. (2003). Simulating energy and carbon fluxes over winter wheat using coupled land surface and terrestrial ecosystem models. *Agricult. For. Meteorol.* 118, 21–47. doi: 10.1016/s0168-1923(03)00073-x

Atkin, O. K., Edwards, E. J., and Loveys, B. R. (2000). Response of root respiration to changes in temperature and its relevance to global warming. *New Phytol.* 147, 141–154. doi: 10.1046/j.1469-8137.2000.00683.x

Bai, J., Ouyang, H., Deng, W., Zhu, Y., Zhang, X., and Wang, Q. (2005). Spatial distribution characteristics of organic matter and total nitrogen of marsh soils in river marginal wetlands. *Geoderma* 124, 181–192. doi: 10.1016/j.geoderma.2004.04.012

Bartholomeus, R. P., Witte, J.-P. M., van Bodegom, P. M., van Dam, J. C., and Aerts, R. (2008). Critical soil conditions for oxygen stress to plant roots: substituting the feddes-function by a process-based model. *J. Hydrol.* 360, 147–165. doi: 10.1016/j.jhydrol.2008.07.029

Blom, C. (1999). Adaptations to flooding stress: from plant community to molecule. *Plant Biol.* 1, 261–273. doi: 10.1055/s-2007-978515

Blume-Werry, G., Milbau, A., Teuber, L. M., Johansson, M., and Dorrepaal, E. (2019). Dwelling in the deep–strongly increased root growth and rooting depth enhance plant interactions with thawing permafrost soil. *New Phytol.* 223, 1328–1339. doi: 10.1111/nph.15903

Booth, E. G., and Loheide, S. P. (2010). Effects of evapotranspiration partitioning, plant water stress response and topsoil removal on the soil moisture regime of a floodplain wetland: implications for restoration. *Hydrol. Process.* 24, 2934–2946. doi: 10.1002/hyp.7707

Byun, C., Nam, J. M., and Kim, J. G. (2017). Effects of flooding regime on wetland plant growth and species dominance in a mesocosm experiment. *Plant Ecol.* 218, 517–527. doi: 10.1007/s11258-017-0707-0

Caffrey, J., and Kemp, W. (1991). Seasonal and spatial patterns of oxygen production, respiration and root-rhizome release in *Potamogeton perfoliatus* l. and *Zostera marina* l. *Aquat. Bot.* 40, 109–128. doi: 10.1016/0304-3770(91)90090-R

Calleja-Cabrera, J., Boter, M., Oñate-Sánchez, L., and Pernas, M. (2020). Root growth adaptation to climate change in crops. *Front. Plant Sci.* 11:544. doi: 10.3389/fpls.2020.00544

Casanova, M. T., and Brock, M. A. (2000). How do depth, duration and frequency of flooding influence the establishment of wetland plant communities? *Plant Ecol.* 147, 237–250. doi: 10.1023/A:1009875226637

Cesarz, S., Ciobanu, M., Wright, A. J., Ebeling, A., Vogel, A., Weisser, W. W., et al. (2017). Plant species richness sustains higher trophic levels of soil nematode communities after consecutive environmental perturbations. *Oecologia* 184, 715–728. doi: 10.1007/s00442-017-3893-5

Coleman, J. M., Huh, O. K., and Braud, D. (2008). Wetland loss in world deltas. *J. Coast. Res.* 24, 1–14. doi: 10.2112/05-0607.1

Colmer, T. (2003). Long-distance transport of gases in plants: a perspective on internal aeration and radial oxygen loss from roots. *Plant Cell Environ.* 26, 17–36. doi: 10.1046/j.1365-3040.2003.00846.x

Cook, F. (1995). One-dimensional oxygen diffusion into soil with exponential respiration: analytical and numerical solutions. *Ecol. Model.* 78, 277–283. doi: 10.1016/0304-3800(94)00179-l

Dalmagro, H. J., Lathuillière, M. J., Vourlitis, G. L., Campos, R. C., Pinto, O. B. Jr., Johnson, M. S., et al. (2016). Physiological responses to extreme hydrological events in the pantanal wetland: heterogeneity of a plant community containing super-dominant species. *J. Veg. Sci.* 27, 568–577. doi: 10.1111/jvs.12379

De Willigen, P., and Van Noordwijk, M. (1984). Mathematical models on diffusion of oxygen to and within plant roots, with special emphasis on effects of soil-root contact. *Plant Soil* 77, 215–231. doi: 10.1007/bf02182925

DeLaune, R., Pezeshki, S., and Pardue, J. (1990). An oxidation-reduction buffer for evaluating the physiological response of plants to root oxygen stress. *Environ. Exp. Bot.* 30, 243–247. doi: 10.1016/0098-8472(90)90070-k

Evans, D. E. (2004). Aerenchyma formation. *New Phytol.* 161, 35–49. doi: 10.1046/j.1469-8137.2003.00907.x

Ewing, K. (1996). Tolerance of four wetland plant species to flooding and sediment deposition. *Environ. Exp. Bot.* 36, 131–146. doi: 10.1016/0098-8472(96)01000-3

Fischer, F. M., Wright, A. J., Eisenhauer, N., Ebeling, A., Roscher, C., Wagg, C., et al. (2016). Plant species richness and functional traits affect community stability after a flood event. *Philos. Transac. R. Soc. B Biol. Sci.* 371, 20150276. doi: 10.1098/rstb.2015.0276

Gardner, R. C., and Davidson, N. C. (2011). "The ramsar convention," in *Wetlands*, ed. B. LePage (Dordrecht: Springer), doi: 10.1007/978-94-007-0551-7_11.

Gattringer, J. P., Donath, T. W., Eckstein, R. L., Ludewig, K., Otte, A., and Harvolk-Schöning, S. (2017). Flooding tolerance of four floodplain meadow species depends on age. *PLoS One* 12:e0176869. doi: 10.1371/journal.pone.0176869

Gattringer, J. P., Ludewig, K., Harvolk-Schöning, S., Donath, T. W., and Otte, A. (2018). Interaction between depth and duration matters: flooding tolerance of 12 floodplain meadow species. *Plant Ecol.* 219, 973–984. doi: 10.1007/s11258-018-0850-2

Glenz, C., Schlaepfer, R., Iorgulescu, I., and Kienast, F. (2006). Flooding tolerance of central european tree and shrub species. *For. Ecol. Manag.* 235, 1–13. doi: 10.1016/j.foreco.2006.05.065

Haak, D. C., Fukao, T., Grene, R., Hua, Z., Ivanov, R., Perrella, G., et al. (2017). Multilevel regulation of abiotic stress responses in plants. *Front. Plant Sci.* 8:1564. doi: 10.3389/fpls.2017.01564

Hammersley, J. (2013). *Monte Carlo Methods*. Berlin: Springer Science & Business Media. doi: 10.1007/978-94-009-5819-7.

Hough-Snee, N., Nackley, L. L., Kim, S.-H., and Ewing, K. (2015). Does plant performance under stress explain divergent life history strategies? The effects of flooding and nutrient stress on two wetland sedges. *Aquat. Bot.* 120, 151–159. doi: 10.1016/j.aquabot.2014.03.001

Isbell, F., Craven, D., Connolly, J., Loreau, M., Schmid, B., Beierkuhnlein, C., et al. (2015). Biodiversity increases the resistance of ecosystem productivity to climate extremes. *Nature* 526:574. doi: 10.1038/nature15374

Jackson, M., and Armstrong, W. (1999). Formation of aerenchyma and the processes of plant ventilation in relation to soil flooding and submergence. *Plant Biol.* 1, 274–287. doi: 10.1111/j.1438-8677.1999.tb00253.x

Jones, C. G., Lawton, J. H., and Shachak, M. (1994). "Organisms as ecosystem engineers," in *Ecosystem Management*, eds F.B. Samson and F. L. Knopf (New York, NY: Springer), doi: 10.1007/978-1-4612-4018-1_14.

Jung, V., Hoffmann, L., and Muller, S. (2008). "Ecophysiological responses of nine floodplain meadow species to changing hydrological conditions," in *Herbaceous Plant Ecology*, ed. A. G. Van der Valk (Dordrecht: Springer). doi: 10.1007/978-90-481-2798-6_18

Kirwan, M. L., and Guntenspergen, G. R. (2015). Response of plant productivity to experimental flooding in a stable and a submerging marsh. *Ecosystems* 18, 903–913. doi: 10.1007/s10021-015-9870-0

Kozlowski, T. T. (2002). Physiological-ecological impacts of flooding on riparian forest ecosystems. *Wetlands* 22, 550–561. doi: 10.1672/0277-5212(2002)022[0550:PEIOFO]2.0.CO;2

Kumari, A., and Gupta, K. J. (2017). "Visisens technique to measure internal oxygen and respiration in barley roots," in *Plant Respiration and Internal Oxygen*, ed. J. G. Kapuganti (New York, NY: Springer), doi: 10.1007/978-1-4939-7292-0_4.

Laan, P., Berrevoets, M., Lythe, S., Armstrong, W., and Blom, C. (1989). Root morphology and aerenchyma formation as indicators of the flood-tolerance of rumex species. *J. Ecol.* 77, 693–703. doi: 10.2307/2260979

Lai, W.-L., Zhang, Y., and Chen, Z.-H. (2012). Radial oxygen loss, photosynthesis, and nutrient removal of 35 wetland plants. *Ecol. Eng.* 39, 24–30. doi: 10.1016/j.ecoleng.2011.11.010

Lai, Z., Lu, S., Zhang, Y., Wu, B., Qin, S., Feng, W., et al. (2016). Diel patterns of fine root respiration in a dryland shrub, measured in situ over different phenological stages. *J. For. Res.* 21, 31–42. doi: 10.1007/s10310-015-0511-4

Lemon, E., and Wiegand, C. (1962). Soil aeration and plant root relations ii. Root respiration 1. *Agron. J.* 54, 171–175. doi: 10.2134/agronj1962.00021962005400020024x

Li, S., Zhou, D., Luan, Z., Pan, Y., and Jiao, C. (2011). Quantitative simulation on soil moisture contents of two typical vegetation communities in Sanjiang Plain, China. *Chinese Geogr. Sci.* 21, 723–733. doi: 10.1007/s11769-011-0507-8

Maricle, B. R., and Lee, R. W. (2002). Aerenchyma development and oxygen transport in the estuarine cordgrasses *Spartina alterniflora* and *S. Anglica*. *Aquat. Bot.* 74, 109–120. doi: 10.1016/S0304-3770(02)00051-7

Montagnoli, A., Terzaghi, M., Chiatante, D., Scippa, G. S., Lasserre, B., and Dumroese, R. K. (2019). Ongoing modifications to root system architecture of pinus ponderosa growing on a sloped site revealed by tree-ring analysis. *Dendrochronologia* 58:125650. doi: 10.1016/j.dendro.2019.125650

Myers-Smith, I. H., Elmendorf, S. C., Beck, P. S., Wilmking, M., Hallinger, M., Blok, D., et al. (2015). Climate sensitivity of shrub growth across the tundra biome. *Nat. Clim. Change* 5, 887–891. doi: 10.1038/nclimate2697

Niu, Z., Zhang, H., Wang, X., Yao, W., Zhou, D., Zhao, K., et al. (2012). Mapping wetland changes in China between 1978 and 2008. *Chinese Sci. Bull.* 57, 2813–2823. doi: 10.1007/s11434-012-5093-3

Pedersen, O., Perata, P., and Voesenek, L. A. (2017). Flooding and low oxygen responses in plants. *Funct. Plant Biol.* 44, iii–vi. doi: 10.1071/fpv44n9_fo

Pedersen, O., Sand-Jensen , K., and Revsbech, N. P. (1995). Diel pulses of o_2 and co_2 in sandy lake sediments inhabited by lobelia dortmanna. *Ecology* 76, 1536–1545. doi: 10.2307/1938155

Pezeshki, S. (1998). Photosynthesis and root growth in spartina alterniflora in relation to root zone aeration. *Photosynthetica* 34, 107–114. doi: 10.1023/a:1006820019220

Pezeshki, S. (2001). Wetland plant responses to soil flooding. *Environ. Exp. Bot.* 46, 299–312. doi: 10.1016/s0098-8472(01)00107-1

Pezeshki, S. R., Finlayson, C. M., Everard, M., Irvine, K., Mcinnes, R. J., Middleton, B. A., et al. (eds) (2018). "Photosynthesis in wetlands," in *The Wetland Book: I: Structure and Function, Management, and Methods*, (Dordrecht: Springer Netherlands). doi: 10.1007/978-90-481-9659-3_64.

Pezeshki, S., DeLaune, R., and Patrick, W. Jr. (1987). Effects of flooding and salinity on photosynthesis of *Sagittaria lancifolia*. *Mar. Ecol. Progr. Ser.* 41, 87–91. doi: 10.3354/meps041087

Pregitzer, K. S., King, J. S., Burton, A. J., and Brown, S. E. (2000). Responses of tree fine roots to temperature. *New Phytol.* 147, 105–115. doi: 10.1046/j.1469-8137.2000.00689.x

Probert, M., Dimes, J., Keating, B., Dalal, R., and Strong, W. (1998). Apsim's water and nitrogen modules and simulation of the dynamics of water and nitrogen in fallow systems. *Agricult. Syst.* 56, 1–28. doi: 10.1016/s0308-521x(97)00028-0

Purcell, A. S., Lee, W. G., Tanentzap, A. J., and Laughlin, D. C. (2019). Fine root traits are correlated with flooding duration while aboveground traits are related to grazing in an ephemeral wetland. *Wetlands* 39, 291–302. doi: 10.1007/s13157-018-1084-8

Reddy, K. R., and DeLaune, R. D. (2008). *Biogeochemistry of Wetlands: Science and Applications*. Boca Raton, FL: CRC press. doi: 10.1201/9780203491454.

Reich, P. B., Knops, J., Tilman, D., Craine, J., Ellsworth, D., Tjoelker, M., et al. (2001). Plant diversity enhances ecosystem responses to elevated CO_2 and nitrogen deposition. *Nature* 410:809. doi: 10.1038/35081122

Rubol, S., Silver, W. L., and Bellin, A. (2012). Hydrologic control on redox and nitrogen dynamics in a peatland soil. *Sci. Total Environ.* 432, 37–46. doi: 10.1016/j.scitotenv.2012.05.073

Simunek, J., Van Genuchten, M. T., and Sejna, M. (2005). *The HYDRUS-1D Software Package for Simulating the One-Dimensional Movement of Water, Heat, and Multiple Solutes in Variably-Saturated Media. Version 3.0. HYDRUS Software Series 1*. Riverside*:* University of California Riverside, 1-240.

Striker, G., Insausti, P., Grimoldi, A., and Vega, A. (2007). Trade-off between root porosity and mechanical strength in species with different types of aerenchyma. *Plant Cell Environ.* 30, 580–589. doi: 10.1111/j.1365-3040.2007.01639.x

Van Genuchten, M. T. (1980). A closed-form equation for predicting the hydraulic conductivity of unsaturated soils 1. *Soil Sci. Soc. Am. J.* 44, 892–898. doi: 10.2136/sssaj1980.03615995004400050002x

Watanabe, K., Takahashi, H., Sato, S., Nishiuchi, S., Omori, F., Malik, A. I., et al. (2017). A major locus involved in the formation of the radial oxygen loss barrier in adventitious roots of teosinte zea nicaraguensis is located on the short-arm of chromosome 3. *Plant Cell Environ.* 40, 304–316. doi: 10.1111/pce.12849

Waters, I., Armstrong, W., Thompson, C., Setter, T., Adkins, S., Gibbs, J., et al. (1989). Diurnal changes in radial oxygen loss and ethanol metabolism in roots of submerged and non-submerged rice seedlings. *New Phytol.* 113, 439–451. doi: 10.1111/j.1469-8137.1989.tb00355.x

Watson, E. B., Andrews, H. M., Fischer, A., Cencer, M., Coiro, L., Kelley, S., et al. (2015). Growth and photosynthesis responses of two co-occurring marsh grasses to inundation and varied nutrients. *Botany* 93, 671–683. doi: 10.1139/cjb-2015-0055

Weiss, R. F. (1970). The solubility of nitrogen, oxygen and argon in water and seawater. *Deep Sea Res. Oceanogr. Abstracts.* 17, 721–735. doi: 10.1016/0011-7471(70)90037-9

Wright, A. J., de Kroon, H., Visser, E. J. W., Buchmann, T., Ebeling, A., Eisenhauer, N., et al. (2017). Plants are less negatively affected by flooding when growing in species-rich plant communities. *New Phytol.* 213, 645–656. doi: 10.1111/nph.14185

Wright, A. J., Ebeling, A., De Kroon, H., Roscher, C., Weigelt, A., Buchmann, N., et al. (2015). Flooding disturbances increase resource availability and productivity but reduce stability in diverse plant communities. *Nat. Commun.* 6:6092. doi: 10.1038/ncomms7092

Yamauchi, T., Colmer, T. D., Pedersen, O., and Nakazono, M. (2018). Regulation of root traits for internal aeration and tolerance to soil waterlogging-flooding stress. *Plant Physiol.* 176, 1118–1130. doi: 10.1104/pp.17.01157

Yan, K., Zhao, S., Cui, M., Han, G., and Wen, P. (2018). Vulnerability of photosynthesis and photosystem i in Jerusalem artichoke (*Helianthus tuberosus* l.) exposed to waterlogging. *Plant Physiol. Biochem.* 125, 239–246. doi: 10.1016/j.plaphy.2018.02.017

Zeng, Y. (eds) (2013). "Diurnal pattern of coupled moisture and heat transport process," in *Coupled Dynamics in Soil*, (New York, NY: Springer), doi: 10.1007/978-3-642-34073-4_2.

Zeng, Y., Su, Z., Wan, L., and Wen, J. (2011). A simulation analysis of the advective effect on evaporation using a two-phase heat and mass flow model. *Water Resourc. Res.* 47:W10529. doi: 10.1029/2011WR010701

Zhang, D., Qi, Q., Wang, X., Tong, S., Lv, X., An, Y., et al. (2019). Physiological responses of *Carex schmidtii* meinsh to alternating flooding-drought conditions in the Momoge wetland, Northeast China. *Aquat. Bot.* 153, 33–39. doi: 10.1016/j.aquabot.2018.11.010

Zhang, Y., Niu, J., Yu, X., Zhu, W., and Du, X. (2015). Effects of fine root length density and root biomass on soil preferential flow in forest ecosystems. *For. Syst.* 24:12. doi: 10.5424/fs/2015241-06048

Zhou, D., Gong, H., Wang, Y., Khan, S., and Zhao, K. (2009). Driving forces for the marsh wetland degradation in the honghe national nature reserve in Sanjiang Plain, Northeast China. *Environ. Model. Assess.* 14, 101–111. doi: 10.1007/s10666-007-9135-1

Zhou, D., Wang, Z., Tang, T., Li, S., and Liu, C. (2013). Prediction of the changes in ecological pattern of wetlands due to a new dam establishment in China. *Ecohydrol. Hydrobiol.* 13, 52–61. doi: 10.1016/j.ecohyd.2013.03.002

Zhou, D., Zhang, H., and Liu, C. (2016). Wetland ecohydrology and its challenges. *Ecohydrol. Hydrobiol.* 16, 26–32. doi: 10.1016/j.ecohyd.2015.08.004

Conflict of Interest: The authors declare that the research was conducted in the absence of any commercial or financial relationships that could be construed as a potential conflict of interest.

Publisher's Note: All claims expressed in this article are solely those of the authors and do not necessarily represent those of their affiliated organizations, or those of the publisher, the editors and the reviewers. Any product that may be evaluated in this article, or claim that may be made by its manufacturer, is not guaranteed or endorsed by the publisher.

frontiers | Frontiers in Ecology and Evolution

ORIGINAL RESEARCH
published: 27 April 2022
doi: 10.3389/fevo.2022.872816

Salinity Effects on Microbial Derived-C of Coastal Wetland Soils in the Yellow River Delta

*Pengshuai Shao[1], Hongyan Han[1], Jingkuan Sun[1], Hongjun Yang[1] and Hongtu Xie[2]**

[1] Shandong Key Laboratory of Eco-Environmental Science for the Yellow River Delta, Binzhou University, Binzhou, China,
[2] Institute of Applied Ecology, Chinese Academy of Sciences, Shenyang, China

Microorganisms play a crucial role in regulating the turnover and transformation of soil organic carbon (SOC), whereas microbial contribution to SOC formation and storage is still unclear in coastal wetlands. In this study, we collected topsoil (0–20 cm) with 7 salinity concentrations and explored the shifts in microbial residues [represented by amino sugar (AS)] and their contribution to the SOC pool of coastal wetlands in the Yellow River delta. The gradually increasing soil salinity reduced soil water content (SWC), SOC, and soil nitrogen (N), especially in high salinity soils of coastal wetlands. Total ASs and their ratio to SOC, respectively, decreased by 90.56 and 66.35% from low salinity to high salinity soils, indicating that coastal wetlands with high salinity restrained microbial residue accumulation and microbial residue-C retention in the SOC pool. Together with redundancy analysis and path analysis, we found that SWC, pH, SOC, soil N, and glucosamine/muramic arid were positively associated with the ratio of ASs to SOC. The higher available soil resource (i.e., water, C substrate, and nutrient) increased microbial residue accumulation, promoting microbial derived-C contribution to SOC in low salinity coastal wetlands. The greatly decreased microbial residue contribution to SOC might be ascribed to microbial stress strategy and low available C substrate in coastal wetlands with high salinity concentration. Additionally, the gradually increasing salinity reduced fungal residue contribution to SOC but did not change bacterial residue contribution to SOC. These findings indicated that changed fungal residues would substantially influence SOC storage. Our study elucidates microbial contribution to SOC pool through residue reservoir in coastal wetlands and pushes microbial metabolites to a new application in global wetland SOC cycling.

Keywords: amino sugar, soil salinity, soil organic carbon, microbial necromass, coastal wetland

OPEN ACCESS

Edited by:
Yijian Zeng,
University of Twente, Netherlands

Reviewed by:
Yuntao Hu,
Lawrence Berkeley National Laboratory, United States
Ying Huang,
East China Normal University, China

****Correspondence:***
Hongtu Xie
xieht@iae.ac.cn

Specialty section:
This article was submitted to Conservation and Restoration Ecology, a section of the journal Frontiers in Ecology and Evolution

Received: *10 February 2022*
Accepted: *28 March 2022*
Published: *27 April 2022*

Citation:
Shao P, Han H, Sun J, Yang H and Xie H (2022) Salinity Effects on Microbial Derived-C of Coastal Wetland Soils in the Yellow River Delta. Front. Ecol. Evol. 10:872816. doi: 10.3389/fevo.2022.872816

INTRODUCTION

Coastal wetlands act as the important carbon (C) sink, which plays a crucial role in contributing to soil organic carbon (SOC) storage and regulating global C cycling (Chmura et al., 2003; Macreadie et al., 2019). However, the disturbance would greatly influence the structure and function of coastal wetlands. Naturally environmental disturbances (e.g., climate change and sea-level rise) or anthropogenic activities (e.g., agricultural reclamation and dam construction) result in the degradation of coastal wetlands, aggravating soil salinization (Xu et al., 2019; Haywood et al., 2020).

Increased salinity stress results in the decline in biodiversity, loss of soil nutrients, and SOC and alters plant and microbial mediation in SOC transformation and accumulation (Crooks et al., 2018; Lewis et al., 2019; Chen et al., 2021).

Coastal wetlands are the transitional zone between terrestrial and aquatic ecosystems. The drastically changing habitats alter water and salt conditions, soil nutrition, and plant community, influencing soil microbial community structure and functions in coastal wetlands (Hu et al., 2014; Spivak et al., 2019). To date, the studies on microorganisms in coastal wetlands mainly focus on active soil microbial community structure and functions using the technologies and methods of phospholipid fatty acid, enzyme, high-throughput sequencing, and metagenome (Bossio et al., 2006; Wang et al., 2020). Soil microorganisms are key participants and drivers in SOC transformation, formation, and storage through microbial metabolic processes (Trivedi et al., 2013; Spivak et al., 2019). Microbial community composition (e.g., fungi and bacteria) and extracellular enzymes govern litter decomposition, soil nutrient release, and recycling, which further influence SOC turnover in coastal wetlands (Hill et al., 2018; Zhao et al., 2020). However, it is not clear how microbes directly contribute to SOC accumulation through microbial metabolites (e.g., microbial necromass) in coastal wetlands.

Microorganisms utilize plant and soil C substrates to synthesize microbial cells, and the dead microbial cell that persists in the soil as relative stable soil organic matter (SOM) contributes to the SOC pool *via* microbial residues (Angst et al., 2021). Microbial residues can account for 30–60% of SOC in the forest, grassland, and agricultural ecosystems (Liang et al., 2019). Coastal wetlands have special soil conditions, such as low oxygen, high salinity, or dramatically fluctuant hydrology, which are different from terrestrial ecosystems (Lyu et al., 2018; Steinmuller et al., 2019). Therefore, it is necessary to explore the contribution of microbial residues to the SOC pool in coastal wetlands.

Amino sugars (ASs), as the main components of microbial cell walls, are usually used to represent microbial residues (Ding et al., 2019). As the biomarker of microbial residues, AS, such as glucosamine (GluN), galactosamine (GalN), and muramic acid (MurA), are derived from different soil microbial communities. GluN is mainly detected in fungi; MurA is solely extracted in bacteria; whereas GalN can be synthesized by fungi and bacteria (Glaser et al., 2004; Joergensen, 2018). Based on the origin of AS monomer, the ratio of AS monomer not only represents the ratio of fungal residues to bacterial residues but also reflects the changes in fungi and bacteria (Joergensen, 2018).

Salinity is the main limiting factor, affecting soil microbial community structure and functions in coastal wetlands (Ma et al., 2017; Zhang et al., 2021). *Phragmites australis* is widely distributed in coastal wetlands due to their salt-rejection and salt-adaption, which is a suitable plant community to study the responses of microbial residues to salinity. Using the biomarker of AS, we explored the dynamic of microbial residues and their contribution to SOC under coastal wetlands along a natural salinity gradient in the Yellow River delta, China. The goals of this study were (1) to detect the impacts of salinity on microbial residues and their contributions to SOC; (2) to examine the variation in fungal and bacterial residues and their contributions to microbial residues; and (3) to clarify how abiotic and biotic parameters drive microbial residue-C retention in wetland soils.

MATERIALS AND METHODS

Site Description and Sampling

Our study sites were located in the Yellow River Delta National Nature Reserve (118°33′–119°20′E, 37°35′–38°12′N), near Bohai and Laizhou Bay, China (**Figure 1**). Mean annual temperature and precipitation are approximately 12.4°C and 550 mm, respectively. Soil types are classified as fluvial soil formed by alluvial sediment of the Yellow River and saline soil formed by long-term seawater intrusion. In the water-salt interaction regions, we selected seven salinity concentrations (represented by electrical conductivity), including S1 (1.61 dS m^{-1}), S2 (2.47 dS m^{-1}), S3 (3.67 dS m^{-1}), S4 (5.21 dS m^{-1}), S5 (9.24 dS m^{-1}), S6 (14.53 dS m^{-1}), and S7 (29.90 dS m^{-1}) (**Table 1** and **Figure 1**). The sites of S1 and S2 are the interaction regions of the Yellow River and Bohai bay; S3 and S4 are affected by the seasonal tide; and S5, S6, and S7 are the degraded wetlands due to dam construction. Plant communities are dominated by *Phragmites australis,* following *Suaeda glauca*, *Tamarix chinensis*, *Cynanchum*, etc. We established study plots in August 2019 using a randomized within-wetland nested design. In each of the seven salinity concentrations, four plots (each approximately 10 m × 10 m) were randomly selected to collect soil samples (0–20 cm), with at least a 100-m distance between each plot. To alleviate spatial heterogeneity, we randomly took five soil cores using a soil auger (diameter of 5 cm) within each plot and pooled them into one soil sample (n = 4 samples per salinity concentration). After sieving soils to 2 mm to remove fine root, plant, and animal debris, soils were homogenized, and analyzed as below.

Soil Physicochemical Analysis

Air-dried soils (sieved to 2 mm) were used to prepare soil slurries (1:5 w/v), oscillate for 30 min, and subsequently measure electrical conductivity (EC) and pH on an electrode meter (Jenco 6173, Jenco, United States). Fresh soil samples (sieved to 2 mm) were oven-dried (105°C for 48 h) to determine soil water content (SWC). Air-dried soil samples (sieved to 0.15 mm) were prepared to analyze SOC using the potassium dichromate oxidation method (Nelson and Sommers, 1982). Total nitrogen (TN) was measured on a Vario MACRO Cube (Elementar vario EL III, Germany). Total phosphorus (TP) was detected using a UV-VIS spectrophotometer (PERSEE, WA, United States) after soil digestion using H_2SO_4 and $HClO_4$ (Cheng et al., 2016).

Soil Amino Sugar Analysis

Soil ASs, including GluN, GalN, and MurA, were determined according to a modified procedure referring to Zhang and Amelung (1996). In brief, air-dried soil samples (sieved to 0.15 mm) containing 0.3 mg N at least were hydrolyzed using 15 ml 6 M HCl at 105°C for 8 h. Each hydrolysate was filtered and dried at 52°C on a rotary vacuum evaporator after adding 100 μl of myoinositol (internal standard 1 with response factors, Rf of 1). The dried residue was dissolved using deionized water and

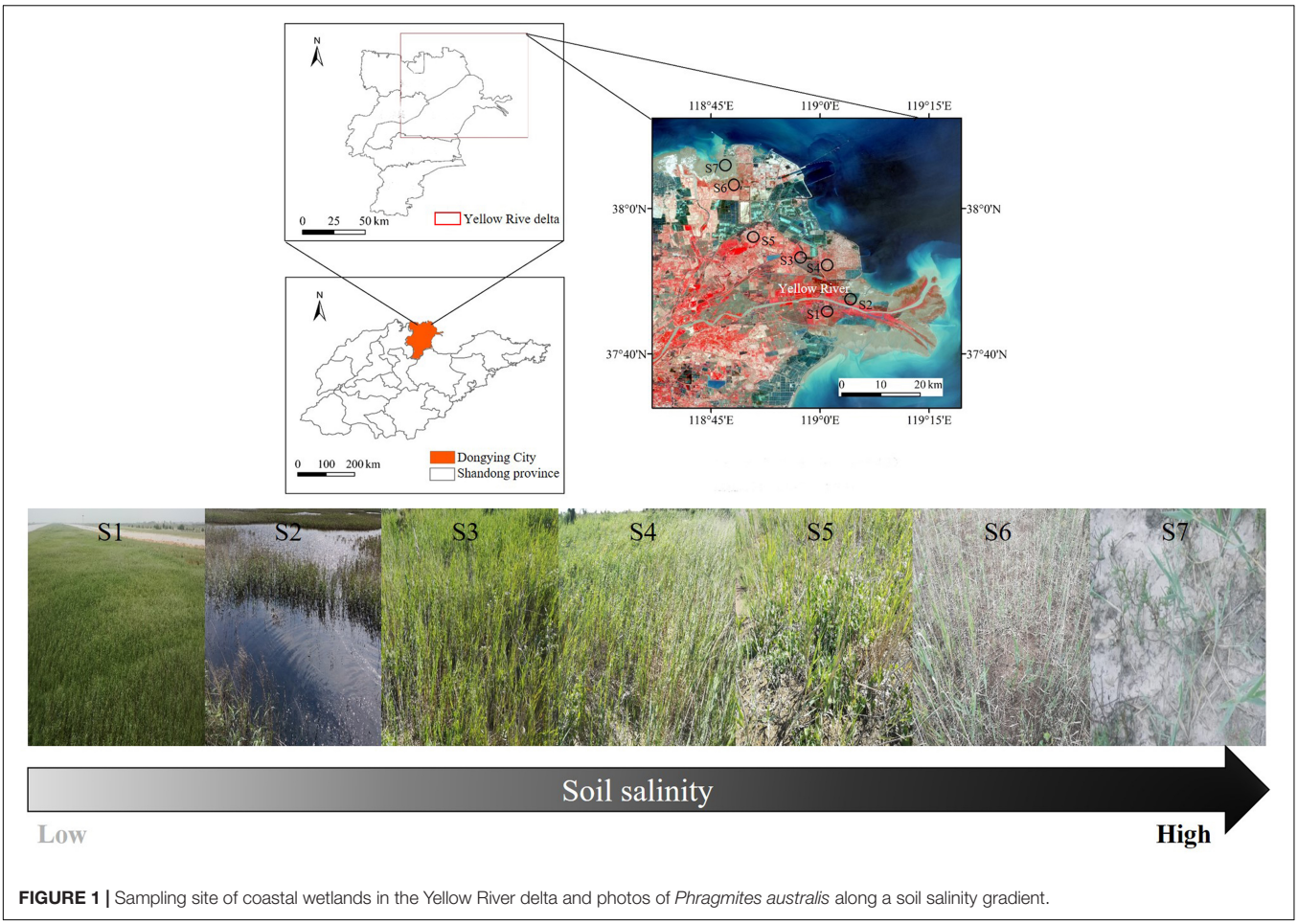

FIGURE 1 | Sampling site of coastal wetlands in the Yellow River delta and photos of *Phragmites australis* along a soil salinity gradient.

TABLE 1 | Soil physicochemical properties with 7 salinity concentrations under coastal wetlands in the Yellow River delta.

	Salinity gradient							Statistical value	
	S1	S2	S3	S4	S5	S6	S7	*F*	*P*
EC (dS m^{-1})	1.61 ± 0.13^{d}	2.47 ± 0.19^{d}	3.67 ± 0.11^{d}	5.21 ± 0.47^{d}	9.24 ± 0.31^{c}	14.53 ± 1.63^{b}	29.90 ± 2.71^{a}	68.06	<0.001
pH	7.83 ± 0.06^{a}	7.57 ± 0.06^{ab}	7.64 ± 0.10^{ab}	7.69 ± 0.09^{ab}	7.36 ± 0.13^{b}	7.38 ± 0.156^{b}	7.40 ± 0.12^{b}	2.84	0.04
SWC (%)	29.41 ± 0.40^{ab}	32.03 ± 3.19^{a}	30.94 ± 3.63^{a}	30.22 ± 1.28^{a}	28.93 ± 4.21^{ab}	25.03 ± 1.34^{ab}	21.73 ± 1.58^{b}	2.2	0.08
SOC (g kg^{-1})	10.13 ± 1.64^{a}	8.12 ± 0.50^{a}	5.13 ± 0.28^{b}	4.98 ± 0.60^{b}	3.83 ± 0.32^{b}	3.05 ± 0.22^{b}	2.93 ± 0.40^{b}	13.89	<0.001
TN (g kg^{-1})	1.07 ± 0.12^{a}	0.92 ± 0.06^{ab}	0.65 ± 0.06^{bc}	0.70 ± 0.10^{bc}	0.54 ± 0.05^{cd}	0.41 ± 0.02^{d}	0.47 ± 0.04^{d}	11.24	<0.001
SOC/TN	9.62 ± 1.60^{a}	8.83 ± 0.31^{a}	7.99 ± 0.21^{a}	7.47 ± 1.22^{a}	8.11 ± 1.50^{a}	7.41 ± 0.38^{a}	6.34 ± 1.00^{a}	1.08	0.41
TP (g kg^{-1})	0.59 ± 0.07^{a}	0.55 ± 0.07^{a}	0.47 ± 0.03^{a}	0.50 ± 0.06^{a}	0.53 ± 0.08^{a}	0.56 ± 0.09^{a}	0.51 ± 0.06^{a}	0.29	0.94

EC, electrical conductivity; SWC, soil water content; SOC, soil organic carbon; TN, total nitrogen; SOC/TN ratio of SOC to TN; TP, total phosphorus. The superscript letters represent statistical significance.

purified with KOH neutralization. The solution was fully dried and dissolved with absolute methanol. The dissolved residue was dried by N_2 gas at 45°C, subsequently redissolved with 1 ml deionized water and 100 μl N-methylglucamine (internal standard 2), and then lyophilized.

Each lyophilized residue was derivatized with a 300-μl derivatization reagent. The reactive solution was completely mixed and heated at 75–80°C for 35 min. The derivative was heated (75–80°C, 25 min) for acetylation after cooling and adding 1 ml acetic anhydride. After cooling to room temperature, we orderly added 1.5 ml dichloromethane and 1 ml 1 M HCl and fully mixed to isolate the organic phase. The organic phase was washed with deionized water three times to absolutely remove residual anhydride. The remaining organic phase was dried with N_2 gas at 45°C and then dissolved with 100 μl ethyl acetate-hexane (1:1 v/v). Finally, the extracted ASs were detected and analyzed on an Agilent 7890B GC (Agilent Technologies, Santa Clara, CA, United States). In terms of the response factors of

standards (i.e., GluN, GalN, MurA, and mannosamine) relative to the internal standard 1 (Rf = 1), we can calculate the concentration of soil ASs; the internal standard 2 is used to check the derivatization process and calculate the recovery of soil ASs (Zhang and Amelung, 1996; Liang et al., 2012).

Statistical Analysis

One-way ANOVA was conducted to assess the effects of salinity on soil physicochemical properties and AS parameters using R software (R version 3.6.0). We performed redundancy analysis to detect the relationships of GluN/MurA, GluN/SOC, GalN/SOC, and MurA/SOC (log-transformed) with soil physicochemical properties on Canoco (version 4.5 for Windows; Ithaca, NY, United States). Path analysis was used to evaluate the causality among soil physicochemical properties and ASs along a salinity gradient, using AMOS software (AMOS 17.0.2 student version; Amos Development, Crawfordville, FL, United States). The maximum likelihood method was used to fit measured data to the model. The adequate model goodness of fit was tested using root-mean-square error of approximation (RMSEA).

RESULTS

Variation of Soil Physicochemical Properties Along a Salinity Gradient

Salinity resulted in the significant changes in soil pH (F = 2.84, P = 0.04), SOC (F = 13.89, $P < 0.001$), and TN (F = 11.24, $P < 0.001$), whereas there was no change in SWC, SOC/TN, and TP (**Table 1**). High salinity soils (S5, S6, and S7) had lower pH than low salinity soils (S1), decreasing by 5.82%. SOC and TN gradually decreased along with increased salinity, from 10.13 to 2.93 g kg^{-1} and from 1.07 to 0.41 g kg^{-1}, respectively. Although salinity did not change SWC, high salinity coastal wetlands had low SWC (**Table 1**).

Effects of Salinity on Soil Amino Sugar Content and Their Contributions to Soil Organic Carbon

Salinity greatly influenced the contents of soil AS (F = 29.37, $P < 0.001$), GluN (F = 25.84, $P < 0.001$), GalN (F = 35.65, $P < 0.001$), and MurA (F = 10.77, $P < 0.001$) (**Figure 2**). The contents of AS, GluN, and GalN gradually declined across a salinity gradient, which decreased by 90.56% (**Figure 2A**), 91.11% (**Figure 2B**), and 90.62% (**Figure 2C**), respectively. The contents of MurA were higher in low salinity soils (S1 and S2) than that of other soil salinity concentrations. Additionally, MurA showed no change from S3 to S7 (**Figure 2D**).

The ratios of AS, GluN, and GalN to SOC showed significant responses to salinity ($P < 0.001$), whereas there was no change in the ratio of MurA to SOC (**Figure 3**). The ratios of AS, GluN, and GalN to SOC showed the similar trend with AS content across a salinity gradient. The AS/SOC decreased from 36.62 to 12.32 g kg^{-1} (**Figure 3A**; F = 39.20, $P < 0.001$); GluN/SOC showed a decline from 24.22 to 7.76 g kg^{-1} (**Figure 3B**; F = 43.27, $P < 0.001$); and GalN/SOC reduced from 11.50 to 3.75 g kg^{-1} (**Figure 3C**; F = 24.00, $P < 0.001$) from S1 to S7.

Shifts in GluN/GalN and GluN/MurA Under Different Salinity Concentrations

Salinity resulted in a significant change in GluN/MurA (**Figure 4B**; F = 31.32, $P < 0.001$), but there was no change in GluN/MurA (**Figure 4A**). Low salinity soils had high GluN/MurA, and high salinity lowered GluN/MurA in soils (**Figure 4B**).

Relationships Between Soil Physicochemical Properties and Amino Sugar

Redundancy analysis demonstrated that soil physicochemical properties explained 82.19% (axis 1 of 80.1% and axis 2 of 2.1%) variation of the GluN/MurA, GluN/SOC, GalN/SOC, and MurA/SOC (**Figure 5**). The ratios of GluN/SOC, GalN/SOC, and GluN/MurA were negatively related to soil salinity (represented by EC) and positively associated with SWC, pH, SOC, and TN, whereas not related to SOC/TN and TP. Soil physicochemical properties showed no impact on the MurA/SOC (**Figure 5**).

Path analysis further evaluated the causal relationships among soil physicochemical properties, GluN/MurA, and AS/SOC across a salinity gradient in coastal wetlands and elucidated the relative contributions of these soil variables to explain changed AS/SOC (**Figure 6**). Salinity, pH, SOC, TN, and GluN/MurA were the main abiotic and biotic factors influencing AS/SOC, accounting for 84% variation of the AS/SOC. Soil salinity showed a negative effect on soil chemical properties and AS/SOC; soil pH and TN indirectly and positively influenced AS/SOC *via* changing the GluN/MurA; and SOC showed a positive direct impact on AS/SOC (**Figure 6**).

DISCUSSION

Responses of Soil Microbial Residues to Salinity in Coastal Wetlands

In this study, we found that the AS content was 34.82–368.6 mg kg^{-1} along a salinity gradient under coastal wetlands in the Yellow River delta, which was several or even tens of times lower than AS content in terrestrial ecosystems (i.e., forest, grassland, and agriculture) (Lauer et al., 2011; Xia et al., 2019; Chen et al., 2020). Coastal wetlands are predominately controlled by water and salinity due to tides and underground seawater (Ma et al., 2017; Steinmuller et al., 2019). The restrained plant productivity leads to low SOM (Zhao et al., 2020), decreasing the accumulation of microbial AS. Also, plant phenology shows a quick response to changed soil salinity (Sun et al., 2021). High salinity negatively influences plant phenology and alters the seasonality of plant photosynthesis or productivity. Especially in dry seasons, the exacerbated soil salinity stress restrains aboveground plant growth, root germination, and reproduction (related to plant reproduction the next year) (Baldwin et al., 2014; Sun et al., 2021), reducing C input to soils, consequently resulting

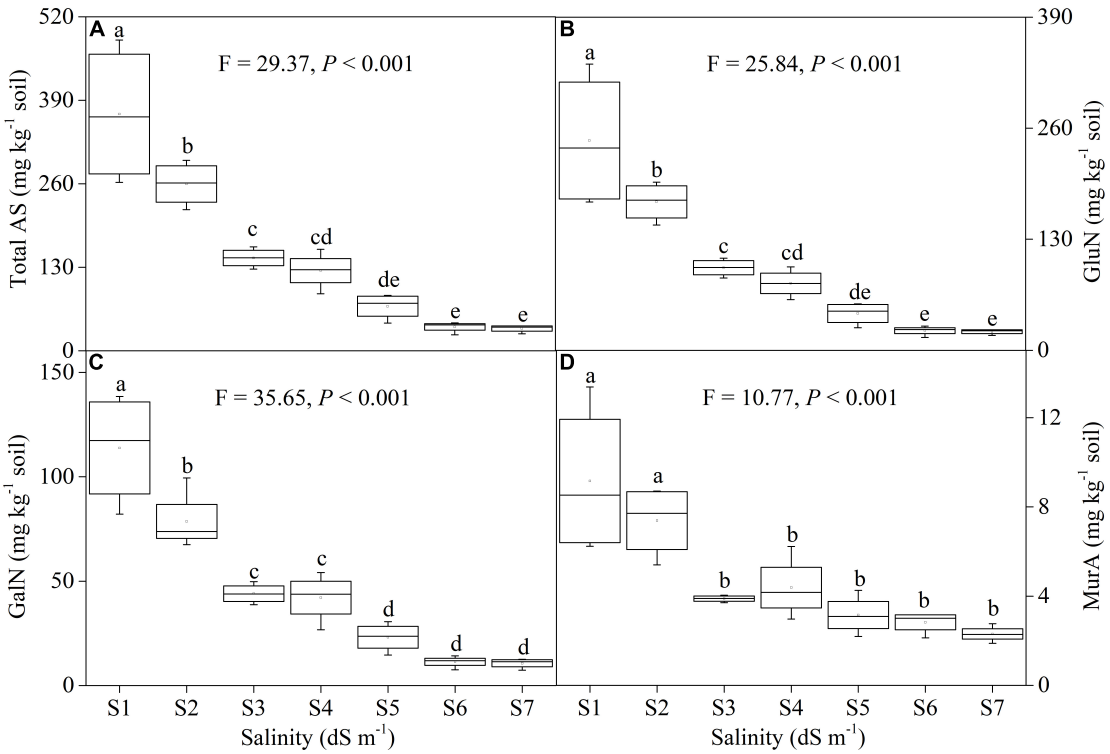

FIGURE 2 | Changes in the content of soil total amino sugar (AS, **A**), glucosamine (GluN, **B**), galactosamine (GalN, **C**), and muramic acid (MurA, **D**) along a soil salinity gradient.

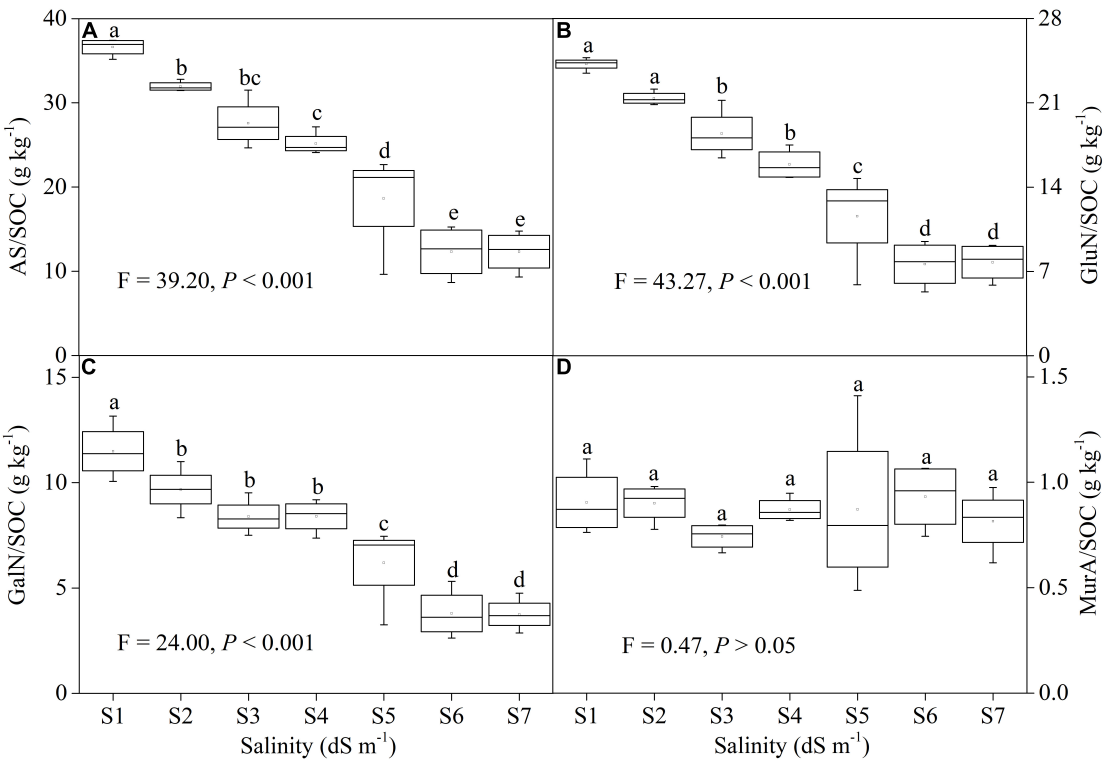

FIGURE 3 | The ratio of total AS **(A)**, GluN **(B)**, GalN **(C)**, and MurA **(D)** to SOC across a soil salinity gradient.

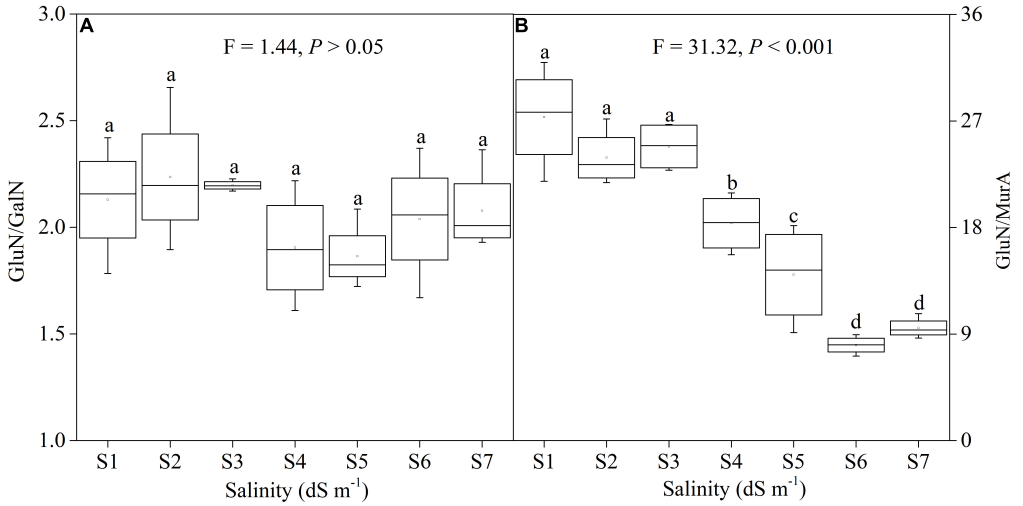

FIGURE 4 | Variation of GluN/GalN **(A)** and GluN/MurA **(B)** under different salinity concentrations.

in the decrease in microbial AS. In addition, the SOM was not easily utilized by soil microorganisms with a low decomposition rate (Steinmuller and Chambers, 2019; Ward, 2020), which is likely to result in low AS synthesis.

As the main component of the microbial cell wall, soil AS has certain specificity and stability, which cannot only represent microbial residues but also reflect the dynamic changes of ecosystems (Lauer et al., 2011; Shao et al., 2019). Increased soil

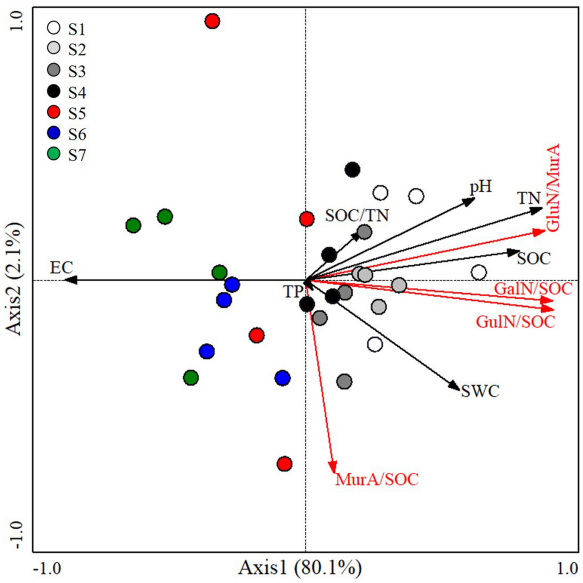

FIGURE 5 | Redundancy analysis detecting the relationships of AS parameters with soil physicochemical properties along a salinity gradient (white circle, S1; light gray circle, S2; gray circle, S3; black circle, S4; red circle, S5; blue circle, S6; green circle, S7). Black vectors indicate trajectories of soil chemical parameters as independent variables; red vectors indicate AS parameters, including the ratio of GluN, GalN, and MurA to SOC and GluN/MurA. The acute and obtuse angles among variables represent positive and negative relationships, respectively. The numbers in brackets indicate the percentage of the total variance explained by the first and second axes. Soil physicochemical properties with significant effects on AS parameters are evaluated at the 0.05 level (Monte Carlo tests with 499 permutations).

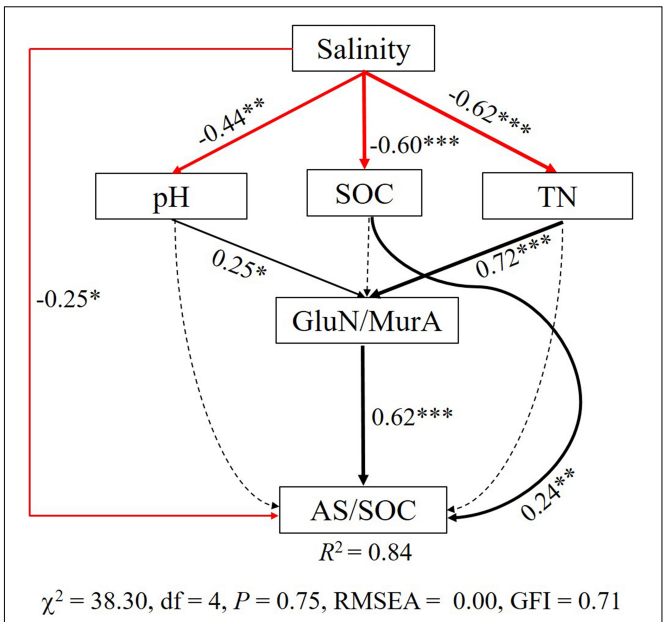

FIGURE 6 | Path analysis evaluating the underlying causality between soil physicochemical properties and AS/SOC along a salinity gradient under coastal wetlands in the Yellow River delta. Solid and dashed lines indicate significant ($P < 0.05$) and non-significant ($P > 0.05$) effects (*P*-values inside brackets), respectively. Standardized path coefficients are listed beside each path (black and red lines represent positive and negative paths, respectively; line width indicates the proportion of factorial contribution). R^2 values indicate the strength of explanation by independent variables. The symbols of ***, **, *represent statistical significance with $p < 0.001$, $p < 0.01$, and $p < 0.05$, respectively.

salinity decreased AS content, indicating that salinity stress would suppress microbial residue accumulation in coastal wetland soils. Microbial residues are mainly originated from the fast iteration of microbial cell production and death, thus high microbial biomass could promote microbial residue retention in soils (Liang et al., 2017). A recent study has reported that increased salinity results in a decline in microbial biomass, associated with the decreased microbial residues in the saline-alkali soils (Chen et al., 2021). In addition, microorganisms utilize more SOM to synthesize several stress-resistant substances (e.g., extracellular polysaccharides) to maintain microbial survival and integrity and less SOM investment in microbial cell growth and metabolism (Malik et al., 2020), thus resulting in low microbial residues in high salinity soils.

The GluN and MurA can be used to represent fungal and bacterial residues, respectively (Joergensen, 2018). The GluN accounted for 65.67% of total AS; MurA accounted for 3.19% of total AS; and the content of GluN was approximately 20 times of MurA in coastal wetland soils. These findings are similar to the previous studies that the content of soil GluN was approximately 15–20 times of MurA in terrestrial ecosystems (Shao et al., 2019; Wang et al., 2021). Although increased salinity stress greatly decreased the contents of GluN and MurA, the proportion of GluN and MurA in total AS showed an increment and decline, respectively. The inconsistent changes in fungal and bacterial residues are probably ascribed to the different responses of fungal and bacterial communities to salinity. The 80% of fungi in soil systems are symbiotic with plants; and changed plant productivity and traits would influence fungal activity and biomass (Zheng et al., 2021). In our studied regions, increased soil salinity inhibits the growth and photosynthate synthesis of *Phragmites australis*; and few *Phragmites australis* survive in high or extreme salinity soils (Guan et al., 2017). The decreased plant litterfall and root exudates lead to less available C input to soil fungi, particularly plant symbiotic fungi, to assimilate less C into fungal biomass, thus reducing fungal residue retention in soils. MurA is uniquely derived from bacteria, which can reflect the change in the bacterial community (Glaser et al., 2004). Low salinity soils had higher bacterial residues, and there was no change in bacterial residues from medium salinity to high salinity. The dynamic of bacterial residues along with soil salinity gradient may be attributed to the salinity tolerance of the bacterial community. Some specific bacterial taxa (e.g., *Halomonas* and *Chloroflexi*) can survive in high salinity soil (Xu et al., 2021), which maintains the balance between production and degradation of bacterial residues, resulting in no change in bacterial residues.

Microbial Residue Contributions to Soil Organic Carbon Pool Along a Salinity Gradient in Coastal Wetlands

With the developments of microbial biomarkers (i.e., AS) and microbial C pump theory (Zhang and Amelung, 1996; Liang et al., 2017), more studies concentrate on microbial residue contribution to SOC pool (Kallenbach et al., 2016; Ma et al., 2018; Deng and Liang, 2022). The AS extracted from soils accounts for a major percentage of dead microbial biomass (Joergensen, 2018). Therefore, AS levels are used to evaluate the extent to which microbial residue contributes to the SOC pool, providing significant information on the "chronic" responses of microbial residues to changing ecosystems (Shao et al., 2019). The AS/SOC can represent microbial residue contributions to SOC. The AS/SOC was gradually declined with increasing salinity, approximately decreasing by 70% from low salinity to high salinity, indicating that high salinity stress greatly inhibits microbial residue contributions to the SOC pool. We found that salinity negatively affected fungal residue contributions to SOC, and there was no change in bacterial residue contributions to SOC. These findings imply that fungal residues predominately drive SOC storage, which is consistent with previous views (Wang et al., 2021). The different effects of salinity on fungal and bacterial residue contributions to SOC are likely ascribed to change soil physicochemical properties. Our study shows the positive relationship of GluN/SOC with SWC, pH, SOC, and TN, suggesting that changed soil water and nutrient conditions regulate fungal residue accumulation in the SOC pool. Additionally, the chemical stability of bacterial residues is lower than fungal residues, which are easily decomposed and assimilated by soil microorganisms (Joergensen, 2018; Ma et al., 2022). The fast turnover of bacterial residues is not conducive to the retention of microbial residue-C belowground in coastal wetlands.

Current studies pay more attention to the plant community effect on SOC cycling, and plant-derived C mainly drives wetland soil C storage (Duarte et al., 2013; Xia et al., 2021). Microbial C pump theory has proposed that microorganisms utilize the decomposed plant detritus and micromolecular SOM to synthesize microbial cells, contributing to the SOC pool *via* microbial necromass (Kästner and Miltner, 2018). Low salinity held high AS/SOC, which indicates more soil microbial residue-C accumulation in low salinity coastal wetlands. Abundant soil water, SOC, and N promote the synthesis of microbial products, enhancing the contribution of microbial residues to existing SOC stocks. High soil water and nutrient stimulate plant growth and photosynthetic C input into soils (Chu et al., 2019); and microbes assimilate more plant-derived C to synthesize microbial biomass, ultimately increasing microbial residue-C storage in coastal wetland soils. In addition, we also found that AS/SOC was positively related to pH. Some studies have clarified that pH is tightly associated with soil cation, such as calcium and aluminum ions (Gruba and Mulder, 2015). Microbial residues can persist in soils for decades or even centuries in the form of stable SOM through mineral association (Sokol et al., 2019; Buckeridge et al., 2020), substantially enhancing soil C storage. Overall, the abundant soil resource (i.e., water, C substrate, and N nutrient) can promote SOC storage by increasing microbial residue accumulation and stability in low salinity coastal wetlands.

In high salinity coastal wetlands, salinity stress greatly restrained the contribution of microbial residues to SOC. This might be explained by the two mechanisms, namely, microbial stress tolerance strategy and low available C. In extreme environmental stress (e.g., high salinity or drought), microorganisms select a stress tolerance strategy

responding to environmental changes (Krause et al., 2014; Malik et al., 2020). Microorganisms invest more C to synthesize osmolytes (e.g., mycose) or extracellular polymeric substances (e.g., polysaccharides) to protect microbial cell integrity and to enhance microbial stress-resistance in high salinity soils. Meanwhile, less C was used for microbial cell growth and proliferation, thus reducing the source of microbial residues. The low microbial cell death and microbial residue production both lower the retention of microbial residues in the SOC pool of coastal wetlands. In addition, high salinity soils held few SOC and low SOC/TN, which decrease microbial C availability. Low soil available C inhibits the production of microbial biomass and residues, resulting in the low contribution of microbial residues to SOC storage in high salinity coastal wetlands.

Path analysis was used to evaluate the causal relationships among microbial residue-C contribution, soil physicochemical properties, and fungal/bacterial residues, clarifying the main factors driving microbial residue contribution to SOC. Changed soil salinity, pH, SOC, TN, and GluN/MurA explained 84% variation of microbial residue-C contribution to SOC. Soil nutrient regulates microbial residue contribution to SOC through varied fungal and bacterial residues associated with their stability along a salinity gradient in coastal wetlands.

Although soil physicochemical properties (e.g., salinity, water, SOC, and N) were substantially different among coastal wetlands with different salinity concentrations, the changes in microbial residues and their contributions to SOC were influenced. However, we cannot neglect the impacts of system experience conditions (e.g., hydrology, microclimate, and topography) on microbial residues in different geographical locations. Together, our study presents supporting evidence on how salinity affects the fate and magnitude of microbial residues in coastal wetlands through changed soil properties. Further research is needed to accurately assess microbial residues in changing wetlands considering system experience conditions and other fluctuant environmental variants.

Responses of Fungal/Bacterial Residues to Salinity in Coastal Wetlands

The ratio of GluN to MurA cannot only indicate the responses of fungal and bacterial communities to environmental changes but also represent the relative contributions of fungal and bacterial residues to the SOC pool (Liang et al., 2015; Joergensen, 2018). We found a gradual reduction in GluN/MurA across increasing salinity, implying that fungi are more competitive in low salinity soils, and bacteria are more tolerant in high salinity soils of coastal wetlands. The positive relationships of GluN/MurA to SWC, SOC, and TN indicate that suitable soil water, salinity, and nutrients favor fungi and stimulate fungal residue accumulation, reserving more microbial residue-C in the SOC pool.

CONCLUSION

Microbial residues (represented by AS) play a crucial role in coastal wetland SOC accumulation. In our study, we found that low-salinity soils held high microbial residues and microbial residue contribution to SOC, while high-salinity stress greatly inhibited microbial residue accumulation and microbial residue retention in the SOC pool in coastal wetlands. Changed soil resource (i.e., water, C substrate, and nitrogen) availability and microbial strategy to salinity stress explained the accumulation of microbial residues along a salinity gradient in coastal wetlands. Additionally, the different responses of fungal and bacterial residues to salinity and the positive relationship between fungal/bacterial residues and microbial residue C contribution indicate that fungal residues predominately contributed to the SOC pool. We suggest that clarifying microbial necromass contribution to SOC pool will strengthen the C persistence in soils and a more accurate understanding of global wetland soil C cycling.

DATA AVAILABILITY STATEMENT

The raw data supporting the conclusions of this article will be made available by the authors, without undue reservation.

AUTHOR CONTRIBUTIONS

PS wrote the manuscript. HH, JS, HY, and HX revised the manuscript. All authors contributed to the article and approved the submitted version.

FUNDING

This study was supported by the National Natural Science Foundation of China (32101387, 32001134, and 42171059) and the Natural Science Foundation of Shandong Province (ZR2020QD004, ZR2020MD005, and ZR2020QC040).

REFERENCES

Angst, G., Mueller, K. E., Nierop, K. G., and Simpson, M. J. (2021). Plant- or microbial-derived? A review on the molecular composition of stabilized soil organic matter. *Soil Biol. Biochem.* 156:108189. doi: 10.1016/j.soilbio.2021.108189

Baldwin, A. H., Jensen, K., and Schönfeldt, M. (2014). Warming increases plant biomass and reduces diversity across continents, latitudes, and species migration scenarios in experimental wetland communities. *Glob. Chang. Biol.* 20, 835–850. doi: 10.1111/gcb.12378

Bossio, D. A., Fleck, J. A., Scow, K. M., and Fujii, R. (2006). Alteration of soil microbial communities and water quality in restored wetlands. *Soil Biol. Biochem.* 38, 1223–1233. doi: 10.1016/j.soilbio.2005.09.027

Buckeridge, K. M., La Rosa, A. F., Mason, K. E., Whitaker, J., McNamara, N. P., Grant, H. K., et al. (2020). Sticky dead microbes: rapid abiotic retention of microbial necromass in soil. *Soil Biol. Biochem.* 149:107929. doi: 10.1016/j.soilbio.2020.107929

Chen, G., Ma, S., Tian, D., Xiao, W., Jiang, L., Xing, A., et al. (2020). Patterns and determinants of soil microbial residues from tropical to boreal forests. *Soil Biol. Biochem.* 151:108059. doi: 10.1016/j.soilbio.2020.108059

Chen, J., Wang, H., Hu, G., Li, X., Dong, Y., Zhuge, Y., et al. (2021). Distinct accumulation of bacterial and fungal residues along a salinity gradient in coastal salt-affected soils. *Soil Biol. Biochem.* 158:108266. doi: 10.1016/j.soilbio.2021.108266

Cheng, Y., Li, P., Xu, G., and Gao, H. (2016). Spatial distribution of soil total phosphorus in Yingwugou watershed of the Dan River, China. *Catena* 136, 175–181. doi: 10.1016/j.catena.2015.02.015

Chmura, G. L., Anisfeld, S. C., Cahoon, D. R., and Lynch, J. C. (2003). Global carbon sequestration in tidal, saline wetland soils. *Glob. Biogeochem. Cycles* 17:1111.

Chu, X., Han, G., Xing, Q., Xia, J., Sun, B., Li, X., et al. (2019). Changes in plant biomass induced by soil moisture variability drive interannual variation in the net ecosystem CO_2 exchange over a reclaimed coastal wetland. *Agric. For. Meteorol.* 264, 138–148. doi: 10.1016/j.agrformet.2018.09.013

Crooks, S., Sutton-Grier, A. E., Troxler, T. G., Herold, N., Bernal, B., Schile-Beers, L., et al. (2018). Coastal wetland management as a contribution to the US National Greenhouse Gas Inventory. *Nat. Clim. Change* 8, 1109–1112. doi: 10.1038/s41558-018-0345-0

Deng, F., and Liang, C. (2022). Revisiting the quantitative contribution of microbial necromass to soil carbon pool: stoichiometric control by microbes and soil. *Soil Biol. Biochem.* 165:108486. doi: 10.1016/j.soilbio.2021.108486

Ding, X., Zhang, B., Filley, T. R., Tian, C., Zhang, X., and He, H. (2019). Changes of microbial residues after wetland cultivation and restoration. *Biol. Fertil. Soils* 55, 405–409. doi: 10.1007/s00374-019-01341-2

Duarte, C. M., Losada, I. J., Hendriks, I. E., Mazarrasa, I., and Marbà, N. (2013). The role of coastal plant communities for climate change mitigation and adaptation. *Nat. Clim. Change* 3, 961–968. doi: 10.1038/nclimate1970

Glaser, B., Turrión, M.-B., and Alef, K. (2004). Amino sugars and muramic acid—biomarkers for soil microbial community structure analysis. *Soil Biol. Biochem.* 36, 399–407. doi: 10.1016/j.soilbio.2003.10.013

Gruba, P., and Mulder, J. (2015). Tree species affect cation exchange capacity (CEC) and cation binding properties of organic matter in acid forest soils. *Sci. Total Environ.* 511, 655–662. doi: 10.1016/j.scitotenv.2015.01.013

Guan, B., Yu, J., Hou, A., Han, G., Wang, G., Qu, F., et al. (2017). The ecological adaptability of *Phragmites australis* to interactive effects of water level and salt stress in the Yellow River Delta. *Aquat. Ecol.* 51, 107–116. doi: 10.1007/s10452-016-9602-3

Haywood, B. J., Hayes, M. P., White, J. R., and Cook, R. L. (2020). Potential fate of wetland soil carbon in a deltaic coastal wetland subjected to high relative sea level rise. *Sci. Total Environ.* 711:135185. doi: 10.1016/j.scitotenv.2019.135185

Hill, B. H., Elonen, C. M., Herlihy, A. T., Jicha, T. M., and Serenbetz, G. (2018). Microbial ecoenzyme stoichiometry, nutrient limitation, and organic matter decomposition in wetlands of the conterminous United States. *Wetl. Ecol. Manage.* 26, 425–439. doi: 10.1007/s11273-017-9584-5

Hu, Y., Wang, L., Tang, Y., Li, Y., Chen, J., Xi, X., et al. (2014). Variability in soil microbial community and activity between coastal and riparian wetlands in the Yangtze River estuary–Potential impacts on carbon sequestration. *Soil Biol. Biochem.* 70, 221–228. doi: 10.1016/j.soilbio.2013.12.025

Joergensen, R. G. (2018). Amino sugars as specific indices for fungal and bacterial residues in soil. *Biol. Fertil. Soils* 54, 559–568. doi: 10.1007/s00374-018-1288-3

Kallenbach, C. M., Frey, S. D., and Grandy, A. S. (2016). Direct evidence for microbial-derived soil organic matter formation and its ecophysiological controls. *Nat. Commun.* 7:13630.

Kästner, M., and Miltner, A. (2018). "SOM and Microbes-What is Left from Microbial Life," in *The Future of Soil Carbon*, eds C. Garcia, P. Nannipieri, T. Hernandez (Cambridge, MA: Academic Press), 125–163. doi: 10.1016/b978-0-12-811687-6.00005-5

Krause, S., Le Roux, X., Niklaus, P. A., Van Bodegom, P. M., Lennon, J. T., Bertilsson, S., et al. (2014). Trait-based approaches for understanding microbial biodiversity and ecosystem functioning. *Front. Microbiol.* 5:251. doi: 10.3389/fmicb.2014.00251

Lauer, F., Kösters, R., Du Preez, C. C., and Amelung, W. (2011). Microbial residues as indicators of soil restoration in South African secondary pastures. *Soil Biol. Biochem.* 43, 787–794. doi: 10.1016/j.soilbio.2010.12.012

Lewis, C. J. E., Baldock, J. A., Hawke, B., Gadd, P. S., Zawadzki, A., Heijnis, H., et al. (2019). Impacts of land reclamation on tidal marsh 'blue carbon'stocks. *Sci. Total Environ.* 672, 427–437. doi: 10.1016/j.scitotenv.2019.03.345

Liang, C., Amelung, W., Lehmann, J., and Kästner, M. (2019). Quantitative assessment of microbial necromass contribution to soil organic matter. *Glob. Chang. Biol.* 25, 3578–3590. doi: 10.1111/gcb.14781

Liang, C., Gutknecht, J., and Balser, T. (2015). Microbial lipid and amino sugar responses to long-term simulated global environmental changes in a California annual grassland. *Front. Microbiol.* 6:385. doi: 10.3389/fmicb.2015.00385

Liang, C., Read, H. W., and Balser, T. C. (2012). GC-based detection of aldononitrile acetate derivatized glucosamine and muramic acid for microbial residue determination in soil. *J. Vis. Exp.* 63:e3767. doi: 10.3791/3767

Liang, C., Schimel, J. P., and Jastrow, J. D. (2017). The importance of anabolism in microbial control over soil carbon storage. *Nat. Microbiol.* 2:17105. doi: 10.1038/nmicrobiol.2017.105

Lyu, Z., Genet, H., He, Y., Zhuang, Q., McGuire, A. D., Bennett, A., et al. (2018). The role of environmental driving factors in historical and projected carbon dynamics of wetland ecosystems in Alaska. *Ecol. Appl.* 28, 1377–1395. doi: 10.1002/eap.1755

Ma, T., Zhu, S., Wang, Z., Chen, D., Dai, G., Feng, B., et al. (2018). Divergent accumulation of microbial necromass and plant lignin components in grassland soils. *Nat. Commun.* 9:3480. doi: 10.1038/s41467-018-05891-1

Ma, X., Zhang, W., Zhang, X., Bao, X., Xie, H., Li, J., et al. (2022). Dynamics of microbial necromass in response to reduced fertilizer application mediated by crop residue return. *Soil Biol. Biochem.* 165:108512. doi: 10.1016/j.soilbio.2021.108512

Ma, Z., Zhang, M., Xiao, R., Cui, Y., and Yu, F. (2017). Changes in soil microbial biomass and community composition in coastal wetlands affected by restoration projects in a Chinese delta. *Geoderma* 289, 124–134. doi: 10.1016/j.geoderma.2016.11.037

Macreadie, P. I., Anton, A., Raven, J. A., Beaumont, N., Connolly, R. M., Friess, D. A., et al. (2019). The future of Blue Carbon science. *Nat. Commun.* 10:3998.

Malik, A. A., Martiny, J. B., Brodie, E. L., Martiny, A. C., Treseder, K. K., and Allison, S. D. (2020). Defining trait-based microbial strategies with consequences for soil carbon cycling under climate change. *ISME J.* 14, 1–9. doi: 10.1038/s41396-019-0510-0

Nelson, D. W., and Sommers, L. E. (1982). "Total carbon, organic carbon and organic matter. In Methods of Soil Analysis Part 3-Chemical Methods," in *Methods of Soil Analysis. Part 2. Chemical and Microbiological Properties,* ed. A. L. Page (Madison: SSSA)

Shao, P., Liang, C., Lynch, L., Xie, H., and Bao, X. (2019). Reforestation accelerates soil organic carbon accumulation: evidence from microbial biomarkers. *Soil Biol. Biochem.* 131, 182–190. doi: 10.1016/j.soilbio.2019.01.012

Sokol, N. W., Sanderman, J., and Bradford, M. A. (2019). Pathways of mineral-associated soil organic matter formation: integrating the role of plant carbon source, chemistry, and point of entry. *Glob. Chang. Biol.* 25, 12–24. doi: 10.1111/gcb.14482

Spivak, A. C., Sanderman, J., Bowen, J. L., Canuel, E. A., and Hopkinson, C. S. (2019). Global-change controls on soil-carbon accumulation and loss in coastal vegetated ecosystems. *Nat. Geosci.* 12, 685–692. doi: 10.1038/s41561-019-0435-2

Steinmuller, H. E., and Chambers, L. G. (2019). Characterization of coastal wetland soil organic matter: implications for wetland submergence. *Sci. Total Environ.* 677, 648–659. doi: 10.1016/j.scitotenv.2019.04.405

Steinmuller, H. E., Dittmer, K. M., White, J. R., and Chambers, L. G. (2019). Understanding the fate of soil organic matter in submerging coastal wetland soils: a microcosm approach. *Geoderma* 337, 1267–1277. doi: 10.1016/j.geoderma.2018.08.020

Sun, B., Yan, L., Jiang, M., Li, X., Han, G., and Xia, J. (2021). Reduced magnitude and shifted seasonality of CO_2 sink by experimental warming in a coastal wetland. *Ecology* 102:e03236. doi: 10.1002/ecy.3236

Trivedi, P., Anderson, I. C., and Singh, B. K. (2013). Microbial modulators of soil carbon storage: integrating genomic and metabolic knowledge for global prediction. *Trends Microbiol.* 21, 641–651. doi: 10.1016/j.tim.2013.09.005

Wang, B., An, S., Liang, C., Liu, Y., and Kuzyakov, Y. (2021). Microbial necromass as the source of soil organic carbon in global ecosystems. *Soil Biol. Biochem.* 162:108422. doi: 10.1111/gcb.14070

Wang, J., Wang, J., Zhang, Z., Li, Z., Zhang, Z., Zhao, D., et al. (2020). Shifts in the bacterial population and ecosystem functions in response to vegetation in the

Yellow River Delta wetlands. *mSystems* 5:e00412-20. doi: 10.1128/mSystems.00412-20

Ward, R. D. (2020). Carbon sequestration and storage in Norwegian Arctic coastal wetlands: impacts of climate change. *Sci. Total Environ.* 748:141343. doi: 10.1016/j.scitotenv.2020.141343

Xia, S., Song, Z., Li, Q., Guo, L., Yu, C., Singh, B. P., et al. (2021). Distribution, sources, and decomposition of soil organic matter along a salinity gradient in estuarine wetlands characterized by C: N ratio, $d^{13}C$-$d^{15}N$, and lignin biomarker. *Glob. Chang. Biol.* 27, 417–434. doi: 10.1111/gcb.15403

Xia, Y., Chen, X., Hu, Y., Zheng, S., Ning, Z., Guggenberger, G., et al. (2019). Contrasting contribution of fungal and bacterial residues to organic carbon accumulation in paddy soils across eastern China. *Biol. Fertil. Soils* 55, 767–776. doi: 10.1007/s00374-019-01390-7

Xu, J., Gao, W., Zhao, B., Chen, M., Ma, L., Jia, Z., et al. (2021). Bacterial community composition and assembly along a natural sodicity/salinity gradient in surface and subsurface soils. *Appl. Soil Ecol.* 157:103731. doi: 10.1016/j.apsoil.2020.103731

Xu, W., Fan, X., Ma, J., Pimm, S. L., Kong, L., Zeng, Y., et al. (2019). Hidden loss of wetlands in China. *Curr. Biol.* 29, 3065–3071. doi: 10.1016/j.cub.2019.07.053

Zhang, G., Bai, J., Tebbe, C. C., Zhao, Q., Jia, J., Wang, W., et al. (2021). Salinity controls soil microbial community structure and function in coastal estuarine wetlands. *Environ. Microbiol.* 23, 1020–1037. doi: 10.1111/1462-2920.15281

Zhang, X., and Amelung, W. (1996). Gas chromatographic determination of muramic acid, glucosamine, mannosamine, and galactosamine in soils. *Soil Biol. Biochem.* 28, 1201–1206.

Zhao, Q., Zhao, H., Gao, Y., Zheng, L., Wang, J., and Bai, J. (2020). Alterations of bacterial and archaeal communities by freshwater input in coastal wetlands of the Yellow River Delta, China. *Appl. Soil Ecol.* 153:103581. doi: 10.1016/j.apsoil.2020.103581

Zheng, Y., Chen, L., Ji, N. N., Wang, Y. L., Gao, C., Jin, S. S., et al. (2021). Assembly processes lead to divergent soil fungal communities within and among twelve forest ecosystems along a latitudinal gradient. *New Phytol.* 231, 1183–1194. doi: 10.1111/nph.17457

Conflict of Interest: The authors declare that the research was conducted in the absence of any commercial or financial relationships that could be construed as a potential conflict of interest.

Publisher's Note: All claims expressed in this article are solely those of the authors and do not necessarily represent those of their affiliated organizations, or those of the publisher, the editors and the reviewers. Any product that may be evaluated in this article, or claim that may be made by its manufacturer, is not guaranteed or endorsed by the publisher.

frontiers | Frontiers in Ecology and Evolution

ORIGINAL RESEARCH
published: 25 May 2022
doi: 10.3389/fevo.2022.837747

The Effects of Drainage on the Soil Fungal Community in Freshwater Wetlands

Qingqing Zhao[1], Junhong Bai[2], Jia Jia[3]*, Guangliang Zhang[2], Jianing Wang[1] and Yongchao Gao[1]*

[1] Shandong Provincial Key Laboratory of Applied Microbiology, Ecology Institute, Qilu University of Technology (Shandong Academy of Sciences), Jinan, China, [2] State Key Laboratory of Water Environment Simulation, School of Environment, Beijing Normal University, Beijing, China, [3] Henan Key Laboratory of Ecological Environment Protection and Restoration of Yellow River Basin, Yellow River Institute of Hydraulic Research, Zhengzhou, China

Wetland drainage has been intensively implemented globally, and it has exerted significant effects on wetland ecosystems. The effects of wetland drainage on the soil fungal community remain to be clarified. Soil samples were collected at depths of 0–5 and 5–10 cm in freshwater *Phragmites australis* wetlands to investigate changes in the fungal community before and after drainage (termed FW and DFW, respectively) using high-throughput sequencing of the fungal-specific internal transcribed spacer 1 (ITS1) gene region. No significant differences in the α diversity of the soil fungal community were found in 0–10 cm soils between FW and DFW ($p > 0.05$), except for the abundance-based coverage estimator (ACE) and Chao1 indices in 5–10 cm soils. Significantly higher values of ACE and Chao1 in 5–10 cm soils in FW than in DFW indicated that wetland drainage may reduce fungal community richness in 5–10 cm soils. Ascomycota, Sordariomycetes, and Cephalothecaceae were the dominant fungal phylum, class, and family, respectively, in 0–5 and 5–10 cm soils of both FW and DFW, representing as high as 76.17, 58.22, and 45.21% of the fungal community in 5–10 FW soils, respectively. Saprotrophic fungi predominated in both FW and DFW. Drainage altered both the fungal community structure and some edaphic factors. Mantel tests and Spearman correlation analyses implied that edaphic factors [i.e., soil organic matter (SOM), electronic conductivity (EC), pH, and clay] also affected soil fungal community structure. Overall, wetland drainage altered the community structure of the fungal community in the freshwater wetlands.

Keywords: wetland drainage, fungal community, diversity, community structure, freshwater wetlands

OPEN ACCESS

Edited by:
Haitao Wu,
Northeast Institute of Geography and Agroecology (CAS), China

Reviewed by:
Fei-Hai Yu,
Taizhou University, China
Mingxiang Zhang,
Beijing Forestry University, China

****Correspondence:***
Qingqing Zhao
qingqingzhao@qlu.edu.cn
Jia Jia
jiajiast@126.com

Specialty section:
This article was submitted to Conservation and Restoration Ecology, a section of the journal Frontiers in Ecology and Evolution

Received: *17 December 2021*
Accepted: *07 March 2022*
Published: *25 May 2022*

Citation:
Zhao Q, Bai J, Jia J, Zhang G, Wang J and Gao Y (2022) The Effects of Drainage on the Soil Fungal Community in Freshwater Wetlands. Front. Ecol. Evol. 10:837747. doi: 10.3389/fevo.2022.837747

INTRODUCTION

Due to anthropogenic activities (i.e., overexploitation), and the ecosystem services they provide have been strongly impacted (Jones et al., 2018). Specifically, extensive wetland drainage for agriculture or other land uses has been conducted throughout the world and has increased dramatically (Drexler et al., 2009; Cortus et al., 2011; Xue et al., 2020).

Wetland drainage is one of the primary reasons for wetland loss, for example, causing the loss of more than 40% of prairie wetlands in Alberta (Canada), more than 90% of the wetland area in some states of the midwestern and eastern United States, and even turning 90.5% of fens into seasonally inundated wetlands (Cortus et al., 2011; Jones et al., 2018; Zhang et al., 2019). Wetland drainage will cause drastic changes in the structure and function of wetland soils and further lead to landscape modifications such as land-surface subsidence and loss of water storage capacity (Wiltermuth and Anteau, 2016; Jones et al., 2018). Consequently, the loss of soil mass, the changes in soil physiochemical properties, reduced soil fertility, and the reduction of ecosystem services will result from the drainage of wetlands (Drexler et al., 2009). Additionally, the oxidation of organic matter caused by drainage will result in secondary subsidence in wetlands (Drexler et al., 2009). Historical data also indicate that the landscape modifications by drainage have altered the exchange of energy and moisture at the surface, finally affecting local and regional climate (Schneider and Eugster, 2007). Undoubtedly, drainage induces inevitable variation in the water table, thereby changing hydraulic conductivity and hydrologic processes in wetlands (Brunet and Westbrook, 2012; Jones et al., 2018). However, drainage in depressional wetlands has turned temporarily flooded wetlands into permanently flooded areas with higher water levels (McCauley et al., 2015). It has been reported that the drainage accelerated wetland degradation in the Zoige Plateau (Li et al., 2012; Xue et al., 2020) as the stability of the hydrology maintains the structure and function of wetlands (Zedler, 2000). It is worth noting that the hydrologic modifications may further lead to changes in wetland sedimentation and nutrification as well as community composition (Wiltermuth and Anteau, 2016). Thus, the biota in wetlands, including vegetation and microbes, will certainly be affected by drainage (Brunet and Westbrook, 2012; McCauley et al., 2015).

Fungi are substantially involved in vital ecosystem services (i.e., nutrient cycling, production of clean water, pollutant degradation, compound transformations, suppression of disease-causing soil organisms, and ecological restoration), and they affect global biogeochemical cycles on a large scale due to their important roles as plant symbionts, primary decomposers of organic material, key regulators of soil carbon balance, and the meditation in phosphorus and nitrogen cycles through secreting extracellular enzymes (Treseder and Lennon, 2015; Xu et al., 2017; Guan et al., 2018; Xiao et al., 2020). Fungal biodiversity has been shown to essentially influence the maintenance of wetland ecosystems due to its functions involved in soil health, resilience to perturbations, and capacity for coevolution, interpreting biogeographic patterns, and screening natural products (Mueller and Schmit, 2007; Frąc et al., 2018; Xie et al., 2020). Moreover, the variation in soil fungal community composition can signify environmental changes (Xu et al., 2017). Dini-Andreote et al. (2016) highlighted the importance of fungal community composition in reflecting the successional stages of a marine environment being transformed into a terrestrial system. Onufrak et al. (2020) reported that the variations in fungal community structure contributed to wetland quality assessments with support from the Ohio Rapid Assessment Method (ORAM), and this will further facilitate better management of wetland ecosystems. In addition, Almeida et al. (2020) emphasized that the diversity and composition of the fungal community can be utilized to evaluate and improve restoration success. Thus, the important roles played by fungi necessitate identifying the important factors determining the diversity and composition of the fungal community. Therefore, more exploration of soil fungi is needed, as fungi still exist in a kind of "Earth's dark matter" (Xu et al., 2017).

The effects of anthropogenic activities on the soil fungal community have been reported by numerous researchers. For example, Hui et al. (2018) found that reforestation of farmland restored the transitional fungal communities and decreased soil fungal diversity. Liu et al. (2020) demonstrated that afforestation of cropland altered functional groups of fungi and reduced fungal diversity. Xiao et al. (2020) found that freshwater restoration reduced the diversity of soil fungi but strengthened the network connectivity. However, how wetland drainage affects the soil fungal community has rarely been reported. As fungi are primarily aerobic heterotrophs and are sensitive to soil oxygen conditions, it can be predicted that the water table drawdown and the consequent increase in oxygen availability brought by wetland drainage will affect the soil fungal community (Asemaninejad et al., 2018; Bergsveinson et al., 2019; Xue et al., 2020). Previous studies have indicated that soil characteristics (i.e., salinity, pH, soil organic carbon, and soil moisture), geographic conditions, and vegetation types impact the diversity of the fungal community (Guan et al., 2018; Hui et al., 2018; Xie et al., 2020). Liu et al. (2018) reported that soil physicochemical characteristics could be reshaped by water table drawdown in Zoige peatlands. Therefore, this study focused on the changes in the diversity and community structure of the soil fungal community before and after drainage to investigate the effects of wetland drainage on the soil fungal community.

MATERIALS AND METHODS

Sampling Sites, Soil Sample Collection, and Soil Analysis

Close to the north bank of the Yellow River, the studied freshwater *Phragmites australis* wetlands (FW) are located in the Nature Reserve of the Yellow River Delta. FW were created in 2002 to restore degraded salt marshes by channeling freshwater from the Yellow River. The soils of FW have been inundated by freshwater since then. However, FW has been drained for the construction project of artificial islands since November 2018. Consequently, no standing water exists where *P. australis* grows, but the soils were still saturated in December 2018.

Soil samples with three replicates were taken from 0–5 and 5–10 cm depths of FW before (October 2018) and after (December 2018) the wetland drainage. As we intended to investigate whether there were differences in the fungal community from 0–5 and 5–10 cm soils, we selected these two soil layers instead of just 0–10 cm soils. After drainage, the wetlands were named drained freshwater *P. australis* wetlands (DFW). Soils for sequencing

were placed in an ice cooler box and stored in a refrigerator at −80°C after being brought to the laboratory. Sequencing and data processing were conducted by Beijing Novogene Co. Ltd. (Beijing, China). Soils for the determination of water content (WC) were dried using a drying oven. Soils for the measurement of other soil properties were air-dried and sieved through a 10-mesh sieve (soil particle analysis), a 20-mesh sieve [pH and electronic conductivity (EC)], or a 100-mesh sieve [including soil organic matter (SOM) and TN], respectively. The specific methods for the determination of soil properties can be found in Zhao et al. (2020).

DNA Extraction, Internal Transcribed Spacer Amplification, and Illumina MiSeq Sequencing

Soil DNA was extracted from approximately 0.5 g soil using a TIANGEN®Magnetic Soil and Stool DNA Kit (Qiagen, Valencia, CA, United States). The DNA concentration and purity were monitored on 1% agarose gels. According to the concentration, DNA was diluted to 1 ng/μl using sterile water. The internal transcribed spacer 1 (ITS1) region was amplified using the primer pair ITS1-1F-F (5′-CTTGG TCATTTAGAGGAAGTAA-3′) and ITS1-1F-R (5′-GCTGCGTT CTTCATCGATGC-3′). All PCR reactions were carried out in 30 μl reactions with 15 μl of Phusion® High-Fidelity PCR Master Mix (New England Biolabs, Ipswich, MA, United States); 0.2 μM of forward and reverse primers, and about 10 ng template DNA. Thermal cycling consisted of initial denaturation at 98°C for 1 min, followed by 30 cycles of denaturation at 98°C for 10 s, annealing at 50°C for 30 s, elongation at 72°C for 30 s, and final extension at 72°C for 5 min.

Equal volumes of 1X loading buffer (containing SYB green) were mixed with PCR products and subjected to electrophoresis on 2% agarose gels for detection. Samples with a bright main strip between 400 and 450 bp were chosen for further analysis. PCR products were mixed in equidensity ratios. Then, the PCR products were purified using the GeneJET Gel Extraction Kit (Thermo Scientific, Belmont, MA, United States). Sequencing libraries were generated using an Illumina TruSeq DNA PCR-Free Sample Preparation Kit (Illumina, San Diego, CA, United States) following the manufacturer's recommendations, and index codes were added. The library quality was assessed on the Qubit@ 2.0 Fluorometer (Thermo Scientific, Belmont, MA, United States) and Agilent Bioanalyzer 2100 system. Finally, the library was sequenced on an Illumina NovaSeq 6000 platform and 250 bp paired-end reads were generated.

Sequence Processing and Taxonomic Assignment

Sequencing of purified amplicon products was conducted on the Illumina MiSeq PE300 platform in Beijing Novogene Biotech Co. Ltd. (Beijing, China). Paired-end reads were assigned to samples based on their unique barcode and truncated by cutting off the barcode and primer sequence. FLASH (version 1.2.7[1]) was used to merge paired-end reads, and then raw tags were obtained. Quality filtering on the raw tags was performed under specific filtering conditions to obtain the high-quality clean tags according to the QIIME (Quantitative Insights into Microbial Ecology, version 1.9.1[2]) quality control process. The tags were compared with the UNITE database (version 8.0[3]) using the UCHIME algorithm (UCHIME[4]) to detect and remove chimera sequences. Then, the effective tags were finally obtained. Sequence analyses were performed using Uparse software (Uparse version 7.0.1001[5]). Sequences with ≥ 97% similarity were assigned to the same OTUs. A representative sequence for each OTU was screened for further annotation. For each representative sequence, the UNITE Database[6] was used based on the Mothur algorithm to annotate taxonomic information. The phylogenetic relationships of different OTUs and the difference in the dominant species in different samples (groups) of multiple sequence alignment were identified using the MUSCLE software (version 3.8.31[7]). All raw sequencing data of this study are deposited into the NCBI database with the Short Read Archive (SRA) accession number PRJNA814347.

The α diversity indices, including observed species (S_{obs}), abundance-based coverage estimator (ACE), Chao1, and Shannon diversity, were calculated using QIIME. The β-diversity indices, including principal component analysis (PCA) and principal coordinate analysis (PCoA), were calculated using QIIME software to evaluate the differences in bacterial community composition before and after drainage. Both PCA and PCoA were assessed on the basis of the Bray–Curtis distance of OTUs.

Statistical Analyses

Student's *t*-test was conducted to test the difference in soil properties and soil α-diversity indices between the same soil layer of different sites and different soil layers from the same site at $p < 0.05$ level. Sequencing data were processed on the cloud platform of Novegene. Based on the Bray–Curtis distance, the similarity percentage (SIMPER) analysis was performed using R software to evaluate the contribution of fungal species to the difference in the fungal community between FW and DFW. The Mantel test between the fungal communities and soil properties was conducted at the OTUs, phylum, and class levels based on the Bray–Curtis distance algorithm, to determine environmental variables that structure these communities. Spearman correlation analysis was used to identify the relationships between environmental variables and selected fungal taxa by calculating the correlation coefficients. Mantel test, and Spearman correlation analysis were performed using R software. The trophic model of the fungal community was categorized by subjecting the taxonomic data to the FUNGuild database[8].

[1]http://ccb.jhu.edu/software/FLASH/

[2]http://qiime.org/scripts/split_libraries_fastq.html

[3]http://unite.ut.ee/

[4]http://www.drive5.com/usearch/manual/uchime_algo.html

[5]http://drive5.com/uparse/

[6]http://www.arb-silva.de/

[7]http://www.drive5.com/muscle/

[8]http://www.stbates.org/guilds/app.php

RESULTS

The Changes in Edaphic Factors After Drainage

Soil properties in different soil layers before and after drainage are shown in **Table 1**. Soil EC, Mg^{2+}, Ca^{2+}, SO_4^{2-}, and silt content in 0–5 cm soils were significantly lower in FW than in DFW ($p < 0.05$), while sand content in 0–5 cm soils was significantly higher in FW than in DFW ($p < 0.05$). In 5–10 cm soils, soil Mg^{2+} and SO_4^{2-} were higher in DFW than in FW ($p < 0.05$), whereas soil pH was lower in DFW than in FW ($p < 0.05$). However, EC, Ca^{2+}, SO_4^{2-}, and clay content between FW and DFW showed significant differences ($p < 0.05$). Vertically, soil Na^+, K^+, Mg^{2+}, Ca^{2+}, SO_4^{2-}, and WC in 0–5 cm soils were significantly higher than in 5–10 cm soils in FW ($p < 0.05$), while soil SOM, EC, Mg^{2+}, Ca^{2+}, and SO_4^{2-} in 0–5 cm soils were significantly lower than those in 5–10 cm soils in DFW ($p < 0.05$).

The α and β Diversities of Soil Fungal Community Before and After Drainage

The comparison of α diversity indices of the fungal community between FW and DFW is shown in **Table 2**. The coverage index of the fungal communities in FW and DFW both exceeded 99%, indicating that the sequencing could reflect the fungal communities of both sites. The values of Sobs in 0–5 cm soils showed no significant differences between FW and DFW ($p > 0.05$). However, significantly higher values of Sobs in FW compared with DFW were observed in 5–10 cm soils ($p < 0.05$), with mean values of 416 and 272 in soils in FW and DFW, respectively. Similar to Sobs, the ACE and Chao1 showed significant differences in 5–10 cm soils between FW and DFW ($p < 0.05$), with higher values occurring in FW. As for the Shannon index, no significant differences between FW and DFW in 0–5 or 5–10 cm soils ($p < 0.05$) were found. Besides, no significant differences in Sobs, ACE, Chao1, or Shannon indices were observed between 0–5 and 5–10 cm soils in either FW or DFW.

The PCA and PCoA plots, based on the Bray-Curtis distance of OTUs between FW and DFW, are shown in **Figures 1A,B**, respectively. In the PCA plot, PC1 and PC2 explained 19.1 and 12.15% of the total variance, respectively. Fungi in the soils of DFW were distributed on the upper axis of PC2. However, fungi in soils of FW were scattered on the lower axis of PC2, except for fungi from one soil sample, which showed a closer relationship with samples of DFW. This indicated that the fungal communities between soils from FW and DFW can be separated to a great degree. Similar to PCA, the PCoA plot showed that the fungal communities of most soil samples from DFW can be distinguished from those of soil samples from FW (**Figure 1B**), as soil samples from FW and DFW are mainly distributed on the upper and lower axis of PCoA 2, respectively.

The Fungal Community Structure Before and After Drainage

The fungal community structure at phylum level in 0–5 and 5–10 cm soils of FW and DFW is illustrated in **Figure 2A**. More ITS reads in 0–10 cm soils of DFW (>40%) than in those of FW (<30%) could not be assigned to known fungal phyla. In total, 15 fungal phyla were identified in the soils of FW and DFW. Ascomycota was recognized as the most predominant fungal phylum in both 0–5 and 5–10 cm soils of FW and DFW, with the relative abundance exceeding 50% in 0–10 cm soils of FW and 5–10 cm soils of DFW. The highest relative abundance of Ascomycota was found in 5–10 cm soils of FW, reaching 76.17%. The rest of the 14 fungal phyla occupied less than 1% of the fungal community in 0–10 cm soils of both FW and DFW, except for Rozellomycota,

TABLE 1 | The changes of soil properties before and after drainage.

	FW (0–5 cm)	DFW (0–5 cm)	FW (5–10 cm)	DFW (5–10 cm)
SOM (%)	1.06 ± 0.46^{aA}	0.98 ± 0.39^{aA}	0.38 ± 0.09^{aA}	0.24 ± 0.11^{aB}
TN (g/kg)	0.70 ± 0.32^{aA}	1.04 ± 0.34^{aA}	0.28 ± 0.06^{aA}	0.39 ± 0.08^{aA}
C/N ratio	10.60 ± 2.14^{aA}	10.81 ± 1.10^{aA}	9.13 ± 0.47^{aA}	7.08 ± 2.22^{aA}
EC (mS/cm)	0.61 ± 0.06^{bA}	1.20 ± 0.04^{aA}	0.50 ± 0.09^{aA}	0.67 ± 0.10^{aB}
Na^+ (g/kg)	0.51 ± 0.11^{aA}	0.44 ± 0.12^{aA}	0.25 ± 0.04^{aB}	0.29 ± 0.10^{aA}
K^+ (mg/kg)	36.43 ± 6.20^{aA}	58.59 ± 18.32^{aA}	22.09 ± 1.77^{aB}	32.14 ± 9.09^{aB}
Mg^{2+} (mg/kg)	56.30 ± 11.64^{bA}	141.15 ± 50.05^{aA}	20.32 ± 1.69^{bB}	53.49 ± 20.09^{aB}
Ca^{2+} (g/kg)	0.14 ± 0.02^{bA}	0.39 ± 0.11^{aA}	0.08 ± 0.01^{aB}	0.15 ± 0.05^{aB}
Cl^- (g/kg)	0.51 ± 0.14^{aA}	0.32 ± 0.06^{aA}	0.30 ± 0.04^{aA}	0.18 ± 0.05^{bB}
SO_4^{2-} (g/kg)	0.39 ± 0.03^{bA}	1.60 ± 0.38^{aA}	0.07 ± 0.007^{bB}	0.42 ± 0.11^{aB}
pH	7.93 ± 0.76^{aA}	7.64 ± 0.04^{aA}	8.33 ± 0.09^{aA}	7.96 ± 0.19^{bA}
WC (%)	34.25 ± 0.97^{aA}	33.34 ± 2.95^{aA}	29.94 ± 4.61^{aB}	26.53 ± 3.09^{aA}
Clay (%)	0.39 ± 0.67^{aA}	8.60 ± 3.74^{aA}	0.00 ± 0.00^{aA}	6.87 ± 9.07^{aA}
Silt (%)	17.57 ± 8.43^{bA}	38.27 ± 1.83^{aA}	22.57 ± 2.89^{aA}	24.16 ± 18.96^{aA}
Sand (%)	82.04 ± 8.82^{aA}	53.13 ± 4.92^{bA}	77.43 ± 2.89^{aA}	68.97 ± 27.85^{aA}

^{ab}Different letters represent significant differences between the same soil layer of different sites at $p < 0.05$ level.
^{AB}Different letters represent significant differences between 0–5 cm and 5–10 cm soils at the same site at $p < 0.05$ level.

TABLE 2 | The α diversity indices of fugal community in FW and DFW.

	FW (0–5 cm)	DFW (0–5 cm)	FW (5–10 cm)	DFW (5–10 cm)
Coverage (%)	99.87 ± 0.04	99.90 ± 0.02	99.83 ± 0.02	99.93 ± 0.01
Sobs	440 ± 146^{aA}	289 ± 14^{aA}	416 ± 41^{aA}	272 ± 58^{bA}
ACE	479.60 ± 142.56^{aA}	321.74 ± 11.47^{aA}	474.84 ± 50.77^{aA}	291.35 ± 60.38^{bA}
Chao1	477.84 ± 142.38^{aA}	328.31 ± 10.46^{aA}	458.14 ± 48.73^{aA}	287.40 ± 59.58^{bA}
Shannon	4.05 ± 1.44^{aA}	3.58 ± 0.80^{aA}	2.85 ± 0.33^{aA}	3.07 ± 0.82^{aA}

^{ab}*Different letters represent significant differences between microbes in the same soil layer of different sites ($p < 0.05$).*
^{AB}*Different letters represent significant differences between 0-5 cm and 5-10 cm soils at the same site at $p < 0.05$ level.*

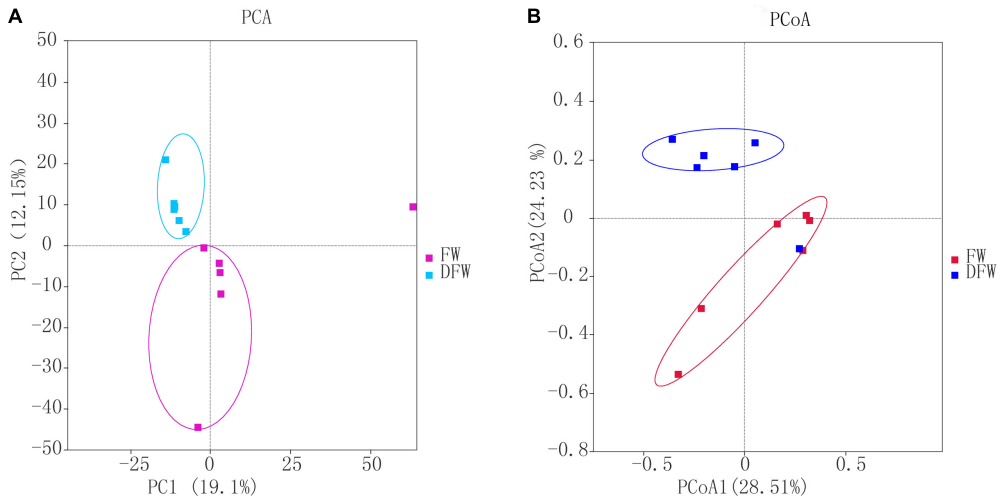

FIGURE 1 | PCA **(A)** and PCoA **(B)** plots.

Chytridiomycota, Basidiomycota, Mortierellomycota, and Glomeromycota. Kickxellomycota was not detected in FW, while Monoblepharomycota, Blastocladiomycota, Neocallimastigomycota, and Basidiobolomycota were only found in FW. Ascomycota and Mortierellomycota in both FW and DFW, Chytridiomycota in DFW, and Glomeromycota, Mucoromycota, Monoblepharomycota, Blastocladiomycota, Neocallimastigomycota, and Basidiobolomycota in FW showed higher abundances in 5–10 cm soils than in 0–5 cm soils. The SIMPER analysis showed that the change in abundance of Ascomycota contributed 43.67 and 43.66% to the dissimilarity in 0–5 and 5–10 cm soils between FW and DFW, respectively (**Table 3**). Additionally, Rozellomycota, Chytridiomycota, Basidiomycota, Mortierellomycota, and Glomeromycota each explained more than 1% of the dissimilarity in 0–5 and 5–10 cm soils between FW and DFW (**Table 3**). At the phylum level, the changes in abundance of these six taxa determined as high as about 61% of the dissimilarity between FW and DFW, among those with individual contributions greater than 1%.

Figures 2B,C show the top 15 fungal classes and families in 0–5 and 5–10 cm soils of FW and DFW, respectively. The dominant soil fungal class was Sordariomycetes in 0–10 cm soils of both FW and DFW. The proportions occupied by Sordariomycetes in FW were 48.16% in 0–5 cm soils and 58.22% in 5–10 cm soils. However, the relative abundance of Sordariomycetes was lower in DFW than in FW, with values of 26.81% in 0–5 cm soils and 45.61% in 5–10 cm soils. Although Leotiomycetes was the second most abundant fungal class, the proportions of Leotiomycetes in the fungal community in 0–5 cm soils of FW and 0–10 cm soils of DFW were less than 10%. Sordariomycetes, Leotiomycetes, Dothideomycetes, Lecanoromycetes, Saccharomycetes, Mortierellomycetes, and Tremellomycetes in both FW and DFW; Glomeromycetes, Pezizomycetes, and Eurotiomycetes in FW; and unidentified Glomeromycotina in DFW showed increasing trends along with the soil profile, while unidentified Rozellomycota sp., Agaricomycetes, Lobulomycetes, and Spizellomycetes in FW and DFW; Glomeromycetes, Pezizomycetes, and Eurotiomycetes in DFW; and unidentified Glomeromycotina in FW were more enriched in 0–5 cm soils than in 5–10 cm soils. Simultaneously, the changes in the abundances of Sordariomycetes, Leotiomycetes, unidentified Rozellomycota sp., Agaricomycetes, Dothideomycetes, Lecanoromycetes, and Saccharomycetes contributed 61.34 and 61.36% of the dissimilarity in 0–5 and 5–10 cm soils between FW and DFW, respectively, among those with individual contributions greater than 1% (**Table 3**). The largest contribution was made by Sordariomycetes (32.89% in 0–5 cm soils and 32.88% in 5–10 cm soils), followed by Leotiomycetes (11.79% in 0–10 cm soils).

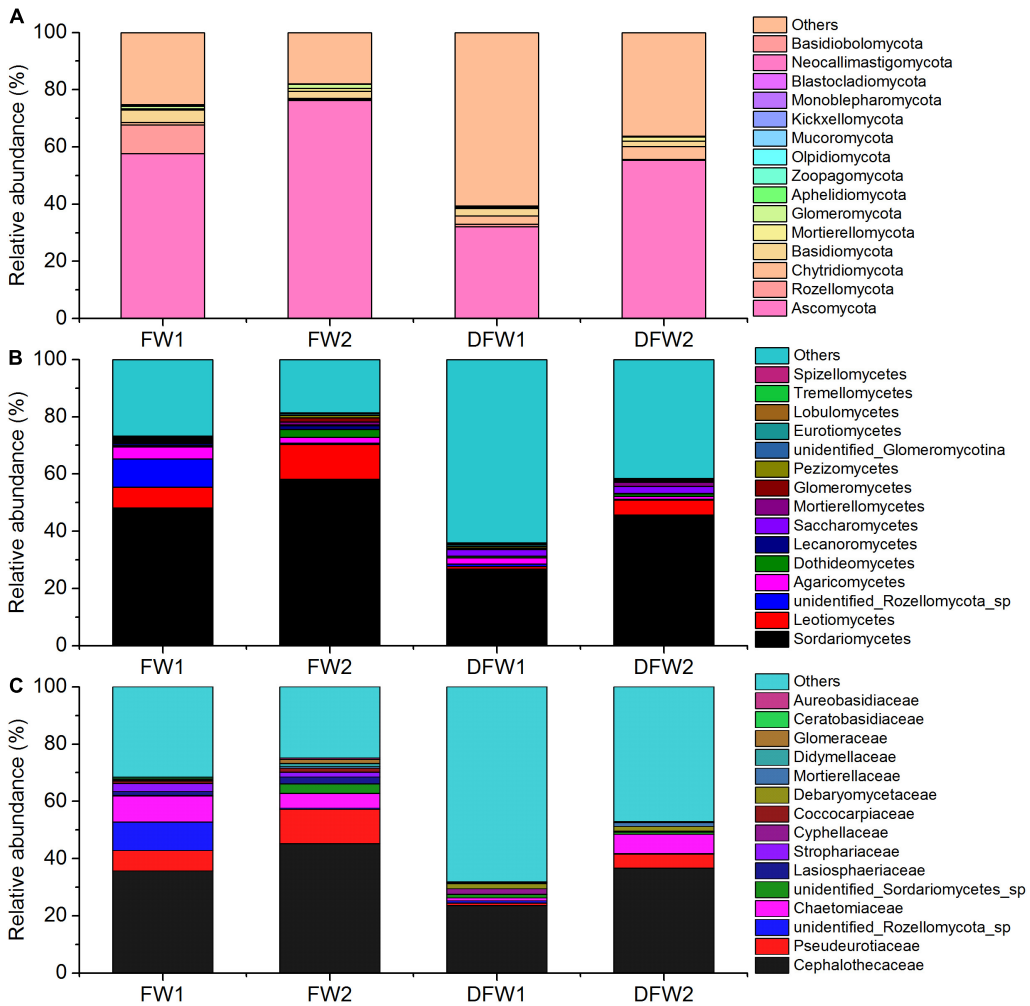

FIGURE 2 | The fungal community structure in 0–5 and 5–10 cm soils of FW and DFW at phylum level **(A)**, at class level **(B)**, and at family level **(C)**. (Note: 1 represents 0–5 cm soils and 2 represents 5–10 cm soils).

At the family level, the relative abundance of Cephalothecaceae was highest in 0–10 cm soils in both FW (35.72% in 0–5 cm soils and 45.20% in 5–10 cm soils) and DFW (23.62% in 0–5 cm soils and 36.62% in 5–10 cm soils), followed by Pseudeurotiaceae (**Figure 2C**). The relative abundance of Pseudeurotiaceae was less than 1% in 0–5 cm soils of DFW but reached 12.00% in 5–10 cm soils of FW. Notably, fungi belonging to Cyphellaceae and Debaryomycetaceae were not detected in 0–10 cm soils in FW. Cephalothecaceae, Pseudeurotiaceae, unidentified Sordariomycetes sp., Lasiosphaeriaceae, Coccocarpiaceae, Mortierellaceae, Didymellaceae, and Aureobasidiaceae in FW and DFW; Chaetomiaceae, Stropharіaceae and Ceratobasidiaceae in DFW; and Glomeraceae in FW showed a lower relative abundance in 0–5 cm soils than in 5–10 cm soils, while the relative abundances of unidentified Rozellomycota sp. in FW and DFW; Chaetomiaceae, Stropharіaceae, and Ceratobasidiaceae in FW; Cyphellaceae, Debaryomycetaceae, and Glomeraceae in DFW were higher in 0–5 cm soils than in 5–10 cm soils. According to the SIMPER analysis (**Table 3**), Cephalothecaceae and Pseudeurotiaceae made the highest (28.46%) and second-highest (10.21%) contributions to the dissimilarity in 0–10 cm soils between FW and DFW at the family level, respectively. Each of the abundances of unidentified Rozellomycota_sp., Chaetomiaceae, unidentified Sordariomycetes sp., Lasiosphaeriaceae, Stropharіaceae, Cyphellaceae, and Coccocarpiaceae explained > 1% of the dissimilarity between FW and DFW, while the sum of the contributions made by these seven taxa reached 59.04% in both 0–5 and 5–10 cm soils.

The Trophic Characterization of Soil Fungal Community Before and After Drainage

The fungal OTUs in 0–10 cm soils of FW and DFW were categorized into eight trophic modes based on FUNGuild (**Figure 3**). The proportion of OTUs that could be classified by

TABLE 3 | The similarity percentage (SIMPER) analysis at phylum, class and family level between FW and DFW.

	Species	Contribution (%) of fungi at different depth	
		0-5 cm	5-10 cm
Phylum	Ascomycota	43.67	43.66
	Rozellomycota	7.22	7.22
	Chytridiomycota	4.06	4.06
	Basidiomycota	3.51	3.50
	Mortierellomycota	1.41	1.41
	Glomeromycota	1.07	1.07
Class	Sordariomycetes	32.89	32.88
	Leotiomycetes	11.79	11.79
	Unidentified_Rozellomycota_sp	5.82	5.82
	Agaricomycetes	2.85	2.85
	Dothideomycetes	1.74	1.75
	Lecanoromycetes	1.46	1.46
	Saccharomycetes	1.28	1.28
Family	Cephalothecaceae	28.46	28.46
	Pseudeurotiaceae	10.21	10.21
	Unidentified_Rozellomycota_sp	5.03	5.03
	Chaetomiaceae	4.55	4.55
	Unidentified_Sordariomycetes_sp	2.31	2.31
	Lasiosphaeriaceae	1.88	1.88
	Strophariaceae	1.83	1.83
	Cyphellaceae	1.25	1.25
	Coccocarpiaceae	1.10	1.10

FUNGuild was higher in FW (>60%) than in DFW (<50%). Saprotroph was the dominant trophic mode in both 0–5 and 5–10 cm soils of FW and DFW, accounting for more than 54.26, 67.16, and 55.98% in 0–5 and 5–10 cm soils of FW and 5–10 cm soils of DFW, respectively. Although Saprotroph just occupied 27.08% of the fungal community in 0–5 cm soils of DFW, its abundance ranked the highest among the OTUs that could be assigned by FUNGuild at 92.79%. Among the remaining seven trophic modes, only the relative abundance of Symbiotroph in 0–10 cm soils of FW and Pathotroph-Saprotroph in 0–5 cm soils of DFW and 5–10 cm soils of FW were higher than 1%. Saprotroph, Pathotroph, Saprotroph-Pathotroph-Symbiotroph, Saprotroph-Symbiotroph, and Saprotroph-Symbiotroph in 0–5 and 5–10 cm soils of FW; Pathotroph-Saprotroph-Symbiotroph and Pathotroph-Symbiotroph in 0–5 cm soils of FW; and Pathotroph-Saprotroph in 5–10 cm soils of FW were more enriched than those of DFW, showing a decreasing trend after drainage.

The Relationship Between the Fungal Community and Environmental Variables

The results of the Mantel tests between the fungal community and environmental variables at OTU, phylum, class, and family level are shown in **Table 4**. EC and pH showed significant correlations with the fungal community at OTU, phylum, class, and family levels ($p < 0.05$) with correlation coefficients ranging from 0.31 to 0.48. However, no significant relationships between the fungal community and other environmental variables were observed ($p > 0.05$).

The Spearman correlations between environmental variables and α diversity of the fungal community and fungal community at phylum, class, and family level are exhibited in **Figures 4A–D**, respectively. Soil clay and Cl^- showed significantly negative and positive relationships with Sobs, ACE, and Chao1 indices ($p < 0.05$), respectively, while soil Ca^{2+} showed a significantly negative relationship with the Chao1 index ($p < 0.05$). At the phylum level, there were significant correlations between Ascomycota, Chytridiomycota, Mortierellomycota, Aphelidiomycota, Zoopagomycota, Olpidiomycota, Mucolomycota, Blastocladiomycota, and Neocallimastigomycota and all soil properties except for silt ($p < 0.05$, **Figure 4B**). At the class level, Dothideomycetes, Saccharomycetes, Mortierellomycetes, Glomeromycetes, Lobulomycetes, Tremellomycetes, and Spizellomycetes were significantly related to all soil properties except for silt and pH ($p < 0.05$, **Figure 4C**). At the family level, soil clay, Cl^-, Ca^{2+}, K^+, Na^+, pH, EC, C/N ratio, TN, and SOM were significantly related to Lasiosphaeriaceae, Strophariaceae, Cyphellaceae, Coccocarpiaceae, Debaryomycetaceae, Mortierellaceae, Didymellaceae, and Aureobasidiaceae ($p < 0.05$, **Figure 4D**).

DISCUSSION

How Drainage Affects the Soil Fungal Community

Drainage caused the disappearance of standing water in FW, turning the long-term flooded soils into a saturated state and temporarily creating a more aerobic soil environment. Hydrology is one of the dominant controlling factors of fungal diversity and community composition, and water table drawdown could induce both positive and negative effects on fungal communities (Asemaninejad et al., 2017; Almeida et al., 2020). The increased oxygen availability by short-term water table drawdown favors the fungal cell energy metabolism (especially for saprotrophs), while long-term water table drawdown results in comprehensive changes in the soil environment (Asemaninejad et al., 2017). Microorganisms are sensitive to the availability of water and oxygen in wetland ecosystems (Xue et al., 2020). Fungi are also capable of compensating for unfavorable soil moisture conditions (Jassey et al., 2017). Soil moisture has been confirmed as one of the main drivers for changes in the fungal community (Zhao et al., 2019). Different oxygen requirements of different fungi in their life cycle possibly render fungal communities altered after drainage (Guan et al., 2018). Almeida et al. (2020) considered that the sensitivity of some fungi to dry conditions or the increased dispersal of spores to wetter sites could explain the decreased fungal diversity and shifted composition as the water level relatively lowered in the Everglades tree islands. Peltoniemi et al. (2009) reported that a short-term water-level drawdown induced an increase in fungal diversity in a boreal peatland in Finland. Tian et al. (2022) found that the composition and size of the fungal community in 0–25 cm soils in Zoige peatlands were

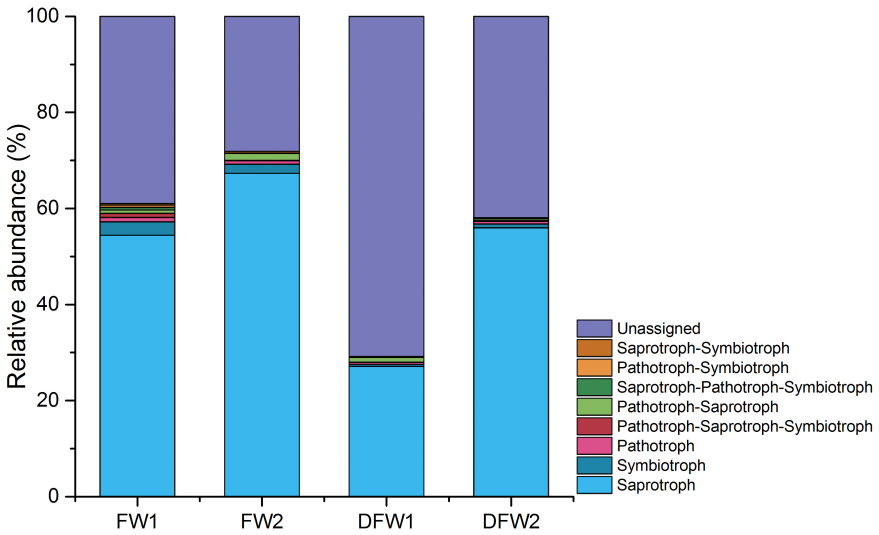

FIGURE 3 | The relative abundance of fungal trophic modes in 0–5 and 5–10 cm soils of FW and DFW. (Note: 1 represents 0–5 cm soils and 2 represents 5–10 cm soils).

not significantly affected by aerobic conditions. A decreasing trend in the richness of the soil fungal community was observed after drainage, but statistically significant differences were only detected for the Sobs, ACE, and Chao1 indices in 5–10 cm soils (**Table 2**). The diversity indicated by the Shannon index in 0–10 cm soils and the abundance of the fungal community in 0–5 cm soils showed no significant differences before and after drainage. The disparity in these studies might be caused by the initial *in situ* water table level, duration time of the water-level drawdown, or the wetland type (Peltoniemi et al., 2009; Tian et al., 2022).

Various studies have reported the influence of soil properties on soil fungal abundance and diversity (Guan et al., 2018; Zhao et al., 2019; Xue et al., 2020; Hou et al., 2021). According to Hou et al. (2021), soil Ca^{2+} was negatively correlated with the Chao1 index of soil fungi. In this study, Spearman correlation analysis showed that soil clay and Ca^{2+} negatively affected the abundance of the fungal community (**Figure 4A**). However, soil Ca^{2+} and clay positively responded to wetland drainage, indicating that drainage possibly causes the decreased abundance of the fungal community in the long run. Guan et al. (2018) found that soil organic carbon negatively affected the diversity of the fungal community due to the competition for organic matter and the increased decomposition ability. No significant differences in SOM were found in 0–10 cm soils of FW or DFW in this study, a factor that might explain the similar α diversity of fungal communities in FW and DFW. Salinity has been reported to negatively affect the fungal Shannon diversity in degraded grasslands (Wu et al., 2021). Xiao et al. (2020) found that EC explained 14.93% of the difference in soil fungal communities between freshwater restored wetlands and natural wetlands. Zhao et al. (2019) reported that salinity could predict changes in the fungal community. Although no significant correlations were observed between fungal α diversity indices or EC and salt ions, these salinity parameters selectively affected some fungal species as shown by the Spearman correlation analysis (**Figure 4**). Simultaneously, soil EC, Mg^{2+}, Ca^{2+}, and SO_4^{2-} responded positively to wetland drainage. Thus, drainage possibly imposes a further decreasing effect on fungal community diversity by affecting soil salinity. Soil pH has been shown to significantly affect soil fungal OTU numbers and community structure, but no significant relationship between the abundance of the fungal community and pH was observed (Wang et al., 2015; Dini-Andreote et al., 2016). In this study, pH significantly affected the soil fungal community at various levels ($p < 0.05$, **Table 4**) and had significant relationships with the abundances of Ascomycota, Chytridiomycota, Olpidiomycota, Strophariaceae, Cyphellaceae, and Debaryomycetaceae ($p < 0.05$, **Figure 4**). Several studies have reported the structuring effect of both silt and sand content on the fungal community (Chen et al., 2017; Zhao et al., 2017; Dos Passos et al., 2021), a pattern that was confirmed in this study. Although a statistically significant difference was only observed in 0–5 cm soils, the silt and sand content increased and decreased after drainage in this study. Higher WC can stimulate an increase in the diversity of the fungal community (Xu et al., 2017). However, drainage did not have any significant effects on the soil WC (**Table 1**), which might be another reason for the similar diversity of the fungal community before and after drainage. Additionally, SOM, TN, C/N ratio, Na^{+}, and WC significantly affected some fungal species despite the fact that there were no significant drainage effects on these factors. Thus, the associated changes caused by drainage in soil properties would alter the soil fungal community. Apart from soil properties, soil depth is considered a non-negligible influencing factor. The variations of the fungal community along the soil profile have been reported at both small and large spatial scales by several researchers. For example, Pagano et al. (2016) found that the abundance of the fungal community showed a clear decreasing tendency as soil

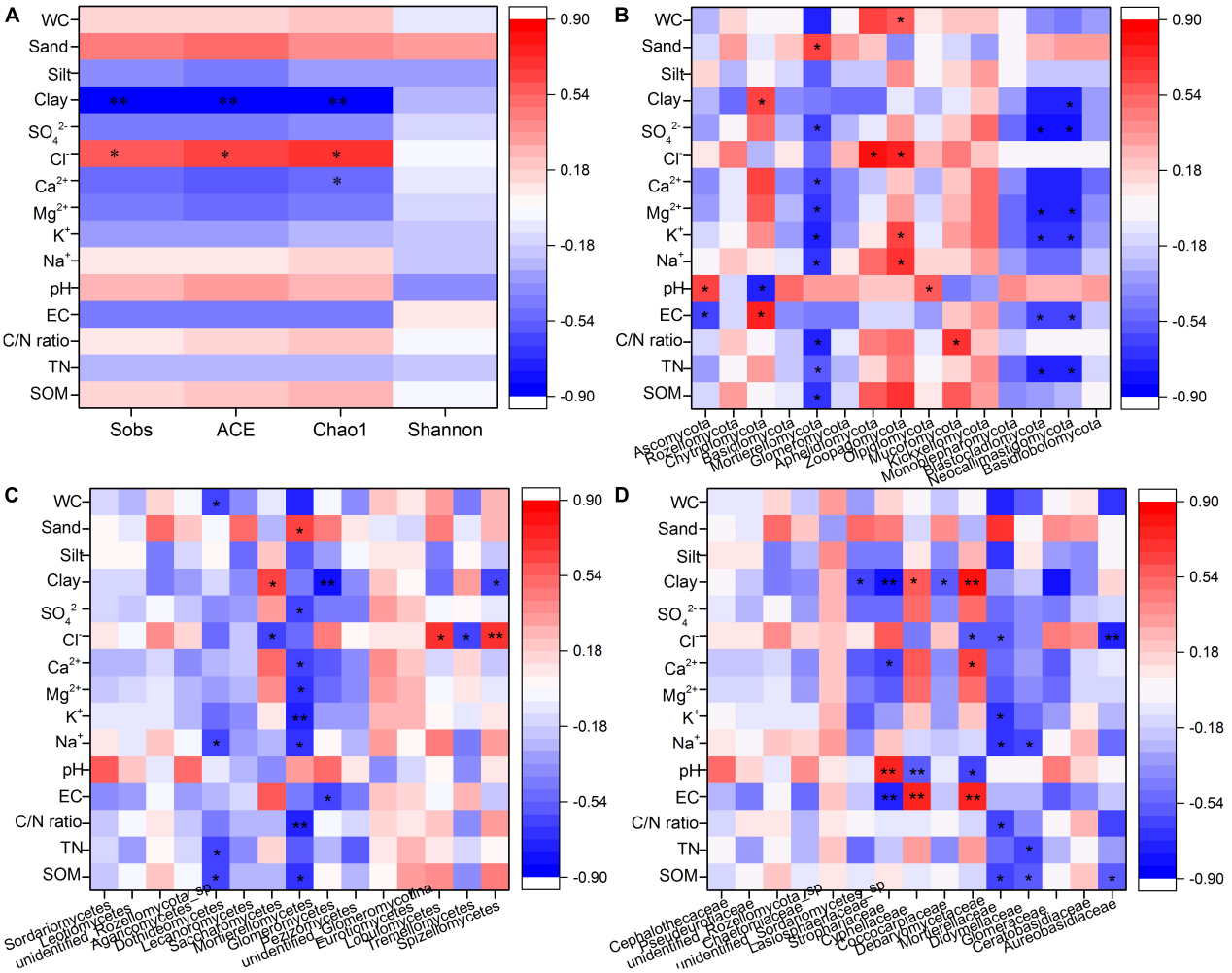

FIGURE 4 | Spearman correlation analyses between environmental variables and α diversity indices **(A)**, fungal community at phylum level **(B)**, selected fungal classes **(C)**, and selected fungal families **(D)**.

depth increased in anthropic Amazonian dark soils. Li et al. (2020) reported that the community structure of soil fungi in paddy fields varied along with soil depth due to the variations of soil organic carbon and nitrogen content in three regions across China. In this study, the fungal community richness showed no significant changes along with the depth, but the community composition varied between 0–5 and 5–10 cm soil depths.

The Specific Effects of Drainage on Fungal Community Structure and the Possible Ecological Impact

The fungal community structure seemed to be more sensitive to drainage than the α diversity indices. The proportions of ITS reads that could not be assigned to any fungal phyla reached up to 60.62% in 0–5 cm soils and 36.24% in 5–10 cm soils of DFW, which were much higher than those in 0–10 cm soils of FW (25.16% for 0–5 cm soil layer and 17.92% for 5–10 cm soil layer). Dini-Andreote et al. (2016) also found that 49.5% of the fungal sequences from sediments of salt marshes with zero year of succession could not be affiliated with any fungal phylum in the database. Recently, Cheung et al. (2018) reported that about 23% of ITS reads cannot be recognized as known fungal phyla, and they considered that these unassigned fungi might be identified as novel early diverging lineages that could facilitate our understanding of the evolution of fungi.

Both compositional and functional shifts in the fungal community associated with water table level changes have been observed by Peltoniemi et al. (2012) and Asemaninejad et al. (2017). In this study, drainage decreased the relative abundances of Saprotroph, Pathotroph, Saprotroph-Pathotroph-Symbiotroph, Saprotroph-Symbiotroph, Saprotroph-Symbiotroph Pathotroph-Saprotroph-Symbiotroph, Pathotroph-Symbiotroph, and Pathotroph-Saprotroph in 0–5 or/and 5–10 cm soils in the freshwater wetlands. Jassey et al. (2017) found that saprotrophic fungi showed a gradually increasing trend as water level decreased, which collaborates with this study. Saprotrophic fungi can boost the process of carbon mineralization and potentially affect long-term carbon

TABLE 4 | The Mantel test between fungal community and environmental variables.

	R(OTU)	R(phylum)	R(class)	R(family)
SOM	0.16	0.13	0.15	0.17
TN	0.10	0.02	0.07	0.08
C/N ratio	0.09	0.03	0.15	0.16
EC	0.33*	0.48*	0.33*	0.36*
pH	0.37*	0.31*	0.40**	0.36*
Na^+	0.10	0.08	0.16	0.15
K^+	0.06	0.00	0.05	0.05
Mg^{2+}	0.03	0.06	0.02	0.01
Ca^{2+}	0.07	0.05	0.03	0.03
Cl^-	0.24	0.24	0.24	0.27
SO_4^{2-}	0.01	0.12	0.03	0.05
Clay	0.08	0.02	0.01	0.03
Silt	0.00	0.07	0.04	0.00
Sand	0.02	0.06	0.05	0.01
WC	0.11	0.11	0.01	0.04

** and ** represent the significant difference at $p < 0.05$ and $p < 0.01$ level, respectively.*

storage through accretion of soil recalcitrant C carbon (Treseder and Lennon, 2015). Moreover, increased saprotrophic fungi improved enzyme activity (Jassey et al., 2017). Thus, the changes in the relative abundance of saprotrophic fungi resulting from wetland drainage will consequently affect wetland carbon storage in the future. At the phylum level, the fungal species contributing more than 1% to the dissimilarity before and after drainage were Ascomycota, Rozellomycota, Chytridiomycota, Basidiomycota, Mortierellomycota, and Glomeromycota. However, the fungal class and family that contributed more than 1% to the difference between the soil fungal communities of FW and DFW belonged to three phyla (Ascomycota, Rozellomycota, and Basidiomycota). Among fungal species (at phylum, class, and family level) that made higher contributions to the dissimilarity before and after drainage, the relative abundances of most species in both 0–5 and 5–10 cm soils decreased after drainage except for Mortierellomycota, Chaetomiaceae, and unidentified Sordariomycetes sp. in 5–10 cm soils of FW, Dothideomycetes, and Saccharomycetes in 0–5 cm soils of FW and Cyphellaceae in both 0–5 and 5–10 cm soils of FW.

As saprotrophic fungal species and important decomposers of cellulose, Ascomycota have been reported as the dominant fungal phylum in various soil types, such as coastal wetlands sediments, alpine wetlands soils, paddy soils, subtropical bamboo forests, and degraded grasslands (Li et al., 2017, 2020; Cheung et al., 2018; Xie et al., 2020; Wu et al., 2021). Consistently, Ascomycota, the Sordariomycetes class, and the Cephalothecaceae family belonging to Ascomycota held the highest proportions in fungal communities in 0–5 and 5–10 cm soils in both FW and DFW in this study, respectively, demonstrating that cellulose-degrading species dominated in the fungal community of both FW and DFW (Li et al., 2017). Dothideomycetes have been reported as the largest class of Ascomycota with the highest ecological diversity (Hongsanan, 2020). Most species of freshwater Dothideomycetes are saprobic fungi, decomposing submerged woody debris and leaves in water (Dong et al., 2020). However, the relative abundance of Dothideomycetes in 0–10 cm soils of FW and DFW was quite low in this study. As the second-largest class of Ascomycota, Sordariomycetes are widely found in various environments and contain functionally diverse members, such as plant pathogens and saprobes (Maharachchikumbura et al., 2016). Freshwater Sordariomycetes contain diverse lignicolous freshwater fungi and thus participate in the functioning of ecosystems (Luo et al., 2019). Similar to Sordariomycetes, Leotiomycetes consist of a large number of non-lichenized ascomycetes fungi and are widely found in various biotopes, producing inoperculate, unitunicate asci in perithecial or apothecial ascomata (Zhang and Wang, 2015). Members of Chaetomiaceae are capable of producing a series of enzymes that possess significant applications in biotechnology and industry, and most members are renowned for breaking down cellulose (Ibrahim et al., 2021). The decrease in the relative abundances of Ascomycota, Sordariomycetes, and Cephalothecaceae after drainage indicated that drainage would affect cellulose decomposition (Li et al., 2017).

Rozellomycota consist of uniflagellated and unwalled zoospores with ready motility acquired from swimming (Dini-Andreote et al., 2016). Thus, the members of Rozellomycota may thrive more in the flooding soil environment of FW than in DFW, explaining the higher relative abundance of Rozellomycota in FW than in DFW. Besides, it has been reported that sand content positively affected the relative abundance of Rozellomycota (Dini-Andreote et al., 2016). The higher sand content in 0–10 cm soils of FW than that of DFW might partly explain why Rozellomycota was more enriched in FW.

Generally, Chytridiomycota (Chytrids) favor aquatic environments and terrestrial habitats with surface water (Peltoniemi et al., 2009). However, many Chytrids can endure short-term desiccation through producing resistant spores, and thus they can survive from water table drawdown for short periods (Asemaninejad et al., 2017). In this study, the relative abundance of Chytridiomycota increased after drainage, perhaps due to the high proportion of desiccation-resistant Chytrids in the freshwater.

Basidiomycota are also involved in carbon cycling through degrading organic substances (especially lignin), and members (especially in the class Agaricomycetes) are typical representatives of cellulose degraders (Treseder and Lennon, 2015; Li et al., 2017; Wu et al., 2021). Xue et al. (2020) reported that the relative abundance of Basidiomycota showed an enormously increasing trend as the water table lowered in drained peatlands of the Zoige Plateau. This might be associated with the differences in drainage duration observed in these two studies, as drainage duration affects the response of microbial communities to the decline of the water table (Xue et al., 2020). In line with the study of Fu et al. (2021), no environmental variables significantly affected the relative abundance of Basidiomycota. Agaricomycetes are the most abundant class within the phylum Basidiomycota are widely distributed in soils due to the high production of atmospheric fungal spores (50%) (Santillán et al., 2021). The relative abundance of Agaricomycetes also showed a negative response to wetland drainage in this study.

Mortierellomycota contain a large group of saprotrophs in the soil that can dissolve soil mineral phosphorus to enhance soil

nutrient levels (Wang et al., 2020). The relative abundance of Mortierellomycota has been reported to be diminished by higher SOM and TN content (Qiu et al., 2020; Wu et al., 2021), which collaborates with the spearman correlation results of this study (**Figure 4**). However, SOM and TN weren't significantly altered by drainage in this study, which might explain why only a quite small change was observed in the relative abundance of Mortierellomycota.

Glomeromycota are a globally distributed fungal phylum, and Glomeromycota fungi that can form arbuscular mycorrhiza are known as Arbuscular mycorrhizal fungi (AMF), importantly affecting plant growth and maintaining soil functions and the sustainability of the soil environment (Rivera-Becerril et al., 2017; Stürmer et al., 2018). Although no significant relationships between Glomeromycota and edaphic factors were observed, the relative abundance of Glomeromycota decreased after drainage.

CONCLUSION

This study has shed light upon the effects of drainage on the fungal community and soil properties in a freshwater wetland in the Yellow River Delta vegetated with *P. australis*. Wetland drainage lowered the water table in freshwater wetlands and turned the flooded soil environment into a saturated state, altering the soil fungal community as well as several edaphic factors. Drainage increased the contents of soil EC, Mg^{2+}, Ca^{2+}, $SO_4{}^{2-}$, and silt but lowered sand content and pH in 0–5 or 5–10 cm soils. The predominant Ascomycota, Sordariomycetes, and Cephalothecaceae at phylum, class, and family level, respectively, all decreased after drainage and also made the highest contribution to the dissimilarity in the fungal community before and after drainage, as revealed by the SIMPER analysis. However, drainage increased the relative abundances of Chytridiomycota and Cyphellaceae in both 0–5 and 5–10 cm soils. Additionally, most of the remaining fungal species caused large changes (1%) in the fungal community before and after drainage exhibited a decrease after drainage in both 0–5 and 5–10 cm soils except for Mortierellomycota, Chaetomiaceae, unidentified Sordariomycetes sp., Dothideomycetes, Saccharomycetes, and Cyphellaceae. Multiple statistical analyses unraveled that SOM, TN, C/N ratio, EC, pH, Cl^-, Na^+, K^+, Mg^{2+}, Ca^{2+}, $SO_4{}^{2-}$, clay, and WC influenced fungal community structure at different levels. Thus, drainage also changed the soil fungal community through altering edaphic factors. The effects of drainage on the soil fungal community potentially change soil nutrient cycling, especially the carbon cycle in wetlands. Therefore, the possible influence of drainage on wetland ecosystems should be taken into consideration when trading off whether to conduct a drainage project.

DATA AVAILABILITY STATEMENT

The original contributions presented in the study are included in the article/supplementary material, further inquiries can be directed to the corresponding author/s.

AUTHOR CONTRIBUTIONS

QZ: methodology, investigation, analysis, draft writing, revision, and funding acquisition. JB: methodology and supervision. JJ: investigation, analysis, draft writing, and revision. GZ: investigation and analysis. JW and YG: literature search and funding acquisition. All authors contributed to the article and approved the submitted version.

FUNDING

This study was financially supported by the Shandong Provincial Natural Science Foundation (ZR2019BD007), Major Scientific and Technological Innovation Projects in Shandong Province (2021CXGC011201), Joint Funds of the National Natural Science Foundation of China (U1806217), and the National Key R&D Program of China (2019YFC1804103).

ACKNOWLEDGMENTS

We are grateful to the editor and two reviewers for their constructive feedback on our article.

REFERENCES

Almeida, B. K., Ross, M. S., Stoffella, S. L., Sah, J. P., Cline, E., Sklar, F., et al. (2020). Diversity and Structure of Soil Fungal Communities across Experimental Everglades Tree Islands. *Diversity* 12:324. doi: 10.3390/d12090324

Asemaninejad, A., Thorn, R. G., Branfireun, B. A., and Lindo, Z. (2018). Climate change favours specific fungal communities in boreal peatlands. *Soil Biol. Biochem.* 120, 28–36. doi: 10.1016/j.soilbio.2018.01.029

Asemaninejad, A., Thorn, R. G., and Lindo, Z. (2017). Experimental climate change modifies degradative succession in boreal peatland fungal communities. *Microbial. Ecol.* 73, 521–531. doi: 10.1007/s00248-016-0875-9

Bergsveinson, J., Perry, B., Simpson, G., Yost, C. K., Schutzman, R. J., Hall, B. D., et al. (2019). Spatial analysis of a hydrocarbon waste-remediating landfarm demonstrates influence of management practices on bacterial and fungal community structure. *Microb. Biotechnol.* 12, 1199–1209. doi: 10.1111/1751-7915.13397

Brunet, N. N., and Westbrook, C. J. (2012). Wetland drainage in the Canadian prairies: Nutrient, salt and bacteria characteristics. *Agric. Ecosyst. Environ.* 146, 1–12. doi: 10.1016/j.agee.2011.09.010

Chen, Y., Xu, T., Veresoglou, S., Hu, H., Hao, Z., Hu, Y., et al. (2017). Plant diversity represents the prevalent determinant of soil fungal community structure across temperate grasslands in northern China. *Soil Biol. Biochem.* 110, 12–21. doi: 10.1016/j.soilbio.2017.02.015

Cheung, M. K., Wong, C. K., Chu, K. H., and Kwan, H. S. (2018). Community Structure, Dynamics and Interactions of Bacteria, Archaea and Fungi in Subtropical Coastal Wetland Sediments. *Sci. Rep.* 8:14397 doi: 10.1038/s41598-018-32529-5

Cortus, B. G., Jeffrey, S. R., Unterschultz, J. R., and Boxall, P. C. (2011). The Economics of Wetland Drainage and Retention in Saskatchewan. *Can. J. Agric. Econ.* 59, 109–126. doi: 10.1111/j.1744-7976.2010.01193.x

Dini-Andreote, F., Pylro, V. S., Baldrian, P., van Elsas, J. D., and Salles, J. F. (2016). Ecological succession reveals potential signatures of marine-terrestrial

transition in salt marsh fungal communities. *ISME J.* 10, 1984–1997. doi: 10.1038/ismej.2015.254

Dong, W., Wang, B., Hyde, K. D., McKenzie, E. H. C., Raja, H. A., Tanaka, K., et al. (2020). Freshwater Dothideomycetes. *Fungal Diver.* 105, 319–575.

Dos Passos, J., Maia, L., de Assis, D., Da Silva, J., Oehl, F., and Da Silva, I. (2021). Arbuscular mycorrhizal fungal community structure in the rhizosphere of three plant species of crystalline and sedimentary areas in the Brazilian dry forest. *Microb. Ecol.* 82, 104–121. doi: 10.1007/s00248-020-01557-y

Drexler, J. Z., de Fontaine, C. S., and Deverel, S. J. (2009). The legacy of wetland drainage on the remaining peat in the Sacramento — San Joaquin Delta, California, USA. *Wetlands* 29, 372–386. doi: 10.1672/08-97.1

Frąc, M., Hannula, S. E., Bełka, M., and Jędryczka, M. (2018). Fungal biodiversity and their role in soil health. *Front. Microbiol.* 9:707. doi: 10.3389/fmicb.2018.00707

Fu, B., Li, Z., Gao, X., Wu, L., Lan, J., and Peng, W. (2021). Effects of subsurface drip irrigation on alfalfa (*Medicago sativa* L.) growth and soil microbial community structures in arid and semi-arid areas of northern China. *Appl. Soil Ecol.* 159:103859. doi: 10.1016/j.apsoil.2020.103859

Guan, M., Pan, X., Wang, S., Wei, X., Zhang, C., Wang, J., et al. (2018). Comparison of fungal communities among ten macrophyte rhizospheres. *Fungal Biol.* 122, 867–874. doi: 10.1016/j.funbio.2018.05.001

Hongsanan, S. (2020). Refined families of Dothideomycetes: Dothideomycetidae and Pleosporomycetidae. *Mycosphere* 11, 1553–2107. doi: 10.5943/mycosphere/11/1/13

Hou, Y., Zeng, W., Hou, M., Wang, Z., Luo, Y., Lei, G., et al. (2021). Responses of the Soil Microbial Community to Salinity Stress in Maize Fields. *Biology* 10:1114. doi: 10.3390/biology10111114

Hui, N., Liu, X., Jumpponen, A., Setälä, H., Kotze, D. J., Biktasheva, L., et al. (2018). Over twenty years farmland reforestation decreases fungal diversity of soils, but stimulates the return of ectomycorrhizal fungal communities. *Plant Soil* 427, 231–244. doi: 10.1007/s11104-018-3647-0

Ibrahim, S. R. M., Mohamed, S. G. A., Sindi, I. A., and Mohamed, G. A. (2021). Biologically active secondary metabolites and biotechnological applications of species of the family Chaetomiaceae (Sordariales): an updated review from 2016 to 2021. *Mycol. Prog.* 20, 595–639. doi: 10.1007/s11557-021-01704-w

Jassey, V. E. J., Reczuga, M. K., Zielińska, M., Słowińska, S., Robroek, B. J. M., Mariotte, P., et al. (2017). Tipping point in plant–fungal interactions under severe drought causes abrupt rise in peatland ecosystem respiration. *Glob. Change Biol.* 24, 972–986. doi: 10.1111/gcb.13928

Jones, C. N., Evenson, G. R., Mclaughlin, D. L., Vanderhoof, M. K., Lang, M. W., Mccarty, G. W., et al. (2018). Estimating restorable wetland water storage at landscape scales. *Hydrol. Proc.* 32, 305–313. doi: 10.1002/hyp.11405

Li, M., Li, L., Liao, H., Huang, Z., Huang, Z., and Huang, W. (2012). The influence of drainage on wetland degradation in Zoige Plateau. *Dis. Adv.* 5, 659–666.

Li, X., Wang, H., Li, X., Li, X., and Zhang, H. (2020). Distribution characteristics of fungal communities with depth in paddy fields of three soil types in China. *J. Microbiol.* 58, 279–287. doi: 10.1007/s12275-020-9409-8

Li, Y., Li, Y., Chang, S. X., Liang, X., Qin, H., Chen, J., et al. (2017). Linking soil fungal community structure and function to soil organic carbon chemical composition in intensively managed subtropical bamboo forests. *Soil Biol. Biochem.* 107, 19–31. doi: 10.1016/j.soilbio.2016.12.024

Liu, J., Le, T. H., Zhu, H., Yao, Y., Zhu, H., Cao, Y., et al. (2020). Afforestation of cropland fundamentally alters the soil fungal community. *Plant Soil* 457, 279–292. doi: 10.1007/s11104-020-04739-2

Liu, L., Chen, H., Jiang, L., Hu, J., and Zhan, W. (2018). Water table drawdown reshapes soil physicochemical characteristics in Zoige peatlands. *Catena* 170, 119–128. doi: 10.1016/j.catena.2018.05.025

Luo, Z., Hyde, K., Liu, J., Maharachchikumbura, S., Jeewon, R., Bao, D., et al. (2019). Freshwater Sordariomycetes. *Fungal Divers.* 99, 451–660. doi: 10.1007/s13225-019-00438-1

Maharachchikumbura, S., Hyde, K., Jones, E., McKenzie, E. H. C., Bhat, J. D., Dayarathne, M. C., et al. (2016). Families of Sordariomycetes. *Fungal Divers.* 79, 1–317. doi: 10.1007/s13225-016-0369-6

McCauley, L. A., Anteau, M. J., van der Burg, M. P., and Wiltermuth, M. T. (2015). Land use and wetland drainage affect water levels and dynamics of remaining wetlands. *Ecosphere* 6, 1–22.

Mueller, G. M., and Schmit, J. P. (2007). Fungal biodiversity: what do we know? What can we predict? *Biodivers. Conserv.* 16, 1–5. doi: 10.1007/s10531-006-9117-7

Onufrak, A., Rúa, M. A., and Hossler, K. (2020). The Missing Metric: An Evaluation of Fungal Importance in Wetland Assessments. *Wetlands* 40, 825–838. doi: 10.1007/s13157-019-01228-w

Pagano, M., Ribeiro-Soares, J., Cançado, L., Falcão, N., Gonçalves, V., Rosa, L., et al. (2016). Depth dependence of black carbon structure, elemental and microbiological composition in anthropic Amazonian dark soil. *Soil Till. Res.* 155, 298–307. doi: 10.1016/j.still.2015.09.001

Peltoniemi, K., Fritze, H., and Laiho, R. (2009). Response of fungal and actinobacterial communities to water-level drawdown in boreal peatland sites. *Soil Biol. Biochem.* 41, 1902–1914. doi: 10.1016/j.soilbio.2009.06.018

Peltoniemi, K., Straková, P., Fritze, H., Iráizoz, P. A., Pennanen, T., and Laiho, R. (2012). How water-level drawdown modifies litter-decomposing fungal and actinobacterial communities in boreal peatlands. *Soil Biol. Biochem.* 51, 20–34. doi: 10.1016/j.soilbio.2012.04.013

Qiu, Y., Lv, W., Wang, X., Xie, Z., and Wang, Y. (2020). Long-term effects of gravel mulching and straw mulching on soil physicochemical properties and bacterial and fungal community composition in the Loess Plateau of China. *Eur. J. Soil Biol.* 98:103188. doi: 10.1016/j.ejsobi.2020.103188

Rivera-Becerril, F., van Tuinen, D., Chatagnier, O., Rouard, N., Béguet, J., Kuszala, C., et al. (2017). Impact of a pesticide cocktail (fenhexamid, folpel, deltamethrin) on the abundance of Glomeromycota in two agricultural soils. *Sci. Total Environ.* 577, 84–93. doi: 10.1016/j.scitotenv.2016.10.098

Santillán, J., López-Martínez, R., Aguilar-Rangel, E., Hernández-García, K., Vásquez-Murrieta, M., Cram, S., et al. (2021). Microbial diversity and physicochemical characteristics of tropical karst soils in the northeastern Yucatan peninsula, Mexico. *Appl. Soil Ecol.* 165:103969. doi: 10.1016/j.apsoil.2021.103969

Schneider, N., and Eugster, W. (2007). Climatic impacts of historical wetland drainage in Switzerland. *Clim. Change* 80, 301–321. doi: 10.1007/s10584-006-9120-8

Stürmer, S., Bever, J., and Morton, J. (2018). Biogeography of arbuscular mycorrhizal fungi (Glomeromycota): a phylogenetic perspective on species distribution patterns. *Mycorrhiza* 28, 587–603. doi: 10.1007/s00572-018-0864-6

Tian, J., Liu, L., Chen, H., Zhong, L., Zhou, X., Jiang, L., et al. (2022). Aerobic environments in combination with substrate additions to soil significantly reshape depth-dependent microbial distribution patterns in Zoige peatlands, China. *Appl. Soil Ecol.* 170:104252. doi: 10.1016/j.apsoil.2021.104252

Treseder, K. K., and Lennon, J. T. (2015). Fungal Traits That Drive Ecosystem Dynamics on Land. *Microbiol. Mol. Biol. Rev.* 79, 243–262. doi: 10.1128/MMBR.00001-15

Wang, J., Zheng, Y., Hu, H., Zhang, L., Li, J., and He, J. (2015). Soil pH determines the alpha diversity but not beta diversity of soil fungal community along altitude in a typical Tibetan forest ecosystem. *J. Soils Sedim.* 15, 1224–1232. doi: 10.1007/s11368-015-1070-1

Wang, S., Cheng, J., Li, T., and Liao, Y. (2020). Response of soil fungal communities to continuous cropping of flue-cured tobacco. *Sci. Rep.* 10:19911 doi: 10.1038/s41598-020-77044-8

Wiltermuth, M., and Anteau, M. (2016). Is consolidation drainage an indirect mechanism for increased abundance of cattail in northern prairie wetlands? *Wetlands Ecol. Manag.* 24, 533–544. doi: 10.1007/s11273-016-9485-z

Wu, X., Yang, J., Ruan, H., Wang, S., Yang, Y., Naeem, I., et al. (2021). The diversity and co-occurrence network of soil bacterial and fungal communities and their implications for a new indicator of grassland degradation. *Ecol. Indic.* 129:107989. doi: 10.1016/j.ecolind.2021.107989

Xiao, R., Guo, Y., Zhang, M., Pan, W., and Wang, J. J. (2020). Stronger network connectivity with lower diversity of soil fungal community was presented in coastal marshes after sixteen years of freshwater restoration. *Sci. Total Environ.* 744:140623. doi: 10.1016/j.scitotenv.2020.140623

Xie, F., Ma, A., Zhou, H., Liang, Y., Yin, J., Ma, K., et al. (2020). Revealing Fungal Communities in Alpine Wetlands through Species Diversity, Functional Diversity and Ecological Network Diversity. *Microorganisms* 8:632 doi: 10.3390/microorganisms8050632

Xu, F., Cai, T., Yang, X., and Sui, W. (2017). Soil fungal community variation by large-scale reclamation in Sanjiang plain, China. *Ann. Microbiol.* 67, 679–689. doi: 10.1007/s13213-017-1296-9

Xue, D., Chen, H., Zhan, W., Huang, X., and Liu, J. (2020). How do water table drawdown, duration of drainage and warming influence greenhouse gas emissions from drained peatlands of the Zoige Plateau? *Land Degradat. Dev.* 32, 3351–3364. doi: 10.1002/ldr.4013

Zedler, J. B. (2000). Progress in wetland restoration ecology. *Trends Ecol. Evol.* 15, 402–407. doi: 10.1016/s0169-5347(00)01959-5

Zhang, H., Yao, Z., Ma, L., Zheng, X., Wang, R., Wang, K., et al. (2019). Annual methane emissions from degraded alpine wetlands in the eastern Tibetan Plateau. *Sci. Total Environ.* 657, 1323–1333. doi: 10.1016/j.scitotenv.2018.11.443

Zhang, N., and Wang, Z. (2015). "3 Pezizomycotina: Sordariomycetes and Leotiomycetes," in *Systematics and Evolution. The Mycota (A Comprehensive Treatise on Fungi as Experimental Systems for Basic and Applied Research)*, eds D. McLaughlin and J. Spatafora (Berlin: Springer), doi: 10.1007/978-3-662-46011-5_3

Zhao, H., Li, X., Zhang, Z., Zhao, Y., Yang, J., and Zhu, Y. (2017). Species diversity and drivers of arbuscular mycorrhizal fungal communities in a semi-arid mountain in China. *PeerJ* 5:e4155. doi: 10.7717/peerj.4155

Zhao, Q., Bai, J., Gao, Y., Zhao, H., Zhang, G., and Cui, B. (2020). Shifts in the soil bacterial community along a salinity gradient in the Yellow River Delta. *Land Degrad. Develop.* 31, 2255–2267. doi: 10.1002/ldr.3594

Zhao, S., Liu, J., Banerjee, S., White, J. F., Zhou, N., Zhao, Z., et al. (2019). Not by Salinity Alone: How Environmental Factors Shape Fungal Communities in Saline Soils. *Soil Sci. Soc. Am. J.* 83, 1387–1398. doi: 10.2136/sssaj2019.03.0082

Conflict of Interest: The authors declare that the research was conducted in the absence of any commercial or financial relationships that could be construed as a potential conflict of interest.

Publisher's Note: All claims expressed in this article are solely those of the authors and do not necessarily represent those of their affiliated organizations, or those of the publisher, the editors and the reviewers. Any product that may be evaluated in this article, or claim that may be made by its manufacturer, is not guaranteed or endorsed by the publisher.

frontiers | Frontiers in Ecology and Evolution

METHODS
published: 09 June 2022
doi: 10.3389/fevo.2022.866597

PSR-BP Neural Network-Based Health Assessment of the Huangshui Plateau Urban Wetlands in China

Lingling Tong[1,2], Xufeng Mao[1,2,3], Xiuhua Song[4], Xiaoyan Wei[5]*, Wenjia Tang[3], Yanfang Deng[6], Hongyan Yu[6], Zhuo Deng[7], Feng Xiao[8], Huakun Zhou[9] and Xinan Yin[10]*

[1] Key Laboratory of Tibetan Plateau Land Surface Processes and Ecological Conservation, Ministry of Education, Qinghai Normal University, Xining, China, [2] Qinghai Province Key Laboratory of Physical Geography and Environmental Process, College of Geographical Science, Qinghai Normal University, Xining, China, [3] State Key Laboratory for Environmental Protection Monitoring and Assessment of the Qinghai-Xizang Plateau, Xining, China, [4] School of Economic and Management, Qinghai Normal University, Xining, China, [5] Management and Service Center for Huangshui National Wetland Park, Xining, China, [6] Management and Service Center of Qilian Mountain National Park, Xining, China, [7] School of Landscape Architecture, Beijing Forestry University, Beijing, China, [8] Forest and Grass Bureau of Qinghai Province, Xining, China, [9] Key Laboratory of Cold Regions Restoration Ecology, Xining, China, [10] School of Environmental Science, Beijing Normal University, Beijing, China

OPEN ACCESS

Edited by:
Haitao Wu,
Northeast Institute of Geography and Agroecology (CAS), China

Reviewed by:
Junhong Bai,
Beijing Normal University, China
Arnaldo Marín,
University of Murcia, Spain

***Correspondence:**
Xufeng Mao
maoxufeng@yeah.net
Xiaoyan Wei
weixiaoyan4477@163.com

Specialty section:
This article was submitted to Conservation and Restoration Ecology, a section of the journal Frontiers in Ecology and Evolution

Received: *31 January 2022*
Accepted: *20 May 2022*
Published: *09 June 2022*

Citation:
Tong L, Mao X, Song X, Wei X, Tang W, Deng Y, Yu H, Deng Z, Xiao F, Zhou H and Yin X (2022) PSR-BP Neural Network-Based Health Assessment of the Huangshui Plateau Urban Wetlands in China. Front. Ecol. Evol. 10:866597. doi: 10.3389/fevo.2022.866597

Wetland health assessment provides important basis for wetland restoration and management. However, it is quite tricky to select proper indicators from multiple assessment indicators that can truly reflect the health state of urban wetlands. In an attempt to address these problems, a pressure-state-response (PSR) and back propagation artificial neural network (BP) conjoined model was established for health assessment of several plateau urban wetlands in Xining City, China. The model was driven and verified through field monitoring and social questionnaire data for 4 consecutive years from 2016 to 2019. Results indicate that: (1) Eight health evaluation indexes, including population density, eutrophication level, increasing humidity, carbon dioxide absorption, air purifying, recreation, wetland management level and investment in ecological construction and protection were selected from 45 input indexes. (2) The health index of Huangshui National Wetland Park has been increasing year by year, with an average of comprehensive health score of 0.746, 0.790, 0.884, and 0.877, respectively. The indicators that contributed the most to the restoration effect were leisure and entertainment service value (2016), carbon dioxide absorption service value (2017), eutrophication (2018), and wetland management level (2019), respecially. (3) Compared with the single PSR method, the advantages of this method include; There are fewer evaluation indicators, more accurate results (excluding the interference of some highly variable indicators) and more sensitive to environmental changes. The current study proposed a novel method that may provide additional accurate and refined indicators for urban wetland health assessment.

Keywords: BP neural network, plateau urban wetland, health evaluation, evaluation index, pressure-state-response (PSR) model

INTRODUCTION

Urban wetlands refer to wetlands distributed in cities and towns (Sun et al., 2004; Robert et al., 2021). As an important part of the urban ecological environment, urban wetlands are public open space dominated by natural landscapes (Bolund and Hunhammar, 1999; Wang et al., 2006). They present many advantages, such as controlling flood and waterlogging, providing leisure and entertainment environments, and fulfilling scientific research and education purposes with their ecosystem-managing and cultural services also playing relatively important roles (Boyer and Polasky, 2004; Ho and Richardson, 2013; McInnes, 2014; Wahlroos et al., 2015; Jonathan et al., 2019; Stefanak, 2019; Wei et al., 2020; Liu et al., 2021; Li et al., 2022). Rapid urbanization has made urban wetlands one of the fastest shrinking ecosystems (Holland et al., 1995; Cui et al., 2004; Lee et al., 2006; Asomani-Boateng, 2019; Jing et al., 2020; Wang, 2020).

People are gradually realizing the importance of wetlands in urban ecological security and ecosystem services. Different scales and types of wetland ecological restoration have been carried out (Asomani-Boateng, 2019), such as the ecological restoration of Xixi National Wetland Park (Liu and Lu, 2021) and the functional restoration of the Yellow River wetland ecosystem (Xia et al., 2006) in China. Traditional wetland health assessment methods mainly include grey clustering analysis (Zhou and Xu, 2006; Zhang et al., 2013; Zou et al., 2013; Jiao et al., 2016; Wang et al., 2018; Asare et al., 2021), comprehensive index analysis and fuzzy comprehensive evaluation analysis (Zhang et al., 2010; Zhang and Yang, 2012; Wu et al., 2015; Sutton-Grier and Sandifer, 2019; Fang et al., 2021). Due to the existence of certain supervision in the weight and weight functions of each evaluation indicator, whether such health evaluation results truly reflect the health situation needs to be further explored.

Huangshui National Wetland Park, located in a plateau city in China, consists of rivers and artificial wetlands. Since a pilot scheme was launched in 2013, a series of restoration projects have been carried out. The transformation of sponge city, that is, the combination of wetland natural ecology and green technology to form a rainwater and flood control and utilization system (Hu et al., 2017; Ahn and Schmidt, 2019), has improved the hydrological cycle and water ecosystem, and the CHI (comprehensive health index) has increased from 0.568 in 2018 to 0.620 in 2019. Bird habitat islands and wetland plant plantings have put in place to create habitats for wild birds. The species of wild birds has increased from 89 in 2017 to 116 in 2019 (an increase of 27 species) at a rate of 30.33% (Mao et al., 2019); Biological monitoring technology, isotope analysis technology, and ecological network analysis technology have been adopted to create large enclosure systems for continuous monitoring, and build a quantitative lake ecological network model. Treatment of algal blooms facilitates the improvement of water quality, and the total phosphorus in water quality has improved from class V to class II and III during the treatment period (Mao and Wei, 2015; Mao et al., 2019; Wu et al., 2021). However, because restoration projects are often carried out with a specific goal, the final restoration effect exhibit significant differences. These differences include (1) time difference: while the initial effect of the restoration project was good, the effect diminished due to a lack of maintenance and investment in the later stage; (2) spatial difference: the effect of the restoration area was superior, but with unacceptable effect of the unrestored area; (3) differences in response indicators: for example, while dredging may bring about an improvement in water quality, it may also have a negative impact on benthic organisms. Thus, eventually, the health evaluation results document significant differences and variations, and it is difficult to find indicators that truly represent the health of wetland ecosystems (Mao et al., 2019).

The BP neural network is a non-linear dynamic system built on artificial intelligence (Rheinhardt et al., 1997; Cao et al., 2006; Bian et al., 2014; Wu and Feng, 2018; Wei et al., 2021). Due to the characteristics of self-learning and self-adaptation, the weights and thresholds of the network are transformed according to the existing information in the data to reduce artificial factors and better fit the relationship between evaluation indicators and wetland health (Kuo et al., 2007; Hanbay et al., 2008; Ferreira et al., 2011; Han et al., 2021). On one hand, if pressure-state-response (PSR) with BP artificial neural networks are combined, the pressure, state, and response indicators are to the greatest extent incorporated into the health evaluation indicators; on the other hand, the self-learning and adaptive ability of the BP artificial neural network are utilized. This indicates the advantage of a stronger and better fitting ability of the relationship between evaluation indicators and wetland health. This strategy may be part of the measures to screen for indicators that truly reflect the health of urban wetland ecosystems. Taking Xining Huangshui Wetlands as the research areas, supported by field plant quadrats, environmental monitoring data, and social survey data from 2016 to 2019, this study used the Analytic Hierarchy Process (AHP) method to provide comprehensive index weight, and construct a comprehensive health evaluation model suitable for plateau city wetlands based on the PSR-BP neural network model. This is aimed at finding the evaluation factors suitable for plateau city wetland health, evaluate the health status of wetland restoration, find the synergy and trade-off relationship between wetland ecosystem evaluation factors, score the key influencing factors of national wetland health in plateau cities, and provide key methods and theoretical support for wetland improvement and protection projects in plateau cities.

STUDY AREA

The study area is located in the urban area of Xining City, Qinghai Province (**Figure 1**). It is located in the eastern part of Qinghai Province and the middle of Hehuang Valley, with an average altitude of around 2,261 m. The terrain is high in the northwest and low in the southeast, belonging to the plateau cold temperate semi-arid climate zone, with low air pressure, long sunshine, and large temperature difference between day and night. The annual average temperature is 5.0°C, and the average precipitation is

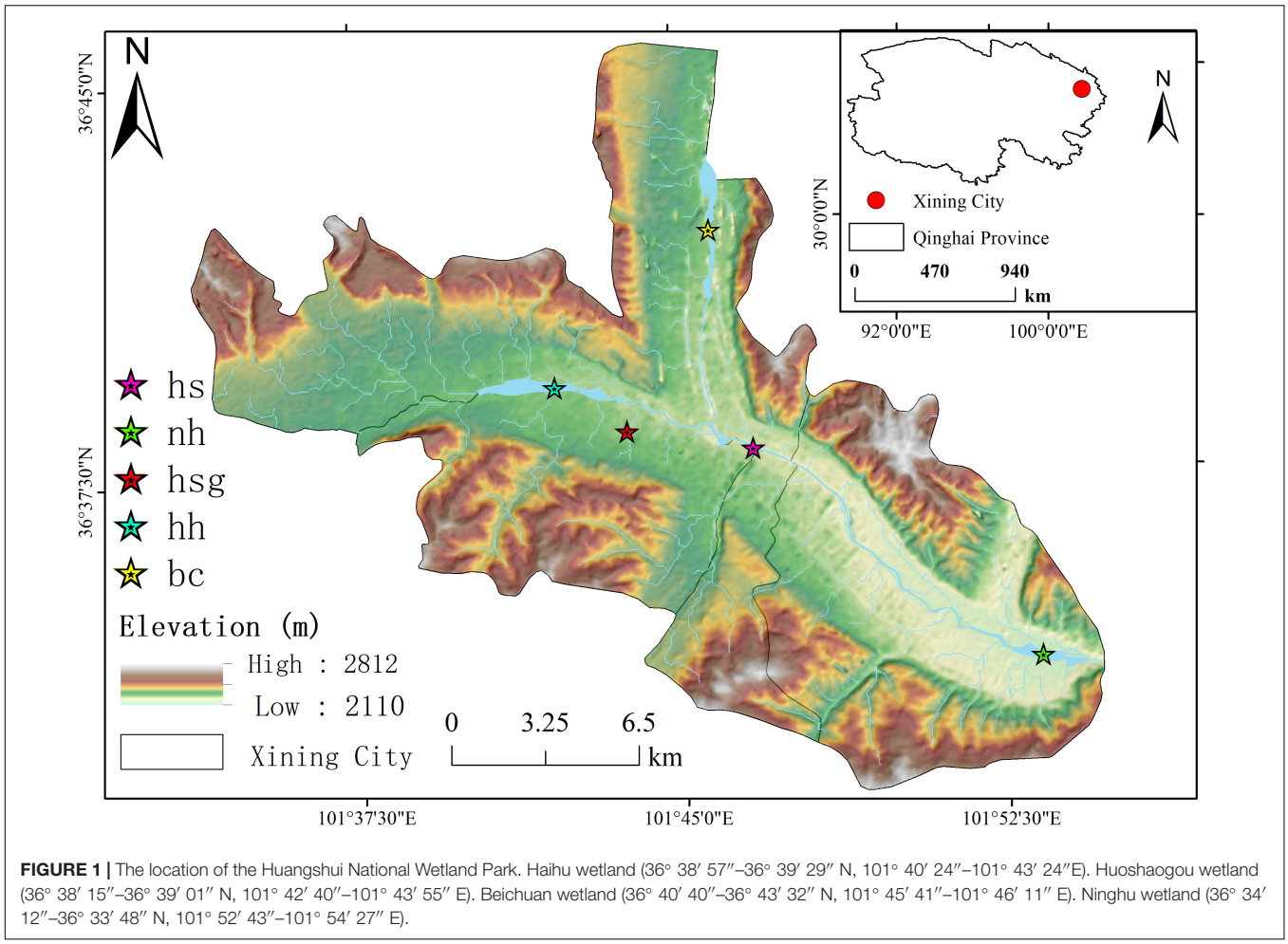

FIGURE 1 | The location of the Huangshui National Wetland Park. Haihu wetland (36° 38′ 57″–36° 39′ 29″ N, 101° 40′ 24″–101° 43′ 24″E). Huoshaogou wetland (36° 38′ 15″–36° 39′ 01″ N, 101° 42′ 40″–101° 43′ 55″ E). Beichuan wetland (36° 40′ 40″–36° 43′ 32″ N, 101° 45′ 41″–101° 46′ 11″ E). Ninghu wetland (36° 34′ 12″–36° 33′ 48″ N, 101° 52′ 43″–101° 54′ 27″ E).

506.4 mm. The annual sunshine time is 2,390.1 h, and the annual average wind speed is 2.0 m/s.

The Huangshui National Wetland Park is located in an urban area. The surrounding residential areas, commercial areas, and roads are dense, with several sources of pollution and poor water quality. Among them, the Haihu wetland and Huoshaogou were transformed into sponge cities in 2016. With purification capacity of the wetland ecological treatment system and the restoration capacity of the water ecosystem, the functioning of the bird habitat strengthened, and the functions of science popularization, publicity and education, leisure and entertainment further improved, wetland ecosystem services have gradually stabilized. Beichuan wetland has a large water area. Ninghu wetland is an artificial wetland. In 2017, wetland vegetation ecological restoration and bird habitat restoration were undertaken for the two wetlands simultaneously, so that the water quality was purified and the biodiversity was improved. However, in this process of sponge city reconstruction, wetland vegetation restoration and bird habitat restoration, along with other ecological restoration projects such as water quality restoration, there are temporal and spatial differences in the effect of ecological restoration. Further impacts of the performance of different indicators may also be good or bad, making it difficult to carry out a scientific evaluation of the effect of wetland restoration.

MATERIALS AND METHODS

The Pressure-State-Response-Back Propagation Neural Network Assessment Model

Pressure-state-response-BP neural network evaluation model is a model established by the combination of PSR model (Zhang et al., 2010) and BP neural network assessment model (Han et al., 2021). According to the PSR model, we selected the pressure-state-response index, a total of 45 wetland evaluation indexes, and gave the index weight according to the AHP method and Delphi method, and established the general PSR wetland health evaluation model to evaluate the wetland health status. 45 indexes selected based on PSR model were used as the input layer of BP neural network model to output the weight of 45 indexes. Finally, 8 wetland evaluation indexes with large weight were selected to establish PSR-BP neural network wetland health evaluation model.

Methods

Normalization Treatment on Pressure-State-Response Indicators

We used the 2016-2019 field monitoring, experimental, and social survey data, as well as Qinghai Provincial Statistical Yearbook data as the basis, and converted them into the pressure, state, and response indicators (**Supplementary Table 1**). According to the above pressure state response index and index scoring standard, data were standardized in combination with the formula (1), so that the value was between 0 and 1.

$$x_i^{'} = \frac{X_i}{\sum_{i=1}^{m} X_i} \quad (1)$$

Where m is the number of samples.

Analytic Hierarchy Process and Delphi Method

Specific evaluation methods: Based on the combination of AHP and Delphi, the judgment matrix of the relative importance of the criteria layer indicators was constructed (**Table 1**). After the consistency test formula passed (CR = 0.03319 < 0.1), the weight of the three-criteria-layer indicators of pressure index, state index, and response index was calculated as 0.258, 0.637, and 0.105, respectively.

$$CI = \frac{\lambda_{max} - n}{n - 1} \quad (2)$$

$$CR = \frac{CI}{RI} \quad (3)$$

Back Propagation Neural Network Methodology

The Huangshui wetland health assessment network model was formed by the Levenberg Marquardt algorithm. The network used the mean square error algorithm to compute the error, and the maximum allowable number of iterations was 1,000. (1) Input layer: the health evaluation indicators of the Huangshui National Wetland Park served as the input layer of the model, and there were 45 input nodes. (2) Output layer: the comprehensive health evaluation index of the Huangshui National Wetland Park was invoked as the output layer of the model, and there was one output node. (3) Hidden layer: as the calculation method of the node number of this layer has not yet displayed a definite regularity, the empirical formula was used. (4) In the formula, the number of hidden layer nodes is n; the number of input layer nodes is m; the number of output layer nodes a; l is a random integer from 1 to 10. The calculated number of hidden layer nodes varied from 7 to 16. When the mean square error (MSE) reached the minimum, the corresponding optimal number of nodes was $n = \sqrt{m + a} + l$(Mo et al., 2009). (2) The average value and standard deviation of the eight selected evaluation indexes are presented in the **Supplementary Material**.

Comprehensive Health Index

Combined with the results of wetland monitoring data from 2016 to 2019, the scoring criteria for the restoration effect of each evaluation index of wetland were probed, and Comprehensive Health Index (CHI) was used for wetland health evaluation. After the BP neural network model determined the index weight of the sub criterion layer, the expert scoring method was used to identify the pressure, state and response index weight of the criterion layer, and complete the weighting of all standardized index values. The CHI of each wetland park was obtained according to the calculation formula (4)

$$CHI = \sum_{i=1}^{m} W_i \cdot X_i \quad (4)$$

Where Wi is the comprehensive weight of each indicator, and Xi is the health index.

A three-layer BP neural network model was established based on the Neural Net Fitting toolbox in MATLAB, and a PSR-BP neural network-based wetland health assessment model was constructed (**Figure 2**).

Trade-Off Analysis and Driving Factors Analysis

The trade-off analysis of urban health assessment indicators mainly adopted the Pearson correlations correlation analysis method. This analysis is primarily used to assess the correlation degree between multiple index factors. SPSS27 was used to analyze the correlation of the weight of Huangshui humidity health assessment index of 45 plateau cities extracted from the BP neural network model.

Data Sources

The monitoring data were collected from March to October every year from 2016 to 2019, and the wetland restoration area was monitored and sampled for details (**Supplementary Table 1**). Remote sensing data were obtained from the Geospatial Data Cloud website. After interpretation of remote sensing images in 2021, the land-use map was obtained. It was split into cultivated land, forest land, grassland, wetland, residential land, unused land and other types of land, and a general map of the study area was drawn (**Figure 1**). Bird data were obtained from the Huangshui National Wetland Park Management Office and their the Shannon-Wiener index and the evenness were calculated (Jiang, 2001). Wetland Park Management Office. Based on PSR wetland health evaluation system, 45 evaluation indexes were passed through MATLAB software when the error value is 2.635×10^{-11}, extracted the weight and threshold vector of the index. After Origin21, the average weight of 45 indicators is presented in the order from large to small, and the weights of pressure, state and response indicators were presented in a comparative bar graph; Based on PSR-BP neural network model, the comprehensive health score of Huangshui wetland were presented by superimposing columnar statistical chart with Origin21 software, and the scores of five wetlands were presented by broken line chart. The evaluation results of PSR model and PSR-BP model were presented by the standard variation curve function of Origin21 software.

TABLE 1 | Relative importance judgment matrix and ranking.

	Pressure index	Status index	Response index	Wi
Pressure index	1.00	0.33	3.00	0.258
Status index	3.00	1.00	5.00	0.637
Response index	0.33	0.20	1.00	0.105

CR = 0.03319 < 0.1.

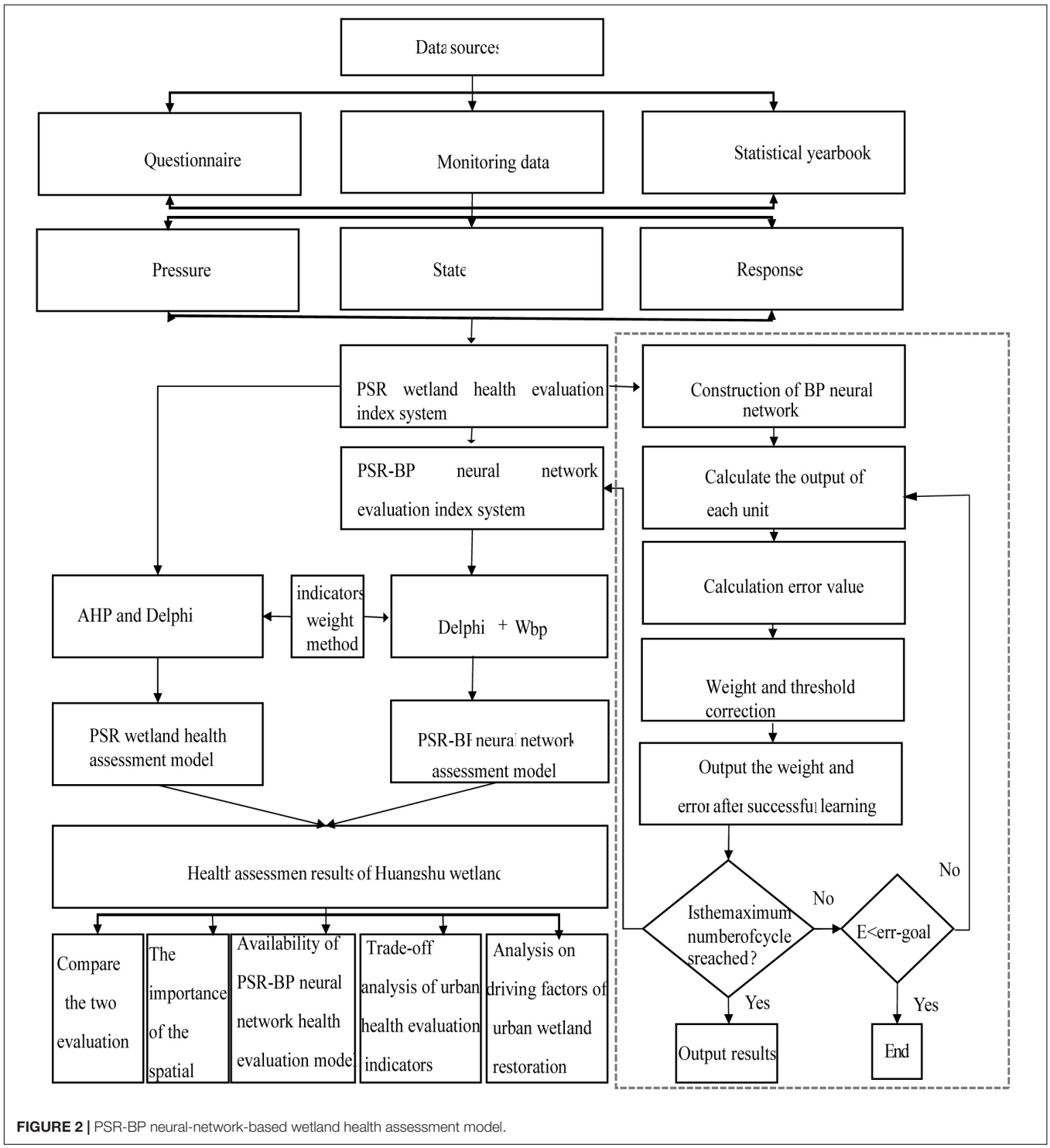

FIGURE 2 | PSR-BP neural-network-based wetland health assessment model.

RESULTS

Screening of Health Evaluation Indicators Based on the Back Propagation Neural Network Model

Based on the trained PSR-BP neural network model, the weight and threshold vector when the error value is 2.635×10^{-11} was extracted using MATLAB, and the weight mean values were presented in descending order using Origin21 (**Figure 3**). We observed that among the 45 Huangshui national wetland health evaluation indicators, the average weight of 21 indicators was positive, indicating that there were 21 evaluation indicators suitable for evaluating the health status of plateau urban wetlands. According to the average weight of the Huangshui national wetland health evaluation indicators from 2016 to 2019, the top eight indicators were identified as increasing humidity > wetland management level > eutrophication > absorption of carbon dioxide > leisure and entertainment > population density > investment in ecological construction and protection > air purification. (1) Pressure indicators: compared with natural pressure, anthropogenic pressure (population density, W = 0.083) had a more marked effect on the plateau wetland ecosystem. (2) Wetland state indicators: increasing humidity services (W = 0.110) played a positive role in promoting the healthy and sustainable development of the plateau urban wetland ecosystem, and this indicator acts jointly with carbon dioxide absorption (W = 0.093), purifying the air (W = 0.065), regulating services and entertainment (W = 0.088) to promote the healthy development of wetlands for cities with arid climates on the plateau. The improvement of water eutrophication (W = 0.093) greatly affected the evaluation index of the wetland. (3) Response indicators: obviously, the management level of wetlands (average weight = 0.107), ecological construction and protection investment (W = 0.071), and other response indicators are positively correlated with the health of wetland ecosystems. Therefore, to improve the management level of wetland factors, it is necessary to increase investment in wetland ecological construction and protection to improve the wetland ecosystem, and to promote sustainable development.

FIGURE 3 | Weights of National Wetland Assessment Indicators in Plateau Cities. For the meaning of EI, please refer to the table notes.

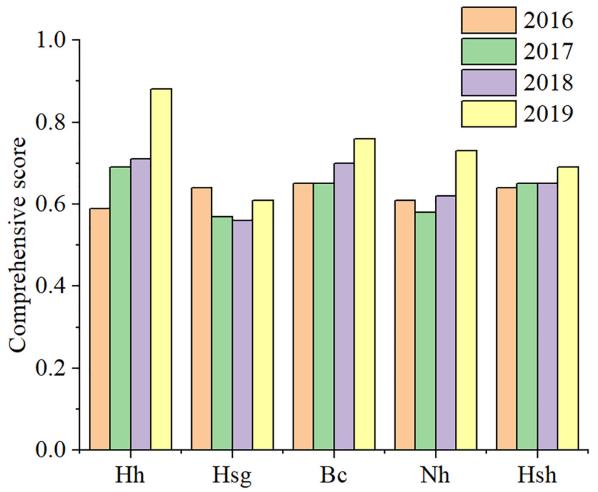

FIGURE 4 | Spatial distribution of the comprehensive health score of the Huangshui wetland based on the PSR-BP neural network. Hh (Haihu Wetland); Hsg (Huoshaogou Wetland); Bc (Beichuan Wetland); Nh (Ninghu Wetland); Hsh (Huangshuihe Wetland). Yellow represents 2016; pink represents 2017; green represents 2018; blue represents 2019.

Health Evaluation Results Using the Pressure-State-Response-Back Propagation Neural Network Method

From the health evaluation results using the PSR-BP artificial network, it can be seen that (1) the health index of the Huangshui National Wetland Park has been increasing year by year, and the comprehensive scores were 0.746 (2016), 0.790 (2017), 0.884 (2018), and 0.877 (2019); (2) the spatial variation of PSR-BP neural network health comprehensive score was Beichuan Wetland > Haihu Wetland > Huoshaogou > Huangshui River > Ninghu Wetland (**Figure 4**); (3) among the three PSR types of indicators, the state indicators had the best recovery, while the comprehensive score of the response indicators increased year by year, showing a gradually increasing impact on the restoration of the Huangshui (**Figure 5**); (4) The top indicators with a major contribution to the restoration were leisure and entertainment service value (2016), carbon dioxide absorption service (2017), eutrophication (2018), and wetland management level (2019).

Comparison Between Pressure-State-Response Based and Pressure-State-Response-Back Propagation-Based Evaluation Results

Compared with the general PSR evaluation results, the PSR-BP neural network evaluation results were found to be

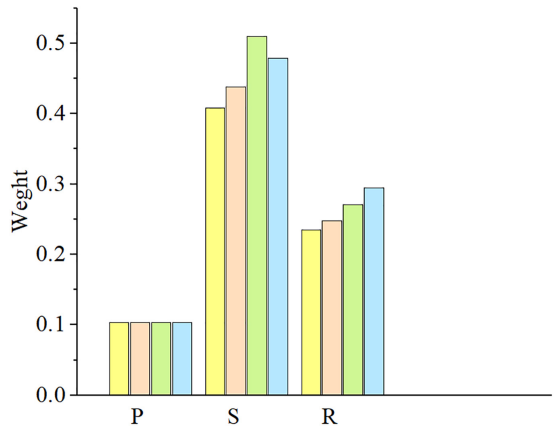

FIGURE 5 | The comprehensive score of Huangshui wetland health based on the PSR-BP neural network. Yellow represents 2016; pink represents 2017; green represents 2018; blue represents 2019. P (Pressure); S (State); R (Response).

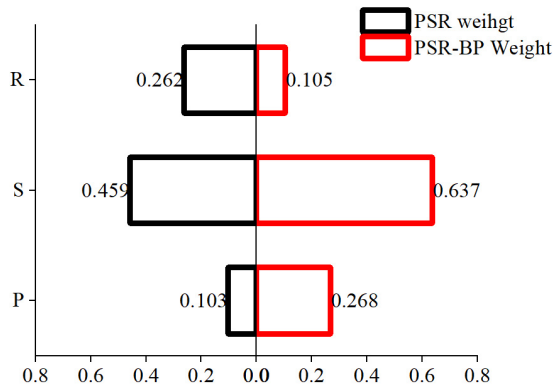

FIGURE 6 | Comprehensive score of health evaluation index of urban wetland. The black trend line A represents the health score of the Huangshui wetland obtained from the PRS-BP neural network model. The red trend line B represents the health score of the Huangshui wetland obtained from the ordinary PRS model. P (Pressure); S (State); R (Response).

parallel. For comparing the scores of the three comprehensive indicators (**Figure 6**), based on the results of the general PSR health evaluation, the weight of the stress, state, and response indicators was 0.258, 0.637, and 0.105, respectively. The status indicators were the most important ones for the health restoration of the Huangshui wetlands (**Figure 6**). The comparison of comprehensive health scores was consistent with the evaluation outcome of the previous result documenting an increase year by year (**Figure 7**). For the comparison of restoration contribution indicators, in the general PSR evaluation results, the indicators that contributed the most to the restoration were leisure and entertainment service value (2016), cumulative soil erosion area, land-use intensity (2017), eutrophication (2018), and plant height (2019). In 2016 and 2018, the indicators with the largest contribution to the annual recovery were consistent.

DISCUSSION

Advantages of Pressure-State-Response-Back Propagation Neural Network in Wetland Evaluation

The advantages of this research method lie in (1) giving the index weight: the PSR-BP neural network wetland health evaluation model adopted the combination of AHP method and BP artificial neural network to give the index weight. Compared with the single PSR model, the index weight reduced subjectivity and was more objective and accurate. (2) screening of indicators: This model was fitted with the indicator data for four consecutive years, so that the selected evaluation indicators were more in line with the recovery characteristics of the study area. (**Figures 8**, **9**) show that the trend of A curve is more in line with the wetland health status, and the evaluation indicators are more targeted and representative; The representative indicators suitable for evaluating the health of plateau urban wetland ecosystem were found: population density, eutrophication level, increasing humidity, carbon dioxide absorption, air purifying, recreation, wetland management level and investment in ecological construction and protection.

New Insights Into the Wetland Management Based on Spatial Distribution of Pressure-State-Response-Back Propagation Neural-Network-Based CHI and Trade-Off Between Indicators

The ecological environment of the wetlands in Huangshui National Wetland Park is divers, and the objectives and effects of restoration projects are different. The bird habitats and the four wetlands vegetation were restored, and the number and diversity of wild birds in the wetland were significantly improved. Among them (**Figure 10**), Beichuan, with the largest water area, had the highest Shannon-Wiener index (H = 2.91). Through the construction of constructed wetland, vegetation ecological restoration combined different vegetation reasonably (merged plants, floating plants, and floating left plants). The average richness and coverage of wetland plants increased dramatically. The average coverage of the four wetlands was up to 81% (Mao et al., 2018), and the vegetation biomass of Ninghu wetland increased significantly; The restoration projects from 2016 to 2017 mainly focused on the water purification project of Haihu wetland, and carried out external pollution control, constructed wetland construction and wetland desilting. The total phosphorus pollution of water quality was decreased, the phenomenon of eutrophication was considerably improved (**Figure 8**), and the improvement rate of wetland score was arrived at 22.10% (**Figure 4**).

Analyze the spatial differences of PSR-BP neural network based on artificial neural network, and draw new the implications for more accurate management,and conservation of alpine urban wetlands:

FIGURE 7 | Interannual variations of health score of wetlands in Huangshui. A represents the health score of the Huangshui wetland obtained from the PRS-BP neural network model. B represents the health score of the Huangshui wetland obtained from the ordinary PRS model. Hh (Haihu Wetland); Hsg (Huoshaogou Wetland); Bc (Beichuan Wetland); Nh (Ninghu Wetland); Hsh (Huangshuihe Wetland).

(1). There are significant differences in the spatial distribution of wetlands. The selection of evaluation indicators should consider the characteristics of wetland ecological environment, regional development status, risks and pressures faced, so as to improve the accuracy of the health evaluation results.

(2). The bird habitat restoration project is appropriate for wetlands with large water area and sufficient living space to ensure the safe distance of birds. At the same time, in order to prevent habitat destruction, it is necessary to reduce the Land use intensity ($P < 0.01$) and limit the water consumption for irrigated agriculture ($P < 0.05$, **Figure 11**) in the wetland, so as to improve the survival rate of birds.

(3). While considering the specific water pollution indicators, the water purification measures should strengthen the external pollution control (domestic sewage, urban road surface rainwater and industrial sewage) to control the source and intercept the sewage, so as to ensure the improvement and play of the ecological purification function of the wetland.

(4). Considering the characteristics of wetland environmental pollution, the vegetation reorganization of constructed wetland fully combines the purification function of wetland on the botanical characteristics of plants. Targeted plant reorganization can purify the main pollutants, improve the green space coverage and improve the carbon dioxide fixation of wetland ($r = 0.746$, $P < 0.01$).

Uncertainty or Deficiency of the Model

Effective evaluation results require accurate analysis and evaluation of the sources uncertainty (Hines et al., 2018). Here we calculated the average values of three secondary level indicators (Pressure, State, and Response) and their standard deviation (± SD) to evaluate the potential uncertainty of the assessment affected by time and space (**Figure 12**).

Time and space lead to the uncertainty of indicators, resulting in the difference of model evaluation results. Because the average uncertainty of spatial distribution index is so 0.5, which is about 4.26% of the average comprehensive score of the study area,

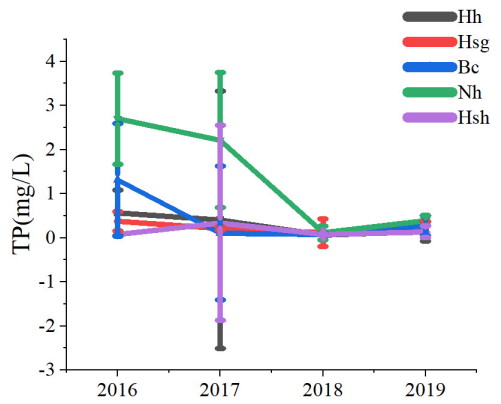

FIGURE 8 | Annual changes of eutrophication in Huangshui wetland. TP (Total Phosphorus), The unit of concentration is mg/L; Hh (Haihu Wetland); Hsg (Huoshaogou Wetland); Bc (Beichuan Wetland); Nh (Ninghu Wetland); Hsh (Huangshuihe Wetland).

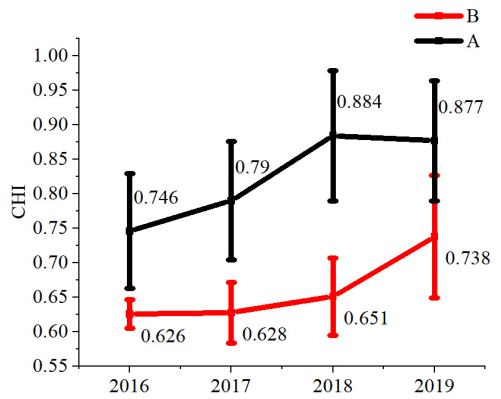

FIGURE 9 | The red trend line indicates the health evaluation results of the ordinary PSR model. The black trend line represents the health evaluation results of the PSR-BP neural network model.

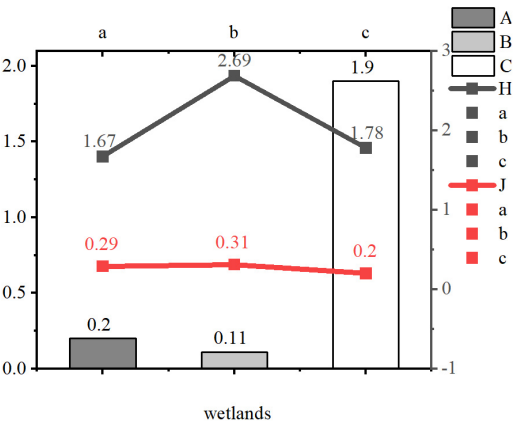

FIGURE 10 | (a): "H" is the Shannon Wiener index of birds in 2019. "J" is the Pielou uniformity index of birds in 2019. "a": Haihu wetland. "b": Beichuan wetland. "c": Ninghu wetland. "A": Increase rate of wild bird species in 2018-2019. "B": Increase rate of waterfowl in 2018-2019. "C": Increase rate of waterfowl in 2018-2019.

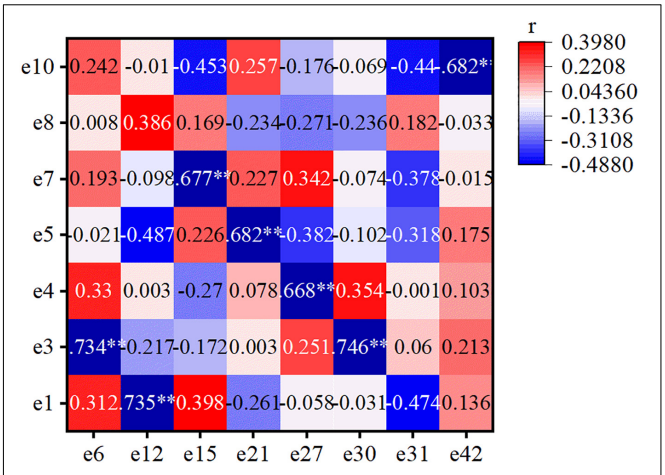

FIGURE 11 | Correlation analysis of the evaluation indicators for the plateau urban national wetland in Huangshui. Population density e1; green coverage rate of the built-up area e3; cumulative area under soil erosion control e4; number of tourists e5; sewage treatment e6; land use intensity e7; sewage discharge e8; ecological environment hydration e10; low temperature e12; wildlife survival rates e15; dissolved oxygen e21; total nitrogen e27; absorb carbon dioxide e30; oxygen release e31; disposition of surrounding population e42.

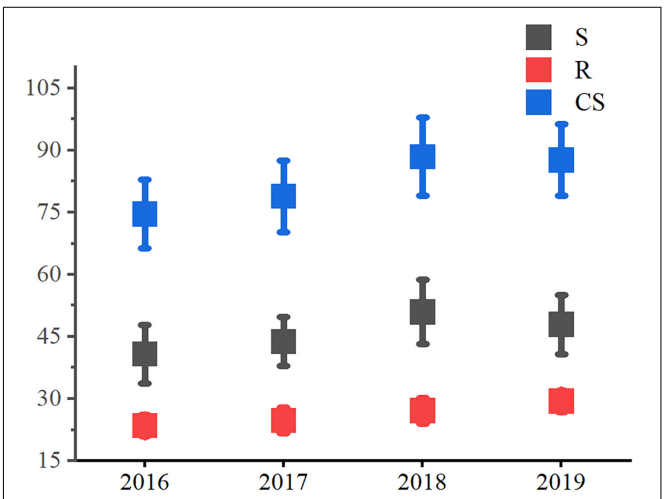

FIGURE 12 | Uncertainty analyses of assessment of four wetlands. "a": Haihu wetland. "b":Huoshaogou wetland. "c": Beichuan wetland. "d": Ninghu wetland. "e": Huangshuihe wetland. "S": Average score of state indexes. "R": Average score of response indexes. "Cs": Average score of comprehensive health score.

the average uncertainty of status index (4.48%) > the average uncertainty of response index (2.51%); Under the influence of time change, the average uncertainty is nd play of thnting for about 6% of the average comprehensive score of the wetland in the study area. The average uncertainty of state index and response index is 6.94 and 2.83% respectively; the error caused by artificial selection of neural network nodes increases the uncertainty of index weight.

Taking Beichuan as an example, its CRS ranges from 75.64 to 91.11, which is owned by a fairly good level. The pressure

of traffic and population around the spatial distribution increases gradually, and the average uncertainty is 7.73%. The climate change over time has an effect on the wetland evaluation results. Owing to the uncertainty, the uncertainty of different evaluation indicators of wetlands with different temporal and spatial distribution is different. In general, the uncertainty of state indicators is the largest.

CONCLUSION

Given China's fast urbanization and eco-desires under the latest discourse on ecological civilization, the exploration focus of researchers is to find suitable ecological evaluation methods for urban wetlands (Wang, 2020). By combining PSR and BP artificial neural network models, a health evaluation model of plateau urban wetlands was built by using AHP and other methods, and a health evaluation model of plateau urban wetlands including 3 comprehensive indices and 45 evaluation indicators was constructed. The fitting results were of high quality, revealing the weight of the evaluation indicators of plateau urban wetlands and their synergy and trade-off relationship, and finding the evaluation factors that can truly evaluate the health of plateau urban wetlands. We used model to evaluate comprehensive health of wetlands from 2016 to 2019.

(1). The proposed method selects seven effective evaluation indexes, including the pressure index in PSR model: population density. Status indicators include humidity, eutrophication, carbon dioxide absorption and entertainment. Response indicators include wetland management level, ecological construction and protection investment.
(2). The evaluation results show that from 2016 to 2019, after taking wetland ecological restoration measures, the interannual comprehensive average score increased from 0.746 (2016) to 0.877 (2019). The overall health index of urban wetlands in the plateau has increased, indicating that ecological restoration has played an active role.
(3). Compared with the single PSR method, the PRS-BP model selects 8 indicators suitable for evaluating the health of plateau wetlands. Therefore, this model only evaluates 8 evaluation indicators, which is simple and operable. The time span of BP neural network model fitting index data is large. According to the output weight of the model, interference of highly variable indexes is eliminated, and the evaluation result is more accurate and reasonable. ”

DATA AVAILABILITY STATEMENT

The datasets presented in this article are not readily available because none. Requests to access the datasets should be directed to LT, https://data.cnki.net/area/Yearbook/Single/N2020110002?z=D29.

ETHICS STATEMENT

The sample collection in this study was approved by the Management Committee of the Huangshui National Constructed Wetland.

AUTHOR CONTRIBUTIONS

LT, XM, and XW wrote the manuscript and performed the statistical analysis. XS, WT, YD, HY, ZD, FX, HZ, and XY contributed to the field and laboratory experiments. All authors contributed model construction, data analysis and manuscript revision.

FUNDING

The study was supported in part by the National Natural Science Foundation of China (Project No. 51669028), "Western Young Scholars" project of the Chinese Academy of Sciences and Qinghai Provincial Key Laboratory of Natural Geography and Environmental Process (2020-zj-y06).

ACKNOWLEDGMENTS

We would appreciate two reviewer's valuable comments on our manuscript. We would also appreciate Xianming Yang, Kai Du, Yanxiang Jin, Xin Jin, and Nana Zhang for their help in field work.

SUPPLEMENTARY MATERIAL

The Supplementary Material for this article can be found online at: https://www.frontiersin.org/articles/10.3389/fevo.2022.866597/full#supplementary-material

REFERENCES

Ahn, C., and Schmidt, S. (2019). Designing wetlands as an essential infrastructural element for urban development in the era of climate change. *Sustainability* 11:1920. doi: 10.3390/su11071920

Asare, E. A., Assim, Z. B., Wahi, R. B., Tahir, R. B., and Droepenu, E. K. (2021). Application of fuzzy evaluation technique and grey clustering method for water quality assessment of the coastal and estuaries of selected rivers in Sarawak. *Bull. Natl. Res. Centre* 45, 156–167. doi: 10.1186/s42269-021-00616-9

Asomani-Boateng, R. (2019). Urban wetland planning and management in Ghana: a disappointing implementation. *Wetlands* 39, 251–261. doi: 10.1007/s13157-018-1105-7

Bian, J. M., Hu, Y. X., Li, Y. S., Ma, Y. X., and Bian, J. (2014). Study on water quality evaluation in the source area of Liaohe River based on BP neural network. *Soil Water Conserv. Res.* 21, 147–151. doi: 10.13869/j.cnki.rswc.2014.01.029

Bolund, P., and Hunhammar, S. (1999). Ecosystem services in urban areas. *Ecol. Econ.* 29, 293–301. doi: 10.1016/S0921-8009(99)00013-0

Boyer, T., and Polasky, S. (2004). Valuing urban wetlands: a review of nonmarket valuations studies. *Wetlands* 24, 744–745. doi: 10.1672/0277-52122004

Cao, J. F., Ping, J. H., Oumar, S., Jiang, J. Y., Shen, Y. Y., and Qin, L. J. (2006). Application of improved BP neural network in groundwater environmental quality assessment. *Adv. Water Resour. Hydropower Sci. Technol.* 26, 21–23.

Costanza, R. (1992). Ecological economics: the science and management of sustainability. *Am. J. Agric. Econ.* 7, 170–171.

Cui, B. S., Yang, Z. F., Li, Y. H., Zhang, K. G., and Zhao, X. S. (2004). Comprehensive protection and development of wetland in urban expansion. *J. Nat. Resour.* 19, 462–471.

Fang, X. S., Liu, S., Chen, W. Z., and Wu, R. Z. (2021). An effective method for wetland park health assessment: a case study of the Guangdong Xinhui National Wetland Park in the Pearl River Delta, China. *Wetlands* 41:44. doi: 10.1007/s13157-021-01418-5

Ferreira, N. C., Bonetti, C., and Seiffert, W. Q. (2011). Hydrological and water quality indices as management tools in marine shrimp culture. *Aquaculture* 318, 425–433. doi: 10.1016/j.aquaculture.2011.05.045

Han, Y., He, F., Chen, Y., Qin, W., Yu, H., and Xu, D. (2021). Quality assessment of protein docking models based on graph neural network. *Front. Bioinform.* 1:693211. doi: 10.3389/fbinf.2021.693211

Hanbay, D., Turkoglu, I., and Demir, Y. (2008). Prediction of wastewater treatment plant performance based on wavelet packet decomposition and neural networks. *Expert Syst. Appl.* 34, 1038–1043. doi: 10.1016/j.eswa.2006.10.030

Hines, D. E., Ray, S., and Borrett, S. R. (2018). Uncertainty analyses for ecological network únalysis enable stronger inferences. *Environ. Model. Softw.* 101, 117–127. doi: 10.1016/j.envsoft.2017.12.011

Ho, M., and Richardson, C. J. (2013). A five year study of floristic succession in a restored urban wetland. *Ecol. Eng.* 61, 511–518. doi: 10.1016/j.ecoleng.2013.05.001

Holland, C. C., Honea, J. E., Gwin, S. E., and Kentula, M. E. (1995). Wetland degradation and loss in the rapidly urbanizing area of Portland, Oregon. *Wetland* 15, 336–345. doi: 10.1007/BF03160888

Hu, S., Niu, Z., Chen, Y., Li, L., and Zhang, H. (2017). Global Wetlands: potential distribution, wetland loss, and status. *Sci. Total Environ.* 586, 319–327. doi: 10.1016/j.scitotenv.2017.02.001

Jiao, J. L., Ren, H. L., and Sun, S. Z. (2016). Assessment of surface ship environment adaptability in seaways: a fuzzy comprehensive evaluation method. *Int. J. Naval Archit. Ocean Eng.* 8, 344–359. doi: 10.1016/j.ijnaoe.2016.05.002

Jiang, T. (2001). Principles of animal ecology. *Acta Ecol. Sin.* 11:1868.

Jing, B. Z., Wu, J., and Gong, Y. Z. (2020). Valuing wetland ecosystem services based on benefit transfer: a meta-analysis of China wetland studies. *J. Clean. Prod.* 276:122988. doi: 10.1016/j.jclepro.2020.122988

Jonathan, P. R., Andrew, T. K., Emily, A. S., Victor, H., Chris, N., Ruth, C., et al. (2019). The application of wearable technology to quantify health and wellbeing co-benefits from urban wetlands. *Front. Psychol.* 10:1840. doi: 10.3389/fpsyg.2019.01840

Kuo, J. T., Hsieh, M. H., Lung, W. S., and She, N. (2007). Using artificial neural network for reservoir eutrophication prediction. *Ecol. Model.* 200, 171–177. doi: 10.1016/j.ecolmodel.2006.06.018

Lee, S. Y., Dunn, R. J. K., Young, R. A., Connolly, R. M., Dale, P. E. R., Dehayr, R., et al. (2006). Impact of urbanization on coastal wetland structure and function. *Austral Ecol.* 31, 149–163. doi: 10.1111/j.1442-9993.2006.01581.x

Li, H., Wang, X., Wei, H., Xia, T., Liu, M., and Ai, S. (2022). Geographical distribution and driving meteorological forces of facial expressions of visitors in urban wetland parks in eastern China. *Front. Earth Sci.* 10:781204. doi: 10.3389/feart.2022.781204

Liu, F., and Lu, J. B. (2021). Ecological engineering approaches to restoring the aquatic biological community of an urban pond ecosystem and its effects on water quality – a case study of the urban Xixi National Wetland Park in China. *Knowl. Manag. Aquat. Ecosyst.* 422:24. doi: 10.1051/kmae/2021024

Liu, P., Liu, M., Xia, T., Wang, Y., and Wei, H. (2021). Can urban forest settings evoke positive emotion? Evidence on facial expressions and detection of driving factors. *Sustainability* 13:8687. doi: 10.3390/su13168687

Mao, X. F., and Wei, X. Y. (2015). The spatial and temporal distribution of chlorophyll a and its influencing factors in an eutrophic lake. *Environ. Monitor. China* 31, 65–70. doi: 10.19316/j.issn.1002-6002.2015.06.012

Mao, X. F., Wei, X. Y., Jin, X., Tao, Y. Q., Zhang, Z. F., Wang, W. Y., et al. (2019). Monitoring urban wetlands restoration in Qinghai Plateau: integrated performance from ecological characters, ecological processes to ecosystem services. *Ecol. Indic.* 101, 623–631. doi: 10.1016/j.ecolind.2019.01.066

Mao, X. F., Wei, X. Y., Yuan, D. H., Jin, Y., and Jin, X. (2018). An ecological-network-analysis based perspective on the biological control of algal blooms in Ulansuhai Lake, China. *Ecol. Model.* 386, 11–19. doi: 10.1016/j.ecolmodel.2018.07.020

McInnes, R. J. (2014). Recognising wetland ecosystem services within urban case studies. *Mar. Freshw. Res.* 65, 575–588. doi: 10.1071/MF13006

Mo, M. H., Wang, X. L., Wu, H. J., Cai, S. M., Zhang, X. Y., and Wang, H. L. (2009). Ecosystem health assessment of Honghu Lake Wetland of China using artificial neural network approach. *Chin. Geograph. Sci.* 19, 349–356. doi: 10.1007/s11769-009-0349-9

Rheinhardt, R. D., Brinson, M. M., and Paul, M. F. (1997). Applying wetland reference data to functional assessment, mitigation and restoration. *Wetlands* 17, 195–215.

Robert, J. R., Donagh, H., and Jennifer, J. R. (2021). Integrating artificial urban wetlands into communities: a pathway to carbon zero? *Front. Built Environ.* 7:777383. doi: 10.3389/fbuil.2021.777383

Stefanak, A. I. (2019). The role of constructed wetlands as green infrastructure for sustainable urban water management. *Sustainability* 11:6981. doi: 10.3390/su11246981

Sun, W. G., Wang, H. X., and Yu, S. P. (2004). The advance of urban wetland study. *Prog. Geogr.* 23, 94–100.

Sutton-Grier, A. E., and Sandifer, P. A. (2019). Conservation of wetlands and other coastal ecosystems: a commentary on their value to protect biodiversity, reduce disaster impacts, and promote human health and well-being. *Wetlands* 39, 1295–1302. doi: 10.1007/s13157-018-1039-0

Wahlroos, O., Valkama, P., Mäkinen, E., Ojala, A., Vasander, H., Väänänen, V. M., et al. (2015). Urban wetland parks in Finland: improving water quality and creating endangered habitats. *Int. J. Biodivers. Sci. Ecosyst. Serv. Manag.* 11, 46–60. doi: 10.1080/21513732.2015.1006681

Wang, H. X., Sun, G. Y., Gong, H. L., and Yu, S. P. (2006). Characteristics of urban wetland and its construction policies upon the sustainable development strategy in Beijing. *J. Arid Land Resour. Environ.* 20, 94–100.

Wang, J., Wang, X., Zhang, X. H., Li, H. C., Lei, X. H., Wang, H., et al. (2018). Application of grey clustering method based on improved analytic hierarchy process in water quality evaluation. *MATEC Web Conf.* 246:02004. doi: 10.1051/matecconf/201824602004

Wang, T. (2020). Wetland governance: contested aspirations and reflexive roles of local professionals toward Worlding cities in tai lake basin. *Front. Environ. Sci.* 8:577357. doi: 10.3389/fenvs.2020.577357

Wei, H., Ma, B., Hauer, R. J., Liu, C., Chen, X., and He, X. (2020). Relationship between environmental factors and facial expressions of visitors during the urban forest experience. *Urban For. Urban Green.* 53:126699. doi: 10.1016/j.ufug.2020.12669

Wei, M., Zheng, Z., Bai, X., Lin, J., and Taghizadeh-Hesary, F. (2021). Application of rough set and neural network in water energy utilization. *Front. Energy Res.* 9:604660. doi: 10.3389/fenrg.2021.604660

Wu, J. M., Xu, D., He, F., He, J., and Wu, Z. B. (2015). Comprehensive evaluation of substrates in vertical-flow constructed wetlands for domestic wastewater treatment. *Water Pract. Technol.* 10, 625–632. doi: 10.2166/wpt.2015.077

Wu, Y., Mao, X. F., Zhang, Z. F., Tang, W. J., Cao, G. C., Zhou, H. K., et al. (2021). Temporal and spatial characteristics of CO_2 flux in plateau urban wetlands and their influencing factors based on eddy covariance technique. *Water* 13:1176. doi: 10.3390/w13091176

Wu, Y. C., and Feng, J. W. (2018). Development and application of artificial neural network. *Wirel. Pers. Commun.* 102, 1645–1656. doi: 10.1007/s11277-017-5224-x

Xia, H. J., Liu, L. S., Bai, J. H., Kong, W. J., Lin, K. X., and Guo, F. (2006). Wetland ecosystem service dynamics in the yellow river estuary under natural and anthropogenic stress in the past 35 years. *Ecol. Eng.* 26, 27–39. doi: 10.1007/s13157-020-01368-4

Zhang, H. Y., Sun, Y. D., Zhang, W. X., Song, Z. Y., Ding, Z. L., and Zhang, X. Q. (2021). Comprehensive evaluation of the eco-environmental vulnerability in the Yellow River Delta wetland. *Ecol. Indic.* 125:107514. doi: 10.1016/j.ecolind.2021.107514

Zhang, L. N., Wu, F. P., and Jia, P. (2013). Grey evaluation model based on reformative triangular whitenization weight function and its application in water rights allocation system. *Open Cybernet. Syst. J.* 7, 1–10. doi: 10.2174/1874110X20130521001

Zhang, M. L., and Yang, W. P. (2012). Fuzzy comprehensive evaluation method applied in the real estate investment risks research. *Phys. Procedia* 24, 1815–1821. doi: 10.1016/j.phpro.2012.02.267

Zhang, M. W., Jin, H. J., Cai, D. S., and Jiang, C. B. (2010). The comparative study on the ecological sensitivity analysis in Huixian karst wetland, China. *Procedia Environ. Sci.* 2, 386–398. doi: 10.1016/j.proenv.2010.10.043

Zhou, L. F., and Xu, S. G. (2006). Application of grey clustering method in eutrophication assessment of wetland. *J. Am. Sci.* 2, 53–58.

Zou, Q., Zhou, J. Z., Zhou, C., Song, L. X., and Guo, J. (2013). Comprehensive flood risk assessment based on set pair analysis-variable fuzzy set model and fuzzy AHP. *Stoch. Environ. Res. Risk Assess.* 27, 525–546. doi: 10.1007/s00477-012-0598-5

Conflict of Interest: The authors declare that the research was conducted in the absence of any commercial or financial relationships that could be construed as a potential conflict of interest.

frontiers | Frontiers in Ecology and Evolution

TYPE Methods
PUBLISHED 06 September 2022
DOI 10.3389/fevo.2022.979415

OPEN ACCESS

EDITED BY
Guangxuan Han,
Yantai Institute of Coastal Zone Research (CAS), China

REVIEWED BY
Maria Flavia Gravina,
University of Rome "Tor Vergata," Italy
Zhenguo Niu,
Aerospace Information Research Institute (CAS), China

*CORRESPONDENCE
Rossella Boscolo Brusà
rossella.boscolo@isprambiente.it
Federica Cacciatore
federica.cacciatore@isprambiente.it

SPECIALTY SECTION
This article was submitted to Conservation and Restoration Ecology, a section of the journal Frontiers in Ecology and Evolution

RECEIVED 27 June 2022
ACCEPTED 12 August 2022
PUBLISHED 06 September 2022

CITATION
Boscolo Brusà R, Feola A, Cacciatore F, Ponis E, Sfriso A, Franzoi P, Lizier M, Peretti P, Matticchio B, Baccetti N, Volpe V, Maniero L and Bonometto A (2022) Conservation actions for restoring the coastal lagoon habitats: Strategy and multidisciplinary approach of LIFE Lagoon Refresh. *Front. Ecol. Evol.* 10:979415. doi: 10.3389/fevo.2022.979415

Conservation actions for restoring the coastal lagoon habitats: Strategy and multidisciplinary approach of LIFE Lagoon Refresh

Rossella Boscolo Brusà[1]*, Alessandra Feola[1], Federica Cacciatore[1]*, Emanuele Ponis[1], Adriano Sfriso[2], Piero Franzoi[2], Matteo Lizier[3], Paolo Peretti[4], Bruno Matticchio[4], Nicola Baccetti[5], Valerio Volpe[6], Luigi Maniero[6] and Andrea Bonometto[1]

[1]ISPRA, Italian National Institute for Environmental Protection and Research, Venice, Italy, [2]Department of Environmental Sciences, Informatics and Statistics (DAIS), University Ca' Foscari of Venice, Venice, Italy, [3]Direzione Progetti Speciali per Venezia, Venice, Italy, [4]IPROS Environmental Engineering s.r.l., Padua, Italy, [5]ISPRA, Italian National Institute for Environmental Protection and Research, Bologna, Italy, [6]Interregional Superintendency for Public Works in Veneto, Venice, Italy

The Habitat Directive of European Union lists Costal Lagoons (habitat code 1150*) among priority habitats because they are in danger of disappearance. Natural ecosystems may recover from anthropogenic perturbations; however, the recovery can follow natural restoration or it can be redirected through ecological restoration by anthropogenic intervention. Accordingly, by collecting the available theoretical indications for restoration of estuarine and coastal areas, a methodological approach was detailed andit can be summarised into five issues: (i) Environmental context from which it began; (ii) Desired state to be achieved; (iii) Policies and socio-economic context; (iv) Typology of recovery and/or improvement of habitats and ecosystems; and (v) Methods for monitoring the impact of the project. The project strategy, management and measures of LIFE Lagoon Refresh were also presented and discussed, as a case study for the implementation of the multidisciplinary approach for restoration ecology in transitional waters. The project takes place in the northern Venice Lagoon (Italy), started in 2017 and it lasts 5 years. In the Venice Lagoon, since the 20th century, strong reductions of the typical salinity gradient of buffer areas between lagoon and mainland, and of reedbed extensions have occurred due to historic human interventions, with negative consequences on coastal lagoon habitats. To improve the conservation status of habitats and biodiversity of the area, the LIFE Lagoon Refresh project included several conservative actions, which are (i) the diversion of a freshwater flow from the Sile River into the lagoon; (ii) the restoration of intertidal morphology, through biodegradable structures; (iii) the reed and aquatic angiosperm transplantations with the involvement of local fishermen

and hunters, and (iv) the reduction of hunting and fishing pressures in the intervention area. To achieve the restoration of the lagoon environment, the strategy of the project covered a combination of different aspects and tools, such as planning activities, through the involvement of local Institutions and communities; stakeholder's involvement to increase awareness of environment conservation and socioeconomic value improvement; an ecological engineering approach; numerical models as supporting tool for planning and managing of conservation actions; environmental monitoring performed before and after the conservation actions.

KEYWORDS

Venice Lagoon, ecological restoration, salinity, reedbeds, habitats directive, birds directive, water framework directive

Introduction

In last decades, many lagoon and coastal marine ecosystems, of exceptional ecological, recreational, and commercial value, have experienced a loss of their environmental status (De Wit et al., 2020).

The European Union (EU) Habitat Directive lists, in Annex I, sites of community interest that require the designation of special areas of conservation. Among these sites, some are considered of priority interest because they are in danger of disappearance, such as the priority habitat of Coastal lagoons (Habitat code: 1150*), defined as expanses of shallow coastal saltwater, of varying salinity and water volume, wholly or partially separated from the sea by sand banks, or, less frequently, by rocks. The Habitat Directive also details information about salinity, which may vary from brackish water to hypersalinity depending on several conditions, such as rainfall, evaporation, tidal exchange, etc. (European Commission, 2013). Moreover, the EU Water Framework Directive (WFD, 2000/60/EC), aims at improving the ecological status of water bodies, such as transitional waters, advocating the pro-active approach of the restoration ecology (De Wit et al., 2020). Multiple stressors, including hydromorphological modifications, pollutants, excess of nutrient inputs, sediment budget unbalance and other ecosystem alterations, which can affect resources through single, cumulative or synergistic processes, can cause their degradation (De Wit et al., 2020). From a morphological and hydrodynamic point of view, each lagoon has peculiar characteristics closely related to the amount of freshwater inputs, tidal fluctuations and human interventions that, very often, have modified these areas either by land reclamation, or by exploitation of fish resources, or for navigation (Facca et al., 2020). The threats and pressures determining the unfavourable/bad status of European coastal lagoons are numerous. Among these, the main are: changes in water bodies conditions, pollution of surface water, fishing and harvesting of aquatic resources, direct destruction or reduction of habitats due to the construction of infrastructure (e.g., ports), dredging of shipping channels, and the creation of facilities for the regulation of hydrodynamism (Newton et al., 2014; European Environment Agency, 2021).

Natural ecosystems may recover from perturbations being able to return to the state before the disturbance (resilience). However, depending upon time scales of duration, extension and intensity of perturbations, the return to the historic trajectory of the ecosystem may: (i) follow natural restoration though secondary succession; (ii) be redirected through ecological restoration by anthropogenic intervention; or (iii) be unattainable (Borja et al., 2010).

Many theoretical indications exist concerning restoring of estuarine and coastal area; the transfer of theoretical approach for the design and actual implementation of restoration project is still an issue of high scientific interest.

The Venice Lagoon is one of the largest and most important coastal transitional ecosystems of the Mediterranean Sea (Tagliapietra et al., 2009). Human presence has constantly modified the original morphology and hydrology since the city's foundation and the Venetians tried to modify the environment in the attempt to preserve economic interests, human health and for defence purposes (Guerzoni and Tagliapietra, 2006; Solidoro et al., 2010). Among anthropogenic actions, the management of freshwater and sediment loads from the drainage-basin tributaries was particularly relevant to prevent sedimentation in marginal areas and to avoid health problems associated with malaria. The main intervention realised from the second half of the 16th century was the diversion of main rivers that flowed into the lagoon (Piave and Sile rivers in the northern lagoon, Brenta and Bacchiglione rivers in the southern lagoon). Those hydrological modifications caused profound changes in morphology and ecology of the lagoon. One of the main effects was a deficit in the sediment budget of the lagoon, that led to prevalence of erosion processes, with a strong

reduction of salt marshes and deepening of tidal flats. The reduction of hundreds cubic metres per second of freshwaters that flowed into the lagoon resulted in an increase of salinity in the inner parts and a loss of the typical salinity gradient of that environment (D'Alpaos, 2010; D'Alpaos and Carniello, 2010). The increase of salinity modified heavily habitats and ecology of those areas, leading to expansion of mudflats instead of typical lagoon oligohaline habitats. Alterations of geomorphological and physical properties clearly affected spatial distribution, structure, and composition of vegetation and fauna communities. The reedbed of *Phragmites australis* disappeared almost everywhere. Historical maps demonstrate a constant decline of salt marshes from 255 km^2 in early 1,600, to 170 km^2 in 1,900 and 47 km^2 in 2000, respectively, mainly in the inner areas, where reeds were dominant (D'Alpaos, 2010). These changes affected heavily biological communities, leading to a replacement of lagoon species with predominantly marine species, and a shift toward assemblages with more tolerance to eutrophic conditions (Solidoro et al., 2010).

In this context, LIFE Lagoon Refresh is the first project aimed at restoring salinity gradient in the Venice Lagoon, and the scope of this manuscript is illustrating the project strategy, management and measures adopted as a case study for the application of the multidisciplinary approach of restoration ecology in transitional waters. The major strengths of the study are the environmental-friendly methodology employed that did not compromise the other uses of the lagoon area, the attainability of the results obtained and the evident potential of long-term strategies of conservation and management; these are especially significant for the Venice Lagoon, which is unique in its configuration, location, ecosystem services, as well as in its historical, artistic, urban, and economic relevance.

Methodological approach

With reference to the approaches proposed by USEPA (2000), Elliott et al. (2007), and De Wit et al. (2020), the planning and execution stages of an ecological restoration project should consider five essential issues: (i) Environmental context from which it began; (ii) Desired state to be achieved; (iii) Policies and socio-economic context; (iv) Typology of recovery and/or improvement of habitats and ecosystems, and (v) Methods for monitoring the impact of the project (**Table 1**).

The collection of information should include not only chemical, physical, hydrological, geomorphological, biological, and ecological data, but also information on the existing impact and pressures, the current socio-economic uses of the area, ongoing and foreseen management plans and programmes, and any constraints and limitations. All these information contribute to the restoration process and define the baseline inventory.

Environmental context

The existing environmental information and data collected with monitoring activities before the project realisation define the site baseline condition at the beginning of the restoration process. The information on biotic and abiotic elements of the site, as well as pressures, threats and impacts, are as a key initial step to understand what the desirable and possible state is considered in terms of restoration target (Gann et al., 2019). At the same time, it is essential to take into account the socio-economic uses (fishing, hunting, farming, and tourism, etc.), the plans and programmes of the area and any constraints and limitations, to prevent further difficulties and barriers for the project implementation.

Desired state to be achieved

In an ecological restoration project, it is fundamental to have clear in mind the desired state to be achieved. As reported by Elliott et al. (2007), ecological restoration should be based on the identification of a reference state, also turning to reference site, namely areas that are comparable in structure and function to the proposed restoration site before it was degraded. When the original condition of the natural habitat is unknown, a combination of qualitative knowledge of the original habitat type with information deriving from still existing habitats can be done to provide a quantitative assessment of the state to be achieved and the expected results (Lewis, 1990). Indeed, it is possible to use both historical information on altered or destroyed sites, and/or those of similar and relatively healthy ones, as a guide for the project (Clewell and Aronson, 2013).

Restoration projects need clear goals and objectives in order to be successful. Direct implementation of goals and objectives provides standards for measuring the success; they must be linked to expected results, which should be measurable with specific indicators (Gann et al., 2019). The expected results for habitat and species restoration are given in a quantitative way, but the quantification can be decided by expert judgement referring to reference sites.

Policies and socio-economic context

Ecological restoration is a solutions-based approach that engages communities, scientists, policymakers, and land managers, thus the analysis of the policies and socio-economic context need to be considered during the development of the restoration project. In their proposal of conceptualisation, placing the ecological restorations in societal context, De Wit et al. (2020) posed two interesting questions. The first is related to the value that human populations, and particularly stakeholders, give to ecological restoration practice; with

TABLE 1 Elaboration of the theoretical elements from literature (see reference in the text).

(1)	**Environmental context from which it began**
	Chemical, physical, hydrological, geomorphological, biological, and ecological data Impacts and pressures Socio-economic uses of the area Plans and programmes of the area Constraints and limitations
(2)	**Desired state to be achieved**
	Which status to refer to? Reference state, historical reference, new status Which are the expected results? Qualitative and/or quantitative Which are the tools available to predict quantitative results? Hydrodynamic models, habitat suitability models, etc.
(3)	**Policies and socio-economic context**
	How is the ecological restoration practice evaluated by human populations and particularly by stakeholders? Involvement of stakeholder, quantification of ecosystem services Is the ecological restoration practice congruent with other type of legislation (local, national, and European, etc.)? Single low or multiple legislation aspects Is there a broader management context? Different measures in the area and/or same measures in different site of the area Is it possible to ensure the long-term viability of the restored area? Minimising the need for maintenance, favouring the self-sustainability
(4)	**Typology of recovery and/or improvement of habitats and ecosystems**
	Natural recovery once the stressor is removed Anthropogenic interventions ○ in response to a degraded or anthropogenically changed environment ○ in responses to a single stressor ○ Habitat enhancement or creation The necessary eco-engineering measures (in the cases of anthropogenic interventions) ○ Is it necessary to restore physical and/or chemical and/or morphological environments? ✓ Change in flow regimes and siltation ✓ Bottom elevation alterations ○ Is it necessary to restore biological and ecological integrity? ✓ Transplanting seagrass ✓ Transplanting reed beds
(5)	**Methods for monitoring the impact of the project**
	Choice or implementation of tools for monitoring physical, chemical, morphological, and biological parameters in a quantitative way (indicators, models, etc.) Monitoring before the project to evaluate the status zero (baseline) Monitoring during the project for finding out whether goals of Methodological approach are being achieved Applied "mid-course" adjustments. Adaptive management Monitoring post-project and evaluate whether additional actions or adjustments are needed

particular regard to their perceptions and wishes for desired states of the ecosystem. The latter is the conflicts that can arise because of different objectives and concepts, as the ecological restoration practice should be congruent with other types of legislation.

The key to ensure that both nature and society mutually benefit is to recognise the expectations and interests of stakeholders, involving them directly. All categories of stakeholders, potentially influenced by the project, such as institutions, local and national management bodies, local community, associations, fishermen, and hunters, should be analysed in the earliest stages, thus addressing to both stakeholders who could benefit or have a negative impact from restoration actions due to conflicting uses. Indeed, as reported by Gann et al. (2019), stakeholders can make or break a project.

Again, to achieve better results with ecological restoration in the policies context, the projects have to integrate strategically within larger restoration programmes. As principles of wetland restoration described by USEPA (2000), it is essential a design based on the entire watershed, not just the part of the waterbody that may be the most degraded site. Restoration plans should identify dispositions for site maintenance after project completion, and ensure the long-term viability of a restored area by minimising the need for continuous maintenance (USEPA, 2000).

Typology of recovery and/or improvement of habitats and ecosystems

Many studies in scientific literature report different typologies of recovery in aquatic habitats and ecosystems (see, e.g., Fonseca et al., 2002; Simenstad et al., 2006; Elliott et al., 2007; Bekkby et al., 2020; De Wit et al., 2020). The term "recovery" implies that a system will return to a previous condition after being in a degraded or disrupted one. The return

to the original state will be with (active recovery) or without (passive/natural recovery) human interventions. As reported by USEPA (2000), restoring the original hydrological regime of wetlands may be enough to re-establish, with time, the native flora and fauna communities.

Eco-engineering is increasingly used to recreate and restore ecosystems degraded by previous human activities by two types of approaches. The Type A approach that consists on restoring the hydrological processes and physico-chemical conditions necessary to a natural Self-improving of ecological structure and functioning, and the Type B approach that consists on a direct intervention on biota with transplanting actions (Elliott et al., 2016).

Methods for monitoring the impact of the project

Design of monitoring schemes occurs at the planning stage of the restoration project to ensure that the project's goals, objectives and indicators are measured. Chosen parameters and tools for monitoring activities depend on the conditions that the project is going to restore. Monitoring plans should be feasible in terms of costs and technologies, and should always provide relevant information to meet the project goals. The monitoring results indicate whether goals are being achieved and if it is necessary to modify actions of restoration by adaptive management. Since restoration efforts may not proceed exactly as planned, adapting a project to at least some changes or new information should be considered as normal (USEPA, 2000).

Application of the methodology to LIFE Lagoon Refresh

Project area, project site, and area of interventions

The project area is located in the northern Venice Lagoon in Italy (NATURA 2000 network codes: Sites for Community Importance, SCI, IT3250031 and Special Protection Area, SPA, IT3250046) (**Figure 1**). The surface of the SCI is 20,365 ha with 18% of the surface characterised by habitat 1,150*, 10% of habitat 1,420 (Mediterranean and thermo-Atlantic halophilous scrubs, *Sarcocornetea fruticosi*) and 8% of habitat 1,140 (Mudflats and sandflats not covered by seawater at low tide). The NATURA 2000 Standard Data Form describes this SCI as an environment characterised by salt marshes, tidal flats, channels, and river mouths with large portions occupied by typical Venetian fish farms. More than 330 species of birds are recorded in the Venice Lagoon and 66 are included in Annex I of Birds Directive (2009/147/EC), 25 of them are documented in the SCI of the northern Venice Lagoon (Bon et al., 2004). The total extension of reedbed in the SCI is of 34 ha and greater extension is close to the Dese river mouth.

The Project Site (**Figure 1**, see red line) has an extension of 1,900 ha and is located in Trezze area from Ca' Zane site to Santa Cristina Island. The Project Site falls into two of the twelve natural water bodies of the Venice Lagoon, identified in the WFD context: EC "Palude Maggiore" and PC1 "Dese," being the first as an euhaline waterbody (average salinity >30) and the latter as a polyhaline waterbody (average salinity 20–30). The freshwater flow from the watershed to the Venice Lagoon is about 34.5 m^3/s for the whole lagoon, and just about 17 m^3/s for the northern lagoon. In this area, the socio economic activities are fishing, hunting, and tourism.

The Area of Interventions (**Figure 2**, see yellow line) is about 70 ha and it is delimited by Sile river in the north, Valle Cesaro in the west, Valle Lanzoni in the east and Valle Ca' Zane in the south. In this area, along the Sile river embankment, a spillway is present. During flood events (about a dozen per year), thousands of cubic metre of freshwater spill from the river into the lagoon, without a buffer zone able to reduce nutrient load.

Hunting activities in the Venice Lagoon are very intense and there are about 600 hunting posts; three of them are placed within the Intervention Area.

The policies and socio economic context

In the Venice Lagoon, the environmental restoration has a long story. The idea of a basin-scale policy (not extended to the mainland) was contained in the "Special law for Venice" (Italian government Law no. 171/1973). During the 20th century, human activities have endangered two of the key habitats of the lagoon, the salt marshes and the aquatic angiosperm beds (Tagliapietra et al., 2018). While environmental conservation and restoration programmes (such as, Morphological plan of the Venice Lagoon; LIFE SeResto, LIFE12 NAT/IT/000331; LIFE VIMINE, LIFE12 NAT/IT/001122) have been put in place for the just cited endangered habitats, almost nothing has been done to recreate the lost salinity gradient. Indeed, LIFE Lagoon Refresh is the first project aimed at restoring salinity gradient and reedbeds in the Venice Lagoon.

The River Basin Management Plans of Eastern Alps District consider as a measure the general idea of restoration of salinity gradient and of ecotonal environments, therefore, as reported in the methodological approach, the project could be considered as a pilot example to replicate in other sites. Before investing in restoration, evidence of potential for long-term conservation management of the site was assessed. Indeed, the developed hydraulic and morphological works are environmental-friendly, having a very low maintenance. Moreover, the principal public authorities, responsible for the

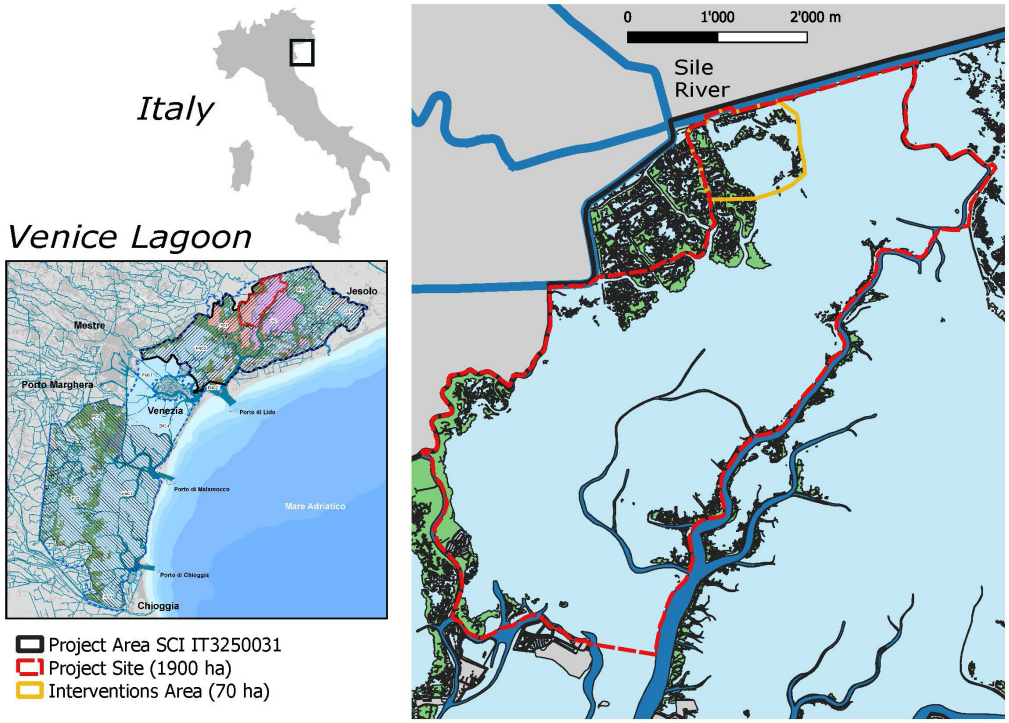

FIGURE 1
Project area, project site, and interventions area of the life lagoon refresh project.

management and safeguard of the Venice Lagoon, are partners of the project and agreed to pursuit their efforts in the area still after the project lifecycle.

Stakeholders' analysis identified a large spectrum of categories potentially interested by the project: national and local authorities, Reclamation Consortia, fishermen's, and hunters' organisations and people attending the northern Venice Lagoon. A Regional Environmental Impact Study was carried out for the Project. The District Authority of the Eastern Alps and Regional Directorate for Environmental Assessments played a fundamental role in the approval process. The environmental regulations they referred to assess the compliance of the project were the WFD, Habitat and Birds Directives, respectively, and all of them refer to river and lagoon environments. Therefore, it was necessary to verify the compliance with minimum in-stream flow of the Water Protection Plan of Veneto Region in accordance with the environmental objectives for rivers defined by WFD. The Sile river waters are also used for drinking and for irrigation purposes in agriculture. Therefore, it was necessary to verify with Water Authority and Reclamation Consortium that the flow of 1,000 l/s would not compromise those uses and the diversion would not worsen salt intrusion.

In the Venice Lagoon, fishing and hunting activities are regulated by a Regional fishing plan and a wildlife-hunting plan, respectively. Any modifications in fishing and hunting rules must be discussed and coordinated with Regional competent institutions.

In the northern Venice Lagoon, there are about twenty-two fishermen's and hunters' organisations for a total of about 4,000 people, therefore sharing the project and its aims was essential. In this context, a kind of wasp-waist strategy was adopted as following. In the planning stages, the project was discussed with two/three key representatives of fishermen and hunters, highly sensitive to environmental issues. They introduced LIFE Lagoon Refresh referents to the presidents of the associations, and a collaboration was established to involve the government boards of the associations. LIFE Lagoon Refresh staff met the boards to explain them the project, the goals, the conservative actions and the intention to involve fishermen and hunters in specific concrete actions of the project, namely in transplantations of reeds and aquatic plants. In this way, the project met consensus among them by working together, and it reached a very important goal, that is to relocate the three hunting posts outside of the project area of interventions.

Restoration goals and expected results

The effective condition of natural habitats in the project area before rivers' diversions could not be known in details, as the anthropic management of the Venice Lagoon and of

10.3389/fevo.2022.979415

FIGURE 2
Overall picture of the identified conservation actions of the Project. (1) Hydraulic works; (2) morphological works; (3) *P. australis* transplantation; (4) aquatic angiosperm transplantation; (5) area of reduction of hunting and fishing pressure.

its watershed started centuries ago. As pragmatically reported by Lewis (1990), in such cases it is not necessary to know the original condition of the natural habitat, but only to know which habitat type was there, and to refer to the same general habitat type. Some historical maps attest the massive presence of a mixed habitat of reedbed/salt marshes/mud flats (see, e.g., D'Alpaos, 2010; D'Alpaos and Carniello, 2010). Nowadays, a residual fraction of that mosaic of habitats is present in the areas close to the small rivers still flowing into the lagoon. The LIFE Lagoon Refresh project has not the ambition to restore the original Sile river mouth before its diversion, but to restore the lagoon oligohaline habitats, by the creation of a new freshwater input. The low salinity and morphological variations would make the environment more suitable for the growing of reedbed and it could provide valuable and diversified ecosystem services, such as the purification of the water by reducing the degree of eutrophication with, consequently, the improvement of benthic biocenosis. Moreover, there will be achievements of the improvement of the conservation status of bird species that use the reed environment during winter period and/or for breeding, foraging or nesting, as well as the increase of the presence of fish species attracted by lower salinity environments. Finally, an improvement of the conservation degree of habitat 1,150*, according to Habitat Directive, and a restore of physical, chemical, morphological, and ecological conditions are expected, too.

In estuarine and coastal ecosystems, Borja et al. (2010) reported that, in some cases, recoveries can take <5 years, whilst the full recovery from over a century of degradation can take a minimum of 15–25 years for attain the original biotic composition and diversity. Despite of a lack of studies that provide the timing for recovery, LIFE Lagoon Refresh proposal provided hypothesis for the necessary time to reach the expected results. Indeed, the salinity gradient is expected to be attained within project duration time, once hydraulic and morphological works are completed and regime water discharge reached, whilst habitat, ecological and target bird species outcomes are expected within 5 years after the end of the project. The response of target fish species (e.g., *Pomatoschistus canestrinii*) to the restoration of the salt gradient should be rapid and expected within project duration time (Scapin et al., 2019a). On the other hand, the outcomes of the fish assemblages to the restoration of aquatic

habitats are expected to take longer than the project time (Scapin et al., 2019b).

Typology of recovery

The LIFE Lagoon Refresh project started in 2017 and lasted 5 years. It considered two different types of conservation actions, following the approaches by Elliott et al. (2016). Two actions for the recovery of the salinity gradient (Type A):

(1) Diversion of a freshwater flow (1,000 l/s) from the Sile river into the lagoon.
(2) Restoration of the intertidal morphology to slow down the fresh water diffusion and sustain the reed development.

In addition, two actions that directly act on the ecosystem (Type B):

(3) Transplanting of *P. australis*.
(4) Transplanting of aquatic angiosperms.

To obtain the greatest chances of success for restoration, the strategy and choices for transplantation actions are consistent with Bekkby et al. (2020), and in particular are:

(1) The choice of the donor and recipient sites: to ensure that the restoration site has suitable physical conditions and biological characteristics, as similar as possible to that of the donor site. In transplantation activities, donor site was chosen in an area of the Venice Lagoon with similar characteristics to intervention area.
(2) The identification of the best transplantation methodology: all transplantations activities are carried out manually preferring a widespread transplant of small clumps.
(3) The specific features of the selected species, *P. australis,* and most of the selected angiosperm species are fast growing species with high reproductive outputs; generally, they have high dispersal, connectivity and number of propagules.

Eco-engineering conservation measures

LIFE Lagoon Refresh is a project of active ecological restoration by using *in situ* eco-engineering. In this case, it was not necessary to remove the stressors of hydrological and physical alterations, but anthropogenic interventions were considered to be necessary to restore physical, chemical, and ecological conditions. To achieve physical expected results, the proposed interventions included the diversion of a freshwater flow from the Sile river into the lagoon, and the creation of an intertidal morphology properly arranged to slow down the freshwater dispersion. Proposed measures to achieve habitat, ecological and species results were: the restoration of the intertidal morphology to favour the reed development; the planting of clumps and rhizomes of *P. australis*; the transplantation of small clumps of aquatic angiosperm species; the implementation of restricting rules to contain the hunting and fishing pressure. **Figure 2** reports the overall picture of the identified conservation actions.

Modelling tools

One of the key elements of the project was the prediction (forecasting) of the optimal freshwater discharge necessary to achieve the expected goal of restoring the salinity gradient. Nevertheless, for the objectives related to the conservation of habitats, a qualitative assessment based on a comparison with similar habitats was enough, whilst for the prediction of the expected variations in terms of salinity, a quantitative approach was essential. In particular, to verify the successful achievement of the project goals, it was necessary to setup, with a proper planning and implementation, a numerical model suitable for operating as a forecasting and hindcasting tool. Indeed, it allowed setting quantitatively the project objectives and it was functional to predict the expected results in terms of variations in space and time of salinity. It also allowed verifying, in analysis mode (hindcasting), the effects of the project actions, integrating modelling results with monitoring data collected as part of the project.

In the writing phase of the proposal, the modelling tool was applied to optimise the design choices related to the construction of the freshwater intake structure and for the realisation of the morphological structures.

The numerical simulations were carried out using the finite element numerical model 2DEF validated in the Venice Lagoon (Viero and Defina, 2016). The model was also applied in 3D baroclinic mode (3DEF model), as it is mostly suitable for simulating salinity transport and mixing in very shallow tidal environments.

According to the project objectives of salinity gradient restoration, simulations were carried out to compare the effects of different discharges of the freshwater input, starting from 300 l/s up to 1,000 l/s, as well as different morphological configurations, differentiated per extension, location and height of the structures designed to slowdown the dispersion of freshwater (**Figure 3**). The different configurations were compared in terms of percentage of salinity variation at a number of checkpoints near and with increasing distances from the intervention area.

Hydraulic works

The hydraulic works were planned considering the requirements and restrictions as following. Technical feasibility related to hydraulic risks of the Sile river; limitation due to

10.3389/fevo.2022.979415

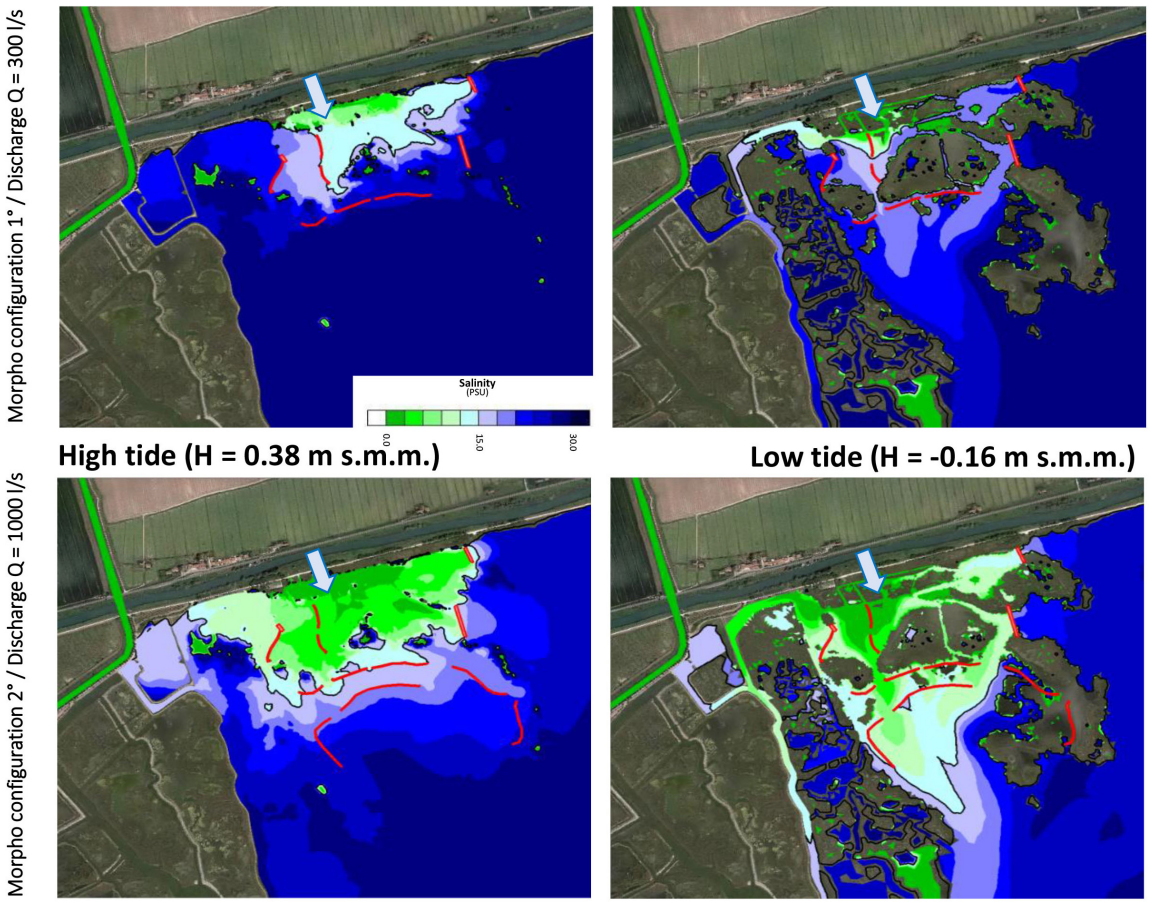

FIGURE 3
Maps of salinity distribution in the surface layer (0.08 m above sea level, a.s.l.) with simulations of freshwater displacement in the design phase. **Top**: with an inflow of 300 l/s and first phase of morphological works. **Bottom**: with an inflow of 1,000 l/s and second phase of morphological works.

other downstream freshwater uses; ensure in the long-term of the designed discharge (including low-maintenance effort); flexibility in regulating the discharge; no energy consumption; integration with the landscape.

The hydraulic works included three elements: (i) a linear channel for intake from the Sile river with a length of 40 m and width of 3 m; (ii) a crossing of the embankment, made by two parallel pipes with a diameter of 0.8 m; (iii) an inflow channel in the lagoon with a length of 20 m, a width of 4 m and two non-return valves at the beginning of the channel (Figure 4).

The freshwater from the Sile river to the lagoon has flowed since May 2020 by gravity according to the differences between the river and the tidal level in the lagoon, and it is adjustable *via* two sluice gates. The flow was gradually increased starting from 300 to 1000 l/s in February 2021. The structure is equipped with two flow metres and measured data are accessible in remotely real time. The low energy needed to make them work is guaranteed by solar panels. The visible structures are covered with bricks recalling typical rural houses.

Morphological works

The morphological works were planned, considering the low bathymetry and fragility of the project area, as well as the following requirements: effectiveness in slowing down the dispersion of freshwater introduced into the lagoon; establishment of a suitable substrate for the reedbed development; all constructions must be carried out manually; no dredging of temporary channels; adaptive management through phases of realisation.

Materials and technical solutions for morphological structures were investigated, considering the characteristics of the bottom of the lagoon, the expected hydrodynamic forcing derived by modelling results, and the function of reed transplanting. Long time was spent investigating solution available on the market, in particular for biodegradable materials. The final choice was to use light and biodegradable materials (coconut fibbers and jute), with modular bags placed manually from small boats, without the need to dredge channels necessary in case of heavy equipment. The works were divided

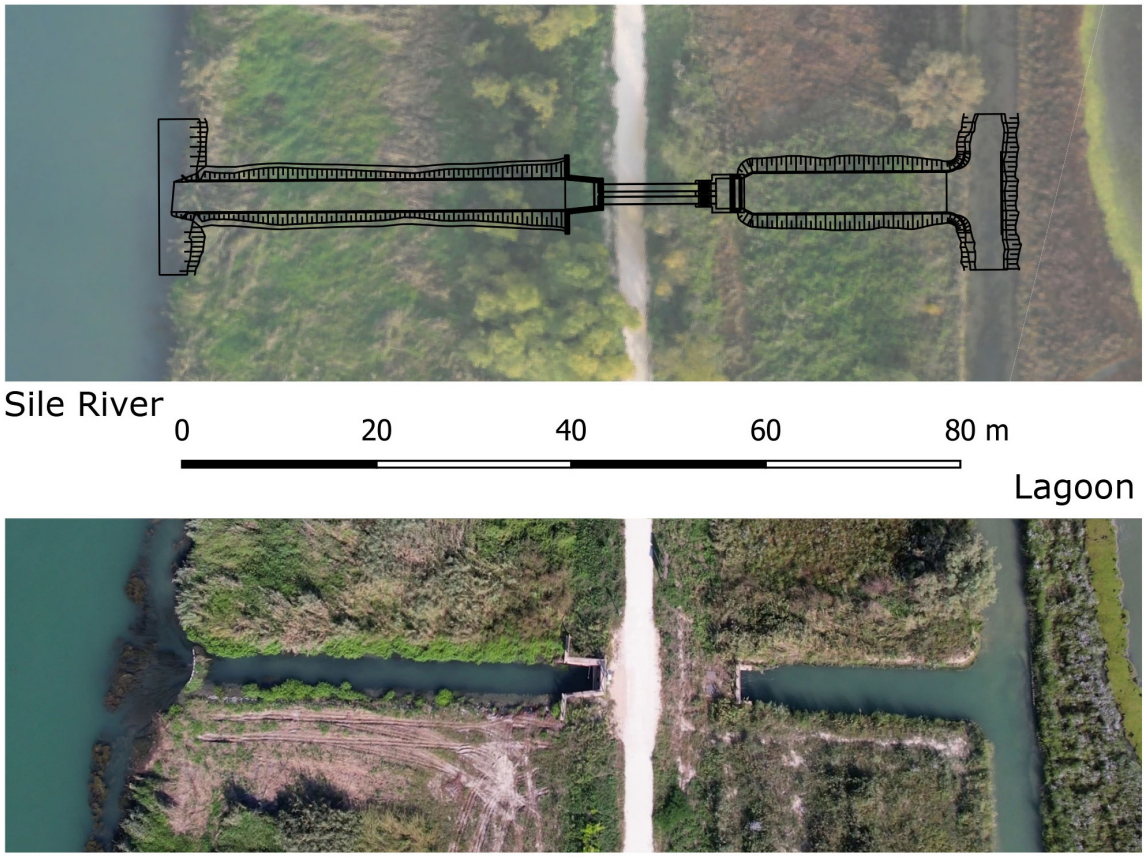

FIGURE 4
Hydraulic works. **Top**: executive design; **bottom**: completed hydraulic works.

into two lines at growing distance from the freshwater input. Considering the novelty of the structures, it was decided to carry out the morphological works in two phases, to allow an adaptive management strategy. Due to the large use of biodegradable materials (chosen as the most environmental-friendly solution) and the risk of bag deterioration before having fully performed their function of slowing down the dispersion of freshwater and of reedbed substrate, the second line of structures was realised about 1 year later, following the increase of the discharge up to 1,000 l/s. In the first phase, 775 m of linear structures were realised near to the freshwater input, with an elevation of approximately 0.10 m above sea level. In the second phase, 400 m of linear structure were realised and placed at greater distance from freshwater input. The second phase was realised starting from the results obtained by the first one in terms of consolidation, salinity monitoring and modelling results, and it was optimised to allow the establishment of suitable salinity conditions for the development of the reedbeds (Figure 5).

Measures to restore biological and ecological integrity

Once the conditions of water salinity and topography required to sustain the target ecosystem were met, approx. 2,500 small clumps and rhizomes of *P. australis* were transplanted to accelerate the natural expanding process of reedbed. The transplant activities were carried out by fishermen and hunters trained during the project. All activities were conducted manually with a very low impact to donor and transplant sites. Clumps of about 10–15 cm in diameter were explanted from healthy and well developed reedbeds near the project site, paying attention to not disturb fauna, especially nesting birds. Reed clumps were transplanted in areas characterised by low salinity (less than 12) and water level higher than −0.20 above sea level, in a portion of the project site close to the freshwater input, both along the margins of the existing salt marshes and on biodegradable bags (Figure 6).

Aquatic angiosperm transplantations started at the end of hydraulic and morphological works. To define the

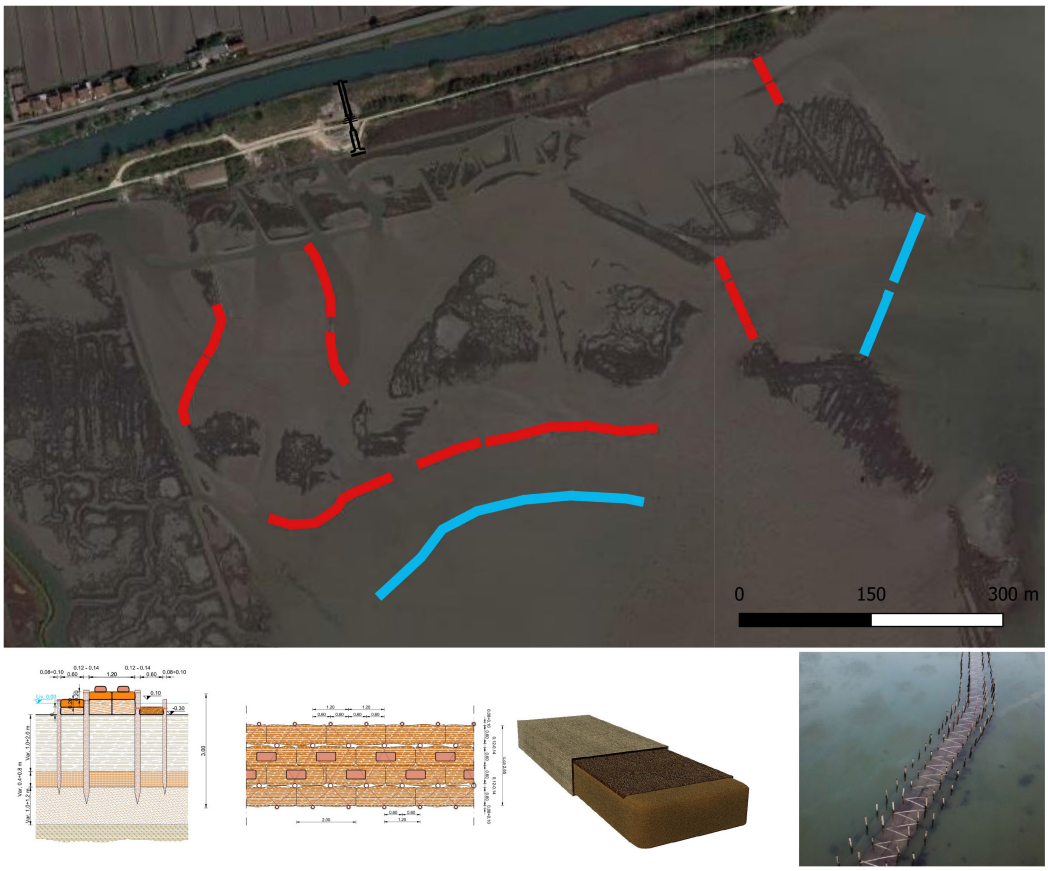

FIGURE 5
Morphological works. **Top**: in red first phase and in blue second phase. **Bottom**: executive design of morphological works, biodegradable module and frame of completed morphological works.

most suitable transplantation techniques and seasons, the experience gained in the LIFE SeResto project was taken into account (Sfriso et al., 2021). Small clumps (15–20 cm) of *Ruppia cirrhosa, Zostera noltei*, and *Zostera marina* were transplanted in the whole project site for a total of approx. 2,000 clumps. As well as for reedbed, angiosperm transplantations were carried out by fishermen and hunters trained during the project, and all activities were conducted manually with a very low impact to donor and transplant sites (**Figure 7**).

Monitor of achievement of project's objectives and goals

To verify the effects of measures, a detailed monitoring plan was scheduled in advance, at the planning stage of the project, to ensure that goals, objectives, and selected indicators would have been measurable. The experimental design included indicators necessary to assess the site condition prior to project initiation (baseline monitoring) and after project implementation to evaluate whether restoration actions met the project's expected results.

Restoration of salinity gradient

As saline gradient restoring is the main goal of the LIFE Lagoon Refresh project, the monitoring strategy aimed at capturing its changes, considering interactions between different hydrological and morphological processes, such as the modification of freshwater discharge, the effect of morphological works, tidal regime, exchanges with sea, etc. To assess whether hydraulic and morphological works were meeting the salinity expected results, a precise quantitative analysis of salinity with adequate resolution in time and space was adopted. Therefore, a combination of environmental monitoring and numerical modelling was applied. Characterisation in time and space of salinity variations, performed before and after the conservative actions, was obtained by the integration of three different tools: moored salinity probes that allow the acquisition, in fixed positions, of continuous measured data; field campaigns with

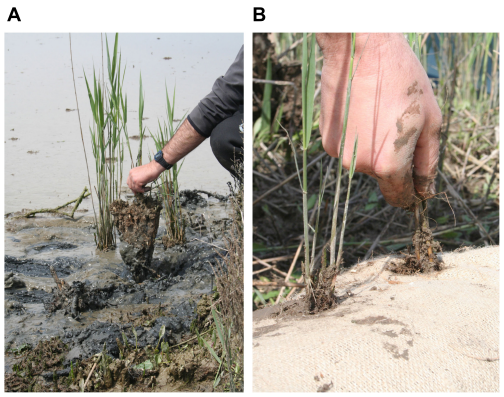

FIGURE 6
Reedbed (*P. australis*) transplantations in mudflat **(A)** and in biodegradable module **(B)**.

conductivity-temperature-depth (CTD) measures profilers that allowed the acquisition of instantaneous/spatially distributed measured data; implementation of numerical modelling that allowed simulation of modelled data with variation in space and time.

As planned, the restoration of salinity gradient was reached in the intervention area of 70 ha. Indeed, starting from >30 (annual mean salinity before project) at the whole area, the salinity has resulted less than 5, in 5 ha; less than 15, in 25 ha; and less than 25, in 70 ha after the interventions (Feola et al., 2022).

Habitat restoration

The assessment of habitat quality, according to the Habitat Directive requirements, is based on the criteria of "habitat structures" and "habitat functions." To assess habitat 1,150* structure, the salinity gradient was considered, as well as the eutrophication degree, evaluated by transitional water quality index (Giordani et al., 2009; Bonometto et al., 2022) and the mapping of submerged angiosperm vegetation. To assess functions, the ecological quality status improvement of macroinvertebrate, fish fauna and macrophyte communities were assessed, as well as water and sediment parameters, as reported in Ecological status improvement.

The period to assess these results was set within 5 years after the end of the project and monitoring activities are still ongoing. Currently the result concerning salinity gradient was achieved (Feola et al., 2022), and the first outcomes of fish fauna assessments indicated a quite positive response (see Species increasing). Based on expectations, the other indicators for habitat structures and functions will take a longer time to respond to the environmental changes. So, part of one of the objectives of the project, which was the consolidation and restoration of 1,250 ha of habitat 1,150* (34% of habitat area within SCI IT3250031) to "B" conservation status (corresponding to "good conservation" according to Habitat Directive) comprising 30% part currently in a "C" status (corresponding to "average or reduced conservation" according to Habitat Directive), was achieved.

The monitoring plan also provided habitat halophyte and reedbed mapping *ante* intervention and after the conclusion of hydraulic and morphologic works and *P. australis* transplantations. The *post operam* monitoring of halophyte and reedbed will last several years. The mapping activities include a combination of field monitoring and drone surveys. Expected results are the creation of reedbed on an area of approximately 20 ha and monitoring activities are still ongoing.

Ecological status improvement

For the ecological status assessment, protocols, defined by the Italian law (Ministerial Decree no. 260/2010) in agreement with the WFD, were applied. Biological Quality Elements (BQEs), such as macroalgae, aquatic angiosperms, macroinvertebrates, and fish fauna were monitored in addition to physico-chemical and hydromorphological quality elements that support the ecological status classification, by confirming or not the assessment provided by the BQEs.

A before-after monitoring strategy was adopted for all the quality elements (ecological, physico-chemical, and hydromorphological) at two spatial scales: at a local scale in the intervention area and at a larger scale in the project area. At larger scale, the monitoring network of the project was also integrated as part of the WFD monitoring network in the Venice Lagoon. Monitoring activities are still ongoing and results are expected within 5 years after the end of the project.

Species increasing

To monitor birds, especially those included in Annex I of Birds Directive, a diversified approach was adopted, considering the different species (migratory, wintering, and breeding) and the annual cycle. Therefore, three different monitoring activities included: (i) abundance detecting of passerines; (ii) total *census* of aquatic birds; (iii) *census* of *Botaurus stellaris* through sunset surveys (Luchetta et al., 2019).

Expected results regard specifically the increase of bird species typical of reeds, in particular *Phalacrocorax pygmeus, B. stellaris, Ardea purpurea, Ixobrychus minutus, Circus aeruginosus, Circus cyaneus,* and *Alcedo atthis*, with progressive structuring of the community.

Fish fauna monitoring aimed at assessing the ecological quality status of the community, as well as the presence of *P. canestrinii*, and other fish fauna species of commercial interest, such as *Dicentrarchus labrax, Anguilla anguilla*, *Chelon*

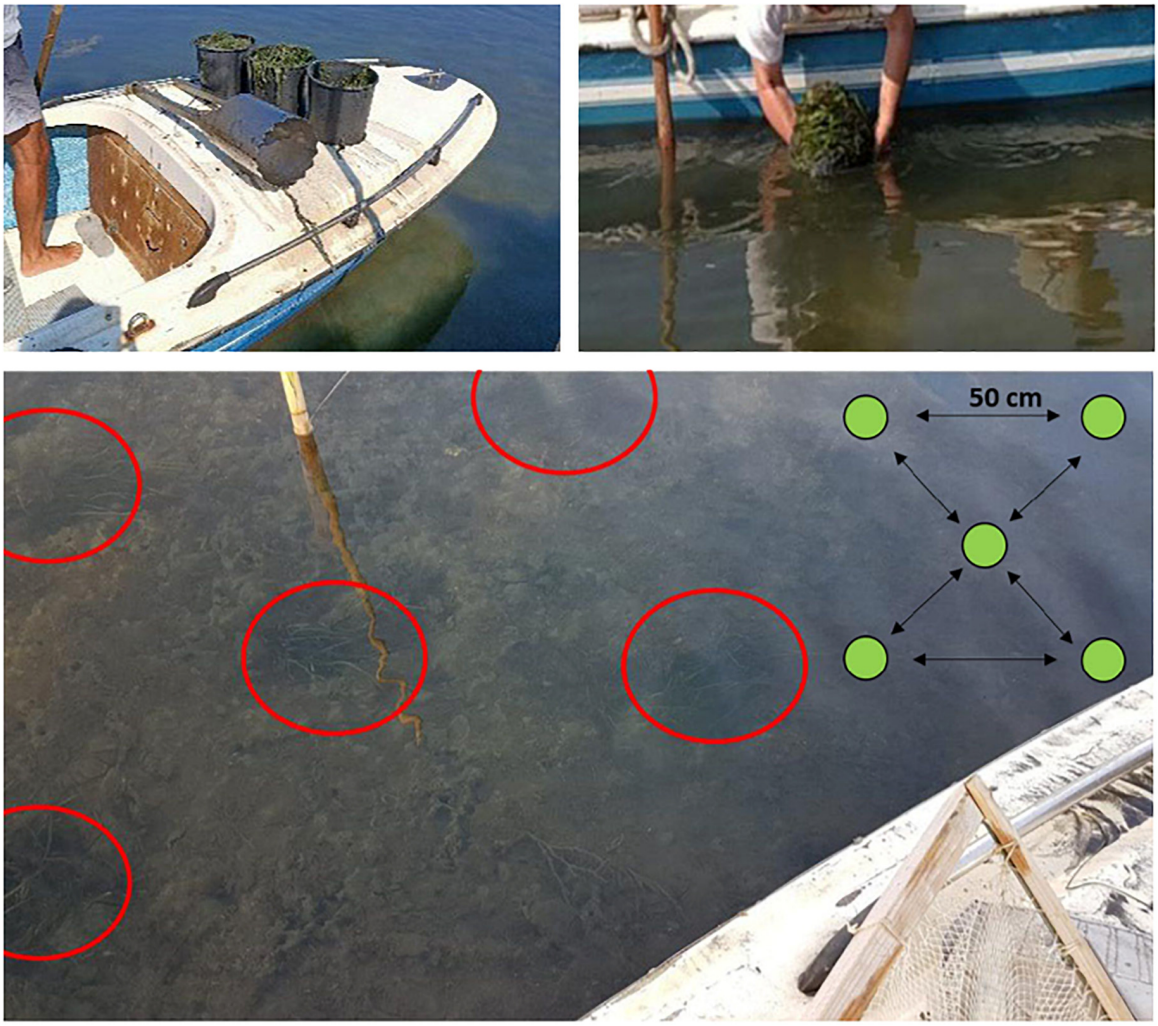

FIGURE 7
Aquatic angiosperm transplantation **(top)**. Scheme of transplantation **(bottom)**.

spp., *Atherina boyeri*, *Platichthys flesus*, and other species. Monitoring surveys were carried out twice a year (spring and autumn) for the entire duration of the project, by seine netting and by "bertovelli" nets before and after interventions.

A predicting model applied to the area assessed expected results (Scapin et al., 2019a). Very preliminary outcomes showed an increase of *P. canestrinii* from 0.1 ind/100 m^2 up to 20 ind/100 m^2 as expected by the project. Moreover, an increase of juveniles of commercial species, mostly mullets (*Chelon* spp.), was observed near the freshwater inflow.

Discussion

The application of the restoration project in the northern Venice Lagoon, LIFE Lagoon Refresh, resulted a clear case and real application of the purposed method, based on the collection of available theoretical indications for restoration projects and produced a methodological approach suitable for transitional waters. The main intervention realised in the Venice Lagoon from the second half of the 16th century was the diversion of main rivers. The reduction of hundreds of cubic metres per second of freshwater that flowed into the lagoon resulted in an increase of salinity and consequently in a heavy modification of its habitats and ecology. LIFE Lagoon Refresh is an active ecological restoration project that adopts an *in situ* eco-engineering approach aimed at recovering, in the northern Venice Lagoon, the salinity gradient, and at re-establishing the physical, chemical and biological processes and, subsequently, the ecotonal environment characterised by large intertidal areas vegetated by reeds *P. australis*. In this work, the strategy of the project and the foreseen conservation actions highlighted the integration of multidisciplinary knowledge on biodiversity and

ecosystem functioning, hydrological and morphological aspects, legislation, as well as socio-economic aspects concerning the involvement of local stakeholders. Each restoration goal was clearly converted into specific objectives and indicators. Starting from the status assessments, as required by European Directives, such as Habitat, Birds, and WFD directives, same indicators were used to properly forecast outcomes. In this context, the desired state to be achieved was assessed by objective, as well as intercalibrated methods that are internationally recognised. Moreover, modelling applications resulted suitable and very useful to provide reasonable and quantitative outcomes to achieve. In addition, times to meet the objectives were also scheduled. Finally, indicators were established to assess progresses during the project, and to eventually adopt mitigation interventions.

The conservation actions were identified through a participatory process to reach the presented goals. Indeed, the Venice Lagoon is a very complex area concerning policies and socioeconomic contexts, from national to local authorities, associations, fishermen, hunters, and people attending the area. Therefore, meeting the agreement of the numerous stakeholders was one of the most important step for the realisation of the project. The key to success was to recognise the expectations and interest of all of them, and directly involving them, as for example including fishermen and hunters in transplanting actions. Currently, as most stakeholders know and share the project objectives, they could be also the keeper and maintainer of them for the future. Moreover, also the partners of the project, as principal authorities of the area, were directly involved in the interventions, and they will be the owner and responsible of the works after the end of the project.

Conclusion remarks

The case study of LIFE Lagoon Refresh project showed the effectiveness of the multidisciplinary method depicted in this manuscript, which met the application of theoretical advice with a methodological approach. This is especially relevant for restoration of coastal lagoon habitats, which are highly productive ecosystems, rich in flora and fauna of conservation interest and, unfortunately, subjected to multiple threats that may endanger their quality status or existence.

As results, this method can be applied to several coastal lagoons in order to reach the desired state, starting from a robust assessment of environmental, policies and socioeconomic context, clearly defining the typology of recovery, identifying the best configuration of conservation actions, and assessing the impact of the project through an integrated monitoring plan. The study could be considered as an innovative pilot example of restoration strategy and application that can provide a baseline for future similar interventions.

Data availability statement

The original contributions presented in this study are included in the article/supplementary material, further inquiries can be directed to the corresponding authors.

Author contributions

RB, AF, FC, and AB: conceptualization and writing—original draft preparation. AF, FC, EP, BM, AS, PF, and NB: investigation. AF: visualization. RB, AB, AS, ML, PP, and VV: resources, project administration, and funding acquisition. RB and AB: supervision. RB, AF, FC, EP, AS, PF, ML, PP, BM, NB, VV, LM, and AB: methodology, writing—review and editing the manuscript, and approved the submitted version.

Funding

This research was funded by the European Union's LIFE program financial instrument 2014–2020 (grant LIFE16 NAT/IT/000663—LIFE Lagoon Refresh, which contributes to the environmental recovery of a Natura 2000 site, SCI IT3250031—Northern Venice Lagoon).

Conflict of interest

PP and BM were employed by IPROS Environmental Engineering s.r.l.

The remaining authors declare that the research was conducted in the absence of any commercial or financial relationships that could be construed as a potential conflict of interest.

Publisher's note

References

Bekkby, T., Papadopoulou, N., Fiorentino, D., McOwen, C. J., Rinde, E., Boström, C., et al. (2020). Habitat features and their influence on the restoration potential of marine habitats in Europe. *Front. Mar. Sci.* 7:184. doi: 10.3389/fmars.2020.00184

Bon, M., Semenzato, M., Scarton, F., Fracasso, G., and Mezzavilla, F. (2004). *Atlante faunistico della provincia di Venezia. Ass. Cacc. Pesc. Poliz. Prov. Protez. Civ*, Vol. XVIII. Venezia: Provincia di Venezia, 257.

Bonometto, A., Ponis, E., Cacciatore, F., Riccardi, E., Pigozzi, S., Parati, P., et al. (2022). A new multi-index method for the eutrophication assessment in transitional waters: Large-scale implementation in Italian lagoons. *Environments* 9:41. doi: 10.3390/environments9040041

Borja, A., Dauer, D. M., Elliott, M., and Simenstad, C. A. (2010). Medium- and Long-term recovery of estuarine and coastal ecosystems: Patterns, rates and restoration effectiveness. *Estuar. Coasts* 33, 1249–1260. doi: 10.1007/s12237-010-9347-5

Clewell, A. F., and Aronson, J. (2013). *Ecological restoration, principles, values, and structure of an emerging profession*, 2nd Edn. Washington, DC: Island Press.

D'Alpaos, L. (2010). *L'evoluzione morfologica della Laguna di Venezia attraverso la lettura di alcune mappe storiche e delle sue carte idrografiche*. Venezia: Comune di Venezia, 110.

D'Alpaos, L., and Carniello, L. (2010). "Sulla reintroduzione di acque dolci nella laguna di Venezia. Salvaguardia di Venezia e della sua Laguna," in *Proceedings of the convegni lincei giornata dell'ambiente, XXVI Giornata dell'Ambiente, in Ricordo di Enrico Marchi ACL*, Vol. 255, (Rome: Accademia Nazionale dei Lincei), 113–146.

De Wit, R., Leruste, A., Le Fur, I., Sy, M. M., Bec, B., Ouisse, V., et al. (2020). A multidisciplinary approach for restoration ecology of shallow coastal lagoons, a case study in South France. *Front. Ecol.* 8:108. doi: 10.3389/fevo.2020.00108

Elliott, M., Burdon, D., Hemingway, K. L., and Apitz, S. E. (2007). Estuarine, coastal and marine ecosystem restoration: Confusing management and science–A revision of concepts. *Estuar. Coast. Shelf Sci.* 74, 349–366. doi: 10.1016/j.ecss.2007.05.034

Elliott, M., Mander, L., Mazik, K., Simenstad, C., Valesini, F., Whitfield, A., et al. (2016). Ecoengineering with Ecohydrology: Successes and failures in estuarine restoration. *Estuar. Coast.* 176, 12–35. doi: 10.1016/j.ecss.2016.04.003

European Commission (2013). *Interpretation manual of European union habitats; EUR 28. E. C.* Bruxelles: DG Environment, 144.

European Environment Agency (2021). *European topic centre on biological diversity—report under the Article 17 of the habitats directive period 2013–2018*. Available online at: https://nature-art17.eionet.europa.eu/article17/ (accessed December 10, 2021).

Facca, C., Cavraro, F., Franzoi, P., and Malavasi, S. (2020). Lagoon resident fish species of conservation interest according to the habitat directive (92/43/CEE): A review on their potential use as ecological indicator species. *Water* 12:2059. doi: 10.3390/w12072059

Feola, A., Ponis, E., Cornello, M., Boscolo Brusà, R., Cacciatore, F., Oselladore, F., et al. (2022). An integrated approach for evaluating the restoration of the salinity gradient in transitional waters: Monitoring and numerical modeling in the life lagoon refresh case study. *Environments* 9:31. doi: 10.3390/environments9030031

Fonseca, M. S., Judson Kenworthy, W., Julius, B. E., Shutler, S., and Fluke, S. (2002). "Seagrasses," in *Handbook of ecological restoration. Restoration in practice*, Vol. 2, eds M. R. Perrow and A. J. Davy (Cambridge: Cambridge University Press), 149–170.

Gann, G. D., McDonald, T., Walder, B., Aronson, J., Nelson, C. R., Jonson, J., et al. (2019). *International principles and standards for the practice of ecological restoration*, 2nd Edn. Washington, DC: Society for Ecological Restoration. doi: 10.1111/rec.13035

Giordani, G., Zaldivar, J. M., and Viaroli, P. (2009). Simple tools for assessing water quality and trophic status in transitional water ecosystems. *Ecol. Ind.* 9, 982–991. doi: 10.1016/j.ecolind.2008.11.007

Guerzoni, S., and Tagliapietra, D. (2006). *Atlas of the lagoon: Venice between land and sea*. Venezia: Marsilio Editori, 242.

Lewis, R. R. (1990). "Marine and estuarine provinces (Florida)," in *Wetland creation and restoration: The status of the science*, eds J. A. Kasler and M. E. Kentula (Washington DC: Island Press), 73–101.

Luchetta, A., Baccetti, N., Bonometto, A., Boscolo Brusà, R., De Faveri, A., Ponis, E., et al. (2019). "LIFE LAGOON REFRESH: Mission and project goals and first analysis of data from the first year of bird monitoring," in *Proceedings of the Conference: Presented at XX CIO, Italian Ornithology Conference in Naples*. Naples, Italy.

Newton, A., Icely, J., Cristina, S., Brito, A., Cardoso, A. C., Colijn, F., et al. (2014). An overview of ecological status, vulnerability and future perspectives of European large shallow, semi-enclosed coastal systems, lagoons and transitional waters. *Estuar. Coast. Shelf Sci.* 140, 95–122. doi: 10.1016/j.ecss.2013.05.023

Scapin, L., Zucchetta, M., Bonometto, A., Feola, A., Boscolo Brusà, R., Sfriso, A., et al. (2019a). Expected shifts in nekton community following salinity reduction: Insights into restoration and management of transitional water habitats. *Water* 11:1354. doi: 10.3390/w11071354

Scapin, L., Zucchetta, M., Sfriso, A., and Franzoi, P. (2019b). Predicting the response of nekton assemblages to seagrass transplantations in the Venice lagoon: An approach to assess ecological restoration. *Aquat. Conserv. Mar. Freshw. Ecosyst.* 29, 849–864. doi: 10.1002/aqc.3071

Sfriso, A., Buosi, A., Facca, C., Sfriso, A. A., Tomio, Y., Juhmani, A.-S., et al. (2021). Environmental restoration by aquatic angiosperm transplants in transitional water systems: The Venice Lagoon as a case study. *Sci. Total Environ.* 795:148859. doi: 10.1016/j.scitotenv.2021.148859

Simenstad, C., Reed, D., and Ford, M. (2006). When is restoration not? Incorporating landscape-scale processes to restore self-sustaining ecosystems in coastal wetland restoration. *Ecol. Eng.* 26, 27–39. doi: 10.1016/j.ecoleng.2005.09.007

Solidoro, C., Bandelj, V., Bernardi Aubry, F., Camatti, E., Ciavatta, S., Cossarini, G., et al. (2010). "Response of Venice Lagoon ecosystem to natural and anthropogenic pressures over the last 50 years," in *Coastal lagoons: Critical habitats of environmental change*, eds M. J. Kennish and H. W. Paerl (Boca Raton, FL: CRC Press), 483–511. doi: 10.1201/EBK1420088304-c19

Tagliapietra, D., Baldan, D., Barausse, A., Buosi, A., Curiel, D., Guarneri, I., et al. (2018). "Protecting and restoring the salt marshes and seagrasses in the lagoon of Venice," in *Management and restoration of Mediterranean coastal lagoons in Europe. Edition Càtedra d'Ecosistemes Litorals Mediterranis Parc Natural del Montgrí, les Illes Medes i el Baix Ter Museu de la Mediterrània; Life Pletora (LIFE13 NAT/ES/001001)*, Vol. 10, eds X. Quintana, D. Boix, S. Gascòn, and J. Sala (Torroella de Montgrí: Càtedra d'Ecosistemes Litorals Mediterranis), 39–65.

Tagliapietra, D., Sigovini, M., and Ghirardini, A. V. (2009). A review of terms and definitions to categorize estuaries, lagoons and associated environments. *Mar. Freshw. Res.* 60, 497–509. doi: 10.1071/MF08088

USEPA (2000). *Principles for the ecological restoration of aquatic resources. EPA841-F-00-003. Office of Water (4501F)*. Washington, DC: United States Environmental Protection Agency, 4.

Viero, D. P., and Defina, A. (2016). Water age, exposure time, and local flushing time in semi-enclosed, tidal basins with negligible freshwater inflow. *J. Mar. Syst.* 156, 16–29. doi: 10.1016/j.jmarsys.2015.11.006

frontiers | Frontiers in Environmental Science

TYPE Original Research
PUBLISHED 07 September 2022
DOI 10.3389/fenvs.2022.889170

OPEN ACCESS

EDITED BY
Orsolya Valkó,
Hungarian Academy of Sciences, Hungary

REVIEWED BY
David Andrew Kaplan,
University of Florida, United States
David Haukos,
Kansas State University, United States

*CORRESPONDENCE
Brian A. Tangen,
btangen@usgs.gov

SPECIALTY SECTION
This article was submitted to Conservation and Restoration Ecology, a section of the journal Frontiers in Environmental Science

RECEIVED 03 March 2022
ACCEPTED 15 August 2022
PUBLISHED 07 September 2022

CITATION
Tangen BA, Bansal S, Jones S, Dixon CS, Nahlik AM, DeKeyser ES, Hargiss CLM and Mushet DM (2022), Using a vegetation index to assess wetland condition in the Prairie Pothole Region of North America.
Front. Environ. Sci. 10:889170.
doi: 10.3389/fenvs.2022.889170

Using a vegetation index to assess wetland condition in the Prairie Pothole Region of North America

Brian A. Tangen[1]*, Sheel Bansal[1], Seth Jones[2], Cami S. Dixon[3], Amanda M. Nahlik[4], Edward S. DeKeyser[2], Christina L. M. Hargiss[2] and David M. Mushet[1]

[1]United States Geological Survey, Northern Prairie Wildlife Research Center, Jamestown, ND, United States, [2]North Dakota State University, School of Natural Resource Sciences, Fargo, ND, United States, [3]United States Fish and Wildlife Service, Chase Lake National Wildlife Refuge, Woodworth, ND, United States, [4]United States Environmental Protection Agency, Office of Research and Development, Center for Public Health and Environmental Assessment, Pacific Ecological Systems Division, Corvallis, OR, United States

Wetlands deliver a suite of ecosystem services to society. Anthropogenic activities, such as wetland drainage, have resulted in considerable wetland loss and degradation, diminishing the intrinsic value of wetland ecosystems worldwide. Protecting remaining wetlands and restoring degraded wetlands are common management practices to preserve and reclaim wetland benefits to society. Accordingly, methods for monitoring and assessing wetlands are required to evaluate their ecologic condition and outcomes of restoration activities. We used an established methodology for conducting vegetation-based assessments and describe a case study consisting of a wetland condition assessment in the Prairie Pothole Region of the North American Great Plains. We provide an overview of an existing method for selecting wetlands to sample across broad geographic distributions using a spatially balanced statistical design. We also describe site assessment protocols, including vegetation survey methods, and how field data were applied to a vegetation index that categorized wetlands according to ecologic condition. Results of the case study indicated that vegetation communities in nearly 50% of the surveyed wetlands were in *very poor* or *poor* condition, while only about 25% were considered *good* or *very good*. Approximately 70% of wetlands in native grasslands were categorized as *good* or *very good* compared to only 12% of those in reseeded grasslands (formerly cropland). In terms of informing restoration and management activities, results indicated that improved restoration practices could include a greater focus on establishing natural vegetation communities, and both restored and native prairie wetlands would benefit from enhanced management of invasive species.

KEYWORDS

ecosystem services, multi-metric index, wetland degradation, wetland restoration, plants

1 Introduction

Wetlands are a globally important natural resource that cover approximately 5–8% of the Earth's land surface (Millennium Ecosystem Assessment, 2005; Zedler and Kercher, 2005; Mitsch and Gosselink, 2015). The societal value of wetlands is widely recognized and generally linked to the ecological condition or quality of a wetland (Murkin, 1998; Millennium Ecosystem Assessment, 2005; Euliss et al., 2006; Gleason et al., 2011). Despite their intrinsic value to society, wetland loss and degradation are commonly linked with human activities. Wetland loss is most often due to drainage associated with urban development and agricultural practices (McCorvie and Lant, 1993; Johnson et al., 2008; Blann et al., 2009; Yan and Zhang, 2019). To preserve or enhance the delivery of wetland ecosystem services, national policies (e.g., Section 404 of the Clean Water Act, "Swampbuster" provision of 1985 Farm Bill) and efforts to conserve remaining wetlands and restore drained or degraded wetlands have become a focal point for many government agencies (e.g., United States Department of Agriculture Agricultural Conservation Easement Program, United States Fish and Wildlife Service [USFWS] wetland easements) and nongovernmental organizations (e.g., Tori et al., 2002; Gleason et al., 2011). Consequently, techniques are needed to assess these activities and guide future conservation efforts and natural resource management. We provide a brief overview of a variety of wetland assessment techniques and describe a vegetation-based wetland assessment method through presentation of a case study conducted in the Prairie Pothole Region (PPR) of central North America.

1.1 Wetland assessments

Effects of anthropogenic activities on aquatic ecosystems, as well as their overall ecologic condition, are typically assessed based on the composition of biotic communities, water quality, hydrologic functions, or degree of anthropogenic impacts (e.g., Karr, 1981; Brinson, 1993; Kerans and Karr, 1994; DeKeyser et al., 2003; Post van der Burg and Tangen, 2015; McMurry et al., 2016; Schwarz et al., 2018). Approaches used to assess various pollutants of aquatic systems (e.g., streams, rivers, wetlands) often focus on chemical analyses (e.g., nutrients, metals, agrichemicals) or various water-quality parameters (e.g., dissolved oxygen, pH, turbidity). Water-quality sampling can be useful for identifying elevated or harmful levels of metals, nutrients, or agrichemicals by comparing observed levels to standards that typically are established by state regulatory agencies. While water-quality assessments can be informative, they do have limitations because standards developed for lakes or streams often do not apply to wetlands; many wetlands have short periods of inundation and even large wetlands dry completely during extended drought (Euliss et al., 2004; Kentula et al., 2020). Concentration of some water-quality parameters can vary widely, both within and among years, because of concentration and dilution associated with precipitation, runoff, and evapotranspiration (Euliss et al., 2014; Mushet et al., 2015; Hayashi et al., 2016). Connection to groundwater (e.g., recharge, discharge), which varies greatly among wetlands, also can have considerable effects on water chemistry (Goldhaber et al., 2011; LaBaugh et al., 2018; Levy et al., 2018). Moreover, many potential contaminants, such as agrichemicals, can have short life spans or residence times, and in the case of riverine systems, contaminants are transported downstream from the source.

Rather than concentrating on specific contaminants or water-quality parameters, many assessments focus on the overall ecologic condition, or "health," of aquatic systems. This approach often involves the development and application of multi-metric indices (e.g., Index of Biotic Integrity; Karr, 1981), in which biotic communities such as fish, macroinvertebrates, or plants are surveyed across an observed stressor gradient, and biological response variables or metrics are identified (e.g., Burton et al., 1999; Lopez and Fennessy, 2002; DeKeyser et al., 2003; Seilheimer and Chow-Fraser, 2006; Lu et al., 2019). Effective metrics that display a predictable response to stressors are then used to reflect the condition of a site by calculating an overall index score, which can then be used to define condition categories such as very poor, poor, fair, good, or excellent. Index scores associated with each condition category are typically determined based on community attributes observed at minimally impacted reference sites. In addition to standard, single-community indices, recent research has explored the utility of multi-community (e.g., plants + birds, plants + phytoplankton + invertebrates) indices (e.g., Gronke, 2004; Wilson and Bayley, 2012), as well as a modeling framework for developing biomonitoring tools (Bolding et al., 2020). These methods, however, may require additional financial resources, as well as more time, labor, and expertise (Wilson and Bayley, 2012; Bolding et al., 2020). Conversely, less complicated indices that require fewer resources and rely on relatively few metrics (e.g., floristic quality) have proven effective for assessing wetland condition, especially when time and resources are limited (Guntenspergen et al., 2002; Lopez and Fennessy, 2002; Mack, 2006; Rebelo et al., 2009; Bourdaghs, 2012; Hargiss et al., 2017). Regardless of the approach chosen, assessing the condition of wetlands can be challenging due to the highly variable nature of many systems (Wilcox et al., 2002; Tangen et al., 2003; Langer et al., 2018; Mushet et al., 2018; McLean et al., 2020; Mushet et al., 2020). Therefore, results of wetland assessments must be viewed in light of current and past climate (e.g., drought) and hydrologic conditions (depth, permanence), which directly affect wetland characteristics (e.g., vegetation, chemistry) regardless of anthropogenic disturbances (Kantrud and Newton, 1996; Wilcox et al., 2002; Euliss et al., 2004; Euliss and Mushet, 2011).

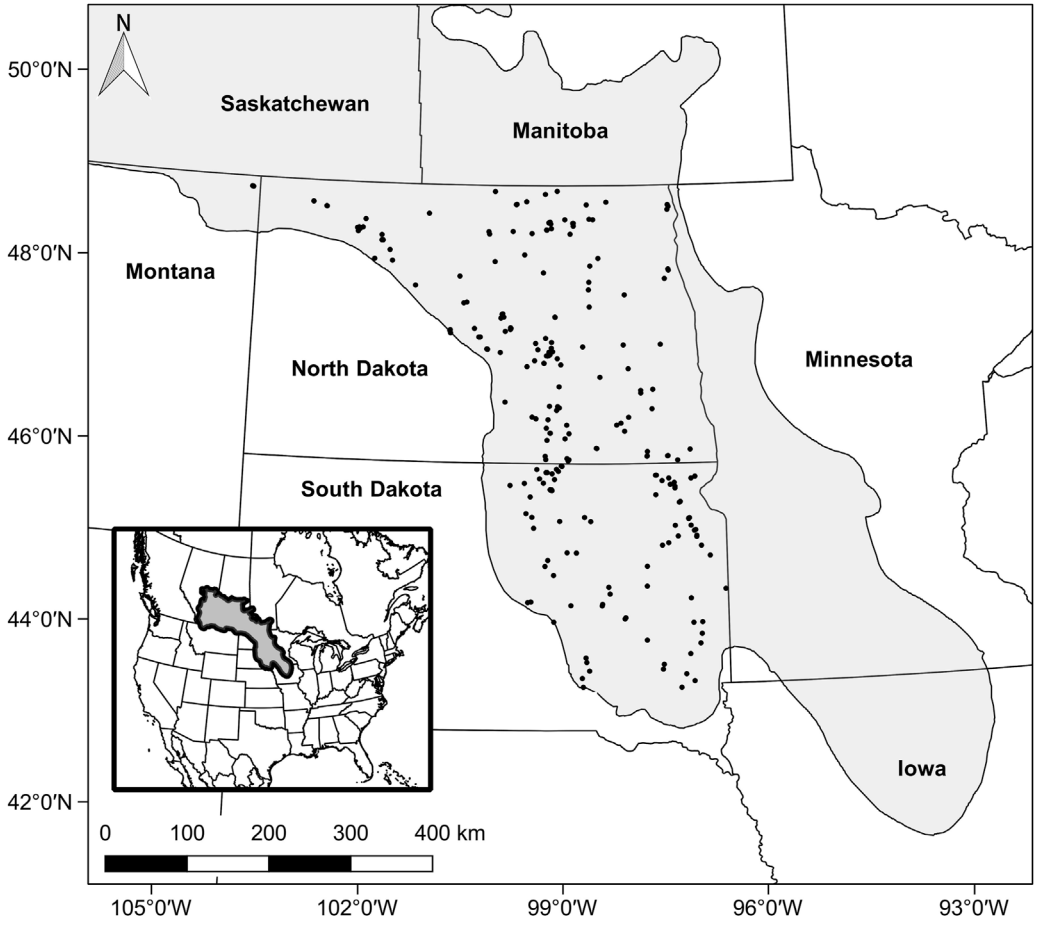

FIGURE 1
The Prairie Pothole Region of North America (shaded area). Dots indicate the location of wetlands selected for the 2020–2021 case study in the United States portion of the region.

While studies that describe the development and validation of various approaches and metrics for assessing aquatic systems are common, there are far fewer studies that describe the practical application of existing biotic indices with the goal of informing management or conservation practices. We present a regional case study that uses established methods to assess plant communities of wetlands embedded within grasslands managed for wildlife habitat, species conservation, and outdoor recreation.

1.2 Prairie Pothole Region wetlands: A case study

The PPR of North America is widely recognized for its agricultural production, abundant wetland resources, and concentration of lands enrolled in conservation programs. Additionally, tracts of native prairie that have not been tilled still exist in the western PPR (e.g., Missouri Coteau ecoregion), although these lands typically are subjected to grazing and frequently impacted by invasive plants. Thus, the region is well suited for developing and demonstrating methods for assessing the ecologic condition of restored, degraded, and natural (although impacted) wetlands. We describe a proven methodology for assessing wetland ecological condition (DeKeyser et al., 2003; Hargiss et al., 2008; Hargiss, 2009; Hargiss et al., 2017) and demonstrate the utility of the method through description of a recent (c. 2020–2021) case study from the PPR (Tangen et al., 2019; Jones, 2021). While the sample methods, plant-based index, and case study are specific to wetlands of the PPR, the general methodology or approach could be adapted to other inland wetlands with varying degrees of effort (e.g., modified sample design, identifying alternative metrics or scoring criteria).

1.2.1 Prairie Pothole Region

The PPR (Figure 1) covers nearly 800,000 km^2 of central North America, including portions of five United States states

and three Canadian provinces (Euliss et al., 2006; Dahl, 2014). The PPR is distinguished by millions of small, depressional, mineral-soil wetlands, hereafter referred to simply as wetlands. Wetlands in the PPR provide a range of ecosystem services that include wildlife habitat, carbon sequestration, flood mitigation, filtration of pollutants, groundwater recharge, nutrient retention, and recreational opportunities (Winter and Rosenberry, 1995; Knutsen and Euliss, 2002; Euliss et al., 2006; Gleason et al., 2008; Badiou et al., 2011; Gleason et al., 2011). Wetlands of the region are particularly well-known for providing breeding, brood-rearing, and migration stop-over habitats for a large proportion of North America's migratory water birds (Batt et al., 1989; Niemuth et al., 2006; Skagen et al., 2008; Niemuth et al., 2018). Estimates suggest that greater than half of the wetlands in the United States have been lost due to human activities, and a considerable number of those that remain are degraded as a result of land-use and climate change (DeKeyser et al., 2003; Johnston, 2013; Dahl, 2014; U.S. Environmental Protection Agency, 2016a; Bourdaghs et al., 2019). The intrinsic value of wetlands to society has led to the PPR becoming a focal region for conservation programs in the United States and Canada. However, despite the considerable resources committed to restoring and preserving wetlands in the PPR, relatively little effort has been dedicated to studying the outcomes of these activities (Galatowitsch and Bohnen, 2020, 2021). Broad studies conducted at state and National levels, which included PPR wetlands, have assessed wetland quality for specific regions and wetland types, but these studies typically lack the resolution required to characterize specific restoration or management practices, as well as particular wetland subclasses (U.S. Environmental Protection Agency, 2016a; Bourdaghs et al., 2019). Thus, future conservation activities, as well as ongoing management, would benefit from recurring assessments of the overall ecologic condition of both natural and restored wetlands in the PPR.

1.2.2 Wetland conservation in the Prairie Pothole Region

Thousands of square kilometers of land in the PPR have been protected from development through land acquisition, establishment of conservation easements, or restoration from a cropland setting to a grassland setting through various governmental and non-governmental conservation programs (Gleason et al., 2011; Doherty et al., 2013; Walker et al., 2013; Niemuth et al., 2014; Dixon et al., 2019). Often, wetland restoration occurs on these protected lands, typically consisting of 1) disrupting surface or subsurface drainage systems to reestablish natural hydrology, and 2) reseeding surrounding uplands (i.e., croplands) to grassland species (Gleason et al., 2011; Dixon et al., 2019). In many instances, intact (i.e., not drained) wetlands embedded within croplands are not specifically targeted for restoration but are essentially restored when adjacent croplands are converted to grasslands. Restoration of both drained and intact wetlands, however, generally does not involve seeding or planting wetland vegetation, or removing accumulated sediment; rather, wetland species typically are established through natural recolonization from remnant seed banks or wind-blown seeds (Galatowitsch and van der Valk, 1996a; b; Mulhouse and Galatowitsch, 2003; Gleason et al., 2011; Smith et al., 2016). This lack of targeted restoration and management can result in reduced water depths from sediment accretion and low-diversity, wetland plant communities composed of annual or invasive species (Kantrud and Newton, 1996; Gleason and Euliss, 1998; Mulhouse and Galatowitsch, 2003; Aronson and Galatowitsch, 2008; Smith et al., 2016; Galatowitsch and Bohnen, 2021).

Although formal assessments of specific restoration activities are sparse, plant communities of restored wetlands in the PPR have been shown to differ from those of native-prairie wetlands that have not been directly affected by tillage and cropping (e.g., Galatowitsch and van der Valk, 1996b; Seabloom and van der Valk, 2003; Aronson and Galatowitsch, 2008; Laubhan and Gleason, 2008; Paradeis et al., 2010; Smith et al., 2016). Restored wetlands in the PPR are often colonized by fewer species than are found in natural sites, their wet-prairie and sedge-meadow zones generally do not redevelop, and many become dominated by invasive perennial species such as *Phalaris arundinacea* (reed canarygrass) and *Typha x glauca* (hybrid cattail) (Seabloom and van der Valk, 2003; Aronson and Galatowitsch, 2008). Based on generalizations from the previous studies in the PPR, periodic regional assessments that target sites of interest could benefit conservation efforts by providing information related to specific wetland types, management practices, or regions.

Within the PPR, the USFWS National Wildlife Refuge System (NWRS) manages thousands of square kilometers consisting of lands such as National Wildlife Refuges (NWRs) and Waterfowl Production Areas (WPAs) (Dixon et al., 2019). These conservation lands preserve and restore grassland/wetland complexes to support the conservation of wildlife, and provide habitat for migratory birds such as waterfowl. In recent years, a focus of the USFWS has been on restoring and reconstructing the grassland portion of these complexes (e.g., Gannon et al., 2013; Igl et al., 2018; Dixon et al., 2019), with less emphasis on the embedded pothole wetlands. At a national level, although a vegetation-based condition assessment indicated that 80% of the wetland area in the United States Interior Plains, which partially overlays the PPR, was in good or fair condition, 19% was considered poor (U.S. Environmental Protection Agency, 2016a). Conversely, a regional vegetation assessment indicated that 82% of the wetlands in western Minnesota were in poor or fair condition, while only 18% were considered good or exceptional (Bourdaghs et al., 2019). These results highlight the need to assess the outcomes of current and previous

management practices, in terms of the ecologic condition of wetlands, to inform management strategies for improving the condition and functioning of restored and natural wetlands.

1.2.3 Biotic indices in the Prairie Pothole Region

All manner of biotic communities of wetlands, along with geochemistry and soils, have been widely studied, but plant and invertebrate communities generally have been promoted as potential indicators of wetland ecologic condition (DeKeyser et al., 2003; Tangen et al., 2003; Hargiss et al., 2008; Gleason and Rooney, 2017; Hargiss et al., 2017; Preston et al., 2018). Aquatic invertebrates are an important component of the food chain, and various taxa have been shown to be sensitive to disturbance or pollution in aquatic systems such as streams (e.g., Kerans and Karr, 1994; Fore et al., 1996; Morley and Karr, 2002). Plants provide habitat for a wide variety of birds, invertebrates, and other wildlife, with species composition closely coupled with soils, hydrology, and water chemistry. Plant communities often respond in predictable patterns to anthropogenic impacts; thus, they also are well-suited to function as indicators of wetland condition. Aquatic invertebrates of wetlands have shown inconsistent and variable responses to stressors, and efforts to incorporate them into biotitic indices have proven largely ineffective (Tangen et al., 2003; Hentges and Stewart, 2010; Batzer, 2013; Gleason and Rooney, 2017; Preston et al., 2018).

Conversely, vegetation-based assessments have resulted in the development and implementation of biotic indices for assessing wetland condition (Kantrud and Newton, 1996; DeKeyser et al., 2003; Reiss, 2006; Hargiss et al., 2008; Reiss et al., 2010; Rooney and Bayley, 2012; Wilson and Bayley, 2012; Wilson et al., 2013). DeKeyser et al. (2003) developed the index of plant community integrity (IPCI) for assessing the quality of wetland plant communities, which can be a surrogate for overall wetland condition. Hargiss et al. (2008) demonstrated the validity of the IPCI as a tool for assessing various classes of wetlands throughout the PPR, indicating its utility for informing wetland management and conservation practices. We synopsize established methods and procedures developed in North and South Dakota for using plants to assess inland wetlands of the PPR. The utility of these vegetation-based assessments is demonstrated through presentation of a case study performed in the PPR of North America, although the information provided should be applicable elsewhere with appropriate modifications. The overall goal was to inform and guide wetland restoration and management, while the overarching objective of this paper was to provide a real-world example of the application of existing methodologies, while discussing important aspects to consider when utilizing and adapting biotic indices to a diversity of aquatic systems.

2 Methods

2.1 Selection of wetlands

The PPR case study focused on temporarily and seasonally ponded wetlands (classification of Stewart and Kantrud, 1971) located on native prairie or reseeded (i.e., restored) former croplands managed by the USFWS (i.e., NWRs and WPAs). Wetlands were classified and identified based on wetland polygons from a modified USFWS National Wetlands Inventory geodatabase (see Tangen et al., 2019). Selection of study wetlands was constrained to the North Dakota, South Dakota, and Montana portions of the United States PPR (Figure 1). These relatively small (<1.0 ha) and shallow (<1 m) wetlands generally have two to three vegetation zones and make up roughly 90% of wetlands throughout the PPR (Stewart and Kantrud, 1971; Niemuth et al., 2010; Dahl, 2014). Spatially balanced designs for populations that are unevenly distributed across the landscape provide spatially distributed samples that are more likely to be representative of the population than the commonly used random sampling approach (Dunn and Harrison, 1993; Stevens and Olsen, 2004; Olsen et al., 2012). Thus, we selected study wetlands using a generalized random tessellation stratified (GRTS) sampling design, following the approach of the United States Environmental Protection Agency's National Wetland Condition Assessment (Stevens and Olsen, 2004; Stevens and Jensen, 2007; U.S. Environmental Protection Agency, 2016b; Olsen et al., 2019). This approach generated a randomly selected, but spatially balanced distribution of 250 wetlands stratified by hydrologic regime (i.e., temporarily, seasonally ponded) and sample year (i.e., Year 1 [2020] and Year 2 [2021]; Tangen et al., 2019). Equal number of wetlands were targeted for each class and sample year. Two hundred of the selected wetlands were designated as primary sample sites, while the remaining 50 were designated as alternates for use when the primary sites were deemed not appropriate for sampling (e.g., misclassified, inaccessible). Of the 200 sampled wetlands, 48 (13 temporarily ponded, 35 seasonally ponded) and 152 (46 temporarily ponded, 106 seasonally ponded) were located within native prairie and reseeded croplands, respectively. Site selection was performed using the 'spsurvey' package (Kincaid and Olsen, 2019) in R (R version 3.0.1; R Core Development Team, Vienna).

2.2 Plant surveys

Plant surveys were performed during summer when most plants were mature enough to be identified to species. One hundred wetlands were surveyed during each of the 2 years of the study (2020–2021; Jones, 2021). Survey and inventory procedures followed an established quadrat method for PPR wetlands (DeKeyser et al., 2003; Hargiss et al., 2008). Upon arrival at a site, the primary concentric wetland vegetation zones

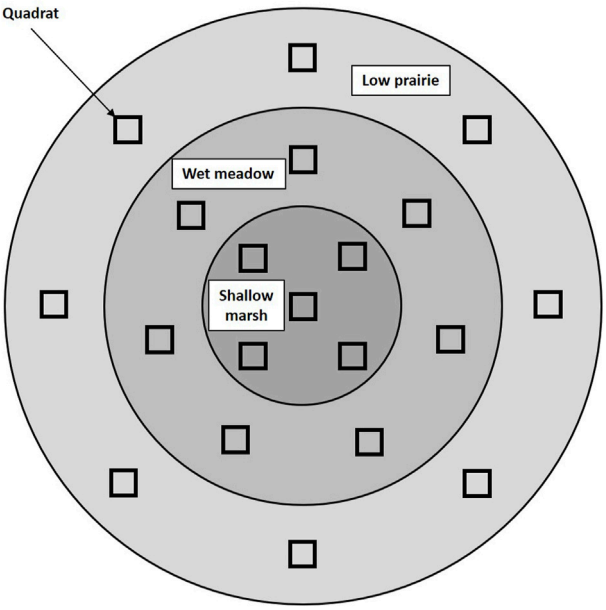

FIGURE 2
General vegetation sample layout for quadrats in the low-prairie, wet-meadow, and shallow-marsh zones of seasonally ponded wetlands of the Prairie Pothole Region of North America (see DeKeyser et al., 2003; Hargiss, 2009). Temporarily ponded wetlands have a similar layout, but only have an exterior low-prairie zone and a central wet-meadow zone.

(Stewart and Kantrud, 1971) were delineated. Both temporarily and seasonally ponded wetlands had an exterior low-prairie zone and an interior wet-meadow zone (central zone for temporarily ponded); additionally, seasonally ponded wetlands had a central, shallow-marsh zone. For seasonally ponded wetlands, eight quadrats (1 m^2) were evenly distributed throughout the low-prairie zone; seven in the wet-meadow zone and five in the shallow-marsh zone. For temporarily ponded wetlands, eight quadrats were distributed throughout the low-prairie zone, and seven quadrats were distributed in the wet-meadow zone. Quadrats were centered in the interior and exterior vegetation zones, and oriented in a spiraled configuration in the central vegetation zone (DeKeyser et al., 2003; Hargiss, 2009; Figure 2). When open water was present in the central zone, quadrats were distributed proportionally to the area of open water and emergent vegetation following DeKeyser et al. (2003) and Hargiss (2009). The entire wetland was surveyed regardless of area; thus, spacing between quadrats varied among wetlands. Plant species within each quadrat were identified. In addition to the primary species within the sample quadrats, species located between, but not within, quadrats were recorded and used to determine IPCI scores (Hargiss et al., 2008). Additional information describing quadrats also was documented, including the percentage of the quadrat covered by standing dead vegetation, open water, or bare ground, and litter thickness and water depth.

2.3 Wetland condition

Data from the plant surveys were used to assess wetland condition using metrics developed for the prairie wetland IPCI by DeKeyser et al. (2003), along with modified metric value ranges and scoring criteria presented by Hargiss et al. (2008). There are several established approaches to metric scoring in the literature that include using ordinal classes (e.g., DeKeyser et al., 2003; Hargiss et al., 2008) and continuous scoring (e.g., U.S. Environmental Protection Agency, 2016b; Magee et al., 2019). We chose to use the established ordinal-class approach to metric scoring for the PPR from DeKeyser et al. (2003) and Hargiss et al. (2008) instead of developing new indices and scoring criteria that a continuous scoring approach would necessitate. In total, nine plant community metrics were used to assign a condition score to each temporarily and seasonally ponded pothole wetland, with a maximum possible score of 99. The nine metrics represent various aspects of species richness, species composition, disturbance tolerance, and floristic quality (Table 1). The species richness and composition metrics focus on the number of native perennial species or genera, and the proportion of annual, biennial, and introduced species. Stress tolerance of native species was determined using a coefficient of conservatism, or 'C-value,' following The Northern Great Plains Floristic Quality Assessment Panel (2001). The C-value was used to calculate three metrics based on a plant's stress tolerance, and one metric based on a floristic quality index (DeKeyser et al., 2003), which was calculated as the average C-value multiplied by the square root of the total number of native plant species (Table 1). Metric scores for each wetland were summed, and wetlands were categorized as very poor, poor, fair, good, or very good following Hargiss et al. (2008; Table 2).

2.4 Data analysis

Condition classes were assigned to each of the 200 sampled wetlands, and the unweighted results were summarized by number and percent of wetlands in each condition category. Condition classes were determined using all species identified, including those not located within the sample quadrats. Because these results are based on the number of wetlands in each category, there are no associated confidence intervals.

3 Results

The wetland selection process resulted in an equal number of temporarily and seasonally ponded wetlands. Wetland classification based on hydrologic and vegetation conditions, however, is temporally variable based on weather and climate (Euliss et al., 2004); thus, spatial wetland databases are inherently associated with some classification variability and error. Based on

TABLE 1 Index of Plant Community Integrity metric value ranges for scores of 0, 4, 7, and 11 for temporarily ponded and seasonally ponded wetlands of the Prairie Pothole Region of North America (see Hargiss et al., 2008).

Metric	0	4	7	11
Temporarily ponded				
Species richness of native perennials	0–16	17–23	24–40	≥41
Number of Genera of native perennials	0–11	12–19	20–26	≥27
Number of native grass and grass-like species	0–8	9–10	11–15	≥16
Percentage of annual, biennial, and introduced species	≥41.1	35.1–41.0	27.1–35.0	0.0–27.0
Number of native perennial species in wet-meadow zone	0–7	8–10	11–13	≥14
Number of species with C value ≥ 5[a]	0–4	5–11	12–16	≥17
Number of species in the wet-meadow zone with C value ≥ 4[a]	0–3	4–9	10–12	≥13
Average C value[a]	0.00–2.50	2.51–3.57	3.58–4.58	≥4.59
Floristic Quality Index (FQI)[b]	0.00–13.60	13.61–21.70	21.71–27.20	≥27.21
Seasonally ponded				
Species richness of native perennials	0–19	20–31	32–41	≥42
Number of Genera of native perennials	0–14	15–24	25–32	≥33
Number of native grass and grass-like species	0–6	7–10	11–17	≥18
Percentage of annual, biennial, and introduced species	≥41.1	30.8–41.0	21.1–30.7	0.0–21.0
Number of native perennial species in wet-meadow zone	0–8	9–16	17–24	≥25
Number of species with C value ≥ 5[a]	0–7	8–17	18–26	≥27
Number of species in the wet-meadow zone with C value ≥ 4[a]	0–4	5–9	10–16	≥17
Average C value[a]	0.00–2.60	2.61–3.12	3.13–3.52	≥3.53
Floristic Quality Index (FQI)[b]	0.00–10.00	10.01–16.11	16.12–22.99	≥23.00

[a]Coefficients of conservatism (C value) follow the Northern Great Plains Floristic Quality Assessment Panel (2001).
[b]FQI, average C-value multiplied by the square root of the total number of native plant species (DeKeyser et al., 2003).

TABLE 2 Score ranges for each Index of Plant Community Integrity condition category for temporarily ponded and seasonally ponded wetlands of the Prairie Pothole Region of North America (see Hargiss et al., 2008).

	Score range	
Wetland condition	Temporarily ponded	Seasonally ponded
Very poor	--	0–19
Poor	0–33	20–39
Fair	34–66	40–59
Good	67–99	60–79
Very good	--	80–99

onsite classification by field personnel (following Stewart and Kantrud, 1971), 59 pothole wetlands were treated as temporarily ponded (two vegetation zones) and 141 as seasonally ponded (three vegetation zones) based on vegetation conditions during 2020–2021. Moreover, 24 of the initial 200 wetlands were replaced with alternates due to factors such as misclassification and difficulty of access. Thus, it is important to select alternate wetlands during the site selection process to avoid potential bias when replacing sites deemed not appropriate for sampling.

When the 200 wetlands from both classes and years were combined, IPCI scores indicated that 49.5% were in very poor or poor condition, 25.0% were in fair condition, and 25.5% were in good or very good condition (Figure 3). When segregated by grassland type, the average (± standard deviation) IPCI score of the wetlands in native grasslands (64 ± 24) was nearly twice that of wetlands in reseeded grasslands (34 ± 21). Approximately 70% of wetlands in native grasslands were categorized as good or very good, while only 12% of pothole wetlands in reseeded grasslands were categorized as good or very good (Figure 4). Conversely, 15% of wetlands in native grasslands were categorized as poor, while >60% of wetlands in reseeded grasslands were categorized as poor or very poor. No wetlands in native grasslands were categorized as very poor (Figure 4). When segregated by wetland class, 54% of seasonal and 42% of temporarily ponded wetlands were categorized as fair, good, or very good. Correspondingly, 46% of seasonally ponded and 58% of temporarily ponded

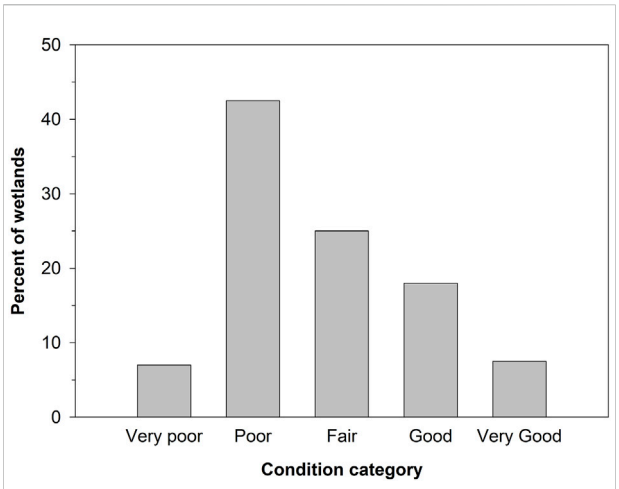

FIGURE 3
Percent of sampled (2020–2021) wetlands assigned to each Index of Plant Community Integrity condition category. Data represent 59 temporarily ponded and 141 seasonally ponded wetlands located within native prairie and reseeded grasslands in the United States portion of the Prairie Pothole Region of North America.

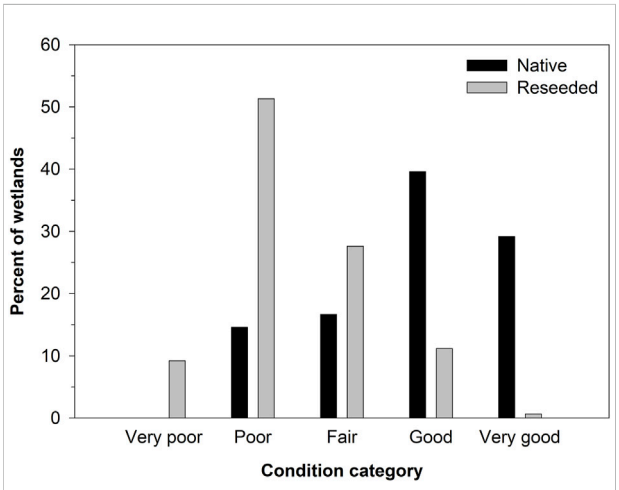

FIGURE 4
Percent of sampled (2020–2021) wetlands within 48 native prairie and 152 reseeded grasslands assigned to each Index of Plant Community Integrity condition category. Data represent 59 temporarily ponded and 141 seasonally ponded potholes in the United States portion of the Prairie Pothole Region of North America.

wetlands were categorized as poor or very poor. Common (i.e., present in ≥50% of wetlands) plants identified in study wetlands included invasive or non-native species such as Canada thistle (*Cirsium arvense*), smooth brome (*Bromus inermis*), Kentucky bluegrass (*Poa pratensis*), reed canarygrass, and hybrid cattail (Jones, 2021). Moreover, disturbed wetlands with low condition scores typically were dominated by smooth brome, Kentucky bluegrass, reed canarygrass, and hybrid cattail (Jones, 2021).

4 Discussion

Through presentation of a case study (see Tangen et al., 2019; Jones, 2021), we demonstrated a method for assessing wetland condition using an established biotic index based on vegetation (DeKeyser et al., 2003; Hargiss et al., 2008). In doing so, we also used a proven method for selecting a representative, spatially balanced sample of wetlands across a broad spatial area (Stevens and Olsen, 2004; Stevens and Jensen, 2007; U.S. Environmental Protection Agency, 2016b; Olsen et al., 2019). While the case study was specific to the PPR, the overall methodologies and approach are applicable to other areas and wetland types, although modifications to metrics and scoring criteria likely would be required.

4.1 Informing wetland management

Wetland condition assessments can provide relevant and timely data to wetland managers and conservation organizations that can be used to inform policy development, guide the allocation of resources, frame the problem of invasive and non-native plants, determine if management and restoration objectives are met, and support overall conservation efforts such as land procurement and habitat improvement. Using data from this field study, Jones (2021) identified USFWS wetland management districts located in north-west North Dakota and north-east South Dakota as having the highest quality (i.e., greatest average IPCI/species richness scores) wetland vegetation communities. In general, these high-quality areas were characterized by greater amounts of native grasslands and less agricultural soil disturbance than areas with low-quality communities. Conservation organizations can use such information to inform and guide management and conservation efforts. For example, areas characterized by relatively high-quality wetlands could be prioritized for establishment of conservation easements to protect wetlands from anthropogenic activities. Similarly, areas characterized by relatively low-quality wetlands could be prioritized for restoration or invasive species management. Information gained from these types of assessments also can be used to refine habitat management practices or prioritize management of specific areas or wetland types associated with degraded habitat conditions.

Results of the PPR case study suggested that plant communities from approximately one-half of the wetlands included in this study were in very poor or poor condition, while only 25% were in good or very good condition. Jones (2021) showed that the wetlands from the PPR case study with low index scores (e.g., very poor, poor) were characterized by fewer plant species than those with larger index scores (e.g., good, very good). Moreover, wetlands with low index scores tended to be dominated by invasive or non-native species.

When results were examined separately for wetlands within native and reseeded grasslands, however, it was evident that most of the restored wetlands were in poor condition, while most of the natural wetlands were in relatively good condition (Figure 4). Nevertheless, roughly 30% of the wetlands embedded within native grasslands were characterized by vegetation communities considered poor or fair, suggesting that both restored and native prairie wetlands would benefit from enhanced management of invasive species. Moreover, results suggest that the USFWS could benefit from allocation of additional resources for monitoring managed lands and assessing restoration and management practices.

These general results, along with findings of previous studies (Kantrud and Newton, 1996; Mulhouse and Galatowitsch, 2003; Aronson and Galatowitsch, 2008; Smith et al., 2016; Galatowitsch and Bohnen, 2021), indicate that wetland restoration techniques and management could benefit from practices that focus not only on re-establishing natural wetland plant communities, but on controlling invasive species (e.g., prescribed burns, herbicide treatments, or grazing). For instance, restoration practices in the PPR, which often focus on re-establishing hydrology and restoring croplands to grassland, could be modified to include seeding native wetland plants when possible. Currently, wetland plants typically establish through natural colonization. While not a common practice, Smith et al. (2016) suggested that removal of accumulated sediment may result in greater quality plant communities for restored wetlands; thus, restoration efforts also could incorporate this practice as well.

4.2 Application to other areas and wetland types

Biotic indices based on a variety of organisms (e.g., plants, invertebrates, fish) have been developed for numerous aquatic systems (e.g., Karr, 1981; Lopez and Fennessy, 2002; Seilheimer and Chow-Fraser, 2006; Lu et al., 2019; Magee et al., 2019). The plant-based IPCI used for this case study has proven useful for assessing wetlands of the PPR (DeKeyser et al., 2003; Hargiss et al., 2008). These concepts and methods should be easily adapted elsewhere. Specific metrics and scoring criteria used for the IPCI (Tables 1, 2), however, likely would not be appropriate for wetland systems outside of the PPR, or even other wetland classes within the PPR (e.g., permanent pond, fen). Furthermore, our metrics rely on presence/absence of species and do not incorporate abundance data, the incorporation of which may result in a more powerful multi-metric index. Thus, initial efforts to adapt the IPCI (or other indices) to other areas and wetland types would require assessing the utility of the PPR metrics, and possibly the development of alternative metrics and scoring criteria. This process may include the sampling of wetlands across a broad degradation gradient to validate existing metrics, or to identify new metrics, including abundance metrics, that display a predictable response to disturbance. Reference wetlands (i.e., least disturbed, best available; Herlihy et al., 2019) also may have to be sampled to facilitate development of index scoring ranges for the various condition categories (e.g., poor, fair, good).

To maximize the provisioning of ecosystem services, conservation personnel require methodologies to assess wetland condition with the purpose of supporting wetland conservation and management. We presented a case study from the PPR to demonstrate the utility of using an existing plant-based biotic index applied with a probabilistic sampling design to assess wetland condition over a broad geographic setting and over different management settings. Methods used for the case study, including site selection, field sampling protocols, plant metrics, and scoring criteria, were developed specifically for PPR wetlands; however, they can provide a baseline for subsequent studies and can be adapted for a variety of wetlands. We also used results of the case study to demonstrate how wetland assessments can inform management and discussed considerations for adapting the method for other systems. Results of this and other studies suggest that plant community characteristics can be appropriate surrogates for assessing the ecologic condition of wetlands, but natural variability and unique traits of specific wetland types should be considered.

Data availability statement

The raw data supporting the conclusion of this article will be made available by the authors, without undue reservation.

Author contributions

BT, SB, SJ, CD, ED, CH, and DM contributed to conception and design of the study. SJ performed field work and organized the data. BT wrote the first draft of the manuscript. All authors contributed to manuscript revision, read, and approved the submitted version.

Funding

This effort was funded by the United States Fish and Wildlife Service and United States Geological Survey Ecosystems Mission Area, Land Change Science Climate Research & Development Program.

Acknowledgments

We thank Rachel Fern for assistance with sample sections for the case study. We thank Patti Meeks and Michael Bourdaghs for comments on a previous version of this manuscript. This manuscript has been subjected to United States. Environmental Protection Agency (EPA) review and has been approved for publication. The views expressed in this paper are those of the authors and do not necessarily reflect the views or policies of the U.S. EPA. Any use of trade, firm, or product names

is for descriptive purposes only and does not imply endorsement by the United States Government.

Conflict of interest

The authors declare that the research was conducted in the absence of any commercial or financial relationships that could be construed as a potential conflict of interest.

Publisher's note

All claims expressed in this article are solely those of the authors and do not necessarily represent those of their affiliated organizations, or those of the publisher, the editors and the reviewers. Any product that may be evaluated in this article, or claim that may be made by its manufacturer, is not guaranteed or endorsed by the publisher.

References

Aronson, M. F. J., and Galatowitsch, S. (2008). Long-term vegetation development of restored prairie pothole wetlands. *Wetlands* 28, 883–895. doi:10.1672/08-142.1

Badiou, P., McDougal, R., Pennock, D., and Clark, B. (2011). Greenhouse gas emissions and carbon sequestration potential in restored wetlands of the Canadian Prairie Pothole Region. *Wetl. Ecol. Manag.* 19, 237–256. doi:10.1007/s11273-011-9214-6

Batt, B. D. J., Anderson, M. G., Anderson, C. D., and Caswell, F. D. (1989). "The use of prairie potholes by North American ducks," in *Northern prairie wetlands*. Editor A. G. van der Valk (Ames: Iowa State University Press), 204–227.

Batzer, D. P. (2013). The seemingly intractable ecological responses of invertebrates in North American wetlands–A review. *Wetlands* 33, 1–15. doi:10.1007/s13157-012-0360-2

Blann, K. L., Anderson, J. L., Sands, G. R., and Vondracek, B. (2009). Effects of agricultural drainage on aquatic ecosystems: A review. *Crit. Rev. Environ. Sci. Technol.* 39, 909–1001. doi:10.1080/10643380801977966

Bolding, M. T., Kraft, A. J., Robinson, D. T., and Rooney, R. C. (2020). Improvements in multi-metric index development using a whole-index approach. *Ecol. Indic.* 113, 106191. doi:10.1016/j.ecolind.2020.106191

Bourdaghs, M. (2012). *Development of a rapid floristic quality assessment. Minnesota Pollution Control Agency*. Available: https://www.pca.state.mn.us/sites/default/files/wq-bwm2-02a.pdf.

Bourdaghs, M., Genet, J., and Gernes, M. (2019). *Status and trends of wetlands in Minnesota: Minnesota wetland condition assessment (2011/12–2016)*. Saint Paul, MN: Minnesota Pollution Control Agency. Available: https://www.pca.state.mn.us/sites/default/files/wq-bwm1-11.pdf.

Brinson, M. M. (1993). *A hydrogeomorphic classification for wetlands*. Washington, DC: U.S. Army Corps of Engineers Technical Report WRP-DE-4. Available: https://wetlands.el.erdc.dren.mil/pdfs/wrpde4.pdf.

Burton, T. M., Uzarski, D. G., Gathman, J. P., Genet, J. A., Keas, B. E., and Stricker, C. A. (1999). Development of a preliminary invertebrate index of biotic integrity for Lake Huron coastal wetlands. *Wetlands* 19, 869–882. doi:10.1007/BF03161789

Dahl, T. E. (2014). *Status and trends of prairie wetlands in the United States 1997 to 2009*. Washington, DC: U.S. Department of the Interior, Fish and Wildlife Service. Available: https://www.fws.gov/wetlands/documents/Status-and-Trends-of-Prairie-Wetlands-in-the-United-States-1997-to-2009.pdf.

DeKeyser, E. S., Kirby, D. R., and Ell, M. J. (2003). An index of plant community integrity: Development of the methodology for assessing prairie wetland plant communities. *Ecol. Indic.* 3, 119–133. doi:10.1016/S1470-160X(03)00015-3

Dixon, C., Vacek, S., and Grant, T. (2019). Evolving management paradigms on U.S. Fish and wildlife service lands in the prairie pothole region. *Rangelands* 41, 36–43. doi:10.1016/j.rala.2018.12.004

Doherty, K. E., Ryba, A. J., Stemler, C. L., Niemuth, N. D., and Meeks, W. A. (2013). Conservation planning in an era of change: State of the U.S. Prairie pothole region. *Wildl. Soc. Bull.* 37, 546–563. doi:10.1002/wsb.284

Dunn, R., and Harrison, A. R. (1993). Two-dimensional systematic sampling of land use. *Appl. Stat.* 42, 585–601. doi:10.2307/2986177

Euliss, N. H., Jr., Gleason, R. A., Olness, A., McDougal, R. L., Murkin, H. R., Robarts, R. D., et al. (2006). North American prairie wetlands are important nonforested land-based carbon storage sites. *Sci. Total Environ.* 361, 179–188. doi:10.1016/j.scitotenv.2005.06.007

Euliss, N. H., Jr., LaBaugh, J. W., Fredrickson, L. H., Mushet, D. M., Laubhan, M. K., Swanson, G. A., et al. (2004). The wetland continuum: A conceptual framework for interpreting biological studies. *Wetlands* 24, 448–458. doi:10.1672/0277-5212(2004)024[0448:TWCACF]2.0.CO;2

Euliss, N. H., Jr., and Mushet, D. M. (2011). A multi-year comparison of IPCI scores for prairie pothole wetlands: Implications of temporal and spatial variation. *Wetlands* 31, 713–723. doi:10.1007/s13157-011-0187-2

Euliss, N. H., Jr., Mushet, D. M., Newton, W. E., Otto, C. R. V., Nelson, R. D., LaBaugh, J. W., et al. (2014). Placing prairie pothole wetlands along spatial and temporal continua to improve integration of wetland function in ecological investigations. *J. Hydrology* 513, 490–503. doi:10.1016/j.jhydrol.2014.04.006

Fore, L. S., Karr, J. R., and Wisseman, R. W. (1996). Assessing invertebrate responses to human activities: Evaluating alternative approaches. *J. North Am. Benthol. Soc.* 15, 212–231. doi:10.2307/1467949

Galatowitsch, S., and Bohnen, J. (2021). Long-term recovery of a restored palustrine wetland: The role of monitoring and adaptive management. *Wetlands* 41, 80. doi:10.1007/s13157-021-01478-7

Galatowitsch, S., and Bohnen, J. (2020). Predicting restoration outcomes based on organizational and ecological factors. *Restor. Ecol.* 28, 1201–1212. doi:10.1111/rec.13187

Galatowitsch, S. M., and van der Valk, A. G. (1996b). The vegetation of restored and natural prairie wetlands. *Ecol. Appl.* 6, 102–112. doi:10.2307/2269557

Galatowitsch, S. M., and van der Valk, A. G. (1996a). Vegetation and environmental conditions in recently restored wetlands in the prairie pothole region of the USA. *Vegetatio* 126, 89–99. doi:10.1007/BF00047764

Gannon, J. J., Shaffer, T. L., and Moore, C. T. (2013). Native prairie adaptive management: A multi region adaptive approach to invasive plant management on fish and wildlife service owned native prairies. *U.S. Geol. Surv.* Open-File Report 2013–1279. doi:10.3133/ofr20131279

Gleason, R. A., Laubhan, M. K., and Euliss, N. H., Jr. (eds) (2008). Ecosystem services derived from wetland conservation practices in the United States Prairie Pothole Region with an emphasis on the US Department of Agriculture Conservation Reserve and Wetlands Reserve Programs. *U.S. Geological Survey Professional Paper* 1745. doi:10.3133/pp1745

Gleason, J. E., and Rooney, R. C. (2017). Aquatic macroinvertebrates are poor indicators of agricultural activity in northern prairie pothole wetlands. *Ecol. Indic.* 81, 333–339. doi:10.1016/j.ecolind.2017.06.013

Gleason, R. A., and Euliss, N. H., Jr. (1998). Sedimentation of prairie wetlands. *Gt. Plains. Res.* 8, 97–112. Available at: http://digitalcommons.unl.edu/greatplainsresearch/363?utm_source=digitalcommons.unl.edu%2Fgreatplainsresearch%2F363&utm_medium=PDF&utm_campaign=PDFCoverPages.

Gleason, R. A., Euliss, N. H., Jr., Tangen, B. A., Laubhan, M. K., and Browne, B. A. (2011). USDA conservation program and practice effects on wetland ecosystem services in the Prairie Pothole Region. *Ecol. Appl.* 21, S65–S81. doi:10.1890/09-0216.1

Goldhaber, M. B., Mills, C., Stricker, C. A., and Morrison, J. M. (2011). The role of critical zone processes in the evolution of the Prairie Pothole Region wetlands. *Appl. Geochem.* 26, S32–S35. doi:10.1016/j.apgeochem.2011.03.022

Gronke, A. L. (2004). *Development of an integrated index of biotic integrity for prairie pothole lakes of eastern South Dakota*. Brookings, SD: South Dakota State University. [master's thesis][Brookings (SD)].

Guntenspergen, G. R., Peterson, S. A., Leibowitz, S. G., and Cowardin, L. M. (2002). Indicators of wetland condition for the prairie pothole region of the United States. *Environ. Monit. Assess.* 78, 229–252. doi:10.1023/A:1019982818231

Hargiss, C. L. M., DeKeyser, E. S., Kirby, D. R., and Ell, M. J. (2008). Regional assessment of wetland plant communities using the index of plant community integrity. *Ecol. Indic.* 8, 303–307. doi:10.1016/j.ecolind.2007.03.003

Hargiss, C. L. M., DeKeyser, E. S., Norland, J. E., and Ell, M. J. (2017). Comparing tiers of a multi-tiered wetland assessment in the Prairie Pothole Region. *Wetl. Ecol. Manag.* 25, 639–647. doi:10.1007/s11273-017-9540-4

Hargiss, C. L. M. (2009). *Estimating wetland quality for the Missouri Coteau ecoregion in North Dakota*. Fargo, ND: North Dakota State University. [dissertation]. [Fargo (ND)].

Hayashi, M., van der Kamp, G., and Rosenberry, D. O. (2016). Hydrology of prairie wetlands: Understanding the integrated surface-water and groundwater processes. *Wetlands* 36, S237–S254. doi:10.1007/s13157-016-0797-9

Hentges, V. A., and Stewart, T. W. (2010). Macroinvertebrate assemblages in Iowa prairie pothole wetlands and relation to environmental features. *Wetlands* 30, 501–511. doi:10.1007/s13157-010-0058-2

Herlihy, A. T., Kentula, M. E., Magee, T. K., Lomnicky, G. A., Nahlik, A. M., and Serenbetz, G. (2019). Striving for consistency in the national wetland condition assessment: Developing a reference condition approach for assessing wetlands at a continental scale. *Environ. Monit. Assess.* 191, 327. doi:10.1007/s10661-019-7325-3

Igl, L. D., Newton, W. E., Grant, T. A., and Dixon, C. S. (2018). Adaptive management in native grasslands managed by the U.S. Fish and wildlife Service—implications for grassland birds. *U.S. Geol. Surv.* Open-File Report 2018–1152. doi:10.3133/ofr20181152

Johnson, R. R., Oslund, F. T., and Hertel, D. R. (2008). The past, present, and future of prairie potholes in the United States. *J. Soil Water Conservation* 63, 84A–87A. doi:10.2489/jswc.63.3.84A

Johnston, C. A. (2013). Wetland losses due to row crop expansion in the Dakota Prairie Pothole Region. *Wetlands* 33, 175–182. doi:10.1007/s13157-012-0365-x

Jones, S. (2021). *Assessment of prairie pothole conditions and plant community composition on FWS fee-title lands*. Fargo, ND: North Dakota State University. [master's thesis]. [Fargo (ND)].

Kantrud, H. A., and Newton, W. E. (1996). A test of vegetation-related indicators of wetland quality in the prairie pothole region. *J. Aquat. Ecosyst. Stress. Recov.* 5, 177–191. doi:10.1007/BF00124105

Karr, J. R. (1981). Assessment of biotic integrity using fish communities. *Fisheries* 6, 212–227. doi:10.1577/1548-8446(1981)006<0021:AOBIUF>2.0.CO

Kentula, M. E., Nahlik, A. M., Paulsen, S. G., and Magee, T. K. (2020). "Wetland assessment: Beyond the traditional water quality perspective," in *Water quality–science, assessments and policy*. Editor K. J. Summers (London: IntechOpen). doi:10.5772/intechopen.92583

Kerans, B. L., and Karr, J. R. (1994). A benthic index of biotic integrity (B-IBI) for rivers of the Tennessee Valley. *Ecol. Appl.* 4, 768–785. doi:10.2307/1942007

Kincaid, T., and Olsen, T. (2019). *spsurvey: spatial survey design and analysis, R package version 4.0.0*. Available: https://cran.r-project.org/web/packages/spsurvey/spsurvey.pdf (Accessed March 15, 2019).

Knutsen, G. A., and Euliss, N. H., Jr. (2002). *Wetland restoration in the prairie pothole region of North America: A literature review*. Reston, VA: U.S. Geological Survey Biological Science. Report USGS/BRD/BSR-2001-0006. Available: http://pubs.er.usgs.gov/publication/2000149.

LaBaugh, J. W., Rosenberry, D. O., Mushet, D. M., Neff, B. P., Nelson, R. D., and Euliss, N. H., Jr. (2018). Long-term changes in pond permanence, size, and salinity in Prairie Pothole Region wetlands: The role of groundwater-pond interaction. *J. Hydrology Regional Stud.* 17, 1–23. doi:10.1016/j.ejrh.2018.03.003

Langer, T. A., Cooper, M. J., Reisinger, L. S., Reisinger, A. J., and Uzarski, D. G. (2018). Water depth and lake-wide water level fluctuation influence on α- and β-diversity of coastal wetland fish communities. *J. Gt. Lakes. Res.* 44, 70–76. doi:10.1016/j.jglr.2017.11.001

Laubhan, M. K., and Gleason, R. A. (2008). "Plant community quality and richness," in *Ecosystem services derived from wetland conservation practices in the United States prairie pothole region with an emphasis on the US department of agriculture conservation Reserve and wetlands Reserve programs*. Editors R. A. Gleason, M. K. Laubhan, and N. H. EulissJr. (Reston, VA: U.S. Geological Survey Professional Paper 1745), 15–22. doi:10.3133/pp1745

Levy, Z. F., Mills, C. T., Lu, Z., Goldhaber, M. B., Rosenberry, D. O., Mushet, D. M., et al. (2018). Using halogens (Cl, Br, I) to understand the hydrogeochemical evolution of drought-derived saline porewater beneath a prairie wetland. *Chem. Geol.* 476, 191–207. doi:10.1016/j.chemgeo.2017.11.017

Lopez, R. D., and Fennessy, M. S. (2002). Testing the floristic quality assessment index as an indicator of wetland condition. *Ecol. Appl.* 12, 487–497. doi:10.1890/1051-0761(2002)012[0487:TTFQAI]2.0.CO;2

Lu, K., Wu, H., Xue, Z., Lu, X., and Batzer, D. P. (2019). Development of a multimetric index based on aquatic invertebrates to assess floodplain wetland condition. *Hydrobiologia* 827, 141–153. doi:10.1007/s10750-018-3761-2

Mack, J. J. (2006). Landscape as a predictor of wetland condition: An evaluation of the Landscape Development Index (LDI) with a large reference wetland dataset from Ohio. *Environ. Monit. Assess.* 120, 221–241. doi:10.1007/s10661-005-9058-8

Magee, T. K., Blocksom, K. A., and Fennessy, M. S. (2019). A national-scale vegetation multimetric index (VMMI) as an indicator of wetland condition across the conterminous United States. *Environ. Monit. Assess.* 191, 322. doi:10.1007/s10661-019-7324-4

McCorvie, M. R., and Lant, C. L. (1993). Drainage district formation and the loss of midwestern wetlands, 1850-1930. *Agric. Hist.* 67, 13–39. Available at: http://www.jstor.org/stable/3744552.

McLean, K. I., Mushet, D. M., Sweetman, J. N., Anteau, M. J., and Wiltermuth, M. T. (2020). Invertebrate communities of Prairie-Pothole wetlands in the age of the aquatic Homogenocene. *Hydrobiologia* 847, 3773–3793. doi:10.1007/s10750-019-04154-4

McMurry, S. T., Belden, J. B., Smith, L. M., Morrison, S. A., Daniel, D. W., Euliss, B. R., et al. (2016). Land use effects on pesticides in sediments of prairie pothole wetlands in North and South Dakota. *Sci. Total Environ.* 565, 682–689. doi:10.1016/j.scitotenv.2016.04.209

Millennium Ecosystem Assessment (2005). *Ecosystems and human well-being: Wetlands and water synthesis*. Washington, DC: World Resources Institute. Available at: https://www.millenniumassessment.org/documents/document.358.aspx.pdf.

Mitsch, W. J., and Gosselink, J. G. (2015). *Wetlands*. Hoboken: John Wiley & Sons.

Morley, S. A., and Karr, J. R. (2002). Assessing and restoring the health of urban streams in the Puget Sound Basin. *Conserv. Biol.* 16, 1498–1509. doi:10.1046/j.1523-1739.2002.01067.x

Mulhouse, J. M., and Galatowitsch, S. M. (2003). Revegetation of prairie pothole wetlands in the mid-continental US: Twelve years post-reflooding. *Plant Ecol.* 169, 143–159. doi:10.1023/A:1026221302606

Murkin, H. R. (1998). Freshwater functions and values of prairie wetlands. *Gt. Plains. Res.* 8, 3–15. Full publication date: Spring 1998. Available: http://www.jstor.org/stable/24156331.

Mushet, D. M., Goldhaber, M. B., Mills, C. T., McLean, K. I., Aparicio, V. M., McCleskey, R. B., et al. (2015). Chemical and biotic characteristics of prairie lakes and large wetlands in south-central North Dakota—effects of a changing climate. *U. S. Geol. Surv. Sci. Investig.* Report 2015-5126. doi:10.3133/sir20155126

Mushet, D. M., McKenna, O. P., LaBaugh, J. W., Euliss, N. H., Jr., and Rosenberry, D. O. (2018). Accommodating state shifts within the conceptual framework of the wetland continuum. *Wetlands* 38, 647–651. doi:10.1007/s13157-018-1004-y

Mushet, D. M., McKenna, O. P., and McLean, K. I. (2020). Alternative stable states in inherently unstable systems. *Ecol. Evol.* 10, 843–850. doi:10.1002/ece3.5944

Niemuth, N. D., Estey, M. E., Reynolds, R. E., Loesch, C. R., and Meeks, W. A. (2006). Use of wetlands by spring-migrant shorebirds in agricultural landscapes of North Dakota's Drift Prairie. *Wetlands* 26, 302–339. doi:10.1672/0277-5212(2006)26[30:UOWBSS]2.0CO

Niemuth, N. D., Fleming, K. K., and Reynolds, R. E. (2014). Waterfowl conservation in the US prairie pothole region: Confronting the complexities of climate change. *PloS one* 9, 100034. doi:10.1371/journal.pone.0100034

Niemuth, N. D., Ryba, A. J., Pearse, A. T., Kvas, S. M., Brandt, D. A., Wangler, B., et al. (2018). Opportunistically collected data reveal habitat selection by migrating Whooping Cranes in the U.S. Northern Plains. *Condor* 120, 343–356. doi:10.1650/condor-17-80.1

Niemuth, N. D., Wangler, B., and Reynolds, R. E. (2010). Spatial and temporal variation in wet area of wetlands in the prairie pothole region of North Dakota and South Dakota. *Wetlands* 30, 1053–1064. doi:10.1007/s13157-010-0111-1

Northern Great Plains Floristic Quality Assessment Panel (2001). *Coefficients of conservatism for the vascular flora of the Dakotas and adjacent grasslands*. Jamestown, ND: U.S. Geological Survey Information and Technology. Report 2001-0001. doi:10.3133/2002366

Olsen, A. R., Kincaid, T. M., Kentula, M. E., and Weber, M. H. (2019). Survey design to assess condition of wetlands in the United States. *Environ. Monit. Assess.* 191, 268. doi:10.1007/s10661-019-7322-6

Olsen, A. R., Kincaid, T. M., and Payton, Q. (2012). "Spatially balanced survey designs for natural resources," in *Design and analysis of long-term ecological monitoring studies*. Editors R. A. Gitzen, J. J. Millspaugh, A. B. Cooper, and D. S. Licht (Cambridge: Cambridge University Press), 126–150. doi:10.1017/CBO9781139022422.010

Paradeis, B. L., DeKeyser, E. S., and Kirby, D. R. (2010). Evaluation of restored and native Prairie Pothole Region plant communities following an environmental gradient. *Nat. Areas J.* 30, 294–304. doi:10.3375/043.030.0305

Post van der Burg, M., and Tangen, B. A. (2015). Monitoring and modeling wetland chloride concentrations in relationship to oil and gas development. *J. Environ. Manag.* 150, 120–127. doi:10.1016/j.jenvman.2014.10.028

Preston, T. M., Borgreen, M. J., and Ray, A. M. (2018). Effects of brine contamination from energy development on wetland macroinvertebrate community structure in the Prairie Pothole Region. *Environ. Pollut.* 239, 722–732. doi:10.1016/j.envpol.2018.04.088

Rebelo, L. M., Finlayson, C. M., and Nagabhatla, N. (2009). Remote sensing and GIS for wetland inventory, mapping and change analysis. *J. Environ. Manag.* 90, 2144–2153. doi:10.1016/j.jenvman.2007.06.027

Reiss, K. C., Brown, M. T., and Lane, C. R. (2010). Characteristic community structure of Florida's subtropical wetlands: The Florida wetland condition index for depressional marshes, depressional forested, and flowing water forested wetlands. *Wetl. Ecol. Manag.* 18, 543–556. doi:10.1007/s11273-009-9132-z

Reiss, K. C. (2006). Florida Wetland Condition Index for depressional forested wetlands. *Ecol. Indic.* 6, 337–352. doi:10.1016/j.ecolind.2005.03.013

Rooney, R. C., and Bayley, S. E. (2012). Development and testing of an index of biotic integrity based on submersed and floating vegetation and its application to assess reclamation wetlands in Alberta's oil sands area, Canada. *Environ. Monit. Assess.* 184, 749–761. doi:10.1007/s10661-011-1999-5

Schwarz, M. S., Davis, D. R., and Kerby, J. L. (2018). *An evaluation of agricultural tile drainage exposure and effects to wetland species and habitat withing Madison Wetland Management District, South Dakota*. Pierre, SD: U.S. Fish and Wildlife Service. Available: https://ecos.fws.gov/ServCat/Reference/Profile/105778.

Seabloom, E. W., and van der Valk, A. G. (2003). Plant diversity, composition, and invasion of restored and natural prairie pothole wetlands: Implications for restoration. *Wetlands* 23, 12. doi:10.1672/0277-5212(2003)023[0001:PDCAIO]2.0.CO;2

Seilheimer, T. S., and Chow-Fraser, P. (2006). Development and use of the wetland fish index to assess the quality of coastal wetlands in the laurentian great lakes. *Can. J. Fish. Aquat. Sci.* 63, 354–366. doi:10.1139/f05-220

Skagen, S. K., Granfors, D. A., and Melcher, C. P. (2008). On determining the significance of ephemeral continental wetlands to North American migratory shorebirds. *Auk* 125, 20–29. doi:10.1525/auk.2008.125.1.20

Smith, C., DeKeyser, E. S., Dixon, C., Kobiela, B., and Little, A. (2016). Effects of sediment removal on prairie pothole wetland plant communities in North Dakota. *Nat. Areas J.* 36, 48–58. doi:10.3375/043.036.0110

Stevens, D. L., and Jensen, S. F. (2007). Sample design, execution, and analysis for wetland assessment. *Wetlands* 27, 5152. doi:10.1672/0277-5212(2007)27[515:SDEAAF]2.0.CO;2

Stevens, D. L., Jr., and Olsen, A. R. (2004). Spatially balanced sampling of natural resources. *J. Am. Stat. Assoc.* 99, 262–278. doi:10.1198/016214504000000250

Stewart, R. E., and Kantrud, H. A. (1971). *Classification of natural ponds and lakes in the glaciated prairie region*. Washington, DCU.S. Department of the Interior, Fish and Wildlife Service Resource Publication, 92. Available: https://pubs.er.usgs.gov/publication/rp92.

Tangen, B. A., Butler, M. G., and Ell, M. J. (2003). Weak correspondence between macroinvertebrate assemblages and land use in Prairie Pothole Region wetlands. *Wetlands* 23, 104–115. doi:10.1672/0277-5212(2003)023[0104:WCBMAA]2.0.CO;2

Tangen, B., Bansal, S., Fern, R. R., DeKeyser, E. S., Hargiss, C. L. M., Mushet, D. M., et al. (2019). *Study design and methods for a wetland condition assessment on U.S. Fish and wildlife service fee-title lands in the prairie pothole region of North Dakota, South Dakota, and Montana*. USA: U.S. Geological Survey Open-File. Report 2019-1118. doi:10.3133/ofr20191118

Tori, G. M., McLeod, S., McKnight, K., Moorman, T., and Reid, F. A. (2002). Wetland conservation and Ducks Unlimited: Real world approaches to multispecies management. *Waterbirds Int. J. Waterbird Biol.* 25, 115–121. Available: http://www.jstor.org/stable/1522457.

U.S. Environmental Protection Agency (2016a). *National wetland condition assessment 2011–A collaborative survey of the Nation's wetlands*. Washington, DC: U.S. Environmental Protection Agency. EPA-843-R-15-005. Available: https://www.epa.gov/national-aquatic-resource-surveys/nwca.

U.S. Environmental Protection Agency (2016b). *National wetland condition assessment: 2011 technical report*. Washington, DC: U.S. Environmental Protection Agency. EPA-843-R-15-006. Available: https://www.epa.gov/national-aquatic-resource-surveys/national-wetland-condition-assessment-2011-technical-report.

Walker, J., Rotella, J. J., Loesch, C. R., Renner, R. W., Ringelman, J. K., Lindberg, M. S., et al. (2013). An integrated strategy for grassland easement acquisition in the Prairie Pothole Region, USA. *J. Fish. Wildl. Manag.* 4, 267–279. doi:10.3996/052013-jfwm-035

Wilcox, D. A., Meeker, J. E., Hudson, P. L., Armitage, B. J., Black, M. G., and Uzarski, D. G. (2002). Hydrologic variability and the application of index of biotic integrity metrics to wetlands: A great lakes evaluation. *Wetlands* 22, 5882–6615. doi:10.1672/0277-5212(2002)022[0588:HVATAO]2.0.CO;2

Wilson, M. J., Bayley, S. E., and Rooney, R. C. (2013). A plant-based index of biological integrity in permanent marsh wetlands yields consistent scores in dry and wet years. *Aquat. Conserv.* 23, 698–709. doi:10.1002/aqc.2354

Wilson, M. J., and Bayley, S. E. (2012). Use of single versus multiple biotic communities as indicators of biological integrity in northern prairie wetlands. *Ecol. Indic.* 20, 187–195. doi:10.1016/j.ecolind.2012.02.009

Winter, T. C., and Rosenberry, D. O. (1995). The interaction of ground water with prairie pothole wetlands in the Cottonwood Lake area, east-central North Dakota, 1979–1990. *Wetlands* 15, 193–211. doi:10.1007/BF03160700

Yan, F., and Zhang, S. (2019). Ecosystem service decline in response to wetland loss in the Sanjiang Plain, Northeast China. *Ecol. Eng.* 130, 117–121. doi:10.1016/j.ecoleng.2019.02.009

Zedler, J. B., and Kercher, S. (2005). Wetland resources: Status, trends, ecosystem services, and restorability. *Annu. Rev. Environ. Resour.* 30, 39–74. doi:10.1146/annurev.energy.30.050504.144248

frontiers | Frontiers in Ecology and Evolution

TYPE Original Research
PUBLISHED 07 February 2023
DOI 10.3389/fevo.2023.1082661

OPEN ACCESS

EDITED BY
Haitao Wu,
Northeast Institute of Geography and Agroecology (CAS), China

REVIEWED BY
Pengshuai Shao,
Binzhou University, China
Xin Sui,
Heilongjiang University, China
Xinhou Zhang,
Nanjing Normal University, China

*CORRESPONDENCE
Jifeng Wang
✉ wjfeng88@163.com

†These authors have contributed equally to this work and share last authorship
‡These authors have contributed equally to this work and share senior authorship

SPECIALTY SECTION
This article was submitted to Conservation and Restoration Ecology, a section of the journal Frontiers in Ecology and Evolution

RECEIVED 28 October 2022
ACCEPTED 16 January 2023
PUBLISHED 07 February 2023

CITATION
Dong H, Xie L, Cao H, Zhang Y, Liu Y, Xing J, Fu X, Wang J, Han D, Zhong H, Luo C, Qu Y, Ni H and Wang J (2023) Propagation strategies of *Deyeuxia angustifolia* in heterogeneous habitats.
Front. Ecol. Evol. 11:1082661.
doi: 10.3389/fevo.2023.1082661

Propagation strategies of *Deyeuxia angustifolia* in heterogeneous habitats

Haipeng Dong[1], Lihong Xie[1†], Hongjie Cao[1], Yu Zhang[1†], Yingnan Liu[1†], Junhui Xing[1†], Xiaoling Fu[1†], Jianbo Wang[1†], Dayong Han[2‡], Haixiu Zhong[1], Chunyu Luo[1], Yi Qu[1], Hongwei Ni[3‡] and Jifeng Wang[1*‡]

[1]Institute of Nature Resources and Ecology, Heilongjiang Academy of Sciences, Harbin, China, [2]College of Biological and Geographical Science, Yili Normal University, Yining, China, [3]Heilongjiang Academy of Forestry, Harbin, China

Plants utilize different strategies in different environments to maximize population expansion. Understanding plant reproductive strategies in heterogeneous habitats is therefore important for explaining plant ecological adaptability, and for effectively managing and conserving ecosystems. We wanted to explore the reproductive strategy transformation of *D. angustifolia* in heterogeneous habitats, as well as the environmental factors driving and affecting its reproductive characteristics. To do this we measured the reproductive characteristics of *D. angustifolia*, as well as the soil physical and chemical properties of these heterogeneous habitats. The density, biomass per unit area, and proportion of aboveground biomass in swampy meadows were significantly higher compared to other habitats. The proportion of rhizome node buds gradually increased from swampy to typical to miscellaneous grass meadows, while the proportion of tillering node buds decreased. The allocation of sexual reproduction within *D. angustifolia* populations was significantly and positively correlated with plant rhizome biomass and negatively correlated with the number of tillering node buds. The propagation strategies of *D. angustifolia* in heterogeneous habitats were consistent with CSR theory (Competitor, Stress-tolerator, and Ruderal). The proportions of inflorescence (2.07±0.52%; 1.01±0.15%) and root (23.8±1.5%; 19.6±1.4%) biomass in miscellaneous and typical meadows were high, which tended toward the "Ruderal" adaptation strategy. In swampy meadow, *D. angustifolia* invested mostly in vegetative growth to produce tiller node buds (14426.67 buds/m^2; 46%) and ramets (1327.11±102.10 plants/m^2), which is characteristic of the "Competitor" strategy. Swamp *D. angustifolia* resisted flooding by maintaining a resource balance in its body, and was therefore biased toward the "Stress-tolerator" strategy. Environmental factors accounted for 74.63% of reproductive characteristic variation, in which the interpretative proportions of soil water content, dissolved organic carbon, ammonia nitrogen, and nitrate nitrogen were significant (p <0.01). When soil water content, dissolved organic carbon, and nitrate nitrogen increased, *D. angustifolia* tended toward the C strategy; in contrast, when soil water content decreased, amine nitrogen and available phosphorus increased, and *D. angustifolia* tended toward the R strategy. In a stressful environment, the escape mechanism constitutes an increased rhizome and sexual reproduction investment. In contrast, for suitable habitats, tillering node buds increased in order to expand the population *via* new plant production, which was the propagation strategy of *D. angustifolia* in heterogeneous habitats.

KEYWORDS

Sanjiang Plain wetland, heterogeneous habitats, propagation strategies, tradeoff, *Deyeuxia angustifolia*

1. Introduction

Wetlands are important ecosystems formed by an interaction between water and land, and play a vitally important role in regulating the water cycle, reducing greenhouse gas emissions, breaking down pollution, and protecting biodiversity (Chen et al., 2018; Zhang et al., 2019). The Sanjiang Plain wetland is the largest freshwater wetland distribution area in northeastern China, and is essential for protecting biodiversity and maintaining an ecological balance (Zhao, 1999; Dong et al., 2022). In recent years, the scale of irrigation has expanded due to the need for agricultural development, and groundwater levels have subsequently experienced an annual decrease (Chen et al., 2018; Qu et al., 2022). Wetland water levels have been lowering continuously, and the wetlands themselves have in turn changed from swamps to swampy-, typical-, or miscellaneous grass meadows (Dong et al., 2022; Luo et al., 2022). As a result, these wetland ecosystems have become spatially heterogeneous. In ecology, spatial heterogeneity is characterized by ecosystem patchiness and changes in environmental gradients (Dong, 2011). Ecosystem patchiness shows that resource levels within patches are relatively consistent; however, large differences exist between patches (Wijesinghe and Handel, 1994). The widespread existence of environmental heterogeneity increases the difficulty in which plants obtain and utilize essential resources (Benton et al., 2003; Chu et al., 2020; Luo et al., 2022). The uptake and utilization of necessary resources for plant growth are linked to environmental suitability, which thus enables plants to develop adaptive strategies for efficiently accessing the necessary resources (Benton et al., 2003; Dong, 2011).

Plants have developed adaptive strategies toward their environments to cope with inter-and intraspecific competition during all their life stages (Sugiyama and Bazzaz, 1998; Pierce et al., 2013, 2017). The study of reproduction has been at the heart of evolutionary ecology (Hodgson et al., 1999; Rüger et al., 2018). The CSR theory, proposed by Grime (1974), greatly promoted the development of a new stage of life-history strategy research, namely from qualitative description to quantitative analysis. A plant life history strategy is the most suitable trade-off strategy between the environment and plant characteristics that gradually formed over long-term evolution (Grime, 2001; Caccianiga et al., 2006). Both environmental and genetic traits influence plant life-history strategies. According to plant productivity levels and the stress intensity produced by the environment, CSR theory classifies plant ecological strategies into three types: C-competitors, S-tolerators, and R-ruderals. C-competitors generally have good competitiveness and plasticity, and their energy utilization is mainly directed toward monopolizing resources quickly in fertile habitats to obtain the highest population competitiveness (Grime, 1974; Dayrell et al., 2018). S-tolerators, which have low population growth rates, short statures, and infrequent flowering events, invest energy into ecological adaptation behaviors, such as stress resistance (Reich, 2014; Dayrell et al., 2018). R-ruderals have a good colonization capacity, and are characterized by rapid germination and flowering rates, which allow them to quickly invest resources and energy into reproduction (Pierce et al., 2017; Dayrell et al., 2018). After years of development and validation, CSR strategies have been heavily supplemented. Hodgson et al. (1999) provide a method for calibrating the classification of CSR strategies: (1) the degree of species dominance in productive and undisturbed habitats provides a C-selection index, (2) variability in leaf traits known to reflect conservative lifestyles provides an S-selection index, and (3) species frequency in potentially productive but disturbed habitats provides an R-selection index (Hodgson et al., 1999). Pierce et al. (2013) used specific quantitative traits for analysis, and applied the method to general vascular plants, while simultaneously adapting it to the comparison of species within a colony and individuals within a population. Based on functional ecology theory, principal component analysis (PCA) is used to transform functional trait variation into a triangular order corresponding to CSR theory, which has a theoretical and practical application value (Pierce et al., 2013).

Reproduction is an important part of a plant's life history. Not only is it the basis of population formation, development, and evolution, but also of the condition of ecosystem evolution (Chen and Wang, 2014; Rüger et al., 2018; Chen et al., 2019). Different plants use different reproduction methods to maintain and expand their populations (Jackson et al., 1985). Resource allocation theory holds that the biomass fixed by photosynthesis is quantitative, and that plants cannot invest an equal amount of biomass into each trait (Cornwell et al., 2014). Thus, trade-offs must be made between traits for plants to adapt to the environment (Jackson et al., 1985). Increased resource allocation to one trait may therefore decrease resource allocation to another trait (Hodgson et al., 1999). For example, a trade-off exists between clonal growth and sexual reproduction such that an increased investment in sexual reproduction will reduce the investment in clonal reproduction (Levins, 1968). This trade-off may be determined by environmental conditions, plant size, population density, and heredity (Abrahamson, 1975; Reekie, 1991). Díaz posited that the trade-off among functional traits determines plant ecological countermeasures (Díaz et al., 2016), and that ecological countermeasures are the basic conditions required to adapt to habitat diversity. The study of plant ecological responses has long been a vital element in plant ecology (Pierce et al., 2012). Only through the rational coordination of resource allocation among traits can plants achieve optimal allocation in complex ecosystems, which provides a competitive advantage for survival and reproduction (Pierce et al., 2017).

Deyeuxia angustifolia is a typical perennial, rhizomatous Poaceae species, and is widely distributed in northeastern China, the Russian Far East, Mongolia, Korea, and Japan. In China, *D. angustifolia* is the most concentrated in the Sanjiang Plain (Ma, 1995; An et al., 2018; Ni et al., 2022). Under suitable environmental conditions, *D. angustifolia* mainly relies on vegetative reproduction. This produces a large area consisting of a single, dominant community, and sexual reproduction only occurs to produce offspring. In the past, *D. angustifolia* research mainly focused on physiological and ecological characteristics, grassland productivity, and the effects of nitrogen deposition (An et al., 2018; Song et al., 2019; Wang et al., 2019). However, a few studies focused on *D. angustifolia* population reproduction in heterogeneous habitats, and more specifically on plant sexual-and asexual reproduction characteristics, as well as reproduction strategies. Four wetland types were studied: swamp, swampy meadow, typical meadow, and miscellaneous grass meadow. These were selected to analyze the reproductive characteristics and trade-offs of *D. angustifolia*, and to explore the following: (1) whether *D. angustifolia* reproductive characteristics significantly change in heterogeneous habitats; (2) whether *D. angustifolia* ecological strategies change in heterogeneous habitats; and (3) which environmental factors dominate the changes in the reproductive characteristics of *D. angustifolia*. This study reveals *D. angustifolia* ecological strategy transformations in heterogeneous habitats, and provides references and a scientific basis for wetland restoration.

2. Materials and methods

2.1. Study site

The Honghe National Nature Reserve, of Heilongjiang Province (47°42′18″ – 47°52′07″ N, 133°34′38″ – 133°46′29″ E), is located in the

northeastern part of the Sanjiang Plain, China (Dong et al., 2022; Luo et al., 2022). The study area has a temperate monsoon climate with an average annual temperature of 2.5°C and an annual average precipitation of 558 mm, which occurs mainly from July to September (Yang et al., 2012; Shi et al., 2015). Furthermore, the elevation is 50–60 m above sea level, with a slope of only 1/1000–1/300. Because of the low and relatively flat terrain, river curvature is large and water flow is unsmooth (Qu et al., 2018). The water level, soil, and nutrients of the wetlands in the Honghe Reserve are very heterogenous (Yang et al., 2012; Qu et al., 2022). A large area of natural wetland, such as typical meadow, swampy meadow, or proper swamp, occurs within the reserve, as well as an island forest which is distributed in the higher lying areas (Dong et al., 2022; Qu et al., 2022).

The sample plots were located in four different habitats, namely: perennial swamp (SW), seasonal swampy meadow (SM), typical meadow (TM) with occasional stagnant water, and miscellaneous grass meadow (MG) on the forest edge. The dominant species in SW is *Carex pseudocuraica,* while the subdominant species is *D. angustifolia*, and the soil is a typical swamp soil (Shi et al., 2015; Dong et al., 2022). In SM and TM, *D. angustifolia* is the dominant species and has an aggregated distribution, while the soil is a typical meadow soil. MG is located on the edge of a *Populus davidiana* forest, and *D. angustifolia* is the dominant species, accompanied by *Spiraea salicifolia*, *Sanguisorba tenuifolia*, and *Anemone dichotoma*. Finally, MG soil is a typical white serous soil (Qu et al., 2018; Dong et al., 2022; Luo et al., 2022; Qu et al., 2022).

2.2. Research methods

In the Sanjiang Plain, rapid *D. angustifolia* growth starts in May, while seeds mature in mid-to-late July; above-ground biomass reaches its maximum at the end of July (Song et al., 2019; Dong et al., 2022). In contrast, rhizomes continue to grow and produce offspring through rhizome buds. At the end of September, underground biomass reaches its maximum. Hereafter, overwintering buds are produced and the number of underground buds reaches its maximum. In mid-July 2020, when above-ground *D. angustifolia* biomass peaked, nine 1 m x 1 m quadrats were randomly placed within each habitat. In each quadrat, five sexual and five asexual *D. angustifolia* plants, each exhibiting healthy growth, were selected. The above-ground parts for each plant were studied by specifically measuring their heights, whereafter the plants were divided into inflorescences, stems, and leaves.

At the beginning of October 2020, nine 1 m x 1 m quadrats were randomly placed within each habitat. In each quadrat, a 0.25 m x 0.25 m sub-quadrat was further placed in the center. The above-and underground *D. angustifolia* parts were excavated together. First, we counted the number of aboveground plants. Underground rhizomes were then separated from excavated plants, their fibrous roots removed, and the number of tiller node buds and rhizome buds of all plants recorded. Lastly, plant parts were dried at 60°C, until a constant weight was obtained, and then weighed. Aboveground biomass was calculated as the sum of inflorescence, stem, and leaf biomass, while total biomass was calculated as the sum of above and belowground biomass. Furthermore, rhizome biomass was calculated as the biomass of the underground parts without fibrous roots, while rhizome bud biomass was calculated as the sum of rhizome internode buds and rhizome apical buds (Figure 1 a). Tiller node buds were considered as all buds on the nodes between roots and aboveground parts (Figure 1 b). Rhizome length was calculated as the total length of all rhizomes connected end-to-end. The total number of buds was calculated as the sum of all rhizome and tiller node buds. The proportion of rhizome biomass was calculated as rhizome biomass divided by total biomass, while the proportion of aboveground biomass was calculated as the aboveground biomass divided by total biomass. Finally, the proportion of inflorescence biomass/reproductive allocation was calculated as inflorescence biomass divided by total biomass.

2.3. Soil factor determination

Soil factor determination was performed according to the Soil Agrochemical Analysis Method (Lu, 2010) and Soil Agrochemical Analysis (Bao, 2000). In each quadrat, we first removed 5 cm of ground litter, then collected soil at a depth of 5–25 cm and mixed it into a soil sample, removed all plant roots inside the soil sample, placed the sample in a plastic bag, and then removed a part of the soil for water content determination. The other part of the soil was air-dried naturally, whereafter the soil index was determined after sieving.

Soil water content (*WC*) was calculated using the drying method. Fresh soil samples were weighed in aluminum boxes and oven-dried at 105°C to a constant weight.

Soil pH (pH) was measured in a soil slurry at a soil-to-water ratio of 1:2.5 by using a calibrated pH meter with a combination electrode.

For available phosphorus (*AP*), 5 g of soil sample was added to 25 ml of 0.5 mol·L^{-1} $NaHCO_3$ and vortexed for 30 min. The filtrate was then used to determine the concentration of available phosphorus by colorimetry (Ade et al., 2018).

For total phosphorus (*TP*), 0.25 g of soil sample was added to 2 g NaOH, and after melting and washing 5 ml molybdenum-antimony anti-color agent was added to determine phosphorus content by a colorimetric method.

FIGURE 1
General morphology of various buds of *Deyeuxia angustifolia*. a, rhizome bud; b, tiller node bud.

TABLE 1 Characteristics of environmental factors in heterogeneous habitats (mean±SE).

Factor	SW	SM	TM	MG
pH	5.07 ± 0.027^{b}	5.07 ± 0.051^{b}	5.31 ± 0.085^{a}	5.18 ± 0.049^{a}
AP ($mg \cdot kg^{-1}$)	60.86 ± 1.61^{c}	72.81 ± 7.21^{b}	71.84 ± 9.58^{b}	113.29 ± 16.08^{a}
TP ($g \cdot kg^{-1}$)	8.42 ± 0.041^{bc}	7.42 ± 1.01^{c}	16.92 ± 2.15^{a}	11.72 ± 1.79^{b}
TK ($g \cdot kg^{-1}$)	17.34 ± 0.12^{b}	18.66 ± 0.53^{a}	14.57 ± 0.55^{c}	18.35 ± 0.30^{ab}
AK ($mg \cdot kg^{-1}$)	241.67 ± 0.23^{b}	136.46 ± 16.13^{c}	299.98 ± 33.14^{a}	202.93 ± 15.51^{b}
DOC ($mg \cdot kg^{-1}$)	643.87 ± 0.76^{b}	690.68 ± 22.65^{ab}	737.00 ± 35.58^{a}	459.68 ± 41.24^{c}
DON ($mg \cdot kg^{-1}$)	31.42 ± 0.19^{b}	37.26 ± 2.26^{ab}	48.11 ± 5.09^{a}	43.62 ± 3.17^{a}
NN ($mg \cdot kg^{-1}$)	4.68 ± 0.16^{b}	5.62 ± 0.19^{a}	6.02 ± 0.11^{a}	4.29 ± 0.35^{b}
AN ($mg \cdot kg^{-1}$)	20.59 ± 0.43^{d}	23.59 ± 0.33^{c}	27.28 ± 0.51^{b}	31.69 ± 0.97^{a}
WC (%)	1.70 ± 0.00^{a}	1.05 ± 0.00^{b}	0.65 ± 0.00^{c}	0.35 ± 0.00^{d}

pH, Soil pH; AP, Available phosphorus; TP, Total phosphorus; TK, Total potassium; AK, Available potassium; DOC, Dissolved organic carbon; DON, Dissolved organic nitrogen; NN, Nitrate nitrogen; AN, Ammonia nitrogen; WC, Soil water content. Different letters in the same column meant significant difference at 0.05 level.

TABLE 2 Population characteristics of *Deyeuxia angustifolia* per unit area in four habitats.

Habitat type	Plant biomass (g)	Density (plant/m^2)	Proportion of rhizome biomass (%)	Proportion of aboveground biomass (%)	Proportion of inflorescence biomass (%)
Swamp	256.6 ± 17.4^{c}	166.2 ± 12.5^{c}	17.8 ± 1.6^{b}	82.2 ± 1.6^{b}	0.33 ± 0.04^{c}
Swampy meadow	1246.1 ± 88.6^{a}	1327.1 ± 102.1^{a}	11.8 ± 0.9^{c}	88.2 ± 0.9^{a}	0.97 ± 0.05^{b}
Typical meadow	927.7 ± 60.9^{b}	870.2 ± 68.5^{b}	19.6 ± 1.4^{b}	80.4 ± 1.4^{b}	1.01 ± 0.15^{b}
Miscellaneous grass meadow	327.1 ± 18.9^{c}	168.9 ± 10.4^{c}	23.8 ± 1.5^{a}	76.2 ± 1.5^{c}	2.07 ± 0.52^{a}

Different letters in the same column meant significant difference at 0.05 level.

Available potassium (*AK*) was determined using 5 g air-dried soil by flame emission technology after vortex and filtration with 1 $mol \cdot L^{-1}$ NH_4OAc.

Total potassium (*TK*) was determined after 0.25 g of dried soil was melted by NaOH and diluted with HCl and H_2SO_4, whereafter total potassium concentration was measured by flame emission technology.

Dissolved organic carbon (*DOC*) and dissolved organic nitrogen (*DON*) were determined by extraction with 0.5% $mol \cdot L^{-1}$ $CaCl_2$ using a TOC/TN analyzer (Shang et al., 2016).

For ammonia nitrogen (*AN*) and nitrate nitrogen (*NN*), soil NH_4^+-N and NO_3^--N were extracted using a 2 $mol \cdot L^{-1}$ KCl solution with a 1 h vortex period. After extraction, NH_4^+-N and NO_3^--N were determined using an AA3 continuous flow chemical analyzer (Table 1).

2.4. Data analysis

All statistical analyses were performed using Excel 2019 and SPSS 25.0. The one-way ANOVA and Least Significant Difference (LSD) methods were used to analyze differences in soil physicochemical properties, plant height, density, biomass, and reproductive characteristics of the different habitats. A correlation analysis was performed to analyze rhizome characteristics, and plots were created with Origin 2018. The R software, with the 'corrplot' package, was used to draw the correlation diagram of reproductive characteristics, and for analyzing the correlation between sexual and asexual reproduction characteristics. The trend correspondence analysis (DCA) was performed with the R software vegan package. The first axis value was less than 3.0, and a redundancy analysis (RDA) was therefore used to analyze the relationship between reproductive characteristics and soil factors. The results were plotted with the ggplot package.

3. Results

3.1. Biomass allocation in heterogeneous habitats

Total biomass was greatly affected by environmental changes. Biomass per unit area and plant density were the highest (1246.1 ± 88.6 g, 1327.1 ± 102.1 plants/m^2) in SM, followed by TM (927.7 ± 60.9 g, 870.2 ± 68.5 plants /m^2), with the lowest being SW (256.6 ± 17.4 g, 166.22 ± 12.5 plants/m^2) (Table 2). There were no significant differences in biomass and density between MG (327.1 ± 18.9 g, 168.9 ± 10.4 plants/m^2) and SW. According to the biomass allocation analysis, the resources invested in the aboveground parts were the highest in SM (88.2 ± 0.9%), while the highest underground investment occurred in MG (23.8 ± 1.5%). There was no significant difference between SW and TM. The proportion of sexual reproduction differed between habitats. The absolute proportion of sexual reproduction was the highest in MG (2.07 ± 0.52%) and the lowest in SW (0.33 ± 0.04%). There was no significant difference in the proportion of absolute investment in sexual reproduction between TM and SM ($p > 0.05$).

The width of the columns and the numbers at the top denote the bud density of *Deyeuxia angustifolia*, and different colors indicate the proportion of different types of buds.

3.2. Quantitative asexual reproduction characteristics in heterogeneous habitats

Deyeuxia angustifolia showed a trade-off between biomass allocation and reproductive allocation in heterogeneous habitats, and the proportion of asexual reproductive buds differed between these habitats. The proportion of tiller node buds was the highest in SM (46.3%) and the lowest in MG (11.4%) (Figure 2). The total number of buds, as well as the number of all bud kinds, differed between heterogeneous habitats. The total number of buds, as well as rhizome and tiller node bud densities, were the highest in SM; specifically, rhizome and tiller node bud densities were 12186.11 ± 573.70 buds/m^2 and 10355.56 ± 840.18 buds/m^2, respectively. Rhizome and tiller node bud densities were lowest in SW and MG, with 1633.33 ± 136.93 buds/m^2 and 558.33 ± 30.46 buds/m^2, respectively. Differences also existed in individual biomass and number of buds per plant between heterogeneous habitats, and individual biomass specifically differed significantly between habitats (p <0.05; Table 3). Individual biomass was the highest in MG (1.942 ± 0.037 g) and the lowest in SW (0.851 ± 0.017). The number of rhizome buds, rhizome length, and rhizome biomass were all lowest in SM (6.18 ± 0.58, 17.68 ± 1.6, 0.11 ± 0.01), while those in MG were the highest (17.45 ± 2.22, 52.8 ± 4.03, 0.47 ± 0.04). By increasing the investment in rhizomes, *D. angustifolia* tends toward a "guerrilla-type" clonal configuration for population expansion, which manifests mainly in an increased number of rhizome buds, as well as increased rhizome biomass. Therefore, the number of rhizome buds, and rhizome biomass, can reflect changing trends in clonal configuration during habitat change. The number of rhizome buds, as well as rhizome biomass, in each habitat was significantly and positively correlated with rhizome length (Figure 3), where regression slope represents the rate at which the number of rhizome buds and rhizome biomass increased with increasing rhizome length. The regression slopes for the four habitats were MG – 0.508, 0.0098, TM – 0.273, 0.0078, SM – 0.257, 0.0044, and SW – 0.255, 0.0072, respectively. The slope of a single regression line cannot fully explain the rhizome strength for all four habitats; that is, the ability of the rhizome to expand outward through clonal reproduction. Thus, we defined rhizome strength as the product of the slopes of the two regression lines. The rhizome strengths of the four habitats were: MG – 0.0050, TM – 0.0020, SM – 0.0011, SW – 0.0018.

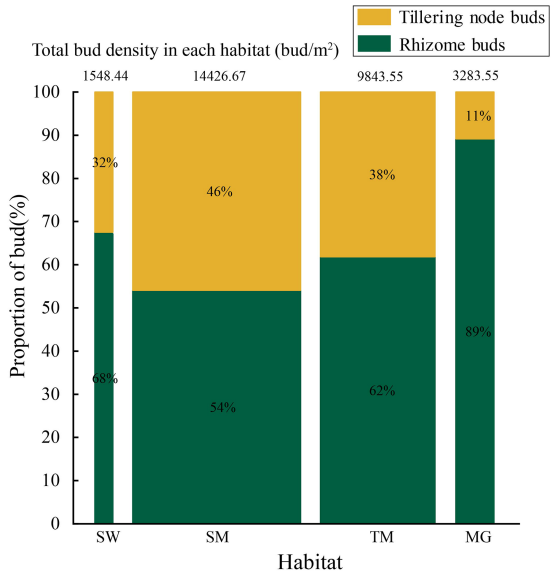

FIGURE 2
Allocation of buds by *Deyeuxia angustifolia* in four habitats.

3.3. Correlation analysis of sexual and asexual reproduction in *Deyeuxia angustifolia*

The correlation analysis between sexual and asexual reproductive characteristics of *D. angustifolia* showed a significant positive correlation among the proportion of rhizome buds, spacer length, number of rhizome buds per plant, rhizome biomass per plant, and rhizome length per plant (p <0.001; Figure 4). The number of rhizome buds per plant, rhizome biomass per plant, and rhizome length per plant were significantly and negatively correlated with the number of tiller node buds per plant, as well as tiller node bud and density (p <0.01). There was a significant positive correlation between sexual reproductive allocation and inflorescence biomass, but not sexual plant biomass. Sexual reproductive allocation was positively correlated with rhizome length per plant, rhizome biomass per plant, proportion of rhizome buds, number of rhizome buds per plant, and spacer length (p <0.01). Sexual reproductive allocation was significantly and negatively correlated with the number of tiller node buds per plant (p <0.05). Inflorescence biomass and sexual plant biomass were positively correlated with population rhizome biomass, but had no correlation with the number of rhizome buds per plant or rhizome biomass per plant.

3.4. Relationship between reproductive characteristics and soil factors

A redundancy analysis of *D. angustifolia* reproductive characteristics and soil factors (Figure 5) showed that the first two axes explained, by 74.63%, the influence of soil factors on the reproductive characteristics

TABLE 3 Characteristics of individual bud of *D. angustifolia* in four habitats.

Habitat type	Biomass(g)	Total bud number(bud)	Axillary rhizome bud(bud)	Rhizome length(cm)	Rhizome biomass(g)
Swamp	0.851 ± 0.017^b	9.57 ± 0.77^b	6.54 ± 0.65^b	23.82 ± 1.68^{bc}	0.15 ± 0.02^c
Swampy meadow	0.943 ± 0.008^b	11.17 ± 0.54^b	6.18 ± 0.58^b	17.68 ± 1.60^c	0.11 ± 0.01^c
Typical meadow	1.076 ± 0.019^b	11.52 ± 0.57^b	7.27 ± 0.61^b	28.91 ± 2.47^b	0.21 ± 0.02^b
Miscellaneous grass meadow	1.942 ± 0.037^a	19.58 ± 2.19^a	17.45 ± 2.22^a	52.81 ± 4.03^a	0.47 ± 0.04^a

Different letters in the same column meant significant difference at 0.05 level.

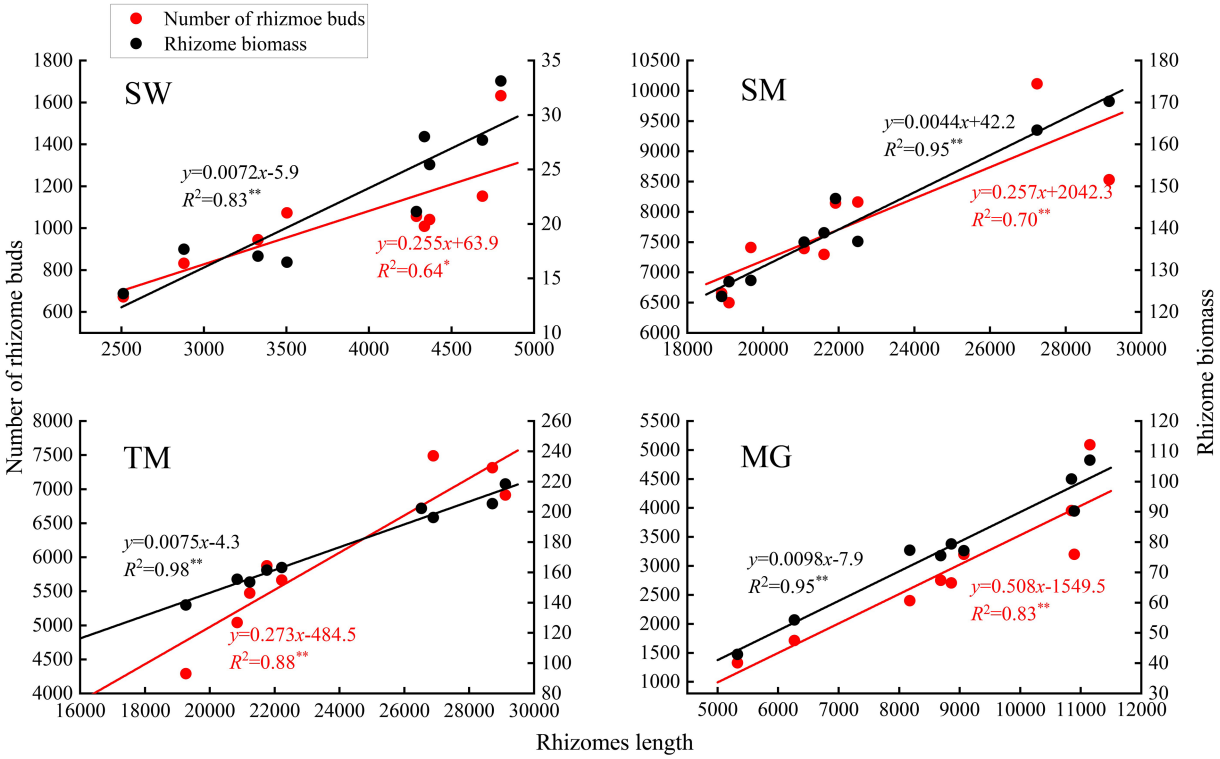

FIGURE 3
Regression of rhizome bud number, rhizome biomass and rhizomes length of *D. angustifolia* in four habitats.

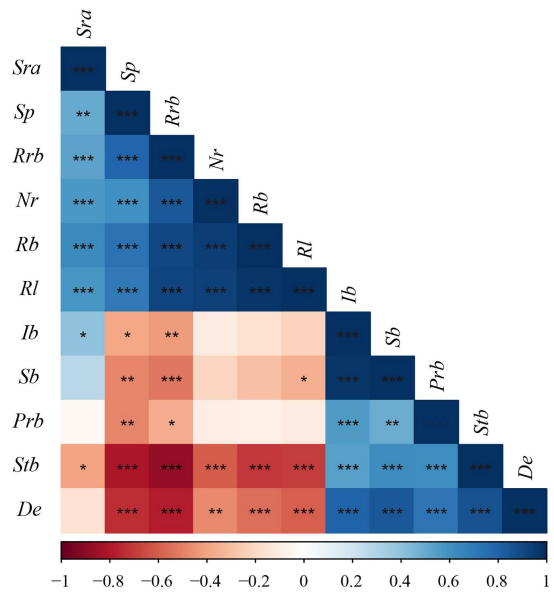

FIGURE 4
Pearson correlation among reproductive characteristics of *D. angustifolia*. *Rl*, rhizome length per plant; *Nr*, number of rhizome buds per plant; *Sp*, spacer; *Rrb*, proportion of rhizome bud; *Rb*, rhizome biomass per plant; *Stb*, tiller node bud per plant; *Sra*, sexual reproduction allocation; *De*, density; *Prb*, population rhizome biomass; *Ib*, inflorescence biomass; *Sb*, sexual plant biomass. * indicate the level of correlation, *p <0.05; **p <0.01; ***p <0.001.

of *D. angustifolia* in which the number of tiller nodes per plant was mainly positively affected by *WC* and *AK*. It was negatively correlated with *NN*, *DON*, pH, *AN*, and *AP* (Table 4). Rhizome length, number of rhizome buds per plant, spacer length, and proportion of rhizome buds were all positively affected by *AP* and negatively affected by *NN*. Sexual plant biomass, rhizome biomass, and inflorescence biomass were positively correlated with *TK*, *AP*, *AN*, *DON*, and pH, but negatively correlated with *WC* ($p < 0.001$), while *AP* was weakly correlated with plant reproductive characteristics ($p < 0.05$). No correlation was found between sexual reproductive allocation and other environmental factors ($p > 0.05$).

Mantel test results for each environmental factor showed that the effects of *DOC*, *NN*, *AN*, and *WC* on *D. angustifolia* reproductive characteristics were highly significant ($p < 0.001$). *AP* also had a significant influence on the reproductive characteristics of *D. angustifolia* ($p < 0.001$; Table 4). Finally, *DON*, *AK*, *TK*, *TP*, and pH did not significantly affect the reproductive characteristics of *D. angustifolia*.

4. Discussion

Deyeuxia angustifolia is a clonal, rhizomatous plant type with well-developed underground rhizomes (Shi et al., 2015; Dong et al., 2022). At the end of each growing season, energy is directed toward rhizome growth, and rhizomes produce terminal-and node buds which develop into new plants (Hutchings and Wijesinghe, 1997; Dong et al., 2022). Rhizomes occupy a specific niche space by elongating away from the mother plant (Dong, 2011). In addition, tiller node buds can also develop into new plants. Therefore, rhizome bud growth is closely related to outward population expansion, while tiller node buds are related to the population's ability to colonize new areas (Chu et al., 2020). Plants develop a variety of life history patterns during environmental

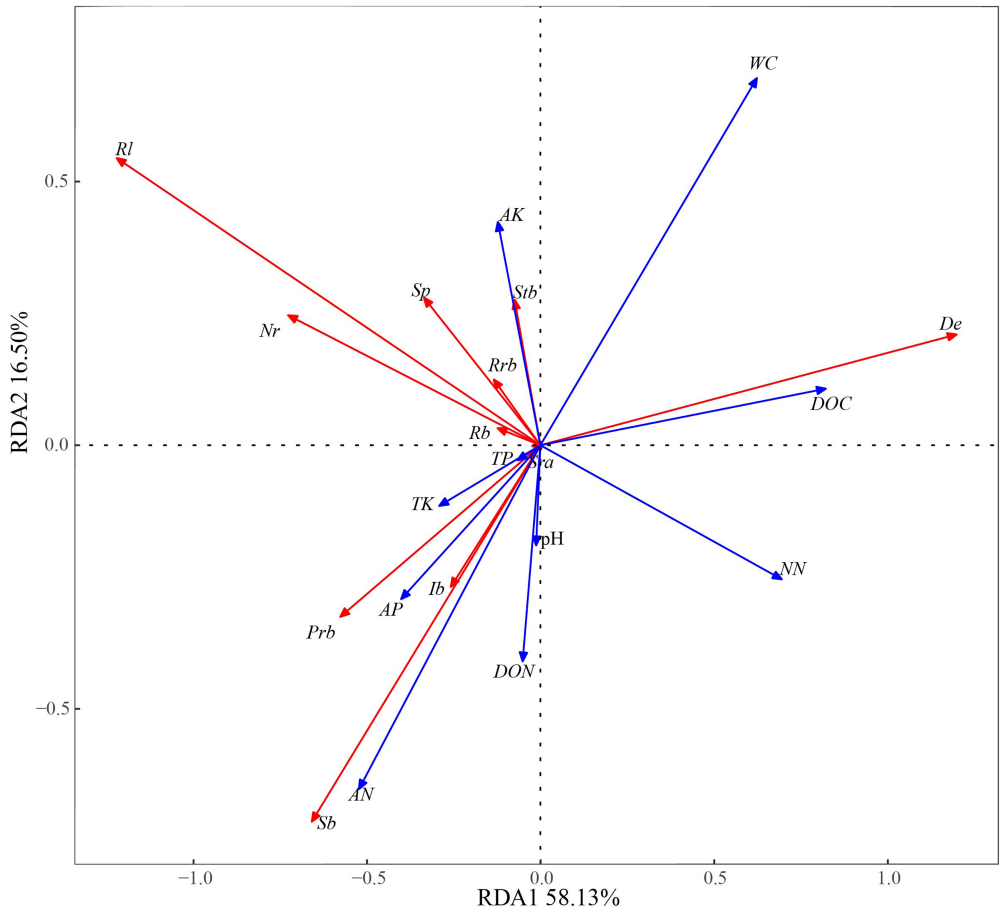

FIGURE 5
Relationship between reproductive characters and soil factors in redundancy analyses. *Rl*, rhizome length per plant; *Nr*, number of rhizome buds per plant; *Sp*, spacer; *Rrb*, proportion of rhizome bud; *Rb*, rhizome biomass per plant; *Stb*, tiller node bud per plant; *Sra*, sexual reproduction allocation; *De*, density; *Prb*, population rhizome biomass; *Ib*, inflorescence biomass; *Sb*, sexual plant biomass. pH, Soil pH; *AP*, Available phosphorus; *TP*, Total phosphorus; *TK*, Total kalium; *AK*, Available kalium; *DOC*, Dissolved organic carbon; *DON*, Dissolved organic nitrogen; *NN*, Nitrate nitrogen; *AN*, Ammonia nitrogen; *WC*, Soil water content.

TABLE 4 Mantel test for the correlation between reproductive characteristics and environmental factors of *D. angustifolia*.

Factor	*r*	*P*
Soil pH (pH)	−0.072	0.913
Available phosphorus (*AP*)	0.114	0.031*
Total phosphorus (*TP*)	−0.016	0.564
Total kalium (*TK*)	−0.041	0.735
Available kalium (*AK*)	0.008	0.397
Dissolved organic carbon (*DOC*)	0.432	0.001***
Dissolved organic nitrogen (*DON*)	−0.024	0.654
Nitrate nitrogen (*NN*)	0.412	0.001***
Ammonia nitrogen (*AN*)	0.354	0.001***
Soil water content (*WC*)	0.579	0.001***

*Indicate the level of correlation, *$P < 0.05$; ***$P < 0.001$.

adaptation. Specifically, out of all four habitats, the water level of SW was too high, which seriously restricted *D. angustifolia* growth, consequently leading to aboveground biomass and plant density being the lowest (Tables 2, 3). The water level of SM was slightly lower, and flooding stress therefore reduced. In this case, biomass per unit area, population density, and all the various bud densities were maximized. Rhizome strength was the highest in MG and the lowest in SM (Figure 3). Wetland clone plant rhizomes are mainly used for population expansion. Thus, stronger rhizomes give *D. angustifolia* an enhanced ability to expand its population (Dong, 2011; Shi et al., 2015; Chu et al., 2020). From SM to TM to MG, *D. angustifolia* density and biomass gradually decreased. When *D. angustifolia* occurred in TM and MG under drought stress, or in SW under flooding stress, the density of all bud types decreased, while the proportion of rhizome node buds, the number of rhizome buds, rhizome length, and rhizome biomass per plant increased. Whether at population or individual level, *D. angustifolia* showed a guerrilla-type clonal configuration in adverse environments. On the one hand, an increased roots biomass increased access to resources and therefore enhanced population competitiveness (Hutchings and Wijesinghe, 1997). On the other hand, rhizomes enabled an escaped from unfavorable habitats (Wijesinghe and Handel, 1994). This result is consistent with Chen et al. (2014) for growth and reproductive responses of two water-holding plants to different water level gradients. Therefore, in a restricted environment, *D. angustifolia* will increase investment in growth and clonal reproduction, thereby reducing the number of individuals per unit area to adapt to environmental stress (Mclntyre

et al., 2009; Dong et al., 2022). This enables it to adapt to a wide range of water gradients.

Life history theory predicts a trade-off between resource allocation among different functional traits (Pierce et al., 2012, 2013; Rüger et al., 2018). This means that, when the total amount of resources is certain, increasing resource allocation to one trait will inevitably reduce resource allocation to other traits (Zhang, 2004; Mclntyre et al., 2009; Dong et al., 2022). Due to competition for nutrient elements, photosynthetic nutrients, and other resources between clonal growth and sexual reproduction, an increased investment in sexual reproduction may weaken the investment in clonal reproduction, and vice versa (Dong, 2011; Shi et al., 2015; Lu et al., 2022). In this study, a significant positive correlation existed between sexual reproductive allocation and rhizome biomass per plant, as well as a significant negative correlation between sexual reproductive allocation and tiller node bud number (Figure 4). In terms of reproductive strategy, an investment in sexual reproduction increases with increased environmental stress, while the investment in asexual reproduction (rhizomes) also increased. In contrast, the investment toward producing tillers and sprouts to form new plants reduced. In a more suitable habitat, *D. angustifolia* increased tiller node output to reduce sexual reproduction input, increased the tillers formed by tiller node bud germination, reduced the production of rhizomes and rhizome node buds, and reduced the investment in sexual reproduction (Figure 2). We can thus classify *D. angustifolia* functional traits into two categories: 1) outgoing rhizomes, rhizome buds, and sexual reproductive characteristics, and 2) *in-situ* growing tillering node buds and population density (Chu et al., 2020). *D. angustifolia* tended toward an "outgoing guerrilla" clonal configuration in stressed environments at both population and individual levels, and thereby produced an escape mechanism. In suitable habitats, *D. angustifolia* tended toward an *in-situ* growing "phalanx" clonal configuration (Jung et al., 2010; Zhang et al., 2022). This is different from Li et al. (2018) on the decrease in sexual reproduction and increase in asexual reproduction of *Vallisneria spinulosa* in stressful environments. The main reason is that different plants have different adaptation strategies to environmental changes.

Plant functional traits result from adaptation to different environments in the long-term evolutionary process, and can objectively express plant adaptability toward external environments (Mclntyre et al., 2009; Jung et al., 2010). In this study, the ecological strategies of *D. angustifolia* and its changing functional characteristic in the four habitats correspond to the CSR strategy proposed by British ecologist Grime (1974). *D. angustifolia* growing in MG and TM corresponded to R-strategies. It allocated resources to reproduction and population expansion mainly by devoting more resources to sexual reproduction and prolonging rhizomes to produce nodal buds (Munoz et al., 2016). It was therefore inclined toward the "Ruderal" adaptation strategy, characterized by a good expanding ability and large investment in reproduction (Grime, 1974). This is similar to Cerabolini et al. in potentially fertile, but disturbed, habitats, where many plants tended toward the R-strategy (Cerabolini et al., 2010). In MG and TM, the investment in sexual reproduction increased ($2.07 \pm 0.52\%$; $1.01 \pm 0.15\%$), and rhizomes from asexual reproduction tended to guerrilla clonal growth ($23.8 \pm 1.5\%$; $19.6 \pm 1.4\%$) so that plants could quickly expand from stressed sites to more suitable habitats (Pierce et al., 2013). *D. angustifolia* growing in SM corresponded to the C-strategy, in which it invested more resources into vegetative growth; that is, by increasing tiller nodes buds and ramets to occupy most of the available resources so that resource utilization could be optimized. The C-strategy dominated in favorable habitats and enabled the maintenance of a relatively high rate of resource acquisition in crowded, fertile, and undisturbed habitats (Grime, 2001; Cerabolini et al., 2010). The progeny formed by increasing tiller node bud germination, produced by clonal reproduction, increased resource utilization efficiency. The clonal configuration tended to the "Competitor" type. *D. angustifolia* therefore corresponded to the S-strategy in SW habitats. Due to the serious stress caused by excessive flooding, most of its resources were spent on maintaining survival, which was mainly reflected in short statured plants with few branches, a low flowering and seed setting rate, and other adaptive characteristics. Most of the previous studies analyzed the functional traits of multiple species and classified plants into various CSR strategies (Caccianiga et al., 2006; Pierce et al., 2013). In this study, we analyzed the functional traits of *D. angustifolia* under fertile, disturbed, and stressed habitats, and found that the adaptation strategies of *D. angustifolia* populations in these different habitats were consistent with the three CSR strategy types.

In heterogeneous habitats, plants can maximize access to resources by adjusting their resource allocation patterns, thus enabling them to have a wider ecological range and higher tolerance (Wijesinghe and Handel, 1994). Plant organs (roots, stems, leaves, flowers, and fruits) are formed by meristem differentiation (Cornwell et al., 2014; Johnson et al., 2016), which exhibits a high level of plasticity. Organ composition changes dramatically when affected by the external environment. Plant resource allocation varies with the environment, and functional traits are prioritized differently to maximize adaptability to different environments (Johnson et al., 2016). The main problem affecting performance during wetland degradation is the lack of adequate soil water, which affects soil nutrient conditions (Dong et al., 2022). By applying the Mantel test to reproductive characteristics and soil environmental factors, it was found that soil *DON*, *DOC*, *AN*, *NN*, *WC*, and *AP* were important factors driving the differences in reproductive characteristics between heterogeneous habitats in the Sanjiang Plain. In this study, *WC* was the most important limiting factor, and *WC* was negatively correlated with rhizome biomass, sexual plant biomass, and inflorescence biomass. This indicated that, when *WC* decreases, *D. angustifolia* increases its investment in rhizome and sexual reproduction. On the one hand, water absorption can be enhanced by increasing the number of rhizome fibrous roots, and on the other hand, the investment in rhizomes and seeds can be increased to avoid environmental stress. When *WC* decreased, and *AN* and *AP* increased, *D. angustifolia* tended toward the R-strategy. Some studies have shown that increased nitrogen levels promote plant sexual reproduction (Hu et al., 2012; Chen et al., 2019). In this study, *AN* and *DON* promoted the biomass of sexual plants, while increased *WC* reduced this effect (Li et al., 2018; Dong et al., 2022). *NN* and *DOC* were significantly and positively correlated with plant density, and when *WC*, *DON*, and *NN* increased simultaneously, *D. angustifolia* tended toward the C-strategy. This result differed from Tomlinson and O'connor (2004). This may be because, in an environment with sufficient soil nutrients, the reproduction strategy of *D. angustifolia* tended to increase the number of plants per unit area through the germination of tiller node buds instead of escaping by increasing rhizome investment (Wang et al., 2019; Dong et al., 2022). *DOC* can be quickly transformed into other components in the soil to provide nutrition for plants. In the habitats with a relatively high soil *WC*, such as SM, this can promote litter decomposition and increase the content of soluble organic carbon in the soil, which in turn promotes *D. angustifolia* growth (Chen et al., 2019).

5. Conclusion

This study focused on the process of habitat change along the SM-TM-MG gradient of heterogeneous habitats. Specifically, *D. angustifolia* produced an escape mechanism from unfavorable environments by increasing individual plant biomass, sexual reproductive investment, and rhizome input, and reducing biomass per unit area, tiller node buds, and plant density. The quantitative variation in reproductive characters, and the trade-off relationship between them, reflected the adaptation strategy of *D. angustifolia* to changes in environmental factors in heterogeneous habitats. In MG and TM, *D. angustifolia* invested more in sexual reproduction and rhizome extension, and tended toward the R-adaptation strategy. Clonal configuration tended to be guerrilla clonal configuration. In SM, *D. angustifolia* invested more in vegetative growth, and tended to the C-adaptation strategy and intensive clonal configuration. *D. angustifolia* resisted the flooded environment by maintaining a balance of resources, and tended toward the S-adaptation strategy. The reproductive strategy of *D. angustifolia* in heterogeneous habitats conforms to CSR theory. Among all the environmental factors, *WC* had the most significant effect on the reproductive characteristics of *D. angustifolia*. In the arid MG environment, it maintained a high uptake of *AN* and *DON*, and increased plant biomass to maintain its adaptation to environmental drought stress. In SM, which had enough water, it increased the number of individuals per unit area to maximize the use of *DOC* and other nutrients, and to maintain maximum productivity. This study provides a scientific explanation for understanding the ecological adaptation strategies of wetland plants in heterogeneous habitats.

Data availability statement

The original contributions presented in the study are included in the article/supplementary materials, further inquiries can be directed to the corresponding author.

Author contributions

HD, HC, JW, YL and HN designed the study. HD, DH, QY and HZ collected the data. HD, LX, YZ and XF analyzed the data. HD, CL, JW and JX lead the writing with all co-authors. All authors gave final approval for publication.

Funding

This research was supported by the Youth Innovation Foundation of Heilongjiang Academy of Science (No. CXJQ2022ZR01), the Central Government Guides Local Science and Technology Development Special Projects (No. ZY20B15), the Heilongjiang Academy of Sciences Double-mention Wild Goose Array Special Program Project-Leading Talents (STYZ2023ZR01), and the Applied Technology Research and Development Program of Heilongjiang Province (GA19C006-5).

Conflict of interest

The authors declare that the research was conducted in the absence of any commercial or financial relationships that could be construed as a potential conflict of interest.

Publisher's note

References

Abrahamson, W. G. (1975). Reproductive strategies in dewberries. *Ecology* 56, 721–726. doi: 10.2307/1935508

Ade, L. J., Hu, L., Zi, H. B., Wang, C. T., Lerdau, M., and Dong, S. K. (2018). Effect of snowpack on the soil bacteria of alpine meadows in the Qinghai-Tibetan Plateau of China. *Catena* 164, 13–22. doi: 10.1016/j.catena.2018.01.004

An, Y., Gao, Y., Tong, S. Z., Lu, X. G., Wang, X. H., Wang, G. D., et al. (2018). Variations in vegetative characteristics of *Deyeuxia angustifolia* wetlands following natural restoration in the Sanjiang plain, China. *Ecol. Eng.* 112, 34–40. doi: 10.1016/j.ecoleng.2017.12.022

Bao, S. D. (2000). *Soil Agrochemical Analysis*. Beijing: Chinese Agriculture Press: 28–91.

Benton, T. G., Vickery, J. A., and Wilson, J. D. (2003). Farmland biodiversity: is habitat heterogeneity the key? *Trends Ecol. Evolut.* 18, 182–188. doi: 10.1016/S0169-5347(03)00011-9

Caccianiga, M., Luzzaro, A., Pierce, S., Ceriani, R. M., and Cerabolini, B. (2006). The functional basis of a primary succession resolved by CSR classification. *Oikos* 112, 10–20. doi: 10.1111/j.0030-1299.2006.14107.x

Cerabolini, B. E. L., Brusa, G., Ceriani, R. M., Andreis, R. D., Luzzaro, A., and Pierce, S. (2010). Can CSR classification be generally applied outside Britain? *Plant Ecol.* 210, 253–261. doi: 10.1007/s11258-010-9753-6

Chen, X. S., Deng, Z. M., Xie, Y. H., Li, F., and Li, X. (2014). Differential growth and vegetative reproduction by two co-occurring emergent macrophytes along a water Table gradient. *Pak. J. Bot.* 46, 881–886.

Chen, T., and Wang, Y. F. (2014). Response of reproductive characteristics of *Saussurea macrota* Franch. To elevation at eastern Qinhai-Tibetan plateau. *Chin. J. Ecol.* 33, 3216–3221. doi: 10.13292/j.1000-4890.2014.0282

Chen, L., Wang, L., Yang, X. G., Song, N. P., Li, Y. F., Su, Y., et al. (2019). Reproductive characteristics of *Artemisia scoparia* and the analysis of the underlying soil drivers in a desert steppe of China. *Chin. J. Plant Ecol.* 43, 65–76. doi: 10.17521/cjpe.2018.0211

Chen, H., Zhang, W. C., Gao, H. R., and Nie, N. (2018). Climate change and anthropogenic impacts on wetland and agriculture in the Songnen and Sanjiang plain, Northeast China. *Remote Sens.* 10:356. doi: 10.3390/rs10030356

Chu, L. S., Li, H. Y., and Yang, Y. F. (2020). Vegetative reproduction characteristics of *Leymus chinensis* in heterogeneous habitats in songnen plain, China. *Chin. J. Appl. Ecol.* 31, 83–88. doi: 10.13287/j.1001-9332.202001.001

Cornwell, W. K., Westoby, M., Falster, D. S., Fitzjohn, R. G., O'Meara, B. C., Pennell, M. W., et al. (2014). Functional distinctiveness of major plant lineages. *J. Ecol.* 102, 345–356. doi: 10.1111/1365-2745.12208

Dayrell, R. L. C., Arruda, A. J., Pierce, S., Negreiros, D., Meyer, P. B., Lambers, H., et al. (2018). Ontogenetic shifts in plant ecological strategies. *Funct. Ecol.* 32, 2730–2741. doi: 10.1111/1365-2435.13221

Díaz, S., Kattge, J., Cornelissen, J. H. C., Wright, L. J., Lavorel, S., Dray, S., et al. (2016). The global spectrum of plant form and function. *Nature* 529, 167–171. doi: 10.1038/nature16489

Dong, M. (2011). *Clonal Plant Ecology*. Beijing: Science Press. 28–123.

Dong, H. P., Cao, H. J., Xie, L. H., Huang, Q. Y., Yang, L. B., Ni, H. W., et al. (2022). Effects of water levels in heterogeneous habitats on sexual reproductive allocation of *Deyeuxia angustifolia*. *Chin. J. Appl. Ecol.* 33, 378–384. doi: 10.13287/j.1001-9332.0202.004

Grime, J. P. (1974). Vegetation classification by reference to strategies. *Nature* 250, 26–31. doi: 10.1038/250026a0

Grime, J. P. (2001). *Plant Strategies, Vegetation Processes and Ecosystem Properties*, *2nd*. Chichester: Wiley.

Hodgson, J. G., Wilson, P. J., Hunt, R., Grime, J. P., and Thompson, K. (1999). Allocating CSR Plant Functional Types: A Soft Approach to a Hard Problem. *Oikos* 85, 282–294. doi: 10.2307/3546494

Hu, Z. X., Mulholland, M. R., Duan, S. S., and Xu, N. (2012). Effects of nitrogen supply and its composition on the growth of *Prorocentrum donghaiense*. *Harmful Algae* 13, 72–82. doi: 10.1016/j.hal.2011.10.004

Hutchings, M. J., and Wijesinghe, D. K. (1997). Patchy habitats, division of labour and growth dividends in clonal plants. *Trends Ecol. Evol.* 12, 390–394. doi: 10.1016/S0169-5347(97)87382-X

Jackson, J. B. C., Buss, L. W., Cook, R. E., and Ashmun, J. W. (1985). *Population Biology and Evolution of Clonal Organisms*. New Haven: Yale University Press: 259–296.

Johnson, B. G., Verburg, P. S., and Arnone, J. A. (2016). Plant species effects on soil nutrients and chemistry in arid ecological zones. *Oecologia* 182, 299–317. doi: 10.1007/s00442-016-3655-9

Jung, V., Violle, C., Mondy, C., Hoffmann, L., and Muller, S. (2010). Intraspecific variability and trait-based community assembly. *J. Ecol.* 98, 1134–1140. doi: 10.1111/j.1365-2745.2010.01687.x

Levins, R. (1968). *Evolution in Changing Environments*. Princeton: Princeton University Press: 27–85.

Li, L., Lan, Z. H., Chen, J. K., and Song, Z. P. (2018). Allocation to clonal and sexual reproduction and its plasticity in *Vallisneria spinulosa* along a water-depth gradient. *Ecosphere* 9:e02070. doi: 10.1002/ecs2.2070

Lu, R. K. (2010). *Soil Agrochemical Analysis Method*. Beijing: Chinese Agriculture Press: 55–163.

Lu, Y. T., Liu, H. L., Chen, Y. F., Zhang, L., Kudusi, K., and Song, J. H. (2022). Effects of drought and salt stress on seed germination of ephemeral plants in desert of Northwest China. *Front. Ecol. Evol.* 10, 01–16. doi: 10.3389/fevo.2022.1026095

Luo, C. Y., Fu, X. L., Zeng, X. Y., Cao, H. J., Wang, J. F., Ni, H. W., et al. (2022). Responses of remnant wetlands in the Sanjiang Plain to farming-landscape patterns. *Ecol. Indic.* 135:108542. doi: 10.1016/j.ecolind.2022.108542

Ma, K. P. (1995). Studies on the structure and function of *Calamagrostis angustifolia* grassland ecosystem I. the basic characteristics of plant community and environment. *Chin. Bull. Bot.* 12, 1–8.

Mclntyre, S., Lavorel, S., Landsberg, J., and Forbes, T. D. A. (2009). Disturbance response in vegetation–towards a global perspective on functional traits. *J. Veg. Sci.* 10, 621–630. doi: 10.2307/3237077

Munoz, F., Violle, C., and Cheptou, P. O. (2016). CSR ecological strategies and plant mating systems: outcrossing increases with competitiveness but stress-tolerance is related to mixed mating. *Oikos* 125, 1296–1303. doi: 10.1111/oik.02328

Ni, B., Zhao, W., Zuo, X. H., You, J., Li, Y. L., Li, J. N., et al. (2022). *Deyeuxia angustifolia* Kom. Encroachment changes soil physicochemical properties and microbial Community in the alpine tundra under climate change. *Sci. Total Environ.* 813:152615. doi: 10.1016/j.scitotenv.2021.152615

Pierce, S., Brusa, G., Sartori, M., and Cerabolini, B. E. L. (2012). Combined use of leaf size and economics traits allows direct comparison of hydrophyte and terrestrial herbaceous adaptive strategies. *Ann. Bot.* 109, 1047–1053. doi: 10.1093/aob/mcs021

Pierce, S., Brusa, G., Vagge, I., and Cerabolini, B. E. L. (2013). Allocating CSR plant functional types: the use of leaf economics and size traits to classify woody and herbaceous vascular plants. *Funct. Ecol.* 27, 1002–1010. doi: 10.1111/1365-2435.12095

Pierce, S., Negreiros, D., Cerabolini, B. E. L., Kattge, J., Díaz, S., Kleyer, M., et al. (2017). A global method for calculating plant CSR ecological strategies applied across biomes world-wide. *Funct. Ecol.* 31, 444–457. doi: 10.1111/1365-2435.12722

Qu, Y., Luo, C. Y., Zhang, H. Q., Ni, H. W., and Xu, N. (2018). Modeling the wetland restorability based on natural and anthropogenic impacts in Sanjiang Plain, China. *Ecol. Indic.* 91, 429–438. doi: 10.1016/j.ecolind.2018.04.008

Qu, Y., Zheng, Y. M., Gong, P., Shi, J. L., Li, L. P., Wang, S. D., et al. (2022). Estimation of wetland biodiversity based on the hydrological patterns and connectivity and its potential application in change detection and monitoring: a case study of the Sanjiang Plain, China. *Sci. Total. Environ.* 805:150291. doi: 10.1016/j.scitotenv.2021.150291

Reekie, E. (1991). Cost of seed versus rhizome production in *Agropyron repens*. *Can. J. Bot.* 69, 2678–2683. doi: 10.1139/b91-336

Reich, P. B. (2014). The world-wide 'fast–slow' plant economics spectrum: a traits manifesto. *J. Ecol.* 102, 275–301. doi: 10.1111/1365-2745.12211

Rüger, N., Comita, L. S., Condit, R., Purves, D., Rosenbaum, B., Visser, M. D., et al. (2018). Beyond the fast–slow continuum: demographic dimensions structuring a tropical tree community. *Ecol. Lett.* 21, 1075–1084. doi: 10.1111/ele.12974

Shang, W., Wu, X. D., Zhao, L., Yue, G. Y., Zhao, Y. H., Qiao, Y. P., et al. (2016). Seasonal variations in labile soil organic matter fractions in permafrost soils with different vegetation types in the Central Qinghai-Tibet Plateau. *Catena* 137, 670–678. doi: 10.1016/j.catena.2015.07.012

Shi, F. X., Song, C. C., Zhang, X. H., Mao, R., Guo, Y. D., and Gao, F. Y. (2015). Plant zonation patterns reflected by the differences in plant growth, biomass partitioning and root traits along a water level gradient among four common vascular plants in freshwater marshes of the Sanjiang Plain, Northeast China. *Ecol. Eng.* 81, 158–164. doi: 10.1016/j.ecoleng.2015.04.054

Song, Y. Y., Song, C. C., Ren, J. S., Zhang, X. H., and Jiang, L. (2019). Nitrogen input increases *Deyeuxia angustifolia* litter decomposition and enzyme activities in a marshland ecosystem in Sanjiang Plain, Northeast China. *Wetlands* 39, 549–557. doi: 10.1007/s13157-018-1102-x

Sugiyama, S., and Bazzaz, F. A. (1998). Size dependence of reproductive allocation: the influence of resource availability, competition and genetic identity. *Funct. Ecol.* 12, 280–288. doi: 10.1046/j.1365-2435.1998.00187.x

Tomlinson, K. W., and O'connor, T. G. (2004). Control of tiller recruitment in bunchgrasses: uniting physiology and ecology. *Funct. Ecol.* 18, 489–496. doi: 10.1111/j.0269-8463.2004.00873.x

Wang, X., Tong, S. Z., Li, Y. Z., Qi, Q., Zhang, D. J., Lyu, X. G., et al. (2019). Plant diversity performance after natural restoration in reclaimed *Deyeuxia angustifolia* wetland. *Chin. Geogr. Sci.* 29, 437–445. doi: 10.1007/s11769-019-1043-1

Wijesinghe, D. K., and Handel, S. N. (1994). Advantages of clonal growth in heterogeneous habitats: an experiment with *Potentilla simplex*. *J. Ecol.* 82, 495–502. doi: 10.2307/2261258

Yang, W. J., Cheng, H. G., Hao, F. H., Ouyang, W., Liu, S. Q., and Lin, C. Y. (2012). The influence of land-use change on the forms of phosphorus in soil profiles from the Sanjiang Plain of China. *Geoderma* 189–190, 207–214. doi: 10.1016/j.geoderma.2012.06.025

Zhang, D. Y. (2004). *Plant Life-History Evolution and Reproductive Ecology Edited*. Beijing: Science Press: 67–98.

Zhang, D. J., Qi, Q., Wang, X. H., Tong, S. Z., Lv, X. G., An, Y., et al. (2019). Physiological responses of *Carex schmidtii* Meinsh to alternating flooding-drought conditions in the Momoge wetland, Northeast China. *Aquat. Bot.* 153, 33–39. doi: 10.1016/j.aquabot.2018.11.010

Zhang, D. J., Xia, J. B., Sun, J. K., Dong, K. K., Shao, P. S., Wang, X. H., et al. (2022). Effect of wetland restoration and degradation on nutrient trade-off of *Carex schmidtii*. *Front. Ecol. Evol.* 9, 1–14. doi: 10.3389/fevo.2021.801608

Zhao, K. Y. (1999). *Chinese Swamp Chronicles*. Beijing: Science Press: 28–76.

Frontiers in
Ecology and Evolution

Ecological and evolutionary research into our natural and anthropogenic world

This multidisciplinary journal covers the spectrum of ecological and evolutionary inquiry. It provides insights into our natural and anthropogenic world, and how it can best be managed.

Discover the latest Research Topics

See more →

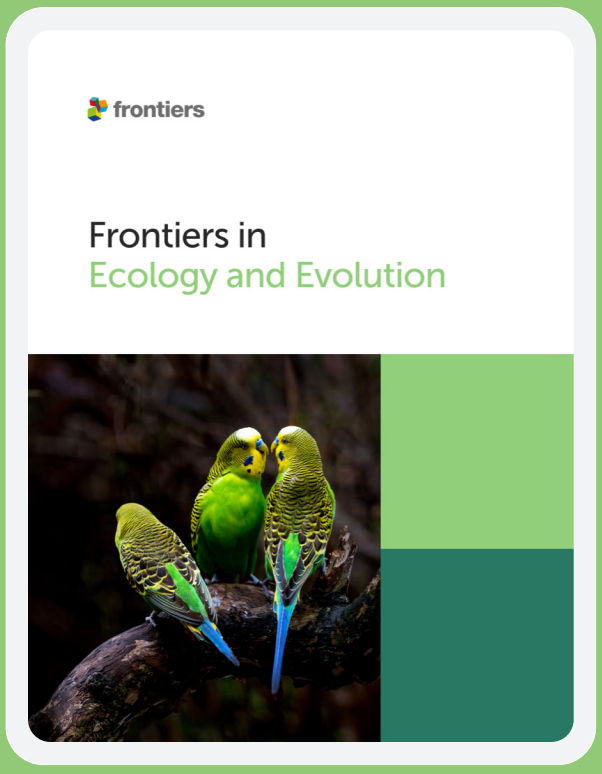

Frontiers

Avenue du Tribunal-Fédéral 34
1005 Lausanne, Switzerland
frontiersin.org

Contact us

+41 (0)21 510 17 00
frontiersin.org/about/contact